P.O.Box 2345, Beijing 100023,China
Fax: +86-10-85381893
E-mail: wjg@wjgnet.com www.wjgnet.com

World J Gastroenterol 2003;9(6):1135-1138
World Journal of Gastroenterology
Copyright ©2003 by The WJG Press ISSN 1007-9327

• REVIEW •

# Severe acute respiratory syndrome and its lesions in digestive system

Jian-Zhong Zhang

**Jian-Zhong Zhang,** Department of Pathology, 306 Hospital of PLA, Beijing 100101, China
**Correspondence to:** Professor Jian-Zhong Zhang, Director of Department of Pathology, Beijing 306 Hospital, 9 North Anxiang Road, P.O.Box 9720, Chaoyang District, Beijing 100101, China. zhangjz55@sina.com
**Telephone:** +86-10-66356237 **Fax:** +86-10-64871261
**Received:** 2003-05-20 **Accepted:** 2003-05-27

## Abstract

Severe acute respiratory syndrome (SARS) is an infectious atypical pneumonia that has recently been recognized in the patients in 32 countries and regions. This brief review summarizes some of the initial etiologic findings, pathological description, and its lesions of digestive system caused by SARS virus. It is an attempt to draw gastroenterologists and hepatologists' attention to this fatal illness, especially when it manifests itself initially as digestive symptoms.

Zhang JZ. Severe acute respiratory syndrome and its lesions in digestive system. *World J Gastroenterol* 2003; 9(6): 1135-1138
http://www.wjgnet.com/1007-9327/9/1135.asp

## INTRODUCTION

In November 2002, a so-called atypical pneumonia with unknown etiology appeared in Guangdong Province, China, followed by reports from Hong Kong, Vietnam, Singapore, Canada and Beijing of severe febrile respiratory illness that spread to household members and health care workers[1-6,23-26]. This disease was designated "severe acute respiratory syndrome (SARS)" later by the World Health Organization (WHO) and global efforts to understand the cause of this illness and prevent its spread were instituted in March 2003. Many cases could be linked through chains of transmission to a health care worker from Guangdong Province, China, who visited Hong Kong, where he was hospitalized with SARS and died. Till May 19, 2003, a cumulative total of 7 864 SARS cases were reported to WHO from 29 countries; 643 deaths (case-fatality proportion: 8.2 %) have been reported, in which most cases occurred in China (7291 cases)[7]. The incubation period for the disease is usually 2 to 7 days. Infection is characterized by fever, non-productive cough, and shortness of breath, and the presence of minimal auscultatory findings with consolidation on chest radiographs. Lymphopenia, leucopenia, thrombocytopenia, and elevated liver enzymes and creatinine kinase may also present in most cases.

In response to this outbreak, WHO coordinated an international collaboration that included clinical, epidemiologic, and laboratory investigation, and initiated efforts to control the spread of SARS. Rapid research progress has been made in last three months. This brief review is to focus on the etiologic and pathologic findings with an emphasis on the known lesions in the liver and intestine.

## ETIOLOGICAL FINDINGS

The isolation of a novel coronavirus was obtained from the respiratory secretions of patients with SARS and subsequently demonstrating this virus or a serologic response to this virus, points to a possible etiologic association with SARS[5,6,17,20,22,27]. The discovery of this new virus occurred through a broad-based and multidisciplinary effort by clinical, epidemiologic, and laboratory investigators.

Researchers around the world have sequenced the genetic codes of SARS virus, and are searching for clues to the virus' s origins, behavior, and future. Science is set to publish online a paper analyzing the genome from the BCCA Genome Sciences Center in Vancouver, as well as one from the Centers for Disease Control and Prevention (CDC) in Atlanta (www.sciencemag.org/feature/data/sars). Now that sequencing technology has become cheap and widely available, almost every country or area affected by SARS is sequencing its own version, including Hong Kong, Singapore and China[8-10]. The viruses themselves are something of an oddity. With a genome of the complete -29 700 nucleotides, coronaviruses are relative giants, and they have a complex two-step replication mechanism. Many RNA virus genomes contain a single, large gene that is translated by the host' s cellular machinery to produce all viral proteins. Coronaviruses, instead, can have up to 10 separate genes. Most ribosomes translate the biggest one of these, called replicase, which by itself is twice the size of many other RNA viral genomes. The replicase gene produces a series of enzymes that use the rest of the genome as a template to produce a set of smaller, overlapping messenger RNA molecules, which are then translated into the so-called structural proteins - the building blocks of new viral particles. Most coronaviruses cause either a respiratory or an enteric disease, and some do both. But the differences among these types can be small. In 1999, for instance, a team led by Luí s Enjuanes of the Autonomous University of Madrid, Spain, showed that just two point mutations can change a mostly enteric virus that can kill piglets into a nondeadly one that excels at the respiratory route but replicates poorly in the gut[11].

Researchers have grouped coronaviruses into three categories based on cross-reactivity of antibodies backed up by genetic data; the two previously known human viruses fell into different groups. Investigators have hoped that the genome sequence of the new virus would help pinpoint its origins. But a first glance at the data has yielded few clues. The new coronavirus does not fit into any of the clusters but is a new one by itself. Phylogenetic analysis of the predicted viral proteins indicates that the virus does not closely resemble any of the three previously known groups of coronaviruses. The genome sequence will aid in the diagnosis of SARS virus infection in humans and potential animal hosts (using PCR and immunological tests), in the development of antivirals (including neutralizing antibodies), and in the identification of putative epitopes for vaccine development.

## PATHOLOGICAL CHANGES IN THE LUNG

Pathological studies of patients who died of SARS from Guangdong, Hongkong, Beijing and Singapore showed diffuse

alveolar damage (DAD) in the lung as the most notable feature[5,6,12,15,21]. In those individuals with severe disease resulting in death, scattered type II pneumocytes showed marked cytologic changes including multinucleation, cytomegaly, nucleomegaly, clearing of nuclear chromatin, and prominent nucleoli. Although these changes were severe, they were within the spectrum of epithelial changes seen in other cases of DAD. Definite viral inclusions were not always found in the cytoplasm of epithelial cells. Nicholis *et al*[12] found that DAD was common but not universal. Morphologic changes identified were bronchial epithelial denudation, loss of cilia, and squamous metaplasia. Other findings included focal intraalveolar hemorrhage, hemophagocytosis, necrotic inflammatory debris in small airways, organizing pneumonia or secondary bacterial pneumonia.

DAD is a pattern of acute lung injury characterized, in the acute phase, by hyaline membranes, interstitial and intraalveolar edema, patchy type II pneumocyte hyperplasia, microthrombi, and scant interstitial infiltrates of mononuclear cells. The acute phase forms a continuum with the proliferative or organizing phase in which proliferation of interstitial fibroblasts and prominent type II pneumocyte hyperplasia are the histologic hallmarks. In addition to DAD, the autopsy cases showed acute bronchopneumonia and variable intravascular thrombosis, all of which are common as terminal events. Biopsy material from milder cases or earlier in the course of illness may better define the initial lesion in SARS.

Multinucleated syncytial cells were identified in the alveolar spaces in a few patients. These cells contained abundant vacuolated cytoplasm with cleaved and convoluted nuclei, which show either CD68 or cytokeratin positive. No obvious intranuclear or intracytoplasmic viral inclusions were identified, and electron-microscopical examination of a limited number of these syncytial cells revealed no coronavirus particles. No definitive immunostaining was identified in tissues from a patient with SARS, with the use of a battery of immunohistochemical stains reactive with coronavirus from antigenic groups I, II, and III. In addition, no staining of patient tissues was identified with the use of immunohistochemical stains for influenza viruses A and B, adenoviruses, Hendra and Nipah viruses, metapneumoviruses, respiratory syncytial virus, measles virus, *Myocoplasma pneumoniae*,and *Chlamydia pneumoniae*[14].

Evaluation of Vero E6 cells infected with coronavirus isolated from a patient with SARS revealed viral cytopathic effect that included occasional multinucleated syncytial cells but no obvious viral inclusions. Immunohistochemical assays with various antibodies reactive with coronavirus from antigenic group I, including human coronavirus 229E, feline infectious peritonitis virus 1, and porcine transmissible gastroenteritis virus, and with an immune serum specimen from a patient with SARS demonstrated strong cytoplasmic and membranous staining of infected cells. No staining was identified with any of several monoclonal or polyclonal antibodies reactive with coronavirus in antigenic group II (human coronavirus OC43, bovine coronavirus, and mouse coronavirus) or group III (turkey coronavirus and infectious bronchitis virus). Electron-microscopical examination of a bronchoalveolar-lavage specimen from one patient revealed many coronavirus-infected cells[14].

Ksiazek and colleagues[5] noticed that the primary histopathological lesions are consistent with a nonspecific acute response to lung injury that can be caused by infections, trauma, drugs, or toxic chemicals. The multinucleated syncytial cells without viral inclusions seen in the lungs of two patients, however, are suggestive of a number of viral infections including measles and parainfluenzavirus, respiratory syncytial virus, and Nipah virus infection. Multinucleated syncytial cells associated with some human coronavirus infections have occasionally been observed in cell culture, but most often in cell cultures inoculated with animal coronaviruses. To detect this novel coronavirus antigen, the investigators used an extensive panel of antibodies against coronaviruses that are representative of the three antigenic groups, including several group 1 antiserum specimens that reacted against Urbani SARS-associated coronavirus infected tissue-culture material. A possible explanation for the failure of this antiserum to react with antigens in these patients on immunohistochemical analysis is that the host immune response has cleared the virus from these tissues. The tissues were available late in the course of the illness, 14 to 20 days after its onset. For many viral respiratory infections, viral antigens and nucleic acids are cleared within two weeks after the onset of disease.

Electron microscopic examination showed that virus-like particles with 100-150 nm in diameter were found in cytoplasm and dilated reticular endoplasm of the infected alveolar epithelial cells and endothelial cells[5, 15-17]. Other agents, such as paramyxovirus, metapneumovirus and chlamydia, were also identified in the pulmonary tissues[16,22]. It could be that the coronavirus may by itself produce the disease but it may also open the door for other viruses, or nonviruses, to aggravate the disease.

The pathogenesis of this disorder remains to be determined. However, the mechanism of acute lung injury could involve direct damage by the virus to the alveolar wall by targeting either endothelial cells or epithelial cells. Alternatively, the virus could infect inflammatory cells with the injury mediated through cytokines, interleukins, or tumor necrosis factor-alpha. It is also possible that the tissue damage in SARS is not directly related to viral infection in tissues but is a secondary effect of cytokines or other factors induced by viral infection proximal to but not within the lung tissue. In influenza infections, viral antigens are seen predominantly in respiratory epithelium of large airways and are only rarely identified in pulmonary parenchyma, despite concomitant and occasionally severe interstitial pneumonitis.

## LESIONS IN DIGESTIVE ORGANS

As previously described, most coronaviruses cause either a respiratory or an enteric disease, which is also transmitted by the faecal-oral route. During this outbreak of SARS, symptoms of gastrointestinal tract in the patients were noticed. Many investigators[13,19,24] found that gastrointestinal symptoms are not uncommon at presentation, including diarrhea (19-50 percent), nausea and vomiting (19.6 percent), and abdominal pain (13 percent) manifested in SARS patients.

As many as 66 % of the patients in the Amoy Garden SARS outbreak in Hong Kong also had diarrhea, contributing to a significant virus load being discharged in the sewerage, which caused 361 cases of SARS[3]. During hospitalization, some patients were present with mildly elevated aminotransferase levels (indicating liver damage), or developed dysfunction of the liver at the later stage of the disease. Some patients presented with severe acute abdominal pain requiring exploratory laparotomy. All these patients developed typical SARS. These clinical findings suggest that SARS virus does involve the digestive system, especially the epithelial cells of intestinal mucosa.

Pathologic evaluation of the fatal cases showed that, except the lung changes, hepatocytes underwent fatty degeneration, cloudy swelling, apoptosis and dot necrosis, with Kupffer cell proliferation and portal infiltrates of lymphocytes[15,16]. There were regional hemorrhages, vascular congestion and lymphocytic infitration in gastrointestinal walls of the patient. Suckling mice inoculated with SARS-infected samples also

demonstrated hepatocytic lesions, including swelling, vacuolar and hydropic degenerations, focal cellular condensation and necrosis. But no coronavirus-like particles were found in hepatocytes.

Epidemiologic investigation also showed that the virus could survive in stools for at least two days and in diarrhoeal stools, which has a higher pH, for up to four days. It can also survive on plastic surfaces for up to 48 hours, but it is not yet known how big a dose of the virus is required to cause infection[18].

According to the experience of Prince of Wales Hospital in Hong Kong[20], where SARS outbreak happened, the difficulty of making a firm diagnosis until chest radiographic changes appear has important implications for health-care personnel and for surveillance. Three major reasons for spread of infection to health-care workers are: failure to apply isolation precautions to cases not yet identified as SARS, breaches of procedure, and inadequate precautions. Every patient must now be assumed to have SARS, which has major long-term implications for the health-care system. Another reason for spread among health-care workers is infected workers continuing to work despite symptoms, such as mild fever. Such individuals must now cease working. However, staying at home can also have disastrous consequences for exposed family members. Potential cases therefore require early isolation from both workplace and household. Extreme measures are required to protect health-care workers, who account for about 20 % of cases. Therefore, gastroenterologists and hepatologists should pay more attention when contacting the patients.

SARS has been appropriately elicited because current knowledge regarding the transmission of this disease is rapidly evolving and clinicians must provide patient care while dealing with a degree of uncertainty. The Centers for Disease Control and Prevention have published and regularly update logical recommendations for preventing the spread of the causative agent. The causative organism appears to spread predominantly by contact and droplets and may spread by airborne routes as well. The use of N-95 masks, gowns, double gloves, hand hygiene, and eye protection seem well advised and appear to have substantially curtailed spread within hospitals.

Global efforts have described this new syndrome with dramatic speed, and identified and sequenced the apparent etiologic agents. With expedited efforts to develop a specific diagnostic test, effective infection-control techniques, and to develop effective therapies and vaccines for SARS-associated coronavirus, and to create a true global health network, there is much reason for optimism. To be prepared for that challenge, health care professionals must not forsake their patients, the research community must help provide answers to the unanswered questions, and health care leadership must take the knowledge from that research to rapidly implement whatever strategies necessary to better combat this newly emerging infectious disease[28].

## REFERENCES


1 **Centers for Disease Control and Prevention**. CDC update: outbreak of severe acute respiratory syndrome-worldwide, 2003. *MMWR* 2003; **52:** 241-248

2 **World health organization**. Situation Update-SARS. Available at http://www.who.int/mediacentre/releases/2003/pr31/en/

3 **Hong Kong Department of Health Report**. Main findings of an investigation into the outbreak of severe acute respiratory syndrome at Amoy Gardens. http://www.info.gov.hk/dh/ap.htm (accessed April 19, 2003)

4 **Booth CM**, Matukas LM, Tomlinson GA, Rachlis AR, Rose DB, Dwosh HA, Walmsley SL, Mazzulli T, Avendano M, Derkach P, Ephtimios LE, Kitai I, Mederski BD, Shadowitz SB, Gold WL, Hawrylurk LA, Rea E, Chenkin JS, Cescon DW, Poutanen SM, Detsky AS. Clinical features and short-term outcomes of 144 patients with SARS in the Greater Toronto Area. *JAMA* 2003; **289**: 1-9

5 **Ksiazek TG,** Erdman D, Goldsmith C, Zaki SR, Peret T, Emery S, Tong S, Urbani C, Comer JA, Lim W, Rolin PE, Dowell S, Ling AE, Humphrey C, Shieh WJ, Guarner J, Paddock CD, Rota P, Fields B, DeRisi J, Yang JY, Cox N, Hughes J, LeDuc JW, Bellini W, Anderson LJ, the SARS Working Group. A Novel Coronavirus Associated with Severe Acute Respiratory Syndrome. New Eng J Med, 2003. http://www.nejm.org, May 10, 2003

6 **Rota PA,** Oberste MS, Monroe SS, Nix A, Campagnoli R, Icenogle JP, Penaranda S, Bankamp B, Maher K, Chen MH, Tong S, Tamin A, Lowe L, Frace M, DeRisi JL, Chen Q, Wang D, Erdam D, Peret TC, Burns C, Ksiazek TG, Rollin PE, Sanchez A, Liffick S, Holloway B, Limor J, McCausland K, Olsen-Rassmussen M, Fouchier R, Gunther S, Osterhaus ADME, Drosten C, Paliansch MA, Anderson LJ, Bellini WJ. Characterization of a novel coronavirus associated with severe acute respiratory syndrome. Science. Available at Sciencexpress/www.sciencexpress.org/1 May 2003/10.1126/science.1085952

7 **World Health Organization.** Cumulative probable cases of severe acute respiratory syndrome (SARS). http://www.who.int/csr/sars/cases (accessed May 19, 2003)

8 **Enserink M**, Vogel G. Hungry for details, scientists zoom in on SARS genomes. *Science* 2003; **300**: 715-716

9 **Marra MA,** Jones SJM, Astel CR, Holt RA, Brooks-Wilson A, Butterfield YS, Khattra J, Asano JK, Barber SA, Chan SY, Cloutier A, Coughlin SM, Freeman D, Girn N, Griffith OL, Leach SR, Mayo M, McDonald H, Montgomery SB, Pandoh PK, Petrescu AS, Robertson AG, Schein JE, Siddiqui A, Smailus DE, Stott JM, Yang GS, Plummer F, Andonov A, Artsob H, Bastien N, Bernard K, Booth TF, Bowness D, Drebot M, Fernando L, Flick R, Garbutt M, Gray M, Grolla A, Jones S, Feldmann H, Meyers A, Kabani A, Li Y, Normand S, Stroher U, Tipples GA, Tyler S, Vogrig R, Ward D, Watson B, Brunham RC, Krajden M, Petric M, Skowronski DM, Upton C, Roper RL. The genome sequence of the SARS-associated coronavirus. Sciencexpress /www. sciencexpress. org/1 May 2003/10.1126/science.1085953

10 **Center for Disease Control and Prevention.** SARS coronavirus sequencing. Availiable at: http://www.cdc.gov/ncidod/sars/sequence.htm

11 **Enserink M**. Calling all coronavirologists. *Science* 2003; **300**: 413-414

12 **Nicholls JM,** Poon LLM, Lee KC, Ng WF, Lai ST, Leung CY, Chu CM, Hui PK, Mak KL. Lung pathology of fatal severe acute respiratory syndrome. Lancet, Published online May 16, 2003/http://image.thelancet.com/extras/03art4347web.pdf

13 **Lee N,** Hui D, Wu A, Chan P, Cameron P, Joynt GM, Ahuja A, Yung MY, Leung CB, To KF, Lui SF, Szeto CC, Chung S, Sung JJY. A Major Outbreak of Severe Acute Respiratory Syndrome in Hong Kong. *N Engl J Med* 2003; **348**:1986-1994

14 **Zhao JM**, Zhou GD, Sun YL, Wang SS, Yang JF, Mao LY, Pan D, Mao PY, Cheng Y, Wang YD, Xin SJ, Zhou XZ, Lu JY, Li L, Chen JM. Pathological and etiological findings in a dead case of severe acute respiratory syndrome in China. *Jifangjun Yixue Zazhi* 2003; **28**: 379-382

15 **Wang CE**, Qin ED, Gan YH, Li YC, Wu XH, Cao JT, Yu M, Si BY, Yan G, Li JF, Zhu QY. Pathological observation on sucking mice and Vero E6 cells inoculated with SARS samples. *Jifangjun Yixue Zazhi* 2003; **28**: 383-384

16 **Hong T**, Wang JW, Sun YL, Duan SM, Chen LB, Qu JG, Ni AP, Liang GD, Ren LL, Yang RQ, Guo L, Zhou WM, Chen J, Li DX, Wen XB Xu H, Guo YJ, Dai SL, Bi SL, Dong XP, Ruan L. Chlamydia-like and coronavirus-like agents found in dead cases of atypical pneumonia by electron microscopy. *Zhonghua Yixue Zazhi* 2003; **83**: 632-636

17 **Ksiazek TG**, Drosten C, Gunther S, Preiser W, Finkelstein S, Rose D, Green K, Tellier R, Draker R, Adachi D, Ayers M, Chan AK, Skowronski DM, Salit I, Simor AE, Slutsky AS, Doyle PW, Krajden M, Petric M, Brunham R, Geer AJ. Identification of a novel coronavirus in patients with severe acute respiratory syndrome. N Eng J Med, 2003 http://www.nejm.org, May 10, 2003

18 **Donnelly CA,** Ghani AC, Leung GM, Hedley AJ, Fraser C, Riley S, Abu-Raddad LJ, Ho ML, Thach TQ, Chau P, Chan KP, Lam TH, Tse LY, Tsang T, Liu SH, Kong JHB, Lau EMC, Ferguson

NM, Roy M, Anderson RM. Epidemiological determinants of spread of causal agent of severe acute respiratory syndrome in Hong Kong. Lancet. Published online May 7, 2003 / http: / / image. thelancet.com / extras / 03art4453web.pdf, t

19 **Tomlinson B**, Cockram C. SARS: experience at Prince of Wales Hospital, Hong Kong, Lancet 2003; **361**: 1486-1487

20 **Poon LLM**, Wong OK, Luk W, Yuen KY, Peris JSM, Guan Y. Rapid diagnosis of a coronavirus associated severe acute respiratory syndrome (SARS). *Clin Chem* 2003; **49**: 1-3

21 **Chan WY**, Hui PK. Pathology of SARS 2003 Hong Kong. Available at http: / / www.eelab.com

22 **Peirs JSM**, Lai ST, Poon LLM, Guan Y, Yam LYC, Lim W, Nicholls J, Yee WKS, Yan WW, Cheung MT, Cheng VCC, Chan K H, Tsang DNC, Yung RWH, Ng TK, Yuen KY, and members of the SARS study group*. Coronavirus as a possible cause of severe acute respiratory syndrome. *Lancet* 2003; **361:** 1319-1325

23 **Poutanen SM**, Low DE, Henry B, Finkelstein S, Rose D, Green K, Tellier R, Draker R, Adachi D, Ayers M, Chan AK, Skowronski DM, Salit I, Simor AE, Slutsky AS, Doyle PW, Krajden M, Petric M, Brunham RC, McGeer AJ. National Microbiology Laboratory, Canada; Canadian Severe Acute Respiratory Syndrome Study Team. Identification of severe acute respiratory syndrome in Canada. *N Engl J Med* 2003; **348**: 1995-2005

24 **Tsang KW**, Ho PL, Ooi GC, Yee WK, Wang T, Chan-Yeung M, Lam WK, Seto WH, Yam LY, Cheung TM, Wong PC, Lam B, Ip MS, Chan J, Yuen KY, Lai KN. A cluster of cases of severe acute respiratory syndrome in Hong Kong. *N Engl J Med* 2003; **348**: 1977-1985

25 **Lee N**, Hui D, Wu A, Chan P, Cameron P, Joynt GM, Ahuja A, Yung MY, Leung CB, To KF, Lui SF, Szeto CC, Chung S, Sung JJ. A major outbreak of severe acute respiratory syndrome in Hong Kong. *N Engl J Med* 2003; **348**: 1986-1994

26 **Drosten C**, Gunther S, Preiser W, Van Der Werf S, Brodt HR, Becker S, Rabenau H, Panning M, Kolesnikova L, Fouchier RA, Berger A, Burguiere AM, Cinatl J, Eickmann M, Escriou N, Grywna K, Kramme S, Manuguerra JC, Muller S, Rickerts V, Sturmer M, Vieth S, Klenk HD, Osterhaus AD, Schmitz H, Doerr HW. Identification of a Novel Coronavirus in Patients with Severe Acute Respiratory Syndrome. *N Engl J Med* 2003; [epub ahead of print]

27 **Fouchier RA**, Kuiken T, Schutten M, Van Amerongen G, Van Doornum GJ, Van Den Hoogen BG, Peiris M, Lim W, Stohr K, Osterhaus AD. Aetiology: Koch's postulates fulfilled for SARS virus. *Nature* 2003; **423**: 240-241

28 **Masur H**, Emanuel E, Lane HC. Severe Acute Respiratory Syndrome: Providing Care in the Face of Uncertainty. *JAMA* 2003; **289**: (DOI 10.1001 / jama.289.21.JED30036)

**Edited by** Zhu LH

P.O.Box 2345, Beijing 100023,China
Fax: +86-10-85381893
E-mail: wjg@wjgnet.com www.wjgnet.com

World J Gastroenterol 2003;9(6):1139-1143
World Journal of Gastroenterology
Copyright ©2003 by The WJG Press ISSN 1007-9327

• REVIEW •

# Advances in clinical diagnosis and treatment of severe acute respiratory syndrome

Qing-He Nie, Xin-Dong Luo, Wu-Li Hui

**Qing-He Nie, Xin-Dong Luo,** The Chinese PLA Center of Diagnosis and Treatment for Infectious Diseases, Tangdu Hospital, Fourth Military Medical University, Xi' an 710038, Shaanxi Province, China
**Wu-Li Hui,** Department of Epidemiology, Chinese People' s Armed Police Force Medical College, Tianjin 300162, China
**Correspondence to:** Dr. Qing-He Nie, The Chinese PLA Center of Diagnosis and Treatment for Infectious Diseases, Tangdu Hospital, Fourth Military Medical University, Xi' an 710038, Shaanxi Province, China. nieqinghe@hotmail.com
Currently, Dr. Qing-He Nie works at Xiao Tang Shan Hospital in Beijing as a member of SARS expert committee
**Telephone:** +86-29-3377452 **Fax:** +86-29-3537377
**Received:** 2003-05-31 **Accepted:** 2003-06-04

## Abstract

It has been proved that severe acute respiratory syndrome (SARS) is caused by SARS-associated coronavirus, a novel coronavirus. SARS originated in Guangdong Province, the People's Republic of China at the end of 2002. At present, it has spread to more than 33 countries or regions all over the world and affected 8 360 people and killed 764 by May 31,2003. Identification of the SARS causative agent and development of a diagnostic test are important. Detecting disease in its early stage, understanding its pathways of transmission and implementing specific prevention measures for the disease are dependent upon swift progress. Due to the efforts of the WHO-led network of laboratories testing for SARS, tests for the novel coronavirus have been developed with unprecedented speed. The genome sequence reveals that this coronavirus is only moderately related to other known coronaviruses. WHO established the definitions of suspected and confirmed and probable cases. But the laboratory tests and definitions are limited. Until now, the primary measures included isolation, ribavirin and corticosteroid therapy, mechanical ventilation, *etc.* Other therapies such as convalescent plasma are being explored. It is necessary to find more effective therapy. There still are many problems to be solved in the course of conquering SARS.

Nie QH, Luo XD, Hui WL. Advances in clinical diagnosis and treatment of severe acute respiratory syndrome. *World J Gastroenterol* 2003; 9(6): 1139-1143
http://www.wjgnet.com/1007-9327/9/1139.asp

## INTRODUCTION

On 12 March 2003, the World Health Organization (WHO) issued a global alert on the atypical pneumonia, also called severe acute respiratory syndrome (SARS), after reports from the Department of Health of Hong Kong of an outbreak of pneumonia in one of its public hospitals. At about the same time, WHO received reports of the syndrome from China, Singapore, Vietnam, Thailand, Indonesia, Taiwan, and the Philippines, as well as from countries in other continents including Canada, the United States, and Germany. The disease originated in Guangdong Province at the end of 2002 and has affected 8 360 people and killed 764 by May 31, 2003. Dr. Carlo Urbani reported the disease first in a Vietnam French Hospital of Hanoi[1]. WHO took prompt measures to avoid wider spread of SARS according to his alarm. It has been proved that a novel coronavirus is associated with SARS (SARS-CoV), and that this virus plays an etiologic role in SARS[2-9]. Because of the death of Dr. Carlo Urbani (46 years old, an expert of infectious diseases, Italian) from SARS, Ksiazek and his colleagues proposed that their first isolate be named the Urbani strain of SARS-associated coronavirus.

On 17 March 2003, WHO called upon 11 laboratories in 9 countries to join a collaborative multi-center research project on SARS diagnosis. This network took advantage of modern communication technologies to share outcomes of investigation of clinical samples from SARS cases in real time. Clinicians from China, Hong Kong and the USA introduced their own experience of treatment on SARS. Scientists have made great progress in the clinical diagnosis and treatment of SARS. However, there are still many difficulties and problems to be solved in the course of conquering SARS.

## DIAGNOSIS

Identification of SARS causative agent and development of a diagnostic test are of paramount importance. Detecting disease in its early stage, understanding its pathways of transmission and implementing disease specific prevention measures are dependent upon swift progress and results in aetiological and diagnostic research.

### *Clinical presentations*

Booth *et al*[10] reported that features of the clinical examination most commonly found in the patients at admission were self-reported fever (99 %), documented elevated temperature (85 %), nonproductive cough (69 %), myalgia (49 %), and dyspnea (42 %). The reports from Zhong[11] and Chan-Yeung *et al*[12] were similar to this.

### *Laboratory tests*

Due to the efforts of the WHO-led international multi-center collaborative network of laboratory testing for SARS, tests for the novel coronavirus have been developed with unprecedented speed[13].

Early in the course of the disease, the absolute lymphocyte count is often decreased. Overall white blood cell counts are generally normal or decreased. At the peak of the respiratory illness, approximately 50 % of patients have leukopenia and thrombocytopenia or low platelet counts within normal range. Early in the respiratory phase, elevated creatine phosphokinase levels (as high as 3 000 IU/L) and hepatic transaminases (two to six times of the upper limits of normal) have been noted. In the majority of patients, renal function is normal. Common laboratory features include elevated lactate dehydrogenase (87 %), hypocalcemia (60 %), and lymphopenia (54 %). Only 2 % of patients have rhinorrhea[10] (Tables 1 and 2).

**Table 1** Earliest symptoms of SARS[a]

| Symptom | No. (%) of patients ($n$=144) |
|---|---|
| Fever ($n$=106) | |
| Alone | 33(23) |
| With prodrome | 33(23) |
| With prodrome and cough or dyspnea | 16(11) |
| With cough or dyspnea | 15(11) |
| With other combinations | 9(6) |
| Prodrome alone | 19(13) |
| Cough or dyspnea alone | 13(9) |
| Symptom reported first | |
| Prodrome | 74(52) |
| Fever | 106(74) |
| Cough or dyspnea | 51(35) |
| Diarrhea | 9(6) |

[a]Prodrome includes headache, malaise, or myalgia.

**Table 2** Laboratory features of SARS at admission and during hospitalization

| | At admission | | During hospitalization[a] | |
|---|---|---|---|---|
| | Median (IQR) | No./Total(%) Abnormal[b] | Median (IQR) | No./Total (%) Abnormal[b] |
| Lymphocytes, /μL | 900 (700-1300) | 104/122 (85) | 500 (400-800) | 106/120 (88) |
| Lactate dehydrogenase, U/L | 396 (219-629) | 86/99 (87) | 630 (363-1156) | 115/123 (94) |
| Creatine kinase, U/L | 157 (70-310) | 43/109 (39) | 370 (208-959) | 64/118 (54) |
| Potassium, mEq/L | 3.7 (3.4-4.0) | 36/137 (26) | 3.2 (2.9-3.4) | 60/140 (43) |
| Calcium, mg/dL[c] | 8.52 (8.2-9.16) | 53/89 (60) | 8.1 (7.76) | 71/101 (70) |
| Magnesium, mg/dL | 1.94 (1.7-2.19) | 12/68 (18) | 1.43 (0.97-1.51) | 55/96 (57) |
| Phosphorus, mg/dL | 3.10 (2.76-3.69) | 17/64 (27) | 2.17 (1.83-2.48) | 41/78 (53) |

Abbreviations: IQR, interquartile range; SI conversions: To convert calcium to mmol/L. multiply by 0.25. To convert magnesium to mmol/L, multiply by 0.411. To convert phosphorus to mmol/L, multiply by 0.323. [a]The most abnormal value recorded used. [b]Defined as lymphocytes <1 500/μL; lactate dehydrogenase >190 U/L; creatine kinase >240 U/L for men and >190 U/L for women; potassium <3.5 mEq/L; calcium <8.8 mg/dL; magnesium <1.70 mg/dL; phosphate <2.79 mg/dL. [c]Calcium values have been corrected for serum albumin.

### *Radiographic findings of SARS*

Wong *et al*[14] found that initial chest radiographs were abnormal in 108 of 138 (78.3 %) patients and showed air-space opacity. Lower lung zone (70 of 108, 64.8 %) and right lung (82 of 108, 75.9 %) were more preferably involved. In most patients, peripheral lung involvement was more common (81 of 108, 75.0 %). Unifocal involvement (59 of 108, 54.6 %) was more frequent than multifocal or bilateral involvement.

### *Molecular test (PCR)*

Sequencing of the about 30000-base genome of the SARS-associated coronavirus has completed[15-21]. The genome sequence revealed that this coronavirus was only moderately related to other known coronaviruses, including two human coronaviruses, HCoV-OC43 and HCoV-229E. A valid positive PCR result indicated that there was genetic material (RNA) from the SARS-CoV in the sample. However, it does not mean the virus present is infectious, or that it is present in a large enough quantity to infect another person. Negative PCR results do not exclude SARS. Besides the possibility of obtaining false-negative test results, specimens may not have been collected at a time when the virus or its genetic material was present.

The SARS-CoV-specific RNA can be detected in various clinical specimens such as blood, stool, respiratory secretions or body tissues by PCR. A number of PCR protocols developed by members of the WHO laboratory network are available on a WHO website[22].

Despite their high sensitivity, the existing PCR tests cannot rule out the presence of the SARS virus in patients on account of possible false negative results. On the other hand, contamination of samples in laboratories may lead to false positive results.

### *SARS-CoV isolation*

The presence of the infectious virus can be detected by inoculating suitable cell cultures (e.g.Vero cells) with patient's specimens (such as respiratory secretions, blood or stool) and propagating the virus *in vitro*. Once isolated, the virus must be identified as SARS-CoV using further tests. Cell culture is a very demanding test, but is currently (with the exception of animal trials) the only means to show the existence of a live virus. Positive cell culture results indicate the presence of live SARS-CoV in the sample. Negative cell culture results do not exclude SARS.

### *Antibody detection*

Various methods provide a means for the detection of antibodies produced in response to infection with SARS-CoV. Different types of antibodies (IgM or IgG) appear and change in level during the course of infection. They can be undetectable in the early stages of infection. IgG usually remains detectable after resolution of the illness. It was reported that IgG would reach peak value 60 days after obvious symptoms and then keep it, while IgM would reach peak value on day 14 after onset of apparent symptoms. Enzyme-linked immunosorbent assay (ELISA), immunofluorescence assay (IFA), neutralisation test are being developed, but are not yet commercially available.

## WHO CASE DEFINATION[23]

The definitions of suspected and confirmed and probable case according to the WHO Case Definition are as follows:

### *Suspect case*

A person presenting after 1 November 2002, with history of: high fever (>38 ℃) and cough or breathing difficulty, and one or more of the following exposures during the 10 days prior to onset of symptoms: (1) close contact, with a person who is a suspect or probable case of SARS; (2) history of travel, to an area with recent local transmission of SARS; (3) residing in an area with recent local transmission of SARS. Close contact means having cared for, lived with, or had direct contact with respiratory secretions or body fluids of a suspect or probable case of SARS.

A person with an unexplained acute respiratory illness resulting in death after 1 November 2002, but on whom no autopsy has been performed, and one or more of the following exposures during the 10 days prior to onset of symptoms: (1) close contact with a person who is a suspect or probable case of SARS; (2) history of travel to an area with recent local transmission of SARS, and (3) residing in an area with recent local transmission of SARS.

### *Probable case*

(1) A suspect case with radiographic evidence of infiltrates

consistent with pneumonia or respiratory distress syndrome (RDS) on chest X-ray (CXR). (2) A suspect case of SARS that is positive for SARS coronavirus by one or more assays. See Use of laboratory methods for SARS diagnosis. (3) A suspect case with autopsy findings consistent with the pathology of RDS without an identifiable cause.

### *Exclusion criteria*

A case should be excluded if an alternative diagnosis can fully explain their illness.

### *Reclassification of cases*

As SARS is currently a diagnosis of exclusion, the status of a reported case may change over time. A patient should always be managed as clinically appropriate, regardless of their case status. (1) A case initially classified as suspect or probable, for whom an alternative diagnosis can fully explain the illness, should be discarded after carefully considering the possibility of co-infection. (2) A suspect case who, after investigation, fulfils the probable case definition should be reclassified as "probable". (3) A suspect case with a normal CXR should be treated, as deemed appropriate, and monitored for 7 days. Those cases in whom recovery is inadequate should be re-evaluated by CXR. (4) Those suspect cases in whom recovery is adequate but whose illness cannot be fully explained by an alternative diagnosis should remain as "suspect". (5) A suspect case who died, on whom no autopsy was conducted, should remain classified as "suspect". However, if this case is identified as being part of a chain transmission of SARS, the case should be reclassified as "probable". (6) If an autopsy was conducted and no pathological evidence of RDS was found, the case should be "discarded".

The surveillance period began on 1 November 2002 to capture cases of atypical pneumonia in China now recognized as SARS. International transmission of SARS was first reported in March 2003 for cases with onset in February 2003. The Centers for Disease Control and Prevention have added laboratory criteria for evidence of infection with SARS-CoV to the interim surveillance case definition[24]. Using the new laboratory criteria, a SARS case is laboratorily confirmed if one of the following is met: detection of the SARS-CoV antibody by indirect fluorescent antibody (IFA) or enzyme-linked immunosorbent assay (ELISA), isolation of SARS-CoV in tissue culture, detection of SARS-CoV RNA by reverse transcriptasepolymerase chain reaction (RT-PCR), which must be confirmed by a second PCR test. Negative laboratory results for PCR, viral culture, or antibody tests obtained within 21 days of illness do not rule out SARS-CoV infection. In these cases, an antibody test of a specimen obtained more than 21 days after the onset of illness is needed to determine infection. Unless PCR confirms the initial suspicion of SARS infection, the diagnosis of SARS is based on the clinical findings of an atypical pneumonia not attributed to any other cause as well as a history of exposure to a suspect or probable case of SARS, or to their respiratory secretions or other body fluids. The initial diagnostic testing for suspected SARS patients should include chest radiography, pulse oximetry, blood cultures, sputum Gram stain and culture, and testing for viral respiratory pathogens, obviously influenza A and B and respiratory syncytial virus. A specimen for Legionella and pneumococcal urinary antigen testing should also be considered.

Clinicians should save any available clinical specimens (respiratory, blood, and serum) for additional testing until a specific diagnosis is made. Acute and convalescent (greater than 21 days after the onset of symptoms) serum samples should be collected from each patient who meets the definition criteria for SARS. Specific instructions for collecting specimens from suspected SARS patients are available on the Internet.

In the early stages, SARS may be hard to differentiate from other viral infections, and diagnostic delays may contribute to the spread of the epidemic. Nevertheless, until standardized reagents for virus and antibody detection become available and methods have been adequately tested, the diagnosis of SARS remains based on clinical and epidemiological findings. The revised case definition for the first time includes laboratory results: a suspected case of SARS, that is positive for SARS-CoV in one or more assays, should be reclassified as a probable case. At present there are no defined criteria for SARS-CoV test results to confirm or reject the diagnosis of SARS.

Positive laboratory test results for other known agents that are able to cause atypical pneumonia such as Legionella pneumophila, influenza and parainfluenza viruses, mycoplasma pneumoniae etc. may serve as exclusion criteria; according to the case definition, a case should be excluded if an alternative diagnosis can fully explain the illness. However, the possibility of dual infection must not be ruled out completely. According to our clinical experience and correlative papers, we think that exact diagnosis of a confirmed case must need a history of close contact and persistent symptoms (fever or influenza-like symptom). To observe the chest x-ray of patient continuously is also necessary.

## TREATMENT

From initial clinical experience, SARS can develop in stages, including acute constitutional symptoms, acute viral pneumonitis, acute lung injury, and even acute respiratory distress syndrome, evolving over 1 to 2 weeks. Initial infection followed by a hyperactive immune response appears to underlie the severe manifestations of SARS. Therefore, corticosteroids can be used to dampen excessive lung damage due to an inflammatory response.

### *Ribavirin and gucocorticoid therapy*

A series of 31 patients with probable SARS were treated according to a treatment protocol consisting of antibacterials and a combination of ribavirin and methylprednisolone in Hong Kong[25]. One patient recovered by antibacterial treatment alone, 17 showed rapid and sustained responses, and 13 achieved improvements with step-up or pulsed methylprednisolone. Four patients required short periods of non-invasive ventilation. No patient required intubation or mechanical ventilation. There was no mortality or treatment morbidity in this series. The following is the standard protocol.

### *Antibacterial treatment*

(1) Levofloxacin 500 mg once daily intravenously or orally; (2) Or clarithromycin 500 mg twice daily orally plus coamoxiclav(amoxicillin and clavulanic acid) , 375 mg three times daily orally if patient is <18 years old, pregnant, or suspected to have tuberculosis.

### *Ribavirin and methylprednisolone*

Combination treatment with ribavirin and methylprednisolone when: (1) Extensive or bilateral chest radiographic involvement; (2) Or persistent chest radiographic involvement and persistent high fever for 2 days; (3) Or clinical, chest radiographic, or laboratory findings suggestive of worsening; (4) Or oxygen saturation <95 % in room air.

### *Standard corticosteroid regimen for 21 days*

(1) Methylprednisolone 1 mg/kg every 8 h (3 mg/kg daily) intravenously for 5 days; (2) Then methylprednisolone 1 mg/kg every 12 h (2 mg/kg daily) intravenously for 5 days; (3) Then prednisolone 0· 5 mg/kg twice daily (1 mg/kg daily) orally

for 5 days; (4) Then prednisolone 0· 5 mg/kg daily orally for 3 days; (5) Then prednisolone 0· 25 mg/kg daily orally for 3 days; (6) Then off.

### *Ribavirin regimen for 10-14 days*

(1) Ribavirin 400 mg every 8 h (1 200 mg daily) intravenously for at least 3 days (or until condition becomes stable); (2) Then ribavirin 1 200 mg twice daily (2 400 mg daily) orally.

### *Pulsed methylprednisolone*

(1) Give pulsed methylprednisolone if clinical condition, chest radiograph, or oxygen saturation worsens (at least two of these), and lymphopenia persists; (2) Give methylprednisolone 500 mg twice daily intravenously for 2 days, then back to standard corticosteroid regimen.

### *Mechanical ventilation*

Traditional approaches to mechanical ventilation use tidal volumes of 10 to 15 ml per kilogram of body weight and may cause stretch-induced lung injury in patients with acute lung injury and the acute respiratory distress syndrome. The Acute Respiratory Distress Syndrome Network therefore conducted a trial. The mean tidal volumes on days 1 to 3 were 6.2±0.8 and 11.8±0.8 ml per kilogram of predicted body weight. They found that in patients with acute lung injury and acute respiratory distress syndrome, mechanical ventilation with a lower tidal volume than traditionally used resulted in decreased mortality and increased number of days without ventilator use[26-29].

Cordingley *et al*[30] suggests that reduced mortality may be achieved by using a strategy that aims at preventing overdistension of the lungs. There is no clinical evidence to support the use of specific $FiO_2$ thresholds, but it is common clinical practice to decrease $FiO_2$ below 0.6 as quickly as possible. $SaO_2$ values of around 90 % are commonly accepted. $PaCO_2$ is allowed to rise during lung protective volume and pressure limited ventilation. $PaCO_2$ levels of 2-3 times 3 normal seem to be well tolerated for prolonged periods. Renal compensation for respiratory acidosis occurs over several days. Many clinicians infuse sodium bicarbonate slowly if arterial pH falls below 7.20, Set PEEP at a relatively high level such as 15 cm $H_2O$ in patients with ARDS. It is common practice during pressure control ventilation to increase the I:E ratio to 1:1 or 2:1 (inverse ratio ventilation) with close monitoring of intrinsic PEEP and haemodynamics.

### *Other therapies being studied*

At present, serum therapy is being studied for SARS patients. 40 patients were divided into two groups in the Medical College of Hong Kong Chinese University. One group was treated with convalescent plasma and another group not. The effect was obviously different among two groups after one month, the therapy group died no patients while another group 3 patients, but it needs more clinical trial to be proved. In their opinion, to use convalescent plasma within earlier two weeks will shorten the in-hospital period and fever time and reduce mortality. Serum therapy was used to dying patients and aged patients with other severe or chronic disease and pregnant women.

As to another trial in Hong Kong[31], treatment of a SARS patient followed by 200 ml convalescent plasma donated by SARS patients in their convalescent phase. No adverse reaction occurred after administration of convalescent plasma. The fever subsided, chest X-ray showed further resolution of basal lung infiltrates, and she made an uneventful recovery. Although no probable SARS case has been ascribed to transmission by labile blood products or blood derivatives, there is a theoretical risk of transmission of the SARS virus through transfusion of labile blood products, since low viraemia has been detected up to approximately 10 days after the onset of symptoms from probable SARS patients[32].

Moller *et al*[33] reported that bovine surfactant therapy in severe ARDS improved oxygenation immediately after administration. This improvement was sustained only in the subgroup of patients without pneumonia but with an initial PaO2/FIO2 ratio higher than 65. The SARS studies on antisense oligonucleotide drug, polypeptide, and vaccine will benefit the treatment of this disease.

It has been proved that a novel coronavirus is the cause of SARS with strong infectivity. Up to now, we have only understood the preliminary pathogenesis and epidemiology of SARS. After all SARS is a disease seen never before in human. To control and defend human being from this disease, further studies are needed, such as: (1) origin, mutation, life cycle, transmission pathways of SARS-CoV; (2) the mechanisms of SARS-CoV replicating and coming into the host cell; (3) pathogenesis of acute lung injury and abnormal immune response; (4) rapid diagnosis and vaccine, and (5) effective medicine such as inhibitory polypeptide. With rapid progress in the basic studies of the disease all over the world, more effective drugs and treatment measures will be discovered in the days to come and SARS will be put under complete control by mankind soon.

## REFERENCES


1 **Reilley B**, Van Herp M, Sermand D, Dentico N. SARS, Carlo Urbani. *N Engl J Med* 2003; **348**: 1951-1952

2 **Ksiazek TG**, Erdman D, Goldsmith CS, Zaki SR, Peret T, Emery S, Tong S, Urbani C, Comer JA, Lim W, Rollin PE, Dowell SF, Ling AE, Humphrey CD, Shieh WJ, Guarner J, Paddock CD, Rota P, Fields B, DeRisi J, Yang JY, Cox N, Hughes JM, LeDuc JW, Bellini WJ, Anderson LJ. A novel coronavirus associated with severe acute respiratory syndrome. *N Engl J Med* 2003; **348**: 1953-1966

3 **Rota PA**, Oberste MS, Monroe SS, Nix WA, Campagnoli R, Icenogle JP, Penaranda S, Bankamp B, Maher K, Chen MH, Tong S, Tamin A, Lowe L, Frace M, DeRisi JL, Chen Q, Wang D, Erdman DD, Peret TC, Burns C, Ksiazek TG, Rollin PE, Sanchez A, Liffick S, Holloway B, Limor J, McCaustland K, Olsen-Rasmussen M, Fouchier R, Gunther S, Osterhaus AD, Drosten C, Pallansch MA, Anderson LJ, Bellini WJ. Characterization of a novel coronavirus associated with severe acute respiratory syndrome. *Science* 2003; **300**: 1394-1399

4 **Falsey AR**, Walsh EE. Novel coronavirus and severe acute respiratory syndrome. *Lancet* 2003; **361**: 1312-1313

5 **Drosten C**, Gunther S, Preiser W, van der Werf S, Brodt HR, Becker S, Rabenau H, Panning M, Kolesnikova L, Fouchier RA, Berger A, Burguiere AM, Cinatl J, Eickmann M, Escriou N, Grywna K, Kramme S, Manuguerra JC, Muller S, Rickerts V, Sturmer M, Vieth S, Klenk HD, Osterhaus AD, Schmitz H, Doerr HW. Identification of a novel coronavirus in patients with severe acute respiratory syndrome. *N Engl J Med* 2003; **348**: 1967-1976

6 **Peiris JS**, Lai ST, Poon LL, Guan Y, Yam LY, Lim W, Nicholls J, Yee WK, Yan WW, Cheung MT, Cheng VC, Chan KH, Tsang DN, Yung RW, Ng TK, Yuen KY. Coronavirus as a possible cause of severe acute respiratory syndrome. *Lancet* 2003; **361**: 1319-1325

7 **No authors listed**. Severe acute respiratory syndrome (SARS) and coronavirus testing-United States, 2003. *Mmwr Morb Mortal Wkly Rep* 2003; **52**: 297-302

8 **No authors listed**. From the centers for disease control and prevention. severe acute respiratory syndrome (SARS) and coronavirus testing-united states, 2003. *JAMA* 2003; **289**: 2203-2206

9 Update 31 - Coronavirus never before seen in humans is the cause of SARS. http://www.who.int/csr/sarsarchive/2003_04_16/en/

10 **Booth CM**, Matukas LM, Tomlinson GA, Rachlis AR, Rose DB, Dwosh HA, Walmsley SL, Mazzulli T, Avendano M, Derkach P, Ephtimios IE, Kitai I, Mederski BD, Shadowitz SB, Gold WL, Hawryluck LA, Rea E, Chenkin JS, Cescon DW, Poutanen SM,

Detsky AS. Clinical features and short-term outcomes of 144 patients with SARS in the greater toronto area. *JAMA* 2003; [epub ahead of print]
11 **Zhong NS**. The Clinical Diagnosis and Treatment of SARS at present. *Zhong Guoyi Xuelun Tanbao* 2003; **4**: 29
12 **Chan-Yeung M**, Yu WC. Outbreak of severe acute respiratory syndrome in hong kong special administrative region: case report. *BMJ* 2003; **326**: 850-852
13 SARS: Laboratory diagnostic tests.29 April 2003.http://www.who.int/csr/sars/diagnostictests/en
14 **Wong KT**, Antonio GE, Hui DS, Lee N, Yuen EH, Wu A, Leung CB, Rainer TH, Cameron P, Chung SS, Sung JJ, Ahuja AT. Severe acute respiratory syndrome: radiographic appearances and pattern of progression in 138 patients. *Radiology* 2003; [epub ahead of print]
15 **Marra MA**, Jones SJ, Astell CR, Holt RA, Brooks-Wilson A, Butterfield YS, Khattra J, Asano JK, Barber SA, Chan SY, Cloutier A, Coughlin SM, Freeman D, Girn N, Griffith OL, Leach SR, Mayo M, McDonald H, Montgomery SB, Pandoh PK, Petrescu AS, Robertson AG, Schein JE, Siddiqui A, Smailus DE, Stott JM, Yang GS, Plummer F, Andonov A, Artsob H, Bastien N, Bernard K, Booth TF, Bowness D, Czub M, Drebot M, Fernando L, Flick R, Garbutt M, Gray M, Grolla A, Jones S, Feldmann H, Meyers A, Kabani A, Li Y, Normand S, Stroher U, Tipples GA, Tyler S, Vogrig R, Ward D, Watson B, Brunham RC, Krajden M, Petric M, Skowronski DM, Upton C, Roper RL. The Genome sequence of the SARS-associated coronavirus. *Science* 2003; **300**: 1399-1404
16 **Dye C**, Gay N. Modeling the SARS Epidemic. *Science* 2003; [epub ahead of print]
17 **Lipsitch M**, Cohen T, Cooper B, Robins JM, Ma S, James L, Gopalakrishna G, Chew SK, Tan CC, Samore MH, Fisman D, Murray M. Transmission dynamics and control of severe acute respiratory syndrome. *Science* 2003; [epub ahead of print]
18 **Riley S**, Fraser C, Donnelly CA, Ghani AC, Abu-Raddad LJ, Hedley AJ, Leung GM, Ho LM, Lam TH, Thach TQ, Chau P, Chan KP, Lo SV, Leung PY, Tsang T, Ho W, Lee KH, Lau EM, Ferguson NM, Anderson RM. Transmission dynamics of the etiological agent of SARS in hong kong: impact of public health interventions. *Science* 2003: [epub ahead of print]
19 **Lipsitch M**, Cohen T, Cooper B, Robins JM, Ma S, James L, Gopalakrishna G, Chew SK, Tan CC, Samore MH, Fisman D, Murray M. Transmission dynamics and control of severe acute respiratory syndrome. *Science* 2003: [epub ahead of print]
20 **Fisher DA**, Chew MH, Lim YT, Tambyah PA. Preventing local transmission of SARS: lessons from singapore. *Med J Aust* 2003; **178**: 555-558
21 **Stohr K**. A multicentre collaboration to investigate the cause of severe acute respiratory syndrome. *Lancet* 2003; **361**: 1730-1733
22 PCR primers for SARS developed by WHO Network Laboratories. 17 April 2003 http://www.who.int/csr/sars/primers/en/
23 Case Definitions for Surveillance of Severe Acute Respiratory Syndrome SARS. http://www.who.int/csr/sars/casedefinition/en/
24 Updated Interim U.S. Case Definition of Severe Acute Respiratory Syndrome (SARS).May 23, 2003, 10:00 PM. http://www.cdc.gov/ncidod/sars/diagnosis.htm
25 **So LK**, Lau AC, Yam LY, Cheung TM, Poon E, Yung RW, Yuen KY. Development of a standard treatment protocol for severe acute respiratory syndrome. *Lancet* 2003; **361**: 1615-1617
26 **The Acute Respiratory Distress Syndrome Network**. Ventilation with lower tidal volumes as compared with traditional tidal volumes for acute lung injury and the acute respiratory distress syndrome. *N Engl J Med* 2000; **342**: 1301-1308
27 **Allegra L**, Blasi F. Problems and perspectives in the treatment of respiratory infections caused by atypical pathogens. *Pulm Pharmacol Ther* 2001; **14**: 21-27
28 **Atabai K**, Matthay MA. The pulmonary physician in critical care. 5: Acute lung injury and the acute respiratory distress syndrome: definitions and epidemiology. *Thorax* 2002; **57**: 452-458
29 **The Acute Respiratory Distress Syndrome Network**. Ventilation with lower tidal volumes as compared with traditional tidal volumes for acute lung injury and the acute respiratory distress syndrome. *N Engl J Med* 2000; **342**: 1301-1308
30 **Cordingley JJ**, Keogh BF. The pulmonary physician in critical care. 8: Ventilatory management of ALI/ARDS. *Thorax* 2002; **57**: 729-734
31 **Wong VWS**, Dai D, Wu AKL, Sung JJY. Treatment of severe acute respiratory syndrome with convalescent plasma. *H K MJ* http://www.hkmj.org.hk/hkmj/update/SARS/cr1606.htm
32 WHO Recommendations on SARS and Blood Safety. http://www.who.int/csr/sars/guidelines/bloodsafety/en/
33 **Moller JC**, Schaible T, Roll C, Schiffmann JH, Bindl L, Schrod L, Reiss I, Kohl M, Demirakca S, Hentschel R, Paul T, Vierzig A, Groneck P, Von Seefeld H, Schumacher H, Gortner L. Treatment with bovine surfactant in severe acute respiratory distress syndrome in children: a randomized multicenter study. *Intensive Care Med* 2003; **29**: 437-446

**Edited by** Zhu LH and Zhang JZ

P.O.Box 2345, Beijing 100023,China
Fax: +86-10-85381893
E-mail: wjg@wjgnet.com www.wjgnet.com

World J Gastroenterol 2003;9(6):1144-1155
World Journal of Gastroenterology
Copyright ©2003 by The WJG Press ISSN 1007-9327

• REVIEW •

# Mechanism and its regulation of tumor-induced angiogenesis

Manoj Kumar Gupta, Ren-Yi Qin

**Manoj Kumar Gupta, Ren-Yi Qin,** Department of Surgery, Tongji Hospital, Tongji Medical College, Huazhong University of Science and Technology, Wuhan, 430030, Hubei Province, China
**Supported by** National Natural Science Foundation of China, No 30271473
**Correspondence to:** Professor Ren-Yi Qin, Department of Surgery, Tongji Hospital, Tongji Medical College, Huazhong University of Science and Technology, Wuhan, 430030, Hubei, China. ryqin@tjh.tjmu.edu.cn
**Telephone:** +86-27-83662389
**Received:** 2002-11-29 **Accepted:** 2003-01-13

## Abstract

Tumor angiogenesis is the proliferation of a network of blood vessels that penetrates into cancerous growths, supplying nutrients and oxygen and removing waste products. The process of angiogenesis plays an important role in many physiological and pathological conditions. Solid tumors depend on angiogenesis for growth and metastasis in a hostile environment. In the prevascular phase, the tumor is rarely larger than 2 to 3 $mm^3$ and may contain a million or more cells. Up to this size, tumor cells can obtain the necessary oxygen and nutrient supplies required for growth and survival by simple passive diffusion. The properties of tumors to release and induce several angiogenic and anti-angiogenic factors which play crucial roles in regulating endothelial cell (EC) proliferation, migration, apoptosis or survival, cell-cell and cell-matrix adhesion through different intracellular signaling are thought to be the essential mechanisms during tumor-induced angiogenesis. Tumor angiogenesis actually starts with tumor cells releasing molecules that send signals to surrounding normal host tissue. This signaling activates certain genes in the host tissue that, in turn, make proteins to encourage growth of new blood vessels. In this review, we focus the mechanisms of tumor-induced angiogenesis, with an emphasis on the regulatory role of several angiogenic and anti-angiogenic agents during the angiogenic process in tumors. Advances in understanding the mechanisms of tumor angiogenesis have led to the development of several most effective anti-angiogenic and anti-metastatic therapeutic agents and also have provided several techniques for the regulation of cancer's angiogenic switch. The suggestion is made that standard cytotoxic chemotherapy and angiogenesis inhibitors used in combination may produce complementary therapeutic benefits in the treatment of cancer.

Gupta MK, Qin RY. Mechanism and its regulation of tumor-induced angiogenesis. *World J Gastroenterol* 2003; 9(6): 1144-1155
http://www.wjgnet.com/1007-9327/9/1144.asp

## MECHANISM OF ANGIOGENESIS

Angiogenesis is a complex multi-step process involving extensive interplay between cells, soluble factors, and extracellular matrix (ECM) components. Four distinct sequential steps in angiogenesis include: (1) degradation of basement membrane by proteases; (2) migration of endothelial cells (ECs) into the interstitial space and sprouting; (3) ECs proliferation at the migrating tip; (4) lumen formation, generation of new basement membrane with the recruitment of pericyte, formation of anastomoses and finally blood flow[1]. The angiogenic response in the microvasculature is associated with changes in cellular adhesive interactions between adjacent ECs, pericytes and surrounding ECM. In the process of active neovascularization, activated ECs reorganize their cytoskeleton, express cell surface adhesion molecules such as integrins and selectins, secrete proteolytic enzymes, and remodel their adjacent ECM. These events are followed by the formation of capillary buds. Autocrine and/or paracrine angiogenic factors must be present to induce EC migration, proliferation, elongation, orientation and differentiation leading to the re-establishment of the basement membrane, lumen formation and anastomosis with other new or pre-existing vessels, eventually leading to the formation of intact microvessels.

## CANCER'S ANGIOGENIC SWITCH

Angiogenic phenotype serves the development of malignant tumor at multiple stages. Tumor cells may overexpress one or more of the positive regulators of angiogenesis, may mobilize an angiogenic protein from the ECM, may recruit host cells such as macrophages (which produce their own angiogenic proteins), or may engage in a combination of these processes. Tumor angiogenesis is mediated by tumor-secreted angiogenic growth factors that interact with their surface receptors expressed on ECs. The most commonly found angiogenic growth factors such as VEGF and bFGF, when encounter ECs, they bind to the tyrosine kinase receptors on ECs membrane. Binding leads to dimerization of the receptors and activation of autophosphorylation of tyrosines on the receptor surface and thereby initiates the several signaling proteins (including PI3-kinase, Src, Grb2/m-SOS-1 (a nucleotide exchange factor for Ras) and signal transducers and activators of transcriptions (STATs) each of which contains src-homology-2 (SH-2) domains[2]. Binding of the SH-2 regions of these proteins to the phosphotyrosines on the receptor tyrosine kinases (RTKs) activates several pathways that are crucial for triggering the cell cycle machinery. The most well studied pathway passes through the GTP-binding protein Ras and activates the mitogen activated protein kinase (MAPK) cascade and subsequently transcription factors in the nucleus[2]. Up-regulation of an angiogenic factor is not sufficient in itself for a tumor cell to become angiogenic, however, certain negative regulators or inhibitors of vessel growth may need to be down-regulated[3]. If there is a preponderance of angiogenic factors in the local milieu, the neovasculature may persist as capillaries, or differentiate into mature venules or arterioles. If instead, the local milieu changes such that there is a preponderance of angiostatic factors, the neovessels can regress. The angiostatic factors that mediate regression can do so either by inducing apoptosis or cell cycle arrest of ECs. Thus, the switch to the angiogenic phenotype is regulated by a change in the local equilibrium between positive and negative regulators of the growth of microvessels[1, 3].

## FACTORS INVOLVED IN TUMOR ANGIOGENESIS

### *Vascular endothelial growth factor and receptors*

Vascular endothelial growth factor (VEGF), also known as

vascular permeability factor (VPF), is a heparin-binding angiogenic growth factor, and is highly expressed in various types of tumors. It may increase ECs permeability by enhancing the activity of vesicular-vacuolar organelles, clustered vesicles in ECs lining small vessels that facilitate transport of metabolites between luminal and abluminal plasma membranes[4]. Alternatively, VEGF may enhance permeability through mitogen-activated protein (MAP) kinase signal transduction cascade by loosening adhering junctions between ECs in a monolayer via rearrangement of cadherin/catenin complexes[5, 6]. In addition, recent studies have shown that VEGF enhances ECs permeability by activating PKB/Akt, endothelial nitric-oxide synthase (eNOS), and MAP kinase dependent pathways using human umbilical vein endothelial cell[7] (Figure 1). Increased vascular permeability may allow the extravasation of plasma proteins and formation of ECM favorable to endothelial and stromal cell migration.

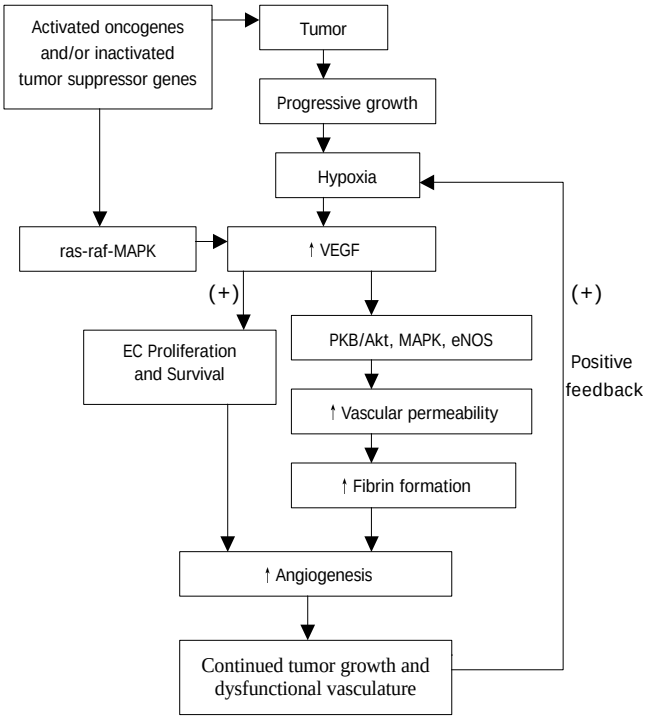


**Figure 1** The triggering mechanism in tumor angiogenesis: inactivated tumor suppressor genes / activated oncogenes versus hypoxia.

VEGF is an EC specific mitogen. VEGF, after binding to its high affinity receptors (Flt-1/VEGFR-1, Flk-1/KDR/VEGFR-2), promotes the formation of the second messenger via hydrolysis of inositol, thus induces the autophosphorylation of the receptors in the presence of heparin-like molecules, and open phosphatidylinositol metabolic signal transduction pathways, activates MAP kinases in EC and thereby VEGF exerts its mitogenic effect by promoting EC proliferation[8, 9].

VEGF induces a balanced system of proteolysis that can remodel ECM components necessary for angiogenesis. VEGF stimulates EC production of urokinase-like plasminogen activator (uPA), tissue type plasminogen activator (tPA) and plasminogen activator inhibitor-1 (PAI-1)[10, 11], proteolytic enzymes, tissue factors, and interstitial collagenase[12]. Plasminogen activators activate plasminogen to plasmin, which can break down ECM components. In addition to remodeling the basement membrane, uPA bound to uPAR also mediates intracellular signal transduction in ECs. Tang *et al*. have demonstrated that uPAR occupancy on ECs results in the phosphorylation of focal adhesion proteins and the activation of MAP kinase[13] through which uPA influences EC migration and proliferation (Figure 2).

Moreover, VEGF has been shown to exhibit its angiogenic effect by inducing expression of the $\alpha_1\beta_1$, $\alpha_2\beta_1$ and $\alpha v\beta_3$-integrins, which promote cell migration, proliferation and matrix reorganization (Figure 2), and $\alpha_1\beta_1$, $\alpha_2\beta_1$ and $\alpha v\beta_3$ antagonists may prove effective on inhibiting VEGF-driven angiogenesis associated with cancers and other pathologies through apoptosis[14, 15]. VEGF, in addition to a very specific mitogen for vascular EC, is a potent pro-survival factor for ECs in newly formed immature vessels. Several endothelial survival factors (VEGF, angiopoietin-1 and $\alpha v\beta_3$) suppress p53, p21, p16 and p27, and proapoptotic protein Bax, whereas they variably activate the survival PI3k/Akt, p42/44 MAP kinases, bcl-2, A1 and survivin pathways[16-20](Figure 2). It was reported that p42/p44 MAP kinases promoted VEGF expression by activating its transcription via recruitment of the AP-2/Sp1 (activator protein-2) complex on the proximal region (-88/-66) of the VEGF promoter and by direct phosphorylation of hypoxia-inducible factor 1 alpha (HIF-1 alpha)[21]. Pharmacological inhibition of PI3K or transfection with a dominant-negative Akt mutant abolished the antiapoptotic effect of VEGF on ECs. In addition to the PI3K/Akt pathway, ras-dependent signaling pathways might also play an important role at least for VEGF signaling. Thus, H-rasV12G down-regulation leads to profound tumor regression, which is initially characterized by massive apoptosis of tumor- and host-derived ECs[22]. Therefore, apoptosis induction is resistant to enforced VEGF expression, suggesting that VEGF requires an intact Ras-dependent signaling pathway to mediate its apoptosis inhibitory effect[22]. And also, VEGF via the KDR/Flt-1 receptor induces enhanced expression of the serine-threonine protein kinase Akt[19], a downstream target of PI3-kinase, which potently blocks apoptosis by interfering with various apoptosis signaling pathways[23, 24], promotes EC migration[25], and enhances the expression of the hypoxia-inducible factor (HIF), which is known to stimulate VEGF expression[26], suggesting a potent proangiogenic effect[27, 28]. These findings have identified the VEGFR2 and the PI3K/Akt signal transduction pathway as crucial elements in promoting EC survival induced by VEGF. The downstream effector pathways mediating the antiapoptotic VEGF effect include Akt-dependent activation of the endothelial nitric oxide synthase (NOS)[29, 30], resulting in an enhanced endothelial NO synthesis, which, in turn promotes EC survival (Figure 2). Gupta *et al*. demonstrated that the VEGF-induced activation of the MAPK/extracellular signal-regulated kinase (ERK) pathway and inhibition of the stress-activated protein kinase/c-Jun amino-terminal kinase pathway is also implicated in the antiapoptotic effect mediated by VEGF[31] (Figure 2). Interestingly, the activation of the PI3K/Akt pathway mediates not only the antiapoptotic effect but also the migratory effect of VEGF on ECs via Akt-dependent phosphorylation and activation of eNOS[32] (Figure 2).

The expression of VEGF mRNA is highest in hypoxic tumor cells adjacent to necrotic areas. Hypoxia-induced transcription of VEGF mRNA is apparently mediated, at least in part, by the binding of hypoxia-inducible factor 1 (HIF-1) to an HIF-1 binding site located in the VEGF promoter, and by the activation of a stress inducible PI3K/Akt pathway[26,33]. In fact, progressive growth of tumor creates ongoing hypoxia, which up-regulates several pro-angiogenic compounds including VEGF, bFGF, IL-8, TNF-α, TGF-β etc. These compounds, via several mechanisms such as increase of vessel hyperpermeability, release of plasma proteins, induction of proteases, fibrin formation, EC proliferation, migration etc, promote angiogenesis and fibrinolysis resulting in continued tumor growth and dysfunctional vasculature, which further positively feedback to create continuing hypoxia inside tumors (Figure 1).

### *Fibroblast growth factors*

Fibroblast growth factors (FGFs) and their receptors are overexpressed in various types of cancers, and are important tumor angiogenic and ECs survival factors. Pardo *et al*. reported that bFGF induced expression of the antiapoptotic proteins bcl-XL and bcl-2 via the MEK/ERK signaling pathway[34] (Figure 2). Expression of VEGF mRNA in the tumor is increased by bFGF overexpression, and the bFGF-induced tumor development is significantly inhibited by treatment with KDR/Flk-1 neutralizing monoclonal antibody (mAb), which suggests that bFGF synergistically augments VEGF-mediated hepatocellular carcinoma development and angiogenesis, at least in part, by induction of VEGF through KDR/Flk-1[35]. In addition, bFGF induces an increase of VEGF mRNA in vascular smooth muscle cells[36] and an increase in VEGF receptors in microvascular ECs[37]. aFGF and bFGF are mitogenic for ECs and stimulate ECs migration as well as ECs production of plasminogen activator (PA) and collagenase that are capable of degrading basement membrane[38] (Figure 2). FGFs are responsible for production of ECM and release of matrix metalloproteinases (MMPs) for selective degradation and organization of ECM[39] (Figure 2).

Binding of FGFs to their high affinity receptors causes the activation of the intrinsic tyrosine kinase and a cascade of events, leading eventually to the induction of immediate early gene transcription, and to cell proliferation. FGFs receptors dimerize upon ligand binding, and transphosphorylate at tyrosine residue. Angiogenic growth factors, like bFGF and VEGF165, require interaction with heparin sulfate (HS) in order to induce a proliferative signal through tyrosine kinase receptors. Binding of bFGF to high affinity cell surface receptor sites can be modulated by heparin-mimicking compounds (i. e. RG-13577) that can modulate abnormal bFGF signaling by disrupting bFGF mediated autocrine loop, compete with heparin sulfate (HS) on binding to bFGF, bind the growth factor, and prevent receptor binding and/or dimerization[40], and by proteolytic enzymes (e.g. MMP-2) that cleave the ectodomain of the receptor. These effects are associated with profound inhibition of bFGF mediated signal transduction (tyrosine phosphorrylation) and proliferation of vascular ECs[40]. Spontaneous migration of ECs is inhibited by neutralizing antibodies to bFGF, suggesting an autocrine of bFGF synthesized and released by the ECs themselves[38]. A dominant-negative receptor, which, when co-expressed with

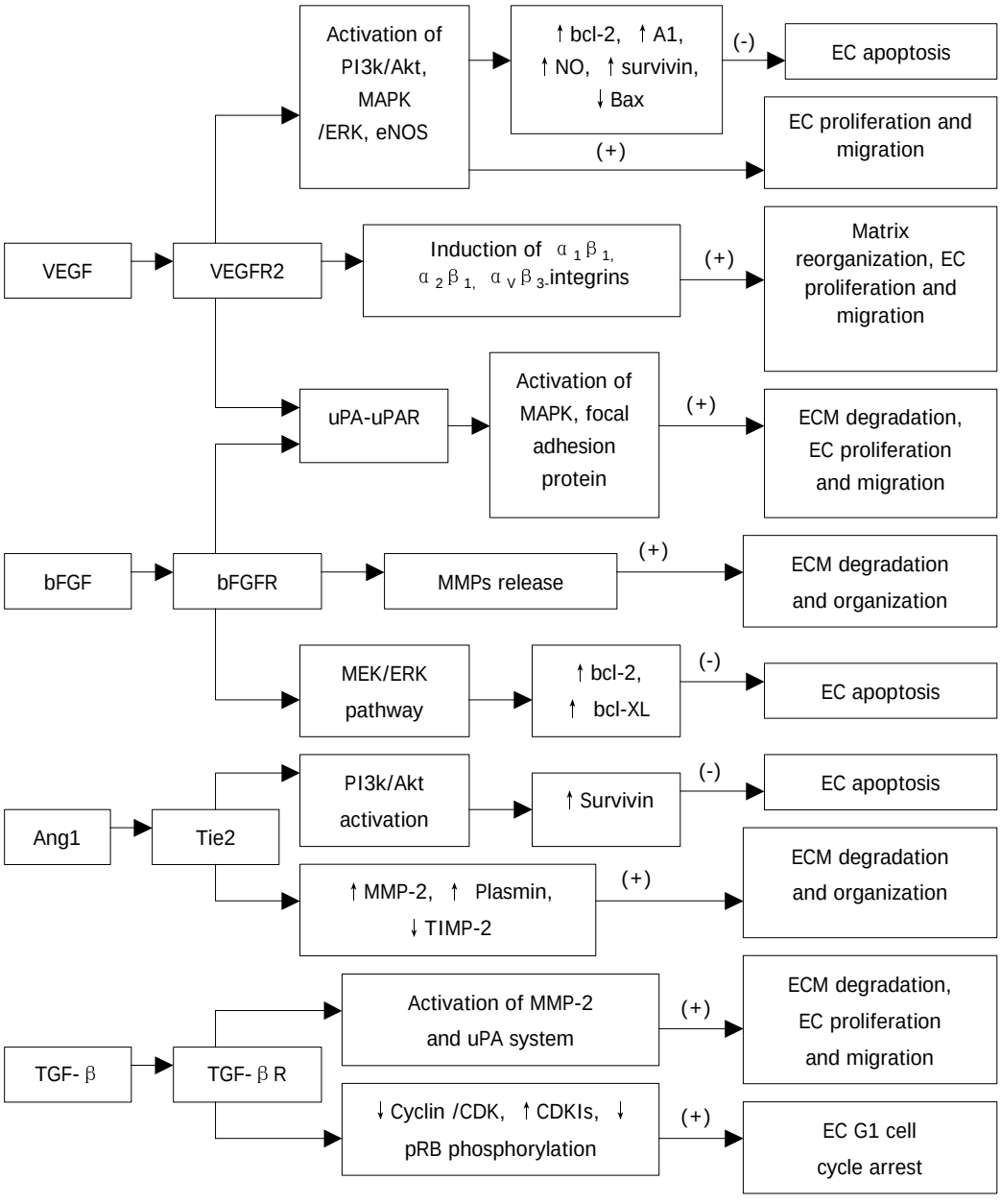


**Figure 2** Mechanism of angiogenesis by angiogenic factors.

FGF receptors (FGFRs), can block the activation and signal transduction. In addition, the ligand-specific targeting of toxin to tumor cells expressing FGFRs and the compounds that bind and inactivate FGF ligands, can block ECs proliferation.

### *Angiopoietins and tie receptors*

It has been proposed that angiopoietin-1 (Ang1) and angiopoietin-2 (Ang2) are pro-angiogenic and anti-angiogenic owing to their respective agonist and antagonist signaling action through the Tie2 receptor[41]. Lobov *et al*. have demonstrated that *in vivo*, in the presence of endogenous VEGF-A, Ang2 promotes a rapid increase in capillary diameter, remodeling of the basal lamina, proliferation and migration of ECs, and stimulates sprouting of new blood vessels[41]. By contrast, Ang2 promotes ECs death and vessel regression if the activity of endogenous VEGF is inhibited[41]. It was reported that Ang1 induced phosphorylation of Tie2 and the p85 subunit of PI 3' -kinase and increased PI 3' -kinase activity in a dose-dependent manner, suggesting that the Tie2 receptor, PI 3' -kinase, and Akt are crucial elements in signal transduction pathway leading to EC survival induced by the paracrine activity of Ang1[42] (Figure 2). Alternatively, Ang1 prevents EC apoptosis via Akt/survivin pathway by activating a critical survival messenger, Akt, and by up-regulating a broad spectrum apoptosis inhibitor, survivin[43, 44] (Figure 2), but has no effect on the expression of bcl-2 and XIAP[44]. Moreover, Ang1-induced migratory effect might be mediated through PI 3' -kinase activity dependent tyrosine phosphorylation of $p125^{FAK}$, which plays a key role in regulating dynamic changes in actin cytoskeleton organization during EC migration[45]. Increased plasmin and MMP-2 secretion, and suppressed TIMP-2 secretion by Ang1 from ECs are also important determinants for inducing ECs sprouting[45] (Figure 2). In contrast, the PI 3' -kinase inhibitors have been found to inhibit Ang1-stimulated tyrosine phosphorylation of $p125^{FAK}$, and secretion of MMP-2 and plasmin from ECs and migration [45]. Ang2 blocks Ang1-mediated Tie2 autophosphorylation in ECs and acts as a check point on Ang1/Tie2-mediated angiogenesis to prevent excessive branching and sprouting of blood vessels by promoting destabilization of blood vessels.

### *Transforming growth factor-b*

Transforming growth factor-betas (TGF-βs) are multifunctional polypeptides that regulate cell growth and differentiation, ECM deposition, cellular adhesion properties, angiogenesis and immune functions. TGF-β1 acts through the TGF-β type I and type II receptors to activate intracellular mediators, such as Smad proteins, the p38 MAPK, and the ERK pathway[46]. TGF-β1 mRNA levels by activin receptor-like kinase 5 (ALK5) independent of p38 MAPK activation[46]. In contrast, TGF-β1 induction of fibronectin (FN) mRNA requires p38 MAPK activity[46]. TGF-β1 induction of PAI-1 and TSP-1 mRNA uses at least ALK5 and possibly the p38 MAPK pathway[46]. TGF-β secreted by most cultured cells is in biologically inactive form, and cannot bind TGF-β receptors; the latent TGF-β is activated by proteases such as plasmin and cathepsin D, low pH, chaotropic agents such as urea, and heat[47, 48]. Several studies suggested that VEGF increases plasminogen activator (PA) activity in vascular ECs[11] and that plasmin is able to activate latent TGF- $\beta_1$[49, 50] which decreases Flk-1 expression and thereby negatively regulates the VEGF/Flk-1 signal transduction pathway in EC[51], raise the possibility that a complex self-regulating mechanism of VEGF signal transduction may exist during angiogenesis[50]. However, immunohistochemical study has shown that TGF-β1 might be associated with tumor progression by indirectly stimulating angiogenesis through the up-regulation of VEGF expression in gastric carcinoma[52]. In addition, TGF-$\beta_1$ inhibits the generation of the anti-angiogenic molecule angiostatin by human pancreatic cancer cells in a time- and dose-dependent manner, and this effect is mediated through modulation of the plasminogen/plasmin system[53].

TGF-β not only inhibits the activity and expression of cyclins and CDKs but also induces the cyclin-dependent kinase inhibitors (CDKIs) p15, p27 and p15, which bind to the cyclin/CDKs, preventing phosphorylation of pRB and thereby arresting most epithelial cells (including ECs) at late G1 phase[54] (Figure 2). The effects of TGF-$\beta_1$ on endothelial tube formation may be mediated through a net antiproteolytic activity by modulating uPA and PAI levels[55]. Ellenrieder *et al*. reported that TGF-β treatment of PANC-1 and IMIM-PC1 cells resulted in strong up-regulation of expression and activity of both matrix metalloproteinase-2 (MMP-2) and the uPA system, and treatment with MMP inhibitors or inhibitors of the uPA system caused significant reduction of TGF-β-induced invasiveness in both cell lines suggesting that TGF-β acts in an autocrine manner to induce tumor cell invasion, which is mediated by MMP-2 and the uPA system[56] (Figure 2). Furthermore, TGF-β indirectly stimulates angiogenesis by the recruitment of inflammatory mediators that secrete angiogenic factors. Thus, TGF-β regulates vascular remodeling through its pleiotropic effects on different cell types.

### *Interleukin-8 and matrix metalloproteinase-2*

Up-regulation of MMP activity, favoring proteolytic degradation of the basement membrane and ECM, has been linked to tumor growth and metastasis, as well as tumor-associated angiogenesis. IL-8 mRNA is up-regulated in neoplastic tissues, such as non-small cell lung cancer[57] and that its expression correlates with the extent of neovascularization, tumor progression and survival. And also, MMP-2 mRNA level is increased in tumor cells transfected with IL-8, but VEGF and bFGF mRNA levels are unchanged[58,59] suggesting that IL-8-induced MMP-2 production is a major mechanism by which tumor cells induce angiogenesis. IL-8 can also be up-regulated by hypoxia, suggesting that the environment plays a major role in regulating IL-8 expression and metastasis[58]. MMPs induce tumor angiogenesis by degrading ECM and thereby release angiogenic mitogens that have been shown to be stored within the matrix. In addition, MMP-2 and MMP-3 are able to release soluble FGF receptor 1 (FGFR1)[60] and soluble 12-kDa immunoreactive and mitogenic heparin-binding epidermal growth factor (HB-EGF)[61], respectively. MMP-2 has been shown to directly modulate melanoma cell adhesion, spreading on ECM and invasion[62], and an inhibitor of MMP-2 significantly inhibits growth and neovascularization of tumors implanted into chick chorioallantoic membrane (CAM) by preventing MMP-2 binding to $\alpha v\beta_3$ and blocking cell surface collagenolytic activity[63]. Furthermore, MMP-9, as well as MMP-2 proteolytically cleave and activate latent TGF-β, and promote tumor invasion and angiogenesis[64].

### *Oncogene and tumor suppressor genes*

Oncogenes are found to be activated and tumor suppressor genes are found to be inactivated in tumor, and hence promote tumor growth and angiogenesis through different mechanisms (Figure 1). It has been shown that VEGF is introduced by K- or H-ras mutant gene, v-src and v-raf in transformed fibroblast and ECs. Other angiogenic factors such as VEGF, TNF-α, TGF-β have been shown to be up-regulated by mutant ras[65]. These effect may be mediated through a ras-raf-MAP kinase signal transduction pathway (Figure 1), which results in activation of promoter regions of genes of angiogenic growth factors[66]. Moreover, expression of ras, either constitutive or transient, potentiated the induction of VEGF by hypoxia[67].

p53 is an important suppressor gene, which inhibits the angiogenic process by inducing thrombospondin-1, down-regulating VEGF and NOS and, in addition, down-regulating hypoxia-induced angiogenesis, either inducing apoptosis or enhancing anti-angiogenic factors[68]. A transient transfection of mutated p53 results in up-regulation of VEGF mRNA in NIH3T3 cells[69]. In contrast, adenovirus-mediated wild-type p53 overexpression down-regulats CD40-induced VEGF expression and transmigration in human multiple myeloma cells expressing mutant p53[70]. And, we have previously demonstrated that the expression of Flt-1 receptor is significantly correlated with p53 mutation gene, not obviously with ras mutation gene in pancreatic carcinoma cells, which suggest that wild type p53, after mutation, might lose the suppressive function to the expression of Flt-1 receptor, thus results in neovascularization of pancreatic neoplasm and promotes the growth of tumor cells, whereas ras mutation may take part in neovascularization through other approaches. Recombinant wild type p53 represses bFGF mRNA translation in rabbit reticulocyte lysate, in a dose- dependent manner via blocking translation initiation by preventing 80S ribosome formation on an mRNA bearing the bFGF mRNA leader sequence[71]. Moreover, adenoviral vector-mediated wild type p53 transduction results in tumor regression, at least in part, via anti-angiogenesis mediated by the down-modulation of FGF binding protein, a secreted protein required for the activation of angiogenic factor bFGF[72]. In addition, wild type p53 gene transfer significantly reduces cell invasiveness *in vitro* via a decrease in the secreted levels of MMP-2 in mutated p53 human melanoma cell lines[73]. Biologically, p53 acts at a G1/S check point, postponding DNA replication after certain cell stress, such as DNA damage[74], and also induces the apoptotic pathway of cell death[75].

## THE ANGIOGENIC INHIBITORS

### *Mechanism of angiogenesis inhibitors*

Leading anti-angiogenic targets that have been identified are[76, 77]: (1) inhibition of the growth factors that promote endothelial proliferation; (2) inhibition of the proteases required for ECs to penetrate basement membrane and form new blood vessels; (3) disruption of specific intracellular signal transduction pathway; (4) induction of EC apoptosis or inhibition of EC survival; (5) inhibition of endothelial bone marrow precursor cells; and (6) inhibition of $\alpha v\beta_3$-integrin-vitronect interaction that is pivotal in mediating ECs adhesion to ECM during neovascularizatioin[77].

### *Inhibitors of angiogenic growth-factors and their receptors*

One broad class of angiogenesis inhibitors is made up of drugs that target growth factors such as bFGF and VEGF. The factors tend to bind to heparin, a property that may trap them within the ECM and may thereby govern their bioavailability. Hence, the early generation of drugs is heparin-like (e.g. Pentosan polysulfate), especially with regard to carrying multiple negative charges that promote growth factor binding. However, receptor targeting agents can impede tumor growth and metastasis by interfering, at specific growth-factor receptors, such as those for FGFs and VEGF, with the transduction of angiogenic stimuli into intracellular responses. In these pathways, the receptors are transmembrane tyrosine kinases, in which ligand binding to an extracellular domain induces autophosphorylation of an intracellular kinase domain. Each kinase then functions as an activator of downstream signals. To disrupt such a sequence, a drug may compete for receptor binding and prevent tyrosine kinase autophosphorylation. Inhibitors of VEGF family include: (1) anti-VEGF mAb[78]: directly neutralizes VEGF proteins, and inhibits biological activities of VEGF; (2) soluble VEGF receptors: specifically bind to VEGF, indirectly block the function of VEGF with receptors; (3) inhibitors of VEGF receptors[79]: bind to VEGF receptors and block their functions with VEGF; (4) inhibitors of VEGF signal transduction: interfere a series of signal transduction pathways by blocking autophosphorylation of VEGF receptors; (5) VEGF antisense[80]: is a specific nucleotide sequence, which binds to VEGF mRNA and thereby interferes VEGF mRNA translation and VEGF protein formation. A recent study has shown that the VEGFR2 DNAzyme can cleave its substrate efficiently in a concentration- and time-dependent manner, inhibit the proliferation of EC with a concomitant reduction of VEGFR2 mRNA, and inhibit tumor growth *in vivo*[81].

### *Endogenous angiogenesis inhibitors*

More than 40 endogenous angiogenesis inhibitors have been characterized, and they are divided into 4 major groups: interferons (IFNs), proteolytic fragments, interleukins (ILs), and tissue inhibitors of metalloproteinases (TIMPs)[82].

**Interferons** The interferons (INF-$\alpha$, -$\beta$, and -$\gamma$) are members of a family of secreted glycoproteins, which have direct or indirect inhibitory effect on tumor angiogenesis and growth. IFN-$\alpha/\beta$ have been reported to down-regulate the expression of pro-angiogenic factor MMP-9 mRNA and protein in different cancers[83-86]. Also, IFN-$\alpha/\beta$ down-regulate IL-8 expression in bladder cancer[83-84]. Several studies demonstrated that the administration of optimal biological dose of IFN-$\alpha/\beta$ decreased the expression of bFGF mRNA and protein and microvessel density in the tumors and, in addition, induced EC apoptosis[83-85, 87]. Sasamura *et al*. demonstrated that IFN-$\gamma$ had mild inhibitory effects on VEGF mRNA and bFGF mRNA expression, whereas IFN-$\alpha$ did not significantly decrease the level of either VEGF mRNA or bFGF mRNA in renal cell carcinoma[88]. However, some studies demonstrated that IFN-$\alpha/\beta$ treatment did not cause the reduction of bFGF and VEGF levels in serum from patients with carcinoid tumours[89] and leukemia[86]. Thus, anti-angiogenic effect of IFNs treatment might be mediated by the regulation of different angiogenic factors in different tumors in dose- and time-dependent manner. Moreover, IFN-$\gamma$ is presumed to induce its anti-angiogenic effects through the secretion of IFN-$\gamma$ inducible protein 10 (IP-10) and monokine induced by IFN-$\gamma$[90]. Finally, IFNs have antitumor properties, which may be mediated through a direct cytotoxic effect on tumor cells, augmentation of immunogenicity of tumor by up-regulation of major histocompatibility (MHC) classes *I and II* and tumor associated antigens, and/or activation of macrophages, T lymphocytes and natural killer cells[89].

**Interleukins** It was reported that interleukins (ILs) having a Glu-Leu-Arg (ELR) motif at the $NH_2$ terminus, such as IL-8, enhance angiogenesis, and those that lack this sequence, such as IL-4, inhibit it[91]. IL-4 inhibits *in vivo* neovascularization induced by bFGF in the rat cornea and blocks the migration of microvascular ECs toward bFGF *in vitro*[92]. However, it has been shown that IL-1$\alpha$, a representative cytokine of activated macrophages, induces angiogenesis through the enhanced expression of various angiogenic factors such as VEGF, IL-8, and bFGF[93]. And also, IL-6 was found to counteract the apoptotic effect mediated by wild type p53[75]. Several studies have reported that IL-12 suppresses the expression of VEGF mRNA[94, 95], bFGF[94] and MMP-9 mRNA[94]. Additionally, IL-12 was found to stimulate mRNA expression of IFN-$\gamma$ and its inducible anti-angiogenic chemokine IFN$\gamma$-inducible protein (IP-10) in ECs cultured with IL-12[95]. IL-12 significantly promotes apoptosis and inhibits proliferation rate of human tumors and extensive necrosis in the murine, and thereby reducing tumor vessel density[95]. Furthermore, the *in vivo* inhibition of neovascularization in IL-10-secreting tumors

might be mediated by the ability of IL-10 to down-regulate the synthesis of VEGF, IL-1β, TNF-α, IL-6, and MMP-9 in tumor-associated macrophages[96]. And also, IL-10 inhibits tumor metastasis through a natural killer (NK) cell-dependent mechanism[96].

**Tissue inhibitors of metalloproteinases** Remodeled ECM components comprise a scaffold upon which ECs can adhere, migrate, and form tubes, and deposition of these components forms the basal lamina that ensheaths endothelial and mural cells. *In vitro* migration of ECs through gelatin is significantly inhibited by overexpressed TIMP-1[97]. Murphy *et al*. reported that TIMP-2, but not TIMP-1, inhibited bFGF-induced EC proliferation[98]. TIMP-2 is able to inhibit soluble FGFR1 released by MMP-2[60]. Transfection of the highly metastatic B6F10 murine melanoma cell line with TIMP-2 cDNA showed the reduced levels of blood vessel formation and diminished induction of EC migration and invasion[99]. Studies have shown that the overexpression of TIMP-3 induces the apoptotic cell death of a number of cancer cell lines and rat vascular smooth muscle cells through the stabilization of TNF-alpha receptors on the cell surface, perhaps by inhibiting a receptor shedding metalloproteinase[100, 101]. Furthermore, anti-angiogenic and antitumor effects of TIMP-3 appear to be mediated, in part, by decreased expression of vascular endothelial (VE)-cadherin by ECs in the presence of TIMP-3 in an *in vitro* assay and in TIMP-3-overexpressing tumors[102]. Finally, TIMP-1, TIMP-2, TIMP-3 and TIMP-4 inhibit neovascularization by inhibiting MMP-1, MMP-2, and MMP-9 induced breakdown of surrounding matrix[103]. Thus, the multiple effects of TIMPs on both endothelial and tumor cells migration render MMPs attractive targets for tumor therapy.

**Proteolytic fragments** Most of these fragments are derived from ECM components, such as collagen or fibronectin, or from enzymes such as plasminogen and MMP-2 that remodel ECM. Perhaps the most characterized inhibitors in this class are angiostatin and endostatin.

**Angiostatin** The anti-angiogenic effect of angiostatin, a 38-kDa internal fragment of plasminogen, may be mediated, at least in part, by their ability to down-regulate VEGF expression within the tumor[104]. Angiostatin inhibits hepatocyte growth factor (HGF)-induced phosphorylation of c-met, Akt, and ERK1/2, and thereby exerts its anti-angiogenic effect via disruption of HGF/c-met signaling[105]. Intraperitoneal administration of angiostatin potently inhibits the neovascularization and metastasis formation in mice observed after a primary tumor has been removed[106]. It has been shown that binding of angiostatin to the α/β-subunits of plasma membrane-localized ATP synthase may suppress endothelial-surface ATP metabolism and thereby mediates its anti-angiogenic effects and the down-regulation of EC proliferation and migration[107, 108] (Figure 3). Further, adenoviral mediated angiostatin gene transfer selectively inhibits EC proliferation and disrupts the $G_2$/M transition induced by M-phase-promoting factors, and that ECs show a significant mitosis arrest that is correlated with the down-regulation of the M-phase phosphoproteins[109]. Other studies have shown that angiostatin treatment significantly increases the apoptosis of EC and tumor cells, and decreases density of tumor blood vessels[109-111]. Angiostatin was found to produce a transient increase in ceramide that correlates with actin stress fiber reorganization, detachment and death[112] and, in addition, treatment with angiostatin or ceramide resulted in the activation of RhoA, an important effector of cytoskeletal structure[112] (Figure 3). Angiostatin can selectively regulate the expression of E-selectin and thereby inhibits the proliferation of ECs.

**Endostatin** It is a 20-kDa fragment of type XVIII collagen that has been identified as a factor produced by hemangioendothelioma cells that inhibits ECs proliferation, angiogenesis and tumor growth. The mechanisms by which endostatin inhibits VEGF-induced proliferation and migration of ECs are (Figure 3): First, endostatin blocks the VEGF-induced tyrosine phosphorylation of KDR/Flk-1 in ECs[113]. Second, endostatin suppresses the VEGF-induced activation of ERK, p38 MAPK, and $p125^{FAK}$, which are downstream events of the KDR/Flk-1 signaling and are involved in the mitogenic and motogenic activities of VEGF in ECs[113]. Third, endostatin inhibits the binding of VEGF to ECs and to its cell surface receptor, KDR/Flk-1[113]. Finally, endostatin directly binds to KDR/Flk-1 but not to VEGF[113]. Endostatin was found to exhibit its anti-migratory effect by reducing VEGF-induced phosphorylation of endothelial NOS (eNOS)[114] (Figure 3). Rehn *et al*. demonstrated that soluble endostatin was capable of binding to $\alpha_v$- and $\alpha_5$-integrins, thereby inhibiting the integrin functions, such as EC migration[115] (Figure 3). In addition, endostatin may exert its antiproliferative and anti-angiogenic effects by competing with bFGF for binding to cell surface heparan sulphate proteoglycans, which could disrupt the mitogenic growth factor signaling[116]. Endostatin induces a significant decrease in EC proliferation in the basal state and after stimulation by neuropeptide Y and bombesin[117]. Endostatin potently inhibits both the extracellular activation of proMMP-2 by inhibition of membrane-type 1 MMP (MT1-MMP) and the catalytic activity of MMP-2 and thereby can block the invasiveness of ECs and tumor cells[118]. The proapoptotic activity of endostatin appears to be mediated via tyrosine kinase signaling[119] and reduction of antiapoptotic proteins bcl-2 and bcl-XL without affecting the level of the proapoptotic Bax protein[120] (Figure 3). Furthermore, the Shb adaptor protein has been suggested to be involved in the mediation of the apoptotic signaling of endostatin[119] (Figure 3).

### *Somatostatin and its analogs*

Somatostatin (SS) and its analogs inhibit the proliferation of somatostatin receptors (SSTRs) positive endocrine neoplasm. The antiproliferative action of SS is signaled via five specific G-protein coupled receptors (SSTR1-SSTR5), which initiate pertussis toxin sensitive-G protein dependent, and tyrosine phosphatase mediated cell growth arrest or apoptosis according to receptor subtypes and target cells. It has been shown that activation of SSTR1, 2, 4, and 5 induce G1 cell cycle arrest through the ability of SS to maintain high levels of CDKIs $p27^{(Kip1)}$ and p21, and inactivate cyclin E-CDK2 complexes, thus leading to hypophosphorylation of pRb[121, 122](Figure 3). Moreover, somatostatin-mediated growth inhibition of normal and cancer pancreatic acinar cells is triggered via an inhibition of PI3-kinase signaling pathway[123]. SS may directly stimulate tumor apoptosis via sstr3-dependent G protein signaling, causing the induction of suppressor gene p53 and proapoptotic protein Bax[124](Figure 3). Our recent investigation reported that the low expression or loss of SSTR2 gene was more negatively correlated with the over-expression of p53 and ras mutation genes, which might take part in the angiogenesis of pancreatic neoplasm, whereas there was no significant relationship between SSTR2 and DPC4 (deleted in pancreatic cancer, locus 4), which suggested that there was different regulatory pathway in neovascularization of pancreatic neoplasm. Albini *et al*. provided evidence that SS inhibits Kaposi sarcoma associated angiogenesis by inhibiting both EC proliferation and invasion, and also by inhibiting migration of monocytes, which are important mediators of the angiogenic cascade, and are able to produce survival factors that, in turn, activate ECs[125]. In addition, SS induces a significant decrease in basal and stimulates EC proliferation in HUVEC, and also decreases number of capillaries[117]. CAM model study showed that unlabeled SS analogs inhibited angiogenesis, which was

proportional to the ability of the analogs to inhibit growth hormone (GH) production[126].

It is defined that SSTR subtypes are responsible for the specific post-receptor signal transduction mechanisms involved in octreotide' s inhibition of angiogenesis[126]. The intracellular signal transduction mechanisms involved in this angiogenic inhibition include the G^sub i^-binding protein, cAMP, and calcium[127]. Further, SS and its analogs induce their biologic effects by interacting with specific receptors that are coupled to a variety of signal transduction pathways involving adenylate cyclase, guanylate cyclase, ionic conductance channels, phospholipase C-β, phospholipase $A_2$, and tyrosine phosphatase and protein dephosphorylation and thereby regulate cell growth[128, 129]. The best characterized pathway involves the inhibition of adenylate cyclase, leading to a reduction in intracellular cAMP levels. Antiproliferative effects that are mediated through SSTR1 and SSTR2, involve the stimulation of tyrosin phosphatases, however SSTR5 appears to be coupled to inositol phospholipid/calcium pathway[130]. Mentlein *et al*. reported that cultivated cells from solid human gliomas of different stages and glioma cell lines secreted variable amounts of VEGF, which was reduced between 25 and 80 % of control levels depending on the glioma by co-incubation with SS or SSTR2-selective agonists (octreotide and L-054 522) in dose-dependent manner[131]. Growth factor-induced (EGF, bFGF) VEGF synthesis could also be suppressed to <50 % by co-incubation with SS or SSTR2-selective agonists, which was less pronounced in hypoxia-induced VEGF synthesis[131]. And also, SS and octreotide diminished the proliferative activity of cultured murine ECs HECa10 *vs.* controls; however, SS and octreotide did not change the release of VEGF into supernatants of 24-h or 72-h EC cultures[132]. A recent study has demonstrated that SS 14 can reduce bFGF-induced corneal angiogenesis[133].

In summary, the mechanisms of action of tumor growth inhibition by SS and its analogs are[134]: (1) inhibition of the secretion of hormones, such as GH, insulin and/or gastrointestinal hormones; (2) direct or indirect (via GH) inhibition of IGF-1 and/or other growth factors that exert a stimulatory effect on tumor growth. On the other hand, SS analogs can selectively stimulate the formation of IGF-binding protein 1, and thereby interfering with IGF-1 action at the receptor level; (3) inhibition of angiogenesis through different mechanisms; (4) direct antimitotic effects of growth factors, which act on tyrosine kinase receptors such as EGF and FGF, via SSTRs on the tumor cells; (5) modulation of immunological activity.

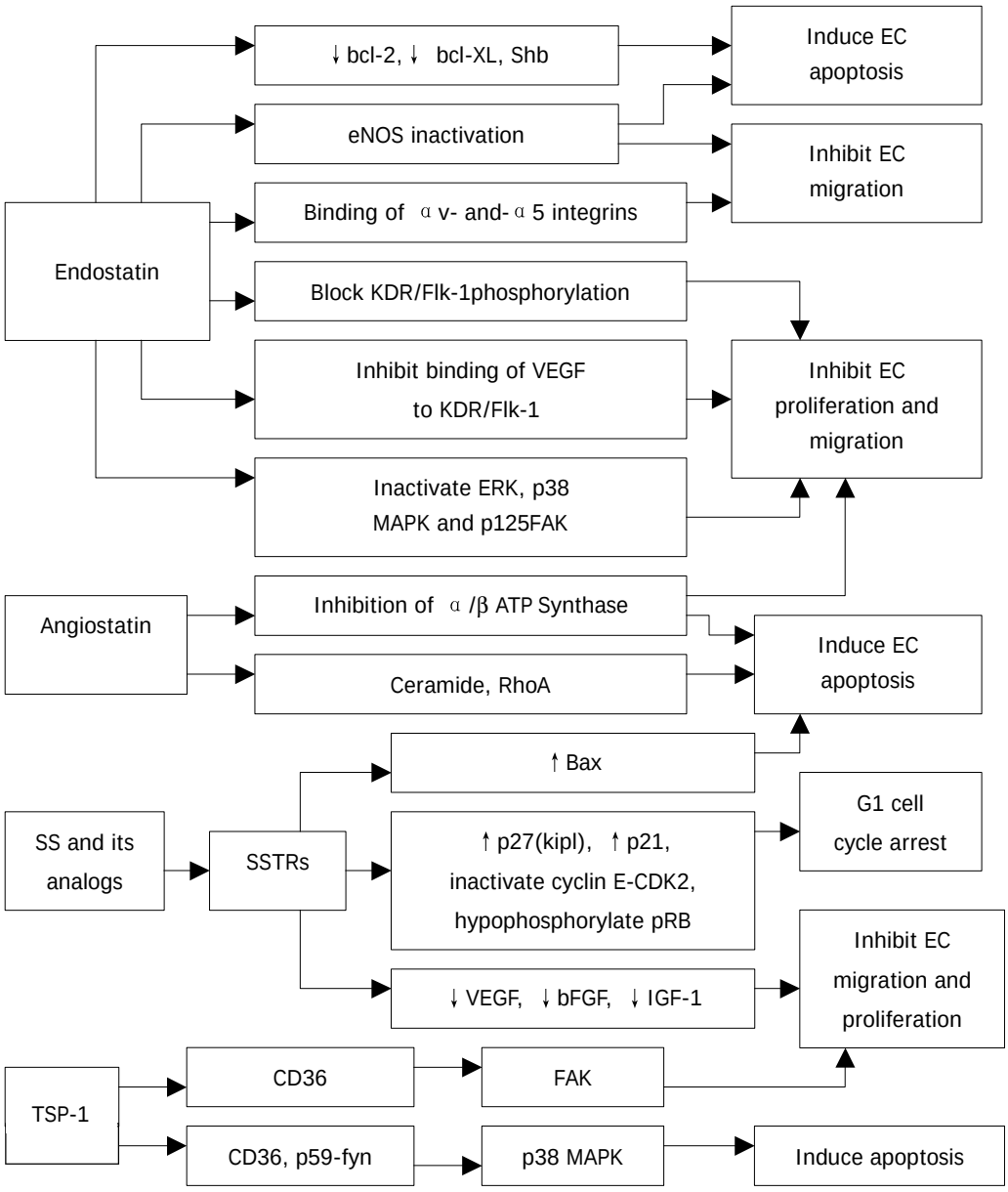


**Figure 3** Proposed effector pathways of angiogenic inhibitors.

### *Thrombospondin-1*

Thrombospondin-1 (TSP-1) is a naturally occurring inhibitor of angiogenesis that limits vessel density in normal tissues and curtails tumor growth. TSP-1 exerts its anti-angiogenic activity via binding to the CD36 receptor by triggering an apoptotic signaling pathway[135]. Binding of TSP-1 to CD36 receptor leads to the recruitment of the Src-related kinase, p59-fyn, and to activation of p38 MAPK. The activation of the p38 MAPK has been shown to be p59-fyn-dependent and to require a caspase-3-like proteolytic activity[135]. Furthermore, activated p38 MAPK leads to the activation of caspase-3 and to apoptosis[135] (Figure 3). Interestingly, the apoptotic effect of TSP-1 is restricted to ECs activated to take part in the angiogenic process and not in quiescent vessels[135]. TSP-1 acts through CD36 to modulate the activity of focal adhesion kinase (FAK) and thus inhibits EC migration and proliferation[136] (Figure 3). TSP-1 can effectively inhibit chemotaxis *in vitro* and neovascularization *in vivo*, induced by several angiogenic stimuli. These include protein that acts via tyrosine kinase receptors (VEGF, bFGF, aFGF, PDGF), via G proteins (IL-8), via serine/threonine kinase receptors (TGF-β), and also lipids (PGE-1)[137, 138].

## SUMMARY AND CONCLUSION

### *Developmental status and evaluation of anti-angiogenic therapy in human clinical trials*

Angiogenesis is a complex process that depends on the coordination of many different activities in several cell types. The angiogenic response in the microvasculature is associated with changes in cellular adhesive interactions between adjacent ECs, pericytes, fibroblasts, and immune mediators express many different cytokines and growth factors that react with other cells or ECM components to affect ECs migration, proliferation, tube formation, and vessel stabilization. As one or more of the positive regulators of angiogenesis are up-regulated, and simultaneously, certain negative regulators of angiogenesis are down-regulated, tumors become angiogenic. Interestingly, different angiogenic regulators, sometimes, function through the same mechanism and a single angiogenic regulator, sometimes, functions through different mechanisms. Hence, the anti-angiogenic therapy can be realized through the regulation of ' angiogenic switch' by interfering with different mechanisms.

Anti-angiogenic agents, if administered before a tumor develops or becomes vascular supply dependent, would therefore theoretically act similarly to a vaccine in preventing tumor development, not just tumor growth. However, it is notable that anti-angiogenic therapy represents a treatment, not a cure, for cancer. A cure for cancer can be realized only by targeting the agents and mechanisms that cause normal cells to become tumorigenic. The anti-angiogenic therapy of cancer, nonetheless, represents a highly effective strategy for destroying tumors because fundamental requirement of tumor growth is dependent on a blood supply. Unlike standard chemotherapy that targets tumor cells and other proliferating cells, angiogenesis inhibitors target dividing ECs that have been recruited into the tumor bed. For example, certain tubulin-binding agents such as combretastin A-4, exhibit a selective toxicity for proliferating ECs *in vitro* and causing a vascular collapse in tumor models *in vivo* via apoptosis and the subsequent death of much larger numbers of tumor cells[139]. Thus, specific anti-angiogenic therapy has little or no toxicities such as gastrointestinal symptoms and myelosuppression that are characteristic of standard chemotherapeutic regimens, does not require that the therapeutic agent enter any tumor cells nor cross the blood brain barrier, controls tumor growth independently of growth fraction or tumor cell heterogeneity or even tumor cell type, and does not induce acquired drug resistance [140]. Further, since normal vasculature in the adult is quiescent, the appropriate use of selective angiogenic inhibitors may be expected to confer a degree of specificity that is not obtainable with the nonspecific modalities of chemotherapy and radiation therapy and to allow for relatively nontoxic, long-term treatment of tumors.

Because anti-angiogenic agents are expected to be cytostatic rather than cytotoxic, they may be particularly effective in combination with cytotoxic agents, even used in advanced cases of pancreatic, colon, and hormone-refractory prostate cancer, thereby targeting not only DNA synthesis and cell division but also the biologic behavior of tumor cells. The following guidelines are suggested to improve the therapeutic efficacy of endogenous angiogenesis inhibitors in clinical trials: (1) after surgery or radiotherapy to prevent recurrence of distant metastases; (2) combinatorial therapies, for example, in combination with conventional chemotherapy, radiotherapy and vaccine therapy or immunotherapy, and also, in combination with several angiogenesis inhibitors rather than a single inhibitor; (3) targeting therapy. Angiogenesis inhibitors may be specifically targeted to the disease locus at high concentrations rather than be widely distributed in the entire body; (4) gene therapy, several advantages including prolonged therapy, low doses of DNA molecules, and less frequent injections may be achieved by anti-angiogenic gene therapy with endogenous angiogenesis inhibitors; (5) more potent angiogenesis inhibitors should be discovered; (6) prolonged half-lives. Slow-release of angiogenesis inhibitors in the body reaches a steady-state level in the circulation.

Remarkably diverse groups of anti-angiogenic drugs are currently undergoing evaluation in phase I, II or III clinical trials. However, there are still some difficulties associated with the clinical evaluation of these drugs efficacy. In the experimental animal model, tumors can be removed and examined for therapeutic efficacy such as changes in the extent of vascularization, vascular structure, EC viability or apoptosis, as well as for markers of angiogenic activity, e.g. VEGF expression. But in the clinical situation, taking serial biopsies of metastatic tumors may not be a particularly practical or desirable approach. For this, reliable surrogate markers of tumor angiogenesis in serum or urine, and non-invasive strategy may be necessary. Several studies have successfully used various non-invasive medical imaging strategies (e.g. MRI, Doppler ultrasound) to monitor changes in tumor blood flow, vascular structure and permeability[141-143]. Indeed, there are considerable research efforts underway in this field. In addition, there are obvious concerns about delayed toxicity associated with long-term anti-angiogenic therapy, and physiological angiogenesis affected by anti-angiogenic drugs such as wound healing in a cancer patient, reproductive angiogenesis (e.g. corpus luteum development in adult females, development of the vasculature in developing embryos), in neonates and children. In this concern, a potentially significant development in the near future could be the use of genomics based technologies to uncover a large number of highly (or even totally) specific molecular markers for the activated ECs of newly formed blood vessels.

In the near future, the outcome of ongoing clinical trials will give us more insights into the potential of anti-angiogenic approaches to treat cancer.

## REFERENCES

1 **Bussolino F**, Mantovani A, Persico G. Molecular mechanisms of blood vessel formation**.** *Trends Biochem Sci* 1997; **22**: 251-256

2 **Sebti SM,** Hamilton AD. Design of growth factor antagonists with antiangiogenic and antitumor properties. *Oncogene* 2000; **19**: 6566-6573

3 **Dameron KM**, Volpert OV, Tainsky MA, Bouck N. Control of angiogenesis in fibroblasts by p53 regulation of thrombospondin-1. *Science* 1994; **265**: 1582-1584

4 **Kohn S**, Nagy JA, Dvorak HF, Dvorak AM. Pathways of macromolecular tracer transport across venules and small veins. Structural basis for the hyperpermeability of tumor blood vessels. *Lab Invest* 1992; **67**: 596-607

5 **Esser S**, Lampugnani MG, Corada M, Dejana E, Risau W. Vascular endothelial growth factor induces VE-cadherin tyrosine phosphorylation in endothelial cells. *J Cell Sci* 1998; **111**: 1853-1865

6 **Kevil CG**, Payne DK, Mire E, Alexander JS. Vascular permeability factor / vascular endothelial cell growth factor-mediated permeability occurs through disorganization of endothelial junctional proteins. *J Biol Chem* 1998; **273**: 15099-15103

7 **Lal BK**, Varma S, Pappas PJ, Hobson RW 2nd, Duran WN. VEGF increases permeability of the endothelial cell monolayer by activation of PKB / akt, endothelial nitric-oxide synthase, and MAP kinase pathways. *Microvasc Res* 2001; **62**: 252-262

8 **Ferrara N**. Role of vascular endothelial growth factor in regulation of physiological angiogenesis. *Am J Physiol Cell Physiol* 2001; **280**: C1358-C1366

9 **Doanes AM**, Hegland DD, Sethi R, Kovesdi I, Bruder JT, Finkel T. VEGF stimulates MAPK through a pathway that is unique for receptor tyrosine kinases. *Biochem Biophys Res Commun* 1999; **255**: 545-548

10 **Mandriota SJ**, Seghezzi G, Vassalli JD, Ferrara N, Wasi S, Mazzieri R, Mignatti P, Pepper MS. Vascular endothelial growth factor increases urokinase receptor expression in vascular endothelial cells. *J Biol Chem* 1995; **270**: 9709-9716

11 **Pepper MS**, Ferrara N, Orci L, Montesano R. Vascular endothelial growth factor (VEGF) induces plasminogen activators and plasminogen activator inhibitor-1 in microvascular endothelial cells. *Biochem Biophys Res Commun* 1991; **181**: 902-906

12 **Unemori EN**, Ferrara N, Bauer EA, Amento EP. Vascular endothelial growth factor induces interstitial collagenase expression in human endothelial cells. *J Cell Physiol* 1992; **153**: 557-562

13 **Tang H**, Kerins DM, Hao Q, Inagami T, Vaughan DE. The urokinase-type plasminogen activator receptor mediates tyrosine phosphorylation of focal adhesion proteins and activation of mitogen-activated protein kinase in cultured endothelial cells. *J Biol Chem* 1998; **273**: 18268-18272

14 **Senger DR**, Claffey KP, Benes JE, Perruzzi CA, Sergiou AP, Detmar M. Angiogenesis promoted by vascular endothelial growth factor: regulation through alpha1beta1 and alpha2beta1 integrins. *Proc Natl Acad Sci U S A* 1997; **94**: 13612-13617

15 **Senger DR**, Ledbetter SR, Claffey KP, Papadopoulos-Sergiou A, Peruzzi CA, Detmar M. Stimulation of endothelial cell migration by vascular permeability factor / vascular endothelial growth factor through cooperative mechanisms involving the alphavbeta3 integrin, osteopontin, and thrombin. *Am J Pathol* 1996; **149**: 293-305

16 **Carmeliet P**. Mechanisms of angiogenesis and arteriogenesis. *Nat Med* 2000; **6**: 389-395

17 **Watanabe Y**, Lee SW, Detmar M, Ajioka I, Dvorak HF. Vascular permeability factor / vascular endothelial growth factor (VPF / VEGF) delays and induces escape from senescence in human dermal microvascular endothelial cells. *Oncogene* 1997; **14**: 2025-2032

18 **Gerber HP**, Dixit V, Ferrara N. Vascular endothelial growth factor induces expression of the antiapoptotic proteins Bcl-2 and Al in vascular endothelial cells. *J Biol Chem* 1998; **273**: 13313-13316

19 **Gerber HP**, McMurtrey A, Kowalski J, Yan M, Keyt BA, Dixit V, Ferrara N. Vascular endothelial growth factor regulates endothelial cell survival through the phosphatidylinositol 3'-kinase / Akt signal transduction pathway. Requirement for Flk-1 / KDR activation. *J Biol Chem* 1998; **273**: 30336–30343

20 **Wheeler-Jones C**, Abu-Ghazaleh R, Cospedal R, Houliston RA, Martin J, Zachary I. Vascular endothelial growth factor stimulates prostacyclin production and activation of cytosolic phospholipase A2 in endothelial cells via p42 / p44 mitogen-activated protein kinase. *FEBS Lett* 1997; **420**: 28-32

21 **Berra E**, Milanini J, Richard DE, Le Gall M, Vinals F, Gothie E, Roux D, Pages G, Pouyssegur J. Signaling angiogenesis via p42 / p44 MAP kinase and hypoxia. Signaling angiogenesis via p42 / p44 MAP kinase and hypoxia. *Biochem Pharmacol* 2000; **60**: 1171-1178

22 **Chin L**, Tam A, Pomerantz J, Wong M, Holash J, Bardeesy N, Shen Q, O'Hagan R, Pantginis J, Zhou H, Horner JW 2nd, Cordon-Cardo C, Yancopoulos GD, DePinho RA. Essential role for oncogenic Ras in tumour maintenance. *Nature* 1999; **400**: 468-472

23 **Khwaja A**. Akt is more than just a Bad kinase. *Nature* 1999; **401**: 33-34

24 **Fujio Y**, Walsh K. Akt mediates cytoprotection of endothelial cells by vascular endothelial growth factor in an anchorage-dependent manner. *J Biol Chem* 1999; **274**: 16349-16354

25 **Morales-Ruiz M**, Fulton D, Sowa G, Languino LR, Fujio Y, Walsh K, Sessa WC. Vascular endothelial growth factor-stimulated actin reorganization and migration of endothelial cells is regulated via the serine / threonine kinase Akt. *Circ Res* 2000; **86**: 892-896

26 **Mazure NM**, Chen EY, Laderoute KR, Giaccia AJ. Induction of vascular endothelial growth factor by hypoxia is modulated by a phosphatidylinositol 3-kinase / Akt signaling pathway in Ha-ras-transformed cells through a hypoxia inducible factor-1 transcriptional element. *Blood* 1997; **90**: 3322-3331

27 **Dimmeler S**, Zeiher AM. Akt takes center stage in angiogenesis signaling. *Circ Res* 2000; **86**: 4-5

28 **Jiang BH**, Zheng JZ, Aoki M, Vogt PK. Phosphatidylinositol 3-kinase signaling mediates angiogenesis and expression of vascular endothelial growth factor in endothelial cells. *Proc Natl Acad Sci U S A* 2000; **97**: 1749-1753

29 **Dimmeler S**, Fleming I, Fisslthaler B, Hermann C, Busse R, Zeiher AM. Activation of nitric oxide synthase in endothelial cells by Akt-dependent phosphorylation. *Nature* 1999; **399**: 601-605

30 **Fulton D**, Gratton JP, McCabe TJ, Fontana J, Fujio Y, Walsh K, Franke TF, Papapetropoulos A, Sessa WC. Regulation of endothelium-derived nitric oxide production by the protein kinase Akt. *Nature* 1999; **399**: 597-601

31 **Gupta K**, Kshirsagar S, Li W, Gui L, Ramakrishnan S, Gupta P, Law PY, Hebbel RP. VEGF prevents apoptosis of human microvascular endothelial cells via opposing effects on MAPK / ERK and SAPK / JNK signaling. *Exp Cell Res* 1999; **247**: 495–504

32 **Dimmeler S**, Dernbach E, Zeiher AM. Phosphorylation of the endothelial nitric oxide synthase at ser-1177 is required for VEGF-induced endothelial cell migration. *FEBS Lett* 2000; **477**: 258-262

33 **Buchler P**, Reber HA, Buchler M, Shrinkante S, Buchler MW, Friess H, Semenza GL, Hines OJ. Hypoxia-inducible factor 1 regulates vascular endothelial growth factor expression in human pancreatic cancer. *Pancreas* 2003; **26**: 56-64

34 **Pardo OE**, Arcaro A, Salerno G, Raguz S, Downward J, Seckl MJ. Fibroblast growth factor-2 induces translational regulation of Bcl-XL and Bcl-2 via a MEK-dependent pathway: correlation with resistance to etoposide-induced apoptosis. *J Biol Chem* 2002; **277**: 12040-12046

35 **Yoshiji H**, Kuriyama S, Yoshii J, Ikenaka Y, Noguchi R, Hicklin DJ, Huber J, Nakatani T, Tsujinoue H, Yanase K, Imazu H, Fukui H. Synergistic effect of basic fibroblast growth factor and vascular endothelial growth factor in murine hepatocellular carcinoma. *Hepatology* 2002; **35**: 834-842

36 **Stavri GT**, Zachary IC, Baskerville PA, Martin JF, Erusalimsky JD. Basic fibroblast growth factor upregulates the expression of vascular endothelial growth factor in vascular smooth muscle cells. Synergistic interaction with hypoxia. *Circulation* 1995; **92**: 11-14

37 **Mandriota SJ**, Pepper MS. Vascular endothelial growth factor-induced in vitro angiogenesis and plasminogen activator expression are dependent on endogenous basic fibroblast growth factor. *J Cell Sci* 1997; **110**: 2293-2302

38 **Sato Y**, Rifkin DB. Autocrine activities of basic fibroblast growth factor: regulation of endothelial cell movement, plasminogen activator synthesis, and DNA synthesis. *J Cell Biol* 1988; **107**: 1199-1205

39 **Ausprunk DH**, Folkman J. Migration and proliferation of endothelial cells in preformed and newly formed blood vessels during tumor angiogenesis. *Microvasc Res* 1977; **14**: 53-65

40 **Miao HQ**, Ornitz DM, Aingorn E, Ben-Sasson SA, Vlodavsky I. Modulation of fibroblast growth factor-2 receptor binding, dimerization, signaling, and angiogenic activity by a synthetic heparin-mimicking polyanionic compound. *J Clin Invest* 1997; **99**: 1565-1575

41 **Lobov IB**, Brooks PC, Lang RA. Angiopoietin-2 displays VEGF-dependent modulation of capillary structure and endothelial cell survival *in vivo*. *Proc Natl Acad Sci U S A* 2002; **99**: 11205-11210

42 **Kim I**, Kim HG, So JN, Kim JH, Kwak HJ, Koh GY. Angiopoietin-1 Regulates Endothelial Cell Survival Through the Phosphatidylinositol 3'-Kinase/Akt Signal Transduction Pathway. *Circulation Research* 2000; **86**: 24-29

43 **Papapetropoulos A**, Fulton D, Mahboubi K, Kalb RG, O'Connor DS, Li F, Altieri DC, Sessa WC. Angiopoietin-1 inhibits endothelial cell apoptosis via the Akt/survivin pathway. *J Biol Chem* 2000; **275**: 9102-9105

44 **Harfouche R**, Hassessian HM, Guo Y, Faivre V, Srikant CB, Yancopoulos GD, Hussain SN. Mechanisms which mediate the antiapoptotic effects of angiopoietin-1 on endothelial cells. *Microvasc Res* 2002; **64**: 135-147

45 **Kim I**, Kim HG, Moon SO, Chae SW, So JN, Koh KN, Ahn BC, Koh GY. Angiopoietin-1 induces endothelial cell sprouting through the activation of focal adhesion kinase and plasmin secretion. *Cir Res* 2000; **86**: 952-959

46 **Laping NJ**, Grygielko E, Mathur A, Butter S, Bomberger J, Tweed C, Martin W, Fornwald J, Lehr R, Harling J, Gaster L, Callahan JF, Olson BA. Inhibition of transforming growth factor (TGF)-beta1-induced extracellular matrix with a novel inhibitor of the TGF-beta type I receptor kinase activity: SB-431542. *Mol Pharmacol* 2002; **62**: 58-64

47 **Lawrence DA**, Pircher R, Jullien P. Conversion of a high molecular weight latent beta-TGF from chicken embryo fibroblasts into a low molecular weight active beta-TGF under acidic conditions. *Biochem Biophys Res Commu* 1985; **133**: 1026-1034

48 **Lyons RM**, Keski-Oja J, Moses HL. Proteolytic activation of latent transforming growth factor-beta from fibroblast-conditioned medium. *J Cell Biol* 1988; **106**: 1659-1665

49 **Lyons RM**, Gentry LE, Purchio AF, Moses HL. Mechanism of activation of latent recombinant transforming growth factor beta 1 by plasmin. *J Cell Biol* 1990; **110**: 1361-1367

50 **Sato Y**, Tsuboi R, Lyons RM, Moses HL, Rifkin DB. Characterization of the activation of latent TGF-beta by co-cultures of endothelial cells and pericytes or smooth muscle cells: a self- regulating system. *J Cell Bio* 1990; **111:** 757-763

51 **Mandriota SJ**, Menoud PA, Pepper MS. Transforming growth factor beta 1 down-regulates vascular endothelial growth factor receptor 2/flk-1 expression in vascular endothelial cells. *J Biol Chem* 1996; **271**: 11500-11505

52 **Saito H**, Tsujitani S, Oka S, Kondo A, Ikeguchi M, Maeta M, Kaibara N. The expression of transforming growth factor-beta1 is significantly correlated with the expression of vascular endothelial growth factor and poor prognosis of patients with advanced gastric carcinoma. *Cancer* 1999; **86**: 1455-1462

53 **O'Mahony CA**, Albo D, Tuszynski GP, Berger DH. Transforming growth factor-beta 1 inhibits generation of angiostatin by human pancreatic cancer cells. *Surgery* 1998; **124**: 388-393

54 **Sherr CJ**. Cancer cell cycle. *Science* 1996; **14**: 309-318

55 **Pepper MS**, Belin D, Montesano R, Orci L, Vassalli JD. Transforming growth factor-beta 1 modulates basic fibroblast growth factor-induced proteolytic and angiogenic properties of endothelial cells *in vitro*. *J Cell Biol* 1990; **111**: 743-755

56 **Ellenrieder V**, Hendler SF, Ruhland C, Boeck W, Adler G, Gress TM. TGF-beta-induced invasiveness of pancreatic cancer cells is mediated by matrix metalloproteinase-2 and the urokinase plasminogen activator system. *Int J Cancer* 2001; **93**: 204-211

57 **Yuan A**, Yang PC, Yu CJ, Chen WJ, Lin FY, Kuo SH, Luh KT. Interleukin-8 messenger ribonucleic acid expression correlates with tumor progression, tumor angiogenesis, patient survival, and timing of relapse in non-small-cell lung cancer. *Am J Respir Crit Care Med* 2000; **162**: 1957-1963

58 **Bar-Eli M**. Role of interleukin-8 in tumor growth and metastasis of human melanoma. *Pathobiology* 1999; **67**: 12-18

59 **Kitadai Y**, Takahashi Y, Haruma K, Naka K, Sumii K, Yokozaki H, Yasui W, Mukaida N, Ohmoto Y, Kajiyama G, Fidler IJ, Tahara E. Transfection of interleukin-8 increases angiogenesis.and tumorigenesis of human gastric carcinoma cells in nude mice. *Br J Cancer* 1999; **81**: 647-653

60 **Levi E**, Fridman R, Miao HQ, Ma YS, Yayon A, Vlodavsky I. Matrix metalloproteinase 2 releases active soluble ectodomain of fibroblast growth factor receptor 1. *Proc Natl Acad Sci U S A* 1996; **93**: 7069-7074

61 **Suzuki M**, Raab G, Moses MA, Fernandez CA, Klagsbrun M. Matrix metalloproteinase-3 releases active heparin-binding EGF-like growth factor by cleavage at a specific juxtamembrane site. *J Biol Chem* 1997; **272**: 31730-31737

62 **Ray JM**, Stetler-Stevenson WG. Gelatinase A activity directly modulates melanoma cell adhesion and spreading. *EMBO J* 1995; **14**: 908-917

63 **Brooks PC**, Silletti S, von Schalscha TL, Friedlander M, Cheresh DA. Disruption of angiogenesis by PEX, a noncatalytic metalloproteinase fragment with integrin binding activity. *Cell* 1998; **92**: 391-400

64 **Yu Q**, Stamenkovic I. Cell surface-localized matrix metalloproteinase-9 proteolytically activates TGF-beta and promotes tumor invasion and angiogenesis. *Genes Dev* 2000; **14**: 163-176

65 **Rak J**, Filmus J, Finkenzeller G, Grugel S, Marme D, Kerbel RS. Oncogenes as inducers of tumor angiogenesis. *Cancer Metastasis Rev* 1995; **14**: 263-277

66 **Relf M**, LeJeune S, Scott PA, Fox S, Smith K, Leek R, Moghaddam A, Whitehouse R, Bicknell R, Harris AL. Expression of the angiogenic factors vascular endothelial cell growth factor, acidic and basic fibroblast growth factor, tumor growth factor beta-1, platelet-derived endothelial cell growth factor, placenta growth factor, and pleiotrophin in human primary breast cancer and its relation to angiogenesis. *Cancer Res* 1997; **57**: 963-969

67 **Mazure NM**, Chen EY, Yeh P, Laderoute KR, Giaccia AJ. Oncogenic transformation and hypoxia synergistically act to modulate vascular endothelial growth factor expression. *Cancer Res* 1996; **56**: 3436-3440

68 **Chiarugi V**, Magnelli L, Gallo O. Cox-2, iNOS and p53 as playmakers of tumor an giogenesis. *Int J Mol Med* 1998; **2**: 715-719

69 **Kieser A**, Weich HA, Brandner G, Marme D, Kolch W. Mutant p53 potentiates protein kinase C induction of vascular endothelial growth factors expression. *Oncogene* 1994; **9**: 963-969

70 **Tai YT**, Podar K, Gupta D, Lin B, Young G, Akiyama M, Anderson KC. CD40 activation induces p53-dependent vascular endothelial growth factor secretion in human multiple myeloma cells. *Blood* 2002; **99**: 1419-1427

71 **Galy B**, Creancier L, Prado-Lourenco L, Prats AC, Prats H. p53 directs conformational change and translation initiation blockade of human fibroblast growth factor 2 mRNA. *Oncogene* 2001; **20**: 4613-4620

72 **Sherif ZA**, Nakai S, Pirollo KF, Rait A, Chang EH. Downmodulation of bFGF-binding protein expression following restoration of p53 function**.** *Cancer Gene Ther* 2001; **8**: 771-782

73 **Toschi E**, Rota R, Antonini A, Melillo G, Capogrossi MC. Wild-type p53 gene transfer inhibits invasion and reduces matrix metalloproteinase-2 levels in p53-mutated human melanoma cells. *J Invest Dermatol* 2000; **114**: 1188-1194

74 **Kastan MB**, Onyekwere O, Sidranski D, Kastan MB, Onyekwere O, Sidranski D. Participation of p53 protein in the cellular response to DNA damage. *Cancer Res* 1991; **51**: 6304-6311

75 **Yonish-Rouach E**, Resnitzky D, Lotem J, Sachs L, Kimchi A, Oren M. Wild-type p53 induceS apoptosis of myeloid leukaemic cells that is inhibited by interleukin-6. *Nature* 1991; **352**: 345-347

76 **Eckhardt SG**. Angiogenesis inhibitors as cancer therapy. *Hosp Pract (Off Ed)* 1999; **34**: 63-68, 77-79, 83-84

77 **Oehler MK**, Bicknell R. The promise of anti-angiogenic cancer therapy. *Br J Cancer* 2000; **82**: 749-752

78 **Zhang W**, Ran S, Sambade M, Huang X, Thorpe PE. A monoclonal antibody that blocks VEGF binding to VEGFR2 (KDR/Flk-1) inhibits vascular expression of Flk-1 and tumor growth in an orthotopic human breast cancer model. *Angiogenesis* 2002; **5**: 35-44

79 **Witte L**, Hicklin DJ, Zhu Z, Pytowski B, Kotanides H, Rockwell P, Bohlen P. Monoclonal antibodies targeting the VEGF receptor-2 (Flk1/KDR) as an anti-angiogenic therapeutic strategy. *Cancer Metastasis Rev* 1998; **17**: 155-161

80 **Im SA**, Gomez-Manzano C, Fueyo J, Liu TJ, Ke LD, Kim JS, Lee HY, Steck PA, Kyritsis AP, Yung WK. Anti-angiogenesis treatment for gliomas: transfer of antisense-vascular endothelial growth factor inhibits tumor growth *in vivo*. *Cancer Res* 1999; **59**: 895-900

81 **Zhang L**, Gasper WJ, Stass SA, Ioffe OB, Davis MA, Mixson AJ. Angiogenic inhibition mediated by a DNAzyme that targets vas-

cular endothelial growth factor receptor 2. *Cancer Res* 2002; **62**: 5463-5469

82 **Feldman AL**, Libutti SK. Progress in antiangiogenic gene therapy of cancer. *Cancer* 2000; **89**: 1181-1194

83 **Slaton JW**, Perrotte P, Inoue K, Dinney CP, Fidler IJ. Interferon-alpha-mediated down-regulation of angiogenesis-related genes and therapy of bladder cancer are dependent on optimization of biological dose and schedule. *Clin Cancer Res* 1999; **5**: 2726-2734

84 **Izawa JI**, Sweeney P, Perrotte P, Kedar D, Dong Z, Slaton JW, Karashima T, Inoue K, Benedict WF, Dinney CP. Inhibition of tumorigenicity and metastasis of human bladder cancer growing in athymic mice by interferon-beta gene therapy results partially from various antiangiogenic effects including endothelial cell apoptosis. *Clin Cancer Res* 2002; **8**: 1258-1270

85 **Ozawa S**, Shinohara H, Kanayama HO, Bruns CJ, Bucana CD, Ellis LM, Davis DW, Fidler IJ. Suppression of angiogenesis and therapy of human colon cancer liver metastasis by systemic administration of interferon-alpha. *Neoplasia* 2001; **3**: 154-164

86 **Bauvois B**, Dumont J, Mathiot C, Kolb JP. Production of matrix metalloproteinase-9 in early stage B-CLL: suppression by interferons. *Leukemia* 2002; **16**: 791-798

87 **Marler JJ**, Rubin JB, Trede NS, Connors S, Grier H, Upton J, Mulliken JB, Folkman J. Successful antiangiogenic therapy of giant cell angioblastoma with interferon alfa 2b: report of 2 cases**.** *Pediatrics* 2002; **109**: E37

88 **Sasamura H**, Takahashi A, Miyao N, Yanase M, Masumori N, Kitamura H, Itoh N, Tsukamoto T. Inhibitory effect on expression of angiogenic factors by antiangiogenic agents in renal cell carcinoma. *Br J Cancer* 2002; **86**: 768-773

89 **Nilsson A**, Janson ET, Eriksson B, Larsson A. Levels of angiogenic peptides in sera from patients with carcinoid tumours during alpha-interferon treatment. *Anticancer Res* 2001; **21**: 4087-4090

90 **Jonasch E**, Haluska FG. Interferon in oncological practice: review of interferon biology, clinical applications, and toxicities. *Oncologist* 2001; **6**: 34-55

91 **Strieter RM**, Polverini PJ, Kunkel SL, Arenberg DA, Burdick MD, Kasper J, Dzuiba J, Van Damme J, Walz A, Marriott D. The functional role of the ELR motif in CXC chemokine-mediated angiogenesis. *J Biol Chem* 1995; **270**: 27348-27357

92 **Volpert OV**, Fong T, Koch AE, Peterson JD, Waltenbaugh C, Tepper RI, Bouck NP. Inhibition of angiogenesis by interleukin 4. *J Exp Med* 1998; **188**: 1039-1046

93 **Torisu H**, Ono M, Kiryu H, Furue M, Ohmoto Y, Nakayama J, Nishioka Y, Sone S, Kuwano M. Macrophage infiltration correlates with tumor stage and angiogenesis in human malignant melanoma. *Int J Cancer* 2000; **85**: 182-188

94 **Oshikawa K**, Rakhmilevich AL, Shi F, Sondel PM, Yang N, Mahvi DM. Interleukin 12 gene transfer into skin distant from the tumor site elicits antimetastatic effects equivalent to local gene transfer. *Hum Gene Ther* 2001; **12**: 149-160

95 **Duda DG**, Sunamura M, Lozonschi L, Kodama T, Egawa S, Matsumoto G, Shimamura H, Shibuya K, Takeda K, Matsuno S. Direct *in vitro* evidence and *in vivo* analysis of the antiangiogenesis effects of interleukin-12. *Cancer Res* 2000; **60**: 1111-1116

96 **Huang S**, Ullrich SE, Bar-Eli M. Regulation of tumor growth and metastasis by interleukin-10: the melanoma experience. *J Interferon Cytokine Res* 1999; **19**: 697-703

97 **Fernandez HA**, Kallenbach K, Seghezzi G, Grossi E, Colvin S, Schneider R, Mignatti P, Galloway A. Inhibition of endothelial cell migration by gene transfer of tissue inhibitor of metalloproteinases-1. *J Surg Res* 1999; **82**: 156-162

98 **Murphy AN**, Unsworth EJ, Stetler-Stevenson WG. Tissue inhibitor of metalloproteinases-2 inhibits bFGF-induced human microvascular endothelial cell proliferation. *J Cell Physiol* 1993; **157**: 351-358

99 **Valente P**, Fassina G, Melchiori A, Masiello L, Cilli M, Vacca A, Onisto M, Santi L, Stetler-Stevenson WG, Albini A. TIMP-2 overexpression reduces invasion and angiogenesis and protects B16F10 melanoma cells from apoptosis. *Int J Cancer* 1998; **75**: 246-253

100 **Smith MR**, Kung H, Durum SK, Colburn NH, Sun Y. TIMP-3 induces cell death by stabilizing TNF-alpha receptors on the surface of human colon carcinoma cells. *Cytokine* 1997; **9**: 770-780

101 **Baker AH**, Zaltsman AB, George SJ, Newby AC. Divergent effects of tissue inhibitor of metalloproteinase-1, -2, or -3 overexpression on rat vascular smooth muscle cell invasion, proliferation, and death in vitro. TIMP-3 promotes apoptosis. *J Clin Invest* 1998; **101**: 1478-1487

102 **Spurbeck WW**, Ng CY, Strom TS, Vanin EF, Davidoff AM. Enforced expression of tissue inhibitor of matrix metalloproteinase-3 affects functional capillary morphogenesis and inhibits tumor growth in a murine tumor model**.** *Blood* 2002; **100**: 3361-3368

103 **Gomez DE**, Alonso DF, Yoshiji H, Thorgeirsson UP. Tissue inhibitors of metalloproteinases: structure, regulation and biological functions. *Eur J Cell Biol* 1997; **74**: 111-122

104 **Hajitou A**, Grignet C, Devy L, Berndt S, Blacher S, Deroanne CF, Bajou K, Fong T, Chiang Y, Foidart JM, Noel A. The antitumoral effect of endostatin and angiostatin is associated with a down-regulation of vascular endothelial growth factor expression in tumor cells. *FASEB J* 2002; **16**: 1802-1804

105 **Wajih N**, Sane DC. Angiostatin selectively inhibits signaling by hepatocyte growth factor in endothelial and smooth muscle cells. *Blood* 2002 oct 24; [epub ahead of print]

106 **Cao Y,** Ji RW, Davidson D, Schaller J, Marti D, Sohndel S, McCance SG, O'Reilly MS, Llinas M, Folkman J. Kringle domains of human angiostatin. Characterization of the anti-proliferative activity on endothelial cells. *J Biol Chem* 1996; **271**: 29461-29467

107 **Moser TL**, Stack MS, Asplin I, Enghild JJ, Hojrup P, Everitt L, Hubchak S, Schnaper HW, Pizzo SV. Angiogenesis binds ATP synthase on the surface of human endothelial cells. *Proc Natl Acad Sci U S A* 1999; **96**: 2811-2816

108 **Moser TL**, Kenan DJ, Ashley TA, Roy JA, Goodman MD, Misra UK, Cheek DJ, Pizzo SV. Endothelial cell surface $F_1$-$F_O$ ATP synthase is active in ATP synthesis and is inhibited by angiostatin. *Proc Natl Acad Sci U S A* 2001; **98**: 6656-6661

109 **Griscelli F**, Li H, Bennaceur-Griscelli A, Soria J, Opolon P, Soria C, Perricaudet M, Yeh P, Lu H. Angiostatin gene transfer: inhibition of tumor growth in vivo by blockage of endothelial cell proliferation associated with a mitosis arrest. *Proc Natl Acad Sci U S A* 1998; **95**: 6367-6372

110 **Sun X**, Kanwar JR, Leung E, Lehnert K, Wang D, Krissansen GW. Angiostatin enhances B7.1-mediated cancer immunotherapy independently of effects on vascular endothelial growth factor expression. *Cancer Gene Ther* 2001; **8**: 719-727

111 **Lucas R**, Holmgren L, Garcia I, Jimenez B, Mandriota SJ, Borlat F, Sim BK, Wu Z, Grau GE, Shing Y, Soff GA, Bouck N, Pepper MS. Multiple forms of angiostatin induce apoptosis in endothelial cells. *Blood* 1998; **92**: 4730-4741

112 **Gupta N**, Nodzenski E, Khodarev NN, Yu J, Khorasani L, Beckett MA, Kufe DW, Weichselbaum RR. Angiostatin effects on endothelial cells mediated by ceramide and RhoA. *EMBO Rep* 2001; **2**: 536-540

113 **Kim YM**, Hwang S, Kim YM, Pyun BJ, Kim TY, Lee ST, Gho YS, Kwon YG. Endostatin Blocks Vascular Endothelial Growth Factor-mediated Signaling via Direct Interaction with KDR/Flk-1. *J Biol Chem* 2002; **277**: 27872-27879

114 **Urbich C**, Reissner A, Chavakis E, Dernbach E, Haendeler J, Fleming I, Zeiher AM, Kaszkin M, Dimmeler S. Dephosphorylation of endothelial nitric oxide synthase contributes to the anti-angiogenic effects of endostatin. *FASEB J* 2002; **16**: 706-708

115 **Rehn M**, Veikkola T, Kukk-Valdre E, Nakamura H, Ilmonen M, Lombardo C, Pihlajaniemi T, Alitalo K, Vuori K. Interaction of endostatin with integrins implicated in angiogenesis. *Proc Natl Acad Sci U S A* 2001; **98**: 1024–1029

116 **Hohenester E**, Sasaki T, Olsen BR, Timpl R. Crystal structure of the angiogenesis inhibitor endostatin at 1.5 angstrom resolution. *EMBO J* 1998; **17**: 1656-1664

117 **Marion-Audibert AM**, Nejjari M, Pourreyron C, Anderson W, Gouysse G, Jacquier MF, Dumortier J, Scoazec JY. Effects of endocrine peptides on proliferation, migration and differentiation of human endothelial cells**.** *Gastroenterol Clin Biol* 2000; **24**: 644-648

118 **Kim YM**, Jang JW, Lee OH, Yeon J, Choi EY, Kim KW, Lee ST, Kwon YG. Endostatin inhibits endothelial and tumor cellular invasion by blocking the activation and catalytic activity of matrix metalloproteinase. *Cancer Res* 2000; **60**: 5410-5413

119 **Dixelius J**, Larsson H, Sasaki T, Holmqvist K, Lu L, Engstrom A, Timpl R, Welsh M, Claesson-Welsh L. Endostatin-induced tyrosine kinase signaling through the shb adaptor protein regulates endothelial cell apoptosis. *Blood* 2000; **95**: 3403-3411

120 **Dhanabal M**, Ramchandran R, Waterman MJ, Lu H, Knebelmann B, Segal M, Sukhatme VP. Endostatin induces endothelial cell apoptosis. *J Biol Chem* 1999; **274**: 11721-11726
121 **Pages P**, Benali N, Saint-Laurent N, Esteve JP, Schally AV, Tkaczuk J, Vaysse N, Susini C, Buscail L. sst2 somatostatin receptor mediates cell cycle arrest and induction of p27(Kip1). Evidence for the role of SHP-1. *J Biol Chem* 1999; **274**: 15186-15193
122 **Sharma K**, Patel YC, Srikant CB. C-terminal region of human somatostatin receptor 5 is required for induction of Rb and G1 cell cycle arrest. *Mol Endocrinol* 1999; **13**: 82-90
123 **Charland S**, Boucher MJ, Houde M, Rivard N. Somatostatin inhibits Akt phosphorylation and cell cycle entry, but not p42/p44 mitogen-activated protein (MAP) kinase activation in normal and tumoral pancreatic acinar cells. *Endocrinology* 2001; **142**: 121-128
124 **Sharma K**, Patel YC, Srikant CB. Subtype-selective induction of wild-type p53 and apoptosis, but not cell cycle arrest, by human somatostatin receptor 3. *Mol Endocrinol* 1996; **10**: 1688-1696
125 **Albini A**, Florio T, Giunciuglio D, Masiello L, Carlone S, Corsaro A, Thellung S, Cai T, Noonan DM, Schettini G. Somatostatin controls Kaposi's sarcoma tumor growth through inhibition of angiogenesis. *FASEB J* 1999; **13**: 647-655
126 **Woltering EA**, Watson JC, Alperin-Lea RC, Sharma C, Keenan E, Kurozawa D, Barrie R. Somatostatin analogs: angiogenesis inhibitors with novel mechanisms of action. *Invest New Drugs* 1997; **15**, 77-86
127 **Gulec SA**, Gaffga CM, Anthony CT, Su LJ, O'Leary JP, Woltering EA, Gulec SA, Gaffga CM, Anthony CT, Su LJ, O'Leary JP, Woltering EA. Antiangiogenic therapy with somatostatin receptor-mediated in situ radiation. *Am Surg* 2001; **67**: 1068-1071
128 **Patel YC**. Molecular pharmacology of somatostatin receptor subtypes. *J Endocrinol Invest* 1997; **20**: 348-367
129 **Lewin MJ**. The somatostatin receptor in the GI tract. *Annu Rev Physiol* 1992; **54**: 455-468
130 **Buscail L**, Esteve JP, Saint-Laurent N, Bertrand V, Reisine T, O'Carroll AM, Bell GI, Schally AV, Vaysse N, Susini C. Inhibition of cell proliferation by the somatostatin analogue RC-160 is mediated by somatostatin receptor subtypes SSTR2 and SSTR5 through different mechanisms. *Proc Natl Acad Sci U S A* 1995; **92**: 1580-1584
131 **Mentlein R**, Eichler O, Forstreuter F, Held-Feindt J. Somatostatin inhibits the production of vascular endothelial growth factor in human glioma cells. *Int J Cancer* 2001; **92**: 545-550
132 **Lawnicka H**, Stepien H, Wyczolkowska J, Kolago B, Kunert-Radek J, Komorowski J. Effect of somatostatin and octreotide on proliferation and vascular endothelial growth factor secretion from murine endothelial cell line (HECa10) culture. *Biochem Biophys Res Commun* 2000; **268**: 567-571
133 **Wu PC**, Liu CC, Chen CH, Kou HK, Shen SC, Lu CY, Chou WY, Sung MT, Yang LC. Inhibition of experimental angiogenesis of cornea by somatostatin. *Graefes Arch Clin Exp Ophthalmol* 2003; **241**: 63-69
134 **Lamberts SW**, Krenning EP, Reubi JC. The role of somatostatin and its analogs in the diagnosis and treatment of tumors. *Endocr Rev* 1991; **12**: 450-482
135 **Jimenez B**, Volpert OV, Crawford SE, Febbraio M, Silverstein RL, Bouck N. Signals leading to apoptosis-dependent inhibition of neovascularization by thrombospondin-1. *Nat Med* 2000; **6**: 41-48
136 **Gilmore AP**, Romer LH. Inhibition of focal kinase protein (FAK) signaling in focal adhesion decreases cell motility and proliferation. *Mol Biol Cell* 1996; **7**: 1209-1224
137 **Volpert OV**, Lawler J, Bouck NP. A human fibrosarcoma inhibits systemic angiogenesis and the growth of experimental metastases via thrombospondin-1. *Proc Natl Acad Sci U S A* 1997; **95**: 6343-6348
138 **Panetti TS**, Chen H, Misenheimer TM, Getzler SB, Mosher DF. Endothelial cell mitogenesis induced by LPA: inhibition by thrombospondin-1 and thrombospondin-2. *J Lab Clin Med* 1997; **129**: 208-216
139 **Iyer S**, Chaplin DJ, Rosenthal DS, Boulares AH, Li LY, Smulson ME. Induction of apoptosis in proliferating human endothelial cells by the tumor-specific antiangiogenesis agent combretastatin A-4. *Cancer Res* 1998; **58**: 4510-4514
140 **Boehm T**, Folkman J, Browder T, O'Reilly MS. Antiangiogenic therapy of experimental cancer does not induce acquired drug resistance. *Nature* 1997; **390**: 404-407
141 **Jayson GC**, Zweit J, Jackson A, Mulatero C, Julyan P, Ranson M, Broughton L, Wagstaff J, Hakannson L, Groenewegen G, Bailey J, Smith N, Hastings D, Lawrance J, Haroon H, Ward T, McGown AT, Tang M, Levitt D, Marreaud S, Lehmann FF, Herold M, Zwierzina H. Molecular imaging and biological evaluation of HuMV833 anti-VEGF antibody: implications for trial design of antiangiogenic antibodies. *J Natl Cancer Inst* 2002; **94**: 1484-1493
142 **Gossmann A**, Helbich TH, Kuriyama N, Ostrowitzki S, Roberts TP, Shames DM, van Bruggen N, Wendland MF, Israel MA, Brasch RC. Dynamic contrast-enhanced magnetic resonance imaging as a surrogate marker of tumor response to anti-angiogenic therapy in a xenograft model of glioblastoma multiforme**.** *J Magn Reson Imaging* 2002; **15**: 233-240
143 **Kim SW**, Park SS, Ahn SJ, Chung KW, Moon WK, Im JG, Yeo JS, Chung JK, Noh DY. Identification of angiogenesis in primary breast carcinoma according to the image analysis. *Breast Cancer Res Treat* 2002; **74**: 121-129

**Edited by** Wu XN

P.O.Box 2345, Beijing 100023,China
Fax: +86-10-85381893
E-mail: wjg@wjgnet.com www.wjgnet.com

World J Gastroenterol 2003;9(6):1156-1164
World Journal of Gastroenterology
Copyright ©2003 by The WJG Press ISSN 1007-9327

• REVIEW •

# Primary adenocarcinomas of lower esophagus, esophagogastric junction and gastric cardia: in special reference to China

Li-Dong Wang, Shu Zheng, Zuo-Yu Zheng, Alan G. Casson

**Li-Dong Wang,** Cancer Institute, Zhejiang University, Hangzhou 310009, Jiangsu Province, China and Laboratory for Cancer Research, College of Medicine, Zhengzhou University, Zhengzhou 450052, Henan Province, China
**Shu Zheng,** Cancer Institute, Zhejiang University, Hangzhou 310009, Jiangsu Province, China
**Zuo-Yu Zheng,** Laboratory for Cancer Research, College of Medicine, Zhengzhou University, Zhengzhou 450052, Henan Province, China
**Alan G. Casson,** Department of Surgery, Dalhousie University, Halifax, Nova Scotia, Canada
**Supported by** National Distinguished Young Scientist Foundation of China, No. 30025016 and Foundation of Henan Education Committee, No. 1999125
**Correspondence to:** Li-Dong Wang, M.D., Professor of Pathology and Oncology, Invited Profesor of Henan Province, Director fo Laboratory for Cancer Research, College of Medicine, Zhengzhou University, Zhengzhou, 450052, Henan Province, China. lidong0823@sina.com
**Telephone:** +86-371-6970165 **Fax:** +86-371-6970165
**Received:** 2003-05-20 **Accepted:** 2003-06-02

## Abstract

Gastric cardia adenocarcinoma (GCA) is an under-studied subject. The pathogenesis, molecular changes in the early stage of carcinogenesis and related risk factors have not been well characterized. There is evidence, however, that GCA differs from cancer of the rest of the stomach in terms of natural history and histopathogenesis. Adenocarcinomas of the lower esophagus, esophagogastric junction (EGJ) and gastric cardia have been given much attention because of their increasing incidences in the past decades, which is in striking contrast with the steady decrease in distal stomach adenocarcinoma. In China, epidemiologically, GCA shares very similar geographic distribution with esophageal squamous cell carcinoma (SCC), especially in Linzhou (formerly Linxian County), Henan Province, North China, the highest incidence area of esophageal SCC in the world. Historically, both GCA and SCC in these areas were referred to as esophageal cancer (EC) by the public because of the common syndrome of dysphagia. In Western countries, Barrett's esophagus is very common and has been considered as an important precancerous lesion of adenocarcinoma at EGJ. Because of the low incidence of Barrett's esophagus in China, it is unlikely to be an important factor in early stage of EGJ adenocarcinoma development. However, Z line up-growth into lower esophagus may be one of the characteristic changes in these areas in early stage of GCA development. Whether intestinal metaplasia (IM) is a premalignant lesion for GCA is still not clear. Higher frequency of IM observed at adjacent GCA tissues in Henan suggests the possibility of IM as a precancerous lesion for GCA in these areas. Molecular information on GCA, especially in early stage, is very limited. The accumulated data about the changes of tumor suppressor gene, such as p53 mutation, and ontogeny, such as C-erbB2, especially the similar alterations in GCA and SCC in the same patient, indicated that there might be some similar risk factors, such as nitrosamine, involved in both GCA and SCC in Henan population. The present observations also suggest that GCA should be considered as a distinct entity.

Wang LD, Zheng S, Zheng ZY, Casson AG. Primary adenocarcinomas of lower esophagus, esophagogastric junction and gastric cardia: in special reference to China. *World J Gastroenterol* 2003; 9(6): 1156-1164
http://www.wjgnet.com/1007-9327/9/1156.asp

## INTRODUCTION

Adenocarcinomas of the gastric cardia are currently classified as gastric cancers[1, 2]. However, recent studies have suggested that these tumors have distinct epidemiological and biological characteristics[3, 4]. In the last two decades, the incidence of primary adenocarcinomas of the lower esophagus, esophagogastric junction (EGJ) and adenocarcinomas of the gastric cardia has increased dramatically in North America and Western European countries[3-6]. In contrast, the incidence of adenocarcinoma of the distal stomach has decreased steadily in recent years.

In China, adenocarcinomas of the gastric cardia have unique epidemiological features distinguishing these tumors from the adenocarcinomas of the distal stomach. Linzhou (formerly Linzhou County), the region with the highest incidence rate of esophageal cancer in the world, also has a high incidence of adenocarcinoma of the gastric cardia. However, the incidence of adenocarcinoma arising from the distal stomach is very low in this area. Therefore, previously, adenocarcinomas arising from the EGJ (gastric cardia) were referred to as esophageal cancers, because they shared similar clinical symptoms such as dysphagia. As most of the adenocarcinomas arising from the cardia are diagnosed at an advanced stage, it is very difficult to accurately define whether these tumors have a primary esophageal or gastric origin. Therefore, adenocarcinomas of the EGJ (gastric cardia) are now generally referred to as gastric cardia adenocarcinomas (GCA). With the exception of Barrett' s esophagus (a well documented premalignant lesion of esophageal adenocarcinoma in Caucasians)[7, 8], the role of other risk factors, such as *H. pylori* infection, diet, alcohol and tobacco exposure, still remains unclear.

Most studies of esophageal carcinoma in Linzhou have evaluated only esophageal squamous cell carcinoma (SCC). Few have studied adenocarcinoma (AC) of the gastric cardia, particularly as a separate pathological entity in China. In this review, recent epidemiological, histopathological and molecular biological advances were summarized to provide clues about the risk factors and the molecular carcinogenosis of adenocarcinomas of the lower esophagus, and EGJ (gastric cardia).

## EPIDEMIOLOGY OF ADENOCARCINOMA OF THE GASTRIC CARDIA

GCA shares several common features with the adenocarcinoma arising from the distal esophagus: a lower mean age of

presentation, a higher incidence in the Caucasian population, a higher male to female ratio, and similar risk factors[4, 9]. Epidemiological studies have demonstrated that smoking, alcohol consumption, increased body mass index (reflecting obesity), and lower socioeconomic status are risk factors for adenocarcinomas of both the distal esophagus and gastric cardia[10-12]. In Linzhou, China, adenocarcinoma of the gastric cardia was previously classified as esophageal cancer by the local registry for the past several decades, primarily because of comparable clinical features and similarity in therapy. Reviewing hospital records of patients with dysphagia, our research group reported that while approximately 60 percent of patients were found to have a diagnosis of SCC, the remaining 40 percent were found to have adenocarcinomas of the lower esophagus or gastric cardia[13]. A case-control study performed on the patients with presumed distal esophageal or gastric cardia cancer in Linzhou found that one third of all these tumors was adenocarcinomas of the gastric cardia[14]. While there is considerable evidence implicating that dietary factors, including certain nutrient deficiencies and consumption of nitrosamine-contaminated food, and drinking water are associated with the development of SCC[15-18], it is not clear whether adenocarcinomas of the gastric cardia share the same risk factors in this high-incidence area in China.

## DIAGNOSTIC CRITERIA FOR ADENOCARCINOMA OF THE GASTRIC CARDIA

It is generally difficult to distinguish where cardia adenocarcinomas originate, as most tumors present in advanced stage at diagnosis, often involving both esophagus and stomach. Imprecise clinical and pathological definitions of adenocarcinomas of the lower esophagus, EGJ or gastric cardia may be the reason underlying inconsistencies between different studies. An adenocarcinoma is considered to be of cardia origin when the epicenter of the tumor is at the esophagogastric junction, or within 2 cm distally[19]. Strict clinicopathologic criteria have been used also to define primary esophageal adenocarcinomas[20]. A new classification for adenocarcinomas of the esophagogastric junction was proposed at a recent conference of the International Gastric Cancer Association (IGCA) and the International Society for Diseases of the Esophagus (ISDE). Adenocarcinomas of the cardia has been defined as tumors that have their centres within 5 cm of the anatomic esophagogastric junction. Three distinct tumor entities (Type I, II and III) have been proposed[21].

## RELAVANT PATHOLOGICAL CONDITIONS OF ADENOCARCINOMA OF THE GASRIC CARDIA

### *Barrett's esophagus*

Barrett's esophagus is the condition in which columnar epithelium replaces the squamous epithelium that normally lines the distal esophagus[22]. The endoscopic appearance is characteristic, with a salmon-pink color and velvety texture. This upward extension may be circumferential, or limited to finger-like projections, or even islands of columnar epithelium that only involve part of the distal esophageal wall[23]. In healthy individuals, the squamo-columnar junction (SCJ) does not always correspond with the anatomic EGJ. The juxtaposition of pale squamous epithelium and reddish columnar epithelium forms a visible line called the Z line, or the SCJ. The EGJ is the most proximate part of gastric folds. The Z line and gastroesophageal junction often coincide. When the Z line is located above the EGJ, there is a columnarly lined segment of esophagus. Barrett's esophagus is diagnosed endoscopically if columnar mucosa extending greater than 3 cm above the EGJ, or by histologic finding of intestinal metaplasia (specialized mucosa) existing at any level of the tubular esophagus[22].

The pathogenesis of Barrett's esophagus is still unclear. Most Barrett's esophagus develops from approximately 10 % of persons who have chronic gastroesophageal reflux[24]. In addition to gastroesophageal reflux diseases (GERD), Barrett's esophagus is associated with several other esophageal disorders, such as hiatal hernia[25], and occasionally familial groupings are reported[26-28].

The significance of Barrett's esophagus is its association with the development of esophageal malignancy[29,30]. Patients with Barrett's esophagus have (by conservative estimates) a 30- to 40-fold higher risk of developing esophageal adenocarcinoma than those without[23]. Since the diagnostic criteria for Barrett's esophagus now include the histological finding of intestinal metaplasia, a columnar-lined esophagus less than 3 cm in length is now recognized as short-segment Barrett's esophagus (SSBE), in contrast to the traditional long-segment Barrett's esophagus (LSBE)[31]. The risk of malignancy in SSBE still needs to be determined[32].

In China, Barrett's esophagus used to be regarded as a rare condition, and consequently has not been studied in detail. However, based on an endoscopic survey performed by our research group in the high-risk population in Linzhou, Barrett's esophagus was detected with a frequency of 0.7 % (3/402); not as rare as it was considered previously[33]. It has been identified that there is an apparent change of Z line upgrowth among symptom free subjects in the high-incidence area for esophageal cancer in Henan Province. Z line upgrowth is related with epithelial cell hyperproliferation both in gastric cardia and lower segment of esophagus. These results suggest that Z line upgrowth may be one of the characteristic changes, or precancerous lesions related with EGJ carcinogenesis in the high-risk population for GCA in Henan[11]. Further characterizing Barrett's Esophagus, Z line upgrowth, and esophageal and gastric reflux esophagitis in this population may provide new insights into understanding of cardia carcinogenesis[34].

### *Intestinal metaplasia*

Since the diagnostic criteria for Barrett's esophagus based on endoscopy are arbitrary, recent definitions of Barrett's esophagus have included the histologic finding of intestinal metaplasia, regardless of the length of the columnar-lined esophagus[35]. Histologically, three types of columnar epithelium have been observed in Barrett's esophagus: gastric fundic type, junctional type and specialized intestinal metaplasia (IM). Based on the mucin content of the columnar and goblet cells, intestinal metaplasia is histopathologically divided into three types: the complete form (Type I), in which the columnar cells are absorptive and contain neutral mucins, and the two incomplete forms, in which the columnar cells are partly secretory and contain acidic sialomucins (Type II) or sulphomucins (Type III)[36,37]. Type I is the predominant form of intestinal metaplasia found in the stomach, including both benign and malignant conditions. Type III is the least common form in the stomach, but the one most strongly associated with gastric cancer[38]. The incomplete form of intestinal metaplasia also termed specialized columnar epithelium (SCE), is the histological mark of Barrett's esophagus[39].

IM is also associated with GERD, and the frequency of IM is increased with the extention of columnar lining in the esophagus[40]. However, gastritis rather than GERD seems to be a risk factor of cardiac intestinal metaplasia[41]. While complete intestinal metaplasia is a manifestation of multifocal atrophic gastritis, the incomplete form may result from carditis and GERD[42].

It has been hypothesized that Barrett' s adenocarcinoma follows the metaplasia-dysplasia-adenocarcinoma sequence (MCS)[43]. Whether intestinal metaplasia is a premalignant lesion for adenocarcinoma of the gastric cardia is still not clear[44]. Several studies showed that dysplasia was infrequently observed in EGJ or gastric cardia with intestinal metaplasia[42, 44, 45]. These suggest that intestinal metaplasia at the EGJ or gastric cardia is not a high-risk precursor lesion for adenocarcinoma. However, progression from intestinal metaplasia at the EGJ or gastric cardia to dysplasia still requires further characterization[46].

Examination of the adjacent gastric cardia cancer tissue by our research group showed that IM was frequently observed in as high as 20 % of the specimens[47]. In contrast, only 0.7 % symptom-free subjects in Linzhou were identified with IM in gastric cardia biopsies[33]. Goblet cell was invariably identified on HE stained specimen. Half of the IM lesion was found to have dysplasia. These suggest that IM may be a precursor of gastric cardia adenocarcinoma in Henan, which is not consistent with that in Western countries. The reason is not clear. Standard histologic evaluation fails to reliably differentiate between IM in the esophagus and IM in native cardiac mucosa. Further characterization for subtypes of IM with biohistochemistry and immunohistochemistry will provide important evidence for elucidating the significance of IM in gastric cardia carcinogenesis.

### *Chronic carditis: H.pylori infection or gastroesophageal reflux disease*

IM in the distal stomach is usually a consequence of chronic inflammation, mainly caused by *H.pylori* infection[48], while the intestinal metaplasia of Barrett' s esophagus has been demonstrated to be associated with GERD[49]. Furthermore, recent studies suggested that gastric infection with *H.pylori* might protect the esophagus from developing of reflux esophagitis and Barrett' s esophagus[50-54]. It is reasonable to hypothesize that intestinal metaplasia at the gastric cardia may develop as a consequence of chronic inflammation due to either GERD or infection. Several recent studies have focused on the relative contribution of *H. pylori* infection and GERD to gastric carditis, however, results have been inconsistent, to date[55-58]. One possible reason may be related to the use of different histopathologic criteria for identification of the gastric cardia. A study of 33 consecutive autopsies in children showed that the length of cardiac epithelium ranged from 1 to 4 mm, with a mean extent of 1.8 mm[59]. Ormsby expanded the study to 223 adult autopsies, finding that the mean extent of cardiac epithelium in patients aged <18, 19-50, and >50 years was 1.7, 2.6, and 3.3 mm, respectively[60]. Such a narrow range makes accurate sampling extremely difficult. Therefore, biopsies from the gastric cardia may have two origins: esophagus or stomach.

## MOLECULAR BASIS FOR ADENOCARCINOMA OF GASTRIC CARDIA

The pathogenesis of carcinoma has been demonstrated to be a progressive, multi-step process, manifested as an uncontrolled cell cycle and abnormal proliferation. The molecular basis of human cancer has been investigated widely in the recent two decades, and has implicated deregulation of tumor suppressor genes, activation of oncogenes, and aberrant expression of growth factors. Different genetic alterations have been observed between the two different histologic sub-types of esophageal cancer. Meanwhile, molecular evidence is also accumulating to support the hypothesis that adenocarcinomas of the gastric cardia are distinct from adenocarcinomas of the esophagus and stomach.

### *Loss of heterozygosity (LOH)*

LOH has been demonstrated to play an important role in tumorigenesis, and to be frequently associated with the loss of tumor suppressor gene function. LOH was initially observed at several tumor suppressor gene loci (17p, 13q, 5q, 18q and 9p for p53, Rb, APC, MSH2, DCC and p16, E-cadherin, 19p, respectively) in human esophageal and gastric cancer[61-67]. At present, LOH has been used to localize putative tumor suppressor genes. LOH has also been reported at 1p, 3p, 4q, 9q, 11p and 17q in esophageal adenocarcinomas[68, 69]. Allelic loss of the tumor suppressor gene p73 on 1p is frequently observed in neuroblastoma[70,71], and hMLH-1, a mismatch repair gene associated with hereditary non-polyposis colorectal cancer, is located on 3q21[72]. The tylosis esophageal cancer (TOC) gene, initially reported in families with autosomal dominant tylosis families who developed esophageal cancer, has been located on chromosome 17q25. Allelic loss at this region has been implicated in both sporadic SCC and Barrett' s adenocarcinoma[73]. BCRA1, associated with susceptibility to breast and ovarian cancer, is located on 17q[74]. Using comparative genomic hybridization (CGH), deletion of a specific region at 14q31-32.1 occurred significantly more frequently in Barrett' s adenocarcinomas in the distal esophagus than in gastric cardia cancers, suggesting genetic divergence in this group of closely related cancers[75]. Allelotype analysis performed on 38 gastric cardia adenocarcinomas even differentiated this allelic imbalance between the intestinal-type and diffuse-type adenocarcinomas, and a higher frequency of allelic imbalance on chromosome 16q was detected in the diffuse-type adenocarcinomas[76].

### *Dysfunction of tumor suppressor genes*

**Tumor suppressor gene p53** P53 is located on chromosome 17p13, encoding a phosphoprotein with a molecular weight of 53kd. Abnormalities in p53 gene function cause uncontrolled cell cycles and abnormal cell proliferation. P53 mutations are the most frequent genetic alterations found in human cancers[77]. Over 90 percent of p53 mutations are observed in exons 5-8, which is the highly conserved region for DNA binding. Comparison of p53 mutations in premalignant (basal cell hypertrophy, BCH; dysplasia, DYS; carcinoma *in situ*, CIS) esophageal tissues matched with corresponding invasive SCC tumor tissues, showed similar p53 mutations in DYS, CIS and tumors[78]. Similar studies with Barrett' s adenocarcinoma showed that p53 mutations in Barrett' s epithelia (metaplasia, non-dysplastic) did not necessarily correspond to the matched adenocarcinoma[20]. The high coincident alterations for P53 in SCC and GCA from the same patient indicate the possibility of similar molecular mechanisms, which provides important molecular basis and etiological clue for similar geographic distribution and risk factors in SCC and GCA[79,80]. These results suggest that some p53 mutations may have a selective tumorigenic advantage during tumor progression. And some findings suggest p53, bcl-2 and caspase-3 may play an important role in the induction of apoptosis in AGS cells[81]. In the course of the formation of gastric carcinoma, proliferation of gastric mucosa can be greatly increased by *H.pylori* infection, which can strengthen the expression of mutated p53 gene[82]. Less aggressive mutations may increase the genetic instability of Barrett' s mucosa, promoting abnormal cellular proliferation, but as they are incapable of transformation independently, additional molecular or epigenetic events are required for tumorigenesis.

About 90 percent of p53 mutations are located within the DNA binding domain (exons 5 to 8). They may occur either at the binding surface or at the hydrophobic core, disrupting the structure for DNA binding. P53 mutations do not distribute in a random manner through the whole encoding region. Several

"hot spot" mutations have been located such as codon 175, 176, 245, 248, 249, 273 and 282 in all the human cancers[83], implying that there may be a general pathway for the pathogenesis of tumors with a high percentage of p53 mutations. However, mutation sites also appear to be organ specific and cell-dependent. In esophageal adenocarcinomas, p53 mutations occur most frequently at codon 175 (9 %), 248 (16 %) and 273 (16 %), which are also hot spot mutations for all human cancers recorded, while mutations at codon 248 and 273 are much less frequently observed, even though the mutation at codon 175 accounts for 8 % in SCC. Relatively high frequencies of p53 mutations at codons 193, 194, 195 and 270 are unique in comparison to other human cancers[77].

P53 mutations may result from endogenous processes or exogenous carcinogens[84], and the spectrum of mutations may be indicative of specific carcinogenic mechanisms. Mutation profiles of p53 also help to identify the DNA damage arising from environmental carcinogens. Approximately 31 % of p53 mutations occur at the A:T base pairs in the SCC, which are usually caused by exogenous carcinogenic compounds. But in esophageal adenocarcinoma, p53 mutations have a very high frequency of transition at the CpG dinucleotides. This alteration is thought to result from spontaneous deamination of 5-methylcytosine, suggesting a defective DNA mismatch repair[77, 85]. Differences in p53 mutation spectra between SCC and esophageal adenocarcinoma are consistent with the results of epidemiological studies, suggesting that SCC and esophageal adenocarcinoma have different etiology.

Adenocarcinomas of gastric cardia share similar epidemiological and histological features to esophageal adenocarcinomas in North America and some European countries. Gleeson *et al*[86] compared the p53 abnormalities in adenocarcinoma of the distal esophagus and gastric cardia, and reported that p53 mutations were detected in 70 % and 63 % of adenocarcinoma of esophagus and gastric cardia, respectively. 85 % of the p53 mutations in esophageal adenocarcinoma occurred as G:C→A:T transitions, with 69 % at the CpG dinucleotides. Similar p53 mutations were observed in adenocarcinoma of the gastric cardia, in which 82 % were base transitions with 55 % occurring at the CpG dinucleotides. One study from Linzhou based on the p53 gene mutation analysis identified 6 mutations among 14 adenocarcinomas of the gastric cardia, 3 of which were G to T transversions, a mutation that is rarely observed in Barrett' s adenocarcinoma[87]. Further investigation and comparison of mutation analysis of p53 gene between SCC and adenocarcinoma of the gastric cardia in this population are needed so to provide more insights into the etiology of both SCC and adenocarcinomas of esophagus and the gastric cardia.

**p53 gene family** Recently, discovery of p53 homologues such as p73 and p63 suggests a more complex pathway. p73 and p63, similar to p53, may result in transactivation, DNA binding and oligomerization domains[88], capable of activating the transcription of p53-responsive genes and inducing apoptosis[89-91]. p73 is located on chromosome 1p36, a region that is frequently deleted in neuroblastoma[73, 74], but unlike p53, p73 mutations have been detected infrequently in other types of tumor, including esophageal and gastric carcinoma[92-100]. Silencing of p73 gene due to hypermethylation at its promoter region was observed in a subset of lymphoblastic leukaemia and Burkett' s lymphoma[101, 102], but increased level of mRNA was more commonly observed in other tumors[95, 103-105]. p73 is characterized by loss of imprinting (LOI), resulting in monoallelic expression in normal tissues. It has been observed that p73 is overexpressed in several tumors, which is thought to be due to the switching from monoallellic to biallelic expression[93, 95]. Meanwhile, p73 isoforms, caused by alternative splicing, have been observed in rare types of brain tumors, suggesting tissue-specificity in the regulation of p73 gene transcription[106]. However, the precise function of p73 isoforms in tumor development is still unclear. Specific mutations of p73 or p63 causing amino acid substitutions are not identified. Neither p53, p73 nor p63 is related to prognosis. p73 and p63 have rarely been found to be mutated in gastric carcinomas, but both proteins are expressed in only a subset of tumors. The status of these p53 homologues is discordant among all patients with multiple simultaneous gastric carcinomas. The increased expression of p63 (TAp63 and black triangleNp63) in less well-differentiated gastric carcinomas may indicate that p63 can act to promote neoplastic growth in the gastric epithelium[107]. In 15 SCC samples from Henan, no p73 mutations were found in exons 4-7, but a high frequency of LOI and LOH was observed in these samples. The SCC samples with p53 defects were significantly correlated with those, which had elevated expression of p73. These results suggest that increased expression of p73, including that by LOI, could be a partial compensatory mechanism for defective p53[100].

The p63 gene also encodes multiple isoforms through alternative splicing with different abilities to transactivate p53-responsive genes. However, p63 is more closely related to p73 than to p53, and p63 mutations have been rarely observed in human tumors[108, 109]. The predominant isoform of p63, lacking in an acidic N-terminus corresponding to the transactivation domain of p53, has been detected in many kinds of epithelial tissue. This truncated protein may act as a dominant-negative agents toward transactivation by p53[110]. Up to date, p63 has not been studied in esophageal adenocarcinoma or adenocarcinomas of the cardia.

**Rb gene** One study compared LOH with the expression of Rb gene in SCC, finding that 90 % of the tumor samples containing LOH showed low or no Rb expression, while only 20 % of those without LOH had altered expression of Rb, suggesting LOH is the principal molecular alteration of Rb in SCC[111]. Recent studies of SCC cell lines demonstrated that the hypophosphorylated Rb protein was also associated with G2 arrest[112]. Besides inhibition of the cell cycle progression, Rb protein appears to have other distinct mechanisms to suppress cellular proliferation[113]. In the gastric carcinogenesis, *H pylori* might cause severe imbalance of proliferation and apoptosis in the precancerous lesions (IMIII and DysIII) first, leading to p53-Rb tumor-suppressor system mutation and telomerase reactivation, and finally causing gastric cancer[114]. Wang *et al*[115] suggested the alteration of Rb protein might play a role in the early stages of gastric cardia carcinogenesis.

**p16INK4a, p15INK4b and p14ARF** LOH of p16INK4a has been detected with high frequencies in both SCC (65 %) and esophageal adenocarcinoma (69 %)[116]. Several studies have demonstrated that hypermethylation of the promoter region of p16INK4a is the main mechanism causing gene silencing rather than point mutation, which rarely occurrs in esophageal carcinomas[116-119]. Distinct from p16INK4a, p15INK4b, which inhibits the cell growth in response to extracellular stimuli such as TGF-β[120], is more frequently deleted, at a frequency of 40 %[118]. Though p16INK4a regulates cell cycle through inhibiting the phosphorylation of Rb protein, p14ARF is closely associated with p53 by attenuating mdm2-mediated degradation of p53[121,122]. Similar to p15INK4b, p14ARF is also deleted frequently in SCC, losing its function to protect p53 from ubiqitin-dependent degradation[123].

**Abnormalities of oncogenes** Point mutation, amplification, rearrangement and overexpression are the most frequent mechanisms for oncogene activation. Amplification of cyclinD1, HER-2/neu(c-erbB2), c-myc, c-ras, Int-2/hst-1 and c-erbB (EGFR) has been observed in gastric and esophageal carcinomas[124-130]. The amplification of c-erbB2 was followed

by overexpression in the same gastric adenocarcinoma tissue[125,129]. No amplification of c-erbB2 was detected in SCC. Amplification of oncogenes that encode growth factor receptors is more commonly found in adenocarcinomas. Int-2 and hst-1, encoding FGF-3 and FGR-4 respectively, are located at chromosome 11q13 with the oncogene cyclinD1. Coamplification of int-2 and hst-1 was observed at a frequency of 28-47 % in primary esophageal carcinomas and much higher in metastatic tumors, suggesting an association with tumor progression and distal metastasis[131, 132]. CyclinD1, a cell cycle protein, facilitates cell cycle progression from G1 to S phase through combining with CDK4. Both the amplification and overexpression of cyclinD1 were detected in esophageal carcinomas[133, 134]. Abnormal expression of cyclin E and p27 may be one of the important molecular changes in the early stage of esophageal carcinogenesis, and the high-expression of cyclin E and low-expression of p27 may be one of the mechanisms driving the mild lesion towards carcinogenesis[135]. In contrast to other gastrointestinal tumors, the ras oncogene is rarely mutated in human esophageal adenocarcinoma[127]. However, overexpression of ras and ras-regulated genes (osteopontin, cathepsin L) has been reported in 58 % of primary esophageal adenocarcinomas[136].

## DIFFERENCES BETWEEN ADENOCARCINOMAS OF LOWER ESOPHAGUS, GASTRIC CARDIA AND SUBCARDIAC STOMACH

Though adenocarcinomas of the lower esophagus and gastric cardia share similar epidemiological characteristics, new clinicopathologic classifications have established criteria to differentiate these two entities. Taniere[137] compared molecular markers in esophageal adenocarcinomas with those in adenocarcinomas of the gastric cardia. The male to female ratio and p53 mutation frequency were higher in esophageal adenocarcinomas, while mdm2 amplification was more frequent in the adenocarcinomas of the gastric cardia. Patterns of cytokeratin immunostaining were also different between these two tumors. Flejou[138] performed a study to compare p53 protein expression immunohistochemically between esophageal and gastric carcinomas, and reported a higher prevalence of p53 protein overexpression was found in esophageal and cardiac adenocarcinomas compared with gastric antral adenocarcinoma. This was confirmed by an additional study, which reported p53 mutation rates in adenocarcinomas of distal stomach were significantly lower than those in adenocarcinomas of esophagus and gastric cardia[139]. These results suggest that adenocarcinoma of the gastric cardia may be a distinct entity from adenocarcinoma of the distal stomach.

### *Comparison between gastric cardia adenocarcinoma and esophageal squamous cell carcinoma, with special reference to Linzhou*

Because of the highly concurrent incidence of gastric cardia adenocarcinoma and esophageal squamous cell carcinoma in Linzhou[140], it is highly desirable to characterize the molecular differences between these tumors of different histological types to explore the possible clues related with etiological risk factors. However, useful information concerning this topic is very limited. In Linzhou, it is not uncommon clinically to identify patients with both gastric cardia adenocarcinoma and esophageal squamous cell carcinoma[141], which is the most common pattern of multiple primary malignant neoplasm (MPN) with an incidence of 0.4-2.5 %[142]. Recent studies from Wang's laboratory showed that there was a highly consistent positive immunostaining rate for p53 in SCC and GCA from the same patient (60 %, 12/25 *vs* 40 %, 10/25)[79] similar results were observed for PCNA. p53 mutation analysis in patients with either SCC or GCA from Linzhou indicated that G:C to A:T transition was the most frequent mutation pattern both in SCC and GCA. The consistency of P53 gene mutation was as high as 64 %[143]. G to A mutation pattern may be resulted from DNA methylation induced by nitrosamine[141]. These results are of important value in explaining the similar geographic distribution of SCC and GCA in this area. Protein file analysis also showed similar expression pattern in SCC and GCA, such as PTEN[144], c-erbB-2 and c-myc[145], MUC1[146], CYP1A1 and 2E1[147], MUC3[148], mEH[149], GSTM1, GSTT1 and GSTP[150], EGFR[151], etc from the samples in Linzhou.

## CONCLUSION

In summary, the incidence of adenocarcinomas arising from the distal esophagus, EGJ and gastric cardia is increasing at a dramatic rate in North America and Europe. It is suggested that adenocarcinomas of the esophagus develop in a metaplasia-dysplasia-carcinoma sequence. Whether adenocarcinomas of the gastric cardia follow the same pattern needs further study. Although both esophageal squamous cell carcinomas and adenocarcinomas of the gastric cardia have a high incidence in the same high-risk population in Linzhou, little information is available on the molecular and etiological differences between these two tumor types. Metaplasia is a frequent finding in the gastric cardia, but its significance in the development of adenocarcinoma of the gastric cardia is not clear. *H.pylori* infection, a main factor causing atrophy of the mucosa of distal stomach, also leads to chronic inflammation of the gastric cardia. Though *H.pylori* has been classified as a Type I carcinogen, the role it plays in gastric cardia carcinogenesis remains unclear. To study adenocarcinoma of the gastric cardia in China, researchers are beginning to evaluate epidemiological, histopathologic and molecular characteristics of the tumor.

## ACKNOWLEDGEMENTS

We acknowledge the help given by graduate students in Laboratory for Cancer Research, College of Medicine, Zhengzhou University (Drs. Dao-Cun Wang, Ning-Bo Wang, Hui-Xing Yi, Xin-Wei He, She-Gan Gao, Xin-Na Yi, Zhi-Wei Chang, Dong-Ling Xie, Ran Wang, Ya-Nan Jiang, Xiao-Dong Lü, Xiao-Li Liu) in preparation of the manuscript.

## REFERENCES

1 **Hermanek P**, Sobin LH. TNM classification of malignant tumors. International Union Against Cancer (UICC). 4th ed. 2nd revision. *Berlin: Springer* 1992; page: 455-460
2 **Beahrs OH**, Henson DE, Hutter RVP, Kennedy BJ, eds. American Joint Committee on Cancer: Manual for Staging of Cancer. 4th ed. *Philadelphia, Pennsylvania: JB Lippincott* 1992; page: 175-200
3 **Powell J**, McConkey CC. Increasing incidence of adenocarcinoma of the gastric cardia and adjacent sites. *Br J Cancer* 1990; **62**: 440-443
4 **Blot WJ**, Devesa SS, Kneller RW, Fraumeni F. Rising incidence of adenocarcinoma of the esophagus and gastric cardia. *JAMA* 1991; **265**: 1287-1289
5 **Blot WJ**, Devesa SS, Fraumeni JF. Continuing climb in rates of esophageal adenocarcinoma: An update. *JAMA* 1993; **270**: 1320-1322
6 **Pera M**, Cameron AJ, Trastek VF, Carpenter HA, Zinsmeister AR. Increasing incidence of adenocarcinoma of the esophagus and esophogastric junction. *Gastroenterology* 1993; **104**: 510-513
7 **Spechler SJ**, Robbins AH, Bloomfield RH, Vincent ME, Heeren T, Doos WG, Colton T, Shimmel EM. Adenocarcinoma and Barrett's esophagus: an overrated risk? *Gastroenterology* 1984; **87**: 927-933
8 **Cameron AJ**, Ott BJ, Payne WS. The incidence of adenocarcinoma in columnar-lined (Barrett's ) esophagus. *N Engl J Med* 1985; **313**: 857-859

9 **Wang HH**, Antonioli DA, Goldman H. Comparative features of esophageal and gastric adenocarcinomas: recent changes in type and frequency. *Hum Pathol* 1986; **17**: 482-487

10 **Vaughan TL**, Davis S, Kristal A, Thomas DB. Obesity, alcohol, and tobacco as risk factors for cancers of the esophagus and gastric cardia: adenocarcinoma versus squamous cell carcinoma. *Cancer Epidemiol Biomarkers Prev* 1995; **2**: 85-92

11 **Zhang ZF**, Kurtz RC, Sun M, Karpeh MJ, Yu GP, Gargon N, Fein JS, Georgopoulos SK, Harlap S. Adenocarcinomas of the esophagus and gastric cardia: medical conditions, tobacco, alcohol, and socio-economic factors. *Cancer Epidemiol Biomarkers Prev* 1996; **1**: 761-768

12 **Gammon MD**, Schoenberg JB, Ahsan H, Risch HA, Vaughan TL, Chow WH, Rotterdam H, West AB, Dubrow R, Stanford JL, Mayne ST, Farrow DC, Niwa S, Blot WJ, Fraumeni JF Jr. Tobacco, alcohol, and socioeconomic status and adenocarcinomas of the esophagus and gastric cardia. *J Natl Cancer Inst* 1997; **89**: 1277-1284

13 **Wang LD**, Gao WJ, Yang WC, Li XF, Li J, Zou JX, Wang DC, Guo RX. Preliminary analysis of the statistics on 3,933 cases with esophageal cancer and gastric cardia cancer from the subjects in People's Hospital of Linzhou in 9 years. *Henan Yike Daxue Xuebao* 1997; **32**: 9-11

14 **Li JY**, Ershow AG, Chen ZJ, Wacholder S, Li GY, Guo W, Li B, Blot WJ. A case-control study of cancer of the esophagus and gastric cardia in Linzhou. *Int J Cancer* 1989; **43**: 755-761

15 **Yang CS**. Research on esophageal cancer in China: a review. *Cancer Res* 1980; **40**: 2633-2644

16 **Lu SH**, Chui SX, Yang WX, Hu XN, Guo LP, Li FM. Relevance of N-nitrosamines to esophageal cancer in China. *IARC Sci Pub* 1991; **105**: 11-17

17 **Yu Y**, Taylor PR, Li JY, Dawsey SM, Wang GQ, Guo WD, Wang W, Liu BQ, Blot WJ, Shen Q. Retrospective cohort study of risk-factors for esophageal cancer in Linzhou, People's Republic of China. *Cancer Causes Control* 1993; **4**: 195-202

18 **Guo W**, Blot WJ, Li JY, Taylor PR, Liu BQ, Wang W, Wu YP, Zheng W, Dawsey SM, Li B. A nested case-control study of oesophageal and stomach cancers in the Linzhou nutrition intervention trial. *Int J Epidemiol* 1994; **23**: 444-450

19 **Wijnhoven BP,** Siersema PD, Hop WC, van Dekken H, Tilanus HW. Adenocarcinomas of the distal oesophagus and gastric cardia are one clinical entity. Rotterdam Esophageal Tumour Study Group. *Br J Surg* 1999; **86**: 529-535

20 **Casson AG**, Muknopadhyay T, Cleary KR, Ro JY, Levin B, Roth JA. P53 gene mutations in Barrett's epithelium and esophageal cancer. *Cancer Res* 1991; **51**: 4495-4499

21 **Siewert JR**, Stein HJ. Classification of adenocarcinoma of the oesophogastric junction. *Br J Sur* 1998; **85**: 1457-1459

22 **Spechler SJ**. Barrett's esophagus and esophageal adenocarcinoma: pathogenesis, diagnosis, and therapy. *Med Clin North Am* 2002; **86**: 1423-1445

23 **Spechler SJ**, Goyal RK. Barrett's esophagus. *N Engl J Med* 1986; **315**: 362-371

24 **Vaughan TL**, Kristal AR, Blount PL, Levine DS, Galipeau PC, Prevo LJ, Sanchez CA, Rabinovitch PS, Reid BJ. Nonsteroidal anti-inflammatory drug use, body mass index, and anthropometry in relation to genetic and flow cytometric abnormalities in Barrett's esophagus. *Cancer Epidemiol Biomarkers Prev* 2002; **11**: 745-752

25 **Spechler SJ**. Clinical practice. Barrett's Esophagus. *N Engl J Med* 2002; **346**: 836-842

26 **Everhart CWJ**, Holzapple PG, Humphries TJ. Barrett's esophagus: inherited epithelium or inherited reflux? *J Clin Gastroenterol* 1983; **5**: 357-358

27 **Crabb DW**, Berk MA, Hall TR, Conneally PM, Biegel AA, Lehman GA. Familial gastroesophageal reflux and development of Barrett's esophagus. *Ann Intern Med* 1985; **103**: 52-54

28 **Smith RRL**, Hamilton SR, Boitnott JK, Rogers EL. The spectrum of carcinoma arising in Barrett's esophagus: a clinicopathologic study of 26 patients. *Am J Surg Pathol* 1984; **8**: 563-557

29 **Bonelli L**. Barrett's esophagus: results of a multicentric survey. *Endoscopy* 1993; **25**: 652-654

30 **Reid BJ**, Sanchez CA, Blount PL, Levine DS. Barrett's esophagus: cell cycle abnormalities in advancing stages of neoplastic progression. *Gastroenterology* 1993; **105**: 119-129

31 **Weston AP**, Krmpotich P, Makdisi WF, Cheriam R, Dixon A, McGregor DH, Banerjee SK. Short segment Barrett's esophagus: clinical and histological features, associated endoscopic findings, and association with gastric intestinal metaplasia. *Am J Gastroenterol* 1996; **91**: 981-986

32 **Hamilton SR**, Smith RR, Cameron JL. Prevalence and characteristics of Barrett's esophagus in patients with adenocarcinoma of the esophagus or esophagogastric junction. *Hum Pathol* 1988; **19**: 942-948

33 **Wang LD**, Feng CW, Zhou Q. Analysis of the screening result of esophageal disease in high risk urban and rural areas of esophageal carcinoma. *Henan Yike Daxue Xuebao* 1997; **32**: 6-8

34 **Wang LD**, Zheng S, Fan ZM, Liu B, Feng CW, Sun C, Gao SG, Zhang YR, Guo HQ, Li JL, Jiao XY. Changes of Z-line at the gastroesophageal junction in symptom-free subjects from high-incidence area for esophageal cancer in Henan. *Zhengzhou Daxue Xuebao Yixueban* 2002; **37**: 733-736

35 **Gottfried MR**, McClave SA, Boyce HW. Incomplete intestinal metaplasia in the diagnosis of columnar lined esophagus (Barrett's esophagus). *Am J Clin Pathol* 1989; **92**: 741-746

36 **Jass JR**. Role of intestinal metaplasia in the histogenesis of gastric carcinoma. *J Clin Pathol* 1980; **33**: 801-810

37 **Filipe MI**, Potet F, Bogomoletz WV, Dawson PA, Fabiani B, Chauveinc P, Fenzy A, Gazzard B, Goldfain D, Zeegen R. Incomplete sulphomucin-secreting intestinal metaplasia for gastric cancer. Preliminary data from a prospective study from three centers. *Gut* 1985; **26**: 1319-1326

38 **Spechler SJ**. The role of gastric carditis in metaplasia and neoplasia at the gastroesophageal junction. *Gastroenterology* 1999; **117**: 218-228

39 **Haggitt RC**. Barrett's esophagus, dysplasia, and adenocarcinoma. *Hum Pathol* 1994; **25**: 982-993

40 **Gulizia JM,** Wang H, Antonioli D, Spechler SJ, Zeroogian J, Goyal R, Shahsafaei A, Chen YY, Odze RD. Proliferative characteristics of intestinalized mucosa in the distal esophagus and gastroesophageal junction (short-segment Barrett's esophagus): a case control study. *Hum Pathol* 1999; **30**: 412-418

41 **El-Serag HB**, Sonnenberg A, Jamal MM, Kunkel D, Crooks L, Feddersen RM. Characteristics of intestinal metaplasia in the gastric cardia. *Am J Gastroenterol* 1999; **94**: 622-627

42 **Voutilaien M**, Farkkila M, Juhola M, Mecklin JP, Sipponen P. The Central Finland Endoscopy Study Group. Complete and incomplete intestinal metaplasia at the esophagogastric junction: prevalences and associations with endoscopic erosive esophagitis and gastritis. *Gut* 1999; **45**: 644-648

43 **Prach AT**, MacDonald TA, Hopwood DA, Johnston DA. Increasing incidence of Barrett's esophagus: education, enthusiasm or epidemiology? *Lancet* 1997; **350**: 933

44 **Morales TG**, Bhattacharyya A, Johnson C, Sampliner R. Is Barrett's esophagus associated with intestinal metaplasia of the gastric cardia? *Am J Gastroenterol* 1997; **92**: 1818-1822

45 **Morales TG**, Sampliner RE, Bhattacharyya A. Intestinal metaplasia of the gastric cardia. *Am J Gastroenterol* 1997; **92**: 414-418

46 **van Sandick JW**, van Lanschot JB, van Felius L, Haringsma J, Tytgat GN, Dekker W, Drillenburg P, Offerhaus GJ, ten Kate FJ. Intestinal metaplasia of the esophagus or esophagogastric junction: Evidence of distinct clinical, pathologic ,and histochemical staining features. *Am Soci Clini Pathol* 2002; **117**: 117-125

47 **Chen H**, Wang LD, Fan ZM, Gao SG, Guo HQ, Guo M. The comparison study of the three histochemical staining methods in gastric cardia intestinal metaplasia staining. *Henan Yixue Yanjiu* 2003; **12**: 10-13

48 **Asaka M**, Takeda H, Sugiyama T, Kato M. What role does *Helicobacter pylori* play in gastric cancer? *Gastroenterology* 1997; **113**: 556-560

49 **Spechler SJ**. Barrett's esophagus. *Semin Oncol* 1994; **21**: 431-437

50 **Oberg S**, Peters JH, DeMeester TR, Chandrasoma P, Hagen JA, Ireland AP, Ritter MP, Mason RJ, Crookes P, Bremner CG. Inflammation and specialized intestinal metaplasia of cardiac mucosa is a manifestation of gastroesophageal reflux disease. *Ann Surg* 1997; **226**: 522-532

51 **Csendes A**, Smok G, Burdiles P, Sagastume H, Rojas J, Puente G, Quezada F, Korn O. "Carditis": an objective histological marker for pathologic gastroesophageal reflux disease. *Dis Esophagus*

1998; **11**: 101-105
52 **Goldblum JR**, Vicari JJ, Falk GW, Rice TW, Peek RM, Easley K, Richter JE. Inflammation and intestinal metaplasia of the gastric cardia: the role of gastroesophageal reflux and *H.pylori* infection. *Gastroenterology* 1998; **114**: 633-639
53 **Chen YY,** Antonioli DA, Spechler SJ, Zeroogian JM, Goyal RK, Wang HH. Gastroesophageal reflux disease versus *Helicobacter pylori* infection as the cause of gastric carditis. *Mod Pathol* 1998; **11**: 950-956
54 **Zhang YR**, Gao SS, Liu G, An JY, Li JL, Jiao XY, Wang LD. Comparison of *Helicobacter pylori* (HP) infection in the cardia and *pylori* parts of the stomach from symptom-free subjects at high-incidence area for esophageal and gastric cardia cancer in Henan. *Zhengzhou Daxue Xuebao Yixueban* 2002; **37**: 777-779
55 **Loffeld RJ,** van der Hulst RW. *Helicobacter pylori* and gastro-oesophageal reflux disease: association and clinical implications. To treat or not to treat with anti-*H. pylori* therapy? *Scand J Gastroenterol Suppl* 2002; **236**: 15-18
56 **Labenz J**, Blum AL, Bayerdorffer E, Meining A, Stolte M, Borsch G. Curing *Helicobacter pylori* infection in patients with duodenal ulcer may provoke reflux esophagitis. *Gastroenterology* 1997; **112**: 1442-1447
57 **Chow WH**, Blaser MJ, Blot WJ, Gammon MD, Vaughan TL, Risch HA, Perez-Perez GI, Schoenberg JB, Stanford JL, Rotterdam H, West AB, Fraumeni JFJ. An inverse relation between cagA+ strains of *Helicobacter pylori* infection and risk of esophageal and gastric cardia adenocarcinoma. *Cancer Res* 1998; **58**: 588-590
58 **Vicari JJ**, Peek RM, Falk GW, Goldblum JR, Easley KA, Schnell J, Perez-Perez GI, Halter SA, Rico TW, Blaser MJ, Richter JE. The seroprevalence of CagA-positive *Helicobacter pylori* strains in the spectrum of gastroesophageal reflux disease. *Gastroenterology* 1998; **115**: 50-57
59 **Ormsby AH,** Kilgore SP, Goldblum JR, Richter JE, Rice TW, Gramlich TL. The location and frequency of intestinal metaplasia at the esophagogastric junction in 223 consecutive autopsies: implications for patient treatment and preventive strategies in Barrett's esophagus. *Mod Pathol* 2000; **13**: 614-620
60 **Ormsby AH,** Goldblum JR, Rice TW, Richter JE, Falk GW, Vaezi MF, Gramlich TL. Cytokeratin subsets can reliably distinguish Barrett's esophagus from intestinal metaplasia of the stomach. *Hum Pathol* 1999; **30**: 288-294
61 **El-Rifai W**, Powell SM. Molecular biology of gastric cancer. *Semin Radiat Oncol* 2002; **12**: 128-140
62 **Zhang QX**, Ding Y, Le XP, Du P. Studies on microsatellite instability in p16 gene and expression of hMSH2 mRNA in human gastric cancer tissues. *World J Gastroenterol* 2003; **9**: 437-441
63 **Chae KS**, Ryu BK, Lee MG, Byun DS, Chi SG. Expression and mutation analyses of MKK4, a candidate tumor suppressor gene encoded by chromosome 17p, in human gastric adenocarcinoma. *Eur J Cancer* 2002; **38**: 2048-2057
64 **Rees BP**, Caspers E, Hausen A, den Brule A, Drillenburg P, Weterman MA, Offerhaus GJ. Different pattern of allelic loss in Epstein-Barr virus-positive gastric cancer with emphasis on the p53 tumor suppressor pathway. *Am J Pathol* 2002; **161**: 1207-1213
65 **Chang YT**, Wu MS, Chang CJ, Huang PH, Hsu SM, Lin JT. Preferential loss of Fhit expression in signet-ring cell and Krukenberg subtypes of gastric cancer. *Lab Invest* 2002; **82**: 1201-1208
66 **Becker KF**, Kremmer E, Eulitz M, Schulz S, Mages J, Handschuh G, Wheelock MJ, Cleton-Jansen AM, Hofler H, Becker I. Functional allelic loss detected at the protein level in archival human tumors using allele-specific E-cadherin monoclonal antibodies. *J Pathol* 2002; **197**: 567-574
67 **Wang Q,** Chen H, Bai J, Wang B, Wang K, Gao H, Wang Z, Wang S, Zhang Q, Fu S. Analysis of loss of heterozygosity on 19p in primary gastric cancer. *Zhonghua Yixue Yichuanxue Zazhi* 2001; **18**: 459-461
68 **Hammoud ZT**, Kaleem Z, Cooper JD, Sundaresan RS, Patterson GA, Goodfellow PJ. Allelotype analysis of esophageal adenocarcinomas: evidence for the involvement of sequences on the long arm of chromosome 4. *Cancer Res* 1996; **56**: 4499-4502
69 **Dolan K**, Garde J, Gosney J, Sissons M, Wright T, Kingsnorth AN, Walker SJ, Sutton R, Meltzer SJ, Field JK. Allelotype analysis of oesophageal adenocarcinoma: loss of heterozygosity occurs at multiple sites. *Br J Cancer* 1998; **78**: 950-957
70 **Kaghad M**, Bonnet H, Yang A, Creancier L, Biscan JC, Valent A, Minty A, Chalon P, Lelias JM, Dumont X, Ferrara P, McKeon F, Caput D. Monoallelically expressed gene related to p53 at 1p36, a region frequently deleted in neuroblastoma and other human cancers. *Cell* 1997; **90**: 809-819
71 **White PS**, Maris JM, Beltinger C, Sulman E, Marshall HN, Fujimori M, Kaufman BA, Biegel JA, AllenC, Hilliard C, Valentine MB, Lod AT, Enomoto H, Skiyama S, Brodeur GM. A region consistent deletion in neuroblastoma maps within human chromosome 1p36.2-36.3. *Proc Natl Acad Sci USA* 1995; **92**: 5520-5524
72 **Papadopoulos N**, Nicolaides NC, Wei YF, Ruben SM, Carter KC, Rosen CA, Haseltine WA, Fleischmann RD, Fraser CM, Adams MD. Mutation of a mutl homolog in hereditary colon cancer. *Science* 1994; **262**: 1625-1629
73 **Risk JM**, Mills HS, Garde J, Dunn JR, Evans KE, Hollstein M, Field JK. The tylosis esophageal cancer (TOC) locus: more than just a familial cancer gene. *Dis Esophagus* 1999; **12**: 173-176
74 **Mori T**, Aoki T, Matsubara T, Iida F, Du X, Nishihira T, Mori S, Nakamura Y. Frequent loss of heterozygosity in the region including BRCA1 on chromosome 17q in squamous cell carcinomas of the esophagus. *Cancer Res* 1994; **54**: 1638-1640
75 **van Dekken H**, Geelen E, Dinjens WN, Wijnhoven BP, Tilanus HW, Tanke HJ, Rosenberg C. Comparative genomic hybridization of cancer of the gastroesophageal junction: deletion of 14Q31-32.1 discriminates between esophageal (Barrett's) and gastric cardia adenocarcinomas. *Cancer Res* 1999; **59**: 748-752
76 **Gleeson CM**, Sloan JM, McGuigan JA, Ritchie AJ, Weber JL, Russel SEH. Allelotype analysis of adenocarcinoma of the gastric cardia. *Br J Cancer* 1997; **76**: 1455-1465
77 **Hollstein M**, Shormer B, Greenblatt M, Soussi T, Hovig E, Montesano R, Harris CC. Somatic point mutations in the p53 gene of human tumors and cell lines: update compilation. *Nucleic Acids Res* 1996; **24**: 141-146
78 **Shi ST**, Yang GY, Wang LD, Xue Z, Feng B, Ding W, Xing EP, Yang CS. Role of p53 gene mutations in human esophageal carcinogenesis: results from immunohistochemical and mutation analysis of carcinomas and nearby non-cancerous lesions. *Carcinogenesis* 1999; **20**: 591-597
79 **Chen H**, Wang LD, Guo M, Gao SG, Guo HQ, Fan ZM, Li JL. Alterations of p53 and PCNA in cancer and adjacent tissues from concurrent carcinomas of the esophagus and gastric cardia in the same patient in Linzhou, a high incidence area for esophageal cancer in northern China. *World J Gastroenterol* 2003; **9**: 16-21
80 **Feng CW**, Wang LD, Jiao LH, Liu B, Zheng S, Xie XJ. Expression of p53, inducible nitric oxide syntheses and vascular endothelial growth factor in gastric precancerous and cancerous lesions: Correlation with clinical features. *BMC Cancer* 2002; **2**: 1-7
81 **Li HL**, Chen DD, Li XH, Zhang HW, Lu YQ, Ye CL, Ren XD. Changes of NF-kB, p53, Bcl-2 and caspase in apoptosis induced by JTE-522 in human gastric adenocarcinoma cell line AGS cells: role of reactive oxygen species. *World J Gastroenterol* 2002; **8**: 431-435
82 **Zhang Z**, Yuan Y, Gao H, Dong M, Wang L, Gong YH. Apoptosis, proliferation and p53 gene expression of *H. pylori* associated gastric epithelial lesions. *World J Gastroenterol* 2001; **7**: 79-82
83 **Wang LD**, Liu B, Zheng S. Analysis of p53 mutational spectra of esophageal squamous cell carcinomas from Linzhou: comparison with esophageal and other cancers from other areas. *Zhonghua Liuxing Bingxue Zazhi* 2003; **24**: 202-205
84 **Greenblatt MS**, Bennett WP, Hollstein M, Harris CC. Mutations in the p3 tumor suppressor gene: clues to cancer etiology and molecular pathogenesis. *Cancer Res* 1994; **54**: 4855-4878
85 **Montesano R**, Hollstein M, Hainaut P. Genetic alterations in esophageal cancer and their relevance to etiology and pathogenesis: a review. *Int J Cancer* 1996; **69**: 225-235
86 **Gleeson CM**, Sloan JM, McManus DT, Maxwell P, Arthur K, McGuigan JA, Ritchie AJ, Russell SEH. Comparison of p53 and DNA content abnormalities in adenocarcinoma of the esophagus and gastric cardia. *Br J Cancer* 1998; **77**: 277-286
87 **Liang YY**, Esteve A, Martel-Planche G, Takahashi S, Lu SH, Montesano R, Hollstein M. p53 mutations in esophageal tumors from high-incidence areas of China. *Int J Cancer* 1995; **61**: 611-614
88 **Arrowsmith CH**. Structure and function in the p53 family. *Cell*

*Death Differ* 1999; **6**: 1169-1173
89 **Kaelin WGJ**. The emerging p53 gene family. *J Natl Cancer Inst* 1999; **91**: 594-598
90 **Sheikh MS**, Fornace AJ Jr. Role of p53 family members in apoptosis. *J Cell Physiol* 2000; **182**: 171-181
91 **Benard J**, Douc-Rasy S, Ahomadegbe JC. TP53 family members and human cancers. *Hum Mut* 2003; **21**: 182-191
92 **Takahashi H**, Ichiniya S, Nimura Y, Watanabe M, Furusato M, Wakui S, Yatani R, Aizawa S, Nakagawara A. Mutation, allelotyping and transcription analyses of the p73 gene in prostatic carcinoma. *Cancer Res* 1998; **58**: 2076-2077
93 **Mai M**, Yokomizo A, Qian C, Yang P, Tindall DJ, Smith DI, Liu W. Activation of p73 silent allele in lung cancer. *Cancer Res* 1998; **58**: 2347-2349
94 **Tsao H**, Zhang X, Majewski P, Haluska FG. Mutational and expression analysis of the p73 gene in melanoma cell lines. *Cancer Res* 1999; **59**: 172-174
95 **Chi SG**, Chang SG, Lee SJ, Lee CH, Kim JI, Park JH. Elevated and biallelic expression of p73 is associated with progression of human bladder cancer. *Cancer Res* 1999; **59**: 2791-2793
96 **Yoshikawa H**, Nagashima M, Knan MA, Mcmenamin MG, Hagiwara K, Harris CC. Mutational analysis of p73 and p53 in human cancer cell lines. *Oncogene* 1999; **18**: 3415-3421
97 **Yokozaki H**, Shitara Y, Fujimoto J, Hiyama T, Yasui W, Tahara E. Alterations of p73 preferentially occur in gastric adenocarcinoms with foveolar epithelial phenotype. *Int J Cancer* 1999; **83**: 192-196
98 **Mihara M**, Nimura Y, Ichimiya S, Sakiyama S, Kajikawa S, Adachi W, Amano J, Nakagawara A. Absence of mutation of the p73 gene localized at chromosome 1p36.3 in hepatocellular carcinoma. *Br J Cancer* 1999; **79**: 164-167
99 **Nimura Y**, Mihara M, Ichimiya S, Sakiyama S, Seki N, Ohira M, Nomura N, Fujimori M, Adachi W, Amano J, He M, Ping YM, Nakagawara A. p73, a gene related to p53, is not mutated in esophageal carcinomas. *Int J Cancer* 1998; **78**: 437-440
100 **Cai YC**, Yang GY, Nie Y, Wang LD, Zhao X, Song Y, Seril D N, Liao J, Xing EP, Yang CS. Molecular alteration of p73 in human esophageal squamous cell carcinomas: loss of heterozygosity occurs frequently; loss of imprinting and elevation of p73 expression may be related to defective p53. *Carcinogenesis* 2000; **21**: 683-689
101 **Kawano S**, Miller CW, Gombart AF, Bartram CR, Matsuo Y, Asou H, Sakashita A, Said J, Tatsumi E, Koeffler HP. Loss of p73 gene expression in leukemias/lymphomas due to hypermethylation. *Blood* 1999; **94**: 1113-1120
102 **Corn PG**, Kuerbitz SJ, van Noesel MM, Esteller M, Compitello N, Baylin SB, Herman JG. Transcriptional silencing of the p73 gene in acute lymphoblastic leukemia and Burkett's lymphoma is associated with 5' CpG island methylation. *Cancer Res* 1999; **59**: 3352-3356
103 **Zaika AI**, Kovalev S, Marchenko ND, Moll UM. Overexpression of the wild type p73 gene in breast cancer tissues and cell lines. *Cancer Res.* 1999; **59**: 3257-3263
104 **Tokuchi Y**, Hashimoto T, Kobayashi Y, Hayashi M, Nishida K, Hayashi S, Imai K, Nakachi K, Ishikawa Y, Nakagawa K, Kawakami Y, Tsuchiya E. The expression of p73 is increased in lung cancer, independent of p53 gene alteration. *Br J Cancer* 1999; **80**: 1623-1629
105 **Yokomizo A**, Mai M, Tindall DJ, Cheng L, Bostwick DG, Naito S, Smith DI, Liu W. Overexpression of the wild type p73 gene in human bladder cancer. *Oncogene* 1999; **18**: 1629-1633
106 **Loiseau H**, Arsaut J, Demotes-Mainard J. p73 gene transcripts in human brain tumors: overexpression and altered splicing in ependymomas. *Neurosci Lett* 1999; **263**: 173-176
107 **Tannapfel A**, Schmelzer S, Benicke M, Klimpfinger M, Kohlhaw K, Mossner J, Engeland K, Wittekind C. Expression of the p53 homologues p63 and p73 in multiple simultaneous gastric cancer. *J Pathol* 2001; **195**: 163-170
108 **Hagiwara K**, McMenamin MG, Miura K, Harris CC. Mutational analysis of the p63/p73L/p51/p40/CUSP/KET gene in human cancer cell lines using intronic primers. *Cancer Res* 1999; **59**: 4165-4169
109 **Kato S**, Shimada A, Osada M, Ikawa S, Obinata M, Nakagawara A, Kanamaru R, Ishioka C. Effects of p51/p63 missense mutations on transcriptional activities of p53 downstream gene promoters. *Cancer Res* 1999; **59**: 5908-5911
110 **Yang A**, Kaghad M, Wang Y, Gillett E, Fleming MD, Dotsch V, Andrews NC, Caput D, McKeon F. p63, a p53 homolog at 3q27-29, encodes multiple products with transactivating, death-inducing, and dominant-negative activities. *Mol Cell* 1998; **2**: 305-316
111 **Xing EP**, Yang GY, Wang LD, Shi ST, Yang CS. Loss of heterozygosity of the Rb gene correlates with pRb protein expression and associates with p53 alteration in human esophageal cancer. *Clin Cancer Res* 1999; **5**: 1231-1240
112 **Rigberg DA**, Kim FS, Sebastian JL, Kazanjian KK, McFadden DW. Hypophosphorylated retinoblastoma protein is associated with G2 arrest in esophageal squamous cell carcinoma. *J Surg Res* 1999; **84**: 101-105
113 **Knudsen KE**, Weber E, Arden KC, Cavenee WK, Feramisco JR, Knudsen ES. The retinoblastoma tumor suppressor inhibits cellular proliferation through two distinct mechanisms: inhibition of cell cycle progression and induction of cell death. *Oncogene* 1999; **18**: 5239-5245
114 **Lan J**, Xiong YY, Lin YX, Wang BC, Gong LL, Xu HS, Guo GS. *Helicobacter pylori* infection generated gastric cancer through p53-Rb tumor-suppressor system mutation and telomerase reactivation. *World J Gastroenterol* 2003; **9**: 54-58
115 **Zhou Y**, Gao SS, Li YX, Fan ZM, Zhao X, Qi YJ, Wei J P, Zou J X, Liu G, Jiao L, Bai YM, Wang LD. Tumor suppressor gene p16 and Rb expression in gastric cardia precancerous lesions from subjects at a high incidence area in northern China. *World J Gastroenterol* 2002; **8**: 423-425
116 **Muzeau F**, Flejou JF, Thomas G, Hamelin R. Loss of heterozygosity on chromosome 9 and p16 (MTS1, CDKN2) gene mutations in esophageal cancers. *Int J Cancer* 1997; **729**: 27-30
117 **Wong DJ**, Barrett MT, Stoger R, Emond MJ, Reid BJ. p16INK4a promoter is hypermethylated at a high frequency in esophageal adenocarcinomas. *Cancer Res* 1997; **57**: 2619-2622
118 **Xing EP**, Nie Y, Wang LD, Yang GY, Yang CS. Aberrant methylation of p16INK4a and deletion of p15INK4b are frequent events in human esophageal cancer in Linzhou, China. *Carcinogenesis* 1999; **20**: 77-84
119 **Tsujimoto H**, Hagiwara A, Sugihara H, Hattori T, Yamagishi H. Promoter methylations of p16INK4a and p14ARF genes in early and advanced gastric cancer. Correlations of the modes of their occurrence with histologic type. *Pathol Res Prac* 2002; **198**: 785-794
120 **Hannon GJ**, Beach D. p15INK4B is a potential effector of TGF-beta-induced cell cycle arrest. *Nature* 1994; **371**: 257-261
121 **Bates S**, Phillips AC, Clark PA, Stott F, Peters G, Ludwig RL, Vousden KH. p14ARF links the tumour suppressors RB and p53. *Nature* 1998; **395**: 124-125
122 **Stott FJ**, Bates S, James MC, McConnell BB, Starborg M, Brookes S, Palmero I, Ryan K, Vousden KH, Peters G. The alternative product from the human CDKN2A locus, p14(ARF), participates in a regulatory feedback loop with p53 and MDM2. *EMBO* 1998; **17**: 5001-5014
123 **Xing EP**, Nie Y, Song YL, Yang GY, Cai YC, Wang LD, Yang CS. Mechanisms of inactivation of p14ARF, p15INK4b and p16INK4a genes in human esophageal squamous cell carcinoma. *Clin Cancer Res* 1999; **5**: 2704-2713
124 **Yokota J**, Yamamoto T, Miyajima N, Toyoshima K, Nomura N, Sakamoto H, Yoshida T, Terada M, Sugimura T. Genetic alterations of the c-erB-2 oncogene occur frequently in tubular adenocarcinoma of the stomach and are often accompanied by amplification of the v-erbA homologue. *Oncogene* 1988; **2**: 283-287
125 **Park JB,** Rhim JS, Park SC, Kimm SW, Kraus MH. Amplification, overexpression, and rearrangement of the erB-2 protooncogene in primary human stomach carcinomas. *Cancer Res* 1989; **49**: 6605-6609
126 **Persons DL**, Croughan WS, Borilli KA, Cherian R. Interphase cytogenetics of esophageal adenocarcinoma and precursor lesions. *Cancer Genet Cytogenet* 1998; **106**: 11-17
127 **Hollstein MC**, Smith AM, Galiana C, Yamasaki H, Bos JL, Mandard A, Partensky C, Montesano R. Amplification of epidermal growth factor receptor gene but no evidence of ras mutation in primary human esophageal cancers. *Cancer Res* 1988; **48**: 5119-5123

128 **Tsuda T**, Tahara E, Kajiyama G, Sakamoto H, Terada M, Sugimura T. High incidence of coamplification of hst-1 and int-2 genes in human esophageal carcinoma. *Cancer Res* 1989; **49**: 5505-5508

129 **Houldsworth J**, Cordon–cardo C, Ladanyi M, Kelsen DP, Chaganti RSK. Gene amplification in gastric and esophageal adenocarcinomas. *Cancer Res* 1990; **50**: 6417-6422

130 **Chen H**, Wang LD, Gao SG, Fan ZM, Guo HQ. Alterations of MUC1, C-erbB2 in concurrent cancers of the esophagus and gastric cardia from the same patient in Linzhou, Henan province, a high incidence area for esophageal cancer. *Zhengzhou Daxue Xuebao (YiXueBan)* 2002; **37**: 758-761

131 **Tsuda T**, Tahara E, Kajiyama G, Sakamoto H, Terada M, Sugimura T. High incidence of coamplification of hst-1 and int-2 genes in human esophageal carcinomas. *Cancer Res* 1989; **49**: 5505-5508

132 **Kitagawa Y**, Ueda M, Anda N, Shinozawa, Y, Shimizu N, Abe O. Significance of int-2 / hst-1 coamplification as a prognostic fact or in patients with esophageal squamous carcinoma. *Cancer Res* 1991; **51**: 1504-1508

133 **Jiang W**, Kahn SM, Tomita N, Zhang YJ, Lu SH, Weinstein IB. Amplification and expression of the human cyclin D gene in esophageal cancer. *Cancer Res* 1992; **52**: 2980-2983

134 **Adelaide J**, Monges G, Derderian C, Seitz JF, Birnbaum D. Oesophageal cancer and amplification of the human cyclin D gene CCND1 / PRAD1. *Br J Cancer* 1995; **71**: 64-68

135 **Qin YR**, Liu Z, Guo HQ, Gao SS, Fan ZM, Li JX. Expression of tumor suppressor gene p27 and cyclinE in esophageal precancerous lesions from the subjects at high-incidence area for esophageal cancer in Henan. *Zhengzhou Daxue Xuebao (Yixueban)* 2002; **37**: 733-736

136 **Casson AG**, Wilson SE, McCart JA, O'Malley FP, Ozcelik H, Tsao MS, Chambers AF. Ras mutation, and expression of the ras regulated genes osteopontin and cathepsin L, in human esophageal cancer. *Int J Cancer* 1997; **72**: 739-745

137 **Tniere P**, Martel-Planche G, Maurici D, Lombard-Bohas C, Scoazec JY, Montesano R, Berger F, Hainaut P. Molecular and clinical differences between adenocarcinomas of the esophagus and of the gastric cardia. *Am J Path* 2001; **158**: 33-40

138 **Flejou JF**, Muzeau F, Potet F, Lepelletier F, Fekete F, Henin D. Overexpression of the p53 tumor suppressor gene product in esophageal and gastric carcinoma. *Path Res Prac* 1994; **190**: 1141-1148

139 **Ireland AP**, Shibata DK, Para Chandrasoma P, Lord RVN, Peters JH, DeMeester TR. Clinical significance of p53 mutations in adenocarcinoma of the esophagus and cardia. *Ann Surg* 2000; **231**: 179-187

140 **Chen H**, Wang LD, Gao SG, Fan ZM, Guo HQ, Li JL, Guo M. Alterations of MUC1, C-erbB2 in concurrent cancers of the esophagus and gastric cardia from the same patient in Linzhou, Henan province, a high incidence area for esophageal cancer. *Zhengzhou Daxue Xuebao (Yixueban)* 2002; **37**: 758-760

141 **Wang LD**, Zheng S. Mechanisms of human esophageal and gastric cardia cancer on the subjects in Henan, the high incidence area for esophageal cancer. *Zhengzhou Daxue Xuebao (Yixueban)* 2002; **37**: 717-729

142 **Zhou Q**, Wang LD. Biological characteristics of gastric cardia adenocarcinoma. *ShiJie Xiaohua Zazhi* 1998; **6**: 636-637

143 **Zhou Q**, Zheng ZY, Wang LD, Liu B, Qin YR, Wang DC, Chang ZW, Yi HX, Fan ZM, Li JL. p53 protein accumulation and p53 gene mutation in esophageal and gastric cardia cancer from the patients at Linzhou, Henan. *Zhengzhou Daxue Xuebao (Yixueban)* 2003; **38**: 313-316

144 **An JY**, Wang LD, He XW, Wang QM, Fan ZM, Gao SS, Guo HQ. Changes of PTEN expression in esophageal squamous cell carcinomas and gastric cardia adenocarcinoma from the patients at high-incidence area for esophageal cancer in Henan. *Zhengzhou Daxue Xuebao (Yixueban)* 2002; **37**: 750-753

145 **Wang LD**, Liu B, Guo RF, Bai YM, Sun C, Yi XN, He XW, Xie DL, Fan ZM, Ding ZH. Changes of c-erbB-2 and c-myc expression in esophageal and gastric cardia carcinogenesis from the subjects at high-incidence area for esophageal cancer in Henan, China. *Zhengzhou Daxue Xuebao (Yixueban)* 2002; **37**: 739-742

146 **Zhuang ZH**, Wang LD, Gao SS, Fan ZM, Song ZB, QI YJ, LI YJ, LI JX. Expression of MUC1 in esophageal and gastric cardiac carcinoma: a study on the subjects at high-incidence area for esophageal cancer in Henan, China. *Zhengzhou Daxue Xuebao (Yixueban)* 2002; **37**: 774-777

147 **Zhou Q**, Zheng ZY, Wang LD, Liu B, Gao SHG, Guo RF, Fan ZM, Guo HQ, Li JL. Prevalence of genetic polymorphisms of CYP1A1 and 2E1 in subjects with gastric cardia adenocarcinoma at Linzhou, Henan. *Zhengzhou Daxue Xuebao (Yixueban)* 2003; **38**: 317-320

148 **Zhou Q**, Bai YM, Wang LD, Liu B, Gao SS, Fan ZM, Guo HQ, Wang QM, Qin YJ, Li JL, Jiao XY. Alterations of MUC3 in gastric-cardia precancerous and cancerous lesions: A comparative study between the high- and low-risk populations. *Zhengzhou Daxue Xuebao (Yixueban)* 2003; **38**: 324-326

149 **Zhou Q**, Zheng ZY, Wang LD, Fan ZM, Guo HQ, Gao SHG, Qin YR, An JY, He XW, Wang QM, Wang DC, Liu B, Li JL. Polymorphism of mEH in gastric cardia carcinogenesis from the subjects at Linzhou, Henan. *Zhengzhou Daxue Xuebao (Yixueban)* 2003; **38**: 321-323

150 **Zhou Q**, Zheng ZY, Wang LD, Yi XN, Wang DC, Chang ZW, Liu B, Li JL. Prevalence of genetic polymorphisms of GSTM1, GSTT1 and GSTP1 in subjects with gastric cardia adenocarcinoma at Linzhou, Henan. *Zhengzhou Daxue Xuebao (Yixueban)* 2003; **38**: 327-329

151 **Zhou Q**, Bai YM, Liu B, He XW, Fan ZM, Li JL, Gao SS, Guo HQ, Wang DC, He XW, Chang ZW, Yih X, Wang NB, Wang LD. Alterations of EGFR in gastric-cardia precancerous and cancerous lesions: A comparative study between the high and low risk populations. *Zhengzhou Daxue Xuebao (Yixueban)* 2003; **38**: 332-334


**Edited by** Zhu LH

P.O.Box 2345, Beijing 100023,China
Fax: +86-10-85381893
E-mail: wjg@wjgnet.com www.wjgnet.com

World J Gastroenterol 2003;9(6):1165-1169
World Journal of Gastroenterology
Copyright ©2003 by The WJG Press ISSN 1007-9327

• REVIEW •

# DNA polymerase ζ: new insight into eukaryotic mutagenesis and mammalian embryonic development

Feng Zhu, Ming Zhang

**Feng Zhu,** Department of Pathophysiology, Zhejiang University School of Medicine, Hangzhou 310031, Zhejiang Province, China
**Ming Zhang,** College of Life Science, Zhejiang University, Hangzhou 310012, Zhejiang Province, China
**Correspondence to:** Professor Ming Zhang, College of Life Science, Zhejiang University, Hangzhou 310012, Zhejiang Province, China. zhangming_ls@zju.edu.cn
**Telephone:** +86-571-88273423 **Fax:** +86-571-88273423
**Received:** 2003-01-04 **Accepted:** 2003-02-17

## Abstract

Information about the mechanisms that generate mutations in eukaryotes is likely to be useful for understanding human health concerns, such as genotoxicity and cancer. Eukaryotic mutagenesis is largely the outcome of attacks by endogenous and environmental agents. Except for DNA repair, cell cycle checkpoints and DNA damage avoidance, cells have also evolved DNA damage tolerance mechanism, by which lesion-targeted mutation might occur in the genome during replication by specific DNA polymerases to bypass the lesions (translesion DNA synthesis, TLS), or mutation on undamaged DNA templates (untargeted mutation) might be induced. DNA polymerase ζ (pol ζ), which was found firstly in budding yeast *Saccharomyces cerevisiae* and consists of catalytic subunit scRev3 and stimulating subunit scRev7, has received more attention in recent years. Pol ζ is a member of DNA polymerase δ subfamily, which belongs to DNA polymerase B family, and exists in almost all eukaryotes. Human homolog of the *scRev3* gene is located in chromosome region 6q21, and the mouse equivalent maps to chromosome 10, distal to the c-*myb* gene and close to the *Macs* gene. Alternative splicing, upstream out-of frame ATG can be found in yeast *scRev3*, mouse and human homologs. Furthermore, the sequence from 253-323 immediate upstream of the AUG initiator codon has the potential to form a stem-loop hairpin secondary structure in *REV3* mRNA, suggesting that human REV3 protein may be expressed at low levels in human cells under normal growth conditions. The functional domain analysis showed that yeast *Rev3*-980 tyrosine in conserved region II is at the polymerase active site. Human REV3 amino acid residues 1 776-2 195 provide a REV7 binding domain, and REV7 amino acid residues 1-211 provide a bind domain for REV1, REV3 and REV7 itself. More interestingly, REV7 interacts with hMAD2 and therefore might function in the cell cycle control by affecting the activation of APC (anaphase promoting complex). Currently it has been known that pol ζ is involved in most spontaneous mutation, lesion-targeted mutation via TLS, chemical carcinogen induced untargeted mutation and somatic hypermutation of antibody genes in mammalian. In TLS pathway, pol ζ acts as a "mismatch extender" with combination of other DNA polymerases, such as pol ι. Unlike in yeast, it was found that pol ζ also functioned in mouse embryonic development more recently. It was hypothesized that the roles of pol ζ in TLS and cell cycle control might contribute to mouse embryonic lethality.

Zhu F, Zhang M. DNA polymerase ζ: new insight into eukaryotic mutagenesis and mammalian embryonic development. *World J Gastroenterol* 2003; 9(6): 1165-1169
http://www.wjgnet.com/1007-9327/9/1165.asp

## INTRODUCTION

The increase of environmental cancer has been received intensive attention in recent years[1-6]. An arresting example is that tobacco smoke significantly increases the risks for oral[7, 8], esophageal[3, 6, 9, 10], bladder[11-14], pancreas[13], gastric[15] and colorectal cancers[16]. To understand the relationship between environmental agents and cancer is a noteworthy hotspot, by which it is possible to establish a system to prevent and control environmental cancers.

Information about the mechanisms that generate mutations in eukaryotes is likely to be useful for understanding human health concerns, such as genotoxicity and cancer. Eukaryotic mutagenesis is largely the outcome of attacks by endogenous and environmental agents. However, the cells have evolved sophisticated systems in response to DNA damage, including DNA repair and cell cycle checkpoints. Even when DNA repair systems and cell cycle checkpoints are fully functional, some damage can still persist in the genome during replication under circumstances such as: (i) when cells sustain significant DNA damage; (ii) when a particular damage is poorly repaired; or (iii) when some genomic regions are inefficiently repaired. DNA damage frequently blocks replication. Such blockage can be overcome by error-free or error-prone translesion DNA synthesis (TLS) bypass, employing specialized DNA polymerases and proteins for promoting continuous nascent strand extension at forks blocked by the presence of unrepaired DNA damage at the cost of increasing mutation frequency[17]. Alternatively, mutation can be avoided by DNA damage avoidance[18], or occur on undamaged DNA template and lead to untargeted mutation via damage tolerance[19].

DNA polymerase ζ (pol ζ), consisting of catalytic subunit scRev3 and stimulating scRev7 in budding yeast *Saccharomyces cerevisiae*, has received more attention in recent years. It is thought to be the major component of error-prone TLS pathway[20-24], although a number of other polymerases might be involved in this process[25]. In Saccharomyces cerevisiae, TLS pathway pasting many types of DNA damage in yeast depends on the activities of pol ζ and Rev1p, which is a major source of DNA-damage-induced substitutions and frameshifts and of spontaneous mutations[21, 22, 26-30]. It has been speculated and demonstrated later that human pol ζ plays a major role in UV-induced mutagenesis and somatic hypermutation in antibody genes[31-34]. More recently, it was found that human pol ζ was also involved in mammalian untargeted mutagenesis, and the expression of human mutator *REV3* could be upregulated at transcriptional level in response to chemical carcinogen *N*-methyl-*N*'-nitro-*N*-nitrosoguanidine (MNNG)[35], which could induce gastric cancer[36-39] and colorectal cancer[40, 41]. Evidences also suggested that pol ζ was concerned with cell cycle control and early

embryonic development[42-45]. The aim of this paper was to review the structural and functional features of pol ζ, and its roles in mutagenesis and embryonic development as well.

## PROPERTIES OF STRUCTURE AND FUNCTION DOMAIN OF POL z

In the budding yeast *Saccharomyces cerevisiae*, the scRev3-scRev7 complex is the sixth eukaryotic DNA polymerase to be described, and is therefore called DNA polymerase ζ[22]. The catalytic subunit Rev3 is a member of family B DNA polymerases, which contains six conserved motifs[46, 47]. Mutation analysis *in vivo* and the X-ray crystal structures of family B polymerases reveal that yeast *scRev3*-980 tyrosine in conserved region II is at the polymerase active site[48]. Investigation suggests that homologues of the yeast *scRev3* gene are found in almost all eukaryotes, including *Arabidopsis thaliana*, *Drosophila melanogaster*, *Schizosaccharomyces pombe*, mouse and specifically humans[30, 31, 49-53].

Human homolog of the *Saccharomyces cerevisiae scRev3* gene is located on chromosome region 6q21, and the mouse equivalent maps to chromosome 10, distal to the c-*myb* gene, and close to the *Macs* gene[50, 52]. The full-length cDNA of human *REV3* consists of 10 919 nucleotides, with a putative open reading frame of 9 390 bp[31, 50, 51]. Human *REV3* gene contains 33 exons in about 200 kb of genomic DNA, in which an additional exon, alternative splicing event and an upstream out-of frame ATG have been demonstrated[31, 50]. The same alternative splicing has also been observed in mouse, with a 128bp exon inserted between nt +139 and +140 in approximately 50 % of the transcripts[52]. An upstream out-of-frame ATG with an ORF that terminates within the main ORF is also found in the yeast gene[21], suggesting that it may be evolutionally conserved in all pol ζ genes. The sequence context of the upstream gene performs a similar function to that of its yeast counterpart. Interestingly, three stretches of sequences, GGCAGTGGCGGC, AGGGGAGGGGGC, and GCCGCCGCCGCTGC, are duplicated in the 5 untranslated region constituting 323 nucleotides. Furthermore, the sequence from 253-323 immediate upstream of the AUG initiator codon has the potential to form a stem-loop hairpin secondary structure in *REV3* mRNA[51]. Such primary structural features and the secondary structure in the 5' untranslated region are expected to reduce the translational efficiency of the message, suggesting that human REV3 protein may be expressed at low levels in human cells under normal growth conditions.

The predicted homogous proteins in human and mouse are a little over twice the length of the yeast scReve protein (1 504 residues), i.e., 3 130 amino acids with an expected mass of 353 kDa and a calculated p *I* of 8.7 in human, and 3 122 amino acids in mouse respectively. The homologous proteins of yeast scRev3 are highly conserved[31, 51, 52]: (i) in the N-terminal part, the overall homology between yeast scRev3/*Drosophila* DmRev3, yeast scRev3/human REV3 and *Drosophila* DmRev3/human REV3 amounts to respectively 33.3 %, 35.0 % and 50.5 % identical amino acids. (ii) in a region of 850 residues at the carboxyl terminus, the overall homology between yeast scRev3/human REV3 amounts to 39 % identical amino acids, and (iii) in a 55-residue region in the middle of both scRev3 and REV3 proteins, with 29 % identity. But little similarity can be found in the intervening regions[31].

The carboxyl terminus region of yeast Rev3 homologue proteins in human, mouse and *Drosophila* contains the six conserved sequence motifs characterized by DNA polymerases in the right order, including the canonical hexapeptide motifs within regions 1 and 2, YGDTDS and SLYPSI, which are found jointly only in type B DNA polymerases[46, 47]. Further alignment shows that pol ζ is a member of DNA polymerase δ family with two specifically conserved motifs ζ I and ζ II in pol ζ, and in the N-terminal part, a conserved glycine repeat motif (G-x4-G-x2-G-x8-G-x3-YFY) in pol δ is also present in the homologues which have been implicated in nucleotide binding[51]. Outside the six DNA polymerase motifs in the C-terminal, both yeast scRev3 and human REV3 proteins contain a putative zinc finger DNA binding region, and the location of this putative zinc finger is also highly conserved from yeast to humans[51]. Such structural features are consistent with the notion that the C-terminal region of scRev3 homologue serves as the catalytic domain during nucleotide polymerization, while its N-terminal region may provide sites for protein-protein interactions with other factors such as a putative yeast scRev7 homologue during translesional DNA synthesis.

However, the existence of a much larger nonhomologous or species-specific region in the expected human protein suggests that pol ζ may perform a wider range of functions in the higher eukaryotes. In *Saccharomyces cerevisiae*, it was found that LexA-scRev3 and Gal4-scRev7 fusions interacted with each other[22]. More recently, studies showed that human REV3 amino acid residues 1 776-2 195 provided a REV7 binding domain, and REV7 amino acid residues 1-211 provided a bind domain for REV1, REV3 and REV7 itself [54, 55]. REV7, the stimulating subunit of pol ζ which is located on chromosome 1p36, displays 23 % identity and 53 % similarity with scRev7, as well as 23 % identity and 54 % similarity with the human mitotic checkpoint protein hMAD2. And yeast two-hybrid assay suggests that REV7 may interact with hMAD2 but not with hMAD1[54]. It is possible that REV3, REV7, and hMAD2 might be capable of forming a stable triprotein complex.

## CHARACTERISTICS AND ROLES OF POL z INVOLVED IN EUKARYOTIC MUTAGENESIS

DNA damage induced elevation of mutations during the course of translesion replication is likely to be an important contributory cause in the development of many cancers[27]. With *in vitro* and *in vivo* investigation, it has been clear that pol ζ plays a role in an error-prone way. Yeast pol ζ can bypass T-T cyclobutane dimer, but not (6-4) T-T photoproduct and abasic site, inserting an incorrect nucleotide with relatively low efficiency *in vitro* ($f_{inc}$ values range from $4.1\times10^{-3}$ to $1.9\times10^{-5}$)[22, 56]. When combined with REV1 (transfers a dCMP residue from dCTP to the 3' end of a DNA primer in a template-dependent reaction opposite abasic site), pol ι (inserts a deoxynucleotide opposite the (6-4) T-T photoproduct and abasic site) or pol η (bypasses T-T cyclobutane dimer with relative high accuracy and efficiency), pol ζ can bypass all three types of lesions with more efficiency ($f^{o}_{ext}$ values range from $10^{-1}$ to $10^{-2}$) at elongating from a mismatched terminus, which develops the TLS two-step model (Figure 1)[56-58].

Mutation caused by TLS is usually designated targeted mutation. However, mutation can also occur on undamaged DNA template and therefore is called untargeted mutation (UTM), which has been described in SOS-induced mutagenesis in *E. coli*[59]. It has been known that untargeted and targeted mutations caused by SOS response in *E. coli* both result from the inhibition of DNA polymerase functions that normally maintain fidelity and the involvement of DNA polymerases with low fidelity, which include DNA pol III, pol IV (dinB), pol V (UmuD' 2C) and other factors (RecA*, β-sliding clamp, γ-clamp loading complex and single-stranded binding protein)[60-64]. Using mating experiments with excision deficient strains of Saccharomyces cerevisiae, Lawrence and Christensen found that up to 40 % of cycl-91 revertants induced by UV were untargeted, showing that a reduction in fidelity of DNA replication[65]. In mouse T-lymphoma cells, stress response induced by DNA damage agents (8-methoxy-psoralen or UVA)

leads to specific, delayed and untargeted mutations[66]. It has been found that low concentration *N*-methyl-*N'*-nitro-*N*-nitrosoguanidine (MNNG), a carcinogen which can induce gastric cancer, could induce mammalian UTM[19]. However, it is not clear which factor capable of inhibiting fidelity can be induced or activated. More recently, it was found that pol ζ might be involved in the mammalian UTM induced by MNNG. The transcriptional level of *REV3* gene is upregulated when human cells are treated by low concentration MNNG. Furthermore, human cells, in which the function of pol ζ is inhibited by antisense *REV3* RNA, display characteristics of both anti UTM and targeted mutation[35].

Pol ζ also functions in somatic hypermutation[33,34]. Accumulation of somatic mutations in the V(H) genes of memory B cells from transgenic mice which express antisense RNA to a portion of mouse REV3 is decreased, particularly among those that generate amino acid replacements enhancing the affinity of the B cell receptor to the hapten[33]. In addition, inhibition of the mouse mRev3 by specific phosphorothioate-modified oligonucleotides impaires Ig and bcl-6 hypermutation and UV damage-induced DNA mutagenesis, without affecting cell cycle or viability[34].

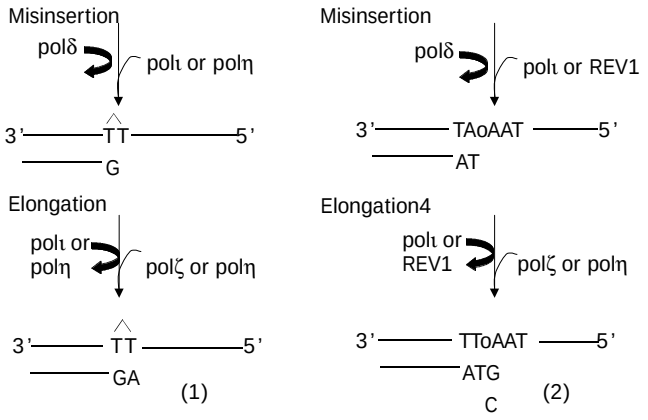


**Figure 1** TLS two-step model in human cells. (1) The main replicase in humans, pol δ, has difficulty in replicating through *cis-syn* T-T cyclobutane dimmer and (6-4) T-T photoproduct. This recruits specialized polymerases such as pol η, pol ι to insert or misinsert deoxynucleotides, and then pol ζ functions as a mismatch extender. (2) Opposite the abasic site, pol ι or REV1 inserts a deoxynucleotide, and bypass of this lesion occurs when combined with pol ζ.

## ROLE OF POL ζ IN MAMMALIAN EMBRYONIC DEVELOPMENT

In *Saccharomyces cerevisiae*, pol ζ is not essential for cell viability, as indicated by the fact that haploids carrying a complete deletion of *Rev3* are viable[21]. Besides, human fibroblast cells expressing high levels of an *REV3* antisense RNA fragment grow normally[31]. However, recent evidences have shown that pol ζ is essential for cell viability during embryonic development in mammals (Table 1)[43-45, 67].

**Table 1** Characteristics of *mRev3*$^{-/-}$ embryo

| Size | Reduced at day 10.5 |
|---|---|
| Viability | Usually aborted around day 12.5 |
| Inner cell mass (ICM) | Diminished expansion |
| Haematopoietic cells | No haematopoietic cells developed other than erythrocytes |
| Morphogenesis of embryo | 1. Abnormalities in the development and maintenance of embryonic mesoderm<br>2. Predominant disorder and lack of integrity mainly in mesenchymal tissues, including heart and large blood vessels |

It has been realized that numerous DNA lesions caused by unavoidable oxidative and hydrolytic processes are constantly formed in genomes[68]. Double-strand breaks can form when DNA replication forks encounter nicked templates, and these stalled replication forks must be reactivated by replication or repair. Unlike cells in adult tissues or in culture, which have mechanisms to cease division or DNA replication temporarily in order to allow accurate and specific DNA repair enzymes to act before proceeding through the cell cycle, embryonic development adheres to a strict temporal program that requires rapid cell division. Under such conditions, enzymes that can rapidly bypass DNA lesions may be expected to be particularly important, and an intolerable load of damaged DNA in critical embryonic or extra-embryonic cells would then lead to death. On the other hand, the proliferating cells in the embryo might gradually accumulate DNA damage and ES cells may be a special case of a cell type primed to undergo apoptosis after accumulated low levels of DNA damage[69]. During the developmental stage of the mRev3-defective mouse embryos before embryonic death, the embryos are still able to propagate rapidly and differentiate through many cell divisions.

It is noteworthy that mouse *mRev3* is most highly expressed in mesodermal tissues and embryonic death coincides with the period of more widely distributed *mRev3l* expression. High-level expression of mouse *mRev3* is developmentally regulated during embryogenesis, occurring first in early somatogenesis and then in other mesodermal tissues up to at least 11.5 days *post coitum*[45]. This differential expression seems likely to account for the predominant disorder and lack of integrity found mainly in mesenchymal tissues. Lack of proper development of the heart and large blood vessels might in itself be the immediate cause of death. Also, as mouse *mRev3* is normally expressed within extraembryonic membranes, the absence of functional mRev3 in mouse *mRev3*$^{-/-}$ embryos could be the cause of the pericardial sac edema, yolk sac fragility and weak attachment to the decidual implantation site. Yolk-sac malfunction can induce osmotic imbalance, leading to edema, whereas delayed and/or suboptimal chorioallantoic fusion can result in an implantation defect. Defects of the chorioallantoic placenta or yolk sac are a common cause of murine lethality *in utero* and could contribute to the embryonic lethality of mouse *mRev3* disruption. Therefore, ES cells may have a special need for the activity of pol ζ if certain types of DNA damage accumulate within them, and bypass of specific types of DNA lesions by pol ζ is essential for cell viability during embryonic development in mammals.

However, it is also possible that mouse mRev3 has an additional unknown function. In view of the fact that yeast scRev7 shares a region of homology, termed the HORMA (Hop1p, Rev7p and Mad2) domain with Mad2, which associates with unattached kinetochores and functions in the spindle assembly mitotic checkpoint[71]. Mad2, Rev3 and Rev7 proteins might therefore have the potential to interact *in vitro*. It has been demonstrated that human REV7 may interact with hMAD2[54]. Interestingly, the tumor suppressor p33*ING1*, which has recently been demonstrated to have no synergistic effect with p53 in camptothecin-induced cell death in melanoma cells[72], strongly associates with mRev3 protein in a two-hybrid assay[30]. It was observed that mouse mRev3$^{-/-}$ embryonic death occurred in a p53-independent pathway indicating mRev3 functions with no direct or indirect interaction with p53[67]. Furthermore, it has been found that *Saccharomyces cerevisiae* lacking Snm1, scRev3 or Rad51 have a normal S-phase but arrest permanently in $G_2$ after cisplatin treatment[42]. Therefore, pol ζ can play a central role in apoptosis, cell proliferation, and the control of cell cycle by protein-protein interaction, and thus affect the embryonic development.

## REFERENCES


1 **Li Y**, Su JJ, Qin LL, Yang C, Luo D, Ban KC, Kensler T, Roebuck B. Chemopreventive effect of oltipraz on AFB(1)-induced hepatocarcinogenesis in tree shrew model. *World J Gastroenterol* 2000; **6**: 647-650

2 **Bollschweiler E**, Holscher AH. Carcinoma of the esophagus-actual epidemiology in Germany. *Onkologie* 2001; **24**: 180-184

3 **Bonnin-Scaon S**, Lafon P, Chasseigne G, Mullet E, Sorum PC. Learning the relationship between smoking, drinking alcohol and the risk of esophageal cancer. *Health Educ Res* 2002; **17**: 415-424

4 **Cai L**, Zheng ZL, Zhang ZF. Risk factors for the gastric cardia cancer: a case-control study in Fujian Province. *World J Gastroenterol* 2003; **9**: 214-218

5 **Xue YW**, Zhang QF, Zhu ZB, Wang Q, Fu SB. Expression of cyclooxygenase-2 and clinicopathologic features in human gastric adenocarcinoma. *World J Gastroenterol* 2003; **9**: 250-253

6 **Wang AH**, Sun CS, Li LS, Huang JY, Chen QS. Relationship of tobacco smoking CYP1A1 GSTM1 gene polymorphism and esophageal cancer in Xi'an. *World J Gastroenterol* 2002; **8**: 49-53

7 **Balaram P**, Sridhar H, Rajkumar T, Vaccarella S, Herrero R, Nandakumar A, Ravichandran K, Ramdas K, Sankaranarayanan R, Gajalakshmi V, Munoz N, Franceschi S. Oral cancer in southern India: the influence of smoking, drinking, paan-chewing and oral hygiene. *Int J Cancer* 2002; **98**: 440-445

8 **Bartal M**. Health effects of tobacco use and exposure. *Monaldi Arch Chest Dis* 2001; **56**: 545-554

9 **Boring CC**, Squires TS, Tong T, Heath CW. Mortality trends for selected smoking-related cancers and breast cancer–United States, 1950-1990. *Morb Mortal Wkly Rep* 1993; **42**: 857, 863-866

10 **Bollschweiler E**, Holscher AH. Carcinoma of the esophagus-actual epidemiology in Germany. *Onkologie* 2001; **24**: 180-184

11 **Badawi AF**, Habib SL, Mohammed MA, Abadi AA, Michael MS. Influence of cigarette smoking on prostaglandin synthesis and cyclooxygenase-2 gene expression in human urinary bladder cancer. *Cancer Invest* 2002; **20**: 651-656

12 **Bernardini S**, Adessi GL, Chezy E, Billerey C, Carbillet JP, Bittard H. Influence of cigarette smoking on P53 gene mutations in bladder carcinomas. *Anticancer Res* 2001; **21**: 3001-3004

13 **Borras J**, Borras JM, Galceran J, Sanchez V, Moreno V, Gonzalez JR. Trends in smoking-related cancer incidence in Tarragona, Spain, 1980-96. *Cancer Causes Control* 2001; **12**: 903-908

14 **Castelao JE**, Yuan JM, Skipper PL, Tannenbaum SR, Gago-Dominguez M, Crowder JS, Ross RK, Yu MC. Gender- and smoking-related bladder cancer risk. *J Natl Cancer Inst* 2001; **93**: 538-545

15 **Chao A**, Thun MJ, Henley SJ, Jacobs EJ, McCullough ML, Calle EE. Cigarette smoking, use of other tobacco products and stomach cancer mortality in US adults: The Cancer Prevention Study II. *Int J Cancer* 2002; **101**: 380-389

16 **Casimiro C**. Etiopathogenic factors in colorectal cancer. Nutritional and life-style aspects. 2. *Nutr Hosp* 2002; **17**: 128-138

17 **Kunz BA**, Straffon AF, Vonarx EJ. DNA damage-induced mutation: tolerance via translesion synthesis. *Mutat Res* 2000; **451**: 169-185

18 **Li Z**, Xiao W, McCormick JJ, Maher VM. Identification of a protein essential for a major pathway used by human cells to avoid UVinduced DNA damage. *Proc Natl Acad Sci USA* 2002; **99**: 4459-4464

19 **Zhang X**, Yu Y, Chen X. Evidence for nontargeted mutagenesis in a monkey kidney cell line and analysis of its sequence specificity using a shuttle-vector plasmid. *Mutat Res* 1994; **323**: 105-112

20 **Quah SK**, Von Borstel RC, Hastings PJ. The origin of spontaneous mutation in Saccharomyces cerevisiae. *Genetics* 1980; **96**: 819-839

21 **Morrison A**, Christensen RB, Alley J, Beck AK, Bernstine EG, Lemontt JF, Lawrence CW. REV3, a Saccharomyces cerevisiae gene whose function is required for induced mutagenesis, is predicted to encode a nonessential DNA polymerase. *J Bacteriol* 1989; **171**: 5659-5667

22 **Nelson JR**, Lawrence CW, Hinkle DC. Thymine-thymine dimer bypass by yeast DNA polymerase zeta. *Science* 1996; **272**: 1646-1649

23 **Baynton K**, Bresson-Roy A, Fuchs RP. Analysis of damage tolerance pathways in Saccharomyces cerevisiae: a requirement for Rev3 DNA polymerase in translesion synthesis. *Mol Cell Biol* 1998; **18**: 960-966

24 **Lawrence CW**, Maher VM. Eukaryotic mutagenesis and translesion replication dependent on DNA polymerase zeta and Rev1 protein. *Biochem Soc Trans* 2001; **29**: 187-191

25 **Rechkoblit O**, Zhang Y, Guo D, Wang Z, Amin S, Krzeminsky J, Louneva N, Geacintov NE. Trans-lesion synthesis past bulky benzo[a]pyrene diol epoxide N2-dG and N6-dA lesions catalyzed by DNA bypass polymerases. *J Biol Chem* 2002; **277**: 30488-30494

26 **Roche H**, Gietz RD, Kunz BA. Specificity of the yeast rev3 delta antimutator and REV3 dependency of the mutator resulting from a defect (rad1 delta) in nucleotide excision repair. *Genetics* 1994; **137**: 637-646

27 **Lawrence CW**, Hinkle DC. DNA polymerase zeta and the control of DNA damage induced mutagenesis in eukaryotes. *Cancer Surv* 1996; **28**: 21-31

28 **Holbeck SL**, Strathern JN. A role for REV3 in mutagenesis during double-strand break repair in Saccharomyces cerevisiae. *Genetics* 1997; **147**: 1017-1024

29 **Xiao W**, Fontanie T, Bawa S, Kohalmi L. REV3 is required for spontaneous but not methylation damage-induced mutagenesis of Saccharomyces cerevisiae cells lacking O6-methylguanine DNA methyltransferase. *Mutat Res* 1999; **431**: 155-165

30 **Lawrence CW**, Maher VM. Mutagenesis in eukaryotes dependent on DNA polymerase zeta and Rev1p. *Philos Trans R Soc Lond B Biol Sci* 2001; **356**: 41-46

31 **Gibbs PE**, McGregor WG, Maher VM, Nisson P, Lawrence CW. A human homolog of the Saccharomyces cerevisiae REV3 gene, which encodes the catalytic subunit of DNA polymerase zeta. *Proc Natl Acad Sci U S A* 1998; **95**: 6876-6880

32 **Diaz M**, Velez J, Singh M, Cerny J, Flajnik MF. Mutational pattern of the nurse shark antigen receptor gene (NAR) is similar to that of mammalian Ig genes and to spontaneous mutations in evolution: the translesion synthesis model of somatic hypermutation. *Int Immunol* 1999; **11**: 825-833

33 **Diaz M**, Verkoczy LK, Flajnik MF, Klinman NR. Decreased frequency of somatic hypermutation and impaired affinity maturation but intact germinal center formation in mice expressing antisense RNA to DNA polymerase zeta. *J Immunol* 2001; **167**: 327-335

34 **Zan H**, Komori A, Li Z, Cerutti A, Schaffer A, Flajnik MF, Diaz M, Casali P. The translesion DNA polymerase zeta plays a major role in Ig and bcl-6 somatic hypermutation. *Immunity* 2001; **14**: 643-653

35 **Zhu F**, Jin C, Song T, Yang J, Guo L, Yu Y. Response of human REV3 gene to gastric cancer inducing carcinogen N-methyl-N'-nitro-N-nitrosoguanidine and its role in mutagenesis. *World J Gastroenterol* 2003; **9**: 888-893 (in press)

36 **Sherenesheva NI**, Mashkovtsev IV. Electron microscopy study of experimental stomach cancer. *Eksp Onkol* 1985; **7**: 29-35

37 **Sasako M**. The effect of Nd:YAG laser irradiation on gastric cancer in rats induced by N-methyl-N'-nitro-N-nitrosoguanidine as a model of endoscopic laser treatment for early gastric cancers. *Nippon Geka Gakkai Zasshi* 1985; **86**: 443-454

38 **Newberne PM**, Charnley G, Adams K, Cantor M, Suphakarn V, Roth D, Schrager TF. Gastric carcinogenesis: a model for the identification of risk factors. *Cancer Lett* 1987; **38**: 149-163

39 **Yamashita S**, Wakazono K, Sugimura T, Ushijima T. Profiling and selection of genes differentially expressed in the pylorus of rat strains with different proliferative responses and stomach cancer susceptibility. *Carcinogenesis* 2002; **23**: 923-928

40 **Amberger H**. Different autochthonous models of colorectal cancer in the rat. *J Cancer Res Clin Oncol* 1986; **111**: 157-159

41 **Narayan S**, Jaiswal AS. Activation of adenomatous polyposis coli (APC) gene expression by the DNA-alkylating agent N-methyl-N'-nitro-N-nitrosoguanidine requires p53. *J Biol Chem* 1997; **272**: 30619-30622

42 **Grossmann KF**, Ward AM, Moses RE. Saccharomyces cerevisiae lacking Snm1, Rev3 or Rad51 have a normal S-phase but arrest permanently in G2 after cisplatin treatment. *Mutat Res* 2000; **461**: 1-13

43 **Bemark M**, Khamlichi AA, Davies SL, Neuberger MS. Disruption of mouse polymerase zeta (Rev3) leads to embryonic lethality and impairs blastocyst development in vitro. *Curr Biol* 2000; **10**: 1213-1216

44 **Esposito G**, Godindagger I, Klein U, Yaspo ML, Cumano A,

Rajewsky K. Disruption of the Rev3l-encoded catalytic subunit of polymerase zeta in mice results in early embryonic lethality. *Curr Biol* 2000; **10**: 1221-1224

45 **Wittschieben J**, Shivji MK, Lalani E, Jacobs MA, Marini F, Gearhart PJ, Rosewell I, Stamp G, Wood RD. Disruption of the developmentally regulated Rev3l gene causes embryonic lethality. *Curr Biol* 2000; **10**: 1217-1220

46 **Braithwaite DK**, Ito J. Compilation, alignment, and phylogenetic relationships of DNA polymerases. *Nucleic Acids Res* 1993; **21**: 787-802

47 **Wong SW**, Wahl AF, Yuan PM, Arai N, Pearson BE, Arai K, Korn D, Hunkapiller MW, Wang TS. Human DNA polymerase alpha gene expression is cell proliferation dependent and its primary structure is similar to both prokaryotic and eukaryotic replicative DNA polymerases. *EMBO J* 1988; **7**: 37-47

48 **Pavlov YI**, Shcherbakova PV, Kunkel TA. *In vivo* consequences of putative active site mutations in yeast DNA polymerases alpha, epsilon, delta, and zeta. *Genetics* 2001; **159**: 47-64

49 **Kajiwara K**, Nagawawa H, Shimizu-Nishikawa S, Ookuri T, Kimura M, Sugaya E. Molecular characterization of seizure-related genes isolated by differential screening. *Biochem Biophys Res Commun* 1996; **219**: 795-799

50 **Morelli C**, Mungall AJ, Negrini M, Barbanti-Brodano G, Croce CM. Alternative splicing, genomic structure, and fine chromosome localization of REV3L. *Cytogenet Cell Genet* 1998; **83**: 18-20

51 **Lin W**, Wu X, Wang Z. A full-length cDNA of hREV3 is predicted to encode DNA polymerase zeta for damage-induced mutagenesis in humans. *Mutat Res* 1999; **433**: 89-98

52 **Van Sloun PP**, Romeijn RJ, Eeken JC. Molecular cloning, expression and chromosomal localisation of the mouse Rev3l gene, encoding the catalytic subunit of polymerase zeta. *Mutat Res* 1999; **433**: 109-116

53 **Eeken JC**, Romeijn RJ, de Jong AW, Pastink A, Lohman PH. Isolation and genetic characterisation of the Drosophila homologue of (SCE) REV3, encoding the catalytic subunit of DNA polymerase zeta. *Mutat Res* 2001; **485**: 237-253

54 **Murakumo Y**, Roth T, Ishii H, Rasio D, Numata S, Croce CM, Fishel R. A human REV7 homolog that interacts with the polymerase zeta catalytic subunit hREV3 and the spindle assembly checkpoint protein hMAD2. *J Biol Chem* 2000; **275**: 4391-4397

55 **Murakumo Y**, Ogura Y, Ishii H, Numata S, Ichihara M, Croce CM, Fishel R, Takahashi M. Interactions in the error-prone postreplication repair proteins hREV1, hREV3, and hREV7. *J Biol Chem* 2001; **276**: 35644-35651

56 **Johnson RE**, Washington MT, Haracska L, Prakash S, Prakash L. Eukaryotic polymerases iota and zeta act sequentially to bypass DNA lesions. *Nature* 2000; **406**: 1015-1019

57 **Nelson JR**, Lawrence CW, Hinkle DC. Deoxycytidyl transferase activity of yeast REV1 protein. *Nature* 1996; **382**: 729-731

58 **Woodgate R**. Evolution of the two-step model for UV-mutagenesis. *Mutat Res* 2001; **485**: 83-92

59 **Maenhaut-Michel G**. Mechanism of SOS-induced targeted and untargeted mutagenesis in *E. coli*. *Biochimie* 1985; **67**: 365-369

60 **Pham P**, Bertram JG, O'Donnell M, Woodgate R, Goodman MF. A model for SOS-lesion-targeted mutations in Escherichia coli. *Nature* 2001; **409**: 366-370

61 **Otterlei M**, Kavli B, Standal R, Skjelbred C, Bharati S, Krokan HE. Repair of chromosomal abasic sites *in vivo* involves at least three different repair pathways. *EMBO J* 2000; **19**: 5542-5551

62 **Kim SR**, Maenhaut-Michel G, Yamada M, Yamamoto Y, Matsui K, Sofuni T, Nohmi T, Ohmori H. Multiple pathways for SOS-induced mutagenesis in Escherichia coli: an overexpression of dinB / dinP results in strongly enhancing mutagenesis in the absence of any exogenous treatment to damage DNA. *Proc Natl Acad Sci USA* 1997; **94**: 13792-13797

63 **Tang M**, Bruck I, Eritja R, Turner J, Frank EG, Woodgate R, O'Donnell M, Goodman MF. Biochemical basis of SOS-induced mutagenesis in Escherichia coli: reconstitution of in vitro lesion bypass dependent on the UmuD'2C mutagenic complex and RecA protein. *Proc Natl Acad Sci U S A* 1998; **95**: 9755-9760

64 **Tang M**, Pham P, Shen X, Taylor JS, O'Donnell M, Woodgate R, Goodman MF. Roles of *E. coli* DNA polymerases IV and V in lesion-targeted and untargeted SOS mutagenesis. *Nature* 2000; **404**: 1014-1018

65 **Lawrence CW**, Christensen RB. The mechanism of untargeted mutagenesis in UV-irradiated yeast. *Mol Gen Genet* 1982; **186**: 1-9

66 **Boesen JJ**, Stuivenberg S, Thyssens CH, Panneman H, Darroudi F, Lohman PH, Simons JW. Stress response induced by DNA damage leads to specific, delayed and untargeted mutations. *Mol Gen Genet* 1992; **234**: 217-227

67 **O-Wang J**, Kajiwara K, Kawamura K, Kimura M, Miyagishima H, Koseki H, Tagawa M. An essential role for REV3 in mammalian cell survival: absence of REV3 induces p53-independent embryonic death. *Biochem Biophys Res Commun* 2002; **293**: 1132-1137

68 **Lindahl T**, Wood RD. Quality control by DNA repair. *Science* 1999; **286**: 1897-1905

69 **Van Sloun PP**, Jansen JG, Weeda G, Mullenders LH, Van Zeeland AA, Lohman PH, Vrieling H. The role of nucleotide excision repair in protecting embryonic stem cells from genotoxic effects of UV-induced DNA damage. *Nucl Acids Res* 1999; **27**: 3276-3282

70 **Copp AJ**. Death before birth: clues from gene knockouts and mutations. *Trends Genet* 1995; **11**: 87-93

71 **Aravind L**, Koonin EV. The HORMA domain: a common structural denominator in mitotic checkpoints, chromosome synapsis and DNA repair. *Trends Biochem Sci* 1998; **23**: 284-286

72 **Cheung KJJr**, Li G. The tumour suppressor p33ING1 does not enhance camptothecin-induced cell death in melanoma cells. *Int J Oncol* 2002; **20**: 1319-1322

**Edited by** Wu XN and Wang XL

P.O.Box 2345, Beijing 100023,China
Fax: +86-10-85381893
E-mail: wjg@wjgnet.com www.wjgnet.com

World J Gastroenterol 2003;9(6):1170-1173
World Journal of Gastroenterology
Copyright ©2003 by The WJG Press ISSN 1007-9327

• ESOPHAGEAL CANCER •

# Detection of human papillomavirus in Chinese esophageal squamous cell carcinoma and its adjacent normal epithelium

Xiao-Bo Zhou, Mei Guo, Lan-Ping Quan, Wei Zhang, Zhe-Ming Lu, Quan-Hong Wang, Yang Ke, Ning-Zhi Xu

**Xiao-Bo Zhou, Lan-Ping Quan, Wei Zhang, Ning-Zhi Xu,** Laboratory of Cell and Molecular Biology, Cancer Institute & Cancer Hospital, Chinese Academy of Medical Sciences, Beijing 100021, China
**Mei Guo, Zhe-Ming Lu, Yang Ke,** Laboratory of Genetics, Beijing Institute for Cancer Research, School of Oncology, Peking University, No. 1 Da Hong Luo Chang St, Beijing 100034, China
**Quan-Hong Wang,** Department of Pathology, the Third People' s Hospital of Shanxi Province, Taiyuan 030013, China
**Supported in part by** grants from the National Natural Science Foundation of China, No. 39925020 and from State Key Basic Research Program, No.G1998051204
**Correspondence to:** Dr Ning-Zhi Xu, Laboratory of Cell and Molecular Biology, Cancer Institute & Cancer Hospital, Chinese Academy of Medical Sciences, Beijing 100021, China. xningzhi@public.bta.net.cn
**Telephone:** +86-10-67738220 **Fax:** +86-10-67767548
Dr Yang Ke, Laboratory of Genetics, Beijing Institute for Cancer Research, School of Oncology, Peking University, No. 1 Da Hong Luo Chang St, Beijing 100034, China. keyang@bjmu.edu.cn
**Telephone**: +86-10-62091204 **Fax**: +86-10-62015681
**Received:** 2002-12-22 **Accepted:** 2003-03-05

## Abstract

**AIM:** To investigate the putative role of human papillomavirus (HPV) infection in the carcinogenesis of esophageal squamous cell carcinoma in China.

**METHODS:** Twenty-three esophageal squamous cell carcinoma samples and the distal normal epithelium from Shanxi Province, and 25 more esophageal squamous cell carcinoma samples from Anyang city, two areas with a high incidence of esophageal cancer in China, were detected for the existence of HPV-16 DNA by PCR, mRNA *in situ* hybridization (ISH) and immunohistochemistry (IHC) targeting HPV-16 E6 gene.

**RESULTS:** There were approximately 64 % (31/48) patients having HPV-16 DNA in tumor samples, among them nearly two-thirds (19/31) samples were detected with mRNA expression of HPV-16 E6. However, in the normal esophageal epithelium from cancer patients, the DNA and mRNA of HPV-16 were found with much less rate: 34.7 % (8/23) and 26.1 % (6/23) respectively. In addition, at protein level detected by IHC assay, 27.1 % (13/48) tumor samples had virus oncoprotein E6 expression, while only one case of normal epithelium was found positive.

**CONCLUSION:** HPV infection, especially type 16, should be considered as a risk factor for esophageal malignancies in China.

Zhou XB, Guo M, Quan LP, Zhang W, Lu ZM, Wang QH, Ke Y, Xu NZ. Detection of human papillomavirus in Chinese esophageal squamous cell carcinoma and its adjacent normal epithelium. *World J Gastroenterol* 2003; 9(6): 1170-1173
http://www.wjgnet.com/1007-9327/9/1170.asp

## INTRODUCTION

Esophageal squamous cell carcinoma (ESCC) is one of the leading causes among Chinese cancer mortality, and the incidence is mainly aggregated in North China, from which Henan and Shanxi Provinces are two high-incidence areas. The distinct geographical distribution suggests a dominant role of environmental factors in the etiology of this disease. Furthermore, other risk factors have been speculated, such as nutrition imbalance (lack or absence of vitamins and minerals), improper life style (cigarette smoking and consumption of pickled food), exposure to nitrosamines, during the carcinogenesis of ESCC in China[1-2]. Nevertheless, the real causes and the mechanism of ESCC have not been elucidated yet.

Human papillomavirus (HPV) as one kind of important tumor-related virus has been firmly recognized in cervical cancer. But its oncogenic role in other tumors is still disputed[3-5]. As to its role in ESCC, it was firstly suggested by Syrjanen 20 years ago, when he found the HPV infection in ESCC by pathological observation[6]. Since then, many reports regarding this topic have been published, but the HPV infection rate in ESCC varied from zero to 67 %[7,8], depending on the specimens obtained from low- or high-risk area around the world and the methods used in each study[9-12]. In our previous study, we found that the prevalence of HPV-16 E6 and E7 genes in high incidence area was higher than that in low incidence area, detected by means of PCR and ISH, from the samples of balloon cytologic examination in Anyang area of China[13]. In order to confirm and further investigate the prevalence of HPV infection in ESCC, the tumor samples and the distal normal epithelia from Shanxi Province, another high incidence region in China, with the tumor samples from Anyang city together, were tested for the existence of HPV-16 DNA.

Based on our previous data[13], in this study, we focused on the HPV-16 E6 gene, a major viral oncogene of high-risk HPV type. In addition to detecting its DNA and mRNA by using PCR and ISH, the E6 protein expression was simultaneously analyzed by IHC for all the samples. Furthermore the status of HPV-16 infection was compared between tumor samples and their adjacent "normal" esophageal epithelium.

## MATERIALS AND METHODS

### *Clinical samples*

A total of 48 primary esophageal carcinoma specimens and 23 normal samples were obtained. Among them, 25 cases were from Anyang City Cancer Hospital and 23 from Shanxi Province Cancer Hospital. Distal end of the 23 surgical samples was pathologically diagnosed as normal esophageal mucous in morphology. Both areas are high incidence region of ESCC in China. The group included 36 males and 12 females with an average age of 57.4 years.

All the samples were esophageal squamous cell carcinomas. None of the patients had radical therapy or chemotherapy before surgery. The paraffin-embedded, formaldehyde fixed samples were cut into 5 μm slides continuously, one for H&E staining and others for DNA extraction, immunohisochemistry and ISH analysis.

### *DNA extraction and PCR*

The methods were as described previously[13]. Briefly, 5-10

slides were deparaffinized in xylene and graded alcohol, then the lysis buffer (300 mmol/l NaCl;50 mmol/l Tris· HCl pH 8.0; 0.2 % SDS) was added into the tube with proteinase K (200 mg/l), and the solution was incubated at 55 ℃ overnight until it became clear. Then DNA was extracted using phenol/ chloroform, precipitated with cold alcohol, and dissolved in ion-free water and the concentration was determined from its optical density. Quality of the extracted DNA was tested by PCR with β-actin primer: 5' GGC GGC ACC ACC ATG TAC CCT 3' and 5' AGG GGC CGG ACT CGT CAT ACT 3' . The usable DNA went through PCR amplification using primer: 5' -CAAGCAACAGTTACTGCGA-3' and 5' -CAACAAG-ACATACATCGACC-3' targeting HPV-16 E6 gene under conditions at 94 ℃ denaturing for 1 min, at 60 ℃ annealing for 1 min, and at 72 ℃ prolonging for 1 min with 30 cycles.

The PCR product was about 321 bp. The plasmid containing full of length of HPV-16 genome as template was the positive control, and the water as template was the negative control.

### *In situ hybridization assay*

HPV-16 E6 gene by PCR from the plasmid containing full length of HPV-16 was obtained and cloned into PGEM-T easy vector (Promega). After Sal I digestion, a digoxin-labelled E6 probe was made via *in vitro* transcription with the kit (Roche, No, 1175025).

The slides were deparaffinized and hydrated in xylene and graded ethanol continuously, then were treated with 0.2 mol/ L HCl for 10 min at room temperature, followed by digestion with proteinase K 100 mg/l at 37 ℃ for 15 min. Twenty-five to fifty ng probe was added into hybridization solution (50 % formamide, 4×SSC, 5 % dextran sulfate, 5×Denhardt' s solution and 200 g/l denatured salmon sperm DNA), then the solution containing E6 probe was dropped on the slides. The hybridization reaction was completed overnight in wet-chamber at 42 ℃. After this, the slides were washed by 2×SSC, 1×SSC orderly twice, 30 min each time. The anti-digoxin antibody conjugated with alkaline phosphatase was added to the samples for 30 min at 37 ℃. The purple-blue ISH signals were developed by adding substrate NBT/ BCIP (Roche, No, 1175041) on the slides. The slides were incubated with hybridizing solution without E6 probe as negative control, and the cervical cancer biopsies were used as positive control.

### *Immunohistochemical staining for HPV-16 E6*

The sections were deparaffinized in xylene and hydrated in graded ethanol continuously. Then the sections were covered with 3 % hydrogen peroxide in PBS to block the endogenous peroxidase activity for 10 min. The sections were pre-treated in citrate buffer (0.01 M, pH=6.0) under microwave heating for 20 min to retrieve the antigen. Normal goat serum was added to the slides for 30 min at room temperature. After that, the sections were incubated overnight at 4 ℃ with mouse monoclonal primary antibody against HPV-16 E6 (Santa Cruez, sc-460#), while the negative control was incubated with PBS instead of primary antibody under the same conditions. After the slides were washed three times in PBS for 5 min each, the biotinylated goat anti-mouse secondary antibody was added for 30 min followed by the avidin-biotinylated peroxidase complex for another 30 min at room temperature. After being washed with PBS, the slides were stained with DAB, and then counterstained in haematoxylin. The cervical cancer biopsies were used as positive control.

### *Evaluation of ISH and IHC results*

If more than 10 % of epithelial cells in one slide showed the positive signals, the case was regarded as positive. And the data were calculated by $\chi^2$-test. $P<0.05$ was regarded as significant.

## RESULTS

### *PCR analysis*

All the extracted DNA samples showed good quality of DNA after PCR with β-actin primer. After PCR amplification using HPV-16 E6 specific primer, HPV infection was found in tumor patients from both regions, with an infection rate of 80 % in Anyang, and 47.8 % in Shanxi Province (Figure 1 and Table 1).

Furthermore, we detected the positive rate of 34.7 % of HPV-16 DNA in the morphologically normal epithelium adjacent to tumor tissue. But comparing the positive rate of cancer and normal samples, the difference of HPV infection in DNA level was significant (Table 1).

### *ISH and IHC assays*

To identify whether HPV-16 infection can definitely cause mRNA transcription and protein expression of E6 oncogene, we further detected these two levels by ISH and IHC.

Using digoxin-labelled HPV-16 E6 specific cRNA probe, a total of 19 samples showed positive ISH signals in the cytoplasm of cancer cells. Among them, only 2 had nuclear positive signals (Figure 1). And 6 samples from adjacent normal esophageal epithelium were positive for HPV-16.

Among 48 cancer samples from both regions, 13 had HPV-16 E6 protein expression, while only one normal epithelium sample showed IHC positive signals. The difference between cancer and normal epithelia was significant ($P<0.05$, Table 1).

The immunohistochemistry dark-brown signals scattered in the infected cancer cells, was similar to those mentioned before[14] (Figure 2).

**Table 1** HPV-16 infection rate detected by PCR, ISH and IHC in normal and tumor esophageal epithelium from two high-incidence regions in China

| Samples | Region | *n* | PCR | ISH | IHC |
|---|---|---|---|---|---|
| Normal | Shanxi | 23 | 8(34.7%)[a] | 6(26.1%) | 1(4.3%)[a] |
| Tumor | Shanxi | 23 | 11(47.8%) | 6(26.1%) | 5(21.7%) |
| | Anyang | 25 | 20(80.0%) | 13(52.0%) | 8(32.0%) |
| Total | | 48 | 31(64.6%) | 19(39.6%) | 13(27.1%) |

[a]$P<0.05$, from PCR and IHC data, HPV infection rate in normal esophageal epithelium was distinctly different from those in esophageal cancer samples.

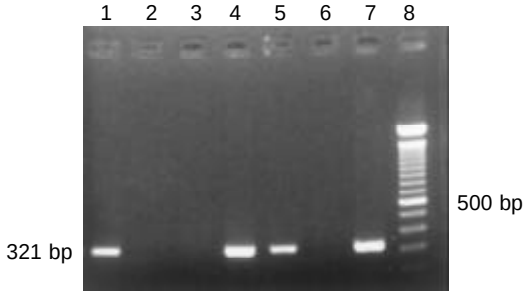


**Figure 1** PCR results of Chinese esophageal cancer samples using HPV-16 E6 specific primer. Lane 1,2 were the positive and negative control; Lane 4,5,7 were the positive samples; Lane 3,6 were the negative samples; Lane 8 was 100 bp ladder.

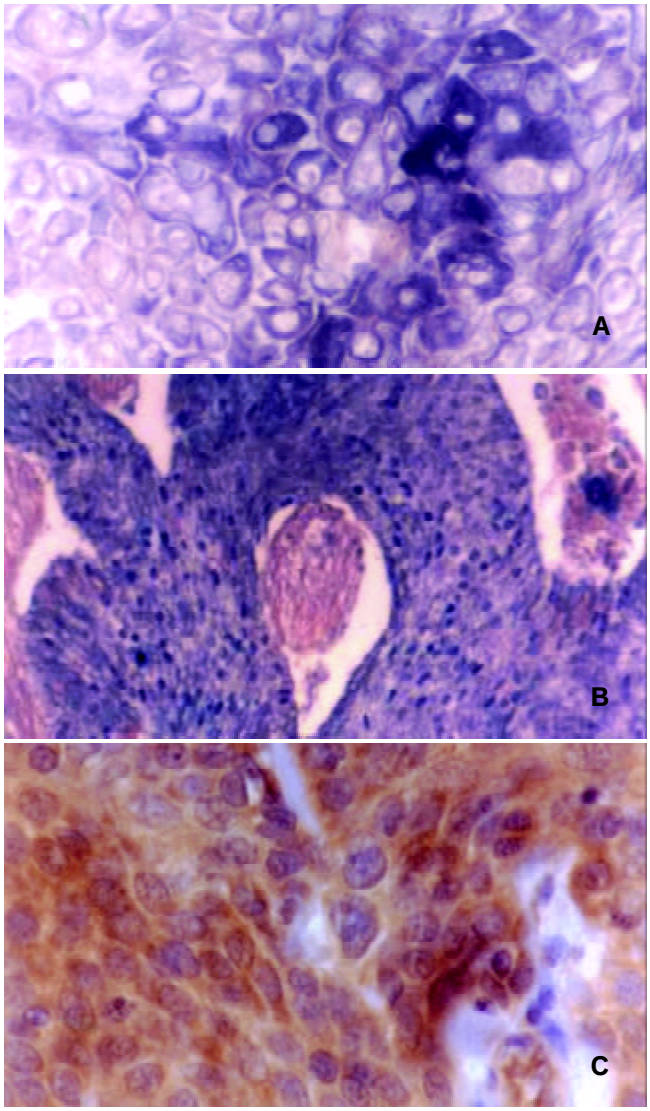


**Figure 2** ISH and IHC results of tumor samples targeting HPV-16 E6 gene. A, the positive purple-blue ISH signal is mainly located in the cytoplasm of esophageal cancer cell. ×200; B, the positive purple-blue ISH signal is mainly located in the nuclear of the carcinoma cell. ×100; C, note the dark-brown IHC signals located mainly in the cytoplasm of cancer cell. SP methods, haematoxylin counterstained ×200.

## DISCUSSION

HPV infection of the esophagus was first suggested by Syrjanen in 1982, who found that 40 % of the esophageal specimens with squamous cell carcinoma presented histological changes identical to those of condylomatous lesions in or around these carcinomas, and demonstrated the presence of HPV antigen in one case of esophageal squamous cell papilloma using immunohistochemistry. This finding was subsequently confirmed by others who demonstrated HPV antigens as well as HPV DNA in benign and malignant esophageal lesions[15-19]. But the infection rate reported in the literature varied largely, such as in India, one of Asian high ESCC regions, the detection rate could reach as high as 67 %[8], while in some Western countries such as France[20], Slovenia[21], Sweden[22], Belgium[23] and Finland[24], the HPV infection rate is close to zero. Based on our previous study[13], and after carefully reviewing the literature, we share the opinion with others[21,25] that HPV infection plays a much more significant role in ESCC in those regions of the world with a high prevalence of disease than in areas with a moderate or low risk[26-28].

Besides the influence of geographic, environmental and racial differences, the sensitivity of the detection techniques and the different methodologies should not be ignored for the variation around the world. For example, consensus L1 primers were frequently used as the proper PCR primers for its ability to detect a wide spectrum of HPV types[12,26,29]. But during virus integration into the host genome, L1 and L2 were often lost. Therefore, the detection using consensus primers against the L1 gene would likely lead to a low rate. This has been demonstrated clearly by our previous and other studies[13,25].

HPV type 16 has been most commonly implicated in ESCC, and in addition, it is known that the E6 amplification system is retained during viral integration into the host genome[25]. In this study, we used specific primer targeting E6 gene of HPV-16 as before[13]. The presence of HPV-16 DNA was found in 65 % tumor patients from Anyang city and Shanxi Province, two high-incidence regions in ESCC in China. Furthermore, E6 mRNA expression of HPV-16 was detected in nearly two-thirds samples among those viral DNA positive patients, while the positive rate of E6 protein expression not found as high as that of mRNA, but still in more than 40 % (13/31) tumor samples, the E6 protein could be detected by IHC when HPV-16 infection occurred among those patients. From this study, it is demonstrated that HPV-16 infection of esophageal epithelium is very common within ESCC patients from Anyang city, and this observation is truly the same as within those from Shanxi Province.

Comparing the status of HPV-16 infection between some adjacent "normal" esophageal epithelium and their tumor samples, the most significant difference was E6 expression at protein level, rather than DNA and mRNA level between them (Table 1). Therefore, it is confirmed that not only existence of the viral DNA, but also the expression of E6 gene may play an important role in the carcinogenesis of ESCC in those high incidence regions.

It is well known that HPV oncogenes expressed in cervical cancer cells are involved in their transformation and immortalization, and are required for the progression towards malignancy[30-35]. In cervical cancer, the knowledge has been firmly established that HPV infection could interfere normal cell cycles by degrading tumor suppressor protein P53 and Rb and cause host genomic instability through its DNA integrating host genome randomly and increasing centrosome number. As for the exact function of HPV infection during the carcinogenesis of ESCC, it is still unclear. But in recent years, more evidences suggested the possible mechanism of high-risk HPV in transforming esophageal epithelial cells, such as induction of HPV on the activity of telomerase[36], interaction of E6 with P53[37] the association of HPV-16 E6 with nuclear matrix[38] and others[39-40].

In conclusion, from our previous study and this study, as well as others, HPV infection should be considered as a risk factor for ESCC, at least in high incidence area in China, and in order to further explore the role of viral DNA infection during the carcinogenesis of ESCC, more works are needed in the future.

## REFERENCES

1 **Wang DX**, Li W. Advances in esophageal neoplasms etiology. *Shijie Huaren Xiaohua Zazhi* 2000; **8**: 1029-1031
2 **Chang F**, Syrjanen S, Wang L, Syrjanen K. Infectious agents in the etiology of esophageal cancer. *Gastroenterology* 1992; **103**: 1336-1348
3 **Heino P**, Eklund C, Fredriksson-Shanazarian V, Goldman S, Schiller JT, Dillner J. Association of serum immunoglobulin G antibodies against human papillomavirus type 16 caspids with anal epidermoid carcinoma. *J Natl Cancer Inst* 1995; **87**: 437-440
4 **Hemminki K**, Jiang Y, Dong C. Second primary cancers after anogenital, skin, oral, esophageal and rectal cancers: etiological links? *Int J Cancer* 2001; **93**: 294-298

5 **Zumbach K**, Hoffmann M, Kahn T, Bosch F, Gottschlich S, Gorogh T, Rudert H, Pawlita M. Antibodies against oncoproteins E6 and E7 of human papillomavirus types 16 and 18 in patients with head-and-neck squamous-cell carcinoma. *Int J Cancer* 2000; **85**: 815-818

6 **Syrjanen KJ**. Histological changes identical to those of condylomatous lesions found in esophageal squamous cell carcinomas. *Arch Geschwustforsch* 1982; **52**: 283-292

7 **Talamini G**, Capelli P, Zamboni G, Mastromauro M, Pasetto M, Castagnini A, Angelini G, Bassi C, Scarpa A. Alcohol, smoking and papillomavirus infection as risk factors for esophageal squamous-cell papilloma and esophageal squamous-cell carcinoma in Italy. *Int J Cancer* 2000; **86**: 874-878

8 **Sobti RC**, Kochar J, Singh K, Bhasin D, Capalash N. Telomerase activation and incidence of HPV in human gastrointestinal tumors in North Indian population. *Mol Cell Biochem* 2001; **217**: 51-56

9 **Han C**, Qiao G, Hubbert NL, Li L, Sun C, Wang Y, Yan M, Xu D, Li Y, Lowy DR, Schiller JT. Serologic association between human papillomavirus type 16 infection and esophageal cancer in Shannxi province, China. *J Natl Cancer Inst* 1996; **88**: 1467-1471

10 **Bjorge T**, Hakulinen T, Engeland A, Jellum E, Koskela P, Lehtinen M, Luostarinen T, Paavonen J, Sapp M, Schiller J, Thoresen S, Wang Z, Youngman L, Dillner J. A prospective, seroepidemiological study of the role of human papillomavirus in esophageal cancer in Norway. *Cancer Res* 1997; **57**: 3989-3992

11 **Tripodi S**, Chang F, Syrjanen S, Shen Q, Cintorino M, Alia L, Santopietro R, Tosi P, Syrjanen K. Quantitative image analysis of oesophageal squamous cell carcinoma from the high-incidence area of China, with special reference to tumour progression and papillomavirus (HPV) involvement. *Anticancer Res* 2000; **20**: 3855-3862

12 **Kawaguchi H**, Ohno S, Araki K, Miyazaki M, Saeki H, Watanabe M, Tanaka S, Sugimachi K. p53 polymorphism in human papillomavirus-associated esophageal cancer. *Cancer Res* 2000; **60**: 2753-2755

13 **Li T**, Lu ZM, Chen KN, Guo M, Xing HP, Mei Q, Yang HH, Lechner JF, Ke Y. Human papillomavirus type 16 is an important infectios factos in the high incidence of esophageal cancer in Anyang area of China. *Carcinogensis* 2001; **22**: 929-934

14 **Kim KH**, Yoon DJ, Moon YA, Kim YS. Expression and localization of human papillomavirus type 16 E6 and E7 open reading frame proteins in human epidermal keratinocyte. *Yonsei Med J* 1994; **35**: 1-9

15 **Chang F**, Syrjanen S, Shen Q, Cintorino M, Santopietro R, Tosi P, Syrjanen K. Human papillomavirus involvement in esophageal carcinogenesis in the high-incidence area of China. A study of 700 cases by screening and type-specific in situ hybridization *Scand J Gastroenterol* 2000; **35**: 123-130

16 **Chang F**, Syrjanen S, Shen Q, Ji HX, Syrjanen K. Human papillomavirus(HPV) DNA in esophageal precancer lesions and squamous cell carcinomas from China. *Int J Cancer* 1990; **45**: 21-25

17 **Ravakhah K**, Midamba F, West BC. Esophageal papillomatosis from human papilloma virus proven by polymerase chain reaction. *Am J Med Sci* 1998; **316**: 285-288

18 **Agarwal SK**, Chatterji A, Bhambhani S, Sharma BK. Immunohistochemical co-expression of human papillomavirus type 16/18 transforming (E6) oncoprotein and p53 tumour suppressor gene proteins in oesophageal cancer. *Indian J Exp Biol* 1998; **36**: 559-563

19 **Syrjanen KJ**. HPV infections and oesophageal cancer. *J Clin Pathol* 2002; **55**: 721-728

20 **Benamouzig R**, Jullian E, Chang F, Robaskiewicz M, Flejou JF, Raoul JL, Coste T, Couturier D, Pompidou A, Rautureau J. Absence of human papillomavirus DNA detected by polymerase chain reaction in French patients with esophageal carcinoma *Gastroenterology* 1995; **109**: 1876-1881

21 **Poljak M**, Cerar A, Seme K. Human papillomavirus infection in esophageal carcinomas: a study of 121 lesions using multiple broad-spectrum polymerase chain reactions and literature review. *Hum Pathol* 1998; **29**: 266-271

22 **Lagergren J**, Wang Z, Bergstrom R, Dillner J, Nyren O. Human papillomavirus infection and esophageal cancer: a nationwide seroepidemiologic case-control study in Sweden. *J Natl Cancer Inst* 1999; **91**: 156-162

23 **Lambot MA**, Haot J, Peny MO, Fayt I, Noel JC. Evaluation of the role of human papillomavirus in oesophageal squamous cell carcinoma in Belgium. *Acta Gastroenterol Belg* 2000; **63**: 154-156

24 **Chang F**, Janatuinen E, Pikkarainen P, Syrjanen S, Syrjanen K. Esophageal squamous cell papillomas. Failure to detect human papillomavirus DNA by in situ hybridization and polymerase chain reaction. *Scand J Gastroenterol* 1991**; 26**: 535-543

25 **Sur M**, Cooper K. The role of the human papillomavirus in esophageal cancer. *Pathology* 1998; **30**: 348-354

26 **Lavergne D**, de Villiers EM. Papillomavirus in esophageal papillomas and carcinomas. *Int J Cancer* 1999; **80**: 681-684

27 **Ma QF**, Jiang H, Feng YQ, Wang XP, Zhou YA, Liu K, Jia ZL. Detection of human papillomavirus DNA in squamous cell carcinoma of the esophagus. *Shijie Huaren Xiaohua Zazhi* 2000; **8**: 1218-1224

28 **Liu J**, Su Qin, Zhang W. Relationship between HPV-E6, p53 protein and esophageal squamous cell carcinoma. *Shijie Huaren Xiaohua Zazhi* 2000; **8**: 494-496

29 **Peixoto Guimaraes D**, Hsin Lu S, Snijders P, Wilmotte R, Herrero R, Lenoir G, Montesano R, Meijer CJ, Walboomers J, Hainaut P. Absence of association between HPV DNA, TP53 codon 72 polymorphism, and risk of oesophageal cancer in a high-risk area of China. *Cancer Lett* 2001; **162**: 231-235

30 **Zur Hausen H**. Immortalization of human cells and their malignant conversion by high risk human papillomavirus genotypes. *Semin Cancer Biol* 1999; **9**: 405-411

31 **Zur Hausen H**. Papillomaviruses and cancer: from basic studies to clinical application. *Nat Rev Cancer* 2002; **2**: 342-350

32 **Duensing S**, Munger K. Human papillomaviruses and centrosome duplication errors: modeling the origins of genomic instability. *Oncogene* 2002; **21**: 6241-6248

33 **Munger K**. The role of human papillomaviruses in human cancers. *Front Biosc* 2002; **7**: d641-649

34 **Cottage A**, Dowen S, Roberts I, Pett M, Coleman N, Stanley M. Early genetic events in HPV immortalized keratinocytes. *Genes Chromosomes Cancer* 2001; **30**: 72-79

35 **Duensing S**, Munger K. Centrosome abnormalities, genomic instability and carcinogenic progression. *Biochim Biophys Acta* 2001; **1471**: M81-88

36 **Shen ZY**, Xu LY, Li C, Cai WJ, Shen J, Chen JY, Zeng Y. A comparative study of telomerase activity and malignant phenotype in multistage carcinogenesis of esophageal epithelial cells induced by human papilomavirus. *Int J Mol Med* 2001; **8**: 633-639

37 **Zou JX**, Wang LD, Shi ST, Yang GY, Xue ZH, Gao SS, Li YX, Yang CS. p53 gene mutations in multifocal esophageal precancerous and cancerous lesions in patients with esophageal cancer in high -risk northern China. *Shijie Huaren Xiaohua Zazhi* 1999**; 7**: 280-284

38 **Chen HB**, Chen L, Zhang JK, Shen ZY, Su ZJ, Cheng SB, Chew EC. Human papillomavirus 16 E6 is associated with the nuclear matrix of esophageal carcinoma cells. *World J Gastroenterol* 2001; **7**: 788-791

39 **Shen Z**, Cen S, Shen J, Cai W, Xu J, Teng Z, Hu Z, Zeng Y. Study of immortalization and malignant transformation of human embryonic esophageal epithelial cells induced by HPV18 E6E7: *J Cancer Res Clin Oncol* 2000; **126**: 589-594

40 **Zou SY**, Liu XM, Tang XP, Wang P. Immunohistochemical and electron microscopic observation on positive HPV-16-E6 protein in esophageal cancer. *Huaren Xiaohua Zazhi* 1998; **6**: 47-48


**Edited by** Ma JY

P.O.Box 2345, Beijing 100023,China
Fax: +86-10-85381893
E-mail: wjg@wjgnet.com www.wjgnet.com

World J Gastroenterol 2003;9(6):1174-1178
World Journal of Gastroenterology
Copyright ©2003 by The WJG Press ISSN 1007-9327

• ESOPHAGEAL CANCER •

# Expression of ECRG4, a novel esophageal cancer-related gene, downregulated by CpG island hypermethylation in human esophageal squamous cell carcinoma

Chun-Mei Yue, Da-Jun Deng, Mei-Xia Bi, Li-Ping Guo, Shih-Hsin Lu

**Chun-Mei Yue, Mei-Xia Bi, Li-Ping Guo, Shih-Hsin Lu,** Department of Etiology and Carcinogenesis, Cancer Institute, Peking Union Medical College and Chinese Academy of Medical Sciences, Beijing, 100021, China
**Da-Jun Deng,** Beijing Institute for Cancer Research, School of Oncology, Peking University, Beijing, 100034, China
**Supported by** grant from State Key Basic Program (G1998051204) and from the Ministry of Education, China
**Correspondence to:** Shih-Hsin Lu, Department of Etiology and Carcinogenesis, Cancer Institute, Chinese Academy of Medical Sciences, Beijing 100021, China. shlu@public.bta.net.cn
**Telephone:** +86-10-67712368 **Fax:** +86-10-67712368
**Received:** 2003-03-02 **Accepted:** 2003-03-29

## Abstract

**AIM:** To study the mechanisms responsible for inactivation of a novel esophageal cancer related gene 4 (ECRG4) in esophageal squamous cell carcinoma (ESCC).

**METHODS:** A pair of primers was designed to amplify a 220 bp fragment, which contains 16 CpG sites in the core promoter region of the *ECRG 4* gene. PCR products of bisulfite-modified CpG islands were analyzed by denaturing high-performance liquid chromatography (DHPLC), which were confirmed by DNA sequencing. The methylation status of *ECRG 4* promoter in 20 cases of esophageal cancer and the adjacent normal tissues, 5 human tumor cell lines (esophageal cancer cell line-NEC, EC109, EC9706; gastric cancer cell line- GLC; human embryo kidney cell line-Hek293) and 2 normal esophagus tissues were detected. The expression level of the *ECRG 4* gene in these samples was examined by RT-PCR.

**RESULTS:** The expression level of *ECRG 4* gene was varied. Of 20 esophageal cancer tissues, nine were unexpressed, six were lowly expressed and five were highly expressed compared with the adjacent tissues and the 2 normal esophageal epithelia. In addition, 4 out of the 5 human cell lines were also unexpressed. A high frequency of methylation was revealed in 12 (8 unexpressed and 4 lowly expressed) of the 15 (80 %) downregulated cancer tissues and 3 of the 4 unexpressed cell lines. No methylation peak was observed in the two highly expressed normal esophageal epithelia and the methylation frequency was low (3/20) among the 20 cases in the highly expressed adjacent tissues. The methylation status of the samples was consistent with the result of DNA sequencing.

**CONCLUSION:** These results indicate that the inactivation of *ECRG 4* gene by hypermethylation is a frequent molecular event in ESCC and may be involved in the carcinogenesis of this cancer.

Yue CM, Deng DJ, Bi MX, Guo LP, Lu SH. Expression of ECRG4, a novel esophageal cancer-related gene, downregulated by CpG island hypermethylation in human esophageal squamous cell carcinoma. *World J Gastroenterol* 2003; 9(6): 1174-1178
http://www.wjgnet.com/1007-9327/9/1174.asp

## INTRODUCTION

Esophageal cancer (EC) is one of the most common malignant tumors in the world. Previous studies have shown several genetic abnormalities including amplification of *c-myc*, *int-2* and *Hst*, mutation and/or deletion of *p53* and *Rb* in human EC and EC cell lines[1,2]. However, the genetic events leading to the development of EC are not clear yet. In recent years, many studies of EC focused on the clone and identification of novel EC-related genes, which might play an important role in the carcinogenesis and development of esophageal cancer[3-5].

Recently, we have cloned and identified a novel tumor candidate suppressor gene, *ECRG 4* (Genbank Accession NO. AF 325503), from human normal esophageal epithelium[6, 7]. The *ECRG 4* gene located in chromosome 2q14.1-14.3 contains 4 exons, spans about 13 kb and has a full-length cDNA of 772 bp. Analysis by bioinformatics has shown that the protein coded by *ECRG 4* shows a 31 % homology with mouse IgG V region. The results of SAGE and RT-PCR detection have demonstrated the *ECRG 4* gene is expressed in adult esophageal epithelium but is downregulated in esophageal squamous cell carcinoma (ESCC) and tumor cell lines. These findings suggest that the *ECRG 4* gene might be involved in the development of ESCC, but the mechanism inactivating it remains to be determined.

According to the result of the sequence analysis in *ECRG 4* gene, we found that there were CpG islands in the promoter region, exon 1 and part of intron 1 of the gene. Many tumor suppressor genes are downregulated by promoter methylation during the development and progression of cancer, and hypermethylation of gene-promoter regions is being revealed as one of the most frequent mechanisms in loss of gene function, thus detection of CpG methylation is important to understand the gene regulation of cancer[8, 9]. It has been reported that the expression of some tumor suppressor genes, such as $p16^{INK4a}$, *p16INK4b*, *FHIT* and *E-cadherin* are commonly downregulated by CpG island hypermethylation in ESCC[10-13]. However, the reason for reducing expression of *ECRG 4* in ESCC is unknown.

In order to determine the mechanism involved in the downregulation of *ECRG 4* in ESCC, we have examined the methylation status of the 5' CpG island in promoter region of the *ECRG 4* gene in 5 human cell lines, which include 3 esophageal cancer cell lines, 2 normal esophageal epithelia and 20 cases with ESCC and adjacent tissues. The methylation status of the cell lines and tissues were compared with the expression of the *ECRG 4* gene in the same samples by RT-PCR respectively.

## MATERIALS AND METHODS

### *Cell lines and tissue samples*

Five cell lines, including 3 esophageal cancer cell line-NEC,

EC109 and EC9706; 1 gastric cancer cell line- GLC and 1 human embryo kidney cell line-Hek293 were used in this study. All cell lines were routinely cultured in 1640 medium (Gibco) supplemented with 10 % fetal bovine serum (Hyclone) at 37 ℃ with 5 % $CO_2$. 20 pairs of ESCC and corresponding tissues adjacent to the tumors were obtained from surgically removed specimens of individual patients who underwent an operation at the Cancer Hospital in Linxian County which has the highest age-adjusted mortality rate of this cancer. Two normal esophageal epithelia were collected from healthy individuals by biopsy. All the samples were frozen at -70 ℃ before RNA and DNA were extracted with standard method as described previously[14].

### *Bisulfite treatment of DNA*

Genomic DNA was treated with sodium bisulfite as described by Herman *et al*[15]. Briefly, 1 g DNA was denatured by adding freshly prepared NaOH with the final concentration 0.3 M for 15 min in a 37 ℃ water bath. The denatured DNA was then diluted in 30 μl freshly prepared 10 mM hydroquinone (Sigma) and 520 μl freshly prepared 3 M sodium bisulfite (Sigma) at pH 5.0. The DNA was incubated at 50 ℃ for 16 h and subsequently purified by the Wizard DNA Clean-Up System Kit (A7280; Promega).

20 μg of human placenta genomic DNA was incubated for 24 h with 20 units of *SssI* (New England Biolabs) as described in the instruction manual and the methylated DNA was treated by bisulfite and purified by the Wizard DNA Clean-Up System Kit (A7280; Promega) as described above.

### *Design of primers and SsPCR condition*

Primers were designed according to the CpG island of the sense strand of the *ECRG 4* gene. The strand-specific primers for the treated CpG island were used to amplify a 220 bp fragment containing 16 CpG sites and 4 cis-acting elements, and they were: 5' -AGT GGG GGA GTT AAG GAG ATA TT -3' (forward), and 5' -CCC CTA AAC TCC AAA ACC AA-3' (reverse). PCR was performed in a GeneAmp 2400 thermocycler (Perkin-Elmer, Norwalk, CT) with a 25 μl reaction mixture containing about 100 ng DNA, 1.6 μmol each primer, 400 μmol each dNTPs, 1.25 U LA Taq with 1× LA reaction buffer (TaKaRa). Thermal cycles were: at 94 ℃ for 2 min, then 40 cycles at 94 ℃ for 30 sec, at 52 ℃ for 30 sec, at 72 ℃ for l min and 30 sec followed by extension at 72 ℃ for 7 min. The PCR products were detected in 1.5 % agarose gels.

### *Analysis for methylation by DHPLC*

The ssPCR products of *ECRG 4* were introduced into the mobile phase at an injection volume of 5 μl by the autosampler on a WAVE DNA Fragment Analysis System (Transgenomic) identical to that described by Deng *et al*[16]. Non-denaturing analysis was conducted at 48 ℃ and partially denaturing analysis was conducted at 56 ℃, which was predicted by WAVEMaker.

The ssPCR product from the *SssI* and bisulfite treated human placenta genomic DNA was the positive control of the experiment.

### *DNA cloning and sequencing*

The PCR products amplified with primers specific either for the methylated or for the unmethylated DNA were purified and cloned into the pMD18-T Easy Vector (Promega) and sequenced on an ABI 377 automated sequencer (Applied Biosystems) by using M13 primers.

### *RT-PCR detection*

Total RNA was isolated from cells and tissues using Trizol reagent (Invitrogen). Reverse transcription was carried out with the SuperScript TM First-Strand Synthesis System (Invitrogen). Approximately 3 μg total RNA was used in each reverse transcription reaction and the final volume was 20 μl. The ORF of *ECRG 4* gene was amplified using the primers 5' -GGT TCT CCC TCG CAG CAC CT-3' (forward), and 5' -CAG CGT GTG GCA AGT CAT GGT TAG T-3' (reverse). PCR was performed in a GeneAmp 2400 thermocycler (Perkin-Elmer, Norwalk, CT) with a 25 μl reaction mixture containing 1 μl reverse transcription products, 200 pmol each primer, 200 μmol each dNTPs, 1.5 mM $Mg^{2+}$, 2.0 U PLATINUM pfx DNA polymerase with 1×reaction buffer (Promega). Thermal cycles were: at 95 ℃ for 2 min, then 30 cycles at 95 ℃ for 30 sec, at 62 ℃ for 30 sec, at 72 ℃ for l min followed by extension at 72 ℃ for 7 min. The β-actin transcripts in each sample were also amplified as internal controls to normalize the amount of *ECRG 4* specific products.

## RESULTS

### *The promoter hypermethylation in ECRG 4 gene*

Based on the flanking DNA sequences of the *ECRG 4*-core promoter region, PCR primers were designed to amplify a 220 bp fragment containing the 16 CpG sites (Figure 1). Using the ssPCR-specific primers, a 220 bp product was successfully obtained from each bisulfite-treated sample, which was detected by 1.5 % agarose gels and DHPLC size analysis, and the specific band (Figure 2) and the single chromatogram peak (Figure 3) were obtained respectively. The agarose gel detection and the size analysis on DHPLC all indicating the quality and quantity of the ssPCR products were high and the products could be used in the methylation analysis on DHPLC. Figure 4a shows the detection of methylated and unmethylated CpG islands in ssPCR products by DHPLC. Compared with the peak of positive control from the *SssI* treated human fetal DNA, the methylated and unmethylated samples could be easily discerned. The different proportion of methylated peak represented the different methylation levels in different samples. To confirm the reliability of the ssPCR products of

agtgg**gggag c**caaggagac acccag**cg**c tgggatc**cg**g caagtcctcc ctc**tgagtgg**
CAAT box CAAT
**ccagg**gggcc t**cg**tcccttc tcc**cg**atgcc ttctgccctt ccttgggtct c**cg**gaaccca
box
gcttgt**ccta accgctttcg ct**g**cg**ggcag **cg**ctggcca**c gcg**gcccc**cg** c**cg**c**cg**g**cg**g
BARBIE box
ttctc**cgtgg ccaagc**atcc ttggccttgg agcccagggg
CAAT box

**Figure 1** The sequence of *ECRG 4* fregment for bisulfite- DHPLC analysis. The fragment contains 4 cis-acting elements and 16 CpG sites in shadow. The 5'and 3' primers are in the frames of the two ends of the fragment respectively.

the *ECRG4* promoter region, either the methylated or the unmethylated DNA was cloned and sequenced (Figure 5). The cytosines in the CpG sites of methylated ssPCR products remained unchanged, but the cytosines of unmethylated products were converted to thymines. The promoter methylation of ECRG4 gene in esophageal tissues is shown in Table 1. A high frequency of methylation was observed in 12 cancer tissues, 3 tumor adjacent tissues and 3 cell lines (EC 9706, EC 109 and GLC). No methylation peak was obtained in the two normal esophageal epithelia, the other tumor and adjacent tissues and the two cell lines (NEC and Hek293).

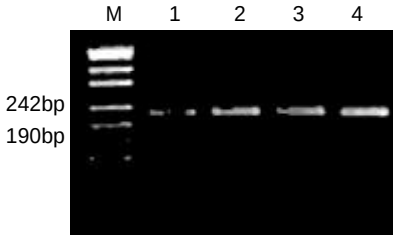


**Figure 2** The 1.5 % agarose gel detection of the ssPCR products of *ECRG 4*. M; pUC19 DNA / *Msp I Hap II)* Marker. 1, 2, 3, 4; four tissue samples.

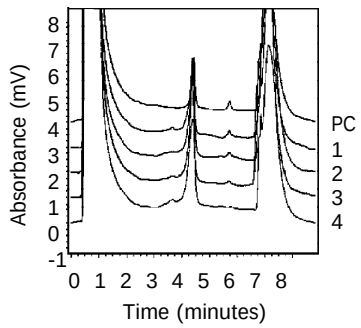


**Figure 3** The sizing analysis of ssPCR products of *ECRG 4* on DHPLC at 48 ℃. PC was the product from the *Sss I* treated human placenta genomic DNA. 1, 2, 3, 4; the same samples as in Figure 2.

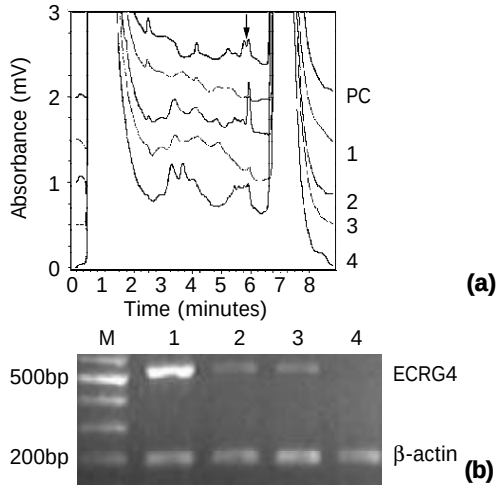


**Figure 4 (a)** The methylation detection of ssPCR products at 56 ℃ on DHPLC. The methylation peak was emphasized by the arrow. PC was the product from the *SssI* treated human placenta genomic DNA. 1, 2, 3, 4; the same samples as Figure 2. **(b)** The expression level of *ECRG 4* by RT-PCR using the primer set flanking the ORF of the gene in the same samples was detected on DHPLC. The β-Actin gene was amplified as internal control. M; 1 kb DNA Ladder Marker. 1, 2, 3, 4; the same samples as Figure 2.

The expression level of *ECRG 4* gene was different, and a high frequency of methylation was revealed in 12 (8 unexpressed and 4 lowly expressed) of the 15 (80 %) cancer tissues and the 3 of the 4 unexpressed cell lines. No methylation peak was observed in the two highly expressed normal esophageal epithelia and the methylation frequency was low (3/20) among the 20 cases in the highly expressed adjacent tissues.

### *Expression of ECRG4 gene related to methylation*

The expression level of the *ECRG 4* gene in the tissues and cell lines was examined by RT-PCR (Figure 4b). Out of 20 esophageal cancer tissues, nine were unexpressed, six were lowly expressed and five were highly expressed compared with the adjacent tissues and the 2 normal esophageal epithelia. In addition, 4 out of the 5 human cell lines were also unexpressed. The methylation was observed in 12 (8 unexpressed and 4 lowly expressed) of the 15 (80.0 %) cancer tissues and the 3 unexpressed cell lines (Table 1 and Table 2). Among the normal tissues corresponding to the 12-methylation cancer tissues, nine were highly expressed and unmethylated; three were lowly expressed or unexpressed and methylated (Table 1). No methylation peak was obtained in the highly expressed samples, including the two normal esophageal epithelia, the cell line Hek293 and the other tumor and adjacent tissues. The results demonstrated that the expression of ECRG4 was downregulated by CpG island hypermethylation in human esophageal squamous cell carcinoma.

**Table 1** The expression and methylation of *ECRG 4* in ESCC

| Cases | Gender | Pathological stage | Expression | | Methylation | |
|---|---|---|---|---|---|---|
| | | | Normal | Cancer | Normal | Cancer |
| N1 | F[a] | | | ++[c] | | - |
| N2 | F | | | ++ | | - |
| 1 | M[b] | Moderate | ++ | +[d] | -[f] | +[g] |
| 2 | F | Moderate | + | - | - | + |
| 3 | M | Moderate | ++ | ++ | - | - |
| 4 | M | Moderate | ++ | ++ | - | - |
| 5 | F | Moderate | ++ | -[e] | - | + |
| 6 | F | Moderate | + | + | + | + |
| 7 | M | Moderate | ++ | ++ | - | - |
| 8 | F | Poor | ++ | - | - | + |
| 9 | M | Moderate | ++ | ++ | - | - |
| 10 | M | Poor | ++ | - | - | + |
| 11 | F | Moderate | + | + | + | + |
| 12 | F | Moderate | ++ | - | - | + |
| 13 | F | Moderate | ++ | ++ | - | - |
| 14 | M | Moderate | ++ | + | - | + |
| 15 | M | Moderate | ++ | - | - | + |
| 16 | F | Moderate | ++ | - | - | + |
| 17 | M | Moderate | - | - | + | - |
| 18 | F | Moderate | ++ | + | - | - |
| 19 | M | Moderate | ++ | + | - | - |
| 20 | M | Moderate | ++ | - | - | + |

[a], Female; [b], Male; [c]++, high expression; [d]+, low expression; [e]-, unexpression; [f]-, unmethylation; [g]+, methylation.

**Table 2** The expression and methylation of *ECRG 4* in cell lines

| Cell lines | Expression | Methylation |
|---|---|---|
| NEC | -[a] | -[c] |
| EC109 | - | +[d] |
| EC9706 | - | + |
| GLC | - | + |
| Hek293 | +[b] | - |

[a]-, unexpression; [b]+, expression; [c]-, unmethylation; [d]+,methylation.

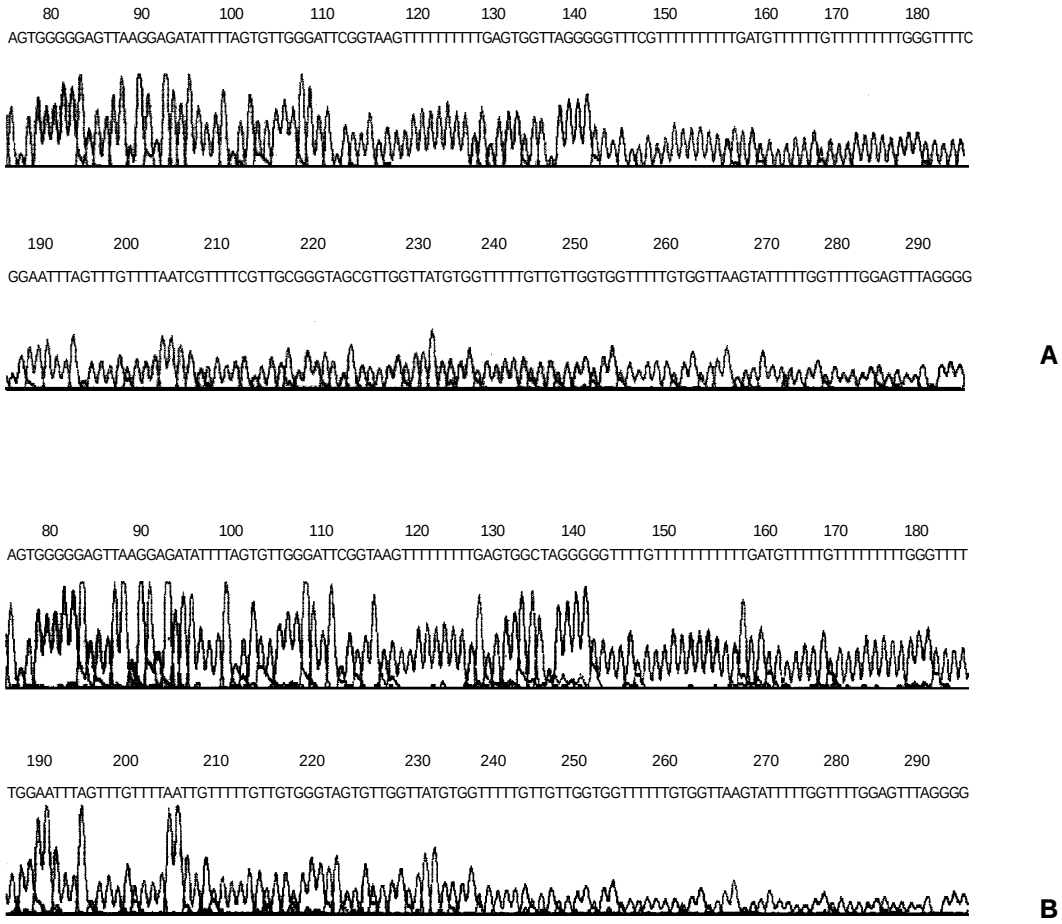


**Figure 5** Sequencing of ssPCR products of the ECRG4 gene promoter region. All cytosines in CpG dinuleotides in the methylated ECRG4 remain as cytosines, indicating methylation (**A**), while all cytosines in unmethylated ECRG4 have been converted to thymidines, indicating unmethylation (**B**).

## DISCUSSION

We used a high-throughout methylation assay, bisulfite-DHPLC assay to examine the methylation status of the *ECRG 4* gene promoter in ESCC. The results demonstrated for the first time that downregulated expression of *ECRG 4* in ESCC was associated with CpG island methylation in the core promoter region of the gene. These findings suggest that inactivation by the promoter hypermethylation of *ECRG 4* is a common molecular event in ESCC and it may be involved in the development of this cancer, since this epigenetic change of the *ECRG 4* gene was not found in the normal epithelium and immortalling cell line Hek293. Eads *et al* reported that DNA hypermethylation was an early epigenetic alteration in the multistep progression of the esophageal adenocarcinoma, because they found that the premalignant tissue was significantly more methylated than the normal tissue[17]. Then, we can speculate that the inactivation by hypermethylation of *ECRG 4* might be an early event in the progression of ESCC carcinogenesis.

Because of the extent of methylation at various CpG sites of most genes, especially a novelly identified gene is unknown, it is hard to design good MSP primers or MethyLight probes for methylated templates, which require full methylation at all CpG sites in their mating region[15,18]. However, the ssPCR for bisulfite-modified templates are not influenced by the extent of methylation of CpGs, because no CpG site exits in the primer sequence and the primer for modified DNA can amplify both methylated and unmethylated templates. Deng *et al* had compared the bisulfite-DHPLC with other methylation detection method, and demonstrated the bisulfite-DHPLC assay could be used to detect methylation in homoallelic and heteroallelic CpG islands in cell lines and tissues rapidly and reliably[16]. In the present study, we also confirmed the reliability of bisulfite-DHPLC assay by DNA sequencing.

Abnormal hypermethylation of CpG islands associated with tumor suppressor genes can lead to repression of gene expression and contribute significantly to tumorigenesis of many kinds of tumors, such as esophageal cancer, gastric cancer, lung cancer, breast cancer and cervical cancer[19-23]. Furthermore, each tumor type has a characteristic set of genes with an increased propensity to become methylated, and an individual tumor within a single patient has a unique epigenetic fingerprint[24]. Determining tumor-type specific and patient-specific fingerprints may provide biomarkers that can be used in diagnosis, such as cancer detection, cancer chemoprediction and prognostics[25, 26]. The recent study has been repleted with the examples of hypermethylation of CpG islands in the promoter region of more than 40 lung cancer related genes to analyse methylation patterns of multiple genes. They want to obtain complex DNA methylation signatures, which can provide a useful and highly specific tool for lung cancer diagnosis[27].

The promoter hypermethlation of the ESCC-related genes such as, *p16$^{INK4a}$*, *p15INK4b*, *hMLH1*, *E-cadherin*, *Chfr* and HLA class I genes, has been shown to be a common epigenetic event in this cancer and the studies of these genes suggest that hypermethylation of key genes may be used in combination with other molecular changes, such as *p53* mutation, in the development of biomarkers for predicting the risk for ESCC[28-30]. Our present study extended the findings of methylation signature in ESCC, and the methylation in more ESCC-related genes was studied, better understaning of the mechanisms underlying tumor progression in this cancer was

obtained, so that improved diagnosis and therapy can be facilitated.

In summary, our study demonstrated that aberrant methylation of CpG islands in the core promoter of the *ECRG 4* gene was a frequent molecular event in ESCC and proved for the first time that loss or lower expression of *ECRG 4* was associated with *ECRG 4* CpG island methylation. These results indicate that the inactivation of *ECRG 4* gene by hypermethylation in ESCC may be involved in the carcinogenesis of the cancer.

## REFERENCES


1 **Lu SH.** Alterations of oncogenes and tumor suppressor genes in esophageal cancer in China. *Mutat Res* 2000; **462:** 343-353

2 **Lu SH,** Hsieh LL, Luo FC, Weinstein IB. Amplification of the EGF receptor and *c-myc* genes in human esophageal cancer. *Int J Cancer* 1988; **42:** 502-505

3 **Yang ZQ,** Imoto I, Fukuda Y, Pimkhaokham A, Shimada Y, Imamura M, Sugano S, Nakamura Y, Inazawa J. Identification of a novel gene, *GASC1*, within an amplicon at 9p23-24 frequently detected in esophageal cancer cell lines. *Cancer Res* 2000; **60:** 4735-4739

4 **Daigo Y,** Nishiwaki T, Kawasoe T, Tamari M, Tsuchiya E, Nakamura Y. Molecular cloning of a candidate tumor suppressor gene, *DLC1*, from chromosome 3p21.3. *Cancer Res* 1999; **59:** 1966-1972

5 **Sasaki S,** Nakamura T, Arakawa H, Mori M, Watanabe T, Nagawa H, Croce CM. Isolation and characterization of a novel gene, *hRFI*, preferentially expressed in esophageal cancer. *Oncogene* 2002; **21:** 5024-5030

6 **Su T,** Liu HL, Lu SX, Zhao XJ, Zhou CX, Jin SQ. Cloning and identification of cDNA fragment related to human esophageal cancer. *Chinese J Oncology* 1998; **20:** 254-257

7 **Bi MX,** Han WD, Lu SX. Using lab on-line to clone and identify the esophageal cancer related gene 4. *Acta Biochimicaet Biophysica Sinica* 2001; **33:** 257-261

8 **Jones PA.** DNA methylation and cancer. *Oncogene* 2002; **21:** 5358-5360

9 **Esteller M.** CpG island hypermethylation and tumor suppressor genes: a booming present, a bright future. *Oncogene* 2002; **21:** 5427-5440

10 **Xing EP,** Nie Y, Song Y, Yang GY, Cai YC, Wang LD, Yang CS. Mechanisms of inactivation of *p14ARF*, *$p15^{INK4b}$* and *p16INK4a* genes in human esophageal squamous cell carcinoma. *Clin Cancer Res* 1999; **5:** 2704-2713

11 **Wong DJ,** Barrett MT, Stoger R, Emond MJ, Reid BJ. *$P16^{INK4a}$* promoter is hypermethylated at a high frequency in esophageal adenocarcinomas. *Cancer Res* 1997; **57:** 2619-2622

12 **Si HX,** Tsao SW, Lam KY, Srivastava G, Liu Y, Wong YC, Shen ZY. E-cadherin expression is commonly downregulated by CpG island hypermethylation in esophageal carcinoma cells. *Cancer Lett* 2001; **173:** 71-78

13 **Tanaka H,** Shimada Y, Harada H, Shinoda M, Hatooka S, Imamura M, Ishizaki K. Methylation of the 5' CpG island of the FHIT gene is closely associated with transcriptional inactivation in esophageal squamous cell carcinomas. *Cancer Res* 1998; **58:** 3429-3434

14 **Blin N,** Stafford DW. A general method for isolation of high molecular weight DNA from eukaryotes. *Nucleic Acid Res* 1976; **3:** 2303-2308

15 **Herman JG,** Graff JR, Myohanen S, Nelkin BD, Baylin SB. Methylation-specific PCR: a novel PCR assay for methylation status of CpG islands. *Proc Natl Acad Sci USA* 1996; **93:** 9821-9826

16 **Deng DJ,** Deng GR, Smith MF, Zhou J, Xin HJ, Powell SM, Lu YY. Simultaneous detection of CpG methylation and single nucleotide polymorphism by denaturing high performance liquid chromatography. *Nucleic Acid Res* 2002; **30:** e13

17 **Eads CA,** Lord RV, Wickramasinghe K, Long TI, Kurumboor SK, Bernstein L, Peters JH, DeMeester SR, DeMeeste TR, Skinner KA, Laird PW. Epigenetic patterns in the progression of esophageal adenocarcinoma. *Cancer Res* 2001; **61:** 3410-3418

18 **Eads CA,** Danenberg KD, Kawakami K, Saltz LB, Blake C, Shibata D, Danenberg PV, Laird PW. MethyLight: a high-throughout assay to measure DNA methylation. *Nucleic Acid Res* 2000; **28:** e32

19 **Tokugawa T,** Sugihara H, Tani T, Hattori T. Modes of silencing of *p16* in development of esophageal squamous cell carcinoma. *Cancer Res* 2002; **62:** 4938-4944

20 **Oue N,** Shigeishi H, Kuniyasu H, Yokozaki H, Yuraoka K, Ito R, Yasui W. Promoter hypermethylation of *MGMT* is associated with protein loss in gastric carcinoma. *Int J Cancer* 2001; **93:** 805-809

21 **Palmisano WA,** Divine KK, Saccomanno G, Gilliland FD, Baylin SB, Herman JG, Belinsky SA. Predicting lung cancer by detecting aberrant promoter methylation in sputum. *Cancer Res* 2000; **60:** 5954-5958

22 **Widschwendter M,** Jones PA. DNA methylation and breast carcinogenesis. *Oncogene* 2002; **21:** 5462-5482

23 **Virmani AK,** Muller C, Rathi A, Zoechbauer-Mueller S, Mathis M, Gazdar AF. Aberrant methylation during cervical carcinogenesis. *Clin Cancer Res* 2001; **7:** 584-589

24 **Costello JF,** Fruhwald MC, Smiraglia DJ, Rush LJ, Robertson GP, Gao X, Wright FA, Feramisco JD, Peltomaki P, Lang JC, Schuller DE, Yu L, Bloomfield CD, Caligiuri MA, Yates A, Nishikawa R, Su HH, Petrelli NJ, Zhang X, O'Dorisio MS, Held WA, Cavenee WK, Plass C. Aberrant CpG-island methylation has non-random and tumor-type-specific patterns. *Nat Genet* 2000; **24:** 132-138

25 **Jones PA,** Laird PW. Cancer epigenetics comes of age. *Nat Genet* 1999; **21:** 163-167

26 **Beck S,** Olek A, Walter J. From genomics to epigenomics: a loftier view of life. *Nat Biotechnol* 1999; **17:** 1144

27 **Tsou JA,** Hagen JA, Carpenter CL, Laird-Offringa IA. DNA methylation analysis: a powerful new tool for lung cancer diagnosis. *Oncogene* 2002; **21:** 5450-5461

28 **Nie Y,** Liao J, Zhao X, Song Y, Yang GY, Wang LD, Yang CS. Detection of multiple gene hypermethylation in the development of esophageal squamous cell carcinoma. *Carcinogenesis* 2002; **23:** 1713-1720

29 **Shibata Y,** Haruki N, Kuwabara Y, Ishiguro H, Shinoda N, Sato A, Kimura M, Koyama H, Toyama T, Nishiwaki T, Kudo J, Terashita Y, Konishi S, Sugiura H, Fujii Y. *Chfr* expression is downregulated by CpG island hypermethylation in esophageal cancer. *Carcinogenesis* 2002; **23:** 1695-1699

30 **Nie Y,** Yang G, Song Y, Zhao X, So C, Liao J, Wang LD, Yang CS. DNA hypermethylation is a mechanism for loss of expression of the HLA class I genes in human esophageal squamous cell carcinomas. *Carcinogenesis* 2001; **22:** 1615-1623


**Edited by** Zhang JZ and Wang XL

P.O.Box 2345, Beijing 100023,China
Fax: +86-10-85381893
E-mail: wjg@wjgnet.com www.wjgnet.com

World J Gastroenterol 2003;9(6):1179-1181
World Journal of Gastroenterology
Copyright ©2003 by The WJG Press ISSN 1007-9327

• ESOPHAGEAL CANCER •

# Expression of a plant-associated human cancer antigen in normal, premalignant and malignant esophageal tissues

Jun Fu, Ping Qu, Mo Li, Hai-Mei Tian, Zhen-Hai Zheng, Xin-Wen Zheng, Wei Zhang

**Jun Fu, Ping Qu, Mo Li, Hai-Mei Tian, Wei Zhang,** Central Laboratory for Tumor Biology, Cancer Hospital (Institute), Peking Union Medical College and Chinese Academy of Medical Sciences, Beijing 100021, China
**Zhen-Hai Zheng, Xin-Wen Zheng,** Zheng' s Cancer Institute, Linshou 050500, HeBei Province, China
**Correspondence to:** Professor Wei Zhang, Central Laboratory for Tumor Biology, Cancer Institute, Peking Union Medical College and Chinese Academy of Medical Sciences, Beijing 100021,China. zhangwe@public.bta.net.cn
**Telephone:** +86-10-67718679 **Fax:** +86-10-67718679
**Received:** 2002-12-24 **Accepted:** 2003-03-05

## Abstract

**AIM:** To study the relationship between the expression profiles of a plant-associated human cancer antigen and carcinogenesis of esophagus and its significance.

**METHODS:** We analyzed expression of a plant-associated human cancer antigen in biopsy specimens of normal ($n$=29), mildly hyperplastic ($n$=29), mildly ($n$=30), moderately ($n$=27) and severely dysplastic ($n$=29) and malignant esophageal ($n$=30) tissues by immunohistochemistry.

**RESULTS:** The plant-associated human cancer antigen was mainly confined to the cytoplasm and showed diffuse type of staining. Positive staining was absent or weak in normal (0/30) and mildly hyperplastic tissue samples (2/29), while strong staining was observed in severe dysplasia (23/29) and carcinoma *in situ* (24/30). There was significant difference of its expression between normal mucosa and severely dysplastic tissues ($P$<0.001) or carcinoma *in situ* ($P$<0.001). Significant difference was also observed between mild dysplasia and severe dysplasia ($P$<0.001) or carcinoma *in situ* ($P$<0.001). An overall trend toward increased staining intensity with increasing grade of dysplasia was found. There was a linear correlation between grade of lesions and staining intensity ($r$=0.794, $P$<0.001). Samples from esophageal cancer showed no higher levels of expression than those in severely dysplastic lesions ($P$>0.05).

**CONCLUSION:** The abnormal expression of this plant-associated human cancer antigen in esophageal lesions is a frequent and early finding in the normal-dysplasia-carcinoma sequence in esophageal carcinogenesis. It might contribute to the carcinogenesis of esophageal cancer. The abnormal expression of this plant-associated human cancer antigen in esophageal lesion tissues may serve as a potential new biomarker for early identification of esophageal cancer.

Fu J, Qu P, Li M, Tian HM, Zheng ZH, Zheng XW, Zhang W. Expression of a plant-associated human cancer antigen in normal, premalignant and malignant esophageal tissues. *World J Gastroenterol* 2003; 9(6): 1179-1181
http://www.wjgnet.com/1007-9327/9/1179.asp

## INTRODUCTION

Despite three decades of progress in cancer treatment, esophageal cancer remains a significant health problem worldwide with a very low 5-year survival rate and a rapid increase in its incidence[1-4]. Esophageal squamous cell carcinoma is believed to develop progressively through a dysplasia-carcinoma sequence[5, 6]. The evolution of sequential histological changes from normal to dysplasia and carcinoma *in situ* suggests that specific biomarkers may be expressed at different points in the evolution of esophageal carcinoma[7]. Therefore, research directed toward the discovery of new biomarkers that can aid in the early detection of esophageal neoplasm has been intensified in recent years.

In the 1990s, Dr. Zhen-Hai Zheng separated and identified a glycoprotein (molecular weight: 46 kilo-dalton) from a lower plant. Early experiments demonstrated its stimulatory activity on the growth of esophageal cancer cells. Recently the differential stimulatory effects of this plant antigen on isolated lymphocytes from patients with dysplasia or breast cancer have been confirmed. Their experiments also suggested that this plant antigen might have an associated counterpart cancer antigen in human.

In this research, we aimed to study the relationship between expression profiles of this human cancer antigen and carcinogenesis of esophagus and its significance.

## MATERIALS AND METHODS

### *Tissue specimens*

Biopsy specimens were obtained from the Cancer Hospital (Chinese Academy of Medical Sciences) in Beijing. These samples were taken from patients with morphologically normal ($n$=29), mildly hyperplastic ($n$=29) esophageal mucosa, mildly ($n$=30), moderately ($n$=27) or severely ($n$=29) dysplastic lesions, or squamous carcinomas *in situ* ($n$=30). All samples were routinely fixed in 10 % buffered formalin, embedded in paraffin, and cut into 4 μm sections. Samples were selected based on the pathological diagnosis and reviewed by a pathologist to ensure the correct diagnosis.

### *Reagents*

SP-ABC kit was purchased from Beijing Zhong Shan Biotechnology Co. Ltd. Rabbit polyclonal antibody anti-plant antigen was kindly provided by professor Zhen-Hai Zheng, diluted to $2\times10^{-2}$g· $L^{-1}$ before use.

### *Immunohistochemistry*

The immunohistochemical localization of the plant-associated human cancer antigen was performed using a modified ABC technique[8]. Briefly, tissue sections were deparaffinized in xylene and rehydrated in a series of ethanol solutions (100-50 %). The sections were then microwaved for 15 min to restore antigens in 0.01M citric acid solutions. The endogenous peroxidase activity was blocked by incubation in a 3 % hydrogen peroxide solution for 20 min at 23 ℃. This was followed by preincubation with 1.5 % normal sheep serum to minimize nonspecific binding of the second antibody. The

sections were incubated at 4 ℃ overnight with rabbit polyclonal antibody anti-plant protein. After being washed three times in PBS, the sections were incubated with biotinylated sheep anti-rabbit IgG for 20 min at 37 ℃ and were washed three times in PBS. Sections were then incubated with streptavidin-peroxidase for 20 min at 37 ℃, followed by 2 min staining with DAB-$H_2O_2$ solution and nuclear counterstained with hematoxylin. For negative controls, the rabbit anti-plant protein polyclonal antibody was replaced by normal rabbit serum.

### *Review and scoring of the section*

The stained sections were reviewed and scored independently by two investigators using an Olympus microscope. The intensity of staining was graded on a scale of 0 to 3 as follows: 0 meaning the amounts of positive cells were less than 10 %; 1, weak positive, the amounts of positive cells were more than 10 %, but less than 30 %; 2, positive, the amounts of positive cells were more than 30 % but less than 50 %; and 3, strong positive, the amounts of positive cells were more than 50 %[9]. The grading for each section used for data analysis was the highest intensity seen on the section.

### *Statistical analysis*

The mean values of the staining intensity for different grades of diseases were compared by analysis of variance. Linear regression analysis was done to evaluate the linear correlation between lesion severity and staining intensity. Statistical analysis was made using Fisher' s exact test to determine the association between normal or dysplastic tissues and tumors. *P* values were generated using SPSS 10.0 for Windows. Statistical significance was accepted at the $P<0.05$ level.

## RESULTS

Our finding suggested that the plant-associated human cancer antigen was mainly confined to the cytoplasma and showed diffuse type of staining, enormous nuclear staining could also be observed in severe dysplastic and carcinoma *in situ* tissue samples. Only background staining was observed in basal layers underlying epithelium. Staining was absent to weak in normal and mildly hyperplastic tissue samples (Figure 1-6). Positive staining was absent to weak in normal (0/30) and mildly hyperplastic tissue samples (2/29), while high positive rate was observed in severe dysplasia (23/29) and carcinoma *in situ* (24/30).

There was significant difference of its expression between normal mucosa and severely dysplastic tissues ($P<0.001$) or esophageal cancer ($P<0.001$). Significant difference was also observed between mild dysplasia and severe dysplasia ($P<0.001$) or esophageal cancer ($P<0.001$) (Table 1). Samples from esophageal cancer showed no higher levels of its expression than seen in severely dysplastic lesions ($P>0.05$). An overall trend toward increased staining intensity with increasing grade of dysplasia was found. There was a linear correlation between grade of lesion and staining intensity ($r=0.794$, $P<0.001$) (Table 2).

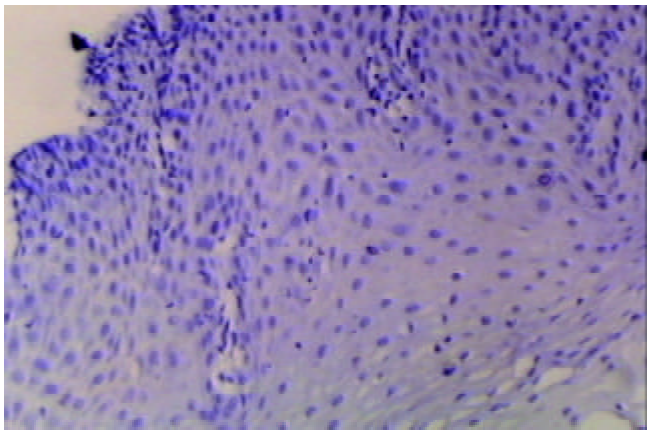

**Figure 1** The expression of plant-associated human cancer antigen in normal esophageal tissues. Avidin-biotin complex staining, ABC, ×100.

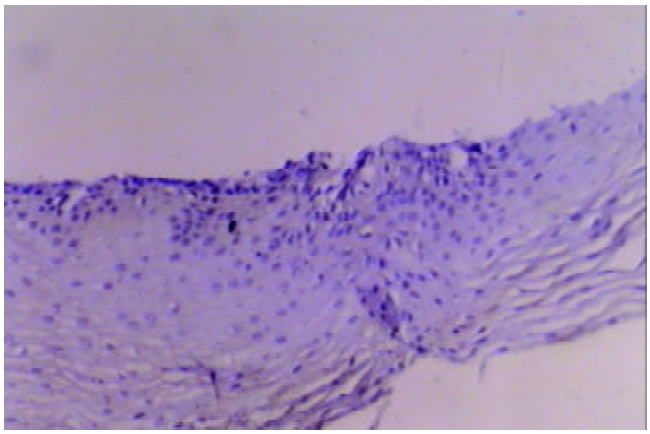

**Figure 3** The expression of plant-associated human cancer antigen in mild dysplasia. Avidin-biotin complex staining, ABC, ×100.

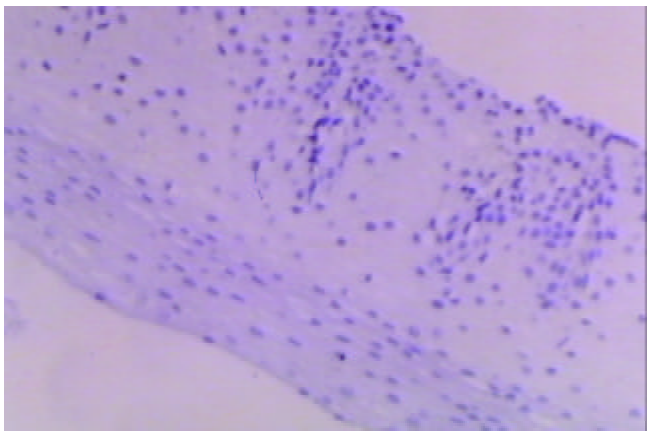

**Figure 2** The expression of plant-associated human cancer antigen in mild hyperplasia. Avidin-biotin complex staining, ABC, ×100.

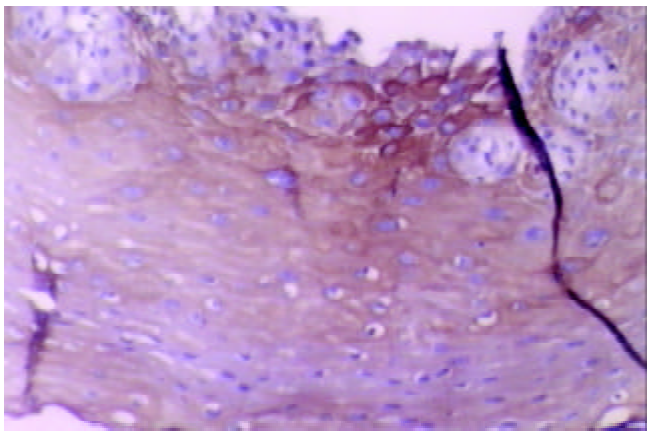

**Figure 4** The expression of plant-associated human cancer antigen in moderate dysplasia. Avidin-biotin complex staining, ABC, ×100.

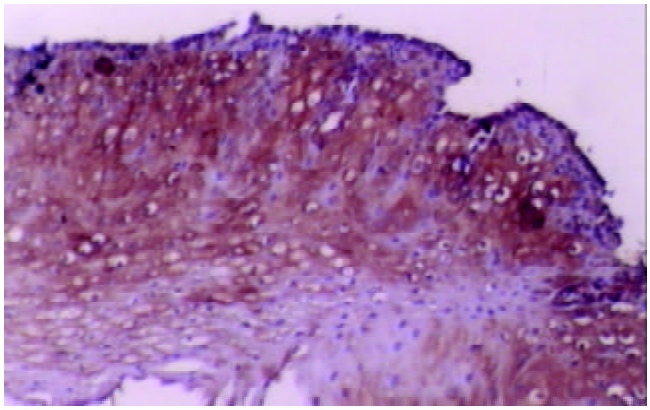

**Figure 5** The expression of plant-associated human cancer antigen in severe dysplasia. Avidin-biotin complex staining, ABC, ×100.

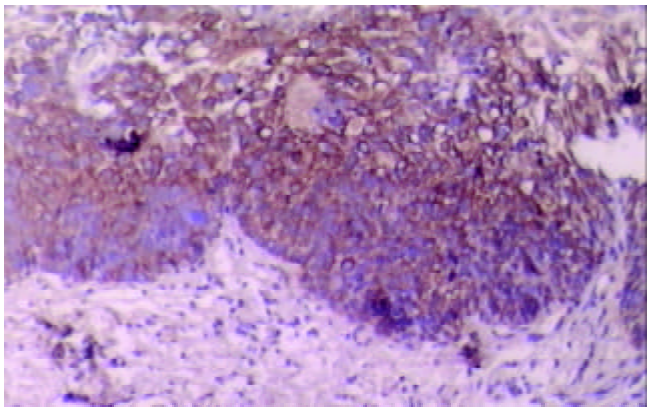

**Figure 6** The expression of plant associated-human cancer antigen in carcinoma *in situ*. Avidin-biotin complex staining, ABC, ×100.

**Table 1** Expression of the plant-associated human cancer antigen in different esophageal tissues

| Esophageal tissues | Total cases | Positive staining | Negative staining | %Positive |
|---|---|---|---|---|
| Normal | 29 | 0 | 18 | 0 |
| Hyperplasia | 29 | 2 | 27 | 6.9 |
| Dysplasia | | | | |
| Mild | 30 | 8 | 22 | 26.7 |
| Moderate | 27 | 17 | 10 | 63.0 |
| Severe | 29 | 23 | 6 | 79.3 |
| [a]CIN | 30 | 24 | 6 | 80.0 |

[a]CIN: Carcinoma *in situ*.

**Table 2** Staining intensity of the plant-associated human cancer antigen expressed in different esophageal tissues

| Histologic diagnisis | Total cases | Staining intensity[a] | Biopsies staining with intensity>2 (%) |
|---|---|---|---|
| Normal | 29 | 0 | 0 |
| Dysplasia | | | |
| Mild | 30 | 0.27±0.52 | 3.3 |
| Moderate | 27 | 1.00±0.93 | 25.9 |
| Severe | 29 | 1.38±0.96 | 41.4 |
| CIN | 30 | 1.33±0.92 | 43.3 |

[a]Expressed as mean staining intensity ± standard deviation. Intensity of staining was graded on a scale of 0 to 3.

## DISCUSSION

We have evaluated esophageal mucosal expression of the plant-associated human cancer antigen in a variety of normal, precancerous or malignant esophageal tissue specimens. Esophageal biopsy specimens with normal histology or low-grade dysplasia did not express significant levels of this human cancer antigen. Its intensive expression was observed in high-grade dysplastic and malignant lesions. There was an overall trend toward increased staining intensity with increasing grade of dysplasia, and the largest difference was observed between mild and severe dysplastic lesions, suggesting that its up-regulation of expression may be involved in esophageal carcinogenesis. Since esophageal carcinogenesis is a multi-stage process, early detection is very crucial[10,11]. This human cancer antigen might be a useful diagnostic marker for advanced dysplasia and could serve as a useful target for biological treatment and for bio-prevention in high-risk patients diagnosed having dysplasia or esophageal carcinoma.

In this report, we also studied the expression distribution of this human cancer antigen in abnormal human sections. Although this antigen was mainly expressed in cytoplasma, enormous nuclear staining could also be observed in severely dysplastic and malignant tissue samples. Combined with previous conclusions, our finding suggested that this protein might be involved in signal transduction pathway or cell cycle control. Its intracellular translocation from cytoplasma to nuclei might play an important role in the transition from low-grade dysplasia to severe lesions and neoplasm. The mechanism of action of this cancer antigen in esophageal carcinogenesis still awaits further studies.

The ability to identify the plant-associated human cancer antigen in esophageal biopsy specimens from patients with dysplasia may provide a useful method for early detection, identification of high-risk patients, monitoring response to therapy. Further studies are needed to separate and identify this protein and its encoding gene in order to fully understand the regulatory mechanism underlying its aberrant expression and its role in esophageal carcinogenesis.

## REFERENCES


1 **Mc Cann J**. Esophageal cancers: changing character, increasing incidence. *J Natl Cancer Inst* 1999; **91**: 497-498
2 **Flood WA**, Forastiere AA. Esophageal cancer. *Curr Opin Oncol* 1995; **7**: 381-386
3 **Flood WA**, Forastiere AA. Esophageal cancer. *Cancer Treat Res* 1998; **98**: 1-40
4 **Blot WJ**. Esophageal cancer trends and risk factors. *Semin Oncol* 1994; **21**: 403-410
5 **Liu FS**, Wang QL, Goldman H. Pathology of the gastrointestinal tract. *Philadelphia: Saunders* 1992: 439-458
6 **Haggitt RC**. Barrette's esophagus, displasia, and adenocarcinoma. *Human Pathol* 1994; **25**: 982-993
7 **Stemmermann G**, Heffelfinger SC, Noffsinger A. The molecular biology of esophageal and gastric cancer and their precursors: oncogenes, tumor suppressor genes, and growth factors. *Hum Pathol* 1994; **25**: 968-981
8 **Zhang W**, Rashid A, Wu H, Xu XC. Differential expression of retinoic acid receptors and P53 protein in normal, premalignant, and malignant esophageal tissues. *J Cancer Res Clin Oncol* 2001; **127**: 237-242
9 **Xu M**, Jin YL, Fu J, Huang H, Chen SZ, Qu P, Tian HM, Liu ZY, Zhang W. The abnormal expression of retinoic acid receptor-β, *P*53 and Ki67 protein in normal, premalignant and malignant esophageal tissues. *World J Gastroenterol* 2002; **8**: 200-202
10 **Kelloff GJ**, Boone CW, Steele VK, Perloff M, Crowell J, Doody LA. Development of chemopreventive agents for lung and upper aerodigestive tract cancers. *J Cell Biochem Suppl* 1993; **17F**: 2-17
11 **Lippman SM**, Lee JJ, Sabichi AL. Cancer chemoprevention: progress and promise. *J Natl Cancer Inst* 1998; **90**: 1514-1515


**Edited by** Ma JY

P.O.Box 2345, Beijing 100023,China
Fax: +86-10-85381893
E-mail: wjg@wjgnet.com www.wjgnet.com

World J Gastroenterol 2003;9(6):1182-1186
World Journal of Gastroenterology
Copyright ©2003 by The WJG Press ISSN 1007-9327

• ESOPHAGEAL CANCER •

# Upregulated expression of Ezrin and invasive phenotype in malignantly transformed esophageal epithelial cells

Zhong-Ying Shen, Li-Yan Xu, Ming-Hua Chen, En-Min Li, Jin-Tao Li, Xian-Ying Wu, Yi Zeng

**Zhong-Ying Shen, Li-Yan Xu, Ming-Hua Chen, Jin-Tao Li, Xian-Ying Wu,** Department of Pathology, Medical College of Shantou University, Shantou, 515031, Guangdong Province China
**En-Min Li,** Department of Biochemistry, Medical College of Shantou University, Shantou, 515031, China
**Yi Zeng,** Institute of Virology, Chinese Academy of Preventive Medicine, Beijing 100052, China
**Supported by** the National Natural Science Foundation of China (No. 39830380, 39900069), Research and Development Foundation of Shantou University (L00012) and the Chinese National Human Genome Center, Beijing
**Correspondence to:** Professor Zhong-Ying Shen, Department of Pathology, Medical College of Shantou University, Shantou 515031, Guangdong Province, China. zhongyingshen@yahoo.com
**Telephone:** +86-754-8538621 **Fax:** +86-754-8537516
**Received:** 2003-03-12 **Accepted:** 2003-04-19

## Abstract

**AIM:** To investigate the correlation between ezrin expression and invasive phenotype formation in malignantly transformed esophageal epithelial cells.

**METHODS:** The experimental cell line employed in the present study was originated form the progressive induction of a human embryonic esophageal epithelial cell line (SHEE) by the E6E7 genes of human papillomavirus (HPV) type 18. The cells at the 35th passage after induction called SHEEIMM were in a state of immortalized phase and used as the control, while that of the 85th passage denominated as SHEEMT represented the status of cells that were malignantly transformed. The expression changes of ezrin and its mRNA in both cell passages were respectively analyzed by RT-PCR and Western blot. Invasive phenotype was assessed *in vivo* by inoculating these cells into the severe combined immunodeficient (SCID) mice via subcutaneous and intraperitoneal injection, and *in vitro* by inoculating them on the surface of the amnion membranes, which then was determined by light microscopy and scanning electron microscopy.

**RESULTS:** Upregulated expression of ezrin protein and its mRNA was observed in SHEEMT compared with that in SHEEIMM cells. The SHEEMT cells inoculated in SCID mice were observed forming tumor masses in both visceral organs and soft tissues in a period of 40 days with a special propensity to invading mesentery and pancreas, but did not exhibit hepatic metastases. Pathologically, these tumor cells harboring larger nucleus, nucleolus and less cytoplasm could infiltrate and destroy adjacent tissues. In the *in vitro* study, the inoculated SHEEMT cells could grow in cluster on the amniotic epithelial surface and intrude into the amniotic stroma. In contrast, unrestricted growth and invasiveness were not found in SHEEIMM cells in both *in vivo* and *in vitro* experiment.

**CONCLUSION:** The upregulated ezrin expression is one of the important factors that are possibly associated with the invasive phenotype formation in malignantly transformed esophageal epithelial cells.

Shen ZY, Xu LY, Chen MH, Li EM, Li JT, Wu XY, Zeng Y. Upregulated expression of Ezrin and invasive phenotype in malignantly transformed esophageal epithelial cells. *World J Gastroenterol* 2003; 9(6): 1182-1186
http://www.wjgnet.com/1007-9327/9/1182.asp

## INTRODUCTION

It has been well known that cancer cells can invade and destroy surrounding tissues by their disseminative potency. This acquired malignant property is believed recently to be determined by the abnormal changes of expression patterns of certain genes such as c-met, urokinase type plasminogen activator receptor or ezrin and so on[1-9]. Therefore, the correlation between the invasive phenotype of tumor cells and the aberrant expression of these genes has become a focus of attention by the worldwide oncologists.

Induced by $E_6E_7$ genes of human papilloma virus (HPV) type 18, we have established both kinds of immortalized and malignantly transformed cells from a human embryonic esophageal epithelial cell line (SHEE)[10]. At early passages after induction, the cell did not display any abnormal growth ability in soft agar and nude mice[11-13]. At the 20th passage, the cell was noted to be immortalized with the appearance of telomerase[14, 15]. At the 30th passage, the cell manifested as a phenotype of biphasic differentiation[16]. While cultivated over 60 passages, the cell exhibited atypical morphological changes and chromosomal alterations that were suspected to be a kind of premalignant transformation[17]. Over 85 passages, the cell was observed having harbored a property of malignant transformation shown by its unrestricted growth in the nude mice and invasion to the surrounding tissues[18, 19]. Obviously, this process of malignant transformation of SHEE cells induced by $E_6E_7$ genes of HPV type 18 possesses a progressive and stepwise characteristic, which is no doubt a good cell model suitable for the study of correlations between abnormal gene expression and corresponding malignant phenotype formation in tumorigenesis.

Differential display analysis of RNA samples isolated from the SHEEIMM and SHEEMT cells has been performed in our previous study. There were 15 up-regulated and 6 down-regulated genes being identified by the cDNA microarray method (Data to be published), in which ezrin was one of the up-regulated genes that have been found existed in certain diseases and tumors. Being a membrane-cytoskeleton linker, ezrin protein is located in cytoplasm and is rich in microvilli and cell surface structures with the function involved in the formation of microvilli and intercellular junctions, as well as the cell motility and invasive behavior of malignant tumors[20-28]. Up to the present, however, there have been few reports concerned about how the ezrin expressed in the malignant transformation of esophageal epithelial cells and what was its relation to the invasiveness formation of tumor cells, which are of both theoretical and practical importance in the

investigation of cancerogenesis. Thus, our present study was conducted to identify the correlation between the ezrin gene expression and invasive phenotype formation in malignantly transformed esophageal epithelial cells.

## MATERIALS AND METHODS

### *Cell lines and cell culture*

The experimental cells came from our laboratory, and were established by the progressive induction of SHEE cell line with the E6E7 genes of HPV type 18. The 35th, 85th passages of induced cells were employed in the present study. The cells at the 35th passage called SHEEIMM were in a state of immortalized phase, while that of the 85th passage denominated as SHEEMT represented the status of cells that were malignantly transformed. Both passages of cells were continuously cultivated in flasks with medium 199 (GIBCO) supplemented by 10 % fetal bovine serum (FBS), 100 U· $ml^{-1}$ penicillin and 100 U· $ml^{-1}$ streptomycin at 37 ℃ in a humidified atmosphere containing 5 % of $CO_2$.

### *RT-PCR*

Total RNA was extracted from SHEEIMM and SHEEMT cells using the Trizol reagent (Invitrogen). The first-strand cDNA synthesis was performed with 1 μg total RNA and carried out at 42 ℃ for 1 h followed by at 95 ℃ for 5 min and at 0-5 ℃ for 5 min according to protocol of reverse transcription system (Promega). The synthesized cDNA was diluted to 100 μl with TE and stored at -20 ℃ until use. In the following experiment, 5 μl of cDNA was amplified in a 25 μl PCR reaction volume with Advantage 2 PCR Kit (CLONTECH). Both of the ezrin primer 5' CGGGCGCTCTAAGGGTTCT3' (sense), 5' TGCCTTTGCAAAGCTTTTATTTCA3' (antisense) and GAPDH primer 5' GAAGGTGAAGGTCGGAGTC 3' (sense), 5' GAAGATGGTGATGGGATTTC 3' (antisense) were synthesized by Genecore Company (Shanghai). After prepared by routine procedures, PCR products were visualized by electrophoresis on 1 % agarose gel stained with ethidium bromide and quantitated with Gelworks 1D Intermediate software (version 3.51, Kodak).

### *Western blot*

Western blot was used to detect ezrin protein expressed by experimental cells. Confluent cells of 3 flasks were washed three times with ice-cold PBS and then lysed in buffer containing 50 mM Tris-HCl (pH 8.0), 150 mM NaCl, 100 μg· $ml^{-1}$ phenyl-methyl-sulfonyl fluoride (PMSF) and 1 % Triton X-100 for 30 min on ice. After removal of cell debris by centrifugation at 12 000 g for 5 min, 50 μl of supernatant was boiled for 5 min in the sample buffer and separated by 10 % SDS-PAGE, which was then transferred onto the nitrocellulose membrane (Pall Corporation). After non-specific reactivity was blocked by 5 % fat-free milk in TBST (10 mM Tris-HCl, pH 7.5, 150 mM NaCl, 0.05 % Tween 20) for 1 h at room temperature, the membrane was incubated in turn with monoclonal antibody of mouse against human ezrin p81 (Maixin-Bio) and anti-mouse IgG-HRP antibody. Reactive protein was finally detected by ECL chemiluminescence system (Santa Cruz).

### *Oncogenesis and invasive potency of SHEE in vivo*

SCID mice (C.B-17/IcrJ-scid nu/nu) were from Animal Laboratory Center, Chinese Academy of Medical Sciences. For the determination of their oncogenesis and invasive potency, SHEEIMM and SHEEMT cells were cultured in flasks with fresh medium to reconstitute their surface protein. After digested and washed twice with PBS, they were counted and resuspended in PBS solution ($10\times10^{6}$· $ml^{-1}$) until use. Then SCID mice were anesthetized with 7 % chloralhydrate followed by intraperitoneal and subcutaneous inoculation with the both passages of cells. That is, $2\times10^{6}$ SHEEMT or SHEEIMM cells in 0.2 ml PBS were injected into the peritoneal cavity in 5 mice and into the right axilla of the same number of animals. Instead, the control mice were injected only with 0.2 ml of PBS. The experimental animals were checked daily and all were killed on after day 40 inoculation by an overdose of anesthetic. Tissues from tumor mass, mesentery, pancreas and gastrointestinal tract were sampled and prepared with the routine method to produce thin paraffin sections (5 μm) stained by hematoxylin and eosin for the assessment of tumor invasion.

### *Invasive potency of SHEE in vitro*

Tumor cell invasion *in vitro* was assessed by using a fresh fetal amnion, which was cultured in 199 medium supplemented with 10 % FBS. In the experiment, a piece of amnion and 50 000 SHEEIMM or SHEEMT cells were in turn added to one well of a 24-well plate and incubated together for 24 h and 72 h, and then were washed for several times with PBS. Then the samples, including the piece of amnion and cells adhering to it, were fixed with 2.5 % glutaraldehyde and post-fixed with 2 % osmium tetraoxide. After full dehydration with gradient concentrations of ethanol, the samples were adhered to an aluminium stub and sprayed plating with gold for 3 minutes (EIKD, IB-3, Hitachi), which were further examined by Hitachi H300 electron microscope with the attachment of scanning apparatus.

## RESULTS

### *Expressive alterations of ezrin and its mRNA*

The ezrin mRNA detected by electrophoresis on 1 % agarose gel was shown as a band of 3 032 bp segment, whose expression was observed to be significantly up-regulated in SHEEMT by RT-PCR assay compared with that expressed in SHEEIMM cells as displayed in Figure 1. The same difference was also noted in the expression of ezrin protein between both of the cell passages (Figure 2).

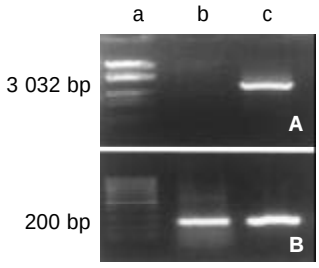


**Figure 1** RT-PCR assay of ezrin mRNA. The expression of ezrin mRNA was significantly increased in SHEEMT compared with that in SHEEIMM cells. A. Ezrin; B. GAPDH: a. Marker; b. SHEEIMM; c. SHEEMT.

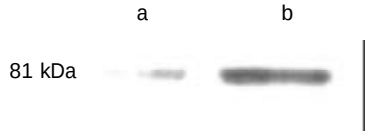


**Figure 2** Western blot analysis of ezrin protein expression. The ezrin protein was exhibited as a band of 81-kDa segment, whose expression was up-regulated in SHEEMT compared with that in SHEEIMM cells. Lane a: SHEEIMM; lane b: SHEEMT.

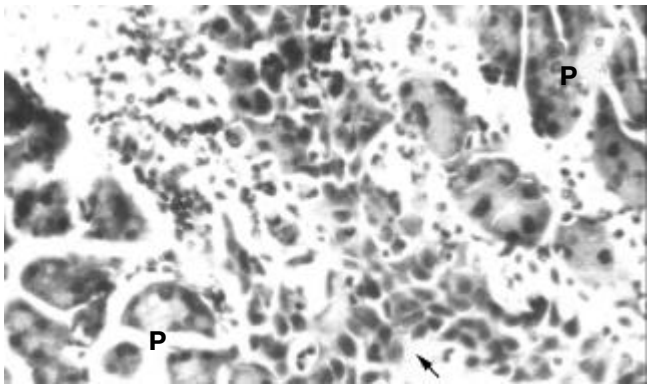


**Figure 3** The inoculated SHEEMT cells (arrow) invaded into the parenchyma of pancreas (P) (HE, ×200).

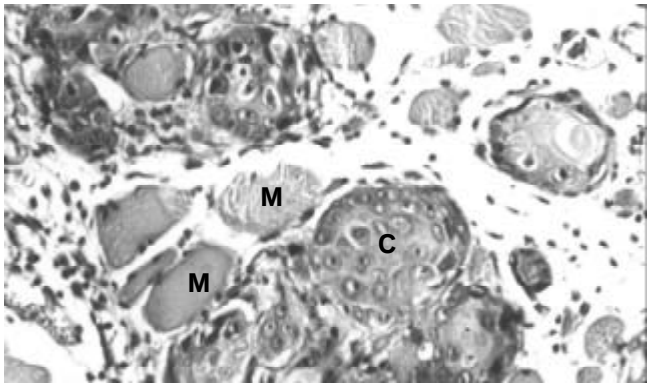


**Figure 4** Tumor formation in subcutaneous tissue inoculated with SHEEMT cells (C), the latter was also shown to invade and destroy nearby muscle fibers (M). (HE, ×200).

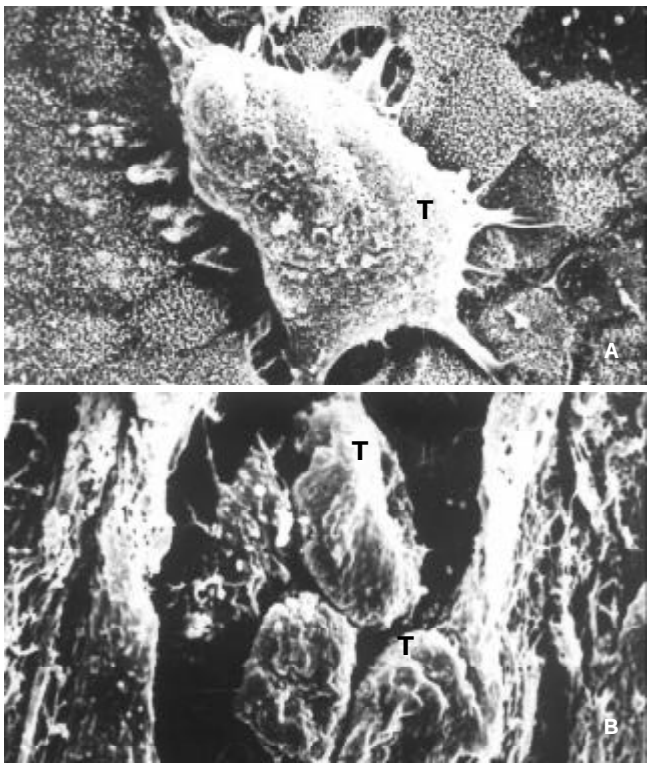


**Figure 5** The invasiveness of inoculated SHEEMT cells on amniotic epithelium was demonstrated by scanning electron microscopy. A. A cluster of SHEEMT cells (T) grew on the amniotic epithelial surface (bar, 5 μ); B. On the cutting surface, SHEEMT cells (T) were observed invading into the amnion stroma (bar, 50 μ).

### *Oncogenesis and invasiveness in SCID mice*

After inoculated into the SCID mice, SHEEMT cells were noted growing rapidly and forming tumor masses in 40 days. In peritoneal cavity, tumors were observed occurring on the mesentery, pancreas, urinary cyst, sub-diaphragm etc. with a special propensity for invading mesentery and pancreas, but did not exhibit any signs of hepatic metastases. Histological examination revealed that these tumor cells did not only grow on the organ surface, but also invade into adjacent tissues (Figure 3). In the subcutaneous tissue of the right axilla, tumor mass was observed macroscopically forming on the thoracic wall and penetrating into the thoracic cavity. Pathologically, these tumor cells harboring larger nucleus, nucleolus and less cytoplasm could infiltrate and destroy adjacent muscular fibers (Figure 4). Once transplanted, tumors could keep be passed to other SCID mice. In contrast, SHEEIMM cells were not found to form tumors in inoculated tissue by gross examination.

### *Invasive potency in vitro*

After inoculated on the amnion, SHEEMT cells were shown growing in cluster on the epithelial surface with the formation of pseudopod that intruded into the gap between intercellular conjunctions (Figure 5A). On the cutting surface, SHEEMT cells were observed invading into the amnion stroma (Figure 5B). It was not found that the inoculated SHEEIMM cells could adhere to or colonize on the amniotic epithelium.

## DISCUSSION

Invasive potency is one of the most important features of malignant tumors and is involved in a critical cascade of events such as extracellular matrix degradation, cell migration and colonization in the assaulted tissue. The invasive phenotype formation of malignant cells requires up-regulated expression of certain adhesive molecules, enzymes and related genes responsible for the interaction between cancer cells and extracellular matrix[29]. Several co-factors have been reported to be involved in the process of invasion and metastasis[30-32] besides ezrin that has been considered as an important molecule contributing to the malignantly transformation of cells. In addition to combining with adhesion molecules such as E-cadherin and catenin implicated in cell-cell and cell-matrix adhesion[33], ezrin plays a critical role in the determination of invasiveness of cancer cells[34].

In the present study, we investigated the expression of ezrin and its mRNA in a malignantly transformed esophageal epithelial cell line SHEEMT and further demonstrated its unrestricted growth and invasive potency in both *in vivo* and *in vitro* circumstances. The experimental results revealed that the expression of ezrin protein and its mRNA was significantly upregulated in SHEEMT compared with that in SHEEIMM cells. The SHEEMT cells inoculated to SCID mice could form tumor masses in both visceral organs and soft tissues in a period of 40 days. Pathologically, these tumor cells harboring larger nucleus, nucleolus and less cytoplasm could infiltrate and destroy adjacent tissues. In the *in vitro* study, the inoculated SHEEMT cells could grow in cluster on the amniotic epithelial surface and intrude into the amniotic stroma. In contrast, unrestricted growth and invasive property were not found in the SHEEIMM cells that were used as the control in both *in vivo* and *in vitro* experiments. As to our knowledge, this is one of the few reports concerned about how the ezrin gene expresses and what is its relation to the invasiveness formation in malignantly transformed esophageal epithelial cells.

New technology in molecular medicine allows global descriptions of complex expression patterns of genes responsible for the malignant properties of tumors[35-38]. With the two representative passages of cells described above, we

have defined the profile of genes involved in the invasiveness of tumor cells using a sensitive cDNA microarray in a previous study. We found that increased expression of ezrin protein in SHEEMT cells was in accordance with their acquisition of the invasive potency[39]. Based on these observations, we therefore speculated that ezrin might be an important candidate of genes in charge of the invasive behaviors of malignantly transformed esophageal epithelial cells, as reported in lymphoma and astrocytic tumors[40, 41]. However, recent work in this field has also focused on the identification of ezrin-binding molecules, including $CD_{44}$, $CD_{43}$, intercellular adhesion molecule[42--44] and syndecan-2[45]. Moreover, modulation of the ERM protein ezrin by Merlin and NF-2 has been reported in other literatures[46-48]. In the meanwhile, we have demonstrated that following expression of $MMP_2$ and $MMP_9$, highly invasive potency was developed in SHEEMT cells (Data to be published). All these suggest the invasiveness of tumor cells is determined by multiple genes and co-factors with complicated cellular signal passways. Therefore, future works are necessitated to demonstrate more exactly the roles of ezrin and related molecules in the formation of invasive potency of cancer cells by the gene knockout technique and other powerful tools.

## REFERENCES


1 **Ueda M,** Terai Y, Yamashita Y, Kumagai K, Ueki K, Yamaguchi H, Akise D, Hung YC, Ueki M. Correlation between vascular endothelial growth factor-C expression and invasion phenotype in cervical carcinomas. *Int J Cancer* 2002; **98:** 335-343

2 **Nestl A,** Von Stein OD, Zatloukal K, Thies WG, Herrlich P, Hofmann M, Sleeman JP. Gene expression patterns associated with the metastatic phenotype in rodent and human tumors. *Cancer Res* 2001; **61:** 1569-1577

3 **Comoglio PM,** Tamagnone L, Boccaccio C. Plasminogen-related growth factor and semaphorin receptors: a gene superfamily controlling invasive growth. *Exp Cell Res* 1999; **253**: 88-99

4 **Janneau JL,** Maldonado-Estrada J, Tachdjian G, Miran I, Motte N, Saulnier P, Sabourin JC, Cote JF, Simon B, Frydman R, Chaouat G, Bellet D. Transcriptional expression of genes involved in cell invasion and migration by normal and tumoral trophoblast cells. *J Clin Endocrinol Metab* 2002; **87:** 5336-5339

5 **Guo Y,** Pakneshan P, Gladu J, Slack A, Szyf M, Rabbani SA. Regulation of DNA methylation in human breast cancer. Effect on the urokinase-type plasminogen activator gene production and tumor invasion. *J Biol Chem* 2002; **277:** 41571-41579

6 **Jiang Y,** Xu W, Lu J, He F, Yang X. Invasiveness of hepatocellular carcinoma cell lines: contribution of hepatocyte growth factor, c-met, and transcription factor Ets-1. *Biochem Biophys Res Commun* 2001; **286:** 1123-1130

7 **Orian-Rousseau V**, Chen L, Sleeman JP, Herrlich P, Ponta H. CD44 is required for two consecutive steps in HGF/c-Met signaling. *Genes Dev* 2002; **16:** 3074-3086

8 **Loktionov A,** Watson MA, Stebbings WS, Speakman CT, Bingham SA. Plasminogen activator inhibitor-1 gene polymorphism and colorectal cancer risk and prognosis. *Cancer Lett* 2003; **189:** 189-196

9 **Tokunou M,** Niki T, Eguchi K, Iba S, Tsuda H, Yamada T, Matsuno Y, Kondo H, Saitoh Y, Imamura H, Hirohashi S. c-MET expression in myofibroblasts: role in autocrine activation and prognostic significance in lung adenocarcinoma. *Am J Pathol* 2001; **158:** 1451-1463

10 **Shen ZY,** Xu LY, Chen MH, Shen J, Cai WJ, Zeng Y. Progressive transformation of immortalized esophageal epithelial cells. *World J Gastroenterol* 2002; **8:** 976-981

11 **Shen ZY,** Cen S, Cai WJ, Teng ZP, Shen J, Hu Z, Zeng Y. Immortalization of human fetal esophageal epithelial cells induced by E6 and E7 genes of human papilloma virus 18. *Zhonghua Shiyan He Linchuang Bingduxue Zazhi* 1999; **13:** 121-123

12 **Shen ZY,** Xu LY, Chen Xh, Cai WJ, Shen J, Chen JY, Huang TH, Zeng Y. The genetic events of HPV-immortalized esophageal epithelium cells. *Int J Mol Med* 2001; **8:** 537-542

13 **Shen ZY,** Shen J, Cai WJ, Cen S, Zeng Y. Biological characteristics of human fetal esophageal epithelial cell line immortalized by the E6 and E7 gene of HPV type 18. *Zhonghua Shiyan He Linchuang Bingduxue Zazhi* 1999; **13:** 209-212

14 **Shen ZY,** Xu LY, Li C, Cai WJ, Shen J, Chen JY, Zeng Y. A comparative study of telomerase activity and malignant phenotype in multistage carcinogenesis of esophageal epithelial cells induced by human papillomavirus. *Int J Mol Med* 2001; **8:** 633-639

15 **Shen ZY,** Xu LY, Li EM, Cai WJ, Chen MH, Shen J, Zeng Y. Telomere and telomerase in the initial stage of immortalization of esophageal epithelial cell. *World J Gastrointerol* 2002; **8:** 357-362

16 **Shen ZY,** Xu LY, Chen MH, Cai WJ, Shen J, Chen JY, Hon CQ, Zeng Y. Biphasic differentiation of immortalized esophageal epitheliums induced by HPV18E6E7. *Bingdu Xuebao* 2001; **17:** 210-214

17 **Shen ZY,** Cen S, Shen J, Cai W, Xu J, Teng Z, Hu Z, Zeng Y. Study of immortalization and malignant transformation of human embryonic esophageal epithelial cells induced by HPV18E6E7. *J Cancer Res Clin Oncol* 2000; **126:** 589-594

18 **Shen ZY,** Cai WJ, Shen J, Xu JJ, Cen S, Teng ZP, Hu Z, Zeng Y. Human papilloma virus 18E6E7 in synergy with TPA induced malignant transformation of human embryonic esophageal epithelial cells. *Bingdu Xuebao* 1999; **15:** 1-6

19 **Shen ZY,** Shen J, Cai WJ, Chen JY, Zeng Y. Identification of malignant transformation in the immortalized esophageal epithelial cells. *Zhonghua Zhongliu Zazhi* 2002; **24:** 107-109

20 **Mangeat P,** Roy C, Martin M. ERM proteins in cell adhesion and membrane dynamics. *Trends Cell Biol* 1999; **9:** 187-192

21 **Scherer SS,** Xu T, Crino P, Arroyo EJ, Gutmann DH. Ezrin, radixin, and moesin are components of Schwann cell microvilli. *J Neurosci Res* 2001; **65:** 150-164

22 **Ohtani K,** Sakamoto H, Rutherford T, Chen Z, Satoh K, Naftolin F. Ezrin, a membrane-cytoskeletal linking protein, is involved in the process of invasion of endometrial cancer cells. *Cancer Lett* 1999; **147:** 31-38

23 **Makitie T,** Carpen O, Vaheri A, Kivela T. Ezrin as a prognostic indicator and its relationship to tumor characteristics in uveal malignant melanoma. *Invest Ophthalmol Vis Sci* 2001; **42:** 2442-2449

24 **Ohtani K,** Sakamoto H, Rutherford T, Chen Z, Kikuchi A, Yamamoto T, Satoh K, Naftolin F. Ezrin, a membrane-cytoskeletal linking protein, is highly expressed in atypical endometrial hyperplasia and uterine endometrioid adenocarcinoma. *Cancer Lett* 2002; **179:** 79-86

25 **Tokunou M,** Niki T, Saitoh Y, Imamura H, Sakamoto M, Hirohashi S. Altered expression of the ERM proteins in lung adenocarcinoma. *Lab Invest* 2000; **80:** 1643-1650

26 **Johnson MW,** Miyata H, Vinters HV. Ezrin and moesin expression within the developing human cerebrum and tuberous sclerosis-associated cortical tubers. *Acta Neuropathol* 2002; **104:** 188-196

27 **Mykkanen OM,** Gronholm M, Ronty M, Lalowski M, Salmikangas P, Suila H, Carpen O. Characterization of human palladin, a microfilament-associated protein. *Mol Biol Cell* 2001; **12:** 3060-3073

28 **Gautreau A,** Poullet P, Louvard D, Arpin M. Ezrin, a plasma membrane-microfilament linker, signals cell survival through the phosphatidylinositol 3-kinase/Akt pathway. *Proc Natl Acad Sci USA* 1999; **96:** 7300-7305

29 **Gonzalez RR,** Devoto L, Campana A, Bischof P. Effects of leptin, interleukin-lalpha, interleukin-6, and transforming growth factor-beta on markers of trophoblast invasive phenotype: integrins and metalloproteinases. *Endocrine* 2001; **15:** 157-164

30 **Chen Z,** Fadiel A, Feng Y, Ohtani K, Rutheford T, Naftolin F. Ovarian epithelial carcinoma tyrosine phosphorylation, cell proliferation, and ezrin translocation are stimulated by interleukin lalpha and epidermal growth factor. *Cancer* 2001; **92:** 3068-3075

31 **Tran Quang C,** Gautreau A, Arpin M, Treisman R. Ezrin function is required for ROCK-mediated fibroblast transformation by the Net and Dbl oncogenes. *EMBO J* 2000; **19:** 4565-4576

32 **Stapleton G,** Malliri A, Ozanne BW. Downregulated AP-1 activity is associated with inhibition of Protein-Kinase-C-dependent CD44 and ezrin localization and upregulation of PKC theta in A431 cells. *J Cell Sci* 2002; **115:** 2713-2724

33 **Si HX,** Tsao SW, Lam KY, Srivastava G, Liu Y, Wong YC, Shen ZY, Cheung AL. E-cadherin expression is commonly downregulated by CpG island hypermethylation in esophageal carcinoma cells. *Cancer Lett* 2001; **173**: 71-78

34 **Hiscox S**, Jiang WG. Ezrin regulates cell-cell and cell-matrix adhesion, a possible role with E-cadherin/beta-catenin. *J Cell Sci* 1999; **112:** 3081-3090

35 **Schindelmann S,** Windisch J, Grundmann R, Kreienberg R, Zeillinger R, Deissler H. Expression profiling of mammary carcinoma cell lines: correlation of in vitro invasiveness with expression of CD24. *Tumour Biol* 2002; **23:** 139-145

36 **Zhan F,** Cao L, Hu C, Li G. Differentially expressed cDNA sequences homologous with known genes in human nasopharyngeal carcinoma. *Hunan Yike Daxue Xuebao* 1999; **24:** 103-106

37 **Khanna C,** Khan J, Nguyen P, Prehn J, Caylor J, Yeung C, Trepel J, Meltzer P, Helman L. Metastasis-associated differences in gene expression in a murine model of osteosarcoma. *Cancer Res* 2001; **61:** 3750-3759

38 **Wang KC,** Cheng AL, Chuang SE, Hsu HC, Su IJ. Retinoic acid-induced apoptotic pathway in T-cell lymphoma: Identification of four groups of genes with differential biological functions. *Exp Hematol* 2000; **28:** 1441-1450

39 **Shen J,** Chen MH, Zheng RM, Chen JJ, Shen ZY. Detection of tumor cell invasion in vitro by scanning electron microscopy. *Dianzi Xianwei Xuebao* 2000; **19:** 313-314

40 **Geiger KD,** Stoldt P, Schlote W, Derouiche A. Ezrin immunoreactivity is associated with increasing malignancy of astrocytic tumors but is absent in oligodendrogliomas. *Am J Pathol* 2000; **157:** 1785-1793

41 **Akisawa N,** Nishimori I, Iwamura T, Onishi S, Hollingsworth MA. High levels of ezrin expressed by human pancreatic adenocarcinoma cell lines with high metastatic potential. *Biochem Biophys Res Commun* 1999; **258:** 395-400

42 **Harrison GM,** Davies G, Martin TA, Jiang WG, Mason MD. Distribution and expression of CD44 isoforms and Ezrin during prostate cancer-endothelium interaction. *Int J Oncol* 2002; **21:** 935-940

43 **Legg JW,** Lewis CA, Parsons M, Ng T, Isacke CM. A novel PKC-regulated mechanism controls CD44 ezrin association and directional cell motility. *Nat Cell Biol* 2002; **4:** 399-407

44 **Guan XQ,** Wang CJ, Li YY. Effects of Ezrin on differentiation and adhesion of hepatocellular carcinoma. *Ai Zheng* 2002; **21:** 281-284

45 **Granes F,** Urena JM, Rocamora N, Vilaro S. Ezrin links syndecan-2 to the cytoskeleton. *J Cell Sci* 2000; **113:** 1267-1276

46 **Gronholm M,** Sainio M, Zhao F, Heiska L, Vaheri A, Carpen O. Homotypic and heterotypic interaction of the neurofibromatosis 2 tumor suppressor protein merlin and the ERM protein ezrin. *J Cell Sci* 1999; **112:** 895-904

47 **Meng JJ,** Lowrie DJ, Sun H, Dorsey E, Pelton PD, Bashour AM, Groden J, Ratner N, Ip W. Interaction between two isoforms of the NF2 tumor suppressor protein, merlin, and between merlin and ezrin, suggests modulation of ERM proteins by merlin. *J Neurosci Res* 2000; **62:** 491-502

48 **Gutmann DH,** Sherman L, Seftor L, Haipek C, Hoang Lu K, Hendrix M. Increased expression of the NF2 tumor suppressor gene product, merlin, impairs cell motility, adhesion and spreading. *Hum Mol Genet* 1999; **8:** 267-275


**Edited by** Zhu L and Wang XL

P.O.Box 2345, Beijing 100023,China
Fax: +86-10-85381893
E-mail: wjg@wjgnet.com www.wjgnet.com

World J Gastroenterol 2003;9(6):1187-1190
World Journal of Gastroenterology
Copyright ©2003 by The WJG Press ISSN 1007-9327

• ESOPHAGEAL CANCER •

# Research and control of well water pollution in high esophageal cancer areas

Xiu-Lan Zhang, Bing Zhang, Xing Zhang, Zhi-Feng Chen, Jun-Zhen Zhang, Shuo-Yuang Liang, Fan-Shu Men, Shu-Liang Zheng, Xiang-Ping Li, Xiu-Lan Bai

**Xiu-Lan Zhang, Zhi-Feng Chen, Shuo-Yuang Liang,** Cancer Institute, the Fourth Hospital of Hebei Medical University, Shijiazhuang 050011, Hebei Province, China
**Bing Zhang, Xing Zhang,** School of Public Health, Hebei Medical University, Shijiazhuang 050017, Hebei Province, China
**Jun-Zhen Zhang,** the Fourth Hospital of Hebei Medical University, Shijiazhuang 050011, Hebei Province, China
**Fan-Shu Men, Shu-Liang Zheng, Xiang-Ping Li,** Cixian Cancer Institute, Cixian County, Hebei Provence, China
**Xiu-Lan Bai,** Chichen Health Center, Chichen County, Hebei Province, China
**Supported by** Ministry of Education of China, No.85-914-01-01
**Correspondence to:** Dr. Xiu-Lan Zhang, Cancer Institute, the Fourth Hospital of Hebei Medical University, 12 Jian Kang Lu, Shijiazhuang 050011, Hebei Province, China. czf@xinhuanet.com
**Telephone:** +86-311-5825709 **Fax:** +86-311-6077634
**Received:** 2002-10-08 **Accepted:** 2002-12-22

## Abstract

**AIM:** In order to detect risk factors for esophageal cancer, a national research program was carried out during the Eighth Five-Year Plan (from 1991 to 1995).

**METHODS:** Cixian County and Chichen County in Hebei Province were selected as the index and the control for the study fields with higher or lower incidence of esophagus cancer in China, respectively. In these areas, we investigated the pollution of three nitrogenous compounds in well water for drinking and the use of nitrogen fertilizer in farming.

**RESULTS:** In well water, nitrate nitrogen, nitrite nitrogen and ammonia nitrogen were 8.77 mg/L, 0.014 mg/L and 0.009 mg/L in Cixian County in 1993, respectively. They were significantly higher than their levels (3.84 mg/L, 0.004 mg/L and 0.004 mg/L) in Chichen County ($P<0.01$, $t=6.281$, $t=3.784$, $t=3.775$). There was a trend that the nitrogenous compounds in well water increased from 1993 to 1996. The amount of nitrogen fertilizer used in farming was 787. 6 kg per hectare land in Cixian County in 1991, significantly higher than 186 kg per hectare in Chichen County ($t=9.603$, $P<0.001$).

**CONCLUSION:** These investigations indicate that the pollution of nitrogenous compounds in well water for drinking is closely related to the use of nitrogen fertilizer in farming, and there is a significantly positive correlation between the level of three nitrogenous compounds in well water and the mortality of esophageal cancer (correlation coefficient =0.5992). We suggest that improvement of well system for drinking water quality should be an effective measure for esophageal cancer prevention and control in rural areas.

Zhang XL, Zhang B, Zhang X, Chen ZF, Zhang JZ, Liang SY, Men FS, Zheng SL, Li XP, Bai XL. Research and control of well water pollution in high esophageal cancer areas. *World J Gastroenterol* 2003; 9(6): 1187-1190
http://www.wjgnet.com/1007-9327/9/1187.asp

## INTRODUCTION

It is well known that the chief causes of most cancers are environmental, dietary and lifestyle factors. In China, there is a special area around the Taihang Mountain with the highest incidence of esophageal cancer. Esophageal cancer has been studied in this rural area for a long time[1-3]. These studies indicate some relationship between local environmental factors and esophageal cancer[4-8]. Among these, nitrogenous compounds in well water for drinking is considered as a possible risk factor for esophageal cancer because of its close relationship with local people' s life[7, 8]. In this rural area, well is the main water source for drinking. It is polluted usually by nitrogenous compounds. In order to identify the effect of nitrogenous compound pollution on esophageal cancer, we designed a 2×2 cross-sectional study for factor analysis during the Eighth Five-Year Plan (from 1991 to 1995). The research program for investigating the relationship between drinking water pollution and esophageal cancer was carried out. It also included a step of improvement in well water quality and pollution control.

## MATERIALS AND METHODS

### *Study fields*

According to mortality, two counties from Hebei Province were selected for the present study fields, Cixian County as index and Chichen County as control, respectively. From 1974 to 1976, the mortality per 100 000 of esophageal cancer standardized by Chinese population in Cixian County and in Chichen County was 147.7 and 8.3 in male, and 79.33 and 2.8 in female, respectively. Cixian County is located at the southern part of Hebei Province and the eastern foot of the Taihang Mountain. There are 354 villages under 35 local town governments in Cixian County. It covers an area of 1 015 $Km^2$ and has a population of 580 000.

### *Well registration*

Before the investigation, a team for the program was organized. The investigators and other work staff were trained based on the program guideline. From the end of 1991 to the beginning of 1992, we completed registration of the wells located in 101 villages (9 towns) in Cixian County and made well file. The registered items of well file included (1) position, (2) type, (3) depth, (4) enclosing wall, (5) wall structure, (6) pipeline, (7) pollution source within 10 meter distance, (8) served population, and (9) served time. According to the well registration, we started a consecutive monitor on the pollution of three nitrogenous compounds (nitrate nitrogen, nitrite nitrogen and ammonia nitrogen) in the selected wells. Meanwhile, we investigated the amount of nitrogen fertilizer used in farming per year in the study fields.

### *Nitrogenous compounds examination*

The level of ammonia nitrogen in water was analyzed by Nessler' s reagent method. The amount of nitrate nitrogen and of nitrite nitrogen was tested in terms of Cadmium column

reduction method. The water samples were collected according to the routine method[9-12].

### *Statistical analysis*

Statistical analysis was performed by *t* test, and linear correlation was used for analysis on the relationship between three nitrogenous compounds and mortality of esophageal cancer. Two-tailed *P* value of less than 0.05 was defined as statistically significant.

## RESULTS

Among 9 towns in Cixian County, there were three types of well served for drinking water, manual-pump well, motor-pump well and non-pump well. Non-pump well was main type, about 554 were built in these areas. This type of well had a big opening mouth without pipe, enclosing wall and cover. Recently, some new motor-pump wells were built. They were 200 meter in depth with brick wall. These old and new wells provided drinking water for 130 952 people. In the control areas, 1/3 of wells was about 8 meters and 2/3 was less than 40 meters in depth. The depth of water varied with season. The served time of wells was different. The oldest one, for example, the Longwangmiao Well of the Xiguanglu Village of the Guanglu Town had a history of 300 years, and the new one was only 2 years.

The pollution of nitrogenous compounds in drinking water was a big health problem. We found that 41.2 % of the motor-pump wells and 88.5 % of non-pump wells existed pollution sources within 10 meter distance, for example, excrement and urine from the residents and animals, and pollution sources increased year by year. The monitoring data from the sampled wells showed that nitrate nitrogen, nitrite nitrogen and ammonia nitrogen in Cixian County were significantly higher than those in Chichen County ($P<0.01$), and the pollution increased gradually from 1993 to 1996 (Table 1). They were 20.6 %, 50.5 % and 33.3 % higher than the state permissive level, respectively. The amount of nitrogen fertilizer used in Cixian County' s farming was significantly higher than in Chichen County ($P<0.01$), and there was an increasing trend (Table 2). The time trend of three nitrogen compounds in relation to the use of nitrogen fertilizer is shown in Figure 1, Figure 2 and Figure 3 for Cixian County and Chichen County, respectively.

**Table 1** Three nitrogenous compounds pollution (mg/L) of the well water in Cixian County and Chichen County from 1993 to 1996

| | Numbers of well | 1993 | 1994 | 1995 | 1996 |
|---|---|---|---|---|---|
| Nitrate nitrogen | | | | | |
| Cixian | 33 | 8.770[b] | 13.381[b] | 14.473[b] | 19.554[b] |
| Chichen | 31 | 3.829 | 4.452 | 4.351 | 8.022 |
| Ratio (Cixian/Chichen) | | 2.29 | 3.00 | 3.33 | 2.44 |
| Nitrite nitrogen | | | | | |
| Cixian | 33 | 0.0144[b] | 0.0629[b] | 0.0407[b] | 0.0101[b] |
| Chichen | 31 | 0.0039 | 0.0094 | 0.0085 | 0.0020 |
| Ratio (Cixian/Chichen) | | 3.69 | 6.69 | 4.79 | 5.05 |
| Ammonia nitrogen | | | | | |
| Cixian | 33 | 0.0094[b] | 0.0256[b] | 0.0237 | 0.0117[b] |
| Chichen | 31 | 0.0039 | 0.0029 | 0.0230 | 0.0028 |
| Ratio (Cixian/Chichen) | | 2.41 | 8.82 | 1.03 | 4.18 |

[b]$P<0.01$, There was a significant difference between two counties.

**Table 2** Farming use of nitrogen fertilizer (kg/hectare) in Cixian County and Chichen County from 1991 to 1996

| | 1991 | 1992 | 1993 | 1994 | 1995 | 1996 |
|---|---|---|---|---|---|---|
| Cixian | 787.6 | 825.1 | 1293.1 | 1213.6 | 1251.1 | 1053.1 |
| Chichen | 186.0[b] | 202.5[b] | 196.5[b] | 201.0[b] | 220.5[b] | 219.0[b] |
| Ratio (Cixian/Chichen) | 4.20 | 4.07 | 6.58 | 6.04 | 5.67 | 4.81 |

[b]$P<0.01$, There was a significant difference between two counties.

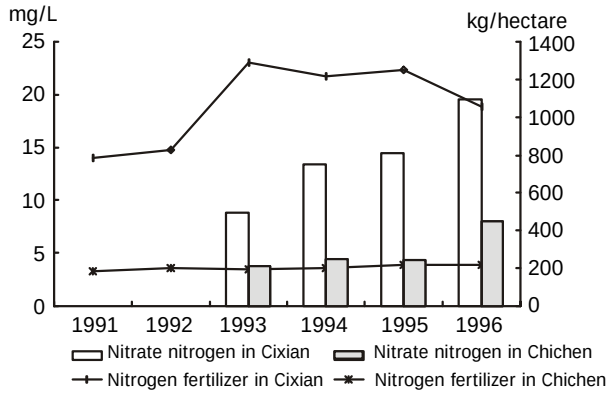


**Figure 1** Time trend of nitrate nitrogen in relation to the farming use of nitrogen fertilizer in Cixian County and Chichen County.

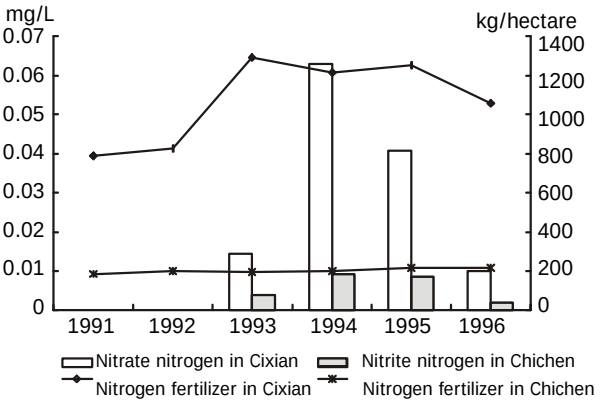


**Figure 2** Time trend of nitrite nitrogen in relation to the farming use of nitrogen fertilizer in Cixian County and Chichen County.

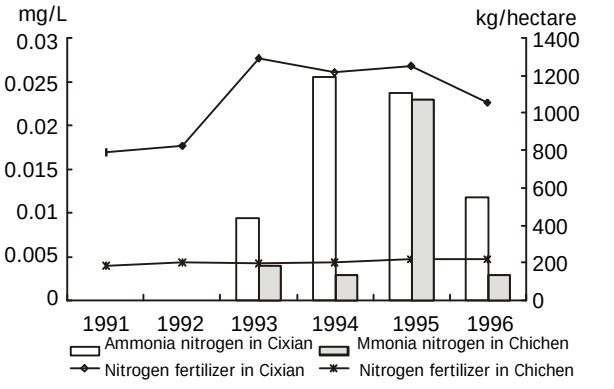


**Figure 3** Time trend of ammonia nitrogen in relation to the farming use of nitrogen fertilizer in Cixian County and Chichen County.

## DISCUSSION

It has been proven in animal experiments that nitrosamine compounds (NOC) are a kind of strong carcinogen and can

cause tumor in different animal tissues and organs[13-21]. The epidemiological investigation has also demonstrated an increased risk of human gastric cancer with food intake polluted by nitrosamine compounds[22,23]. Nitrate and nitrite are precursors of NOC[24,25].

If well water contains a large amount of three nitrogenous compounds, and serve as main water source, there may be two harmful effects on local people' s health. One is that three nitrogenous compounds would accumulate in plants and in crops[25-29]. Usually, nitrate is easily reduced to nitrite, and then it is synthesized into NOC. The other harmful effect is that local people and livestock or poultry would have an increased intake of three nitrogenous compounds through the drinking water[30-32]. These nitrogenous compounds with ammonia can be changed to a strong carcinogen, NOC, in stomach since its pH value is 1-3 from gastric acid[33].

The present investigation showed that the pollution of three nitrogenous compounds in the index area with high risk of esophageal cancer was significantly higher than that in the control area ($P$<0.01). The mortality ratio between Cixian County and Chichen County was 17.9 (147.7 per 100 000 /8. 3 per 100 000) in male, and 28.5 (79.3/2.8) in female in the period of 1974 through 1976. There was a positive correlation between the nitrate nitrogen, nitrite nitrogen in well water and mortality of esophageal cancer in the study fields. The present findings indicate that heavy pollution of nitrogenous compounds in drinking water in the index area is a possible risk factor for esophageal cancer.

There were two possible pollution sources of nitrogenous compounds for well in the investigated fields, living garbage or excrement and farming nitrogen fertilizer. In comparison of the two counties, we found that the amount of nitrogen fertilizer used in farming in Cixian County was significantly higher than that in Chichen County, and the pollution of nitrate nitrogen and nitrite nitrogen in well water had a similar trend (Figure 1 and Figure 2). It can be understood that the nitrate nitrogen and nitrite nitrogen in well water come mainly from the pollution of farming nitrogen fertilizer. The amount of ammonia nitrogen in well has not a regular change. Its pollution to the drinking water is possibly resulted from the excrement of local people and animals other than farming nitrogen fertilizer.

Based on these evidences, well water pollution control of three nitrogenous compounds will be one of the important measures for the primary prevention of esophageal cancer in the higher risk areas. The study revealed that water quality improvement had a beneficial effect on gastric cancer prevention[34]. At the beginning of the Ninth Five-Year Plan (1996-2000), a program for improvement of water supply system in the index area was started. Initial effect was observed (Table 3). There was a significant decline of three nitrogenous compounds in well water after several years' pollution control. These findings indicate that the program for improvement in water supply system is successful for pollution control. Whether pollution control of nitrogenous compounds contributes to incidence decline of esophageal cancer in the higher risk area, needs further study and more evidence.

**Table 3** Three nitrogenous compounds (mg/L) in well water before and after well reconstruction

| No. of well | Nitrate nitrogen | | Nitrite nitrogen | | Ammonia nitrogen | |
|---|---|---|---|---|---|---|
| | Before | After | Before | After | Before | After |
| 12# | 14.9621 | 8.0097 | 0.0077 | 0.0033 | 0.0131 | 0.0048 |
| 14# | 8.9890 | 1.9099 | 0.0208 | 0.0067 | 0.0127 | 0.0053 |
| 29# | 18.4929 | 0.0000 | 0.2929 | 0.0100 | 0.0459 | 0.0087 |

12#, 14#, 29# are the number of the sampled well.

Based on the presently investigated results, measures for pollution prevention and control in the areas with high risk of esophageal cancer should include: (1) The first measure is to improve the health consciousness of local people on drinking water, and to develop the type of deep well with pipeline. (2) The second is to focus on the environmental hygiene surrounding the well. It includes garbage control near water source, and sanitary management of excrement and urine. (3) The third is to establish and to improve the system management of water source, and to supply clean water with pipeline. (4) The fourth is to build high quality lavatory and to prevent its pollution to well water. (5) The fifth is to encourage local farmers to use rational formula fertilization in order to decrease effectively organic nitrogen pollution in the environment.

## REFERENCES


1 **Hou J,** Lin PZ, Chen ZF, Wang GQ, Liu KG, Li SS, Meng FS, Du CL. Survey on esophageal cancer in Cixian County. *Zhongliu Fangzhi Yanjiu* 1998; **25**: 73-75

2 **Yokokawa Y**, Ohta S, Hou J, Zhang XL, Li SS, Ping YM, Nakajima T. Ecological study on the risks of esophageal cancer in Cixian, China: the importance of nutritional status and the use of well water. *Int J Cancer* 1999; **83**: 620-624

3 **Qiao YL**, Hou J, Yang L, He YT, Liu YY, Li LD, Li SS, Lian SY, Dong ZW. The Trends and preventive strategies of esophageal cancer in high-risk areas of Taihang Mountains, China. *Zhongguo Yixue Kexue Yuan Xuebao* 2000; **23**: 10-14

4 **Zhuo XG**, Watanabe S. Factor analysis of digestive cancer mortality and food consumption in 65 Chinese counties. *J Epidemiol* 1999; **9**: 275-284

5 **Li WJ**, Zhu MJ Chen PP, Lu WQ, Wang Q, Shi BQ. Study on dietary pattern and nutrients intakes of residents in areas of high and low incidence of esophageal cancer. *Weisheng Yanjiu* 1997; **26**: 351-355

6 **Wang H**, Wei H, Ma J, Luo X. The fumonisin B1 content in corn from North China, a high risk area of esophageal cancer. *J Environ Pathol Toxicol Oncol* 2000; **19**: 139-141

7 **Li WJ**, Lu WQ, Zhu MJ, Shi BQ, Wang Q. Determination of copper, zinc, iron and calcium in wheat and maize and three nitrogen compounds in high and low risk areas of esophageal cnacer. *Weisheng Yanjiu* 1998; **27**: 69-71

8 **Zhang XL**, Li SS, Zhang WZ. Investigation and study on drinking water in Cixian County. *Zhongguo Zhongliu* 1996; **5**: 12-14

9 **Hao CJ**. The Practical handbook for environmental monitoring and water analysis. *Harbin: Harbin Industrial University Press* 1986

10 **Ministry of Public Health**. The people's republic of China, the standarded method for drinking water testing. *Beijing: China Standard Bureau Press* 1986

11 **Environmental Protective Bureau**. Ministry of urban and rural construction & environment protection analytical method for environmental monitoring. *Beijing*: *Chinese Environmental Science Press* 1986

12 **Chinese Environmental Monitoring Center**. The handbook of quality assurance for environmental monitoring on water. *Beijing*: *Chemical Industry Press* 1984

13 **Opitz OG**, Harada H, Suliman Y, Rhoades B, Sharpless NE, Kent R, Kopelovich L, Nakagawa H, Rustgi AK. A mouse model of human oral- esophageal cancer. *J Clin Invest* 2002; **110**: 761-769

14 **Fong LY**, Nguyen VT, Farber JL. Esophageal cancer prevention in zinc- deficient rats: rapid induction of apoptosis by replenishing zinc. *J Natl Cancer Inst* 2001; **93**: 1525-1533

15 **Straif K**, Weiland SK, Bungers M, Holthenrich D, Taeger D, Yi S, Keil U. Exposure to high concentrations of nitrosamines and cancer mortality among a cohort of rubber workers. *Occup Environ Med* 2000; **57**: 180-187

16 **Qi GY**, Shu SC, You CF, Chen SW, Song Y. A case-control study on the influential factors of esophageal cancer. *Zhongguo Manxingbing Yu Fangyu Kongzhi* 2001; **9**: 15-14,34

17 **Lin K**, Shen ZY, Cai SS, Lu SX, Guo LP. Investigation on nitrosamines in the diets of the inhabitants of high-risk area for esophageal cancer in the southern China and analysis of the correlation factors. *Weisheng Yanjiu* 1997; **26**: 266-269

18 **Lin K**, Shen W, Shen Z, Wu Y, Lu S. Dietary exposure ad urinary excretion of total N- nitroso compounds, nitrosamino acids and volatile nitrosamine in inhabitants of high- and low- risk areas for esophageal cancer in Southern China. *Int J Cancer* 2002; **102**: 207-211
19 **Zhang GS**, He YT, Hou J. A case control study on risk factor of esophageal cancer in Cixian County. *Sichuan Zhongliu FangZhi* 2000; **13**: 65-67
20 **Wilp J**, Zwickenpflug W, Richter E. Nitrosation of dietary myosmine as risk factor of human cancer. *Food Chem Toxicol* 2002; **40**: 1223-1228
21 **Siddiqi M**, Kumar R, Fazili Z, Spiegelhalder B, Preussmann R. Increased expoure to dietary amines and nitrate in a popalation at high risk of oesophageal and gastric cancer in Kashmir. *Carcinogenesis* 1992; **13**: 1331-1335
22 **Cai L**, Zheng ZL, Zhang ZF. Risk factors for the gastric cardia cancer: a case-control study in Fujian Province. *World J Gastroenterol* 2003; **9**: 214-218
23 **Ye WM**, Yi YN, Luo RX, Zhou TS, Lin RT, Chen GD. Diet and gastric cancer: a casecontrol study in Fujian Province, China. *World J Gastroenterol* 1998; **4**: 516-518
24 **Rogers MA**, Vaughan TL, Davis S, Thomas DB. Consumption of nitrate, nitrite, and nitrosodimethylamine and the risk of upper aerodigestive tract cancer. Cancer *Epidemiol Biomarkers Prev* 1995; **4**: 29-36
25 **Yang XF**, Wang KJ, Jia YS, Lian BQ, Li T, Li SD, Du C, Yan JG. Epidemiological investigation on cancer mortality of the workers exposed to nitrite compounds. *Zhonghua Laodongwei Shengzhi Yebing Zazhi* 1996; **14**: 293-295
26 **Li W**, Lu W, Zhu M, Shi B. Determination of copper, zinc, iron and calcium in wheat and maize and three nitrogen compounds in high and low risk areas of esophageal cancer. *Weisheng Yanjiu* 1998; **27**: 69-71
27 **Lu SH**, Camus AM, Ji C, Wang YL, Wang MY, Bartsch H. Mutagenicity in salmonella typhimurium of N-3-methylbutyl- N-1-methyl-acetonyl-nitrosamine and N-methyl-N-benzylnitrosamine, N-nitrosation products isolated from cornbread contaminated with commonly occurring moulds in Linshien County, a high incidence area for oesophageal cancer in Northern China. *Carcinogenesis* 1980; **1**: 867-870
28 **Guo LP**, Zhang FS, Wang XR, Mao DR, Chen XP. Effect of long-term fertilization on soil nitrate distribution. *J Environ Sci* 2001; **13**: 58-63
29 **Ramos C**, Agut A, Lidon AL. Nitrate leaching in important crops of the Valencian Community region. *Environ Pollut* 2002; **118**: 215-223
30 **Barrett JH**, Parslow RC, McKinney PA, Law GR, Forman D. Nitrate in drinking water and the incidence of gastric, esophageal, and brain cancer in Yorkshire, England. *Cancer Causes Control* 1998; **9**: 153-159
31 **Lu WQ**, Chen JL, Li WJ, Wang Y, Ddong WZ, Zhu MJ, Wang Q. Analysis on three nitrogen compounds of the drinking water in high and low risk areas of esophageal cancer. *Zhongguo Zhongliu* 2000; **9**: 227
32 **Shrestha RK**, Ladha JK. Nitrate pollution in groundwater and strategies to reduce pollution. *Water Sci Technol* 2002; **45**: 29-35
33 **Mayne ST**, Risch HA, Dubrow R, Chow WH, Gammon MD, Vaughan TL, Farrow DC, Schoenberg JB, Stanford JL, Ahsan H, West AB, Rotterdam H, Blot WT, Fraumeni JF Jr. Nutrient intake and risk of subtypes of esophageal and gastric cancer. *Cancer Epidemiol Biomarkers Prev* 2001; **10**: 1055-1062
34 **Wang ZQ**, He J, Chen W, Chen Y, Zhou TS, Lin YC. Relationship between different sources of drinking water, water quality improvement and gastric cancer mortality in Changle County-A retrospective-cohort study in high incidence area. *World J Gastroenterol* 1998; **4**: 45-47

**Edited by** Wen CY and Wang XL

P.O.Box 2345, Beijing 100023,China
Fax: +86-10-85381893
E-mail: wjg@wjgnet.com www.wjgnet.com

World J Gastroenterol 2003;9(6):1191-1195
World Journal of Gastroenterology
Copyright ©2003 by The WJG Press ISSN 1007-9327

• GASTRIC CANCER •

# Development of an oral DNA vaccine against MG7-Ag of gastric cancer using attenuated *salmonella typhimurium* as carrier

Chang-Cun Guo, Jie Ding, Bo-Rong Pan, Zhao-Cai Yu, Quan-Li Han, Fan-Ping Meng, Na Liu, Dai-Ming Fan

**Chang-Cun Guo, Jie Ding, Zhao-Cai Yu, Quan-Li Han, Fan-Ping Meng, Na Liu, Dai-Ming Fan,** Institute of Digestive Disease, Xijing Hospital, Fourth Military Medical University, Xi' an 710032, Shaanxi Province, China
**Bo-Rong Pan,** Oncology Center, Xijing Hospital, 127 Changle West Road, Xi' an 710032, Shaanxi Province, China
**Supported by** the National Natural Science Foundation of China, No. 39870742
**Correspondence to:** Professor Dai-Ming Fan, Institute of Digestive Disease, Xijing Hospital, Fourth Military Medical University, Xi' an 710032, Shaanxi Province, China. daimfan@fmmu.edu.cn
**Telephone:** +86-29-3375229
**Received:** 2002-08-24 **Accepted:** 2002-10-21

## Abstract

**AIM:** To develop an oral DNA vaccine against gastric cancer and evaluate its efficacy in mice.

**METHODS:** The genes of the MG7-Ag mimotope and a universal Th epitope (Pan-DR epitope, PADRE) were included in the PCR primers. By PCR, the fusion gene of the two epitopes was amplified. The fusion gene was confirmed by sequencing and was then cloned into pcDNA3.1(+) plasmid. The pcDNA3.1 (+)-MG7/PADRE was used to transfect an attenuated *Salmonella typhimurium*. C57BL/6 mice were orally immunized with $1\times10^8$ cfu *Salmonella* transfectants. *Salmonella* harboring the empty pcDNA3.1(+) plasmid and phosphate buffer saline (PBS) were used as negative controls. At the 6th week, serum titer of MG7-Ag specific antibody was detected by ELISA. At the 8th week cellular immunity was detected by an unprimed proliferation test of the spleenocytes by using a [$^3$H]-thymidine incorporation assay. Ehrlich ascites carcinoma cells expressing MG7-Ag were used as a model in tumor challenge assay to evaluate the protective effect of the vaccine.

**RESULTS:** Serum titer of antibody against MG7-Ag was significantly higher in mice immunized with the vaccine than that in control groups (0.841 *vs* 0.347, $P<0.01$; 0.841 *vs* 0.298, $P<0.01$), while *in vitro* unprimed proliferation assay of the spleenocytes showed no statistical difference between those three groups. Two weeks after tumor challenge, 2 in 7 immunized mice were tumor free, while all the mice in the control groups showed tumor formation.

**CONCLUSION:** Oral DNA vaccine against the MG7-Ag momitope of gastric cancer is immunogenic. It can induce significant humoral immunity against tumor in mice, and the vaccine has partially protective effects.

Guo CC, Ding J, Pan BR, Yu ZC, Han QL, Meng FP, Liu N, Fan DM. Development of an oral DNA vaccine against MG7-Ag of gastric cancer using attenuated *salmonella typhimurium* as carrier. *World J Gastroenterol* 2003; 9(6): 1191-1195

http://www.wjgnet.com/1007-9327/9/1191.asp

## INTRODUCTION

Gastric cancer is the most common malignant tumor in China and the second most common malignancy around the world. Conventional intervention measures such as operation and chemotherapy work poorly in treating gastric cancer. And with few tumor-specific antigens identified, there are few effective vaccines developed to combat gastric cancer. MG7-Ag, discovered by our institute, is a kind of gastric cancer-specific tumor-associated antigen. Detecting the serum anti-MG-Ag antibody serves as a preliminary test in the diagnosis for gastric cancer and could be used for the surveillance of relapse and the appraisal of treatment efficacy[1]. MG7-Ag can be used as an indicator for high risk of malignant change in stomach mucosa dysplasia[2]. Primary study showed that MG7-Ag could elicit significant specific immune response against gastric cancer, suggesting that it could be an excellent target for cancer vaccine development. However, due to its unknown identity, it is much difficult to isolate and purify MG7-Ag from tumor tissues. Recently, we have identified the mimotopes of MG7-Ag by screening the phage display library, and the mimotopes could mimic the primary antigen efficiently, as shown by *in vitro* and *in vivo* assays[3, 4]. We reported here for the first time the development of an oral DNA vaccine by using the MG7-Ag mimotope of gastric cancer.

## MATERIALS AND METHODS

### *Plasmids and bacteria*

The plasmid pcDNA3.1(+) was purchased from Invitrogen Corporation. And the pEGFP plasmid containing the enhanced green fluorescence protein (EGFP) gene was purchased from Clontech Corporation. Attenuated *Salmonella typhimurium* SL3261 strain was used as the oral vector to develop the vaccine.

### *Construction of eukayotic expression vector of MG7-Ag momitope fused with a helper T cell epitope PADRE*

Two pairs of PCR primers ($P_{1.1}$, $P_{1.2}$ and $P_{2.1}$, $P_{2.2}$) were designed by using Primer Premiere 5.0 software. The sense primers ($P_{1.1}$ and $P_{2.1}$) were both 5' -CGATGTACGGGCCAGATATACGCG-3', corresponding to the 209-232 bp sequence of pcDNA3.1(+). Reverse primer $P_{1.2}$ was 5' -ACTTCCTCCTCCTTTTGTATGCACA TGAGGTTTCATGGTGGCAAGCTTCCTACCGCCCATTTGCGT, corresponding to the reverse complementary sequence of 768-785 bp sequence of pcDNA3.1(+), *Hin*d III digestion site, Kozak sequence, and the sequence of the MG7-Ag mimotope. Reverse primer $P_{2.2}$ was 5' -TTAAGCAGCAGCTTTAAGTGTCCAAGCAGCCACAAATTTAGCACTTCCTCCTCCTTTTGTATGCA-3', corresponding to the reverse complementary sequence of the MG7-Ag mimotope and the universal Th epitope PADRE. Two PCR reactions were performed to incorporate the mimotope and the PADRE into a fragment of pcDNA3.1(+) plasmid. In this case, the pcDNA3.1 fragment was used as a carrier to facilitate further manipulations. For the first PCR reaction, template was plasmid pcDNA3.1(+), and primers were $P_{1.1}$ and $P_{1.2}$. By using the product of the first PCR as template, a second PCR was performed with primers $P_{2.1}$ and $P_{2.2}$ to incorporate

the PADRE epitope into the yielding fragment. The final PCR product was visualized by agarose electrophoresis and was then cloned into pUCm-T vector and sequenced on ABI PRISM™ 377 sequencer. Then, the PCR product was subcloned into pcDNA3.1(+) vector from the pUCm-T vector. By restrictive enzyme digestion with *Hin*d III, the non-relevant plasmid fragment was removed from the final recombinant vector pcDNA3.1(+)-MG7/PADRE. The vector was sequenced to confirm the proper encoding sequence.

### *Construction of oral DNA vaccine and in vitro experiment using attenuated Salmonella typhimurium as the oral DNA vector*

To get the oral DNA vaccine, the pcDNA3.1(+)-MG7/PADRE vector was transduced into the attenuated *Salmonella typhimurium* SL3261 by electroporation (2.5 kV, 25 μF, 200 Ω, pulse time 0.0326S). Plasmid in the *Salmonella* transfectant was extracted and used as template, and PCR was performed by using primer $P_{1.1}$ and primer $P_{2.2}$ to verify the successful transfection. The PCR product underwent agarose electrophoresis for visualization. An *in vitro* experiment was performed by using the SL3261 strain as the oral vector of DNA vaccine according to reference[5]. Briefly, eukaryotic expression vector of the enhanced green fluorescence protein was transduced into the attenuated *Salmonella typhimurium* SL3261. The transfectants were coincubated with murine peritoneal macrophage at 37 ℃ for 30 min. SL3261 harboring the empty pcDNA3.1(+) plasmid was used as negative control. Gentamycin was added into the culture media to kill the extracellular beacteria. Four hours later, tetracycline was added to kill the intracellular bacteria. The infected macrophages were cultured for 48 hours, and were then examined by flow cytometry (FCM) for the expression of green fluorescence protein.

### *Immunization of the mice and immune response examination*

Thirty-five female 4-week-aged C57BL/6J mice weighing 15-20g were used in the immunization assay. They were randomly divided into 3 groups, which were orally given the PBS solution (10 mice, PBS control), the attenuated *Salmonella* SL3261 harboring the empty pcDNA3.1(+) plasmid (10 mice, empty control) or the oral DNA vaccine SL3261 strain harboring the pcDNA3.1(+)-MG7/PADRE (15 mice, immunization group). Before immunization, all the mice were starved overnight and pre-administered with 100 μl 10 g/L $NaHCO_3$ solution. Each time, 100 μl PBS (pH7.6) was given to the mice in PBS control group, and $1\times10^8$ *Salmonella typhimurium* were given to the mice in the empty control and immunization group. PBS and *Salmonella typhimurium* were given to the mice by orogastric inoculation. Immunization was repeated every two weeks. At the 6th week after the first immunization, sera from the mice (5 mice from each group) were prepared and 1:80 diluted. By coating KATO III cells expressing the MG7-Ag on the plates, a cellular ELISA was performed to detect the antibody against MG7-Ag. At the 8th week, the splenocyte suspension was prepared, and an unprimed proliferation test of the splenocytes was performed by a [$^3$H]-thymidine incorporation assay[6] with a few modifications. Briefly, splenocyte suspension of the mice from three groups was prepared. $1\times10^6$ cells were plated into each well of 96-well plate. Into each well, $1\times10^5$ mytocin C-pretreated autologous antigen-presenting cells (APC) were added. The cells were incubated with 50 μg/ml synthetic MG7-Ag mimotope peptide for 4 hours. The cells were washed and cultured for 3 days. Then cells were incubated for 6 hours with 74MBq/L of [$^3$H]thymidine. The plates were harvested, and the proliferative response of the splenocytes was examined by measuring the β counts of the cells. To further investigate the efficacy of the oral DNA vaccine, the tumor challenge assay was performed. Ehrlich ascites carcinoma cells (EAC) were immunostained with MG7 antibody to verify the presence of the MG7-Ag. Then $1\times10^7$ EAC cells were injected into the abdominal cavity of the mice in each group. The number of tumor-bearing mice and the survival rate of each group were observed.

## RESULTS

### *Construction of the oral DNA vaccine*

By PCR, MG7-Ag mimotope and PADRE were fused together and incorporated into a fragment of the pcDNA3.1(+) (Figure 1). The proper coding of the epitopes was confirmed by sequencing (Figure 2). The PCR product was subcloned into pcDNA3.1(+). And by Hind III digestion, the fragment of the pcDNA3.1 in the PCR product was removed (Figure 3).

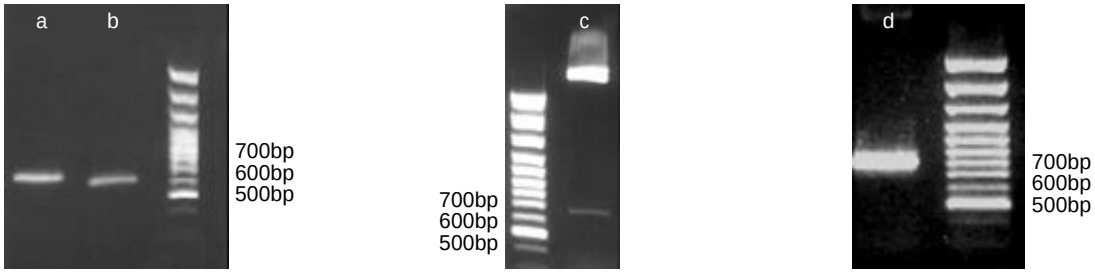


**Figure 1** Incorporation of the epitope gene into the pcDNA3.1 fragment by PCR: A product of 620bp was amplified by the first PCR (a), and a fragment of 660bp was amplified by the second PCR (b).
**Figure 2** Hind III digestion of the recombinant plasmid after subcloning the PCR product into pcDNA3.1(+) from the pUCm-T vector: A fragment of 660bp was released (c), which corresponded to the size of the carrier fragment.
**Figure 4** PCR identification of the pcDNA3.1(+)-MG7/PADRE plasmid harbored by the *Salmonella typhimurium* SL3261: By PCR, a fragment of 800bp was amplified (d), suggesting the existence of epitope genes and removal of carrier fragment.

AAG CTT GCC ACC ATG AAA CCT CAT GTG CAT ACA AAA GGA GGA GGA AGT GCT AAA TTT
Hind III Kozak M K P H V H T K G G G S A K F
GTG GCT GCT TGG ACA CTT AAA GCT GCT GCT TAA
V A A W T L K A A A Z

**Figure 3** Sequencing of PCR product (partial sequence): By PCR, the two epitopes were fused together and incorporated into a pcDNA3.1 fragment. The amino acid sequence of KPHVHTKGGGS correspondeds to the sequence of MG7-Ag mimotope. AKFVAAWTLKAAZ corresponds to the sequence of universal Th epitope PADRE.

The pcDNA3.1(+)-MG7/PADRE was transduced into the attenuated *Salmonella typhimurium* SL3261 by eletroporation. Plasmid from the transfectant was extracted and used as template. By PCR, it was verified that the plasmid harbored by the SL3261 transfectant was pcDNA3.1(+)-MG7/PADRE (Figure 4).

### *In vitro assay using Salmonella typhimurium as oral DNA vaccine vector*

Forty-eight hours after infection with *Salmonella typhimurium*, fluorescence intensity of macrophages infected by the *Salmonella* harbouring the pcDNA3.1(+)-EGFP was 0.927 and the percentage of fluorescent cells was 40.6 %, which was significantly higher than that of than the control (0.345 $P<0.01$ and 3.8 % $P<0.01$ respectively). Our result showed that pcDNA3.1(+)-EGFP plasmid was transferred into the macrophages from the bacteria and was expressed by the macrophages, suggesting that the SL3261 strain could be used as the oral DNA vaccine vector.

### *Immune response induced by the oral DNA vaccine*

No diarrhea was seen in the mice given the *Salmonella typhimurium* harbouring either the vaccine DNA or the empty pcDNA3.1(+) vector. And no *Salmonella* infection-associated death occurred in the end of the experiments. Six weeks after the first immunization, serum titre of the antibody against MG7-Ag was significantly increased in the vaccine-immunized mice, while no significant titre of MG7 antibody was detected in the control groups. There was a significant difference between the vaccine-immunized group and the control groups ($P<0.05$), while no difference was detected between the two control groups ($P<0.05$, Table 1). *In vitro* unprimed proliferation assay of the splenocytes showed no statistical difference between those three groups (Table 2), suggesting no significant cellular immunity was elicited.

**Table 1** Cellular ELISA detection of antibody in the immune serum ($OD_{450}$, $\bar{x}\pm s$)

| Group | $OD_{450}$ |
|---|---|
| PBS control | 0.298±0.017 |
| Empty vector control | 0.347±0.062 |
| Vaccination group | 0.841±0.136 |

Paired Student *t*-test was used to investigate the difference between two groups.

**Table 2** In vitro unprimed assay of spleenocytes (Radiation count/min cpm $\bar{x}\pm s$)

| Group | Radiation count (cpm) |
|---|---|
| PBS control | 2981±389.8 |
| Empty vector control | 3158±416.7 |
| Vaccination group | 2896±335.4 |

Paired student *t*-test was used to investigate the difference between two groups.

By immunohistochemical staining, it was found that MG7-Ag was expressed in the EAC cells, both on the membrane and in the cytoplasm (Figure 5), indicating that the EAC cells can be used to challenge the mice to investigate the protective ability of the oral DNA vaccine. Two weeks after the challenge, all the mice in the control groups developed neoplastic ascites, which was confirmed by microscopic observation of the cells in ascites. However, 2 in the 7 vaccinated mice were tumor free. All the mice in the control group died 4 weeks after the primary challenge, while the tumor-free mice in the immunization group survived 8 weeks after the challenge with no signs of tumor formation. Our results suggested that the oral DNA vaccine was partially protective.

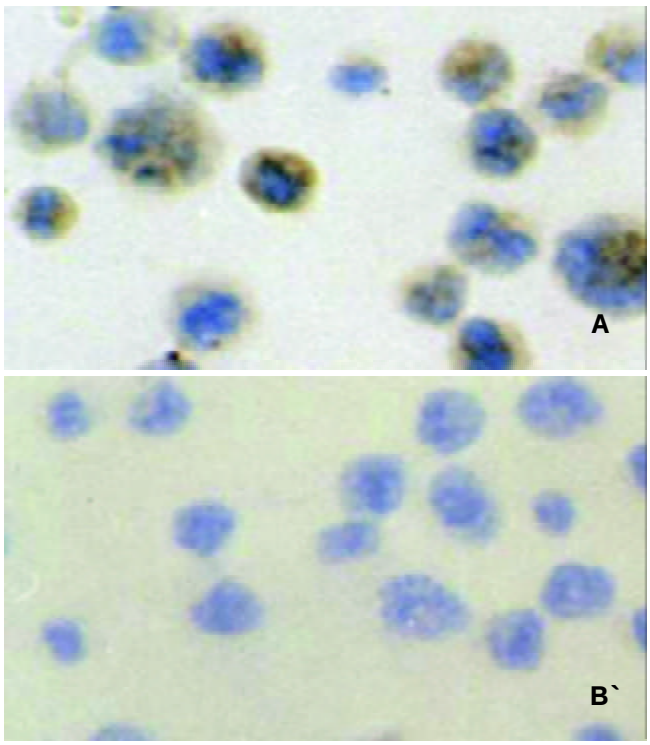


**Figure 5** Immunohistochemical staining of the Ehrlich ascites carcinoma cells (EAC): Positive signal was seen in the cytoplasm and membrane of the EAC cells (A). When stained with a negative control monoclonal antibody (anti-E-tag antibody), the EAC cells showed no positive staining (B).

## DISCUSSION

Attenuated strains of *Salmonella typhimurium* have been widely used as vehicles for delivery and expression of vaccine antigens. Attenuated *Salmonella typhimurium* strains expressing antigens from bacteria, viruses and parasites have been proved efficient as well as safe in combating respective pathogens[7]. Due to mutations in their genome, attenuated *Salmonella typhimurium* lost their pathogenicity but remained to be invasive. When used as the oral vehicle, they can invade the M cells and the intestinal epithelial cells and penetrate the mucosal barrier of the intestine. Subsequently, they can be uptaken by the macrophages and dendritic cells (DC) in the lamina propria and the Peyer' s patch. The intracellular bacteria would not undergo lysis in the lysosomes immediately but survive for a period of time due to unknown reasons. The intracellular bacteria could provide a reservoir of antigen, so these features of the *Salmonella typhimurium* strains make them an excellent vehicle of oral vaccines. The use of attenuated *Salmonella typhimurium* as oral DNA vaccine carrier was first reported by Darji and his colleagues[8]. They found that when used as the carrier of DNA vaccines, the *Salmonella* could deliver the eukaryotic vector to the host cells through the unknown mechanism and the eukaryotic vector could be expressed by the host cells. Further study by Paglia *et al* suggested that attenuated *Salmonella typhimurium* could deliver the eukaryotic vector to the dendritic cells in the spleen[9]. Other studies suggested the expression of eukaryotic vectors in dendritic cells in the mesenteric nodes and Peyer' s patch was detected early after inoculation[10-12]. Oral DNA vaccines developed by using *Salmonella typhimurium* as carrier

can provide a context similar to intracellular bacteria infection and render the body danger signals. Besides, the DC cells are excellent antigen presenting cells and have high expression of costimulatory molecules. So it is not surprising that the oral DNA vaccines can evoke significant immune response, especially CTL response[5, 11, 13, 14]. In this study, we used an attenuated *Salmonella typhimurium* strain SL3261 (S. *typhimurium* WARY hisG46 aroA del407 Fusaricres etc, R+M+), which genotype is much the same as SL7207. We found that it could also act as the carrier of DNA vaccine, which was safe to mice.

CD4+ T cells (T helper cells, Th) play important roles in modulating immune response: They can facilitate the activation of CTL cells by cross-priming, produce various cytokines for the activation of T and B cells, upregulate the costimulatory molecules on APC cells and enhance their ability of antigen processing and presenting. In order to enhance the efficacy of the DNA vaccine, we fused the MG7-Ag mimotope with a universal T helper cell epitope PADRE, which was developed by Alexander *et al*[15]. They introduced the anchoring motif of MHC molecules into the polyalanine backbone and found that the PADRE could bind to most of the human HLA-DR alleles and certain mouse class II alleles and elicit strong CD4+ T cell response; the epitopes were approximately 1000 times more powerful than natural T cell epitopes. PADRE has been used as the adjuvant for various epitopes including B cell epitope, CTL epitope and carbohydrate epitope and was proved to be efficient in enhancing the immunogenicity of these epitopes. Ishioka *et al*[16] developed a minigene vaccine by including PADRE in tandem with multiple CTL epitopes with no spacer between them, and found that though the affinity of the CTL epitopes varied much, PADRE could still provide adjuvant effects on the induction of strong CTL response. Their study suggested that spacers were not necessarily needed in designing the multi-epitope minigene DNA vaccines. Therefore we fused the PADRE directly with the mimotope gene. To guarantee the efficient expression of the minigene, we included a Kozak sequence to right upstream the ATG initiation codon of the fusion gene. Kozak sequence is a specific sequence for the recognition and initiation of the transcription for the eukaryotic ribosome. The study suggested that Kozak sequence was necessary for correct and efficient expression of minigene vaccine[17].

MG7-Ag of gastric cancer was discovered by our institute, and we found that the immonogenicity of the MG7-Ag was located in the carbohydrate chain of the glycoprotein. Due to its unknown identity, MG7-Ag is hard to be isolated from tumor tissue. Our institute has successfully identified the anti-MG-Ag antibodies using phage display method[18,19]. Thus we identified the mimic peptides of MG7-Ag by screening the phage display peptide library with the MG7 antibody and then used it as the target for vaccine development. DNA vaccine of mimotope was first reported by Kieber-Emmons *et al*[20], and the feasibility to develop DNA vaccine of mimotopes was further confirmed by Lesinski *et al*[21]. In both studies, the DNA vaccine of mimotope induced strong humoral immune response. And in the former study, no significant CTL response was elicited. As shown by Monzavi-Karbassi *et al*, the mimic peptides could induce carbohydrate antigen reactive T cell response[22]. Therefore, absence of significant specific T cell response in Kiever-Emmons' s study and our study might be due to the immunogen type of the primary antigen. However, the oral DNA vaccine developed by us was shown to be partially protective as shown by the tumor challenge assay though no significant difference was seen in the $^3$H-Tdr incorporation assay. The inconsistency between the results of tumor challenge assay and the $^3$H-Tdr incorporation assay might be due to the following reasons: (1) The inaccuracy of the $^3$H-Tdr incorporation assay in determining the T cell response. More accurate methods include $^{51}$Cr-releasing assay and ELISPOT. Moreover in our study, we did not purify CD8+ T cells for $^3$H-Tdr incorporation assay. The existence of other types of cells might affect the results. (2) The sample included in the tumor challenge assay was too small. Much larger samples would be needed to further confirm the protective effect of the oral DNA vaccine.

Due to its various mechanisms of multi-drug resistance, gastric cancer often responds poorly to chemotherapy[23, 24]. Cancer vaccines have been proved a powerful adjuvant intervention in gastric cancer management. Study showed that gastric cancer antigens could induce specific immune response[25]. We reported here the first attempt to develop an oral DNA vaccine against gastric cancer antigen mimotope. The oral DNA vaccine against MG7-Ag mimotope is immunogenic. It can induce significant immune response against gastric cancer and may be partially protective in mice. Our results verified the feasibility to develop oral DNA vaccine of mimotopes and efficacy as well as safety of *Salmonella typhimurium* as oral DNA vaccine carriers.

## REFERENCES


1 **Zhang XY.** Some recent works on diagnosis and treatment of gastric cancer. *World J Gastroenterol* 1999; **5: 1**-3

2 **Liu J**, Hu JL, Zhang XY, Qiao TD, Chen XT, Wu KC, Ding J, Fan DM. The value of MG7 antigen in predicting cancerous change in dysplastic gastric mucosa. *Int J Clin Pract* 2002; **56**: 169-172

3 **Xu L**, Qiao T, Chen B. Mimic epitope recognized by monoclonal antibody MG7 against gastric cancer through screening phage displayed random peptide library. *Zhonghua Yixue Zazhi* 2000; **80**: 304-307

4 **Xu L**, Xu H, Ma F. Immunogenicity of phage-displayed tumor antigen-mimic peptide. *Zhonghua Zhongliu Zazhi* 2001; **23**: 187-189

5 **Xiang R**, Lode HN, Chao TH, Ruehlmann JM, Dolman CS, Rodriguez F, Whitton JL, Overwijk WW, Restifo NP, Reisfeld RA. An autologous oral DNA vaccine protects against murine melanoma. *Proc Natl Acad Sci U S A* 2000; **97**: 5492-5497

6 **Pinilla-Ibarz J**, Cathcart K, Korontsvit T, Soignet S, Bocchia M, Caggiano J, Lai L, Jimenez J, Kolitz J, Scheinberg DA. Vaccination of patients with chronic myelogenous leukemia with bcr-abl oncogene breakpoint fusion peptides generates specific immune responses. *Blood* 2000; **95**: 1781-1787

7 **Sirard JC**, Niedergang F, Kraehenbuhl JP. Live attenuated *Salmonella*: a paradigm of mucosal vaccines. *Immunol Rev* 1999; **171**: 5-26

8 **Darji A**, Guzman CA, Gerstel B, Wachholz P, Timmis KN, Wehland J, Chakraborty T, Weiss S. Oral somatic transgene vaccination using attenuated S. typhimurium. *Cell* 1997; **91**: 765-775

9 **Paglia P**, Medina E, Arioli I, Guzman CA, Colombo MP. Gene transfer in dendritic cells, induced by oral DNA vaccination with *Salmonella typhimurium*, results in protective immunity against a murine fibrosarcoma. *Blood* 1998; **92**: 3172-3176

10 **Darji A**, zur Lage S, Garbe AI, Chakraborty T, Weiss S. Oral delivery of DNA vaccines using attenuated *Salmonella typhimurium* as carrier. *FEMS Immunol Med Microbiol* 2000; **27**: 341-349

11 **Cochlovius B**, Stassar MJ, Schreurs MW, Benner A, Adema GJ. Oral DNA vaccination: antigen uptake and presentation by dendritic cells elicits protective immunity. *Immunol Lett* 2002; **80**: 89-96

12 **Hopkins SA**, Niedergang F, Corthesy-Theulaz IE, Kraehenbuhl JP. A recombinant *Salmonella typhimurium* vaccine strain is taken up and survives within murine Peyer's patch dendritic cells. *Cell Microbiol* 2000; **2**: 59-68

13 **Niethammer AG**, Primus FJ, Xiang R, Dolman CS, Ruehlmann JM, Ba Y, Gillies SD, Reisfeld RA. An oral DNA vaccine against human carcinoembryonic antigen (CEA) prevents growth and dissemination of Lewis lung carcinoma in CEA transgenic mice. *Vaccine* 2001; **20**: 421-429

14 **Zheng B**, Woo PC, Ng M, Tsoi H, Wong L, Yuen K. A crucial role of macrophages in the immune responses to oral DNA vaccina-

tion against hepatitis B virus in a murine model. *Vaccine* 2001; **20**: 140-147

15 **Alexander J**, Sidney J, Southwood S, Ruppert J, Oseroff C, Maewal A, Snoke K, Serra HM, Kubo RT, Sette A. Development of high potency universal DR-restricted helper epitopes by modification of high affinity DR-blocking peptides. *Immunity* 1994; **1**: 751-761

16 **Ishioka GY**, Fikes J, Hermanson G, Livingston B, Crimi C, Qin M, del Guercio MF, Oseroff C, Dahlberg C, Alexander J, Chesnut RW, Sette A. Utilization of MHC class I transgenic mice for development of minigene DNA vaccines encoding multiple HLA-restricted CTL epitopes. *J Immunol* 1999; **162**: 3915-3925

17 **An LL**, Rodriguez F, Harkins S, Zhang J, Whitton JL. Quantitative and qualitative analyses of the immune responses induced by a multivalent minigene DNA vaccine. *Vaccine* 2000; **18**: 2132-2141

18 **Yu ZC**, Ding J, Nie YZ, Fan DM, Zhang XY. Preparation of single chain variable fragment of MG(7) mAb by phage display technology. *World J Gastroenterol* 2001; **7**: 510-514

19 **Nie YZ**, He FT, Li ZK, Wu KC, Cao YX, Chen BJ, Fan DM. Identification of tumor associated single-chain Fv by panning and screening antibody phage library using tumor cells. *World J Gastroenterol* 2002; **8**: 619-623

20 **Kieber-Emmons T**, Monzavi-Karbassi B, Wang B, Luo P, Weiner DB. Cutting edge: DNA immunization with minigenes of carbohydrate mimotopes induce functional anti-carbohydrate antibody response. *J Immunol* 2000; **165**: 623-627

21 **Lesinski GB**, Smithson SL, Srivastava N, Chen D, Widera G, Westerink MA. A DNA vaccine encoding a peptide mimic of Streptococcus pneumoniae serotype 4 capsular polysaccharide induces specific anti-carbohydrate antibodies in Balb/c mice. *Vaccine* 2001; **19**: 1717-1726

22 **Monzavi-Karbassi B**, Cunto-Amesty G, Luo P, Lees A, Kieber-Emmons T. Immunological characterization of peptide mimetics of carbohydrate antigens in vaccine design strategies. *Biologicals* 2001; **29**: 249-257

23 **Han Y**, Han ZY, Zhou XM, Shi R, Zheng Y, Shi YQ, Miao JY, Pan BR, Fan DM. Expression and function of classical protein kinase C isoenzymes in gastric cancer cell line and its drug-resistant sublines. *World J Gastroenterol* 2002; **8**: 441-445

24 **Wang X**, Lan M, Shi YQ, Lu J, Zhong YX, Wu HP, Zai HH, Ding J, Wu KC, Pan BR, Jin JP, Fan DM. Differential display of vincristine-resistance-related genes in gastric cancer SGC7901 cell. *World J Gastroenterol* 2002; **8**: 54-59

25 **Chen Q**, Ye YB, Chen Z. Activation of killer cells with soluble gastric cancer antigen combined with anti-CD(3) McAb. *World J Gastroenterol* 1999; **5**: 179-180

**Edited by** Zhang JZ

P.O.Box 2345, Beijing 100023,China
Fax: +86-10-85381893
E-mail: wjg@wjgnet.com www.wjgnet.com

World J Gastroenterol 2003;9(6):1196-1201
World Journal of Gastroenterology
Copyright ©2003 by The WJG Press ISSN 1007-9327

• GASTRIC CANCER •

# A gene encoding an apurinic/apyrimidinic endonuclease-like protein is up-regulated in human gastric cancer

Gang-Shi Wang, Meng-Wei Wang, Ben-Yan Wu, Xiao-Bing Liu, Wei-Di You, Xin-Yan Yang

**Gang-Shi Wang, Meng-Wei Wang, Ben-Yan Wu, Wei-Di You, Xin-Yan Yang,** Department of Gerontal Gastroenterology, General Hospital of Chinese PLA, Beijing 100853, China
**Xiao-Bing Liu,** Department of Pathology, General Hospital of Chinese PLA, Beijing 100853, China
**Supported by** Key Project Grant of Medical Sciences of the Tenth Five-Year Plan of Chinese PLA; Grant number: 01Z035
**Correspondence to:** Gang-Shi Wang, MD., Ph.D., Department of Gerontal Gastroenterology, General Hospital of Chinese PLA, Beijing 100853, China. wanggangshi@hotmail.com
**Received:** 2003-01-14 **Accepted:** 2003-03-03

## Abstract

**AIM:** To identify the gene that may predispose to human gastric cancer and to analyze its expression in gastric cancer and non-tumorous gastric mucosa.

**METHODS:** Cancer, para-tumor, and non-tumor gastric tissues were studied for gene expression profile using fluorescent differential display reverse transcription polymerase chain reaction (DDRT-PCR). The differentially expressed bands of interest were analyzed by cloning, Northern blotting, and sequencing. The sequencing results were compared with the GenBank database for homology and conserved domain analysis. *In situ* hybridization with DIG-labeled cRNA probes was used to detect the expression of gene in paraffin embedded gastric adenocarcinoma and non-cancerous tissues.

**RESULTS:** A gene expressed higher in tumor and para-tumor tissues than in their non-tumor counterparts of all 7 tested gastric adenocarcinoma patients was identified by means of DDRT-PCR analysis. It was named *GCRG213* (gastric cancer related gene 213). Northern blot confirmed the differential expression. *GCRG213* (GenBank No. AY053451) consisted of 1094 base pairs with an open reading frame (ORF) which encoded 142 amino acids. The deduced amino acid sequence contained a putative conserved domain, apurinic/apyrimidinic endonuclease (APE). *In situ* hybridization analysis showed that *GCRG213* was expressed higher in gastric cancer tissues than in their corresponding non-tumor ones. Precancerous leisions of gastric adenocarcinoma showed a high *GCRG213* expression, too. No difference of the expression patterns was found between the early and advanced gastric cancer.

**CONCLUSION:** A gene named *GCRG213* was identified in human gastric adenocarcinoma. It encoded an APE-like protein which was probably a new member of the APE family. *GCRG213* was over-expressed not only in gastric cancer, but also in its precancerous leisions. The role of *GCRG213* expression in carcinogenesis needs further study.

Wang GS, Wang MW, Wu BY, Liu XB, You WD, Yang XY. A gene encoding an apurinic/apyrimidinic endonuclease-like protein is up-regulated in human gastric cancer. *World J Gastroenterol* 2003; 9(6): 1196-1201
http://www.wjgnet.com/1007-9327/9/1196.asp

## INTRODUCTION

Gastric cancer is the second most common cause of cancer-related deaths in the world. It is widely accepted that genetic alterations play an important role in the pathogenesis of gastric cancer[1,2]. The expression of oncogenes such as c-met, c-myc, ras, c-erbB-2[3-5], the inactivation of tumor-suppressor genes, such as p53, p16, Rb, DCC, APC[6-12]; and the abnormal transcription of genes related to metastasis, such as nm23, CD44, and E-cadherin[12,13], have been reported in patients with gastric adenocarcinoma. Recent data showed that cancer related genes such as COX-2[14,15], survivin[16,17], metallothionein II and RUNX3, etc.[18-22] were also expressed abnormally in gastric cancer. With the development of molecular biology techniques, such as cDNA array and differential display reverse transcription polymerase chain reaction (DDRT-PCR), some novel genes or cDNA fragments closely related to the development of human gastric cancer were identified recently[23-32]. However, the genetic factors in human gastric cancer and their mechanisms of carcinogenesis remain uncertain and deserve further study. We, therefore, used DDRT-PCR to screen the human intestinal-type gastric adenocarcinoma and its precursor lesions for the differential expression of gastric cancer related genes (GCRGs).

In our previous reports, we described a cDNA fragment which was upregulated in human gastric cancer tissues. Two subclones, *GCRG213* and *GCRG224*, were subsequently identified. *GCRG224* was overexpressed in almost all gastric mucosal epithelia but only in a small portion of gastric cancer and precancerous leisions[33]. In this study, we investigated the subclone, *GCRG213* and found that it was a gene encoding an apurinic/apyrimidinic endonucleas1(APE)-like protein. *GCRG213* was overexpressed in gastric cancer and in its precancerous leisions.

## MATERIALS AND METHODS

### *Patients and tissue acquisition*

Fresh primary intestinal-type gastric adenocarcinoma, para-tumor tissues and non-cancerous gastric mucosal tissues were collected from 7 patients (male: 4, female: 3; mean age: 51±18 years old) during surgical operation for the differential display analyses of genes. The para-tumor tissues were collected at 1.0 cm away from the tumor mass. Three other sets of fresh gastric adenocarcinoma and non-cancerous gastric tissues were used for Northern blot analysis. Specimens of paraffin embedded gastric adenocarcinoma (male: 21, female: 11; mean age 57±8 years old) and their corresponding noncancerous tissues were collected for *in situ* hybridization analysis. Of the 32 cases of gastric adenocarcinoma, 15 cases were early gastric cancer while the other 17 cases were advanced carcinoma. The diagnosis of cancer was confirmed through histological findings.

### *Differential display, cloning and sequencing*

Total RNA was extracted from tissues using TRIzol reagent (Life Technologies, Inc., Rockville, Maryland) according to the instructions of the manufacturer. The fluorescent differential display was performed as previously described[34]. The primers used in the assay were $T_{12}GG$ *vs.* ARP-8: 5' TGGTAAAGGG3'

(Genomyx Corporation, Foster City, CA). The intensity of differentially expressed bands was quantified by Image Quant software (Molecular Dynamics, Sunnyvale, CA). The differentially expressed cDNA fragments were sub-cloned and sequenced as described previously[33]. The sequenced cDNA was analyzed via the BLAST program for matches in the GenBank database[35], and DNASIS software (Hitachi Software Engineering America Ltd., San Bruno, CA) was used for bioinformatic analysis.

### *Northern blot analysis*

Dig Northern Starter Kit (Roche Diagnostic Corporation, Indianapolis, IN) was used. The procedure of hybridization was performed according to the manufacturer' s protocol. Anti-sense cRNA probe labeled with digoxigenin was generated from a digested cDNA insert by means of *in vitro* transcription. Digoxigenin labeled sense cRNA probe was used as a negative control. The hybridization signals were visualized with chemiluminescence which is recorded on X-ray films. The exposure time was 10 minutes.

### *In situ hybridization*

All specimens were fixed in 10 % neutral buffered formalin and embedded in paraffin. A series of 5 μm thick sections were cut for analysis. *In situ* hybridization (ISH) was performed as previously described[36,37] using anti-sense cRNA probe labeled with digoxigenin. Briefly, the slides were dried at 40 ℃ overnight, dewaxed, rehydrated and pretreated with DEPC-treated PBS containing Triton X-100. The sections were then permeabilized with 20 μg/ml RNase-free proteinase K (Merck, Darmstadt, Germany) for 20 min, incubated at 37 ℃ for at least 20 min with prehybridization buffer. Each section was overlaied with 30 μl of hybridization buffer containing 10 ng of digoxigenin-labeled cRNA probe and incubated at 42 ℃ overnight. The positive signal for GCRG213 mRNA was finally detected by using NBT/BCIP as substrate. Sense cRNA probes were used as negative control. The presentation of blue staining in cytoplasm was considered positive. The positive staining of cytoplasm was semi-quantified as Grade ±: barely detectable light blue, Grade 1+: diffuse light blue, Grade 2+: blue staining, and Grade 3+: dark blue. More than 100 non-tumor or tumor cells were quantified in each measurement, and more than one measurement was required to confirm the diagnosis. Consequent slides with H&E staining were then reviewed to compare the histological patterns to the staining patterns in the ISH preparations.

### *Informed consents*

The study protocol was approved by the Institutional Review Board of the hospital under the guidelines of the 1975 Declaration of Helsinki. Written informed consents were obtained from patients.

## RESULTS

### *Identification of a human gastric cancer related gene*

One differentially expressed cDNA band named W2 was found to be more abundant in the tumor and paratumor samples in all tested patients. W2 was sub-cloned into a pGEM-T easy vector, and confirmed by EcoR I digestion. Two subclones, *GCRG213* and *GCRG224*, were subsequently identified[33]. Sequencing results showed that *GCRG213* consisted of 1094 base pairs with an open reading frame (ORF) which encoded 142 amino acids with an estimated molecular weight of 16.4 kDa (Figure 1). This nucleotide sequence data were submitted to GenBank with accession No. AY053451. BLASTN analysis revealed that *GCRG213* shared 88 % homology with human

```
  3 GTA AAG GGA TCA ATG CAA CAA GAA GAG CTA ACT ATC CTA AAT ATA TAT GCA CCT AAT ACA   62
  1                 M   Q   Q   E   E   L   T   I   L   N   I   Y   A   P   N   T   20
                    .   .   .   .   .   .   .   .   .   .   .   .   .   .   .   .
 63 AGA GCA CCC AGA TTC ATA AAG CAA GTC CTT AGA GAC CTA CAA AGA GAC TTA GAT TCC CAC  122
 21 R   A   P   R   F   I   K   Q   V   L   R   D   L   Q   R   D   L   D   S   H   40
                    .   .   .   .   .   .   .   .   .   .   .   .   .   .   .   .
123 ACA ATA ATA ATG GGA GAC TTT AAC ACC CAA CTG TCA ATA TTA GAA AGA TCA ACA AGG CAG  182
 41 T   I   I   M   G   D   F   N   T   Q   L   S   I   L   E   R   S   T   R   Q   60
                    .   .   .   .   .   .   .   .   .   .   .   .   .   .   .   .
183 AAG GTT AAC AAA GAT ATC CAG GAC CTG AAC TCA GCT CTG CAA CAA ACA GAC CCA ATA GAC  242
 61 K   V   N   K   D   I   Q   D   L   N   S   A   L   Q   Q   T   D   P   I   D   80
                    .   .   .   .   .   .   .   .   .   .   .   .   .   .   .   .
243 ATC CAC AGA ACT CTC CAC CCC AAA TCA ACA GAG TGT ACA TTC TTC TCA GCA CCA CAT CTC  302
 81 I   H   R   T   L   H   P   K   S   T   E   C   T   F   F   S   A   P   H   L   100
                    .   .   .   .   .   .   .   .   .   .   .   .   .   .   .   .
303 ACT TAT TCT AAA TTT GGC CAC ATA ATT GGA AGT AAA GCA CTC CTC ACC AAA TGT AAA AGA  362
101 T   Y   S   K   F   G   H   I   I   G   S   K   A   L   L   T   K   C   K   R   120
                    .   .   .   .   .   .   .   .   .   .   .   .   .   .   .   .
363 ACA GAA ATC ACA ACA GAC TGT CTC TCA GAC CAC AGT GCG ATC AAA TTC GAA CTT AGG ATT  422
121 T   E   I   T   T   D   C   L   S   D   H   S   A   I   K   F   E   L   R   I   140
                    .   .   .   .   .   .   .   .   .   .   .   .   .   .   .   .
423 AAG AAG CTC ACT CAA AAC TGA ACA ACT ACA TGG AAA CTG AAT AAT TTG CTC CTG AAT GAC  482
141 K   K   L   T   Q   N   *                                                       160
                    .   .   .   .   .   .   .   .   .   .   .   .   .   .   .   .
483 TAC TGG GTA AAT AAC AAA ATG AAG GCAGAA ATA AAG ATG TTC TTT GAA ACC AAT GAG AAC  542
543 AAA GAC ACA ATG TAC CAG AAT CTC TGG GAC ACA TTT AAA GCA GTG TGT AGG GGG AAATTG  602
603 ATA GCA CTA AAT GCC CAG AAG AGA AAG CAG GAA AGA TCT AAA ATT GAC CCC CTA ACATCA  662
663 CAA TTA AAA GTA CTA GAG AAG AAA AAG CAA ACA CAT TCA AAAGCTGGCAGA AGG AAA AAA  722
723 TAA GAT CAG AGC AGA GCT GAA GGA GAC AGA GAC ACA AAA AACCCTTCAAAA AAG CAATGA  782
783 ATC CAG GAG CTT GTT TTT TGA AAA GAT CAA CAA AAT TGA TAG ACT GCT AGC AAG ACT AAT  842
843 AAA GAG AAA AGA GAG AGG AAT CAA ATA GAT GCA ATA AAA TGA TAA AGG GGA TAT CAC CAC  902
903 TGA GCC CAG GGA AAT AAA AAC TAC CAT CAG AGA ATA CTA TAA ACG CCT ATA CAC AAA TAA  962
963 ACT TGA ACA TCT GGA AGA AAT GGA TAA ATT CTG GGA CAC ATA CAC CCT TGC AAG ACT AAA 1022
1023 CCA GGA AGA GGT TGA ATC TCT GAA TAG ACC AAT AAC AAG TTC TGA AGT TGA GGC AGT AAT 1082
1083 TAA TAG CCT ACC AAA AAA AAA AAA      1106
```

**Figure 1** Sequence of the human *GCRG213* cDNA. The DNA sequence encoding the predicted start (ATG) and stop (TGA) codons is bolded and underlined. Three possible polyadenylation signals (AATAAA) are in italics. The protein encoded by the open reading frame is indicated in the single-letter code below the DNA sequence.

retrotransposable LINE-1 element LRE2. Through conserved domain database search in GenBank, a putative conserved domain, apurinic/apyrimidinic endonucleas1 (APE), was detected in the deduced amino acid sequence of *GCRG213*-ORF, it shared 61.0 % alignment with the C-terminal region of APE conserved domain (Figure 2). Northern blot analysis showed that *GCRG213* was over-expressed in tumor tissues than in their non-tumor counterparts (Figure 3).


**Figure 2** NCBI conserved domain search results. A: GCRG213 ORF produced significant alignments with gnl | Pfam | pfam 01260 AP_endonucleas1, AP endonuclease family 1; CD-length =250 residues, only 61.0 % aligned; Score=88.2 bits (217), Expect=3e-19. B: Human APE protein produced significant alignments with gnl | Pfam | pfam01260 AP_endonucleas1, AP endonuclease family 1; CD-length=250 residues, 100.0 % aligned. Score=161 bits (407), Expect=1e-40. GCRG213-ORF contained residues such as Y171, D210, N212, D308 and H309 (arrowed) that are important for the endonuclease activity of APE .

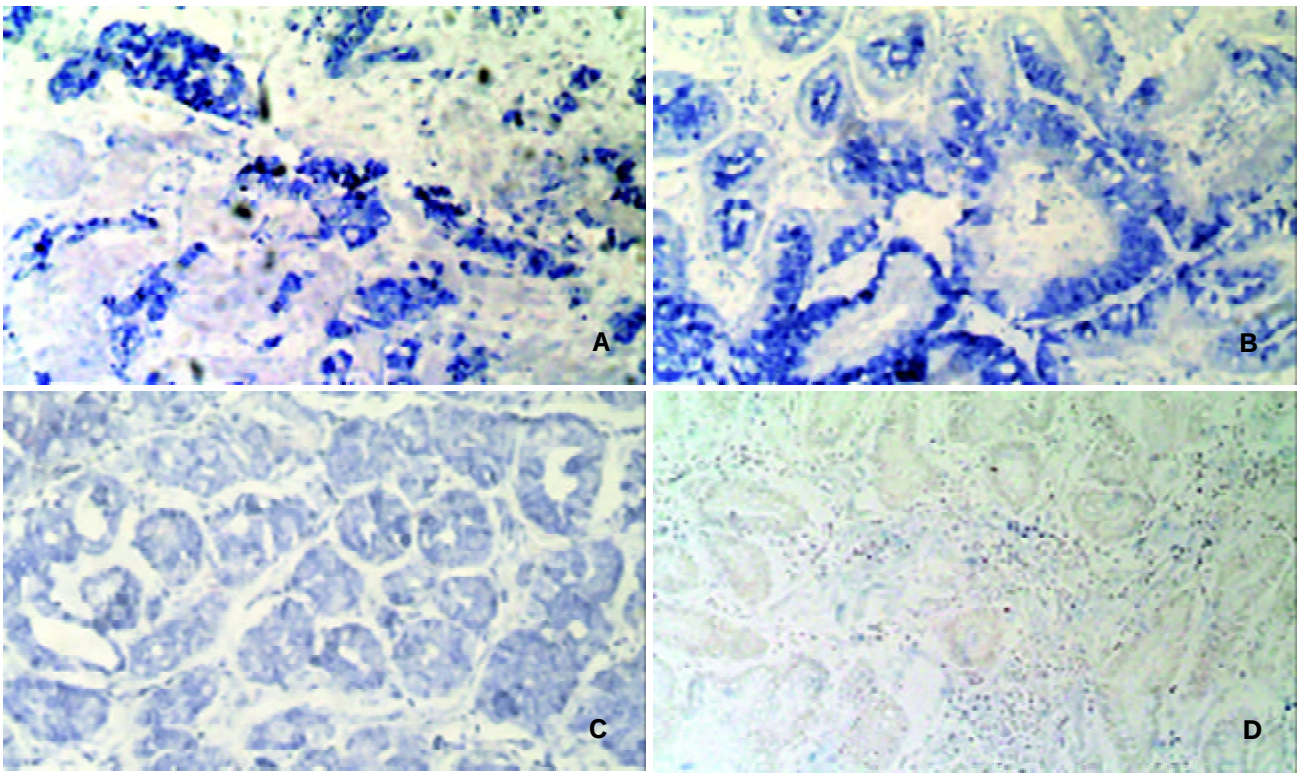


**Figure 4** *In situ* hybridization analysis of *GCRG213* in formalin-fixed, paraffin-embedded tissues with a digoxigenin-labeled anti-sense probe, NBT/BCIP was used as alkaline phosphatase substrates, the expression appeared as cytoplasmic staining (blue precipitates). (A) gastric adenocarcinoma invading into the muscle layer showed grade 2+ ~ 3+ staining, (B) gastric IM epithelium showed grade 2+ ~ 3+ staining, (C) normal gastric glands showed grade ± ~ + staining, (D) negative control. Magnification was 10×10.

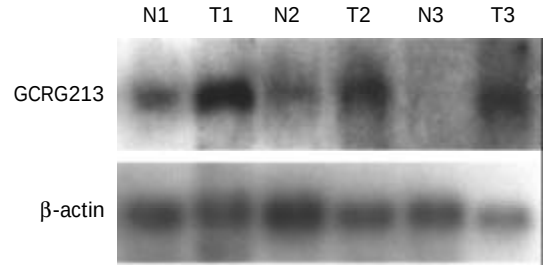


**Figure 3** Northern blot analysis of GCRG213 in human gastric tissues. GCRG213 showed higher expression in tumor tissues than in non-tumorous ones. The expression of β-actin served as an internal control. N: non-tumorous tissue; T: tumor; 1-3: patient number.

### *In situ hybridization*

*GCRG213* expression was analyzed at the mRNA level using *in situ* hybridization. The hybridization signal appeared as a blue color in cytoplasm.

Both the early and advanced gastric cancer tissues were stained grade 2+ ~ 3+. Eight of the 17 cases of advanced adenocarcinoma showed an invasion of cancer into the muscle layer, with all eight cases showing grade 3+ staining in the invading tumor cells (Figure 4A). Dysplasia tissues at the para-tumor region were found in 22 patients. 15/22 dysplasia tissues showed grade 2+ ~ 3+ staining of *GCRG213* expression while the rest showed grade 1+ staining. Nineteen patients had intestinal metaplasia (IM) epithelia at the para-tumor tissue. 9/19 IM showed grade 2+ ~ 3+ staining, the rest showed non-staining to grade 1+ staining (Figure 4B). All normal gastric glands showed grade ± ~ + staining (Figure 4C).

## DISCUSSION

In the present study, we used differential display to study the gene expression profile of human gastric cancer. One cDNA fragment, named by us as gastric cancer related gene 213 (*GCRG213*), was up-regulated in the gastric adenocarcinoma tissues of all 7 tested patients. Northern blot analysis confirmed the differential expression of *GCRG213*. As for the consistent up-regulation in gastric cancer tissues, further studies are necessary to confirm the role of *GCRG213* and its expression pattern in tumors.

The nucleotide sequence of *GCRG213* shared 88 % homology with human retrotransposable LINE1 element LRE2. LINE-1 elements are very ancient, they constitute 20 % or more of some mammalian genomes and presumably play a role in the evolution, structure, and function of mammalian genomes. LINE-1 elements contain regulatory signals and encode two proteins: one is an RNA-binding protein and the other is an APE-like enzyme which has both endonuclease and reverse transcriptase activities[38,39]. BLASTP analysis in this study showed that the deduced amino acid sequence of *GCRG213*-ORF shared 84 % homology with the N terminal of LINE-1 ORF2 where the repair nuclease domain of APE exists.

We proposed that *GCRG213*-ORF be a new APE-like protein based on the following facts. First, APE conserved domain could be detected in *GCRG213*-ORF and the latter shared homology with the C terminal of human APE protein which is of particular relevance to the endonuclease function of APE. Furthermore, *GCRG213*-ORF also contains residues proposed to be important to the endonuclease activity of APE (Y171, D210, N212, D308 and H309)[40-42].

AP endonucleases have been divided into two families based on their amino acid sequence identity to either exonuclease III or Endo IV. Typically, the exonuclease III family of endonucleases accounts for approximately 95 % of the repair activity in the organism. In mammals, the predominant AP endonuclease is APE (also called HAP1 or APEX), an enzyme that belongs to the ExoIII family[42]. Human APE plays an important role in the base excision repair machinery of eukaryotic cells[40]. The DNA repair activity of APE resides in the C-terminal region[41].

Many mechanisms such as hydrolysis of purine or pyrimidine, ionizing radiation, UV irradiation, and N-glycosylases may act on endogenous apurinic/apyrimidinic sites to modify DNA bases[40-43]. Unrepaired apurinic/apyrimidinic sites result in mutations during DNA replication. Apart from its DNA repair function, APE exhibits as Redox-factor-1 which is important for the activation of transcription factors, such as activator protein 1, p53 and nuclear factor kappa B. APE also regulates the transactivation and pro-apoptotic functions of p53[41]. Therefore, a role of APE in human tumorigenesis has been suggested.

APE protein is expressed in a wide range of human cells. Through immunohistochemistry detection, APE can be mainly localized in nucleus or cytoplasm or both[44] depending on the cell type. Elevated expression of APE has been reported in a number of tumors such as prostate, ovarian, cervical, colorectal and germ cell tumors, malignant gliomas, whereas the cellular localization (nuclear/cytoplasmic ratio) differs in some neoplasia (colorectal carcinomas, epithelial ovarian cancers, primary breast carcinomas and thyroid carcinomas)[45-54]. In breast cancer, APE protein expression correlates with lymph node status and angiogenesis[51] while in head-and-neck cancer, nuclear expression of APE is associated with its resistance to chemoradiotherapy and poor outcome[55]. In this study, *GCRG213* overexpressed in gastric intestinal metaplasia and dysplasia of the stomach as well as early and advanced gastric adenocarcinoma. The patterns of *GCRG213* expression in cancerous tissue of the early gastric cancer did not differ significantly from those in the advanced gastric carcinoma. Thus, the *GCRG213* expression appears "early" in the stage of gastric adenocarcinoma. This expression pattern is consistent with that of APE in cervical, prostate, colorectal cancer and their premalignant leisions[45-47] reported.

There are two immediate implications of these findings of elevated *GCRG213* expression in cancers. First, if the expression of *GCRG213* could be modulated downward to, or below normal levels in the cancer cells, there may be an effect on the progression of the cancer or, the cells may become more sensitive to chemotherapeutic treatment. The latter presumes that the increase in AP endonuclease activity result in increased DNA repair activity, protecting more cancer cells against base damage than normal cells.

In conclusion, a gene, GCRG213, overexpressed in tumors was identified in this study. Because of the similarity of the expression pattern in tumors between APE and *GCRG213*, as well as the 61 % alignment between the amino acid sequences of *GCRG213*-ORF and APE conserved domain, it is likely that *GCRG213*-ORF is a new member of the APE family. A greater understanding of alterations in the function of *GCRG213* in human cancers may explore its epidemiological and therapeutic significance.

## ACKNOWLEDGEMENTS

The authors would like to thank Dr. Sien-Sing Yang, the Cathey General Hospital, Taipei, Taiwan and Timothy K Lee, Ph.D., FDA, U.S.A. for their comments.

## REFERENCES

1 **Gonzalez CA**, Sala N, Capella G. Genetic susceptibility and gastric cancer risk. *Int J Cancer* 2002; **100**: 249-260

2 **El-Rifai W**, Powell SM. Molecular biology of gastric cancer. *Semin Radiat Oncol* 2002; **12**: 128-140
3 **Nakajima M**, Sawada H, Yamada Y, Watanabe A, Tatsumi M, Yamashita J, Matsuda M, Sakaguchi T, Hirao T, Nakano H. The prognostic significance of amplification and overexpression of c-met and c-erbB-2 in human gastric carcinomas. *Cancer* 1999; **85**: 1894-1902
4 **Takehana T**, Kunitomo K, Kono K, Kitahara F, Iizuka H, Matsumoto Y, Fujino MA, Ooi A. Status of c-erbB-2 in gastric adenocarcinoma: a comparative study of immunohistochemistry, fluorescence in situ hybridization and enzyme-linked immunosorbent assay. *Int J Cancer* 2002; **98**: 833-837
5 **Yoo J**, Park SY, Robinson RA, Kang SJ, Ahn WS, Kang CS. ras Gene mutations and expression of Ras signal transduction mediators in gastric adenocarcinomas. *Arch Pathol Lab Med* 2002; **126**: 1096-1100
6 **Chang MS**, Kim HS, Kim CW, Kim YI, Lan Lee B, Kim WH. Epstein-Barr virus, p53 protein, and microsatellite instability in the adenoma-carcinoma sequence of the stomach. *Hum Pathol* 2002; **33**: 415-420
7 **Gurel S**, Dolar E, Yerci O, Samli B, Ozturk H, Nak SG, Gulten M, Memik F. Expression of p53 protein and prognosis in gastric carcinoma. *J Int Med Res* 1999; **27**: 85-89
8 **Liu XP**, Tsushimi K, Tsushimi M, Kawauchi S, Oga A, Furuya T, Sasaki K. Expression of p21(WAF1/CIP1) and p53 proteins in gastric carcinoma: its relationships with cell proliferation activity and prognosis. *Cancer Lett* 2001; **170**: 183-189
9 **Sato K**, Tamura G, Tsuchiya T, Endoh Y, Usuba O, Kimura W, Motoyama T. Frequent loss of expression without sequence mutations of the DCC gene in primary gastric cancer. *Br J Cancer* 2001; **85**: 199-203
10 **Lee JH**, Abraham SC, Kim HS, Nam JH, Choi C, Lee MC, Park CS, Juhng SW, Rashid A, Hamilton SR, Wu TT. Inverse relationship between APC gene mutation in gastric adenomas and development of adenocarcinoma. *Am J Pathol* 2002 ;**161**:611-618
11 **Zhou Y**, Gao SS, Li YX, Fan ZM, Zhao X, Qi YJ, Wei JP, Zou JX, Liu G, Jiao LH, Bai YM, Wang LD. Tumor suppressor gene p16 and Rb expression in gastric cardia precancerous lesions from subjects at a high incidence area in northern China. *World J Gastroenterol* 2002; **8**: 423-425
12 **Waki T**, Tamura G, Tsuchiya T, Sato K, Nishizuka S, Motoyama T. Promoter methylation status of E-cadherin, hMLH1, and p16 genes in nonneoplastic gastric epithelia. *Am J Pathol* 2002; **161**: 399-403
13 **Hsieh HF**, Yu JC, Ho LI, Chiu SC, Harn HJ. Molecular studies into the role of CD44 variants in metastasis in gastric cancer. *Mol Pathol* 1999; **52**: 25-28
14 **van Rees BP**, Saukkonen K, Ristimaki A, Polkowski W, Tytgat GN, Drillenburg P, Offerhaus GJ. Cyclooxygenase-2 expression during carcinogenesis in the human stomach. *J Pathol* 2002; **196**: 171-179
15 **Kikuchi T**, Itoh F, Toyota M, Suzuki H, Yamamoto H, Fujita M, Hosokawa M, Imai K. Aberrant methylation and histone deacetylation of cyclooxygenase 2 in gastric cancer. *Int J Cancer* 2002; **97**: 272-277
16 **Krieg A**, Mahotka C, Krieg T, Grabsch H, Muller W, Takeno S, Suschek CV, Heydthausen M, Gabbert HE, Gerharz CD. Expression of different survivin variants in gastric carcinomas: first clues to a role of survivin-2B in tumour progression. *Br J Cancer* 2002; **86**: 737-743
17 **Yu J**, Leung WK, Ebert MP, Ng EK, Go MY, Wang HB, Chung SC, Malfertheiner P, Sung JJ. Increased expression of survivin in gastric cancer patients and in first degree relatives. *Br J Cancer* 2002; **87**: 91-97
18 **Ebert MP**, Gunther T, Hoffmann J, Yu J, Miehlke S, Schulz HU, Roessner A, Korc M, Malfertheiner P. Expression of metallothionein II in intestinal metaplasia, dysplasia, and gastric cancer. *Cancer Res* 2000; **60**: 1995-2001
19 **Li QL**, Ito K, Sakakura C, Fukamachi H, Inoue K, Chi XZ, Lee KY, Nomura S, Lee CW, Han SB, Kim HM, Kim WJ, Yamamoto H, Yamashita N, Yano T, Ikeda T, Itohara S, Inazawa J, Abe T, Hagiwara A, Yamagishi H, Ooe A, Kaneda A, Sugimura T, Ushijima T, Bae SC, Ito Y. Causal relationship between the loss of RUNX3 expression and gastric cancer. *Cell* 2002; **109**: 113-124
20 **Bai YQ**, Yamamoto H, Akiyama Y, Tanaka H, Takizawa T, Koike M, Kenji Yagi O, Saitoh K, Takeshita K, Iwai T, Yuasa Y. Ectopic expression of homeodomain protein CDX2 in intestinal metaplasia and carcinomas of the stomach. *Cancer Lett* 2002; **176**: 47-55
21 **Saitoh T**, Mine T, Katoh M. Up-regulation of WNT8B mRNA in human gastric cancer. *Int J Oncol* 2002; **20**: 343-348
22 **Li Z**, Wang Y, Song J, Kataoka H, Yoshii S, Gao C, Wang Y, Zhou J, Ota S, Tanaka M, Sugimura H. Genomic structure of the human beta-PIX gene and its alteration in gastric cancer. *Cancer Lett* 2002; **177**: 203-208
23 **Yoshikawa Y**, Mukai H, Hino F, Asada K, Kato I. Isolation of two novel genes, down-regulated in gastric cancer. *Jan J Cancer Res* 2000; **91**: 459-463
24 **Wang G**, Wang M, You W, Li H. Cloning and primary expression analyses of down-regulated cDNA fragment in human gastric cancer. *Zhonghua Yixue Yichuanxue Zazhi* 2001; **18**: 43-47
25 **Wang JH**, Chen SS. Screening and identification of gastric adenocarcinoma metastasis-related genes by using cDNA microarray coupled to FDD-PCR. *Shengwu Huaxue Yu Shengwu Wuli Xuebao (Shanghai)* 2002; **34**: 475-481
26 **Wang X**, Lan M, Shi YQ, Lu J, Zhong YX, Wu HP, Zai HH, Ding J, Wu KC, Pan BR, Jin JP, Fan DM. Differential display of vincristine-resistance-related genes in gastric cancer SGC7901 cell. *World J Gastroenterol* 2002; **8**: 54-59
27 **Saitoh T**, Mine T, Katoh M. Molecular cloning and expression of proto-oncogene FRAT1 in human cancer. *Int J Oncol* 2002; **20**: 785-789
28 **Line A**, Stengrevics A, Slucka Z, Li G, Jankevics E, Rees RC. Serological identification and expression analysis of gastric cancer-associated genes. *Br J Cancer* 2002; **86**: 1824-1830
29 **Lee S**, Baek M, Yang H, Bang YJ, Kim WH, Ha JH, Kim DK, Jeoung DI. Identification of genes differentially expressed between gastric cancers and normal gastric mucosa with cDNA microarrays. *Cancer Lett* 2002; **184**: 197-206
30 **Liu LX**, Liu ZH, Jiang HC, Qu X, Zhang WH, Wu LF, Zhu AL, Wang XQ, Wu M. Profiling of differentially expressed genes in human gastric carcinoma by cDNA expression array. *World J Gastroenterol* 2002; **8**: 580-585
31 **El-Rifai W**, Smith MF Jr, Li G, Beckler A, Carl VS, Montgomery E, Knuutila S, Moskaluk CA, Frierson HF Jr, Powell SM. Gastric cancers overexpress DARPP-32 and a novel isoform, t-DARPP. *Cancer Res* 2002; **62**: 4061-4064
32 **Wang GS**, Wang MW, Wu BY, You WD. A lamin-like protein gene is down-regulated in human gastric cancer. *Zhonghua Yixue Yichuanxue Zazhi* 2003; **20**: in press
33 **Wang GS**, Wang MW, Wu BY, You WD, Yang XY. A novel gene, GCRG224, is differentially expressed in human gastric mucosa. *World J Gastroenterol* 2003; **9**: 30-34
34 **Wang GS**, Wang MW, You WD, Wang HF, Feng MF. Fluorescent mRNA differential display technique. *Zhongguo Yingyong Shenglixue Zazhi* 2000; **16**: 373-376
35 **Altschul SF**, Madden TL, Schäffer AA, Zhang J, Zhang Z, Miller W, Lipman DJ. Gapped BLAST and PSI-BLAST: a new generation of protein database search programs. *Nucleic Acids Res* 1997; **25**: 3389-3402
36 **Komminoth P**. Digoxigenin as an alternative probe labeling for *in situ* hybridization. *Diagn Mol Pathol* 1992; **1**: 142-150
37 **Komminoth P**, Merk FB, Leav I, Wolfe HJ, Roth J. Comparison of 35S- and digoxigenin-labeled RNA and oligonucleotide probes for *In situ* hybridization. Expression of mRNA of the seminal vesicle secretion protein II and androgen receptor genes in the rat prostate. *Histochemistry* 1992; **98**: 217-228
38 **Furano AV**. The biological properties and evolutionary dynamics of mammalian LINE-1 retrotransposons. *Prog Nucleic Acid Res Mol Biol* 2000; **64**: 255-294
39 **Volff JN**, Korting C, Froschauer A, Sweeney K, Schartl M. Non-LTR retrotransposons encoding a restriction enzyme-like endonuclease in vertebrates. *J Mol Evol* 2001; **52**: 351-360
40 **Fritz G**. Human APE/Ref-1 protein. *Int J Biochem Cell Biol* 2000; **32**: 925-929
41 **Evans AR**, Limp-Foster M, Kelley MR. Going APE over ref-1. *Mutat Res* 2000; **461**: 83-108
42 **Wilson DM 3rd**, Barsky D. The major human abasic endonuclease:

formation, consequences and repair of abasic leisions in DNA. *Mutat Res* 2001; **485**: 283-307

43 **Meira LB**, Devaraj S, Kisby GE, Burns DK, Daniel RL, Hammer RE, Grundy S, Jialal I, Friedberg EC. Heterozygosity for the mouse Apex gene results in phenotypes associated with oxidative stress. *Cancer Res* 2001; **61**: 5552-5557

44 **Duguid JR**, Eble JN, Wilson TM, Kelley MR. Differential cellular and subcellular expression of the human multifunctional apurinic/apyrimidinic endonuclease (APE/ref-1) DNA repair enzyme. *Cancer Res* 1995; **55**: 6097-6102

45 **Kakolyris S**, Kaklamanis L, Engels K, Turley H, Hickson ID, Gatter KC, Harris AL. Human apurinic endonuclease 1 expression in a colorectal adenoma-carcinoma sequence. *Cancer Res* 1997; **57**: 1794-1797

46 **Kelley MR**, Cheng L, Foster R, Tritt R, Jiang JZ, Broshears J, Koch M. Eleveted and altered expression of the multifunctional DNA base excision repair and redox enzyme Ape1/ref-1 in prostate cancer. *Clin Cancer Res* 2001; **7**: 824-830

47 **Xu Y**, Moore DH, Broshears J, Liu L, Wilson TM, Kelley MR. The apurinic/apyrimidinic endonucleases (APE/ref-1) DNA repair enzyme is elevated in premalignant and malignant cervical cancer. *Anticancer Res* 1997; **17**: 3713-3719

48 **Schindl M**, Oberhuber G, Pichlbauer EG, Obermair A, Birner P, Kelley MR. DNA repair-redox enzyme apurinic endonuclease in cervical cancer: evaluation of redox control of HIF-1alpha and prognostic significance. *Int J Oncol* 2001; **19**: 799-802

49 **Herring CJ**, West CM, Wilks DP, Davidson SE, Hunter RD, Berry P, Forster G, MacKinnon J, Rafferty JA, Elder RH, Hendry JH, Margison GP. Levels of the DNA repair enzyme human apurinic/apyrimidinic endonuclease (APE1, APEX, Ref-1) are associated with the intrinsic radiosensitivity of cervical cancers. *Br J Cancer* 1998; **78**: 1128-1133

50 **Moore DH**, Michael H, Tritt R, Parsons SH, Kelly MR. Alterations in the expression of the DNA repair/redox enzyme APE/ref-1 in epithelial ovarian cancers. *Clin Cancer Res* 2000; **6**: 602-609

51 **Kakolyris S**, Kaklamanis L, Engels K, Fox SB, Taylor M, Hickson ID, Gatter KC, Harris AL. Human AP endonuclease 1 (HAP1) protein expression in breast cancer correlates with lymph node status and angiogenesis. *Br J Cancer* 1998; **77**: 1169-1173

52 **Robertson KA**, Bullock HA, Tritt R, Zimmerman E, Ulbright TM, Foster RS, Einhorn LH, Kelley MR. Altered expression of Ape1/ref-1 in germ cell tumors and overexpression in NT2 cells confers resistance to bleomycin and radiation. *Cancer Res* 2001; **61**: 2220-2225

53 **Bobola MS**, Blank A, Berger MS, Stevens BA, Silber JR. Apurinic/apyrimidinic endonuclease activity is elevated in human adult gliomas. *Clin Cancer Res* 2001; **7**: 3510-3518

54 **Russo D**, Arturi F, Bulotta S, Pellizzari L, Filetti S, Manzini G, Damante G, Tell G. Ape1/Ref-1 expression and cellular localization in human thyroid carcinoma cell lines. *J Endocrinol Invest* 2001; **24**: RC10-RC12

55 **Koukourakis MI**, Giatromanolaki A, Kakolyris S, Sivridis E, Georgoulias V, Funtzilas G, Joclspm ID, Gatter KC, Harris AL. Nuclear expression of human apurinic/apyrimidinic endonuclease (HAP1/Ref-1) in head-and-neck cancer is associated with resistance to chemoradiotherapy and poor outcome. *Int J Radiat Oncol Biol Phys* 2001; **50**: 27-36

**Edited by** Zhao P

P.O.Box 2345, Beijing 100023,China
Fax: +86-10-85381893
E-mail: wjg@wjgnet.com www.wjgnet.com

World J Gastroenterol 2003;9(6):1202-1207
World Journal of Gastroenterology
Copyright ©2003 by The WJG Press ISSN 1007-9327

• LIVER CANCER •

# Is p53 gene mutation an indicatior of the biological behaviors of recurrence of hepatocellular carcinoma?

I-Shyan Sheen, Kuo-Shyang Jeng, Ju-Yann Wu

**I-Shyan Sheen**, Liver Research Unit, Chang Gung Memorial Hospital, Taipei, Taiwan
**Kuo-Shyang Jeng**, Department of Surgery, Mackay Memorial Hospital, Mackay Junior School of Nursing, Taipei, Taiwan
**Ju-Yann Wu**, Medical Research, Mackay Memorial Hospital, Taipei, Taiwan
**Supported by** grants from the Department of Health National Science Council, Executive Yuan, Taiwan. No. NSC 84-2331-B-195-002
**Correspondence to:** Kuo-Shyang Jeng, M.D., F.A.C.S., Department of Surgery, Mackay Memorial Hospital, No. 92, Sec 2, Chung-San North Road, Taipei, Taiwan. issheen.jks@msa.hinet.net
**Telephone:** +86-2-25433535 **Fax:** +86-2-27065704
**Received:** 2003-03-04 **Accepted:** 2003-03-21

## Abstract

**AIM:** To evaluate mutant p53 gene in primary hepatocellular carcinoma and to investigate the correlation between it and the recurrence of hepatocellular carcinoma.

**METHODS:** Mutations of p53 gene were examined using anti-human p53 monoclonal antibody and immunohistochemical staining in 79 resected hepatocellular carcinomas. The correlations among variables of p53 positivity and invasiveness, disease free interval and survival were studied. In addition, in those who developed recurrence, the correlation among p53 positivity, clinical features and post-recurrence survival were also studied.

**RESULTS:** Of these 79 cases, 64 (81 %) had p53 mutation. Those patients with mutant p53 positivity had significantly more tumor recurrence (76.6 % *vs* 40.0 %, *P*=0.0107). However, the COX proportional hazards model showed that p53 overexpression had only weak correlations with recurrence free interval and survival time (*P*=0.088 and 0.081), which was probably related to the short duration of follow-up. The invasiveness variables may be predictors of HCC recurrence. On univariate analysis, more patients with mutant p53 positivity had vascular permeation [78.1 *vs* 40.0 %, *P*=0.0088, O.R. (odds ratio) =5.3], grade II-IV differentiation (98.4 *vs* 80.0 %, *P*=0.0203, O.R. =15.7), no complete capsule (82.8 *vs* 53.3 %, *P*=0.0346, O.R. =4.2) and daughter nodules (60.9 *vs.* 33.3 %, *P*=0.0527, O.R. =3.1) than patients with negative p53 staining. On multivariate analysis, only vascular permeation and grade of differentiation remained significant (*P*=0.042 and 0.012). There was no statistically significant correlation between the status of p53 in the primary lesion and the clinical features of recurrent hepatocellular carcinomas examined, including extrahepatic metastasis (*P*=0.1103) and the number of recurrent tumors (*P*=1.000) except for disease over more than one segment in the extent of recurrent tumors (*P*=0.0043). The post-recurrence median survival was lower in patients in whom p53 mutation had been detected in the primary lesion with a weak significance (3.42 months *vs* 11.0 months, *P*=0.051).

**CONCLUSION:** Our findings suggest that p53 mutation correlates significantly with invasiveness including vascular permeation, grade of cellular differentiation, incomplete capsule and multinodular lesions. Hepatocellular carcinomas with p53 mutations had more tumor recurrence and p53 mutation may also influence disease recurrence interval and survival time. Hepatocellular carcinomas with p53 mutations recur more extensively with a shorter survival. Therefore, p53 mutation in the primary lesion is useful as an indicator of the biological behavior of recurrent hepatocellular carcinomas.

Sheen IS, Jeng KS, Wu JY. Is p53 gene mutation an indicatior of the biological behaviors of recurrence of hepatocellular carcinoma? *World J Gastroenterol* 2003; 9(6): 1202-1207
http://www.wjgnet.com/1007-9327/9/1202.asp

## INTRODUCTION

Hepatocellular carcinoma (HCC) is one of the most common types of malignant tumors that carry a poor prognosis. During the last 10 years, efforts have been made worldwide toward earlier detection and safer surgical resection of HCC. However, despite these recent diagnostic and therapeutic advances, postoperative recurrence is still common[1-4]. How to predict recurrence before resection is a challenging problem for surgeons. Certain characteristics related to HCC recurrence have been reported widely and variably in the literatures[1-11]. Risk factors which have been mentioned include vascular permeation, absence of capsule, presence of daughter nodules, histological grade of tumor differentiation, tumor size, associated cirrhosis, hepatitis B virus (HBV) infection, hepatitis C virus (HCV) infection, daughter nodules, and adequate section margin, etc.

The cellular wild-type p53 gene on chromosome 17p is an established tumor suppressor gene[12-14]. It regulates the cell cycle of DNA repair and synthesis, and also programmed cell death. Once it is mutated, loss of normal function leads to the evolution of neoplasm. Moreover, the speed of tumor growth and invasion may also be enhanced. When mutated, this gene may have transforming properties and can be stained immunohistochemically[15-21]. Its prognostic significance in some types of human cancer has been reported. The relationship between hepatocellular carcinoma (HCC) and overexpression of the mutant p53 gene have been studied in different countries[15-32]. The results are varied. In addition, mutation of the p53 gene was emphasized in advanced but not in early hepatocellular carcinoma[33,34]. However, the correlation between the clinical significance of such p53 mutations and the clinical recurrence of HCC has rarely been clarified.

In this study, we did immunohistochemical staining to investigate the overexpression of p53 protein in HCC in a series of patients. The correlation of the clinical and pathological variables of HCC, recurrence of HCC and the biological behaviors of the mutant p53 gene were studied. The goal of this study was to elucidate the possible role of p53 mutations in the prediction of recurrent HCCs.

## MATERIALS AND METHODS

### *Patients*

One hundred patients with HCC who underwent hepatectomy at Mackay Memorial Hospital, between January 1993 and December 1997 whose tissue specimens (formalin fixed, paraffin wax embedded) were histopathologically found to have no degeneration or necrosis were selected for this study. Clinical details were available from medical records of all patients. Seventy-nine patients entered this study and twenty-one cases were excluded for the following reasons: (1) immediate operative mortality, (2) failure to obtain p53 results due to severe, extensive tumor necrosis, some of which probably resulted from preoperative transcatheter hepatic arterial chemoembolization (TACE), (3) incomplete follow-up, and (4) causes of death not related to liver disease. The mean age of patients was 52.4±16.6 years (range 16-82) with a male to female ratio of 2:1 (52:27). All received curative resections. The surgical operations included major resections (15 partial lobectomies, 31 lobectomies and 9 extended lobectomies) and minor resections (19 segmentectomies, 3 subsegmentectomies and 2 wedge resections). After resection, all patients were followed up at our out-patient-clinic receiving regular clinical assessment, periodic abdominal ultrasonography (every 2 to 3 months during the first 5 years, then every 4 to 6 months thereafter) to detect tumor recurrence, serum alpha-fetoprotein (AFP) and liver biochemistry (every 2 months during the first 2 years, then every 4 months during the following 3 years, and every 6 months thereafter). Abdominal computed tomography was also done (every 6 months during the first year, then every year).

### *Methods*

Five-micron-thick formalin-fixed and paraffin embedded sections were cut, deparaffinized and rehydrated with graded alcohol and xylene. Endogenous peroxidase was blocked using 3 % $H_2O_2$ for 5 minutes, followed by a brief wash in Tris buffer, pH 7.2. Sections were rehydrated and heated in citrate buffer, pH6.0, in a microwave oven at 500 watts for 10 minutes to retrieve the antigen. The tissues were stained with a monoclonal mouse anti-human p53 antibody (DAKO-p53, clone DO-7, Dako Corp, Carpinteria, Calif. U.S.A.) and a labeled streptavidin-biotin staining kit (DAKO LSAB kit, alkaline phosphatase system 40). They were incubated with the antibody at a dilution of 1:100 (in Tris-HCl buffer) for one hour at room temperature. The peroxidase reaction used 3,3-diaminobenzidine tetrahydrochloride as chromogen and the slides were counterstained with hematoxylin. Two independent, blinded observers evaluated all tissue sections. Only nuclear staining was regarded as positive. Cases were scored as negative when no cell was stained even at a concentration as high as 1:10 in a triplicate study. A known colon adenocarcinoma with diffuse p53 nuclear accumulation was stained in parallel as the positive control. For negative controls, we used buffer instead of the specific primary antibody.

We used light microscopy to search for the highest concentration of reactive staining nuclei in each p53 staining section and counted 1 000 cells from the most aggressive area of the tumor to represent the tumor' s behavior and reduce count variability. Specific staining was identified by the presence of a red reaction product in the nuclei and was graded as negative (0), slight (+), moderate (++), or strong (+++) immunostaining, with the distribution as diffuse or focal. The percentage of nuclei immunostained was estimated and was scored without knowledge of the grade of tumor differentiation.

The differences of p53 overexpression in diverse clinicopathologic parameters were evaluated. Parameters included the presence of associated liver cirrhosis (confirmed from the operative findings and also from the pathological examination of the specimen), HBV surface antigen (HBsAg), hepatitis C virus (HCV) infection (antibody to HCV, anti-HCV), Child-Pugh classification of liver reserve, serum alpha fetoprotein (AFP) titer, tumor size (<3 cm, 3-10 cm, >10 cm), cell differentiation grade (Edmondson and Steiner grade I *vs* II-IV), encapsulation (complete, infiltration by HCC or absent), vascular permeation (including vascular invasion and/or tumor thrombi within the portal vein or hepatic vein), and presence of daughter nodules (Table 1). The time lapse between the postoperation till the detection of recurrence is defined as the recurrence free interval. During the follow-up (median 3 years, range 2 to 5 years), 55 patients had tumor recurrence (48 intrahepatic, and 7 both intrahepatic and extrahepatic) and 43 patients died. We also correlated the p53 overexpression with the outcomes. In these 55 patients with recurrence, the correlation between p53 mutation of the primary lesion (presence or absence) and recurrence was studied. The following prognostic factors after recurrence were also analyzed: extrahepatic metastasis (presence or absence), the number (solitary or multiple) and the extent of recurrent tumors (affecting more than or less than one segment), treatment for recurrent tumor (surgical or nonsurgical treatment), and survival time after recurrence.

**Table 1** Characteristics of 79 patients with HCC

| Characteristics | *n* (%) |
|---|---|
| Age (years, mean±S.D.) | 52.4±16.6 |
| Male | 52 (65.8) |
| Liver cirrhosis | 57 (72.2) |
| Child class A:B | 55:24 (70:30) |
| Tumor size small (<3 cm): median (3-10 cm): large (>10 cm) | 24:25:30 (30.4:31.6:38.0) |
| HBsAg (+) | 60 (75.9) |
| Anti-HCV (+) | 41 (51.9) |
| AFP: normal: >1000ng / ml | 30:20(38.0:25.3) |
| Edmondson grade: I:II:III:IV | 4:30:42:3(5.1:38.0:53.2:3.8) |
| Capsule: absent: incomplete: complete | 54:7:18(68.4:8.9:22.8) |
| Vascular permeation | 56 (70.9) |
| Daughter nodules | 44 (55.7) |
| Resection, major: minor | 55:24 (69.6:30.4) |

Notes: HCC: hepatocellular carcinoma; HBsAg: hepatitis B surface antigen; Anti-HCV: antibody to hepatitis C virus; AFP: alpha-fetoprotein; Edmondson grade: Edmondson-Steiner grade of cellular differentiation.

### *Statistical analysis*

The data were tested with statistical programs (BMDP), Student' s *t*-test or Mann-Whitney test for continuous variables, chi-square test or Fisher' s exact test for categorical variables, and logistic regression and COX proportional hazards model for multivariate analysis. $P$ value<0.05 was defined as statistically and significantly different.

## RESULTS

Among the 79 patients, 64 (81 %) patients had a p53-positive result. Among the 64 patients with immunopositivity, 29 patients (45 %) had moderate (++) immunostaining and 3 patients (4.7 %) had strong (++++) immunostaining. The correlations between a positive oncoprotein p53 and patient characteristics are shown in Table 2. Age, gender, positivity of HBsAg or Anti-HCV, levels of AFP, liver cirrhosis, Child-Pugh class A or B, and size of the HCC showed no statistically

significant difference between p53 positive and negative groups. From univariate analysis, a significant correlation was found between p53 over-expression and vascular permeation (78.1 *vs* 40.0 %, *P*=0.0088, odds ratio (O.R.)=5.357), grade of differentiation (Edmondson-Steiner grade I *vs*. II to IV, 98.4 *vs* 80.0 %, *P*=0.0203, O.R.=15.750), complete capsule *vs* infiltration or absent capsule (82.8 *vs* 53.3 %, *P*=0.0346, O.R. =4.200), and presence of daughter nodules (60.9 *vs* 33.3 %, *P*=0.0527, O.R.=3.120) (Table 2). From multivariate analysis, only vascular permeation and grade of differentiation remained significant (*P*= 0.042 and 0.012, respectively).

**Table 2** Comparison of characteristics between p53 positive and negative groups

| Characteristics | P53 Positive (*n*=64) | P53 Negative (*n*=15) | *P* (UV) |
|---|---|---|---|
| Age (years) | 52.8 | 48.3 | n.s. |
| Male | 65.6 % | 66.7 % | n.s. |
| Liver cirrhosis | 76.6 % | 53.3 % | n.s. |
| Child class A | 68.8 % | 73.3 % | n.s. |
| Tumor ≤3 cm | 34.4 % | 13.3 % | n.s. |
| >10 cm | 35.9 % | 40.0 % | n.s. |
| HBsAg (+) | 78.1 % | 66.7 % | n.s. |
| Anti-HCV (+) | 53.1 % | 46.6 % | n.s. |
| AFP <20 ng/mL | 37.5 % | 40.0 % | n.s. |
| >1 000 ng/mL | 21.9 % | 40.0 % | n.s. |
| Edmondson grade I[a] | 1.6 % | 20.0 % | 0.0203 |
| Capsule complete | 17.2 % | 46.7 % | 0.0346 |
| Daughter nodules | 60.9 % | 33.3 % | 0.0527 |
| Vascular permeation[b] | 78.1 % | 40.0 % | 0.0088 |

Notes: *P* (UV): The *P* value by univariate analysis; In multivariate analysis, the significant variables of [a] and [b]: *P* values were 0.0120 and 0.0420 respectively; HBsAg: hepatitis B surface antigen; Anti-HCV: antibody to hepatitis C virus; AFP: alpha-fetoprotein; Edmondson grade: Edmondson-Steiner grade of cellular differentiation; n.s.: no statistical significance; O.R.: odds ratio.

Table 3 shows that patients with p53 positivity had more tumor recurrence (76.6 % *vs* 40.0 %, *P*=0.0107) and more death (59.4 % *vs* 33.3 %, *P*=0.0683). After analysis with the COX proportional hazards model, p53 overexpression had only a weak correlation with recurrence free interval and survival time (*P*=0.088 and 0.081). Factors influencing HCC recurrence and time lapse to recurrence were vascular permeation (*P*=0.0002, O.R.=5.36), complete capsule (*P*=0.0160, O.R. =3.10), and p53 positivity (*P*=0.088, O.R.=2.29) (Table 4). The significant variables affecting death resulting from recurrence included vascular permeation (*P* <0.0001, O.R.=8.35) and p53 positivity (*P*=0.081, O.R.=2.38).

**Table 3** Correlation of p53 with the outcome of patients with HCC

| Outcome | p53 positive (*n*=64) | p53 negative (*n*=15) | *P* value |
|---|---|---|---|
| Morbidity of surgery (%) | 6.3 | 6.7 | n.s. |
| Recurrence (%) (number) | 76.6 (49) | 40.0 (6) | 0.0107 |
| Death[a] (%) | 59.4 | 33.3 | 0.0683 |
| Recurrence free interval (median, months) | 8.3 | 39.1 | 0.0880 |
| Duration of survival (median, months) | 11.8 | 41.9 | 0.0810 |

Notes: n.s.: no statistical significance; Death[a]: patients died of recurrence.

**Table 4** Factors influencing tumor recurrence and death of patients in multivariate analysis

| Variables | *P* | O.R. |
|---|---|---|
| Recurrence | | |
| Vascular permeation | 0.0002 | 5.36 |
| Complete capsule | 0.0160 | 3.10 |
| *p*53 positivity | 0.0880 | 2.29 |
| Death | | |
| Vascular permeation | <0.0001 | 8.35 |
| *p*53 positivity | 0.0810 | 2.38 |

Note: O.R: odds ratio.

In 55 patients with recurrent HCCs, there was no statistically significant correlation between the status of mutant p53 positivity in the primary lesion and the treatment for recurrent tumors, and the clinical features of recurrent HCCs examined, i.e. the existence of extrahepatic metastasis (*P*=0.113), and the number of recurrent tumors (*P*=1.000), except for the extent of recurrent tumors over one hepatic segment (*P*=0.0043). The median survival after recurrence was shorter (3.42 months *vs* 11 months) in those with p53 mutation with a weak significance (*P*=0.051) (Table 5).

**Table 5** Correlation between the clinical features of recurrent hepatocellular carcinoma and the presence of a p53 mutation in the primary lesion

| The clinical features | P53 Positive (*n*=49) | P53 Negative (*n*=6) | *P* |
|---|---|---|---|
| Extrahepatic metastasis (number) (%) | 24 (49.0) | 3 (50.0) | 0.1130 |
| Multiple-recurrent tumors (number) (%) | 34 (69.4) | 4 (66.7) | 1.0000 |
| Extent of recurrent tumors: | 34 (69.4) | 5 (83.3) | 0.0043 |
| More than one segment (number) (%) | | | |
| Median survival after recurrence (Months) | 3.4 | 11.0 | 0.0510 |
| Treatment for recurrent tumors | | | |
| Surgery (number) (%) | 0 | 1[a] (16.7) | n.s. |
| Non-surgical[b](number) (%) | 20 (40.8) | 3 (50.0) | |
| No treatment (number) (%) | 29 (59.2) | 2 (33.3) | |

Notes: n.s.: no statistical significant; [a]: A 55 year old man had a resection of segment II and III; [b]: The Non-surgical treatments included transcatheter arterial chemoembolization and percutaneous ethanol injection.

## DISCUSSION

P53 gene mutation has been identified in over half of human tumors, including HCC, and is the most common genetic abnormality in human cancers[13, 17, 20, 25, 34-42]. Its inactivation by mutation is thought to be a fundamentally important step in carcinogenesis. In addition, the correlation among p53 gene alteration and diagnosis, assessment of tumor progression, recurrence, or cancer prognosis has been investigated and reported[24,28,33]. Recently, Nagao *et al*[43] and Saegusa *et al*[44] found p53 overexpression to be strongly associated with proliferation activity of HCC cells by immunohistochemical studies. Lowe *et al*. demonstrated that a few point mutations on p53 which thus inactivated the gene produced treatment-resistant tumors[45,46]. They suggested p53 status was an important determinant of tumor response to therapy. This indicates that recurrent HCCs with p53 mutation therefore either have a high proliferation rate or are resistant to treatment. Our results supported theirs from a clinical point of view, and also suggested that the high malignant potential was caused by the

p53 mutation. The positive rate of the mutant p53 gene in our HCC patients was 81 %. A wide range in the incidence of p53 mutations from 0 to over 70 % has been reported, with a lower frequency than in other types of cancer, except for special populations in China and Africa. Factors related to the wide variation in positivity may include different thresholds of positivity adopted, different anti-p53 antibodies used, geographical variations and differences in the molecular mechanisms of hepatocarcinogenesis, such as aflatoxin exposure. Some authors have raised a question of whether p53 protein over-expression can represent p53 gene mutation in neoplasms[47]. Hall mentioned a very close correlation between p53 expression and mutations of the p53 gene and found that most antibodies gave the same results[48]. The high recurrence rate after resection is one of the main factors in the poor outcome for HCC patients[1-6, 10, 11]. Tumor recurrence limits the long-term survival. However, tumor recurrence is well correlated with tumor invasiveness. Tumor invasiveness may be determined from vascular permeation, the grade of cell differentiation, infiltration or absence of capsule and presence of daughter lesion. According to our study, they are also all compatible with oncoprotein p53 positivity. In our study, p53 protein over-expression correlated well with tumor recurrence ($P$=0.0107). To analyze the factors relating to HCC recurrence and death, vascular invasion, complete capsule, and p53 positivity correlated well with recurrence and only vascular permeation and p53 positivity correlated with death. A weak association with both recurrence free interval and duration of survival with mutation of the p53 gene was found. The weak correlation may be attributed to the short duration of follow-up (2 to 5 years, median 3 years) in this study.

Vascular permeation indicating tumor invasiveness, consists of either tumor invasion of the hepatic vein, portal vein and/or hepatic artery, or tumor thrombi within the vessels. It may be detected preoperatively by ultrasonography, arteriography or portography, intraoperative ultrasonography or direct observation, or postoperative pathological examination of surgical specimens. Vascular permeation is the most consistent significant prognostic factor of postoperative tumor recurrence[10]. In our univariate analysis, the positive p53 status was significantly related to vascular permeation and in the COX model, patients with vascular permeation had significantly shorter recurrence free intervals and survival periods.

Whether the grade of differentiation of HCC is a determinant of recurrence after resection has been debated for a long time. The association of grade of anaplasia (Edmondson-Steiner' s classification) with p53 positivity also varied in reports[28,49,50]. In our series, less overexpression of p53 and less recurrence were found in patients with well differentiated tumors (Edmondson-Steiner' s grade I) than in those with grade II to IV tumors. The histological differentiation of the HCCs in this study correlated with p53 mutations, and the incidence of p53 mutations increased with increased dedifferentiation. Our findings were consistent with previous reports showing p53 mutation to be associated with the progression of HCC as a late event in hepatocarcinogenesis[33, 34].

The exact mechanism of capsular formation is not known. A tumor capsule may act as a barricade preventing the spread of cancer cells and has a positive role in the prognosis of HCC. The invaded capsule was regarded as incomplete in our series. We found the overexpression rate of p53 was similar in patients with no capsule and incomplete capsule (87.1 % *vs* 85.7 %), but was significantly lower in those with a complete capsule (17.2 %, $P$=0.0346) (Table 2). Other authors had different findings[23,24,49,50]. Multifocal HCCs are also a controversial issue. Some consider them an early metastasis via the portal vein, but some consider them multicentric. The former is a poor prognostic factor but the latter might not be[51]. Without the aid of molecular biology, it is difficult to differentiate daughter nodules, intrahepatic metastatic nodules and multicentric HCC. In the present study, we selected daughter nodules as intrahepatic metastasis according to the criteria of the Liver Cancer Study Group of Japan in order to assess the clinical outcome after recurrence. As for the evaluation of prognosis after recurrence, Ikeda *et al*.[1] reported that the most significant factor affecting the survival time of patients with intrahepatic recurrence was the number of tumor nodules at the time of recurrence. Those with daughter nodules showed a higher mutant p53 positive rate than the group with solitary HCC ($P$=0.0527). This might suggest that most daughter nodules favor intrahepatic metastasis.

Tumor size has been emphasized as one of the significant prognostic factors[2-5] because vascular invasion and daughter lesions may increasingly develop as the tumor grows. In our study, no significant correlation between p53 positivity and tumor size was found. In addition, tumor size also had no significant correlation with histological grade, vascular invasion, recurrence free interval or survival in our patients. From our experience, some large HCCs may be the result of expansive growth and may have slow intraportal or distant spread.

The implications of our results, nevertheless, are that the immunohistochemical detection of p53 is a valuable tool for prediction of recurrence in patients after resection or for identifying subgroups of patients who may be at higher risk. There is some discrepancy between our results and the findings of previous studies on the role of p53 expression in determining the prognosis of patients with HCC. These discrepancies, however, might reflect important variables of selection, such as number of patients, histological type of tumors, tumor stage, period of follow-up, and type of antibody used. All the patients entering our study had received curative resections.

Prognosis after recurrence in relation to p53 mutations in the primary lesion is rarely reported in the literatures. Our findings suggest that HCCs with p53 mutations have a higher malignant potential. Matsuda *et al*.[52] found that the postrecurrence survival of patients with repeat surgery was better than that of patients who were treated conservatively. However, from our study, the type of treatment for recurrent HCCs did not affect the postrecurrent survival because the choice of treatment was closely related to the number and extent of recurrent tumors and the liver function of the remnant. The majority of our patients had diffused multiple recurrent nodules over the liver remnant. Repeat surgery was undertaken on only one patient. In our study, the postrecurrent survival was weakly lower ($P$=0.051) in patients with p53 mutations in their primary lesion than in those without them.

We thus consider the status of p53 mutations in the primary lesion to be useful as a predictor affecting both the recurrence after resection and the prognosis after recurrence, even before the pathologic findings of recurrent HCCs are known. Therefore, it is important in the follow-up of patients after resection of HCCs. In conclusion, patients with p53 mutations have a worse prognosis than patients without such mutations, including survival after recurrence. Therefore, p53 mutation in the primary lesion is considered useful as an indicator of the biological behavior of recurrent HCCs.

## REFERENCES

1 **Ikeda K**, Saitoh S, Tsubota A, Arase Y, Chayama K, Kumada H, Watanabe G, Tsurumaru M. Risk factors for tumor recurrence and prognosis after curative resection of hepatocellular carcinoma. *Cancer* 1993; **71**: 19-25

2 **Arii S**, Tanaka J, Yamazoe Y, Minematsu S, Morino T, Fujita K, Maetani S, Tobe T. Predictive factors for intrahepatic recurrence of hepatocellular carcinoma after partial hepatectomy. *Cancer* 1992; **69**: 913-919

3 **Shirabe K**, Kanematsu T, Matsumata T, Adachi E, Akazawa K, Sugimachi K. Factors linked to early recurrence of small hepatocellular carcinoma after hepatectomy: univariate and multivariate analysis. *Hepatology* 1991; **14**: 802-805

4 **Jwo SC**, Chiu JH, Chau GY, Loong CC, Lui WY. Risk factors linked to tumor recurrence of human hepatocellular carcinoma after hepatic resection. *Hepatology* 1992; **16**: 1367-1371

5 **Nagao T**, Inoue S, Goto S, Mizuta T, Omori Y, Kawano N, Morioka Y. Hepatic resection for hepatocellular carcinoma. *Ann Surg* 1987; **205**: 33-40

6 **Sasaki Y**, Imaoka S, Masutani S, Ohashi I, Ishikawa O, Koyama H, Iwanaga T. Influence of coexisting cirrhosis on long-term prognosis after surgery in patients with hepatocellular carcinoma. *Surgery* 1992; **112**: 515-521

7 **Lai EC**, Ng IO, Ng MM, Lok AS, Tam PC, Fan ST, Choi TK, Wong J. Long-term results of resection for large hepatocellular carcinoma: a multivariate analysis of clinicopathological features. *Hepatology* 1990; **11**: 815-818

8 **Hsu HC**, Wu TT, Wu MZ, Sheu JC, Lee CS, Chen DS. Tumor invasiveness and prognosis in resected hepatocellular carcinoma. *Cancer* 1988; **61**: 2095-2099

9 **Hsu HC**, Sheu JC, Lin YH, Chen DS, Lee CS, Hwang LY, Beasley RP. Prognostic histologic features of resected small hepatocellular carcinoma (HCC) in Taiwan. *Cancer* 1985; **56**: 672-680

10 **el-Assal ON**, Yamanoi A, Soda Y, Yamaguchi M, Yu L, Nagasue N. Proposal of invasiveness score to predict recurrence and survival after curative hepatic resection for hepatocellular carcinoma. *Surgery* 1997; **122**: 571-577

11 **Jeng KS**, Chen BF, Lin HF. En bloc resection for extensive hepatocellular carcinoma: is it advisable? *World J Surg* 1994; **18**: 834-839

12 **Bartek J**, Bartkova J, Vojtesek B, Staskova Z, Lukas J, Rejthar A, Kovarik J, Midgley CA, Gannon JV, Lane DP. Aberrant expression of the p53 oncoprotein is a common feature of a wide spectrum of human malignancies. *Oncogene* 1991; **6**: 1699-1703

13 **Hollstein M**, Sidransky D, Vogelstein B, Harris CC. p53 mutations in human cancers. *Science* 1991; **253**: 49-53

14 **Baker SJ**, Fearon ER, Nigo JM, Hamilton SR, Preisinger AC, Jessup JM, vanTuinen P, Ledbetter DH, Barker DF, Nakamura Y. Chromosome 17 deletions and p53gene mutations in colorectal carcinomas. *Science* 1989; **244**: 217-221

15 **Collier JD**, Carpenter M, Burt AD, Bassendine MF. Expression of mutant p53 protein in hepatocellular carcinoma. *Gut* 1994; **35**: 98-100

16 **Livni N**, Eid A, Ilan Y, Rivkind A, Rosenmann E, Blendis LM, Shouval D, Galun E. p53 expression in patients with cirrhosis with and without hepatocellular carcinoma. *Cancer* 1995; **75**: 2420-2426

17 **Saegusa M**, Takano Y, Kishimoto H, Wakabayashi G, Nohga K, Okudaira M. Comparative analysis of p53 and c-myc expression and cell proliferation in human hepatocellular carcinomas- an enhanced immunohistochemical approach. *J Cancer Res Clin Oncol* 1993; **119**: 737-744

18 **D'Errico A**, Grigioni WF, Fiorentino M, Baccarini P, Grazi GL, Mancini AM. Overexpression of p53 protein and Ki67 proliferative index in hepatocellular carcinoma: an immunohistochemical study on 109 Italian patients. *Pathol Int* 1994; **44**: 682-687

19 **Ng IOL**, Srivastava G, Chung LP, Tsang SW, Ng MM. Overexpression and point mutations of p53 tumor suppressor gene in hepatocellular carcinomas in Hong Kong Chinese people. *Cancer* 1994; **74**: 30-37

20 **Cohen C**, DeRose PB. Immunohistochemical p53 in hepatocellular carcinoma and liver cell dysplasia. *Mod Pathol* 1994; **7**: 536-539

21 **Zhao M**, Zhang NX, Laissue JA, Zimmermann A. Immunohistochemical analysis of p53 protein overexpression in liver cell dysplasia and in hepatocellular carcinoma. *Virchows Arch* 1994; **424**: 613-621

22 **Hollstein MC**, Wild CP, Bleicher F, Chutimataewin S, Harris CC, Srivatanakul P, Montesano R. p53 mutations and aflatoxin B1 exposure in hepatocellular carcinoma patients from Thailand. *Int J Cancer* 1993; **53**: 51-55

23 **Vesey DA**, Hayward NK, Cooksley WGE. p53 gene in hepatocellular carcinomas from Australia. *Cancer Detect Prev* 1994; **18**: 123-130

24 **Pierre LP**, Flejou JF, Fabre M, Bedossa P, Belghiti J, Gayral F, Franco D. Overexpression of p53: a rare event in a large series of white patients with hepatocellular carcinoma. *Hepatology* 1992; **16**: 1171-1175

25 **Sheu JC**, Huang GT, Lee PH, Chung JC, Chou HC, Lai MY, Wang JT, Lee HS, Shih LN, Yang PM. Mutation of p53 gene in hepatocellular carcinoma in Taiwan. *Cancer Res* 1992; **52**: 6098-6100

26 **Kress S**, Jahn UR, Buchmann A, Bannasch P, Schwarz M. p53 mutations in human hepatocellular carcinomas from Germany. *Cancer Res* 1992; **52**: 3220-3223

27 **Wee A**, The M, Raju C. p53 expression in hepatocellular carcinoma in a population in Singapore with endemic hepatitis B virus infection. *J Clin Pathol* 1995; **48**: 236-238

28 **Hsu HC**, Tseng HJ, Lai PL, Lee PH, Peng SY. Expression of p53 gene in 184 unifocal hepatocellular carcinomas: association with tumor growth and invasiveness. *Cancer Res* 1993; **53**: 4691-4694

29 **Debuire B**, Paterlini P, Pontisso P, Basso G, May E. Analysis of the p53 gene in European hepatocellular carcinomas and hepatoblastomas. *Oncogene* 1993; **8**: 2303-2306

30 **Shieh YSC**, Nguyen C, Vocal MV, Chu HW. Tumor suppressor p53gene in hepatitis C and B virus-associated human hepatocellular carcinoma. *Int J Cancer* 1993; **54**: 558-562

31 **Nishida N**, Fukuda Y, Kokuryu H, Toguchida J, Yandell DW, Ikenega M. Role and mutational heterogeneity of the p53 gene in hepatocellular carcinoma. *Cancer Res* 1993; **53**: 368-372

32 **Bressac B**, Kew M, Wands J, Ozturk M. Selective G to T mutations of p53 gene in hepatocellular carcinoma from southern Africa. *Nature* 1991; **350**: 429-431

33 **Tanaka S**, Toh Y, Adachi E, Matsumata T, Mori R, Sugimachi K. Tumor progression in hepatocellular carcinoma may be mediated by p53 mutation. *Cancer Res* 1993; **53**: 2884-2887

34 **Oda T**, Tsuda H, Scarpa A, Sakamoto M, Hirohashi S. p53 gene mutation spectrum in hepatocelllular carcinoma. *Cancer Res* 1992; **52**: 6358-6364

35 **Puisieux A**, Ponchel F, Ozturk M. p53 as a growth suppressor gene in HBV-related hepatocellular carcinoma cells. *Oncogene* 1993; **8**: 487-490

36 **Bressac B**, Galvin KM, Liang TJ, Isselbacher KJ, Wands JR, Ozturk M. Abnormal structure and expression of p53 gene in human hepatocellular carcinoma. *Proc Natl Acad Sci USA* 1990; **87**: 1973-1977

37 **Slagle BL**. p53 mutations and hepatitis B virus: cofactors in hepatocellular carcinoma. *Hepatology* 1995; **21**: 597-599

38 **Nishida N**, Fukuda Y, Kokuryu H, Toguchida J, Yandell DW, Ikenega M. Role and mutational heterogeneity of the p53 gene in hepatocellular carcinoma. *Cancer Res* 1993; **53**: 368-372

39 **Scorsone KA**, Zhou YZ, Butel JS, Slagle BL. p53 mutations cluster at codon 249 in hepatitis B virus-positive hepatocellular carcinomas from China. *Cancer Res* 1992; **52**: 1635-1638

40 **Goldblum JR**, Bartos RE, Carr KA, Frank TS. Hepatitis B and alterations of the p53 tumor suppressor gene in hepatocellular carcinoma. *Am J Surg Pathol* 1993; **17**: 1244-1251

41 **Harris CC**, Hollstein M. Clinical implications of the p53 tumor-suppressor gene. *NEJM* 1993; **329**: 1318-1327

42 **Finlay CA**, Hinds PW, Levine AJ. The p53 proto-oncogene can act as a suppressor of transformation. *Cell* 1989; **57**: 1083-1093

43 **Nagao T**, Kondo F, Sato T, Nagato Y, Kondo Y. Immunohistochemical detection of aberrant p53 expression in hepatocellular carcinoma: correlation with cell proliferative activity indices, including mitotic index and MIB-1 immunostaining. *Hum Pathol* 1995; **26**: 326-333

44 **Saegusa M**, Takano Y, Kishimoto H, Wakabayashi G, Nohga K, Okudaira M. Comparative analysis of p53 and c-myc expression and cell proliferation in human hepatocellular carcinomas- an enhanced immunihistochemical approach. *J Cancer Res Clin Oncol* 1993; **119**: 737-744

45 **Lowe SW**, Ruley HE, Jacks T, Housman DE. p53-depedent apotosis modulates the cytotoxicity of anticancer agents. *Cell* 1993; **74**: 957-967

46 **Lowe SW**, Bodis S, McClatchey A, Remington L, Ruley HE, Fisher DE, Housman DE, Jacks T. p53 status and the efficacy of cancer therapy *in vivo*. *Science* 1994; **266**: 807-810
47 **Wynford-Thomas D**. P53 in tumor pathology: can we trust immunocytochemistry? *J Pathol* 1992; **166**: 329-330
48 **Hall PA**, Lane DP. p53 in tumor pathology: can we trust immunohistochemistry? *J Pathol* 1994; **172**: 1-4
49 **Sugo H**, Takamori S, Kojima K, Beppu T, Futagawa S. The significance of p53 mutations as an indicator of the biological behavior of recurrent hepatocellular carcinomas. *Surg Today* 1999; **29**: 849-855
50 **Hayashi H**, Sugio K, Matsumata T, Adachi E, Takenaka K, Sugimachi K. The clinical significance of p53 gene mutation in hepatocellular carcinomas from Japan. *Hepatology* 1995; **22**: 1702-1707
51 **Nakano S**, Haratake J, Okamoto K, Takeda S. Investigation of resected multinodular hepatocellular carcinoma: assessment of unicentric or multicentric genesis from histological and prognosis viewpoint. *Am J Gastroenterol* 1994; **9**: 189-193
52 **Matsuda Y**, Ito T, Oguchi Y, Nakajima K, Izukura T. Rationale of surgical management for recurrent hepatocellular carcinoma. *Ann Surg* 1993; **217**: 28-34

**Edited by** Xu XQ

P.O.Box 2345, Beijing 100023,China
Fax: +86-10-85381893
E-mail: wjg@wjgnet.com www.wjgnet.com

World J Gastroenterol 2003;9(6):1208-1211
World Journal of Gastroenterology
Copyright ©2003 by The WJG Press ISSN 1007-9327

• LIVER CANCER •

# Transcatheter arterial embolization treatment in patients with hepatocellular carcinoma and risk of pulmonary metastasis

Shee-Chan Lin, Shou-Chuan Shih, Chin-Roa Kao, Sun-Yen Chou

**Shee-Chan Lin, Shou-Chuan Shih, Chin-Roa Kao, Sun-Yen Chou,** Division of Gastroenterology, Department of Internal Medicine, Mackay Memorial Hospital, Taipei, Taiwan, China
**Correspondence to:** Dr. Shee-Chan Lin, Chief of Division of Gastroenterology, Department of Internal Medicine, Mackay Memorial Hospital. 92, Sec. 2, Chung San North Road, Taipei, Taiwan, China. sheechan@ms2.mmh.org.tw
**Telephone:** +86-2-25433535 **Fax:** +86-2-25433642
**Received:** 2003-02-25 **Accepted:** 2003-03-16

## Abstract

**AIM:** To investigate the relationship between transcatheter arterial embolization (TAE) and pulmonary metastasis in subjects with hepatocellular carcinoma (HCC).

**METHODS:** A total of 287 patients with HCC followed up for more than 1 week were included. 102 patients underwent transcatheter arterial embolization (TAE group) and 185 received conservative treatment (control group). The patients' chest x-rays and chest CT scans were examined for pulmonary metastasis.

**RESULTS:** Patients with TAE had a median survival of 19.3 months while that of the control group was only 10.0 months ($P<0.05$). Pulmonary metastasis occurred in 14 (13.7 %) patients in the TAE group and 14 (7.6 %) patients in the control group, there was no significant difference ($P>0.05$). The 1-year, 2-year and 5-year cumulative incidence of pulmonary metastasis was 11.8 %, 17.6 % and 24.0 % in the TAE group and 7.0 %, 13.0 % and 21.7 % in the control group, respectively ($P>0.05$). On the univariate analysis, tumor size, abnormal serum alanine aminotransferase levels and heterogeneity on sonography were significantly associated with pulmonary metastasis. However, on the multivariate analysis, only tumor size was significantly predictive of pulmonary metastasis.

**CONCLUSION:** TAE is effective on prolonging survival of patients with HCC. It does not significantly increase the risk of pulmonary metastasis. Tumor size is the only significant predictive factor associated with lung metastasis.

Lin SC, Shih SC, Kao CR, Chou SY. Transcatheter arterial embolization treatment in patients with hepatocellular carcinoma and risk of pulmonary metastasis. *World J Gastroenterol* 2003; 9(6): 1208-1211
http://www.wjgnet.com/1007-9327/9/1208.asp

## INTRODUCTION

Hepatocellular carcinoma (HCC) is the most common cancer in Taiwan and certain other parts of the world where hepatitis B virus infection is hyperendemic[1]. HCC has a dismal overall prognosis, with 94 % of affected individuals dying of the disease[2]. Treatment leading to long-term survival generally includes resection or ablative therapy for small or localized hepatic tumors[3-6]. Unfortunately, patients with HCC are usually diagnosed at a late stage when few can be treated with surgical resection. Factors indicating unresectability are (1) large or multicentric liver tumors, (2) the presence of metastatic disease, and (3) insufficient functional hepatic reserve[3]. Therapies other than surgical resection include systemic or infusional chemotherapy, hepatic artery ligation or embolization, and radiolabeled antibodies[7]. Transcatheter arterial embolization (TAE) has been performed for the treatment of unresectable HCC[8,9] and has been shown to be able to prolong survival[7, 10-11]. One study found survival of post-TAE to be comparable to that of post-hepatectomy[12].

However, it has been suggested that TAE-induced necrosis might result in hematogenous dissemination from the primary tumor[13]. The lung is the most common site of extrahepatic metastasis in HCC[14]. A higher incidence of pulmonary metastasis following TAE in patients with HCC has been reported. However, the subjects who developed lung metastasis in that series were followed for a longer period than those without metastasis[15]. We designed this case control study to evaluate the risk of pulmonary metastasis in patients with HCC following TAE, taking into account duration of follow up.

## MATERIALS AND METHODS

### *Patients*

Patients with HCC diagnosed from January 1996 to December 1999 at our hospital were included in this study. Diagnosis of HCC was based on high serum alpha-fetoprotein (AFP) values, ultrasonography, computed tomography (CT), and angiographic findings with or without needle biopsy or aspiration cytological examination. Patients who had pulmonary metastasis before or within 1 week after admission or who died within 1 week after admission were excluded, as were those eligible for surgical resection or percutaneous ethanol injection. There were 102 patients receiving TAE treatment during the study period. We selected another 185 patients with HCC who had refused either TAE or chemotherapy as a control group.

### *Methods*

TAE was performed with lipiodol mixed with gelatin particles at an interval of 12 to 16 weeks. All patients were followed until death or December 31, 2000. Chest x-rays were taken at each admission or every 3 months in the outpatient clinic. Multiple nodules in the lung fields on chest x-ray and chest CT scans were diagnosed as pulmonary metastasis. Liver ultrasonography was performed every 3 months. Tumor size and sonographic patterns were recorded. Tumors with both hyper-echoic and hypo-echoic patterns were classified as heterogeneous. The presence of portal vein thrombosis was evaluated with a combination of ultrasonography, angiography and CT. Tumor stage was assessed according to the staging system described by Okuda *et al*[8].

### *Statistical analysis*

Statistical analysis was performed using the $\chi^2$ test to compare

differences between groups. Results were given as the mean ± standard deviation. Comparisons between group means were performed using Student's *t* test. Survival time was calculated from the time of cancer diagnosis until death or December 31, 2000. The time from the date of the diagnosis of cancer to the date of pulmonary metastasis or December 31, 2000 was calculated for analysis of cumulative incidence of pulmonary metastasis. The cumulative probability of survival and the cumulative incidence of pulmonary metastasis were calculated using the Kaplan-Meier method, and the difference between groups was compared using the log-rank test[16]. Univariate and multivariate analyses using Cox proportional hazard models were performed to evaluate clinical parameters associated with pulmonary metastasis and calculate odds ratios (OR). The parameters included in the analysis were age, sex, serum albumin levels, bilirubin levels, AST and ALT values, AFP value, presence of cirrhosis, presence of ascites, presence of encephalopathy, Child scores, tumor size, sonographic pattern, uni- or multifocal tumor, presence of tumor halo, presence of portal vein thrombosis, stage of the disease, and TAE therapy. Significant parameters in the univariate analyses were analyzed with multivariate analysis. The level of significance was set at $P<0.05$.

## RESULTS

Demographic and clinical characteristics, liver function tests, and tumor characteristics did not differ significantly between the TAE and control groups (Table 1). Patients who had received TAE had a median survival time of 19.3 months compared with only 10.0 months for controls. The 6 month, one-year and two-year survival rate was 83 %, 59.1 % and 47.5 % respectively, in the TAE group, and 66.8 %, 43.7 % and 25.7 %, respectively, in the control group ($P<0.001$, Figure 1). Pulmonary metastasis developed in 14 (13.7 %) patients in the TAE group and 14 (7.6 %) patients in the control group ($P>0.05$). There was no significant difference in the cumulative incidence of pulmonary metastasis between these two groups. The 1-year, 2-year, 3-year, and 5-year cumulative incidence of pulmonary metastasis was 11.8 %, 17.6 %, 17.6 % and 24 % in the TAE group, 7 %, 13 %, 21.7 % and 21.7 % in the control group, respectively ($P>0.05$, Figure 2).

**Table 1** Clinical characteristics of patients with hepatocellular carcinoma

| Parameters | TAE group ($n$=102) | Control group ($n$=185) | $P$ |
|---|---|---|---|
| Male (%) | 75 (74.3%) | 148 (80%) | NS |
| Age (years)* | 56.7±10.5 | 56.8±13.7 | NS |
| Albumin (g/dl)* | 3.51±0.57 | 3.40±0.61 | NS |
| Bilirubin (mg/dl)* | 2.02±7.17 | 1.30±1.25 | NS |
| ALT (IU/ml)* | 68.4±63.6 | 63.0±57.1 | NS |
| Prolonged Prothrombin time* | 1.38±1.25 | 1.48±1.11 | NS |
| Encephalopathy (%) | 6 (5.9%) | 14 (7.6%) | NS |
| Cirrhosis (%) | 76 (74.5%) | 121 (65.4%) | NS |
| Ascites (%) | 14 (13.7%) | 32 (17.3%) | NS |
| Multicentric tumors (%) | 19 (18.6%) | 39 (21.1%) | NS |
| Heterogeneous echopattern (%) | 34 (33.4%) | 72 (39.1%) | NS |
| Encapsulated tumors (%) | 49 (48.0%) | 76 41.1%) | NS |
| PV thrombosis (%) | 23 (22.5%) | 58 (31.4%) | NS |
| Large tumor size (%) | 56 (54.9%) | 103 (55.7%) | NS |

Data expressed as means ± standard deviation, comparison with unpaired Student's *t* test. NS=not significant.

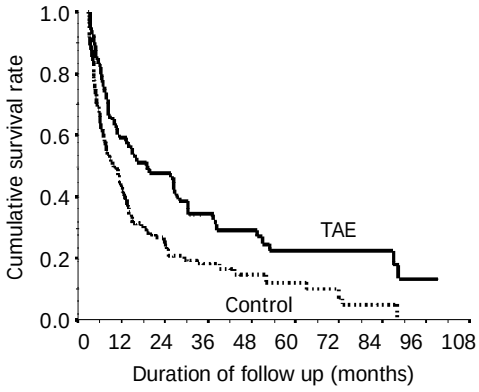


**Figure 1** Survival curves of patients with HCC treated with TAE and untreated controls.

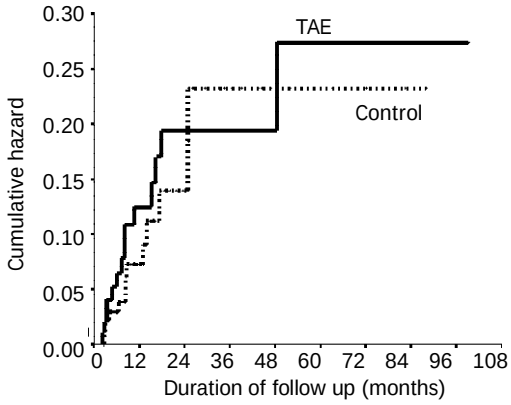


**Figure 2** Cumulative incidence of pulmonary metastasis in patients with HCC treated with TAE or untreated controls.

On the univariate analysis using the Cox proportional hazard model, tumor size (OR 2.34), abnormal serum ALT levels (OR 1.94) and heterogeneous sonographic pattern (OR 2.08) were significantly associated with the risk of pulmonary metastasis. However, on multivariate analysis only tumor size was significantly predictive of pulmonary metastasis (OR 2.24, 95 % CI 1.37 to 6.45).

## DISCUSSION

It is believed that manipulation of tumor with TAE will increase the risk of hematogenous metastasis due to an increase in activity of serum type IV collagen-degrading enzyme[17], or a decrease in activity of the tumor invasion-inhibiting factor[18]. The disruption of tissue architecture resulting from ischemic necrosis after the TAE treatment may facilitate the dissemination of neoplastic cells[19]. The incidence of extrahepatic recurrence of HCC is increased in patients who receive preoperative TAE treatment compared to those who undergo surgery alone[20]. However, in our study, the incidence of pulmonary metastasis after the TAE therapy was not significantly increased. TAE patients also experienced longer survival and were followed longer than untreated controls (Figure 1). The 1-year, 2-year, 3-year and 5-year cumulative incidence of lung metastasis did not differ between the two groups.

The overall incidence of pulmonary metastasis in our series was 7.2 %, lower than that from an autopsy series of HCC reported in Japan[21]. There may be several reasons for this discrepancy. We excluded patients with obvious pulmonary metastasis within 1 month after the diagnosis of cancer, although we could not exclude the presence of micro-metastasis. Our diagnosis of metastatic disease was based on

multi-nodular lesions on the chest x-ray and confirmed by chest CT. Most of our patients with metastasis had lesions larger than 3 mm on the chest film. Peters reported that pulmonary metastasis larger than 1 cm in size was rare and that, in 55 % of cases, lung metastasis was only recognizable microscopically[22]. We would expect the actual incidence of pulmonary metastasis in our series to be more than 10 %, but this could not be documented, in part because autopsy is not well accepted in Taiwan. However, as both TAE and control groups initially included patients without clinically detectable metastasis, we believe that our results are still valid, as the subjects were similar at baseline.

It has been reported in an autopsy study that the HCC tumor size and invasion of the portal vein were associated with pulmonary metastasis[21]. In another study of patients with long survival, the same association was found, with the coexistence of pulmonary metastasis, a large tumor size and portal vein invasion being the final event leading to death[23]. In our series, on univariate analysis only large tumor size, a heterogeneous echo pattern, or abnormal alanine aminotransferase levels were associated with an increased incidence of pulmonary metastasis.

When HCC is small, the sonographic pattern is homogeneous and hypo-echoic. Most small hepatomas progress from hypoechoic to heterogeneous hyperechoic patterns when they grow larger[24]. In general, small hepatomas without necrosis are hypoechoic; medium-sized tumors have a hypoechoic periphery and a hyperechoic center. The hypoechoic periphery corresponds to viable tumor and the hyperechoic core corresponds to central coagulation necrosis. Large tumors with extensive necrosis have an irregular mixed-echo pattern[25]. A significant correlation between the incidence of metastasis and extent of necrosis in the primary tumor has been reported[26]. The heterogeneous sonographic pattern of the tumor therefore implies later stage disease with more potential of extrahepatic metastasis. The serum alanine aminotransferase level correlates with hepatocellular damage. Tumor necrosis releases alanine aminotransferase enzymes into the blood flow. These observations likely explain our finding of an association on the univariate analysis between these factors and pulmonary metastasis. The fact that tumor size was the only independent predictor of metastasis on the multivariate analysis is thus understandable, as large tumors are almost invariable heterogeneous on sonography and associated with abnormal alanine aminotransferase levels.

Unfortunately, about 80 % of all our patients with HCC were not treated (data not shown). The reasons for lack of specific treatment in the control group varied. Most of them did not have regular serum AFP screening or sonographic examination and some already had late-stage HCC with a poor general condition and were thus too unwell for any specific treatment. Some did not trust Western medicine and tried Chinese herbal medicine instead. Only 20 % of our patients with HCC received treatment, 21 % undergoing surgical resection or percutaneous ethanol injection and 75 % of them being treated with TAE. More frequent sonographic screening of patients at high risk for HCC is important for earlier detection of smaller tumors.

In conclusion, TAE therapy is effective on prolonging survival of some patients with HCC. In our series, TAE did not increase the incidence of pulmonary metastasis. The larger the tumor, the higher the risk for pulmonary metastasis.

## REFERENCES


1 **Beasley RP,** Hwang LY, Lin CC, Chien CS. Hepatocellular carcinoma and hepatitis B virus. A prospective study of 22 707 men in Taiwan. *Lancet* 1981; **2**: 1129-1133

2 **Rustgi V**. Epidemiology of hepatocellular cancer. *Ann Intern Med* 1988; **108**: 390-397

3 **Curley SA**, Levin B, Rich TA. Liver and bile ducts. In: Abeloff MD, Armitage JO, Lichter AS. eds. Clinical Oncology. *New York: Churchill Livingstone, Inc*, 1995: 1305-1372

4 **Nagasue N**, Kohno H, Chang YC, Taniura H, Yamanoi A, Uchida M, Kimoto T, Takemoto Y, Nakamura T, Yukaya H. Liver resection for hepatocellular carcinoma: results of 229 consecutive patients during 11 years. *Ann Surg* 1993; **217**: 375-384

5 **Curley SA**, Izzo F, Ellis LM, Nicolas Vauthey J, Vallone P. Radiofrequency ablation of hepatocellular cancer in 110 patients with cirrhosis. *Ann Surg* 2000; **232**: 381-391

6 **Livraghi T**, Bolondi L, Lazzaroni S, Marin G, Morabito A, Rapaccini GL, Salmi A, Torzilli G. Percutaneous ethanol injection in the treatment of hepatocellular carcinoma in cirrhosis. *Cancer* 1992; **69**: 925-929

7 **Di Bisceglie AM**, Rustgi VK, Hoofnagle JH, Dusheiko GM, Lotze MT. NIH conference: hepatocellular carcinoma. *Ann Intern Med* 1988; **108**: 390-401

8 **Okuda K**, Ohtsuki T, Obata H, Tomimatsu M, Okazaki N, Hasegawa H, Nakajima Y, Ohnishi K. Natural history of hepatocellular carcinoma and prognosis in relation to treatment: study of 850 patients. *Cancer* 1985; **56**: 918-928

9 **Yamada R**, Sato M, Kawabata M, Nakatsuka H, Nakamura K, Takashima S. Hepatic artery embolization in 120 patients with unresectable hepatoma. *Radiology* 1983; **148**: 397-401

10 **Mondazzi L**, Bottelli R, Brambilla G, Rampoldi A, Rezakovic I, Zavaglia C, Alberti A, Ideo G. Transarterial oily chemoembolization for the treatment of hepatocellular carcinoma: a multivariate analysis of prognostic factors. *Hepatology* 1994; **19**: 1115-1123

11 **Hsieh MY**, Chang WY, Wang LY, Chen SC, Chuang WL, Lu SN, Wu DK. Treatment of hepatocellular carcinoma by transcatheter arterial chemoembolization and analysis of prognostic factors. *Cancer Chemotherapy & Pharmacology* 1992; **31**: S82-85

12 **Yoshimi F**, Nagao T, Inoue S, Kawano N, Muto T, Gunji T, Ohnishi S, Imawari M. Comparison of hepatectomy and transcatheter arterial chemoembolization for the treatment of hepatocellular carcinoma: necessity for prospective randomized trial. *Hepatology* 1992; **16**: 702-706

13 **Bonfil RD,** Bustuoabad OD, Ruggiero RA, Meiss RP, Pasqualini CD. Tumor necrosis can facilitate the appearance of metastasis. *Clin Exp Metastasis* 1988; **6**: 121-129

14 **Lee YT**, Geer DA. Primary liver cancer: pattern of metastasis. *J Surg Oncol* 1987; **36**: 26-31

15 **Liou TC**, Shih SC, Kao CR, Chou SY, Lin SC, Wang HY. Pulmonary metastasis of hepatocellular carcinoma associated with transarterial chemoembolization. *J Hepatol* 1995; **23**: 563-568

16 **Peto R**, Pike MC, Armitage P, Breslow NE, Cox DR, Howard SV, Mantel N, McPherson K, Peto J, Smith PG. Design and analysis of randomized clinical trials requiring prolonged observation of each patient: II. Analysis and examples. *Br J Cancer* 1977; **35**: 1-39

17 **Hashimoto N**, Kobayashi M, Tsuji T. Serum type IV collagen-degrading enzyme in hepatocellular carcinoma with metastasis. *Acta Med Okayama* 1988; **42**: 1-6

18 **Isoai A**, Giga-Hama Y, Shinkai K, Mukai M, Akedo H, Kumagai H. Tumor invasion-inhibiting factor 2: primary structure and inhibitory effect on invasion in vitro and pulmonary metastasis of tumor cells. *Cancer Res* 1992; **52**: 1422-1426

19 **Boix L**, Bruix J, Castells A. Circulating mRNA for alpha-fetoprotein in patients with hepatocellular carcinoma. Evidence of tumor dissemination after transarterial embolization. *Hepatology* 1996; **24**: 349

20 **Peters RL**. Pathology of hepatocellular carcinoma. Okuda K, Peters, RL, eds. Hepatocellular carcinoma. *New York*: *John Wiley & Son Inc*, 1976: 107-168

21 **Wu CC**, Ho YZ, Ho WL, Wu TC, Liu TJ, Peng FK. Preoperative transcatheter arterial chemoembolization for resectable large hepatocellular carcinoma: a reappraisal. *Br J Surg* 1995; **82**: 122-126

22 **Sawabe M**, Nakamura T, Kanno J, Kasuga T. Analysis of mor-

phological factors of hepatocellular carcinoma in 98 autopsy cases with respect to pulmonary metastasis. *Acta Pathol Jpn* 1987; **37**: 1389-1404

23 **Falkson G**, Cnaan A, Schutt AJ, Ryan LM, Falkson HC. Prognostic factors for survival in hepatocellular carcinoma. *Cancer Res* 1988; **48**: 7314-7318

24 **Sheu JC**, Chen DS, Sung JL, Chuang CN, Yang PM, Lin JT, Yang PC. Hepatocellular carcinoma: US evolution in the early stage. *Radiology* 1985; **155**: 463-467

25 **Yang R**, Kopecky KK, Rescorla FJ, Galliani CA, Grosfeld JL. Changes of hepatoma echo patterns with tumor growth. A study of the microanatomic basis in a rat model. *Invest Radiol* 1993; **28**: 507-512

26 **Nishizaki T**, Matsumata T, Kanematsu T, Yasunaga C, Sugimachi K. Surgical manipulation of VX2 carcinoma in the rabbit liver evokes enhancement of metastasis. *J Surg Res* 1990; **49**: 92-97

**Edited by** Xu XQ

P.O.Box 2345, Beijing 100023,China
Fax: +86-10-85381893
E-mail: wjg@wjgnet.com www.wjgnet.com

World J Gastroenterol 2003;9(6):1212-1215
World Journal of Gastroenterology
Copyright ©2003 by The WJG Press ISSN 1007-9327

• LIVER CANCER •

# Changes in survival patterns in urban Chinese patients with liver cancer

Xi-Shan Hao, Ke-Xin Chen, Peizhong Peter Wang, Tom Rohan

**Xi-Shan Hao, Ke-Xin Chen,** Tianjin Cancer Institute and Hospital, Tianjin Medical University, Tianjin 300060, China
**Peizhong Peter Wang,** Department of Public Health Sciences, University of Toronto, Toronto, Canada
**Tom Rohan,** Department of Epidemiology and Social Medicine, Albert Einstein College of Medicine, Bronx, U.S.A
**Correspondence to:** Dr. P. Peter Wang, ACREU, Toronto Western Hospital Research Institute, University Health Network, MP 10-327, 399 Bathurst Street, Toronto, Ontario M5T 2S8, Canada. wang@uhnres.utoronto.ca
**Telephone:** +1-416-603-5800 Ext: 3174 **Fax:** +1-416-603-6288
**Received:** 2003-02-26 **Accepted:** 2003-03-16

## Abstract

**AIM:** To examine the survival patterns and determinants of primary liver cancer in a geographically defined Chinese population.

**METHODS:** Primary liver cancer cases ($n$=13 685) diagnosed between 1981 and 2000 were identified by the Tianjin Cancer Registry. Age-adjusted and age-specific incidence rates were examined in both males and females. Proportional hazards (Cox) regression was utilized to explore the effects of time of diagnosis, sex, age, occupation, residence, and hospital of diagnosis on survival.

**RESULTS:** Crude and age-adjusted incidence rates in the study period were: 27.4/100 000 and 26.3/100 000 in males; and 11.5/100 000 and 10.4/100 000 in females, respectively. Cox regression analyses indicated that there was a significant improvement in survival rates over time. Industrial workers and older people had relatively poor survival rates. The hospital in which the liver cancer was diagnosed was a statistically significant predictor of survival; patients diagnosed in city hospitals were more likely to have better survival than those diagnosed in community/district hospitals.

**CONCLUSION:** Patients diagnosed in recent years appeared to have a better outcome than those diagnosed in early times. There were also significant survival disparities with respect to occupation and hospital of diagnosis, which suggest that socioeconomic status may play an important role in determining prognosis.

Hao XS, Chen KX, Wang PP, Rohan T. Changes in survival patterns in urban Chinese patients with liver cancer. *World J Gastroenterol* 2003; 9(6): 1212-1215
http://www.wjgnet.com/1007-9327/9/1212.asp

## INTRODUCTION

Liver cancer is a fairly common malignancy world wide[1-5], especially in developing countries[6-9]. In China, primary liver cancer is the third and fourth most common cancer in men and women with the age-adjusted incidence rates of 28.2/100 000 and 9.8/100 000 respectively in Shanghai[10]. Population-based survival data on cancer are indispensable in providing real, unbiased, average outcome of cancer patients. While liver cancer is a major cause of cancer-related mortality in China, little is known about its survival patterns over time. The objective of this study was two-fold: (1) to examine a specific hypothesis regarding the survival patterns of liver cancer in the studied urban Chinese population; (2) to examine the factors affecting such survival patterns. The objectives were achieved by analysing the data from the Tianjin Cancer Registry. The Tianjin Cancer Registry Centre is one of the members of the International Agency for Research on Cancer (IARC) of the World Health Organization. The cancer incidence data from Tianjin have been included in IARC official publications: "Cancer Incidence in Five Continents" since 1981. As Tianjin Cancer Registry is one of the few internationally accredited cancer registries in China, the results have important implications.

## MATERIALS AND METHODS

### *Data*

Tianjin, the third largest city in China, has a population about 10 million, of which about 98 % belongs to the Han ethnic group. The Tianjin Cancer Registry was established in 1978 and became operational in 1981[11-13]. While the registry covers the whole city, data from six urban districts, which include approximately 4-million people, have been computerized and evaluated here. A city by-law requires that all physicians are responsible for filling out a report form for each new diagnosis of cancer. Practically, the task of cancer reporting is delegated to the medical record unit at each hospital. Thus, cancer cases are normally reported when patients are discharged from or die in the hospital. Information collected on the cancer reporting card includes name, sex, current age or date of birth, address, reporting hospital or medical institute, date (month and year) of diagnosis, four digit ICD-9 codes, and occupation. The Centre for Disease Control in Tianjin performs an annual quality control examination in at least 20 randomly selected hospitals in Tianjin to ensure that each hospital meets the standard cancer case reporting protocol. The evaluation results are used as part of the overall hospital report card, which is further used for hospital excellence ranking. A monetary incentive is offered for each cancer case reported, which is normally paid to the medical record unit rather than to individual physicians. Patients from other parts of China or those without permanent residence in Tianjin are not reflected in the current registry data.

All death certificates, which are the second source of cancer registration, are registered both at the district public health unit (DPHU) and the local police station. The DPHU routinely reviews all death certificates and identifies deaths, which are directly or indirectly caused by cancers. All cancer cases identified through death certificates are checked against the existing database at the Tianjin Cancer Institute for possible double or multiple reporting. In this study, we included all primary liver cancer patients (ICD-9 codes 155.1, 155.2). Numbers in each age-sex specific population for the six urban districts were obtained from the Tianjin Police Head Office,

which enumerates the Tianjin urban population based on people' s unique resident cards.

### *Analyses*

Univariate and bivariate descriptive analyses were performed prior to multivariate analyses. Proportional hazards regression (Cox model)[14-20] was used to examine the effects of various factors on survival time for the study population. The proportional hazards model can be expressed as:

$$h(t;X)=h_0(t)exp(b'X)$$

where h(t; X) is the hazard function of T at time t given a regression vector X; $h_0$ is the unspecified baseline hazard function. The SAS PROC PHREG procedure was used to examine the specified survival model. The time variable (in days) was defined as the interval between the date of diagnosis and date of death. The covariates included in the survival analyses were age, sex, occupation, year of diagnosis, and residence. To best capture the impact of age on survival time, we explored different ways to categorize it in our regression models. As the incidence rates of liver cancer are very low in children, in our final model, we used ages 0-19 years as one group (baseline) and 10-year intervals thereafter to get stable estimates for the regression coefficients. Treating age categories as dummy variables in the model did not result in a better goodness of fit than simply introducing age as an ordered categorical variable with one degree of freedom.

Residence was introduced as a binary variable. As Hexi district is generally regarded as the best neighbourhood in Tianjin, it was used as a reference group and coded as "0". Other districts were coded as "1" and compared to Hexi district. Self-reported occupations were collapsed into 4-broad mutually exclusive categories: professionals and managers (such as teachers, medical doctors), service industry workers (such as salespeople), industry workers, and others. The professional and manager group was treated as the reference category. Year of diagnosis was treated as single year in Poisson regression and grouped into four categories in Cox regression analysis: 1981-1985 (reference category), 1986-1990, 1991-1995, and 1996-2000. Hospital of diagnosis was dichotomized to community/district hospitals (reference category) and city hospitals. Community hospitals normally provide walk-in service in their districts but do not provide surgical operations. District hospitals provide in-patient service and day-surgery operations in their districts. City general hospitals and speciality hospitals, which normally have advanced technology and research programs, provide a wide range of service to all Tianjin residents referred by community or district hospitals and sometimes patients from other parts of China.

## RESULTS

In total, 13 685 cancer cases were identified during the study period (1981-2000) and 70.6 % occurred in males. The mean age at diagnosis for the study population was 62.2 years (61.3 and 64.3 years for males and females, respectively) with a median survival time of 151 days. As shown in Table 1, diagnosis based on death certificate only (DCO) was less than 1 %. Most cancer cases were reported from city (75.1 %) or district hospitals (15.5 %) and most cases were diagnosed based on either medical imaging (60.6 %) or histology (28.4 %). While there are few gender differences with respect to the age at diagnosis and types of hospitals of diagnosis, males were more likely than females to be administrators or professionals.

The crude and age-adjusted incidence rates for the entire study period were 27.4/100 000 and 26.3/100 000 respectively for males. The corresponding rates were 11.5/100 000 and 10.4/100 000 for females.

**Table 1** Characteristics of liver cancer cases diagnosed during 1981 to 2000, Tianjin, China

| Variable | Category | Male | | Female | | Total | |
|---|---|---|---|---|---|---|---|
| | | *n* | % | *n* | % | *n* | % |
| Sex | Male | - | - | - | - | 9666 | 70.63 |
| | Female | - | - | - | - | 4019 | 29.37 |
| Age | 0-19 | 19 | 0.20 | 18 | 0.45 | 37 | 0.27 |
| | 20-29 | 64 | 0.66 | 24 | 0.60 | 88 | 0.64 |
| | 30-39 | 360 | 3.72 | 119 | 2.96 | 479 | 3.50 |
| | 40-49 | 1118 | 11.57 | 284 | 7.07 | 1402 | 10.24 |
| | 50-59 | 2443 | 25.27 | 728 | 18.11 | 3171 | 23.17 |
| | 60-69 | 3155 | 32.64 | 1395 | 34.71 | 4550 | 33.25 |
| | 70-79 | 2009 | 20.78 | 1129 | 28.09 | 3138 | 22.93 |
| | 80+ | 498 | 5.15 | 322 | 8.1 | 820 | 5.99 |
| Type of diagnosis | Clinical only | 981 | 10.15 | 473 | 11.77 | 1454 | 10.62 |
| | Medical imaging only | 5934 | 61.39 | 2353 | 58.55 | 8287 | 60.56 |
| | Histology at local site | 2710 | 28.04 | 1176 | 29.26 | 3886 | 28.40 |
| | Surgical examination or autopsy | 14 | 0.14 | 8 | 0.20 | 22 | 0.16 |
| | Death certificate only | 1 | 0.01 | 1 | 0.02 | 2 | 0.01 |
| | Unknown | 26 | 0.27 | 8 | 0.20 | 34 | 0.25 |
| Occupation | Professionals and administrators | 3193 | 33.03 | 390 | 9.7 | 3583 | 26.18 |
| | Service industry workers | 1220 | 12.62 | 334 | 8.31 | 1554 | 11.36 |
| | Industry workers | 3937 | 40.73 | 989 | 24.61 | 4926 | 36.00 |
| | All others | 1316 | 13.62 | 2306 | 57.38 | 3622 | 26.46 |
| Type of reporting hospital | City general or specified hospitals | 7306 | 75.58 | 2968 | 73.85 | 10274 | 75.07 |
| | District general hospital | 1495 | 15.47 | 624 | 15.53 | 2119 | 15.48 |
| | Community hospital | 865 | 8.95 | 427 | 10.62 | 1292 | 9.44 |

Table 2 displays the results from the proportional hazard regression analyses. Older age and female gender were associated with poor survival rates, with relative risks of 1.06 (95 % CI: 1.01, 1.11) and 1.08 (95 % CI: 1.05, 1.09) respectively. Hospital of diagnosis was a statistically significant predictor of survival time. Patients diagnosed in city hospitals tended to live longer than those diagnosed in district or community hospitals, with relative risk of death of 0.76 (95 % CI: 0.73, 0.79). The results showed that period of diagnosis was a statistically significant predictor of patients' survival time. Patients diagnosed in more recent years were likely to live longer than those diagnosed in earlier years with a relative risk of 0.85 (95 % CI: 0.83, 0.86) for every 5-year increment.

**Table 2** Proportional hazards analyses of liver cancer diagnosed between 1981 and 2000 in Tianjin urban districts

| Variable | Category | Relative risk | 95 % CI |
|---|---|---|---|
| Sex | Male | 1 | |
| | Female | 1.06 | 1.01, 1.11 |
| Age | 0-19 | 1 | |
| | Every 10-years increase | 1.08 | 1.05, 1.09 |
| Period of | 1981-1985 | 1 | |
| diagnosis | Every 5-years increase | 0.85 | 0.83, 0.86 |
| Residence | Hexi District (advantaged) | 1 | |
| | Other districts | 1.02 | 0.97, 1.08 |
| Occupation | Administrators | 1 | |
| | Service industry workers | 1.06 | 0.99, 1.13 |
| | Industry workers | 1.08 | 1.03, 1.13 |
| | All others | 0.97 | 0.91, .102 |
| Hospital | District or community hospitals | 1 | |
| | City general or speciality hospitals | 0.76 | 0.73, 0.79 |

## DISCUSSION

In this study, we described the survival patterns for primary liver cancer in a Chinese urban population over the last 20 years. To the best of our knowledge, this was the first study of its kind ever reported from China. Given the inconsistencies in the literature regarding liver cancer incidence trends[21-26] and survival patterns[27-32], this study provides another piece of useful information for this disease. As Tianjin has a first-class cancer treatment centre and facilities, patients from other parts of China often seek treatment in Tianjin. It is relatively uncommon that Tianjin residents travel to other parts of China for treatment. There is no conceivable reason that this pattern had changed during the study period. Moreover, regardless of where a Tianjin patient gets treated, his/her cancer status would eventually be reflected in the death certificates, which are one source of our cancer registration data.

Based on clinical patients in Qidong, which has the highest liver cancer incidence rates in China, Chen *et al*[31] reported that females had a more favourable prognosis than males. In this study, we found that females had slightly poor survival rate than males. As the magnitude of the reported survival difference was small, the results were unlikely to be conclusive. Nevertheless, the discrepancy between the two studies may be related to the differences in study population, such as, clinical setting versus population based or rural (Qidong) versus urban (Tianjin). The last four decades have seen a significant improvement in liver cancer treatment in China[33]. While the current study only had a span of 20 years, the improvement in survival was apparent. The changes may be explained by improvements in liver cancer clinical management in this city. For example, unpublished data indicate the proportion of liver cancer patients who undergo surgery for their condition has increased substantially in Tianjin.

This study has several limitations. First, we only included urban residents and were unable to compare the differences between rural and urban populations. Since China is a vast country with significant variations in economic conditions, the reported results may only be applicable to urban Chinese residents. Second, as the Tianjin Cancer Registry only records cancer related deaths (direct and indirect), it is possible that liver cancer patients who died from other causes, such as traffic accidents, were not reflected in our data bases. As a result, the observed survival time as reflected in the cancer registry data, might have been inflated. However, given that liver cancer is a fast progressive condition and a dominant majority of liver cancer patients die from it or its complications, it is unlikely that the problem related to non-liver cancer deaths would have altered the observed survival patterns greatly. Furthermore, since the possible artificially better survival caused by omission of non-liver cancer deaths would have been more in evidence for patients diagnosed in early periods, the true survival advantage for the patients diagnosed in recent years could be even greater. Third, we did not have information on cancer stage and treatment and were unable to estimate their impact on the observed survival pattern. It was possible that some of the observed survival advantage in later periods could be attributed to the cancer stage shift over time. Thus, studies on the changes in cancer stage and treatment over time are needed to address these questions.

## ACKNOWLEDGEMENTS

Tianjin Cancer Registry is jointly funded by the Tianjin Health Bureau and the Tianjin Cancer Institute. All computations were prepared at Tianjin Cancer Institute and the responsibility for the use and interpretation of these data is entirely that of the authors. The authors thank the International Agency for Research on Cancer (IARC) for their technological support. We are grateful to Dr. Qi-Long Yi, University of Toronto, for his statistical advice.

## REFERENCES

1 **Benhamiche AM,** Faivre C, Minello A, Clinard F, Mitry E, Hillon P, Faivre J. Time trends and age-period-cohort effects on the incidence of primary liver cancer in a well-defined French population: 1976-1995. *J Hepatol* 1998; **29**: 802-806

2 **Anderson IB,** Sorensen TI, Prener A. Increase in incidence of disease due to diagnostic drift: primary liver cancer in Denmark, 1943-85. *Bmj* 1991; **302**: 437-440

3 **Chiesa R,** Donato F, Portolani N, Favret M, Tomasoni V, Nardi G. Primary liver cancer in a high-incidence area in north Italy: etiological hypotheses arising from routinely collected data. *Eur J Epidemiol* 1995; **11**: 435-442

4 **El-Serag HB,** Mason AC. Rising incidence of hepatocellular carcinoma in the United States. *N Engl J Med* 1999; **340**: 745-750

5 **Kobayashi M,** Ikeda K, Saitoh S, Suzuki F, Tsubota A, Suzuki Y, Arase Y, Murashima N, Chayama K, Kumada H. Incidence of primary cholangiocellular carcinoma of the liver in japanese patients with hepatitis C virus-related cirrhosis. *Cancer* 2000; **88**: 2471-2477

6 **Miyakawa Y,** Yoshizawa H. Increasing incidence of hepatocellular carcinoma associated with hepatitis C virus infection in Japan. *Indian J Gastroenterol* 2001; **20**: C95-96

7 **Parkin DM,** Srivatanakul P, Khlat M, Chenvidhya D, Chotiwan P, Insiripong S, L'Abbe KA, Wild CP. Liver cancer in Thailand. I. A case-control study of cholangiocarcinoma. *Int J Cancer* 1991; **48**: 323-328

8 **Srivatanakul P,** Parkin DM, Khlat M, Chenvidhya D, Chotiwan P, Insiripong S, L'Abbe KA, Wild CP. Liver cancer in Thailand. II. A case-control study of hepatocellular carcinoma. *Int J Cancer* 1991; **48**: 329-332

9 **Shea KA,** Fleming LE, Wilkinson JD, Wohler-Torres B, McKinnon

JA. Hepatocellular carcinoma incidence in Florida. Ethnic and racial distribution. *Cancer* 2001; **91**: 1046-1051

10 **International Agency for Reseach on Cancer.** Cancer Incidence in Five Continents, Vol. VII. *Lyon, IARC* 1997

11 **Chen KX,** He M, Dong SF, Wang JF. Incidence, mortality and survival rates of female breast cancer in Tianjin, China. *Zhonghua Zhongliu Zazhi* 2002; **24**: 573-579

12 **Wang QS,** Lin XP. An approach to use cancer registration to assess cancer risks by occupation and industry. *Zhonghua Liuxing Bingxue Zazhi* 1997; **18**: 331-333

13 **Guo Z.** Mortality analysis of malignant neoplasms and cardiovascular diseases 1979-1983 in Tianjin. *Zhonghua Liuxing Bingxue Zazhi* 1985; **6**: 353-355

14 **Wang PP,** Haines CS. Childhood and adolescent leukaemia in a North American population. *Int J Epidemiol* 1995; **24**: 1100-1109

15 **Contal C,** Mallet A. Checking the Cox model in a real situation. *Rev Epidemiol Sante Publique* 2000; **48**: 490-501

16 **Fu JH,** Rong TH, Li XD, Ma GW, Hu Y, Min HQ. Cox regression analysis of the prognostic factors of unresectable esophageal carcinoma after stenting. *Ai Zheng* 2003; 22: 91-94

17 **Averbook BJ,** Fu P, Rao JS, Mansour EG. A long-term analysis of 1018 patients with melanoma by classic Cox regression and tree-structured survival analysis at a major referral center: Implications on the future of cancer staging. *Surgery* 2002; **132**: 589-602; discussion 602-604

18 **Steinbach D,** Hermann J, Littlewood T, Zintl F. Risk group definition in children with acute myeloid leukemia by calculating individual risk factors on the basis of a multivariate stepwise Cox regression analysis. *Leuk Lymphoma* 2001; **42**: 1289-1295

19 **Boberg KM,** Rocca G, Egeland T, Bergquist A, Broome U, Caballeria L, Chapman R, Hultcrantz R, Mitchell S, Pares A, Rosina F, Schrumpf E. Time-dependent Cox regression model is superior in prediction of prognosis in primary sclerosing cholangitis. *Hepatology* 2002; **35**: 652-657

20 **de Bruijne MH,** le Cessie S, Kluin-Nelemans HC, van Houwelingen HC. On the use of Cox regression in the presence of an irregularly observed time-dependent covariate. *Stat Med* 2001; **20**: 3817-3829

21 **Law MG,** Roberts SK, Dore GJ, Kaldor JM. Primary hepatocellular carcinoma in Australia, 1978-1997: increasing incidence and mortality. *Med J Aust* 2000; **173**: 403-405

22 **Saracci R,** Repetto F. Time trends of primary liver cancer: indication of increased incidence in selected cancer registry populations. *J Natl Cancer Inst* 1980; **65**: 241-247

23 **Yu MC,** Yuan JM, Govindarajan S, Ross RK. Epidemiology of hepatocellular carcinoma. *Can J Gastroenterol* 2000; **14**: 703-709

24 **Bosch FX,** Ribes J. Epidemiology of liver cancer in Europe. *Can J Gastroenterol* 2000; **14**: 621-630

25 **Bosch FX,** Ribes J, Borras J. Epidemiology of primary liver cancer. *Semin Liver Dis* 1999; **19**: 271-285

26 **Taylor-Robinson SD,** Foster GR, Arora S, Hargreaves S, Thomas HC. Increase in primary liver cancer in the UK, 1979-94. *Lancet* 1997; **350**: 1142-1143

27 **Lee CL,** Ko YC. Survival and distribution pattern of childhood liver cancer in Taiwan. *Eur J Cancer* 1998; **34**: 2064-2067

28 **Tang ZY,** Yu YQ, Zhou XD, Chen QM. Factors influencing primary liver cancer resection survival rate. *Chin Med J (Engl)* 1981; **94**: 749-754

29 **Walker AR,** Walker BF, Serobe W, Paterson A, Isaacson C, Segal I. Survival of blacks with liver cancer in Soweto, Johannesburg, South Africa. *Trop Gastroenterol* 1986; **7**: 169-172

30 **Zhou X,** Tang Z, Yu Y. Changing prognosis of primary liver cancer: some aspects to improve long-term survival. *Zhonghua Zhongliu Zazhi* 1996; **18**: 211-213

31 **Chen J,** Sankaranrayanan R, Li W. Population-based survival analysis of primary liver cancer in a high-incidence area-Qidong, China during 1972-1991. *Zhonghua Yufang Yixue Zazhi* 1997; **31**: 149-152

32 **Faivre J,** Forman D, Esteve J, Obradovic M, Sant M. Survival of patients with primary liver cancer, pancreatic cancer and biliary tract cancer in Europe. *Eur J Cancer* 1998; **34**: 2184-2190

33 **Wu M.** Clinical advances in primary liver cancer in China. *Hepatogastroenterology* 2001; **48**: 29-32

**Edited by** Zhang JZ

P.O.Box 2345, Beijing 100023,China
Fax: +86-10-85381893
E-mail: wjg@wjgnet.com www.wjgnet.com

World J Gastroenterol 2003;9(6):1216-1219
World Journal of Gastroenterology
Copyright ©2003 by The WJG Press ISSN 1007-9327

• LIVER CANCER •

# Loss of fragile histidine triad protein in human hepatocellular carcinoma

Po Zhao, Xin Song, Yuan-Yuan Nin, Ya-Li Lu, Xiang-Hong Li

**Po Zhao, Xin Song, Yuan-Yuan Nin, Ya-Li Lu, Xiang-Hong Li,** Department of Pathology, Chinese PLA General Hospital, Beijing 100853, China
**Correspondence to:** Dr. Po Zhao, Department of Pathology, Chinese PLA General Hospital, 28 Fuxing Road, Beijing 100853, Beijing China. zhaopo@plagh.com.cn
**Telephone:** +86-10-66937954
**Received:** 2002-12-22 **Accepted:** 2003-02-11

## Abstract

**AIM:** To investigate the expression of fragile histidine triad (FHIT) gene protein, Fhit, which is recently thought to be a candidate tumor suppressor. Abnormal expression of fragile histidine triad has been found in a variety of human cancers, but little is known about its expression in human hepatocellular carcinogenesis and evolution.

**METHODS:** Sections of 83 primary human hepatocellular carcionoma with corresponding para-neoplastic liver tissue and 10 normal liver tissue were evaluated immunohistochemically for Fhit protein expression.

**RESULTS:** All normal liver tissue and para-neoplastic liver tissue showed a strong expression of Fhit, whereas 50 of 83 (65.0 %) carcinomas showed a marked loss or absence of Fhit expression. The differences of Fhit expression between carcinoma and normal or para-neoplastic liver tissue were highly significant ($P$=0.000). The proportion of carcinomas with reduced Fhit expression showed an increasing trend (a) with decreasing differentiation or higher histological grade ($P$=0.219); (b) in tumors with higher clinical stage III and IV (91.3 %, $P$=0.000), compared with tumors with lower stage I and II (27.6 %); and (c) in cancers with bigger tumor size (>50 mm) (75.0 %, $P$=0.017), compared with smaller tumor size ($\leqslant$ 50 mm).

**CONCLUSION:** FHIT inactivation seems to be both an early and a later event, associated with carcinogenesis and progression to more aggressive hepatocellular carcinomas. Thus, evaluation of Fhit expression by immunohistochemistry in hepatocellular carcinoma may provide important diagnostic and prognostic information in clinical application.

Zhao P, Song X, Nin YY, Lu YL, Li XH. Loss of fragile histidine triad protein in human hepatocellular carcinoma. *World J Gastroenterol* 2003; 9(6): 1216-1219
http://www.wjgnet.com/1007-9327/9/1216.asp

## INTRODUCTION

Fragile histidine triad gene (FHIT) has been cloned and mapped to chromosomal region 3p14.2[1]. It spans the t(3:8)+(p14.2;q24) translocation breakpoint found in familial renal cell carcinoma and encompasses the most common human fragile site, FRA3B[2,3]. Alterations of FHIT and its expression have been found in primary tumors and cell lines of the lung[4,5], breast[6-8], head and neck[9], esophageal[10-12], stomach[13-15], colon and rectum[16-18], pancreas[19], kidney[20,21], cervix[22-25], and hepatocellular carcinomas[26-30]. Allelic deletion of FHIT and abnormal expression of FHIT protein (Fhit) in lung cancer are associated with smoking history and poor prognosis[31, 32]. The finding of decreased expression of Fhit in 93 % of precancerous lesions of the lung suggests that this gene may be used as a molecular marker for early diagnosis and prognosis of lung cancers[32]. However, there are only a few reports that evaluated FHIT in hepatocellular carcinoma in a small number of cases so far[30] and further investigation of Fhit protein expression during hepatocellular carcinogenesis is required. Liver cancer, like lung cancer, is thought to be induced by carcinogens such as major viral and environmental risk factors. Therefore, it is imperative to determine whether FHIT plays a role in the development of hepatocellular carcinoma which has been ranked the second in cancer mortality in China since 1990s and is increasing in the rate of its incidence among males in many countries. In this study, 10 normal liver tissues and 83 hepatocellular carcinomas with their corresponding para-neoplastic liver tissues were examined for Fhit expression by immunohistochemistry. It was found that the expression of Fhit was altered in a high proportion of hepatocellular carcinomas and the loss of Fhit expression was associated with more advanced stage of the tumor.

## MATERIALS AND METHODS

### *Specimens*

Paraffin embedded sections of 83 hepatocellular carcinomas with corresponding para-neoplastic tissues and 10 normal liver tissues as controls were obtained from the Department of Pathology, Chinese People's Liberation Army General Hospital. The patients included 71 men and 12 women with the mean age of 52±9.67 years (range 10-76 years). Of these patients, 15 were at grade I, 39 at grade II and 29 at grade III according to histological grading; and 4 were at stage I, 33 at stage II, 46 at stage III and 4 at stage IV according to clinical staging of UICC. In terms of size, 44 tumors were bigger than and 39 were equal to or smaller than 50 mm in diameter.

### *Immunohistochemical determination of Fhit*

All specimens were fixed in 10 % buffered formalin and embedded in paraffin. Paraffin blocks were sectioned into 4-μm thickness and the sections were mounted onto APES-coated glass slides. The slides were deparaffinized in xylene twice for 10 minutes, rehydrated through graded ethanol to distilled water, incubated for 30 minutes with 3 % hydrogen peroxidase-methanol to inhibit endogenous peroxidase activity, and heated in 0.01M citrate buffer (pH 6.0) in a microwave oven for 5 minutes at 100 ℃ for antigen retrieval. After cooled down at room temperature for 30 minutes, the slides were blocked for 15 minutes in PBS containing 10 % normal goat serum, incubated at 4 ℃ overnight in a humidified chamber with rabbit polyclonal antibody to human Fhit (Zymed Laboratories Inc., South San Francisco, CA) at 1:200 dilution in blocking solution. The sections were then rinsed in PBS and incubated

for 30 minutes with biotinylated secondary antibody (Histostain-SP, Zymed), rinsed again in PBS and incubated for 30 minutes in streptavidin-HRP (Histostain-SP, Zymed). 3, 3' -Diaminobenzidine was used as the chromogen. Slides were counterstained for 3 minutes with hematoxylin solution. Normal liver tissue was used as the positive control for each lesion, whereas the primary antibody was replaced by normal rabbit serum IgG with a similar dilution or PBS for the negative control.

### *Evaluation of score*

Both the extent and intensity of immunostaining were considered when scoring Fhit protein expression according to Hao *et al*[18]. The intensity of positive staining was scored as 0, negative; 1, weak; 2, moderate; 3, strong as in normal liver. The extent of positive staining was scored as 0, <5; 1, >5-25 %; 2, >25-50 %; 3, >50-75 %; 4, >75 % of the hepatocytes in the respective lesions. The final score was determined by multiplying the intensity score and the extent score, yielding a range from 0 to 12. Scores 9-12 were defined as preserved or strong staining (++), 5-8 as weak staining (+) and 0-4 as markedly reduced or negative expression (-).

### *Statistical analysis*

Fisher' s exact test (two sided) and Pearson Chi square' s test for trends in proportions were used to assess the associations between Fhit expression and pathological indices. A $P<0.05$ was considered statistically significant.

## RESULTS

### *Fhit expression in normal, para-neoplastic tissue and carcinoma*

Fhit was strongly expressed in the cytoplasm of hepatocytes in all 10 normal liver and 83 para-neoplastic tissues (Figure 1A). Some stromal cells, such as lymphocytes, plasma cells and macrophages, also expressed Fhit in both nucleus and cytoplasm. The expression of Fhit was strong in 33, weak in 21 and negative in 29 hepatocellular carcinomas (Table 1). The carcinomas with markedly reduced or loss of Fhit expression were observed in 50 (65.2 %) cases, whereas those with expression of Fhit equal to normal liver were observed in 33 (34.8 %) cases. In cases with reduced expression of Fhit, both the extent and intensity of Fhit staining were reduced markedly (Figure 1B).

**Table 1** Levels of Fhit expression in heptocellular carcinomas, para-neoplastic tissues and normal liver tissues

| | Fhit score | | | |
|---|---|---|---|---|
| | *n* | - | + | ++ |
| HCC | 83 | 29 | 21 | 33 |
| Para-neoplastic tissue[b] | 83 | 0 | 0 | 83 |
| Normal liver tissue[b] | 10 | 0 | 0 | 10 |

[b]$P=0.000$, *vs* hepatocellular carcinomas.

### *Relationship between Fhit expression and histological grade, clinical stage and tumor size*

The percentage of carcinomas with reduced expression of Fhit increased from 46.7 % (7 of 15) in well-differentiated cancers (grade I) to 53.8 % (21 of 39) in moderately differentiated cancers (grade II) and to 75.8 % (22 of 29) in poorly differentiated cancers (grade III), although this association of increased histological grade of tumors with decreased Fhit expression was not statistically significant ($P>0.05$, Table 2). Nevertheless, the decrease in expression of Fhit was significantly associated with more advanced clinical stage of the tumors. Whereas 21.6 % (8 of 37) stage I and II cases showed reduced expression of Fhit, the percentage of stage III and IV cases with reduced expression of Hhit increased to 91.3 % (42 of 46) ($P=0.000$, Table 2). In addition, the carcinomas with reduced expression of Fhit protein were found in 75 % (33 of 44) of tumors greater than 50 mm in diameter, compared with 43.6 % (17 of 39) of tumors 50 mm or smaller in diameter ($P=0.017$).

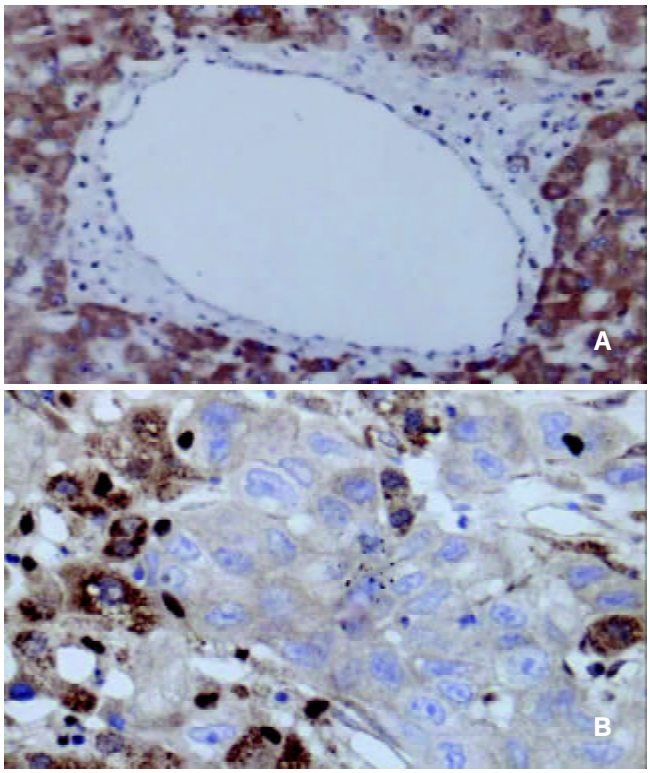


**Figure 1** (A) Strong positive staining of Fhit in normal liver tissue SP×100 (B) Negative staining of Fhit in invading hepatocellular carcinoma (upper right) compared with strong positive staining of Fhit in para-neoplastic liver tissue (lower left) (SP×400).

**Table 2** Relationship between Fhit expression and clinicopathological indice

| | Fhit score | | | |
|---|---|---|---|---|
| | *n* | - | + | ++ |
| Histological grade | | | | |
| Grade I | 15 | 3 | 4 | 8 |
| Grade II | 39 | 12 | 9 | 18 |
| Grade III | 29 | 14 | 8 | 7 |
| Clinical stage | | | | |
| Stage I-II | 37 | 4 | 4 | 29 |
| Stage III-IV | 46 | 25 | 17 | 4 |
| Size (mm) | | | | |
| ≤50 | 39 | 10 | 7 | 22 |
| >50 | 44 | 19 | 14 | 11 |

## DISCUSSION

Fhit protein is expressed in most types of normal human tissues but has been found to be frequently reduced or lost in a variety of human tumors due to alterations in its gene transcription or gene deletion[1]. It has thus been suggested that FHIT gene is a candidate tumor suppressor gene for multiple carcinomas. Fhit,

the FHIT gene protein, is a member of histidine triad family and the mechanism of its suppression on tumor cells remains obscure[1-3]. The following possible mechanisms have been considered as a tumor suppressor[33]: First, the tumor-suppressing function of Fhit might be to catabolize ApppA ($Ap_3A$) or related substrates. $Ap_3A$ is an analogue of ATP, which can provide phosphates as a substrate to raise the activity of protein kinase. Loss of Fhit protein may lead to the loss of $Ap_3A$ hydrolase activity and the resulting elevated levels of $Ap_3A$ or similar compounds may enhance the transductive signals of growth, thus contribute to carcinogenesis. Second, the activity of Fhit on mRNA cap analogs raises the possibility that failure of a decapping function might be tumorigenic, however, the properties of Fhit are quite different from those of enzymes known to decap mRNA, making this an unlikely mechanism. Third, the tumor-suppressing function of Fhit might be signaling by Fhit-substrate complexes or compounds as an active form of Fhit, which may be more important than its role of hydrolase. Fourth, Fhit might have a nucleotide-independent role as a tumor suppressor[33].

Yuan *et al*.[30] found that 4 of 9 cell lines and 5 of 10 primary hepatocellular carcinomas did not express Fhit protein or only expressed reduced levels of Fhit. Consistent with their results, we found that 50 of 83 (65.2 %) primary hepatocellular carcinomas showed markedly reduced or loss of expression of Fhit, suggesting that loss of Fhit protein might be related to the carcinogenesis of hepatocytes. Furthermore, decreasing expression of Fhit protein with higher histological grading, and more significantly with advanced clinical stages (stage III and IV) of primary tumors and bigger tumor size (>50 mm in diameter) suggests that loss of Fhit expression is strongly associated with the development and progression of hepatocellular carcinoma. Similar association between loss of FHIT function and the stage, grade and poor prognosis of tumors has been noted in lung cancer[4-5], colorectal carcinoma[18] and advanced breast cancer[8].

In summary, expression of Fhit is reduced or lost in a significant proportion of hepatocellular carcinomas and especially in more advanced stages of primary tumors. Thus, detection of Fhit protein expression by immunohistochemistry in hepatocellular lesions may provide important diagnostic and prognostic information in practical clinical application.

## REFERENCES


1 **Croce CM**, Sozzi G, Huebner K. Role of FHIT in human cancer. *J Clin Oncol* 1999; **17**: 1618-1624

2 **Huebner K**, Druck T, Siprashvili Z, Croce CM, Kovatich A, McCue PA. The role of deletions at the FRA3B/FHIT locus in carcinogenesis. *Recent Results Cancer Res* 1998; **154**: 200-215

3 **Druck T**, Berk L, Huebner K. FHITness and cancer. *Oncol Res* 1998; **10**: 341-345

4 **Fong KM**, Biesterveld EJ, Virmani A, Wistuba I, Sekido Y, Bader SA, Ahmadian M, Ong ST, Rassool FV, Zimmerman PV, Giaccone G, Gazdar AF, Minna JD. FHIT and FRA3B 3p14.2 allele loss are common in lung cancer and preneoplastic bronchial lesions and are associated with cancer-related FHIT cDNA splicing aberrations. *Cancer Res* 1997; **57**: 2256-2267

5 **Sozzi G**, Tornielli S, Tagliabue E, Sard L, Pezzella F, Pastorino U, Minoletti F, Pilotti S, Ratcliffe C, Veronese ML, Goldstraw P, Huebner K, Croce CM, Pierotti MA. Absence of Fhit protein in primary lung tumors and cell lines with FHIT gene abnormalities. *Cancer Res* 1997; **57**: 5207-5212

6 **Negrini M**, Monaco C, Vorechovsky I, Ohta M, Druck T, Baffa R, Huebner K, Croce CM. The FHIT gene at 3p14.2 is abnormal in breast carcinomas. *Cancer Res* 1996; **56**: 3173-3179

7 **Bieche I**, Latil A, Becette V, Lidereau R. Study of FHIT transcripts in normal and malignant breast tissue. *Genes Chromosomes Cancer* 1998; **23**: 292-299

8 **Campiglio M**, Pekarsky Y, Menard S, Tagliabue E, Pilotti S, Croce CM. FHIT loss of function in human primary breast cancer correlates with advanced stage of the disease. *Cancer Res* 1999; **59**: 3866-3869

9 **Virgilio L**, Shuster M, Gollin SM, Veronese ML, Ohta M, Huebner K, Croce CM. FHIT gene alterations in head and neck squamous cell carcinomas. *Proc Natl Acad Sci U S A* 1996; **93**: 9770-9775

10 **Zou TT**, Lei J, Shi YQ, Yin J, Wang S, Souza RF, Kong D, Shimada Y, Smolinski KN, Greenwald BD, Abraham JM, Harpaz N, Meltzer SJ. FHIT gene alterations in esophageal cancer and ulcerative colitis (UC). *Oncogene* 1997; **15**: 101-105

11 **Michael D**, Beer DG, Wilke CW, Miller DE, Glover TW. Frequent deletions of FHIT and FRA3B in Barrett's metaplasia and esophageal adenocarcinomas. *Oncogene* 1997; **15**: 1653-1659

12 **Menin C**, Santacatterina M, Zambon A, Montagna M, Parenti A, Ruol A, D'Andrea E. Anomalous transcripts and allelic deletions of the FHIT gene in human esophageal cancer. *Cancer Genet Cytogenet* 2000; **119**: 56-61

13 **Tamura G**, Sakata K, Nishizuka S, Maesawa C, Suzuki Y, Iwaya T, Terashima M, Saito K, Satodate R. Analysis of the fragile histidine triad gene in primary gastric carcinomas and gastric carcinoma cell lines. *Genes Chromosomes Cancer* 1997; **20**: 98-102

14 **Baffa R**, Veronese ML, Santoro R, Mandes B, Palazzo JP, Rugge M, Santoro E, Croce CM, Huebner K. Loss of FHIT expression in gastric carcinoma. *Cancer Res* 1998; **58**: 4708-4714

15 **Lee SH**, Kim WH, Kim HK, Woo KM, Nam HS, Kim HS, Kim JG, Cho MH. Altered expression of the fragile histidine triad gene in primary gastric adenocarcinomas. *Biochem Biophys Res Commun* 2001; **284**: 850-855

16 **Ohta M**, Inoue H, Cotticelli MG, Kastury K, Baffa R, Palazzo J, Siprashvili Z, Mori M, McCue P, Druck T. The FHIT gene, spanning the chromosome 3p14.2 fragile site and renal carcinoma-associated t (3;8) breakpoint, is abnormal in digestive tract cancers. *Cell* 1996; **84**: 587-597

17 **Thiagalingam S**, Lisitsyn NA, Hamaguchi M, Wigler MH, Willson JK, Markowitz SD, Leach FS, Kinzler KW, Vogelstein B. Evaluation of the FHIT gene in colorectal cancers. *Cancer Res* 1996; **56**: 2936-2939

18 **Hao XP**, Willis JE, Pretlow TG, Rao JS, MacLennan GT, Talbot IC, Pretlow TP. Loss of fragile histidine triad epression in colorectal carcinomas and premalignant lesions. *Cancer Res* 2000; **60**:18-21

19 **Sorio C**, Baron A, Orlandini S, Zamboni G, Pederzoli P, Huebner K, Scarpa A. The FHIT gene is expressed in pancreatic ductular cells and is altered in pancreatic cancers. *Cancer Res* 1999; **59**: 1308-1314

20 **Hadaczek P**, Siprashvili Z, Markiewski M, Domagala W, Druck T, McCue PA, Pekarsky Y, Ohta M, Huebner K, Lubinski J. Absence or reduction of Fhit expression in most clear cell renal carcinomas. *Cancer Res* 1998; **58**: 2946-2951

21 **Werner NS**, Siprashvili Z, Fong LY, Marquitan G, Schroder JK, Bardenheuer W, Seeber S, Huebner K, Schutte J, Opalka B. Differential susceptibility of renal carcinoma cell lines to tumor suppression by exogenous Fhit expression. *Cancer Res* 2000; **60**: 2780-2785

22 **Greenspan DL**, Connolly DC, Wu R, Lei RY, Vogelstein JT, Kim YT, Mok JE, Munoz N, Bosch FX, Shah K, Cho KR. Loss of FHIT expression in cervical carcinoma cell lines and primary tumors. *Cancer Res* 1997; **57**: 4692-4698

23 **Yoshino K**, Enomoto T, Nakamura T, Nakashima R, Wada H, Saitoh J, Noda K, Murata Y. Aberrant FHIT transcripts in squamous cell carcinoma of the uterine cervix. *Int J Cancer* 1998; **76**: 176-181

24 **Birrer MJ**, Hendricks D, Farley J, Sundborg MJ, Bonome T, Walts MJ, Geradts J. Abnormal Fhit expression in malignant and premalignant lesions of the cervix. *Cancer Res* 1999; **59**: 5270-5274

25 **Wu R**, Connolly DC, Dunn RL, Cho KR. Restored expression of fragile histidine triad protein and tumorigenicity of cervical carcinoma cells. *J Natl Cancer Inst* 2000; **92**: 338-344

26 **Chen YJ**, Chen PH, Chang JG. Aberrant FHIT transcripts in hepatocellular carcinomas. *Br J Cancer* 1998; **77**: 417-420

27 **Schlott T**, Ahrens K, Ruschenburg I, Reimer S, Hartmann H, Droese M. Different gene expression of MDM2, GAGE-1, -2 and FHIT in hepatocellular carcinoma and focal nodular hyperplasia. *Br J Cancer* 1999; **80**: 73-78

28 **Keck CL**, Zimonjic DB, Yuan BZ, Thorgeirsson SS, Popescu NC.

Nonrandom breakpoints of unbalanced chromosome translocations in human hepatocellular carcinoma cell lines. *Cancer Genet Cytogenet* 1999; **111**: 37-44

29 **Gramantieri L**, Chieco P, Di Tomaso M, Masi L, Piscaglia F, Brillanti S, Gaiani S, Valgimigli M, Mazziotti A, Bolondi L. Aberrant fragile histidine triad gene transcripts in primary hepatocellular carcinoma and liver cirrhosis. *Clin Cancer Res* 1999; **5**: 3468-3475

30 **Yuan BZ**, Keck-Waggoner C, Zimonjic DB, Thorgeirsson SS, Popescu NC. Alterations of the FHIT gene in human hepatocellular carcinoma. *Cancer Res* 2000; **60**: 1049-1053

31 **Burke L**, Khan MA, Freedman AN, Gemma A, Rusin M, Guinee DG, Bennett WP, Caporaso NE, Fleming MV, Travis WD, Colby TV, Trastek V, Pairolero PC, Tazelaar HD, Midthun DE, Liotta LA, Harris CC. Allelic deletion analysis of the FHIT gene predicts poor survival in non-small cell lung cancer. *Cancer Res* 1998; **58**: 2533-2536

32 **Sozzi G**, Pastorino U, Moiraghi L, Tagliabue E, Pezzella F, Ghirelli C, Tornielli S, Sard L, Huebner K, Pierotti MA, Croce CM, Pilotti S. Loss of FHIT function in lung cancer and preinvasive bronchial lesions. *Cancer Res* 1998; **58**: 5032-5037

33 **Pace HC**, Garrison PN, Robinson AK, Barnes LD, Draganescu A, Rosler A, Blackburn GM, Siprashvili Z, Croce CM, Huebner K, Brenner C. Genetic, biochemical, and crystallographic characterization of Fhit-substrate complexes as the active signaling form of Fhit. *Proc Natl Acad Sci U S A* 1998; **95**: 5484-5489

**Edited by** Liu HX

P.O.Box 2345, Beijing 100023,China
Fax: +86-10-85381893
E-mail: wjg@wjgnet.com www.wjgnet.com

World J Gastroenterol 2003;9(6):1220-1226
World Journal of Gastroenterology
Copyright ©2003 by The WJG Press ISSN 1007-9327

• LIVER CANCER •

# PPARg pathway activation results in apoptosis and COX-2 inhibition in HepG2 cells

Ming-Yi Li, Hua Deng, Jia-Ming Zhao, Dong Dai, Xiao-Yu Tan

**Ming-Yi Li, Dong Dai, Xiao-Yu Tan,** Department of General Surgery, Affiliated Hospital of Guangdong Medical College, Zhanjiang 524001, Guangdong Province, China
**Hua Deng,** Department of Biochemistry & Molecular Biology, Beijing Institute for Cancer Research, Da Hong-Luo Chang Street, Beijing 100034, China
**Jia-Ming Zhao**, Central Laboratory, Affiliated Hospital of Guangdong Medical College, Zhanjiang 524001,Guangdong Province, China
**Correspondence to:** Ming-Yi Li, Department of General Surgery, Affiliated Hospital of Guangdong Medical College, Zhanjiang 524001, Guangdong Province, China. zjmyli@sohu.com
**Telephone:** +86-759-2387613
**Received:** 2002-11-06 **Accepted:** 2003-01-28

## Abstract

**AIM:** To investigate whether troglitazone (TGZ), the peroxisome proliferator-activated receptor (PPAR) gamma ligand, can induce apoptosis and inhibit cell proliferation in human liver cancer cell line HepG2 and to explore the molecular mechanisms.

**METHODS:** [3-(4,5)-dimethylthiazol-2-yl]-2,5-diphenyl tetrazolium bromide (MTT), [$^3$H] Thymidine incorporation, Hochest33258 staining, DNA ladder, enzyme-linked immunosorbent assay (ELISA), RT-PCR, Northern and Western blotting analyses were employed to investigate the effect of TGZ on HepG2 cells and related molecular mechanisms.

**RESULTS:** TGZ was found to inhibit the growth of HepG2 cells and to induce apoptosis. During the process, the expression of COX-2 mRNA and protein and Bcl-2 protein was down-regulated, while that of Bax and Bak proteins was up-regulated, and the activity of caspase-3 was elevated. Furthermore, the level of $PGE_2$ was decreased transiently after 12 h of treatment with 30 μM troglitazone.

**CONCLUSION:** TGZ inhibits cell proliferation and induces apoptosis in HepG2 cells, which may be associated with the activation of caspase-3-like proteases, down-regulation of the expression of COX-2 mRNA and protein, Bcl-2 protein, the elevation of PGE2 levels, and up-regulation of the expressions of Bax and Bak proteins,

Li MY, Deng H, Zhao JM, Dai D, Tan XY. PPARγ pathway activation results in apoptosis and COX-2 inhibition in HepG2 cells. *World J Gastroenterol* 2003; 9(6): 1220-1226
http://www.wjgnet.com/1007-9327/9/1220.asp

## INTRODUCTION

Peroxisome proliferator-activated receptors (PPARs) are transcription factors belonging to the nuclear receptor gene family. PPARs bind to specific response elements as heterodimers with the retinoid X receptor and activate transcription in response to a variety of endogenous and exogenous ligands, including some polyunsaturated fatty acids, arachidonic acid metabolites, and some anti-diabetic drugs and non-steroidal anti-inflammatory drugs[1-6]. Recently, PPARs subfamily has been defined as PPARα, PPARβ and PPARγ. Three PPAR isoforms differ in their tissue distribution and ligand specificity. PPARα is predominantly expressed in tissues exhibiting high catabolic rate of fatty acids, whereas PPARβ expression is ubiquitous, and its physiological role is not clear. PPARγ is expressed predominantly in adipose tissue, the adrenal gland, spleen, large colon and the immune system. Several lines of evidence indicate that PPARγ plays an important role in regulating adipocyte differentiation and glucose homeostasis. Both PPARα and PPARγ have been shown to be involved in anti-inflammatory reactions mediated by arachidonic acid metabolites. PPARα binds to, and is activated by leukotriene B4, and its level is regulated at the transcriptional level by anti-flammatory glucocorticoids[7-15]. PPARγ is activated by prostaglandin $D_2$ metabolite 15-deoxy-Ä[12, 14] prostaglandin $J_2$ (15 d-$PGJ_2$) and synthetic anti-diabetic thiazolidinedione drugs, resulting in down-regulation of the expression of pro-inflammatory genes and inhibition of tumor cell growth[16,17].

Cyclooyxgenase (COX) is a rate-limiting enzyme, catalyzing the initial step in biosynthesis of prostaglandins (PGs) from arachidonic acid[18,19]. COX is encoded by two separate genes, COX-1 and COX-2, both of which participate in formation of a variety of eicosanoids including $PGD_2$, $PGE_2$, $PGI_2$, $PGF_{2\alpha}$, and thromboxane A. COX-1 is expressed constitutionally in most tissues and has been proposed to be a house-keeping gene, which is involved in cytoprotection of gastric mucosa, vasodilation in kidney, and control of platelet aggregation. In contrast, COX-2 is an inducible immediate-early gene that is upregulated by various stimuli including mitogens, cytokines, growth factors, and tumor promoters. Previous studies have demonstrated that COX-2 expression is aberrantly increased in (various) human epithelial cancers in colorectum, esophagus, stomach, lung, and bladder[20-39]. These findings suggest that up-regulation of COX-2 may be a common mechanism in epithelial carcinogenesis. Recently, PPARγ ligands was found to suppress COX-2 expression in fetal hepatocytes[40] and in macrophage-like differentiated U937 cells[41]. However, other authors reported that 15d-$PGJ_2$ induced the expression of COX-2 in immortalized epithelial[42] and colorectal cancer cells[43]. The mechanisms for the different regulation of COX-2 expression by PPARγ ligands remain to be elucidated. In the present study, we wanted to investigate the effect of PPARγ activation on cell growth and apoptosis, and to investigate underlying mechanism in regard to the expression of COX-2 and Bcl-2 members in HepG2 cells.

## MATERIALS AND METHODS

### *Cell culture*

Human liver cancer cell line HepG2 was provided by the American Type Culture Collection. Cells were grown in RPMI-1640 medium supplemented with 15 % new born bovine serum, penicillin G (100 kU· $L^{-1}$) and kanamycin (0.1g/L) at 37 ℃ in

the 5 % $CO_2$ incubator. Cells were grown on 96-well plates for MTT assay, [$^3$H] thymidine incorporation and DNA fragmentation enzyme-linked immunosorbent assay (ELISA). For the experiment, cells were grown in fresh serum-free medium, incubated for 6 hours, and treated with experimental reagents.

### MTT cell viability assay

Cell growth was assessed by a modified MTT assay. About $2\times10^5$ cells/well were plated in 96-well microtiter plates and incubated overnight. Cells were then treated with troglitazone for 48 h in various concentrations. Then 10 μl stock MTT (0.5 g/L) was added to each well, and the cells were further incubated at 37 ℃ for 4 h. After supernatant was removed, 100 μl of 0.04 M HCl in isopropanol was added to each well to solubilize the formazan products. The absorbance at the wavelength of 570 nm was measured by a micro-ELISA reader. The negative control well contained medium only. The ratios of the absorbance of treated cells relative to those of the control wells were calculated and expressed as percentage of growth inhibition.

### [$^3$H] thymidine incorporation

Cells were planted in 96-well plates and grown for 24 h after being starved by growing in the serum-free medium for 48 h. Then, they were treated with troglitazone for 48 h and labeled with 5 μCi of [$^3$H] thymidine for 4 h. Radioactivity was detected using a Beckman L5 counter, after the reaction was washed and stopped with 5 % trichloro acetic acid and the cells solubilized in 0.5 % of 0.25 N sodium hydroxide. Each experiment was done in quadruplicates and repeated at least three times.

### Hoechst 33258 staining

Cells were fixed with 4 % formaldehyde in phosphate-buffered saline (PBS) for 10 min, stained by Hoechst 33258 (10 mg/L) for 1 hour, and subjected to fluorescence microscopy. After treatment with troglitazone, morphologic changes, including reduction in cell size and nuclear chromatin condensation, were observed.

### DNA ladder demonstration

After induction of apoptosis, cells ($7\times10^6$/sample, both attached and detached cells) were lyzed with 150 μl hypotonic lysis buffer (edetic acid 10 mM, 0.5 % Triton X-100, Tris-HCl, pH7. 4) for 15 min on ice and were precipitated with 2.5 % polyethylene glycol and 1 M NaCl for 15 min at 4 ℃. After centrifugation at 16 000×g for 10 min at room temperature, the supernatant was treated with proteinase K (0.3 g/L) at 37 ℃ for 1 h and precipitated with isopropanol at -20 ℃. After centrifugation, each pellet was dissolved in 10 μl of Tris-EDTA (pH 7.6) and electrophoresed on a 1.5 % agarose gel containing ethidium bromide. DNA ladder pattern was identified under ultraviolet light.

### Detection of DNA fragmentation

HepG2 cells were grown in 96-well plates. The cells were incubated with various dose of troglitazone for 48 h. DNA fragmentation was detected using an enzyme-linked immunosorbent assay (ELISA) kit (Roche). This assay was based on a quantitative sandwich enzyme-immunoassay directed against cytoplasmic histone-associated DNA fragments. Briefly, the cells were incubated in 200 μl of lysis buffer. After centrifugation, 20 μl of the supernatant was reacted overnight at 4 ℃ in streptavidin-coated wells with 80 μl of biotinylated anti-histone antibody and peroxidase-conjugated anti-DNA antibody. After washing, the immunocomplex-bound peroxidase was probed with 2,2' -azino-di[3-ethylbenzthiazoline sulfonate] for spectrophotometric detection at 405 nm.

### TUENL reaction

TUNEL reaction was done using apoptosis detection system (Cayman). Cells were fixed overnight at 4 ℃ with 4 % paraformaldehyde in PBS. The samples were washed three times with PBS and permeabilized by 0.2 % Triton X-100 in PBS for 15 min on ice. After washed twice, cells were equilibrated at room temperature for 15 to 30 min in equilibration buffer (potassium cacodylate 200 mM, dithiothreitol 0.2 mM, bovine serum albumin 0.25 g/L, and cobalt chloride 2.5 mM in 25 mM Tris-HCl, pH 6.6), and then incubated in a solution containing 5 μM pluorescein-12-dUTP, 10 μM dATP, 100 μM edetic acid, and terminal deoxynucleotidyl transferase at 37 ℃ for 1.5 h in a dark chamber. The tailing reaction was terminated by 2×standard saline citrate (SSC). The samples were washed three times with PBS and analyzed by fluorescence microscopy. At least 1000 cells were counted, and the percentage of TUNEL-positive cells was determined.

### RNA isolation and northern blotting

After incubation with different doses of troglitazone for 6 h, cells were washed with RPMI. Total RNA was extrcted from adherent cells using Rneasy Mini kits (Sigma) as described previously[37]. 30 mg of total RNA from each sample was separated on agarose/formaldehyde gels and transferred to nylon membranes. The membrane was hybridized with probes for COX-2 and for GAPDH as a reference.

### RT-PCR for COX-2

Total RNA was extracted from cells using TRIzol™ (Sigma). COX-2 and beta-actin mRNA were detected by polymerase-chain-reaction following reverse transcription- (RT-PCR) as described[37]. Primers for beta-actin were: sense 5' -ATCT-GGCACCACACCTTCTACAATGAGCTGCG-3' , antisense 5' -CGTCATACTCCTGCTTGCTGATCCACATCTGC-3' .

### Western blotting analysis

The cells were lysed in a lysis buffer (hepes 25 mM, Triton X-100 1.5 %, sodium deoxycholate 1 %, SDS 0.1 %, NaCl 0.5 M, edetic acid 5 mM, NaF 50 mM, sodium vanadate 0.1 mM, phenylmethylsulfonyl fluoride (PMSF) 1 mM and leupeptin 0.1 g/L, pH7.8) at 4 ℃ with sonication. The lysates were centrifuged at 15 000 g for 15 min and the concentration of the protein in each lysate was determined with Coomassie brilliant blue G-250. Loading buffer (42 mM Tris-HCl, containing 10 % glycerol, 2.3 % SDS, 5 % 2-mercaptoethanol and 0.002 % bromophenol blue) was then added to each lysate, which was subsequently boiled for 3 min and then electrophoresed on a SDS-polyacrylamide gel. Proteins were transferred onto a nitrocellulose filter and incubated separately with the antibodies against Bcl-2, Bax, Bak, Bcl-$x_L$ and COX-2, and then labeled with peroxidase-conjugated secondary antibodies. The reactions were visualized using the enhanced chemiluminescence reagent (Sigma). The results were approved by repeating the reactions 2 times.

### Evaluation of PGE2 production

To determine the levels of PGE2, HepG2 cells were treated with different concentrations of troglitazone for 24 h. The quantity of PGE2 in supernatants was immediately determined with the PGE2 Enzyme Immunoassay kit (Caymen Chemical) according to the manufacturer' s instructions. Data were recorded using a Dynatech MR50000 microplate reader and normalized to micrograms of protein.

### *Assessment of caspase-3 activity*

Caspase-3 activity was evaluated using a caspase assay kit following instructions of the manufacturer. In brief, caspase-3 fluorogenic substrate (Ac-DEVD-AMC or Ac-IETD-AMC) was incubated with JTE522-treated cell for 1 h at 37 ℃, then AMC released from Ac-DEVD-AMC or Ac-IETD-AMC was detected using a fluorometric plate reader with an excitation wavelength of 380nm and an emission wavelength of 420-460nm.

### *Statistical analysis*

Data were presented as the mean ± standard error, unless otherwise indicated. Multiple comparisons were examined for significant differences using analysis of variance, followed by individual comparisons with the Bonferroni post-test. Comparisons between two groups were made with the Student *t* test. $P<0.05$ was considered significant.

## RESULTS

### *Effects of PPARg activation on cell proliferation and cell viability*

HepG2 cells were incubated with various does of troglitazone for 48 h. MTT assay showed that troglitazone significantly inhibited cell viability. The inhibition was dependent on dose of troglitazone administered (Figure 1A). Application of troglitazone also resulted in a reduction of [$^3$H] thymidine uptake in a dose-dependent manner (Figure 1B).

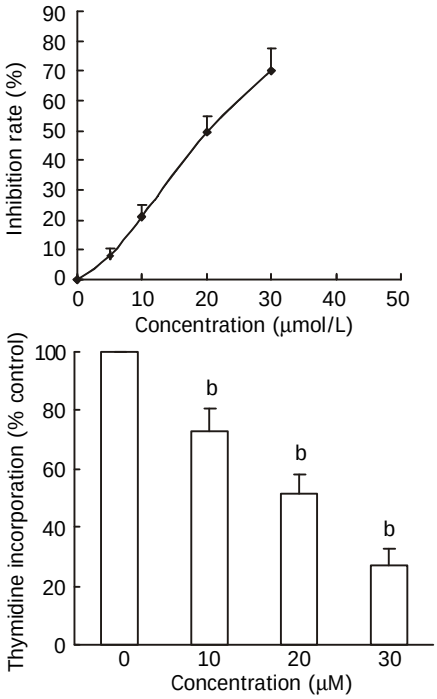


**Figure 1** Effect of TGZ on growth of HepG2 cells. HepG2 cells were incubated with various concentrations of TGZ for 48 h: (A) MTT assay; (B) [$^3$H] thymidine uptake assay. The value was represented as mean ±SEM ($n$=3). $^bP<0.01$ versus corresponding control group.

### *Influence of PPARg activation on apoptosis*

Effect of PPARγ activation on apoptosis was assessed by staining with Hoechst 33258, TUNEL reaction, DNAfragmentation demonstration on an agarose gel and by ELISA. The initiating effect of PPARγ activation on apoptosis was confirmed in HepG2 cell, the morphologic changes included reduction in cell size and nuclear chromation condensation visualized by Hoechst 33258 staining. The apoptotic index was also increased by treatment with different concentration of troglitazone from 3.2±1.2 % to 53±2.6 %. Agarose gel electrophoresis showed DNA ladder pattern in the exposed HepG2 cells (Figure 2). The PPARγ pathway-induced apoptosis was further demonstrated in quantitative measurement of cytoplasmic histone-associated DNA fragment by ELISA. As shown in Figure 3, troglitazone induced significant increase in DNA fragmentation in a dose-dependent manner.

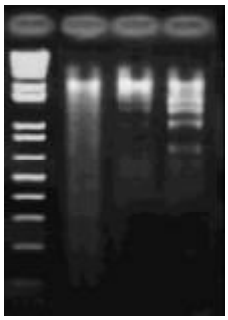

**Figure 2** DNA ladder pattern formation in HepG2 cells after treatment with TGZ. Cells were treated with TGZ for 48 h and the formation of oligonucleosomal fragments was determined by 1.5 % agarose gel electrophoresis: M) DNA markers; 1) control; 2) 10 μM TGZ; 3) 30 μM TGZ.

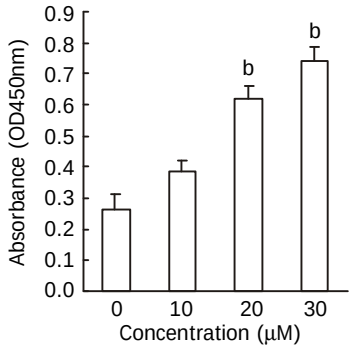


**Figure 3** DNA fragmentation by ELISA assay, as measured by absorbance (OD 450 values). HepG2 cells cultured for 48 h in the presence of TGZ resulted in dose dependent DNA fragmentation. $^aP<0.05$, $^bP<0.01$ compared to respective control.

### *Down-regulation of COX-2 associated with the PPARg activation*

The fact that the COX-2 promoter contains a PPRE indicates that COX-2 might be one of the downstream targets of the PPARγ pathway. In the present study, COX-2 expression was observed in HepG2 cells treated with vehicle or 30 μM troglitazone. After 6, 12, 24 and 48 h of the treatment, cells were harvested. COX-2 mRNA was analysed by RT-PCR (4A) and Northern blotting (4B), and its translation product was demonstrated by Western blotting (4C). As shown in Figure 4, no significant change was detected during the first 6 h of treatment when compared with the control. After treatment with 30 μM troglitazone for 12 h, the expression of COX-2 was inhibited.

### *Effects of PPARg activation on expression levels of Bcl-2, Bcl-$x_L$, Bax and Bak*

To further elucidate the mechanisms of troglitazone-induced apoptosis in HepG2 cells, we assessed the involvement of bcl-2 family proteins in the process by Western blotting. Expression of Bax protein was up-regulated 6 h after 20 μM troglitazone treatment and remained elevated to 24 h. Expression level of Bak protein was also elevated 12 h after the treatment with 30 μM troglitazone and declined at 48 h. On the controry, Bcl-2

protein expression was down-regulated at 6 h and undetectable at 24 h. No significant change was observed in the expression of bcl-$x_L$ protein (Figure 5).

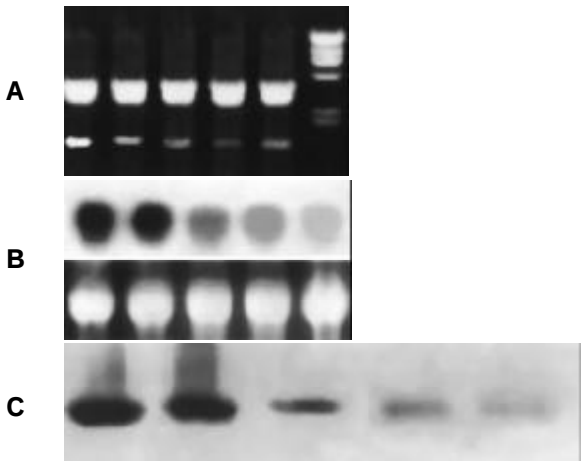


**Figure 4** Effect of TGZ on the expression of COX-2 mRNA and protein in human liver cancer cell line HepG2 cells: (A) RT-PCR; (B) Northern blot; (C): Western blot.

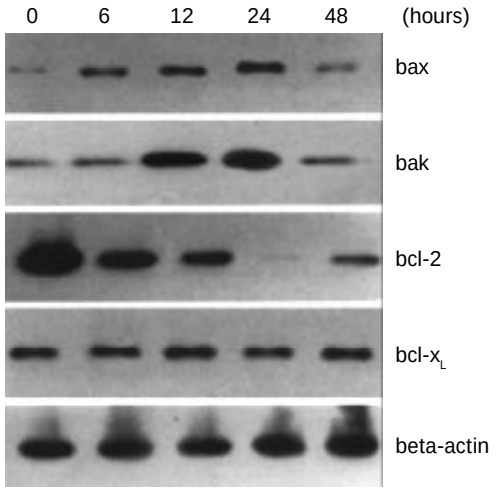


**Figure 5** Effects of TGZ on the levels of bcl-2, bcl-$x_L$, bax and bak proteins in HepG2 cells at indicated time.

### *Effects of PPARg activation on $PGE_2$ production*

The levels of $PGE_2$ in vehicle controls were always high throughout the culture. When HepG2 cells were treated with 30 μM troglitazone, $PGE_2$ concentration decreased transiently at 12 h (Figure 6).

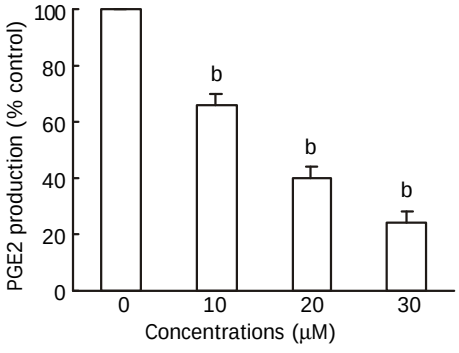


**Figure 6** Effect of TGZ on the production of PGE2. The value was represented as mean ±SEM ($n$=3). $^bP$<0.01 compared to respective control.

### *Change in caspase-3 activity associated with PPARg activation*

In consideration of frequent involvement of caspaes activation in apoptosis, caspase-3 activity was assessed in HepG2 cell, treated with 20 μM troglitazone. As shown in Figure 7, the caspase-3 activity increased with the treatment, the reaction was time-dependent.

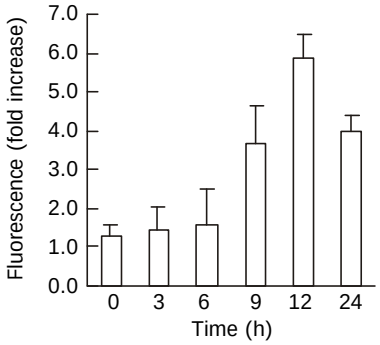


**Figure 7** Effect of TGZ on the activity of caspase-3. The value was represented as mean ± SEM ($n$=3).

## DISCUSSION

Potent effects of PPARγ on cell proliferation and cell cycling have been described. PPARγ ligands can trigger cell cycle arrest in NIH3T3 cells and HIB-1B cells[44]. PPARγ ligands can also induce terminal differentiation and withdrawal of human liposarcoma cells from the cell cycle[45]. Importantly, PPARγ ligands have been found to slow down the progression of advanced liposarcoma in humans[46]. Given the expression of PPARγ in nonadipose tissues, the effect of PPARγ on human breast cancer, gastric cancer, prostate cancer, colon cancer and transtitional cell, bladder cancer have been explored. Treatment of cultured breast cancer cells with troglitazone results in cell growth arrest and promotes differentiation[47]. Troglitazone has also been shown to inhibit tumor growth and induce apoptosis in human breast cancer cells *in vitro* and in BNX mice. Moreover, another PPARγ ligand, GW7845, has been shown to decrease tumor incidence, tumor growth and tumor burden I, the NMU induced mammary carcinoma[48]. These data suggest that PPARγ ligands may be used as novel, nontoxic and selective chemotherapeutic agents for human breast cancers. In the present study, our results have shown that activation of PPARγ by troglitazone inhibits cell growth and induces apoptosis in human liver cancer HepG2 cells. We confirmed that the induction of apoptosis was mediated through down-regulation of COX-2 and Bcl-2 expression, and up-regulation of Bax and Bak expression. The down-regulation of COX-2 was coincident with down-regulation of the production of $PGE_2$. The activity of Caspase-3 was increased after treatment with 30 μM PPARγ ligand troglitazone in a time-dependent manner.

Meade *et al.* have demonstrated that COX-2 expression is enhanced by peroxisome proliferators, including some fatty acids, PGs and NSAIDs, as well as the prototypical peroxisome proliferator WY-14, 643, in mammary and colonic epithelial cells, presumably through PPARα[49]. Yang *et al.* showed that activation of PPAR pathway by ciglitazone induced apoptosis and inhibition of COX-2 expression in human colon cancer cells HT-29[50], but the result was not approved in an observation by Lefebvre *et al*[51]. Our data showed that PPARγ activation inhibited the expression of COX-2. The discrepancy may be caused by different cell types used in these groups.

Overexpression of COX-2 plays important roles in cell adhesion, apoptosis and angiogenesis. Numerous epidemiological studies suggest that use of nonsteroidal anti-inflammatory drugs

(NSAIDs) decreases the incidence of gastrointestinal cancers and COX-2 is recognized as a major target of NSAIDs[52-64]. Inhibition of COX-2 by NSAIDs or COX-2 specific inhibitors causes cell death in cancer cells, indicating that COX-2 may be used as an important molecular target for prevention and therapy in gastrointestinal cancers[65-70]. The mechanism of COX-2 expression remains unclear. Subbaramaiah and colleagues have shown that PPARγ can inhibit COX-2 expression.

In the present study, the levels of $PGE_2$ were decreased in a time-dependent manner after the treatment with 30 μM troglitazone, and were correlated with the change in COX-2 expression. This is in agreement with previous observations in other cell lines[71-73]. Thus, excessively synthesized $PGE_2$ mediated by overexpression of COX-2 is believed to play an important role in neoplasma formation. Inhibition of COX-2 activity may at least partly explain the chemopreventative effect of activated PPAR pathway in human liver cancer.

Apoptosis is characterized by a series of distinct morphological and biochemical changes. Several apoptosis-related genes have been found. One group of apoptosis regulatory genes is the Bcl-2 family[74-79]. Of these genes, Bcl-2, Bcl-$x_L$ are antiapoptotic, whereas Bax, Bcl-$x_s$, Bak, Bad and Bik are proapoptotic. In this study, overexpression of Bax and Bak, and suppression of the expression of Bcl-2 were found during the apoptosis induced by PPARγ activation. These data confirm the role of these proteins in troglitazone-induced apoptosis in HepG2 cells. In addition, the activity of caspase-3 was also found to be elevated during the apoptotic process induced by PPARγ activation.

In summary, we have shown that activation of PPARγ by troglitazone induces apoptosis in HepG2 cells through down-regulation of the expression of COX-2 and bcl-2, up-regulation of bax and bak, and activation of caspase-3. Consistent with other potential chemopreventive agents in human liver cancer model, we believe that COX-2, bak, bax, bcl-2 and caspase-3 play some roles in the process of PPARγ activation-induced apoptosis. These serve as potential targets for future drugs or therapies for prevention and treatment of liver cancer.

## REFERENCES


1 **Evans RM**. The steroid and thyroid hormone receptor superfamily. *Science* 1988; **240**: 889-895
2 **Spiegelman BM**. PPAR gamma: adipogenic regulator and thiazolidinedione receptor. *Diabetes* 1998; **47**: 507-514
3 **Blumberg B**, Evans RM. Orphan unclear receptors-new ligands and new possibilities. *Genes Dev* 1998; **12**: 3149-3155
4 **Desvergne B**, Wahli W. Peroxisome proliferator-activated receptors: nuclear control of metabolism. *Endocr Rev* 1999; **20**: 649-688
5 **Murao K**, Ohyama T, Imachi H, Ishida T, Cao WM, Takahara J. Ealpha stimulation of MCP-1 expression is mediated by the Akt/PKB signal transduction pathway in vascular endothelial cells. *Biochem Biophys Res Commun* 2000; **276**: 791-796
6 **Willson TM**, Brown PJ, Sternbach DD, Henke BR. The PPARs: from orphan receptors to drug discovery. *J Med Chem* 2000; **43**: 527-550
7 **Wu GD**. Nuclear receptor to prevent colon cancer. *N Engl J Med* 2000; **342**: 651-653
8 **Zhu Y**, Qi C, Korenberg JR. Structural organization of mouse peroxisome proliferatior-activated receptor γ (mRNAγ) gene: alternative promoter use and different splicing yield two mPPARγ isoforms. *Pro Natl Acad Sci USA* 1995; **92**: 7921-7925
9 **Fajas L**, Fruchart JC, Auwerx J. PPARγ mRNA: A distinct PPARγ mRNA subtype transcribed from an independent promoter. *FEBS Lett* 1998; **438**: 55-60
10 **Fajas L**, Auboeuf D, Raspe E. The organization, promoter analysis, and expression of the human PPARγ gene. *J Biol Chem* 1997; **272**: 18779-18789
11 **Escher P**, Wahli W. Peroxisome proliferator-activated receptors: Insight into mutiple cellular functions. *Mut Res* 2000; **448**: 121-138
12 **Shao D**, Rangwala SM, Bailey ST. Interdomain communication regulating ligand binding by PPAR. *Nature* 1998; **396**: 377-380
13 **Moras D**, Gronemeyer H. The nuclear receptor ligand-binding domain: Structure and function. *Curr Opin Cell Biol* 1998; **3**: 384-391
14 **Leibowitz MD**, Fievet C, Hennuyer N. Activation of PPARdelta alters lipid metabolism in db/db mice. *FEBS Lett* 2000; **473**: 333-336
15 **Liang YC**, Tsai SH, Tsai DC, Lin-Shiau SY, Lin JK. Suppression of inducible cyclooxygenase and nitric oxide synthase through activation of Peroxisome proliferator-activated receptorγ by flavonoids in mouse macrophages. *FEBS Lett* 2001; **496**: 12-18
16 **Kubuta T**, Koshizuka K, Williamson EA. Ligand for Peroxisome proliferator-activated receptorã has potent antitumor effect against human prostate cancer both *in vitro* and *in vivo*. *Cancer Res* 1998; **58**: 3344-3352
17 **Takahashi N**, Okumaura T, Motomura W. Activation of PPARgamma inhibits cell growth and induces apoptosis in human gastric cancer cells. *FEBS Lett* 1999; **455**: 135-139
18 **Dubois RN**, Abramson SB, Crofford L. Cyclooxygenase in biology and disease. *FASEB J* 1993; **12**: 1063-1073
19 **Herschman HR**. Prostaglandin synthase 2. *Biochem Bioph Acta* 1996; **1299**: 125-140
20 **Eberhart CE**, Coffey RJ, Radhika A. Up-regulation of cyclooxygenase-2 during sporadic colorectal carcinogenesis. *J Pathol* 1999; **187**: 295-301
21 **Ristimaki A**, Honkonen N, Jankala H. Expression of cyclooxygenase-2 in human gastric carcinoma. *Cancer Res* 1998; **58**: 2929-2934
22 **Mahammed SI**, Knapp DW, Bostwick DG. Expression of cyclooxygenase-2 in human invasive transitional cell carcinoma of the urinary bladder. *Cancer Res* 1999; **59**: 5647-5650
23 **Yang ZY**, Rorison KA. Cyclooxygenase-2-selective antagonists do not inhibit growth of colorectal carcinoma cell lines. *Cancer Letters* 1998; **122**: 25-30
24 **Kusuhara H**, Komatsu H, Sugahara K. Reactive oxygen species are involved in the apoptosis induced by NSAIDs in cultured gastric cells. *Eur J Pharmacol* 1999; **383**: 331-337
25 **Tanaka K**, Pracyk JB, Takeda K, Yu ZX, Finkel T. Expression of IdI results in apoptosis of cardiac myocytes through a redox-dependent mechanism. *J Biol Chem* 1998; **273**: 25922-25828
26 **Kim YB**, Kim GE, Cho NH, Pyo HR, Shim SJ, Chang SK, Park HC, Suh CO, Park TK, Kim BS. Overexpression of cyclooxygenase-2 is associated with a poor prognosis in patients with squamous cell carcinoma of the uterine cervix treated with radiation and concurrent chemotherapy. *Cancer* 2002; **95**: 531-539
27 **Ferrandina G**, Legge F, Ranelletti FO, Zannoni GF, Maggiano N, Evangelisti A, Mancuso S, Scambia G, Lauriola L. Cyclooxygenase-2 expression in endometrial carcinoma. *Cancer* 2002; **95**: 801-807
28 **Tang X**, Sun YJ, Half E, Kuo MT, Sinicrope F. Cyclooxygenase-2 overexpression inhibits death receptor 5 expression and confers resistance to tumor necrosis factor-related apoptosis-inducing ligand-induced apoptosis in human colon cancer cells. *Cancer Res* 2002; **62**: 4903-4908
29 **Staats P**. Pain Management and beyond. evolving concepts and treatments involving cyclooxygenase inhibition. *J Pain Symptom Manage* 2002; **24**: S4
30 **Lin DT**, Subbaramaiah K, Shah JP, Dannenberg AJ, Boyle JO. Cyclooxygenase-2: A novel molecular target for the prevention and treatment of head and neck cancer. *Head Neck* 2002; **24**: 792-799
31 **Jiang XH**, Lam SK, Lin MC, Jiang SH, Kung HF, Slosberg ED, Soh JW, Weinstein IB, Wong BC. Novel target for induction of apoptosis by cyclo-oxygenase-2 inhibitor SC-236 through a protein kinase C-beta(1)-dependent pathway. *Oncogene* 2002; **21**: 6113-6122
32 **He Q**, Luo X, Huang Y, Sheikh MS. Apo2L/TRAIL differentially modulates the apoptotic effects of sulindac and a COX-2 selective non-steroidal anti-inflammatory agent in Bax-deficient cells. *Oncogene* 2002; **21**: 6032-6040

33 **Kirkpatrick K**, Ogunkolade W, Elkak A, Bustin S, Jenkins P, Ghilchik M, Mokbel K. The mRNA expression of cyclo-oxygenase-2 (COX-2) and vascular endothelial growth factor (VEGF) in human breast cancer. *Curr Med Res Opin* 2002; **18:** 237-241

34 **Tapiero H**, Ba GN, Couvreur P, Tew KD. Polyunsaturated fatty acids (PUFA) and eicosanoids in human health and pathologies. *Biomed Pharmacother* 2002; **56**: 215-222

35 **Badawi AF**, Habib SL, Mohammed MA, Abadi AA, Michael MS. Influence of cigarette smoking on prostaglandin synthesis and cyclooxygenase-2 gene expression in human urinary bladder cancer. *Cancer Invest* 2002; **20**: 651-656

36 **Gallo O**, Masini E, Bianchi B, Bruschini L, Paglierani M, Franchi A. Prognostic significance of cyclooxygenase-2 pathway and angiogenesis in head and neck squamous cell carcinoma. *Hum Pathol* 2002; **33**: 708-714

37 **Li HL**, Zhang HW, Chen DD, Zhong L, Ren XD, Si-Tu R. JTE-522, a selective COX-2 inhibitor, inhibits cell proliferation and induces apoptosis in RL95-2 cells. *Acta Pharmacol Sin* 2002; **23**: 631-637

38 **Li HL**, Chen DD, Li XH, Zhang HW, Lu YQ, Ye CL, Ren XD. Changes of NF-kB, p53, Bcl-2 and caspase in apoptosis induced by JTE-522 in human gastric adenocarcinoma cell line AGS cells: role of reactive oxygen species. *World J Gastroenterol* 2002; **8**: 431-435

39 **Li HL**, Chen DD, Li XH, Zhang HW, Lu JH, Ren XD, Wang CC. JTE-522-induced apoptosis in human gastric adenocarcinoma cell line AGS cells by caspase activation accompanying cytochrome C release, membrane translocation of Bax and loss of mitochondrial membrane potential. *World J Gastroenterol* 2002; **8**: 217-223

40 **Callejas NA**, Castrillo A, Bosca L, Martin-Sanz P. *J Pharmacol Exp Ther* 1999; **288**: 1235-1241

41 **Inoue H**, Tanabe T, Umeson K. Feedback control of cyclooxygenase-2 expression through PPARã. *J Biol Chem* 2000; **275**: 28028-28032

42 **Meadc EA**, Mclntyre M, Zimmerman GA, Prescott SM. *J Biol Chem* 1999; **274**: 8328-8334

43 **Chinery R,** Coffey RJ, Graves-Deal R, Kirkland SC, Sanchez SC, Morrow JD. Prostaglandin J2 and 15-deoxy-delta12,14-prostaglandin J2 induce proliferation of cyclooxygenase-depleted colorectal cancer cells. *Cancer Res* 1999; **59**: 2739-2746

44 **Altiok S**, Xu M, Spiegelman BM. PPARγ induces cell cycle withdrawal: inhibition of E2F/DP DNA-binding activity via down-regulation of PP2A. *Genes & Dev* 1997; **11**: 1987-1998

45 **Tontonoz P,** Singer S, Forman BM. Terminal differentiation of human liposarcoma cell induced by ligands for peroxisome proliferator-activated receptorγ and the retinoid X receptor. *Prol Natl Acad USA* 1997; **94**: 237-241

46 **Demetri GD**, Fletcher CD, Mueller E. Induction of solid tumor differentiation by the peroxisome proliferator-activated receptor-gamma ligand trogliatzone in patients with liposarcoma. *Prol Natl Acad USA* 1999; **96**: 3951-3956

47 **Mueller E**, Sarraf P, Tontonoz P. Terminal differentiation of human breast cancer through PPARγ. *Mol Cell* 1998; **1**: 465-470

48 **Suh N**, Wang Y, Williams CR. A new ligand for the peroxisome proliferator-activated receptor-gamma, GW7845, inhibits rat mammary carcinogenesis. *Cancer Res* 1999; **59**: 5671-5673

49 **He TC**, Chan TA, Vogelstein B, Kinzler KW. PPARδ is a APC-regulated target of nonsteroidal anti-inflammatory drugs. *Cell* 1999; **99**: 335-345

50 **Yang LW**, Frucht H. Activation of the PPAR pathway induces apoptosis and COX-2 inhibition in HT-29 human colon cancer cells. *Carcinogenesis* 2001; **22**: 1379-1383

51 **Lefebvre AM**, Chen I, Desreuaux P, Najib I, Auwerx J. Activation of peroxisome proliferator-activated receptor gamma promotes the development of colon tumors in C57BL/6J-APC$^{Min}$/+ mice. *Nature Med* 1998; **4**: 1053-1057

52 **Lednicer D**. Tracing the Origins of COX-2 Inhibitors' Structures. *Curr Med Chem* 2002; **9**: 1457-1461

53 **Kawabe A**, Shimada Y, Uchida S, Maeda M, Yamasaki S, Kato M, Hashimoto Y, Ohshio G, Matsumoto M, Imamura M. Expression of cyclooxygenase-2 in primary and remnant gastric carcinoma: comparing it with p53 accumulation, *Helicobacter pylori* infection, and vascular endothelial growth factor expression. *J Surg Oncol* 2002; **80**: 79-88

54 **Kong G**, Kim EK, Kim WS, Lee KT, Lee YW, Lee JK, Paik SW, Rhee JC. Role of cyclooxygenase-2 and inducible nitric oxide synthase in pancreatic cancer. *J Gastroenterol Hepato* 2002; **17**: 914-921

55 **Liu CM**, Hong CY, Shun CT, Hsiao TY, Wang CC, Wang JS, Hsiao M, Lin SK. Inducible cyclooxygenase and interleukin 6 gene expressions in nasal polyp fibroblasts: possible implication in the pathogenesis of nasal polyposis. *Arch Otolaryngol Head Neck Surg* 2002; **128**: 945-951

56 **Maitra A**, Ashfaq R, Gunn CR, Rahman A, Yeo CJ, Sohn TA, Cameron JL, Hruban RH, Wilentz RE. Cyclooxygenase 2 expression in pancreatic adenocarcinoma and pancreatic intraepithelial neoplasia: an immunohistochemical analysis with automated cellular imaging. *Am J Clin Pathol* 2002; **118**: 194-201

57 **Carlton PS**, Gopalakrishnan R, Gupta A, Habib S, Morse MA, Stoner GD. Piroxicam is an ineffective inhibitor of N-nitrosomethylbenzylamine-induced tumorigenesis in the rat esophagus. *Cancer Res* 2002; **62**: 4376-4382

58 **Hoozemans JJ**, Bruckner MK, Rozemuller AJ, Veerhuis R, Eikelenboom P, Arendt T. Cyclin D1 and cyclin E are co-localized with cyclo-oxygenase 2 (COX-2) in pyramidal neurons in Alzheimer disease temporal cortex. *J Neuropathol Exp Neurol* 2002; **61**: 678-688

59 **Wei M**, Wanibuchi H, Morimura K, Iwai S, Yoshida K, Endo G, Nakae D, Fukushima S. Carcinogenicity of dimethylarsinic acid in male F344 rats and genetic alterations in induced urinary bladder tumors. *Carcinogenesis* 2002; **23**: 1387-1397

60 **Sunayama K**, Konno H, Nakamura T, Kashiwabara H, Shoji T, Tsuneyoshi T, Nakamura S. The role of cyclooxygenase-2 (COX-2) in two different morphological stages of intestinal polyps in APC (Delta474) knockout mice. *Carcinogenesis* 2002; **23**: 1351-1359

61 **Wu T**, Han C, Lunz JG, Michalopoulos G, Shelhamer JH, Demetris AJ. Involvement of 85-kd cytosolic phospholipase A (2) and cyclooxygenase-2 in the proliferation of human cholangiocarcinoma cells. *Hepatology* 2002; **36**: 363-373

62 **Wardlaw SA**, Zhang N, Belinsky SA. Transcriptional regulation of basal cyclooxygenase-2 expression in murine lung tumor-derived cell lines by CCAAT/enhancer-binding protein and activating transcription factor/cAMP response element-binding protein. *Mol Pharmacol* 2002; **62**: 326-333

63 **Shah T**, Ryu S, Lee HJ, Brown S, Kim JH. Pronounced radiosensitization of cultured human cancer cells by COX inhibitor under acidic microenvironment. *Int J Radiat Oncol Biol Phys* 2002; **53**: 1314-1318

64 **Lew JI**, Guo Y, Kim RK, Vargish L, Michelassi F, Arenas RB. Reduction of Intestinal Neoplasia With Adenomatous Polyposis Coli Gene Replacement and COX-2 Inhibition Is Additive. *J Gastrointest Surg* 2002; **6**: 563-568

65 **Qiu DK**, Ma X, Peng YS, Chen XY. Significance of cyclooxygenase-2 expression in human primary hepatocellular carcinoma. *World J Gastroenterol* 2002; **8**: 815-817

66 **Tian G**, Yu JP, Luo HS, Yu BP, Yue H, Li JY, Mei Q. Effect of nimesulide on proliferation and apoptosis of human hepatoma SMMC-7721 cells. *World J Gastroenterol* 2002; **8**: 483-487

67 **Wu YL**, Sun B, Zhang XJ, Wang SN, He HY, Qiao MM, Zhong J, Xu JY. Growth inhibition and apoptosis induction of Sulindac on Human gastric cancer cells. *World J Gastroenterol* 2001; **7**: 796-800

68 **Wang X**, Lan M, Wu HP, Shi YQ, Lu J, Ding J, Wu KC, Jin JP, Fan DM. Direct effect of croton oil on intestinal epithelial cells and colonic smooth muscle cells. *World J Gastroenterol* 2002; **8**: 103-107

69 **Niu ZS**, Li BK,Wang M. Expression of p53 and C-myc genes and its clinical relevance in the hepatocellular carcinomatous and pericarcinomatous tissues. *World J Gastoenterol* 2002; **8**: 822-826

70 **Chen Q**, Yang GW, An LG. Apoptosis of hepatoma cells SMMC-7721 induced by Ginkgo biloba seed polysaccharide. *World J Gastroenterol* 2002; **8**: 832-836

71 **Taketo MM**. Cyclooxygenase-2 inhibitors in tumorigenesis. *J Natl Cancer Inst* 1998; **90**: 1529-1536

72 **Zimmermann KC,** Sarbia M, Weber AA, Borchard F, Gabbert HE, Schror K. Cyclooxygenase-2 expression in human esophageal carcinoma. *Cancer Res* 1999; **59**: 198-204
73 **Tjandrawinata RR**, Dahiya R, Hughes FM. Induction of cyclooxygenase-2 mRNA by prostaglandin E2 in human prostatic carcinoma cells. *Br J Cancer* 1997; **75**: 1111-1118
74 **Zhao AG**, Zhao HL, Jin XJ, Yang JK, Tang LD. Effects of Chinese Jianpi herbs on cell apoptosis and related gene expression in human gastric cancer grafted onto nude mice. *World J Gastroenterol* 2002; **8**: 792-796
75 **Liu S**, Wu Q, Ye XF, Cai JH, Huang ZW, Su WJ. Induction of apoptosis by TPA and VP-16 is through translocation of TR3. *World J Gastroenterol* 2002; **8:** 446-450
76 **Xu CT**, Huang LT, Pan BR. Current gene therapy for stomach carcinoma. *World J Gastroenterol* 2001; **7**: 752-759
77 **Wu YL**, Sun B, Zhang XJ, Wang SN, He HY, Qiao MM, Zhong J, Xu JY. Growth inhibition and apoptosis induction of Sulindac on Human gastric cancer cells. *World J Gastroenterol* 2001; **7**: 796-800
78 **Hou L**, Li Y, Jia YH, Wang B, Xin Y, Ling MY. Molecular mechanism about lymphogenous metastasis of hepatocarcinoma cells in mice. *World J Gastroenterol* 2001; **7**: 532-536
79 **Xu AG**, Li SG, Liu JH, Gan AH. Function of apoptosis and expression of the proteins Bcl-2, p53 and C-myc in the development of gastric cancer. *World J Gastroenterol*. 2001; **7**: 403-406

**Edited by** Su Q and Wang XL

P.O.Box 2345, Beijing 100023,China
Fax: +86-10-85381893
E-mail: wjg@wjgnet.com www.wjgnet.com

World J Gastroenterol 2003;9(6):1227-1230
World Journal of Gastroenterology
Copyright ©2003 by The WJG Press ISSN 1007-9327

• COLORECTAL CANCER •

# Clinical significance of vascular endothelial growth factor expression and neovascularization in colorectal carcinoma

Shu Zheng, Ming-Yong Han, Zuo-Xiang Xiao, Jia-Ping Peng, Qi Dong

**Shu Zheng, Ming-Yong Han, Zuo-Xiang Xiao, Jia-Ping Peng, Qi Dong,** Cancer Institute, Zhejiang University, Hangzhou 310009, Zhejiang Province, China
**Correspondence to:** Professor Shu Zheng, Cancer Institute, Zhejiang University, Hangzhou 310009, Zhejiang Province, China
**Telephone:** +86-571-87214404 **Fax:** +86-571-87214404
**Received:** 2003-03-02 **Accepted:** 2003-04-01

## Abstract

**AIM:** To clarify the association of vascular endothelial growth factor (VEGF) and microvascular density (MVD) expression with the angiogenesis and prognosis of colorectal cancer.

**METHODS:** A total of 97 cases of colorectal carcinomas were examined by immunohistochemical staining (SP method), using anti-VEGF and anti-factor $CD34^+$ monoclonal antibodies.

**RESULTS:** VEGF positive staining was obtained in 68 out of 97 cases (70.1 %), and observed mainly in the cytoplasm of tumor cells, and also frequently in stromal cells. VEGF expression was more intense in poorly differentiated adenocarcinoma in comparison with others, but there was no significant correlation between VEGF expression and age, sex and stage. A significant correlation was found between the MVD and grades, and there was no significant relationship between the MVD and age, sex, and stage. The MVD in the VEGF positive group (68 cases) was higher than that in the negative group. Upon multivariate analysis, the significant variables were stage, tumor grade and MVD; VEGF expression was not an independent prognostic factor.

**CONCLUSION:** The expression of VEGF has a significant correlation with MVD; MVD expression has prognostic value but VEGF has not in colon cancer.

Zheng S, Han MY, Xiao ZX, Peng JP, Dong Q. Clinical significance of vascular endothelial growth factor expression and neovascularization in colorectal carcinoma. *World J Gastroenterol* 2003; 9(6): 1227-1230
http://www.wjgnet.com/1007-9327/9/1227.asp

## INTRODUCTION

Angiogenesis is an essential process required for the growth and metastatic ability of solid tumors[1]. Some studies demonstrated that an increase in microvascular density (MVD) was found to be closely associated with the expression of vascular endothelial growth factor (VEGF), and that MVD and VEGF expression had a prognostic value in predicting metastasis of various malignant solid tumors[2,3]. Several studies have noted that the level of VEGF expression, a strong angiogenic factor, correlates with neovascularity and tumor progression in human breast and brain cancers and experimental tumor models[4,5]. In this study, we investigated the correlation of the VEGF and MVD in the tumor tissue of patients with colon cancer.

## MATERIALS AND METHODS

### *Patients and tumor specimens*

Tumor specimens from 97 patients resected for colorectal cancers, from the Second Affiliated Hospital of Zhejiang University (Hangzhou, China) from March 1993 to September 1995 were assessed. The age of the patients ranged from 36 to 74 years; 58 were male and 39 were female; average age, male 57.5 years old, female 61.5 years old. The patients were staged according to operation and pathological findings with UICC TNM classification: 9 (9.3 %) in stage I, 38 (39.2 %) in stage II, 32 (32.9 %) in stage III, and 18 (18.6) in stage IV.

### *Immunohistochemistry*

Specimens were fixed in a 10 % formaldehyde solution and embedded in paraffin. Sections, 5 μm thick, were cut and mounted on glass slides. Immunohistochemical staining was performed using the avidin-biotin method. Staining for VEGF was performed using an anti-VEGF monoclonal antibody (MAb) (Calbiochem, Cambridge, UK). Staining for vascular endothelial cells was performed using an anti-CD34 MAb (DAKO, Copenhagen, Denmark). Briefly, formalin-fixed, paraffin-embedded 5 μm tissue sections were deparaffinised with xylene, dehydrated in ethanol and incubated with 3 % hydrogen peroxidase for 5 min. After washed with phosphate-buffered saline (PBS), tissue sections were incubated in 10 % normal bovine serum for 20 min, followed by an overnight incubation with anti-VEGF (1:50) antibody or anti-CD34 antibody (1:50). Biotinylated goat antimouse and antirabbit immunoglobulins were used as secondary antibodies. Peroxidase-conjugated avidin was used as a dilution of 1:500. Finally, 0.02 % diaminobenzidine and 1 % hydrogen peroxide in PBS were used as the substrate. Normal mouse IgG diluted to an equivalent protein concentration was used as a control in place of the primary antibody. Counterstaining was performed with haematoxylin.

Any single brown-stained cell that indicates an endothelial cell stained with CD34 was counted as a single vessel. Branching structures were counted as a single vessel, unless there was a break in the continuity of the structure. The stained sections were screened at 5 times magnification, to identify the areas of highest vascular density. After the area of highest neovascularization was identified, individual vessel counts were performed at ×200 magnification.

### *Evaluation of VEGF expression*

For the evaluation of VEGF expression, immunostaining was classified in two groups, corresponding to the percentage of immunoreactive cells; the cut-off point to distinguish low from high VEGF expression was 25 % of positive carcinoma cells.

### *Statistical analysis*

Statistical comparisons for significance were made with the Student's *t* test and $\chi^2$ test. Multivariate analysis was performed

using the Cox' s regression multiple hazard model. $P<0.05$ was considered statistically significant.

## RESULTS

### VEGF expression

Positive staining was obtained in 68 out of 97 cases (70.1 %) and a typical immunohistochemical staining is shown in Figure 1. VEGF immunoreactivity was observed mainly in the cytoplasm of tumor cells, and also frequently in stromal cells. The distribution of VEGF-staining was not continuous in the whole slide of the specimen. VEGF expression was more intense in poorly differentiated adenocarcinoma in comparison with other tumors ($P=0.014$), but there was no significant correlation between VEGF expression and age, sex and stage (Table 1).

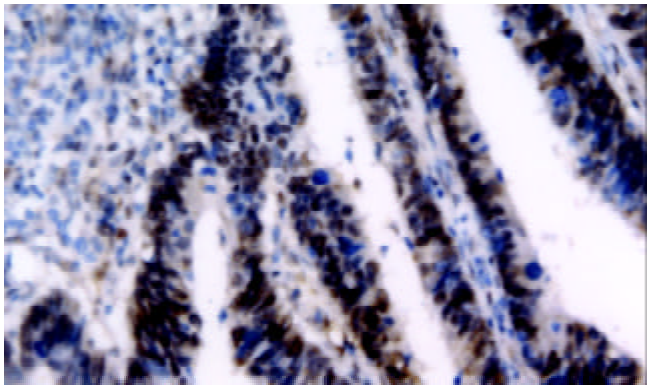

**Figure 1** VEGF expression in colorectal cancer specimen. VEGF immunoreactivity was observed mainly in the cytoplasm of tumor cells, and also frequently in stromal cells.

**Table 1** Relationship between clinicopathologic factors and VEGF expression ($n=97$)

| Variables | *n* (%) | VEGF expression | | |
|---|---|---|---|---|
| | | + *n*(%) | - *n*(%) | *P* value |
| Age | | | | |
| <45 years | 36 | 26(72.2) | 10(27.8) | |
| >45 years | 61 | 42(68.8) | 19(31.2) | |
| Sex | | | | |
| Male | 58 | 41(74.1) | 17(25.9) | |
| Female | 39 | 27(68.9) | 12(31.1) | |
| Different differentiation | | | | |
| Well | 28 | 15(51.1) | 13(48.9) | |
| Moderate | 36 | 26(72.2) | 10(27.8) | |
| Poor | 33 | 27(81.8) | 6(18.2) | 0.014 |
| Stage | | | | |
| I | 9 | 7(77.8) | 2(22.2) | |
| II | 38 | 27(71.1) | 11(28.9) | |
| III | 32 | 23(72.2) | 9(27.8) | |
| IV | 18 | 11(61.5) | 7(38.5) | |

$P<0.05$ *vs* Well differentiated group.

### Microvascular density (MVD)

Any single brown-stained cell that indicates an endothelial cell stained with CD34 was counted as a single vessel (Figure 2). The median MVD was 187.6±17.3. A significant correlation was found between the MVD and different grade (0.028), and there was no significant relationship between the MVD and age, sex, and stage (Table 2).

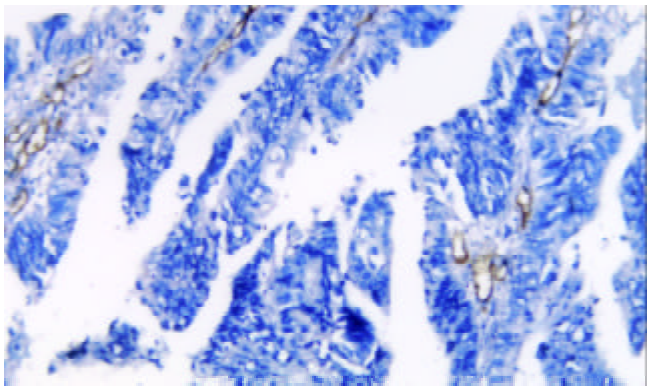

**Figure 2** Microvascular density in colorectal cancer specimen. The single brown-stained cell indicates an endothelial cell that was stained for the presence of CD34.

**Table 2** Relationship between clinicopathologic factors and MVD ($n=97$)

| Variables | *n* | MVD | | |
|---|---|---|---|---|
| | | high MVD | low MVD | *P* value |
| Age | | | | |
| <45 years | 36 | 20(55.6) | 16(44.4) | |
| >45 years | 61 | 33(54.3) | 28(45.7) | |
| Sex | | | | |
| Male | 58 | 32(55.2) | 26(44.8) | |
| Female | 39 | 21(53.8) | 18(46.2) | |
| Different differentiation | | | | |
| Well | 28 | 12(42.9) | 16(57.1) | |
| Moderate | 36 | 20(55.6) | 16(44.4) | |
| Poor | 33 | 21(63.6) | 12(36.4) | 0.028 |
| Stage | | | | |
| I | 9 | 5(55.6) | 4(44.4) | |
| II | 38 | 20(52.6) | 18(47.4) | |
| III | 32 | 18(56.3) | 14(43.7) | |
| IV | 18 | 10(55.6) | 8(44.4) | |

$P<0.05$ *vs* Well differentiated group.

**Table 3** Relationship between MVD and VEGF expression

| Variable | | MVD | *P* value |
|---|---|---|---|
| VEGF | (+) | 213.4±12.8 | |
| Expression | (-) | 138.7±19.4 | 0.027 |

$P<0.05$ *vs* VEGF (-) group.

**Table 4** Multivariate analysis of overall survival by Cox proportional hazards model

| Variable | Categories | Hazard ratio | SEM | *P* value |
|---|---|---|---|---|
| Age | >45 years versus <45 years | 1.877 | 0.3796 | |
| Sex | Male versus female | 1.216 | 0.4071 | |
| Differentiation | Poor versus others | 2.361 | 0.2438 | 0.0217 |
| Stage | I, II versus III, IV | 2.973 | 0.1976 | 0.0012 |
| VEGF | (+) versus (-) | 1.164 | 0.3874 | |
| MVD | >187.6 versus <187.6 | 2.526 | 0.2126 | 0.0314 |

$P<0.05$ *vs* Stage I, II group.

### Association between VEGF expression and MVD

The MVD in the VEGF positive group was 213.4±12.8, and that in the negative group was 138.7±19.4. MVD in the VEGF

positive group was higher than that in the negative group ($P$=0.027) (Table 3).

### *Multivariate analysis*

Upon multivariate analysis of all patients, the significant variables were stage, tumor grade and MVD. Age, sex, VEGF expression were not independent prognostic factors (Table 4).

## DISCUSSION

Microvascularity is important in cancer growth and metastasis because it is involved in the transport of various nutrients to the tumor cells[1,2]. In this process of tumor growth and angiogenesis numerous angiogenic factors are involved. In recent years several of these factors have been identified[3-6]. One of the most important regulators of angiogenesis is VEGF. It induces the vascular stroma not only as a direct endothelial cell mitogen, but also as a potent mediator of microvessel permeability. This ability of VEGF to induce fenestrations on microvessels has been demonstrated in experimental tumors[7,8].

The VEGF is overexpressed in a variety of benign tissues and malignant human tumors. The expression of VEGF suggests that it plays a role in luminal secretion by increasing local vascular permeability[9]. In neuroendocrine tumors the high levels of VEGF expression could indicate a role for VEGF in the release of gastrointestinal hormones through the regulation of baseline permeability of the normal microcirculation[10]. The high level of VEGF expression in some malignant tumors, such as breast cancer, non-small cell lung cancer, bladder cancer and gastric cancer, is a characteristic feature of these tumors. Several studies have demonstrated that high microvessel density is a useful indicator for poor prognosis in these cancers[11-15].

CD34 antigen is expressed on immature human haematopoietic precursor cells and is progressively lost during maturation[16,17]. In normal resting tissues, anti-CD34 antibodies are predominantly neated with the luminal endothelial membrane, whereas the abluminal membrane is negative or only weakly positive. In contrast, significant staining of the endothelial abluminal microprocesses (EAM) has been found in tumor stroma[18]. It has been shown that CD34 is a marker for EAM during angiogenesis and the antigenicity of CD34 is preserved by freezing, or ethanol, and formalin fixation[19].

Microvessel density (MVD) and expression of VEGF act as a highly specific inducer of angiogenesis. Strong VEGF expression and high MVD are considered important parameters of tumor angiogenesis and related to poor survival probability in vulvar cancer patients[20,21]. In primary breast cancer, MVD and VEGF serve as a parameter for determining tumor biological, metastatic potential and prognosis[22]. VEGF is highly related to angiogenesis of gastric carcinoma and promotes growth, invasion and metastasis of gastric carcinoma, VEGF expression and MVD are predictors for the biological behavior of gastric carcinoma[21,23]. In primary liver cancer, besides tumor stage, satellite nodules and portal vein embolus, the MVD and VEGF expressions are also of prognostic significance[24]. Intense VEGF staining was found in the majority of advanced primary SCCs, lymph node metastases, and human SCCs in severe combined immunodeficent mice, where no dysplasia, CIS, or early SCCs showed intense immunostaining. Suggesting a role for VEGF in both clinical and experimental HNSCC[25,26]. By univariate analysis, VEGF expression and MVD in the biopsy specimens were significant predictors of bladder cancer recurrence. By multivariate analysis, only VEGF expression was an independent prognostic factor[27]. The metastatic potency of NPC tissue and the prognosis of the patients with NPC could be estimated by measuring MVD and the expression of VEGF in NPC tissue[28]. Previously it was demonstrated that in prostate tumors, angiogenesis measured as microvessel density (MVD) was associated with tumor stage as well as WHO grade and was an independent predictor of clinical outcome. Vascular endothelial growth factor (VEGF) is a major inducer of angiogenesis[29]. The relationship between VEGF expression and MVD in ovarian carcinoma suggests that in conjunction with the established clinicopathologic prognostic parameters of ovarian carcinoma, VEGF expression may enhance the predictability of patients at high risk for tumor progression who are potential candidates for further aggressive therapy[30]. But MVD in synovial sarcomas did not correlate with prognosis or VEGF expression, angiogensis in synovial sarcoma might be controlled by angiogenesis activators other than VEGF[31]. In patients with invasive cervical cancer VEGF expression has no prognostic value in contrast with the MVD[32].

In this study, we found positive VEGF staining was obtained in 68 out of 97 cases (70.1 %), VEGF immunoactivity was observed mainly in the cytoplasm of tumor cells, and also frequently in stromal cells. VEGF expression was more intense in poorly differentiated adenocarcinoma in comparison with other tumors, but there was no significant correlation between VEGF expression and age, sex and stage. A significant correlation was found between the MVD and different grade, and there was no significant relationship between the MVD and age, sex, and stage. MVD in the VEGF positive group was higher than that in the negative group. Upon multivariate analysis, the significant variables were stage, tumor grade and MVD; VEGF expression was not an independent prognostic factor. We conclude that MVD but not VEGF expression has prognostic value in colon cancer.

## REFERENCES


1 **Folkman J**. Tumor angiogenesis. *Adv Cancer Res* 1985; **43**: 175-203

2 **Decaussin M,** Sartelet H, Robert C, Moro D, Claraz C, Brambilla C, Brambilla E. Expression of vascular endothelial growth factor (VEGF) and its two receptors in non-small cell lung carcinoma (NSCLCs): correlation with angiogenesis and survival. *J Pathol* 1999; **188**: 369-377

3 **Folkman J**, Klagsbrun M. Angiogenic factors. *Science* 1987; **235**: 442-447

4 **Burian M**, Quint C, Neuchrist C. Angiogenic factors in laryngeal carcinomas: do they have prognostic relevance? *Acta Otolaryngol* 1999; **119**: 289-292

5 **Giatromanolaki A,** Koukourakis MI, Stathopoulos GP, Kapsoritakis A, Paspatis G, Kakolyris S, Sivridis E, Georgolias V, Harris AL, Gatter KC. Angiogenic interactions of vascular endothelial growth factor, of thymidine phosphorylase, and of p53 protein expression in locally advanced gastric cancer. *Oncol Res* 2000; **12**: 33-41

6 **Li Z,** Shimada Y, Uchida S, Maeda M, Kawabe A, Mori A, Itami A, Kano M, Watanabe G, Imaura M. TGF-alpha as well as VEGF, PD-ECGF and bFGF contribute to angiogenesis of esophageal squamous cell carcinoma. *Int J Oncol* 2000; **17**: 453-460

7 **Roberts WG**, Palade GE. Increased microvascular permeability and endothelial fenestration induced by vascular endothelial growth factor. *J Cell Sci* 1995; **108**: 2369-2379

8 **Fujimoto K,** Hosotani R, Wada M, Lee JU, Koshiba T, Miyamoto Y, Tsuji S, Nakajima S, Doi R, Imamura M. Expression of two angiogenic factors, vascular endothelial growth factor and platelet-derived endothelial cell growth factor in human pancreatic cancer, and its relationship to angiogenesis. *Eu J Cancer* 1998; **34**: 1439-1447

9 **Zhang L**, Scott PA, Turley H, Leek R, Lewis CE, Gatter KC, Harris AL, Mackenzie IZ, Rees MC, Bicknell R. Validation of anti-vascular endothelial growth factor antibodies for immunohistochemical localization of VEGF in tissue sections: expression of VEGF in the human endometrium. *J Pathol* 1998; **185**: 402-408

10 **Terris B**, Scozec JY, Rubbia L, Bregeaud L, Pepper MS,

Ruszniewski P, Belghiti J, Flejou J, Degott C. Expression of vascular endothelial growth factor in digestive neuroendocrine tumours. *Histopathology* 1998; **32**: 133-138

11 **Uchida S,** Shimada Y, Watanabe G, Tanaka H, Shibagaki I, Miyahara T, Ishigami S, Imamura M. In oesophageal squamous cell carcinoma vascular endothelial growth factor is associated with p53 mutation, advanced stage and poor prognosis. *Br J Cancer* 1998; **77**: 1704-1709

12 **de-Jong JS,** van-Diest PJ, van-der-Valk P, Baak JP. Expression of growth factors, growth-inhibiting factors, and their receptors in invasive breast cancer. *J Pathol* 1998; **184**: 53-57

13 **Koomagi R,** Volm M. Tissue-factor expression in human non-small-cell lung carcinoma measured by immunohistochemistry: correlation between tissue factor and angiogenesis. *Int-J-Cancer* 1998; **79**: 19-22

14 **Aikawa H,** Takahashi H, Fujimura S, Sato M, Endo C, Sakurada A, Kondo T, Tanita T, Matsumura Y, Ono S, Saito Y, Sagawa M. Immunohistochemical study on tumor angiogenic factors in non-small cell lung cancer. *Anticancer Res* 1999; **19**: 4305-4309

15 **Neuchrist C,** Quint C, PammerA, Burian M. Vascular endothelial growth factor (VEGF) and microvessel density in squamous cell carcinomas of the larynx: an immunohistochemical study. *Acta Otolaryng* 1999; **119**: 732-738

16 **Watt SM**, Karhi K, Gatter K, Furley AJ, Katz FE, Healy LE, Altass LJ, Bradley NJ, Sutherland DR, Levinsky R. Distribution and epitope analysis of the cell membrane glycoprotein associated with human hematopoietic progenitor cells. *Leukemia* 1987; **1**: 417-426

**17 El-Assal ON**, Yamanoi A, Soda Y, Yamagchi M, Igarashi M, Yamamoto A, Nabika T, Nagasue N. Clinical significance of microvessel density and vascular endothelial growth factor expression in hepatocellular carcinoma and surrounding liver: possible involvement of vascular endothelial growth factor in the angiogenesis of cirrhotic liver. *Hepatology* 1998; **27**: 1554-1562

18 **Schlingemann RO**, Rietveld FJ, de Waal RM, Bradley NJ, Skene AI, Davies AJ, Greaves MF, Denekamp J, Ruiter DJ. Leukocyte antigen CD34 is expressed by a subset of cultured endothelial cells and on endothelial abluminal microprocesses in the tumor stroma. *Lab Invest* 1990; **62**: 690-696

19 **Traweek ST**, Kandalaft PL, Mehta P, Battifora H. The human hematopoietic progenitor cell antigen (CD34) in vascular neoplasia. *Am J Clin Pathol* 1991; **96**: 25-31

20 **Ogura Y,** Sato K, Kato T, Saito K, Enomoto K. Immunohistochemical analysis of expression of angiogenic factors and tumor angiogenesis in superficial bladder cancer. *Nippon Hinyokika Gakkai Zasshi* 1998; **89**: 529-537

21 **Obermair A,** KohlbergerP, Bancher Todesca D, Tempfer C, Sliutz G, Leodolter S, Reinthaller A, Kainz C, Breitenecker G, Gitsch G. Influence of microvessel density and vascular permeability factor/vascular endothelial growth factor expression on prognosis in vulvar cancer. *Gynecol Oncol* 1996; **63**: 204-209

22 **Jiang X,** Huang X, Li J. The correlation between tumor angiogenesis and lymph node metastasis in primary breast carcinoma. *Zhonghua Waike Zazhi* 1997; **35**: 583-585

23 **Lu M,** Jiang Y, Wang R. The relationship of vascular endothelial growth factor and angiogenesis to the progression of gastric carcinoma. *Zhonghua Binglixue Zazhi* 1998; **27**: 278-281

24 **Xia J,** Yang B, Ye S. Clinico-pathological significance of microvessel density and VEGF expression in primary liver cancer. *Zhonghua Zhongliu Zazhi* 1998; **20**: 440-442

25 **Ikeguchi M,** Oka S, Saito H, Kondo A, Tsujitani S, Maeta M, Kaibara N. The expression of vascular endothelial growth factor and proliferative activity of cancer cells in gastric cancer. *Langenbecks Arch Surg* 1999; **384**: 264-270

26 **Sauter ER,** Nesbit M, Watson JC, Klein-Szanto A, Litwin S, Herlyn M. Vascular endothelial growth factor is a marker of tumor invasion and metastasis in squamous cell carcinoma of the head and neck. *Clin Cancer Res* 1999; **5**: 775-782

27 **Inoue K,** Slaton JW, Karashima T, Yoshikawa C, Shuin T, Sweeney P, Millikan R, Dinney CP. The prognostic value of angiogenesis factor expression for predicting recurrence and metastasis of bladder cancer after neoadjuvant chemotherapy and radical cystectomy. *Clin Cancer Res* 2000; **6**: 4866-4873

28 **Guang WH**, Sunagawa M, Jie En L, Shimada S, Gang Z, Tskeshi Y, Kosugi T. The relationship between microvessel density, the expression of vascular endothelial growth factor ,and the extension of nasopharyngeal carcinoma. *Laryngoscope* 2000; **110**: 2066-2069

29 **Strohmeyer D,** Rossing C, Bauerfeind A, Kaufmann O, Schlechte H, Bartsch, G, Loening S. Vascular endothelial growth factor and its correlation with angiogenesis and p53 expression in prostate cancer. *Prostate* 2000; **45**: 216-224

30 **Shen GH,** Ghazizadeh M, Kawanami O, Shimizu H, Jin E, Araki T, Sugisaki Y. Prognostic significance of vascular endothelial growth factor expression in human ovarian carcinoma. *Br J Cancer* 2000; **83**: 196-203

31 **Kawauchi S,** Fukuda T, Tsuneyoshi M. Angiogenesis does not correlate with prognosis or expression of vascular endothelial growth factor in synovial sarcomas. *Oncol Rep* 1999; **6**: 959-964

32 **Tjalma W,** Weyler J, Weyn B, Van-Marck E, Van-Daele A, Van-Dam P, Goovaerts G, Buytaert P. The association between vascular endothelial growth factor, microvessel density and clinicopathological features in invasive cervical cancer. *Eur J Obstet Gynecol Reprod Biol* 2000; **92**: 251-257

**Edited by** Zhang JZ

P.O.Box 2345, Beijing 100023,China
Fax: +86-10-85381893
E-mail: wjg@wjgnet.com www.wjgnet.com

World J Gastroenterol 2003;9(6):1231-1236
World Journal of Gastroenterology
Copyright ©2003 by The WJG Press ISSN 1007-9327

• COLORECTAL CANCER •

# Effects of KAI1/CD82 on biological behavior of human colorectal carcinoma cell line

Li Liu, De-Hua Wu, Zu-Guo Li, Guang-Zhi Yang, Yan-Qing Ding

**Li Liu, Zu-Guo Li, Guang-Zhi Yang, Yan-Qing Ding,** Department of Pathology, the First Military Medical University, Guangzhou 510515, Guangdong Province, China
**De-Hua Wu,** Department of Radiation Oncology, Nanfang Hospital, the First Military Medical University, Guangzhou 510515, Guangdong Province, China
**Supported by** the National Natural Science Foundation, No. 31070423, the Natural Science Foundation of Guangdong Province, No. 990385, 970335 and the Natural Science Foundation of PLA of China, No. 01MA128
**Correspondence to:** Dr Yang-Qing Ding, Department of Pathology, the First Military Medical University, Guangzhou 510515 Guangdong Province, China. dyq@fimmu.com
**Telephone:** +86-20-61642148 **Fax:** +86-20-61642148
**Received:** 2002-12-22 **Accepted:** 2003-02-11

## Abstract

**AIM:** To investigate the effects of KAI1/CD82 on biological behavior of colorectal carcinoma cells.

**METHODS:** KAI1 cDNA was transfected into highly malignant colorectal carcinoma cell line, LoVo, which had low level of endogenous KAI1 expression, and established stable transfectant clones with high KAI1/CD82 expression. The cell-cell adhesion, cell aggregation, cell-matrix adhesion and cell invasion assay were performed to determine whether KAI1 transfectant could have an effect on proliferation, adhesion and tumor metastasis in comparison with the control transfectant cells.

**RESULTS:** KAI1 expression did not alter *in vitro* cell proliferation. But the KAI1 transfectant cells exhibited significantly increased homotypic cell-cell adhesion and cell aggregation in comparison with the control transfectant cells ($P<0.05$). Furthermore, KAI1 expression significantly suppressed the cell adhesion to extracellular matrix components and *in vitro* cell invasion in KAI1-transfected LoVo cells. The data indicated that KAI1 expression significantly suppressed the metastatic potential of KAI1-transfected LoVo cells.

**CONCLUSION:** Our results suggest that KAI1 might function as a negative regulator of colorectal carcinoma metastasis.

Liu L, Wu DH, Li ZG, Yang GZ, Ding YQ. Effects of KAI1/CD82 on biological behavior of human colorectal carcinoma cell line. *World J Gastroenterol* 2003; 9(6): 1231-1236
http://www.wjgnet.com/1007-9327/9/1231.asp

## INTRODUCTION

KAI1, a newly identified metastatic suppressor gene for prostatic cancer, is located on human chromosome 11p11.2. It was originally isolated by Dong in 1995[1,2]. KAI1 mRNA, is ubiquitously expressed with abundant expression in the surface epithelium of the major epithelial tissues, including prostate, breast, bladder, and gastrointestinal tract[3,4]. Its protein product, CD82, belongs to TM4SF (transmembrane four superfamily) or TST (tetra span transmembrane) superfamily, many of which, including KAI1, are CD antigens present on the surface of leukocytes[5,6]. Four hydrophobic transmembrane domains and one large extracellular hydrophilic domain containing 3 potential N-glycosylation sites are thought to function in cell-cell and cell-matrix interactions. At least three TM4SF members are implicated in metastasis, including CD9/MRP-1, CD63/ME491, and CD82/KAI1[7]. KAI1 and other TM4SF members have been demonstrated to bind to each other, integrins, and E-cadherin, and other surface molecules to relay extracellular signals to signal transduction pathways that are important in cellular adhesion, invasive motility, and metastasis suppression[8-10].

The role of KAI1 in tumor progression may not be limited to prostatic cancer. It was reported to be important in preventing the development of metastases in a wide variety of human tumor types, including several cancers such as cervical[11], breast[12], pancreatic[13], esophageal[14], and ovarian cancer[15]. Therefore, we transfected KAI1 plasmid into highly malignant colorectal carcinoma cell line, LoVo, and examined cell proliferation, adhesion and invasion. The aim of this study was to determine whether KAI1could suppress the invasive or metastatic ability of colorectal carcinoma cells.

## MATERIALS AND METHODS

### *Cell lines and culture conditions*

LoVo cell line was derived from human colon adenocarcinoma established from the metastatic nodule resected from a 56-year-old Caucasian man with colon adenocarcinoma in 1972. ECV304 cell line was derived from human umbilical cord transformed endothelium. Both cell lines were cultured in RPMI-1640 medium supplemented with 10 % heat-inactivated fetal bovine serum (FBS) and 100 U/ml penicillin/streptomycin. All cells were grown in 5 % $CO_2$ humidified atmosphere at 37 ℃, and harvested for analysis at 80-90 % confluency.

### *Transfection and selection of the expressing cells*

pCMV-KAI1 plasmid was a generous gift from Carl Barrett. 1.6 kb KAI1cDNA inserting at salI sites was inserted into the xhoI site of pCMV-neo-xhoI vector to construct pCMV-KAI1. This plasmid was transfected into LoVo cell using the cationic polymer transfection reagent(jetPEI trasfection reagent was purchased from Dakewe Biotechnology Company). The transfection proposal was as follows: the cells were plated at 6-well plate 1d before the transfection. 3 μg pCMV-KAI1 plasmid was diluted to 100 μl 150 mM NaCl and 6 μl jetPEI solution was diluted to 100 μl 150 mM NaCl. 100 μl jetPEI solution was added to the 100 μl DNA solution and vortex the solution immediately. Then the mixture was added drop-wise onto the serum containing medium in each well after incubated for 30 min at room temperature. After incubated for 48 h at 37 ℃, 5 % $CO_2$ in a humidified atmosphere, the transfectants named LoVo-KAI1 were isolated by growing them in G418-containing medium (700 μg/ml) and G418-resistant clones

were established in two weeks. The pCMV-neo (purchased from Stratagene Company) vector alone was also transfected into LoVo cells to generate neo transfected control clones, designated as LoVo-neo.

### *In situ hybridization (ISH) assay*

To prepare digoxigenin-labeled KAI1-DNA probes for *in situ* hybridization, PCR amplification was performed with a forward primer 5' -AGTCCTCCCTGCTGCTGTGTG-3' and reverse primer 5' -TCAGTCAGGGTGGGCAAGAGG-3' and a 1 030 bp KAI1 fragment was achieved[16]. The probes was labeled by Dig DNA Labeling and detecting Kit (purchased from Roche Company). Blot hybridization of Dig-labeled probe showed the labeling efficiency. ISH was performed according to the description of the enhanced sensitive ISH detection kit (purchased from Boster Biotechnology Company). Briefly, the cells that were incubated in cover slip for 24 hour and fixed with 95 % ethanol were washed with PBS (phosphate-buffered saline) three times. The endogenous peroxidases were blocked by incubating with 0.5 % $H_2O_2$ for 30 min at room temperature. The cells were subsequently treated for 10 min with triton X-100 and for 40 s with 3 % pepsin. At 37 ℃ the cells were prehybridized for 3 h and hybridized overnight. The final concentrations of the labeled probes were 150 pg/μl. After hybridization, excess probe was removed by washing in 2×SSC, 0.5×SSC, 0.2×SSC respectively. The cells were incubated with an antidigoxigenin antibody conjugated biotin for 120 min at room temperature and then added strept-avidin biotin complex for 30 min. For color reaction, diaminobenzidine (DAB) was used. If the ISH signals were present, the cytoplasm would be full of brown granules. The control was LoVo-neo cell group.

### *Immunohistochemistry (IHC) assay*

The fixed cells were subjected to immunostaining by using an ultrasensitive S-P technique (Maixin Biotechnology Company). Endogenous peroxidases were blocked by incubating with 0.5 % $H_2O_2$ for 30 min at room temperature. The cells were subsequently treated for 10 min with triton X-100 and for 40 s with 3 % pepsin. The cells were incubated for 30 min at 37 ℃ with normal nonimmune serum before incubation at 4 ℃ with specific monoclonal KAI1-antibody (BD Pharmingen Technical Company) used at a dilution of 1:100 overnight. The cells were then treated with biotin-conjugated second antibody before adding streptavidin-peroxidase. For color reaction, diaminobenzidine was used. If the IHC signals were present, the cytoplasm and membrane were stained brown. The control was LoVo-neo cell group.

### *Growth curve*

LoVo-KAI1 Cells were prepared by trypsinization. The cells were resuspended at a concentration of $10^4$ cells/ml in RPMI 1640 10 % FCS and then 100 μl aliquots were dispensed into 96 well microtiter plates. The cells were incubated for 1,2,3,4,5,6 day respectively and MTT assay was performed by adding 20 μl MTT (5 mg/ml) for 4 h. When the MTT incubation was completed, the supernatants were removed. 150 μl dimethyl sulfoxide (DMSO) was added to each well. The A value of each well was measured with a microplate reader at 570 nm 15 min later. All experiments were performed in triplicate. The control was LoVo-neo cell group.

### *Cell-cell adhesion assay*

Cell-cell adhesion assays were performed using 96-well plates. The cells were cultured in 96-well plates and in confluence without vacant space. Other homotypic cells were harvested with 0.25 % trypsin and resuspended to a density of $10^5$ cells/ml in RPMI-1640 without FCS. Then the cells of 100 μl were added into each well with already cultured homotypic cells and recoverd for 60 min,90 min at 37 ℃. Non-adherent cells were collected by gentle washing with PBS and the washed cells were counted. The number of cell-cell adhesion was calculated using the following formula: The number of cell-cell adhesion=total number of added cells- the number of cells being washed. The experments were performed in triplicate and repeated three times. The control was LoVo-neo cell group.

### *Cell-cell aggregation assay*[17]

12-well plate was coated with 1 % agar. And then single cell suspension ($10^5$/ml) was washed by PBS three time after the cells were detached from the culture flasks with 0.25 % trypsin. The cells (1 ml) were added to 12-well plate and incubated at 37 ℃ with rotary shaking (70 r/min) for 5 h. The number of single cell was counted by haemocytometer. The cell-cell aggregation rate was then measured as ((total number of cells- single cells)/(total number of cells))×100 %.

### *Cell-matrix adhesion*[18]

96-well plates were incubated with 75 μl fibronectin (50 μg/ml) for 45 min and blocked with BSA(10 mg/ml). The cells were harvested as described for cell-cell adhesion assay. The cells ($10^5$ cells/ml) of 100 μl were added to each well and allowed to attach 2 h at 37 ℃. After washed with PBS twice to withdraw the non-adherent cells, 20 μl MTT was added for 4 h and 200 μl DMSO was added as above. The value of each well was measured with a microplate reader at 570 nm 15 min later. The experments were performed in triplicate. The control was LoVo-neo cell group.

### *In vitro invasion assay*

This assay was based on the principle of Boyden chamber[19]. The top and bottom of Boyden chamber (Corning Company) were separated by polycarbonate filter with 8 μm pore size. The top chamber was prepared by coating the filter with 50 μg of diluted matrigel and incubated for 30 min. The bottom chamber was prepared with 5 % FBS as a chemoattactant. After 24 h, 48 h incubation, the noninvasive cells were removed with a cotton swab. The cells that had migrated through the membrane and stuck to the lower surface of the membrane were fixed with methanol and stained with hematoxylin. For quantification, the cells were counted under a microscope in five predetermined fields at ×200. The control was LoVo-neo cell group.

### *Monolayer cells invasion assay*

ECV304 cells were cultured in cover slip and confluence without vacant space. LoVo-KAI1 cells were harvested with 0.25 % trypsin and resuspended to a density of $10^5$ cells/ml in RPMI-1640 with 2 % FBS and $10^5$ cells were added to the surface of ECV304 cells. After interaction for 24 h, the cells were washed with PBS and fixed immediately with 95 % ethanol. The cells that had migrated through the ECV304 cells and grown under ECV304 cells were counted. For quantification, the cells were counted under a microscope in five random fields at ×200. The experments were performed in triplicate and the control was LoVo-neo cell group.

### *Statistical analysis*

The comparison was made using Student *t*-test with a single contrast of LoVo-neo. The *P* value <0.05 was considered to be significant.

## RESULTS

### *Transfection of KAI1 cDNA and selection of stable clones*

To clarify whether KAI1 could suppress colorectal cancer

invasion and metastasis, we transfected KAI1 full-length cDNA into colorectal carcinoma LoVo cell lines. An expression vector was transfected as a negative control. After transfection and G418 selection for two weeks, 10 of each growing clone were picked and screened to confirm the transgene by *in situ* hybridization and immunohistochemistry. The probes for ISH were about 1 000 bp. (Figure 1). The blot hybridization was used to evaluate the efficiency of Dig-labeling probe (Figure 2). KAI1 mRNA expression in LoVo-KAI1 cell was located in the cytoplasm by *in situ* hybridization. LoVo-KAI1 cells were full of brown granules, but the LoVo-neo cells were negative (Figure 3). KAI1 protein expression was detected by immunohistochemistry and located in the cytoplasm and membrane. LoVo-KAI1 cells displayed positive immunostaining and LoVo-neo cells displayed negative staining (Figure 4). The results suggested that KAI1 was expressed in mRNA and protein level.

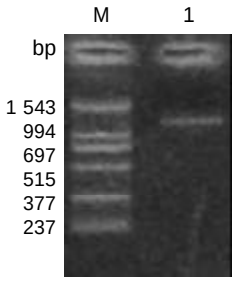


**Figure 1** 1 % gelose electrophoretogram of the product of PCR (1 030 bp). M: PCR marker; 1: PCR procuct.

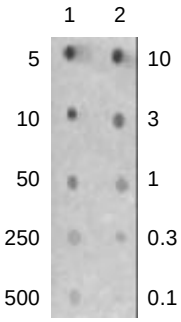


**Figure 2** Blot hybridization of Dig-labeled probe to show the labeling efficiency. Column 1: Dig-labeling probe; Column 2: standard control (unit: pg/μl).

### *Growth curve*

Growth curve showed LoVo-KAI1 cells and LoVo-neo cells existing no difference in proliferation ability (Figure 5). The result demonstrated that KAI1 gene had no effect on cell proliferation ability.

### *Cell-cell adhesion assay*

After interaction of homotypic cells in 60 min and 90 min, cell-cell adhesion was analyzed (Figure 6). These data suggested KAI1 gene could increase adhesion of homotypic cells.

### *Cell-cell aggregation assay*

Aggregation observed in the LoVo-KAI1 cells was very different from that of the LoVo-neo cells. The LoVo-KAI1 cells formed large multicellular aggregates containing many cells, whereas the aggregates formed by LoVo-neo cells were much smaller and rarely contained more than a few cells (Figure 7).The number of LoVo-KAI1 cells aggregation (64.8±4.4) was much larger than that of LoVo-neo cells (58.6±3.5) ($P$<0.05).

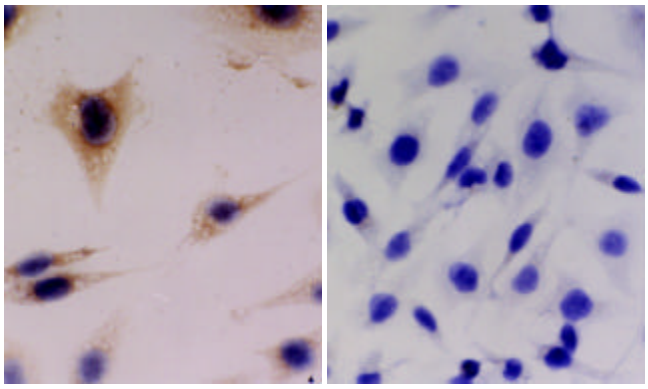

**Figure 3** Expression of KAI1 in LoVo-KAI1 cell and LoVo-neo cell by *in situ* hybridization. The left picture: Expression of LoVo-KAI1 cells (×400) showed that the positive expression (brown granule) located in cytoplasm. The right picture: Expression of LoVo-neo cells (×400) was negative.

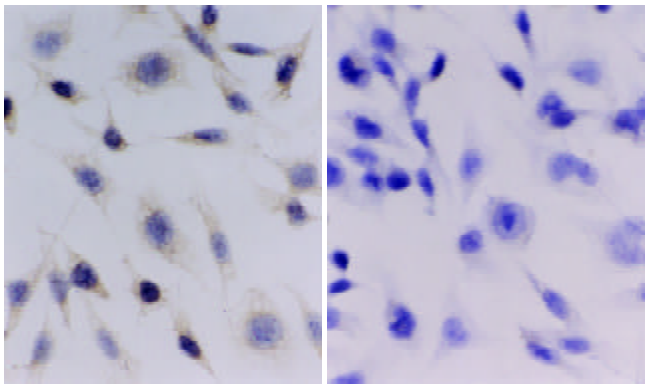

**Figure 4** Expression of CD82 in LoVo-KAI1 cells and LoVo-neo cells by immunohistochemistry. The left picture: Detection of LoVo-KAI1 cells (×400) was positive, the cytoplasm and the membrane were stained brown. The right picture: Detection of LoVo-neo cells (×400) was negative.

### *Cell-matrix adhesion assay*

All LoVo-neo cells attached to fibronectin and the surface of fibronectin appeared the phenomena of degradation while most LoVo-KAI1 cells attached to fibronectin and no degradation occurred. MTT assay showed $OD_{570}$ in LoVo-KAI1 cells was 0.164±0.011 and $OD_{570}$ in LoVo-neo cells was 0.499±0.023. Attachment of LoVo-neo cells to fibronectin were demonstrated to be much higher compared to attachment of LoVo-KAI1 cells ($P$<0.01).

### *In vitro invasion assay*

An *in vitro* cell invasion assay was performed based on the principle of the Boyden chamber assay. The matrigel matrix served as a reconstituted basement membrane *in vitro*. The number of cells migrating through the Matrigel matrix was counted and the result was presented in Figure 8, 9. The LoVo-KAI1 cells showed significantly reduced invasiveness as compared with LoVo-neo cells ($P$<0.01). These data indicated that the enhanced expression of KAI1in LoVo-KAI1 cells was associated with reduced invasive ability.

### *Monolayer cells invasion assay*

After cultured for 24 h, some tumor cells had invaded the ECV304 cells and migrated through the monolayer cells of ECV304. The invasive number of LoVo-KAI1 cells was 6.33±1.74 and that of LoVo-neo was 17.67±4.73. The invasive ability of the LoVo-KAI1 cells was significantly reduced compared with that of the LoVo-neo cells ($P$<0.05).

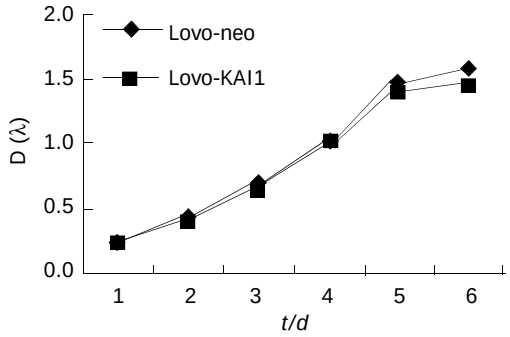


**Figure 5** Growth curve of LoVo-KAI1 and LoVo-neo ($P$<0.05).

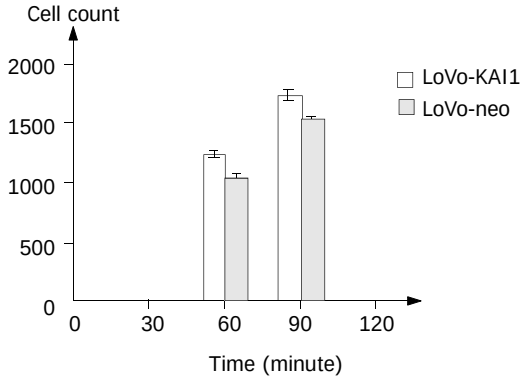


**Figure 6** Adhesion of homotypic cells: The cell-cell adhesion ability in LoVo-KAI1 cells was significantly increased as compared with that of LoVo-neo cells ($P$<0.01).

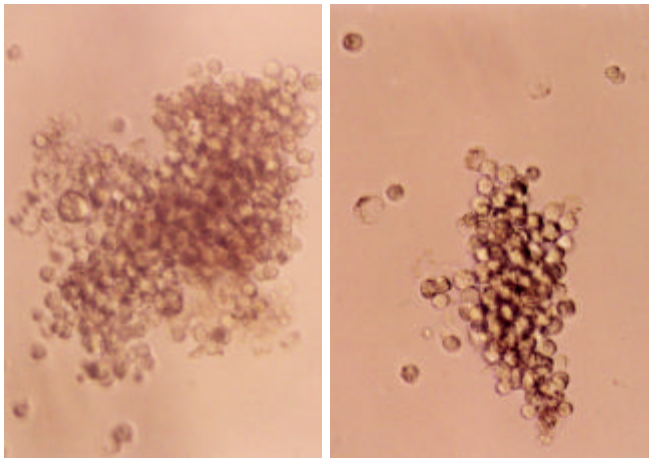

**Figure 7** The cells aggregation pictures. The left picture: The LoVo-KAI1 cells formed large multicellular aggregates. The right picture: The LoVo-neo cells formed smaller aggregates.

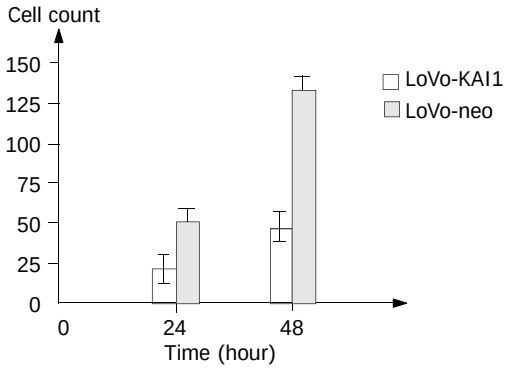


**Figure 8** The invasion assay: The invasive number of LoVo-KAI1 cells was significantly reduced compared with that of LoVo-neo cells ($P$<0.01).

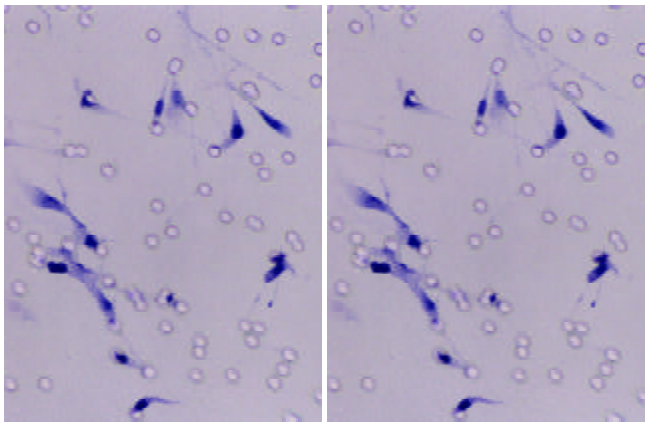

**Figure 9** The invasion ability of LoVo-KAI1 cells and LoVo-neo cells by modified Boyden chamber. The left picture: LoVo-KAI1 cell invasion picture (×200). The right picture: LoVo-neo cell invasion picture (×200).

## DISCUSSION

Loss of the function of metastasis suppressor genes is an important step in the progression of a tumor type. KAI1 is thought to be one of such metastasis suppressor genes because it has been shown to suppress the ability of human prostatic cancer cells to metastasize when the tumor is transplanted into nude mice[1] and because KAI1 mRNA expression is reduced in advanced pancreatic cancer[20], it enables the pancreatic cancer cells to spread to lymph nodes and distant organs. Furthermore, transfer of the KAI1 gene into mammary cancer cells has been shown to lead to suppression of their metastatic potential, whereas their primary tumor growth is not affected.

In our previous studies, KAI1 gene expression at protein level was inversely correlated with the metastatic potential of some established colorectal carcinoma cell lines. Maurer *et al* also demonstrated that the progression of colorectal cancer was associated with decreased expression of KAI1[21]. To further elucidate the effect of KAI1 on colorectal carcinoma cell behavior, we transfected KAI1 cDNA into highly malignant colon adenocarcinoma cell lines, LoVo, which have low level of endogenous KAI1 expression. Consistent with the studies of prostatic cancer[2], breast cancer[12] cells by Dong and Yang, our data also indicated that KAI1 expression did not alter *in vitro* cell proliferation.

To determine if KAI1 expression was reflected in changes of intercellular adhesion, we used cell-cell adhesion assay and cell-cell aggregation assay. We found KAI1 could increase homotypic cells adhesion and the transfectants formed large multicellular aggregates than non-transfected cells. In terms of cell-matrix, our results showed that KAI1 could reduce the transfected cells adhesion to fibronectin as compared with the controls. Member of the TM4SF family of proteins associated with each other and specific integrins[22], suggesting that they might be involved in cell-cell and cell-matrix interactions. Current thinking suggests that these interactions are involved in the formation of multiprotein complexes within the cell membrane that include cell surface receptors, specific integrins and TM4SF proteins. Consequently, a reduced expression of TM4SF proteins might reasonably be expected to have profound effects on cell-cell and cell-matrix interactions. An important avenue of further investigation will be to determine precisely the functions and location of TM4SF-integrin complexes. In this context, Berditchevski[23] has recently provided evidence that TM4SF can modulate integrin signaling and point to a mechanism by which TM4SF proteins regulate cell adhesion.

Our data showed KAI1 could decrease invasive ability in

the transfected cells to a reconstituted basement membrane and endothelium compared to the controls. And there is also accumulated evidence that KAI1 is involved in the reduction of invasive tumor cells. Imai demonstrated that decreased KAI1 gene expression might be associated with increased invasive ability of oral squamous cell carcinoma[24]. Takaoka' s study also suggested that reduced KAI1 gene expression might contribute to the invasiveness and metastatic ability of colon cancer cells[25]. How does reduced TM4SF expression cause changes of invasive ability in tumor cells? It was hypothesized that tetraspanins might be implicated in the assembly of integrin-containing signaling complexes, thus modulating the function of integrin receptors in cell migration[26]. Sugiura' s results indicated that integrin-tetraspanin protein complexes played an important role in regulating protrusive activity of the tumor cells and contributed to ECM-induced production of MMP-2, and as a consequence, the invasive ability of cells[27].

Our *in vitro* study are consistent with *in vivo* observations that reduced KAI1 expression is associated with invasive human colorectal carcinoma. Muneyuki and Lombardi found that KAI1 expression was closely correlated with clinicopathological factors for colorectal cancers and appeared to be a useful prognostic marker[28-30].

KAI1 has been extensively studied for its involvement in the progression of different human cancers. The mechanism of down-regulation is also analyzed although it exists much debate. Mashimo recently found a putative p53 consensus-binding site within the promoter region of KAI1 and demonstrated that the loss of p53 function, which is commonly observed in many types of cancer, leads to the down-regulation of KAI1 gene, which may result in the progression of metastasis[31]. But Uzawa' s data suggest that the down-regulation of KAI1 is not associated with either mutation, allelic loss, methylation of the promoter, or p53 regulation[32]. Our previous study also demonstrated that mutation of KAI1 gene, methylation of CpG islands and abnormality of p53 were not related to low expression of KAI1.

Our results demonstrated a significantly increased adhesion to homotypic cells and decreased adhesion to extracellular matrix components and lower level of invasiveness. In conclusion, KAI1 has a close relationship with tumor adhesion and invasion and the effect of KAI1 appears to be directly targeted on tumor metastasis. Through our studies, we wish colorectal carcinoma cells would be more homotypical adheson, less adhesive to matrix, less invasive[33] that are necessary for metastasis.

## REFERENCES


1 **Dong JT**, Lamb PW, Rinker-Schaeffer CW, Vukanovic J, Ichikawa T, Isaacs JT, Barrett JC. KAI1, a metastasis suppressor gene for prostate cancer on human chromosome 11p11.2. *Science* 1995; **268**: 884-886

2 **Dong JT,** Isaacs WB, Barrett JC, Isaacs JT. Genomic organization of the human KAI1 metastasis-suppressor gene. *Genomics* 1997; **41**: 25-32

3 **Petty HR**, Worth RG, Todd R F 3rd. Interactions of integrins with their partner proteins in leukocyte membranes. *Immunol Res* 2002; **25**: 75-95

4 **Maecker HT**, Todd SC, Levy S. The tetraspanin superfamily: molecular facilitators. *FASEB J* 1997; **11**: 428-442

5 **White A**, Lamb PW, Barrett JC. Frequent downregulation of the KAI1(CD82) metastasis suppressor protein in human cancer cell lines. *Oncogene* 1998; **16**: 3143-3149

6 **Okochi H**, Mine T, Nashiro K, Suzuki J, Fujita T, Furue M. Expression of tetraspans transmembrane family in the epithelium of the gastrointestinal tract. *J Clin Gastroenterol* 1999; **29**: 63-67

7 **Adachi M**, Taki T, Konishi T, Huang CI, Higashiyama M, Miyake M. Novel staging protocol for non-small-cell lung cancers according to MRP-1 / CD9 and KAI1 / CD82 gene expression. *J Clin Oncol* 1998; **16**: 1397-1406

8 **Rubinstein E**, Le Naour F, Lagaudriere Gesbert C, Billard M, Conjeaud H, Boucheix C. CD9, CD63, CD81, and CD82 are components of a surface tetraspan network connected to HLA-DR and VLA integrins. *Eur J Immunol* 1996; **26**: 2657-2665

9 **Bienstock RJ**, Barrett JC. KAI1, a prostate metastasis suppressor: prediction of solvated structure and interactions with binding partners; integrins, cadherins, and cell-surface receptor proteins. *Mol Carcinog* 2001; **32**: 139-153

10 **Hashida H,** Takabayashi A, Tokuhara T, Taki T, Keiichi K, Kohno N, Yamaoka Y, Migake M. Integrin alpha3 expression as a prognostic factor in colon cancer: association with MRP-1 / CD9 and KAI1 / CD82. *Int J Cancer* 2002; **97**: 518-525

11 **Liu FS**, Chen JT, Dong JT, Hsieh YT, Lin AJ, Ho ES, Hung MJ, Lu CH. KAI1 metastasis suppressor gene is frequently down-regulated in cervical carcinoma. *Am J Pathol* 2001; **159**: 1629-1634

12 **Yang X**, Wei LL, Tang C, Slack R, Mueller S, Lippman ME. Overexpression of KAI1 suppresses *in vitro* invasiveness and *in vivo* metastasis in breast cancer cells. *Cancer Res* 2001; **61**: 5284-5288

13 **Friess H**, Guo XZ, Tempia Caliera AA, Fukuda A, Martignoni ME, Zimmermann A, Korc M, Buchler MW. Differential expression of metastasis-associated genes in papilla of vater and pancreatic cancer correlates with disease stage. *J Clin Oncol* 2001; **19**: 2422-2432

14 **Miyazaki T**, Kato H, Shitara Y, Yoshikawa M, Tajima K, Masuda N, Shouji H, Tsukada K, Nakajima T, Kuwano H. Mutation and expression of the metastasis suppressor gene KAI1 in esophageal squamous cell carcinoma. *Cancer* 2000; **89**: 955-962

15 **Liu FS**, Dong JT, Chen JT, Hsieh YT, Ho ES, Hung MJ. Frequent down-regulation and lack of mutation of the KAI1 metastasis suppressor gene in epithelial ovarian carcinoma. *Gynecol Oncol* 2000; **78**: 10-15

16 **Tagawa K**, Arihiro K, Takeshima Y, Hiyama E, Yamasaki M, Inai K. Down-regulation of KAI1 messenger RNA expression is not associated with loss of heterozygosity of the KAI1 gene region in lung adenocarcinoma. *Jpn J Cancer Res* 1999; **90**: 970-976

17 **Whittard JD**, Akiyama SK. Activation of beta1 integrins induces cell-cell adhesion. *Exp Cell Res* 2001; **263**: 65-76

18 **Jackson P**, Kingsley EA, Russell PJ. Inverse correlation between KAI1 mRNA levels and invasive behaviour in bladder cancer cell lines. *Cancer Lett* 2000; **156**: 9-17

19 **Itoh F**, Yamamoto H, Hinoda Y, Imai K. Enhanced secretion and activation of matrilysin during malignant conversion of human colorectal epithelium and its relationship with invasive potential of colon cancer cells. *Cancer* 1996; **77**: 1717-1721

20 **Guo X**, Friess H, Graber HU, Kashiwagi M, Zimmermann A, Korc M, Buchler MW. KAI1 expression is up-regulated in early pancreatic cancer and decreased in the presence of metastases. *Cancer Res* 1996; **56**: 4876-4880

21 **Maurer CA**, Graber HU, Friess H, Beyermann B, Willi D, Netzer P, Zimmermann A, Buchler MW. Reduced expression of the metastasis suppressor gene KAI1 in advanced colon cancer and its metastases. *Surgery* 1999; **126**: 869-880

22 **Shibagaki N**, Hanada K, Yamashita H, Shimada S, Hamada H. Overexpression of CD82 on human T cells enhances LFA-1 / ICAM-1-mediated cell-cell adhesion: functional association between CD82 and LFA-1 in T cell activation. *Eur J Immunol* 1999; **29**: 4081-4091

23 **Berditchevski F**, Odintsova E. Characterization of integrin-tetraspanin adhesion complexes: role of tetraspanins in integrin signaling. *J Cell Biol* 1999; **146**: 477-492

24 **Imai Y**, Sasaki T, Shinagawa Y, Akimoto K, Fujibayashi T. Expression of metastasis suppressor gene (KAI1 / CD82) in oral squamous cell carcinoma and its clinico-pathological significance. *Oral Oncol* 2002; **38**: 557-561

25 **Takaoka A**, Hinoda Y, Satoh S, Adachi Y, Itoh F, Adachi M, Imai K. Suppression of invasive properties of colon cancer cells by a metastasis suppressor KAI1 gene. *Oncogene* 1998; **16**: 1443-1453

26 **Hemler ME**, Mannion BA, Berditchevski F. Association of TM4SF proteins with integrins: relevance to cancer. *Biochim Biophys Acta* 1996; **1287**: 67-71

27 **Muneyuki T**, Watanabe M, Yamanaka M, Shiraishi T, Isaji S. KAIL / CD82 expression as a prognosic factor in sporadic colorectal cancer. *Anticancer Res* 2001; **21**: 3581-3587
28 **Mikami T**, Ookawa K, Shimoyama T, Fukuda S, Saito H, Munakata A. KAI1, CAR, and Smad4 expression in the progression of colorectal tumor. *J Gastroenterol* 2001; **36**: 465-469
29 **Lombardi DP**, Geradts J, Foley JF, Chiao C, Lamb PW, Barrett JC. Loss of KAI1 expression in the progression of colorectal cancer. *Cancer Res* 1999; **59**: 5724-5731
30 **Sugiura T**, Berditchevski F. Function of alpha3 beta1-tetraspanin protein complexes complexes in tumor cell invasion. Evidence for the role of the complexes in production of matrix metalloproteinase 2(MMP-2). *J Cell Biol* 1999; **146**: 1375-1389
31 **Mashimo T**, Watabe M, Hirota S, Hosobe S, Miura K, Tegtmeyer PJ, Rinker-Shaeffer CW, Watabe K. The expression of the KAI1 gene, a tumor metastasis suppressor, is directly activated by p53. *Proc Natl Acad Sci USA* 1998; **95**: 11307-11311
32 **Uzawa K**, Ono K, Suzuki H, Tanaka C, Yakushiji T, Yamamoto N, Yokoe H, Tanzawa H. High prevalence of decreased expression of KAI1 metastasis suppressor in human oral carcinogenesis. *Clin Cancer Res* 2002; **8**: 828-835
33 **Geradts J**, Maynard R, Birrer MJ, Hendricks D, Abbondanzo SL, Fong KM, Barrett JC, Lombardi DP. Frequent loss of KAI1 expression in squamous and lymphoid neoplasms. An immunohistochemical study of archival tissues. *Am J Pathol* 1999; **154**: 1665-1671

**Edited by** Wu XN

P.O.Box 2345, Beijing 100023,China
Fax: +86-10-85381893
E-mail: wjg@wjgnet.com www.wjgnet.com

World J Gastroenterol 2003;9(6):1237-1240
World Journal of Gastroenterology
Copyright ©2003 by The WJG Press ISSN 1007-9327

• COLORECTAL CANCER •

# Cyclooxygenase-2 expression and angiogenesis in colorectal cancer

Bin Xiong, Tao-Jiao Sun, Hong-Yin Yuan, Ming-Bo Hu, Wei-Dong Hu, Fu-Lin Cheng

**Bin Xiong, Tao-Jiao Sun, Hong-Yin Yuan, Ming-Bo Hu, Wei-Dong Hu, Fu-Lin Cheng,** Department of Oncology, Affiliated Zhongnan Hospital of Wuhan University, Wuhan 430071, Hubei Province, China
**Supported by** Hubei Province Natural Science Foundation, No.2000J054
**Correspondence to:** Dr. Bin Xiong, Department of Oncology, Affiliated Zhongnan Hospital of Wuhan University,Wuhan 430071, Hubei Province, China. xbxh@public.wh.hb.cn
**Telephone:** +86-27-87325716
**Received:** 2003-01-11 **Accepted:** 2003-03-10

## Abstract

**AIM:** Cyclooxygenase-2 is involved in a variety of important cellular functions, including cell growth and differentiation, cancer cell motility and invasion, angiogenesis and immune function. However, the role of cyclooxygenase-2 as an angiogenic factor in colorectal cancer tissue is still unclear. We investigated the relationship between cyclooxygenase-2 and angiogenesis by analyzing the expression of cyclooxygenase-2 in colorectal cancer tissue, as well as its association with vascular endothelial growth factor (VEGF) and microvascular density (MVD).

**METHODS:** The expression of cyclooxygenase-2, VEGF, as well as MVD was detected in 128 cases of colorectal cancer by immunohistochemical staining. The relationship between the cyclooxygenase-2 and VEGF expression and MVD was evaluated. Our objective was to determine the effect of cyclooxygenase-2 on the angiogenesis of colorectal cancer tissue.

**RESULTS:** Among 128 cases of colorectal cancer, 87 were positive for cyclooxygenase-2 (67.9 %), and 49 for VEGF (38.3 %), respectively. The microvessel counts ranged from 23 to 142, with a mean of 51.7 (standard deviation, 19.8). The expression of cyclooxygenase-2 was correlated significantly with the depth of invasion, stage of disease, metastasis (lymph node and liver), VEGF expression and MVD. Patients in T3-T4, stage III-IV and with metastasis had much higher expression of cyclooxygenase-2 than patients in T1-T2, stage I-II and without metastasis ($P<0.05$). The positive expression rate of VEGF (81.6 %) in the cyclooxygenase-2 positive group was higher than that in the cyclooxygenase-2 negative group (18.4 %, $P<0.05$). Also, the microvessel count (56±16) in cyclooxygenase-2 positive group was significantly higher than that in cyclooxygenase-2 negative group (43±12, $P<0.05$). The microvessel count in tumors with positive cyclooxygenase-2 and VEGF was the highest (60±18, 41-142, $P<0.05$), whereas that in tumors with negative cyclooxygenase-2 and VEGF was the lowest (39±16, 23-68, $P<0.05$).

**CONCLUSION:** Cyclooxygenase-2 may be associated with tumor progression by madulating the angiogenesis in colorectal cancer tissue and used as a possible biomarker.

Xiong B, Sun TJ, Yuan HY, Hu MB, Hu WD, Cheng FL. Cyclooxygenase-2 expression and angiogenesis in colorectal cancer. *World J Gastroenterol* 2003; 9(6): 1237-1240
http://www.wjgnet.com/1007-9327/9/1237.asp

## INTRODUCTION

Angiogenesis has been postulated to play an important role in the development of malignant tumors[1-5]. Increased vascularity may allow not only an increase in tumor growth but also a greater chance of hematogenous tumor embolization[6]. An association between poor prognosis and increase in microvascular density (MVD) of tumor has been reported in certain tumors[7-10]. This neoangiogenesis depends on the production of angiogenic factors by tumor cells and normal cells[11-15].

Cyclooxygenase (COX) is a key enzyme in prostaglandin biosynthesis[16]. Two COX isoforms, COX-1 and COX-2, have been identified. COX-1 is constitutively expressed and involved in general cell functions, whereas COX-2 is an inducible enzyme that is up-regulated in response to various stimuli, including growth factors and mitogens[17-22]. An enhanced expression of COX-2 has been found in many tumors, such as the lung, the breast, the esophagus and colon cancer[23-26]. Recent studies have demonstrated that COX-2 could affect carcinogenesis via several different mechanisms[27-35]. COX-2 has been also reported to induce angiogenesis[36-39]. COX-2 may be related to development of colorectal cancer, however, its association with angiogenesis in colorectal cancer tissue still remains unclear. To determine the role of COX-2 expression in angiogenesis of colorectal cancer, we examined the VEGF and MVD in colorectal cancer tissue, and then compared the findings with the expression of COX-2 protein.

## MATERIALS AND METHODS

### *Patients*

A total of 128 cases of colorectal adenocarcinoma patients who had undergone surgical resection in the Affiliated Zhongnan Hospital of Wuhan University (Wuhan, China) from January 1999 to September 2002 were included, COX-2, VEGF immunohistochemical staining and MVD counting were performed. There were 73 men and 55 women, and their age ranged from 23 to 74 years (means, 56±11 years). Among the 128 patients, 26 were well differentiated adenocarcinoma, 57 moderately differentiated adenocarcinoma and 45 poorly differentiated adenocarcinoma. According to Duke' s staging criteria, 37 cases were stage I,41 stage II, 39 stage III and 11 stage IV.

### *Methods*

Immunohistochemistry: All the tissue specimens were fixed in 100 $mL \cdot L^{-1}$ neutral formalin and embedded in paraffin. Five-μm thick sections were dewaxed in xylene and dehydrated in ethanol. Tissue sections were washed three times in 0.05 $moL \cdot L^{-1}$ PBS, and incubated in endogenous peroxidase blocking solution. Non-specific antibody binding was blocked by pretreatment with PBS containing 5 $g \cdot L^{-1}$ bovin serum albumin. Sections were then rinsed in PBS and incubated overnight at 4 ℃ with diluted anti-COX-2, anti-VEGF and anti-CD34 antibodies. The steps were performed using immunostain kit according to the manufacturer' s

instructions. PBS was used as substitutes of antibody for negative control. The sections were examined under light microscope. Anti-VEGF polyclonal antibody and anti-CD34 monoclonal antibody were purchased from Bosden Co. (Wuhan, China). Anti-COX-2 polyclonal antibody was purchased from Santa Cruz Co. (USA). S-P detection kit was purchased from Fuzhou Maixin Co. (Fuzhou, China). Anti-COX-2 polyclonal antibody was diluted to 1:75. Anti-VEGF polyclonal antibody and anti-CD34 monoclonal antibody were impromptu type.

Results: Positive evaluation for COX-2 was performed according to the following scoring system[16]: staining intensity was graded as weak (1), moderate (2), or strong (3), and area of staining positivity as <10 percent (0) of all cells stained in the cytoplasm as viewed by microscope, 10 to 40 percent (1), 40 to 70 percent (2), or ⩾70 percent (3). A total for grade and area of 3 or more was defined as positive expression and less than 3 as negative. Positive signal for VEGF was located in the cytoplasm or/and cell membrane[2]. Immunoreactivity was graded as follows: +, ⩾10 percent stained tumor cells; -, <10 percent stained tumor cells[2]. The microvessel counting procedures have been described in the published studies[2]. Briefly, the stained sections were screened at a magnification of ×100 (×10 objective and ×10 ocular lens) under a light microscope to identify 3 regions of the section with the highest microvessel density. Microvessels were counted in these areas at a magnification of ×200, and the average numbers of microvessels were recorded. The average number is known as MVD of the tumor.

### *Statistical analysis*

The difference between each group was analyzed by Chi-square test. $P<0.05$ was considered significant.

## RESULTS

### *COX-2 expression in colorectal cancer and clinicopathologic findings*

COX-2 was expressed in the cytoplasm of cancer cells (Figure 1). COX-2 expression in primary tumor was noted in 67.9 % (87/128). The correlation between COX-2 expression and the clinicopathologic findings is shown in Table 1. The expression of COX-2 was significantly correlated with depth of invasion, stage of disease, metastasis (lymph node and liver). Patients in T3-T4, stage III-IV, with metastasis had much higher COX-2 expression than patients in T1-T2, stage I-II, without metastasis ($P<0.05$). The expression of COX-2 was not correlated with age, gender and differentiation degree of the tumor ($P>0.05$).

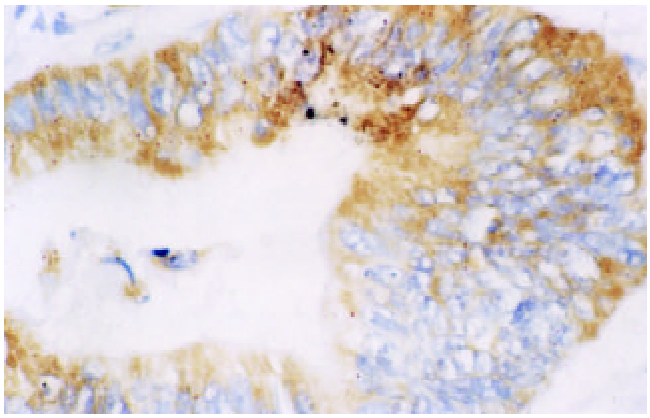

**Figure 1** Expression of COX-2 mainly in cytoplasm of tumor cells, S-P, ×400.

**Table 1** Clinicopathologic characteristics of colorectal cancer with expression of COX-2

| Variable | *n* | COX-2 Positive *n*(%) | COX-2 Negative *n*(%) |
|---|---|---|---|
| Sex | | | |
| Male | 73 | 50(68.5) | 23(31.5) |
| Female | 55 | 37(67.3) | 18(32.7) |
| Age(y) | | 54±12 | 56±15 |
| Histological differentiation | | | |
| Well | 26 | 17(65.4) | 9 (34.6) |
| Moderate | 57 | 40(70.2) | 17(29.8) |
| Poor | 45 | 30(66.7) | 15(33.3) |
| Depth of invasion | | | |
| T1-T2 | 81 | 48(59.3) | 33(40.7) |
| T3-T4 | 47 | 39(83.0) | 8 (17.0)[a] |
| Metastasis | | | |
| Present | 50 | 42(84.0) | 8 (16.0) |
| Absent | 78 | 45(57.7) | 33(42.3)[a] |
| Duke's stage | | | |
| A | 37 | 15(40.5) | 22(59.5) |
| B | 41 | 28(68.3) | 13(31.7) |
| C+D | 50 | 44(88.0) | 6 (12.0)[a] |
| VEGF expression | | | |
| Positive | 49 | 40(81.6) | 9 (18.4) |
| Negative | 79 | 47(59.5) | 32(40.5)[a] |
| MVD ($\bar{x}\pm s$) | | 56±16 | 43±12[a] |

[a]$P<0.05$, *vs* positive.

### *Relationship between COX-2 and VEGF expression and MVD*

VEGF was localized mainly in the cytoplasm and cell membrane of the tumor cells (Figure 2). VEGF expression was detected in 49 tumors (38.3 %), and COX-2 expression was correlated closely with VEGF expression (Table 1). The positive expression rate of VEGF (81.6 %) in the COX-2 positive group was higher than that in the COX-2 negative group (18.4 %) ($P<0.05$).

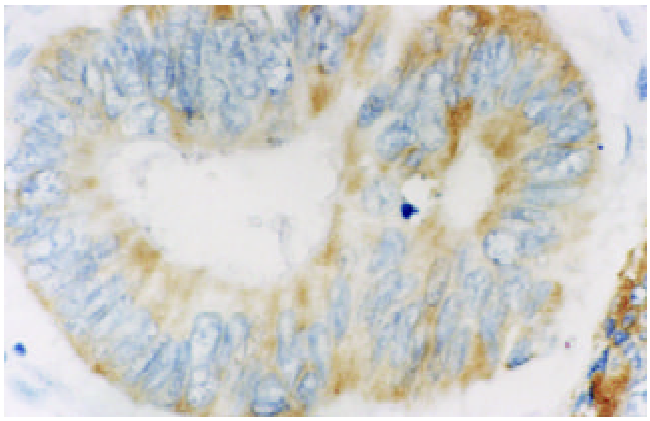

**Figure 2** VEGF expression mainly in cytoplasm and membrane of tumor cell, S-P, ×400.

The number of microvessel counts in all cases was 23-142 ($\bar{x}\pm s$, 50±19). Moreover, the microvessel counts were 56±16 in COX-2 positive tumors and 43±12 in COX-2 negative tumors ($P<0.05$, Table 1). COX-2 expression, VEGF expression and MVD were significantly correlated with one another ($r$=0.5635, 0.2812, 0.5253, respectively. $P<0.05$). The microvessel counts in tumors with both positive COX-2 and VEGF were the highest (60±18, 41-142; $P<0.05$).The

microvessel counts in tumors with both negative COX-2 and VEGF were the lowest (39±16, 23-68; $P<0.05$). The microvessel counts in tumors with positive COX-2 and negative VEGF were 50±16 (29-130), and that in tumors with negative COX-2 and positive VEGF were 51±18 (30-132), lower than that in tumors with both positive COX-2 and VEGF ($P<0.05$). The microvessel counts in tumors with positive COX-2 and negative VEGF were not different from that in tumors with negative COX-2 and positive VEGF ($P>0.05$).

## DISCUSSION

Angiogenesis is essential for tumor growth and metastasis. The process of angiogenesis is the outcome of an imbalance between positive and negative angiogenic factors produced by both tumor cells and normal cells. Numerous angiogenic factors have been described. Of these, VEGF plays a key role in the angiogenesis in colorectal cancer[1-15]. VEGF is a multifunctional cytokine, and has direct relationship with angiogenesis. The factors that regulate VEGF expression in tumor and non-tumor cells have now been elucidated[10-28]. COX-2 is an inducible enzyme catalyzing the conversion of arachidonic acid to biologically active prostanoids. COX-2 modulates the growth and function of many cells, including those with malignant transformation. The over-expression of COX-2 has been reported in tissue from patients with different carcinoma, and is believed to play a role in tumor transformation and progression, as well as in tumor regression[23-33]. Recent experimental studies showed that COX-2 could inhibit cell apoptosis, regulate angiogenesis, and was associated with matrix metalloproteinases (MMP)[16-48]. Uefuji *et al*[45] studied the correlation of COX-2 and angiogenesis of gastric cancer, and found COX-2 might regulate angiogenesis.

COX-2 was overexpressed in approximatly 80 percent of colorectal cancer cases[16], but the role of COX-2 in angiogenesis of colorectal cancer tissue has not been identified yet. This study found that the expression of VEGF and MVD in positive COX-2 group was significantly higher than that in COX-2 negative group. The expression of COX-2 was significantly correlated with the expression of VEGF. It demonstrated that COX-2 might be correlated indirectly with angiogenesis through an up-regulation of the expression of VEGF. The expression of COX-2 was also significantly correlated with MVD in colorectal cancer. It indicates that COX-2 may modulate angiogenesis directly or indirectly through up-regulating the expression of other angiogenic factors. The microvessel counts in tumors that were both positive COX-2 and VEGF were the highest of all. It suggests that COX-2 and VEGF may co-modulate angiogenesis.

COX-2 expression was detected in 87 tumors (67.9 %). The expression of COX-2 was correlated significantly with the depth of invasion, stage of disease and metastasis (lymph node and liver). Patients in T3-T4, stage C-D and with metastasis had much higher expression of COX-2 than patients in T1-T2, stage A-B and without metastasis ($P<0.05$). It suggests that COX-2 is closely related to the invasion and metastasis of colorectal cancer, and COX-2 may be used as a possible biomarker.

## REFERENCES


1 **Gunsilius E**, Tschmelitsch J, Eberwein M, Schwelberger H, Spizzo G, Kahier CM, Stockhammer G, Lang A, Petzer AL, Gastl G. In vivo release of vascular endothelial growth factor from colorectal carcinomas. *Oncology* 2002; **62**: 313-317

2 **Xiong B**, Gong LL, Zhang F, Hu MB, Yuan HY. TGFβ1 expression and angiogenesis in colorectal cancer tissue. *World J Gastroenterol* 2002; **8**: 496-498

3 **Tsuji T**, Sasaki Y, Tanaka M, Hanabata N, Hada R, Munakata A. Microvessel morphology and vascular endothelial growth factor expression in human colonic carcinoma with or without metastasis. *Lab Invest* 2002; **82**: 555-562

4 **Uthoff SM**, Duchrow M, Schmidt MH, Broll R, Bruch HP, Strik MW, Galandiuk S. VEGF isoforms and mutations in human colorectal cancer. *Int J Cancer* 2002; **101**: 32-36

5 **Shaheen RM**, Tseng WW, Davis DW, Liu W, Reinmuth N, Vellagas R, Wieczorek AA, Ogura Y, McConkey DJ, Drazan KE, Bucana CD, McMahon G, Ellis LM. Tyrosine kinase inhibition of multiple angiogenesis growth factor receptors improves survival in mice bearing colon cancer liver metastasis by inhibition of endothelial cell survival mechanisms. *Cancer Res* 2001; **61**: 1464-1468

6 **Dachs GU**, Tozer GM. Hypoxia modulated gene expression: angiogenesis, metastasis and therapeutic exploitation. *Eur J Cancer* 2000; **36**: 1649-1660

7 **Sumiyoshi Y**, Yamashita Y, Maekawa T, Sakai N, Shirakusa T, Kikuchi M. Expression of CD44, vascular endothelial growth factor, and proliferating cell nuclear antigen in severe venous invasional colorectal cancer and its relationship to liver metastasis. *Surg Today* 2000; **30**: 323-327

8 **Kondo Y**, Arii S, Mori A, Furutani M, Chiba T, Imamura M. Enhancement of angiogenesis, tumor growth, and metastasis by transfection of vascular endothelial growth factor into LoVo human colon cancer cell line. *Clin Cancer Res* 2000; **6**: 622-630

9 **Ellis LM**, Takahashi Y, Liu W, Shaheen RM. Vascular endothelial growth factor in human colon cancer: biology and therapeutic implications. *Oncologist* 2000; **5**(Suppl 1): 11-15

10 **Jia L**, Chen TX, Sun JW, Na ZM, Zhang HH. Relationship between microvessel density and proliferating cell nuclear antigen and prognosis in colorectal cancer. *Shijie Huaren Xiaohua Zazhi* 2000; **8**: 74-76

11 **Teraoka H**, Sawada T, Nishihara T, Yashiro M, Ohira M, Ishikawa T, Nishino H, Hirakawa K. Enhanced VEGF production and decreased immunogenicity induced by TGF-β1 promote liver metastasis of pancreatic cancer. *Br J Cancer* 2001; **85**: 612-617

12 **Mancuso P**, Burlini A, Pruneri G, Goldhirsch A, Martinelli G, Bertolini F. Resting and activated endothelial cells are increased in the peripheral blood of cancer patients. *Blood* 2001; **97**: 3658-3661

13 **Carmeliet P**, Jain RK. Angiogenesis in cancer and other diseases. *Nature* 2000; **407**: 249-257

14 **Liu DH**, Zhang W, Su YP, Zhang XY, Huang YX. Constructions of eukaryotic expression vector of sense and antisense VEGF165 and its expression regulation. *Shije Huaren Xiaohua Zazhi* 2001; **9**: 886-891

15 **Yamauchi T**, Watanabe M, Kubota T, Hasegawa H, Ishii Y, Endo T, Kabeshima Y, Yorozuya K, Yamamoto K, Mukai M, Kitajima M. Cyclooxygenase-2 expression as a new marker for patients with colorectal cancer. *Dis Colon Rectum* 2002; **45**; 98-103

16 **Qiu DK**, Ma X, Peng YS, Chen XY. Significance of cyclooxygenase-2 expression in human primary hepatocellular carcinoma. *World J Gastroenterol* 2002; **8**: 815-817

17 **Wu QM**, Li SB, Wang Q, Wang DH, Li XB, Liu CZ. The expression of COX-2 in esophageal carcinoma and its relation to clinicopathologic characteristics. *Shijie Huaren Xiaohua Zazhi* 2001; **9**: 11-14

18 **Wu HP**, Wu KC, Li L, Yao LP, Lan M, Wang X, Fan DM. Cloning of human cyclooxygenase-2 (COX-2) encoding gene and study of gastic cancer cell transfected with its antisense vector. *Shijie Huaren Xiaohua Zazhi* 2000; **8**: 1211-1217

19 **Cao Y**, Prescott SM. Many actions of cycooxygenase-2 in cellular dynamics and in cancer. *J Cell Physiol* 2002; **190**: 279-286

20 **Koki AT**, Masferrer JL. Celecoxib: A specific COX-2 inhibitor with anticancer properties. *Cancer Control* 2002; **9**(Suppl 2): 28-35

21 **Kakiuchi Y**, Tsuji S, Tsujii M, Murata H, Kawai N, Yasumaru M, Kimura A, Komori M, Irie T, Miyoshi E, Sasaki Y, Hayashi N, Kawano S, Hori M. Cyclooxygenase-2 activity altered the cell-surface carbohydrate antigens on colon cancer cells and enhanced liver metastasis. *Cancer Res* 2002; **62**: 1567-1572

22 **Hida T**, Kozaki K, Ito H, Miyaishi O, Tatematsu Y, Suzuki T, Matsuo K, Sugiura T, Ogawa M, Takahashi T, Takahashi T. Significant growth inhibition of human lung cancer cells both *in vitro* and *in vivo* by the combined use of a selective cyclooxygenase-2 inhibitor, JTE-522, and conventional anticancer agents. *Clin Cancer Res* 2002; **8**: 2443-2447

23 **Yamada H**, Kuroda E, Matsumoto S, Matsumoto T, Yamada T, Yamashita U. Prostaglandin E2 down-regulates viable bacilli calmette-guerin-induced macrophage cytotoxicity against murine bladder cancer cell MBT-2 *in vitro*. *Clin Exp Immunol* 2002; **128**: 52-58

24 **Harizi H**, Juzan M, Pitard V, Moreau JF, Gualde N. Cyclooxygenase-2-issued prostaglandin E2 enhances the production of endogenous IL-10, which down-regulates dendritic cell functions. *J Immunology* 2002; **168**: 2255-2263

25 **Kundu N**, Fulton AM. Selective cyclooxygenase(COX)-1 or COX-2 inhibitors control metastasis disease in a murine model of breast cancer. *Cancer Res* 2002; **62**: 2343-2346

26 **Leahy KM**, Ornberg RL, Wang Y, Zweifel BS, Koki AT, Masferrer JL. Cyclooxygenase-2 inhibition by celecoxib reduces proliferation and induces apoptosis in angiogenic endothelial cells *in vivo*. *Cancer Res* 2002; **62**: 625-631

27 **Hansen-Petrik MB**, McEntee MF, Jull B, Shi H, Zemel MB, Whelan J. Prostaglandin E2 protects intestinal tumors from nonsteroidal anti-inflammatory drug-induced regression in $Apc^{Min/+}$ Mice. *Cancer Res* 2002; **62**: 403-408

28 **Waskewich C**, Blumenthal RD, Li H, Stein R, Goldenberg DM, Burton J. Celecoxib exhibits the greatest potency amongst cyclooxygenase(COX) inhibitors for growth inhibition of COX-2-negative hematopoietic and epithelial cell lines. *Cancer Res* 2002; **62**: 2029-2033

29 **Jones MK**, Szabo IL, Kawanaka H, Husain SS, Tarnawski AS. von Hippel Lindau tumor suppressor and HIF-1α: new targets of NSAIDs inhibition of hypoxia-induced angiogenesis. *FASEB J* 2002; **16**: 264-266

30 **Kvirkvelia N**, Vojnovic I, Warner TD, Athie-Morales V, Free P, Rayment N, Chain BM, Rademacher TW, Lund T, Roitt IM, Delves PJ. Placentally derived prostaglandin E2 acts via the EP4 receptor to inhibit IL-2 dependent proliferation of CTLL-2 T cell. *Clin Exp Immunol* 2002; **127**: 263-269

31 **Adam L**, Mazumdar A, Sharma T, Jones TR, Kumar R. A three-dimensional and temporo-spatial model to study invasiveness of cancer cells by heregulin and prostaglandin E2. *Cancer Res* 2001; **61**: 81-87

32 **Dannhardt G**, Ulbrich H. In-vitro test system for the evaluation of cyclooxygenase-1(COX-1) and cyclooxygenase-2(COX-2) inhibitors based on a single HPLC run with UV detection using bovine aortic coronary endothelial cells(BAECs). *Inflamm Res* 2001; **50**: 262-269

33 **Bae SH**, Jung ES, Park YM, Kim BS, Kim BK, Kim DG, Ryu WS. Expression of cyclooxygenase-2(COX-2) in hepatocellular carcinoma and growth inhibition of hepatoma cell lines by a COX-2 inhibitor, NS-398. *Clin Cancer Res* 2001; **7**: 1410-1418

34 **Yang WL**, Frucht H. Activation of the PPAR pathway induces apoptosis and COX-2 inhibition in HT-29 human colon cancer cells. *Carciniogenesis* 2001; **22**: 1379-1383

35 **Dohadwala M**, Luo J, Zhu L, Lin Y, Dougherty GJ, Sharma S, Huang M, Pold M, Batra RK, Dubinett SM. Non-small cell lung cancer cyclooxygenase-2 dependent invasion is mediated by CD44. *J Biol Chem* 2001; **276**: 20809-20812

36 **Dempke W**, Rie C, Grothey A, Schmoll HJ. Cycloxygenase-2: a novel target for cancer chemotherapy? *J Cancer Res Clin Oncol* 2001; **127**: 411-417

37 **Gilroy DW**, Saunders MA, Wu KK. COX-2 expression and cell cycle progression in human fibroblasts. *Am J Physiol Cell Physiol* 2001; **281**: C188-194

38 **Chen WS**, Wei SJ, Liu JM, Hsiao M, Kou-Lin J, Yang WK. Tumor invasiveness and liver metastasis of colon cancer cells correlated with cyclooxygenase-2(COX-2) expression and inhibited by a COX-2 selective inhibitor, *Etodolac. Int J Cancer* 2001; **91**: 894-899

39 **Rozic JG**, Chakraborty C, Lala PK. Cyclooxygenase inhibitors retard murine mammary tumor progression by reducing tumor cell migration, invasiveness and angiogenesis. *Int J Cancer* 2001; **93**: 497-506

40 **Williams CS**, Tsujii M, Reese J, Dey SK, DuBois RN. Host cyclooxygenase-2 modulates carcinoma growth. *J Clin Invest* 2000; **105**: 1589-1594

41 **Marrogi A**, Pass HI, Khan M, Metheng-Barlow LJ, Harris CC, Gerwin BI. Human meaothelioma sample overexpress both cyclooxygenase-2(COX-2) and inducible nitric oxide synthase (NOS2): *In vitro* antiproliferative effects of a COX-2 inhibitor. *Cancer Res* 2000; **60**: 3696-3700

42 **Uefuji K**, Ichikura T, Mochizuki H. Cyclooxygenase-2 expression is related to prostaglandin biosynthesis and angiogenesis in human gastric cancer. *Clin Cancer Res* 2000; **6**: 135-138

43 **Attiga FA**, Fernandez PM, Weeraratna AT, Manyak MJ, Patierno SR. Inhibitors of prostaglandin synthesis inhibit human prostate tumor cell invasiveness and reduce the release of matrix metalloproteinases. *Cancer Res* 2000; **60**: 4629-4637

44 **Shao J**, Sheng H, Inoue H, Morrow JD, DuBois RN. Regulation of constitutive cyclooxygenase-2 expression in colon carcinoma cells. *J Biol Chem* 2000; **275**: 33951-33956

45 **Masferrer JL**, Leahy KM, Koki AT, Zweifel BS, Settle SL, Woerner BM, Edwards DA, Flickinger AG, Moore RJ, Seibert K. Antiangiogenic and antitumor activities of cyclooxygenase-2 inhibitors. *Cancer Res* 2000; **60**: 1306-1311

46 **Reddy BS**, Hirose Y, Lubet R, Steele V, Kelloff G, Paulson S, Seibert K, Rao CV. Chemoprevention of colon cancer by specific cyclooxygenase-2 inhibitor, Celecoxib, administered during different stages of carcinogenesis. *Cancer Res* 2000; **60**: 293-297

47 **Hsueh CT**, Chiu CF, Kelsen DP, Schwartz GK. Selective inhibition of cyclooxygenase-2 enhances mitomycin-C induced apoptosis. *Cancer Chemother Pharmacol* 2000; **45**: 389-396

48 **Hida T**, Kozaki K, Muramatsu H, Masuda A, Shimizu S, Mitsudomi T, Sugiura T, Ogawa M, Takahashi T. Cyclooxygenase-2 inhibitor induces apoptosis and enhances cytotoxicity of various anticancer agents in non-small cell lung cancer cell lines. *Clin Cancer Res* 2000; **6**: 2006-2011


**Edited by** Zhang JZ

P.O.Box 2345, Beijing 100023,China
Fax: +86-10-85381893
E-mail: wjg@wjgnet.com www.wjgnet.com

World J Gastroenterol 2003;9(6):1241-1245
World Journal of Gastroenterology
Copyright ©2003 by The WJG Press ISSN 1007-9327

• COLORECTAL CANCER •

# Synergistic antitumor effect of TRAIL and doxorubicin on colon cancer cell line SW480

Li-Hong Xu, Chang-Sheng Deng, You-Qing Zhu, Shi-Quan Liu, Dong-Zhou Liu

**Li-Hong Xu, Chang-Sheng Deng, You-Qing Zhu,** Department of Gastroenterology, Zhongnan Hospital of Wuhan University, Wuhan 430071, Hubei Province China
**Shi-Quan Liu,** Department of Oncology, Zhongnan Hospital of Wuhan University, Wuhan 430071, Hubei Province China
**Dong-Zhou Liu,** Department of Nephrology, Renmin Hospotal of Wuhan University, Wuhan 430060, Hubei Province China
**Correspondence to:** Li-Hong Xu, Department of Gastroenterology, Zhongnan Hospital of Wuhan University, Donghu Road 169, Wuhan 430071, Hubei Province China. hqy222@yahoo.com.cn
**Telephone:** +86-27-87330254
**Received:** 2002-12-28 **Accepted:** 2003-02-15

## Abstract

**AIM:** TRAIL (tumor necrosis factor-related apoptosis-inducing ligand) has been reported to specifically induce apoptosis of cancer cells although only a small percentage of cell lines were sensitive to it. Cell lines not responding to TRAIL *in vitro* were said to be more prone to apoptosis when TRAIL was combined with another anticancer agent. Generally, factors affecting drug-sensitivity involve many apoptosis-related proteins, including p53. The expression of wild-type p53 gene was proposed as an important premise for tumor cells responding to chemotherapy. The present study was to investigate the cell killing action of TRAIL on colon cancer cell line SW480, its synergistic effect with doxorubicin, and the possible mechanisms.

**METHODS:** SW480 cells were cultured in the regular condition and incubated with different levels of agents. Morphologic changes in these cells after treatment were observed under phase-contrast microscope and cytotoxicity by TRAIL alone and in combination with doxorubicin was quantified by a 1-day microculture tetrazolium dye (MTT) assay. In addition, flow cytometry assay (FCM) and transmission electron microscopy were used to detect apoptosis among these cells. Variation of p53 protein level among different groups according to concentrations of agents was measured by Western blot assay.

**RESULTS:** (1) SW480 cells were not sensitive to TRAIL, with $IC_{50}$>1 mg·$L^{-1}$ and dose-independent cytotoxicity. (2) SW480 cells were sensitive to doxorubicin at a certain degree, with dose-dependent cytotoxicity and $IC_{50}$=65.25±3.48 μmol·$L^{-1}$. (3) TRAIL could synergize with doxorubicin to kill SW480 cells effectively, which was represented by the boosted killing effect of doxorubicin on theses cells. $IC_{50}$ of doxorubicin against SW480 cells sharply reduced when it was combined with TRAIL. (4) Subtoxic TRAIL (100 μg·$L^{-1}$), combined with subtoxic doxorubicin (0.86 μmol·$L^{-1}$), could kill SW480 cells sufficiently. Cytotoxicity by MTT assay arrived at 80.12±2.67 %, which was significantly higher than that by TRAIL or doxorubicin alone, with $P$=0.006 and 0.003 respectively. This killing effect was partly due to apoptosis. It was proved by large amounts of apoptotic cells under phase-contrast microscopy, cell apoptosis rate of 76.82±1.93 % by FCM assay and typical apoptotic morphology observed through transmission electron microscopy. Increase of apoptosis after combined treatment had no relation with protein level of p53 ($P$>0.05).

**CONCLUSION:** SW480 cells are not sensitive to TRAIL, but TRAIL can synergize with lower concentration of doxorubicin to induce apoptosis effectively. The status of p53 protein is not involved in the mechanism of synergistic apoptosis. It suggests the potential therapeutic applicability of the combination of TRAIL with doxorubicin against colon cancers.

Xu LH, Deng CS, Zhu YQ, Liu SQ, Liu DZ. Synergistic antitumor effect of TRAIL and doxorubicin on colon cancer cell line SW480. *World J Gastroenterol* 2003; 9(6): 1241-1245
http://www.wjgnet.com/1007-9327/9/1241.asp

## INTRODUCTION

The rapid induction of apoptosis by TRAIL (tumor necrosis factor-related apoptosis-inducing ligand) preferentially in tumor cells but not in normal cells has implied its potential use in therapy of malignancies[1,2]. Recent studies indicated that many cancer cells *in vitro* were resistant to apoptosis-inducing effect of TRAIL[3,4]. Enhancement of the antitumor activity of TRAIL by metabolic inhibitors has led to later studies encompassing the augmentation of antitumor effects of several kinds of chemotherapy or radiation therapy by TRAIL[5-13].

Doxorubicin has been the regular chemotherapeutic agents for its strong cell killing ability. But severe systemic toxicity limited its use in the clinical treatment of cancer. Reduction of its dose and maintenance of its high efficacy will be necessary in the future treatment of tumors. More efforts have been made to explore the combination of chemodrugs with some other agents[14].

## MATERIALS AND METHODS

### Materials

SW480 cell line was purchased from ATCC and maintained in Roswell Park Memorial Institute (RPMI)-1640 medium (Gibco) supplemented with 2 mmol· $L^{-1}$ L-glutamine (Gibco), 100 kU· $L^{-1}$ penicillin (Gibco), 100 g· $L^{-1}$ streptomycin (Gibco) and 100 ml· $L^{-1}$ heat-inactivated fetal bovine serum (Gibco), hereafter referred to as complete medium. Recombinant human soluble TRAIL (rhsTRAIL) was purchased from Pepro Tech, USA. Doxorubicin, p53 Mab and MTT were respectively from Sigma Co, Santa Cruz Company and Amresco Co.

### Methods

**Cytotoxicity assay** Cytotoxicity was determined by MTT assay. In brief, the cells were cultured in 96-well microtiter plates under 50 ml· $L^{-1}$ $CO_2$ in a humidified atmosphere at 37 ℃. Each well was then incubated for 4 h with MTT solution (final concentration 0.45 g· $L^{-1}$, Sigma Chemical, St.Louis, MO) under the same condition. Culture medium in each well was discarded and replaced with 100 μL of dissolving solution (DMSO). The absorbance of each well was determined by a spectrophotometer

with a 490 nm wavelength. The percentage of cell viability was calculated by multiplying the ratio absorbance of the sample versus the control by 100. Doxorubicin $IC_{50}$ was determined as a doxorubicin concentration showing 50 % cell growth inhibition as compared with control cell growth.

**Antitumor activity of doxorubicin and/or TRAIL** The cells were placed at $4\times10^4$ cells/well in 96-well microtiter plates. After 24 h culture for cell adherence to the plate, doxorubicin and/or TRAIL were added to each well at a given concentration. Detection of cell viability by MTT assay was performed following further incubation of the cells with doxorubicin and/or TRAIL for another 24 h. One well treated by the complete medium with neither doxorubicin nor TRAIL served as a control. The experiments were repeated in triplicate, and the percentage of cell viability was expressed as mean ± standard deviation.

**Flow cytometry** This analysis was conducted with a Facscan flow cytometer (Becton Dickinson, Mountain View, CA). It was to quantify cell apoptosis by the propidium iodide method. In brief, the cells were harvested by trypsinization at 24 hours after treatment and washed twice with PBS (pH 7.2). The medium and PBS were placed in tubes and centrifuged. A total of 1 ml of hypotonic buffer (propidium iodide, 50 mg· $L^{-1}$, in 1 ml· $L^{-1}$ sodium citrate, Rnase plus 1 ml· $L^{-1}$ Triton X-100; sigma) was added directly to the tubes and gently pipetted off. The tubes were placed at 4 ℃ in the dark for half an hour before flow cytometry analysis. The propidium iodide fluorescence of individual nuclei was measured in the red fluorescence and the data were registered in a logarithmic scale. At least $10^4$ cells of each sample were analyzed each time. Apoptotic nuclei appeared as a broad hypodiploid DNA peak before the $G_1$ phase of cell cycle, which was easily distinguished from the narrow hyperdiploid DNA peak at the $G_1$ phase or later $G_2$ and S phase.

**Transmission electron microscopy** Transmission electron microscopy was used to observe apoptosis directly through morphological changes at the subcellular level. In brief, the cells were cultured in the regular condition for 24 h. Then, TRAIL (100 μg· $L^{-1}$), doxorubicin (0.86 μmol· $L^{-1}$), their combination or the complete culture medium was added to them and maintained for another 24 h. After these, the cells were subsequently trypsinized, harvested, fixed in glutaral, immersed with Epon 821, imbedded in capsules and converged. Ultrathin sections of 60 nm were finally prepared and stained with uranyl acetate and lead citrate. Cell morphology was measured by transmission electron microscope.

**Western blot analysis for p53 protein expression** p53 levels following treatment with doxorubicin and/or TRAIL were investigated by Western blot analysis. The cells were incubated with the medium alone, doxorubicin alone, TRAIL alone, or the combination of doxorubicin and TRAIL at 37 ℃ for 24 h. The cells were lysed in a lysis buffer consisting of 1 mmol· $L^{-1}$ dithiothreitol, 1 mmol· $L^{-1}$ phenylmethyl sulphonyl fluoride, 5 mg· $L^{-1}$ leupiptin, 1 mmol· $L^{-1}$ NaF, 10 mmol· $L^{-1}$ β-glycerophosphate, 2 mmol· $L^{-1}$ Natrium orthovanadate, 50 mmol· $L^{-1}$ HEPES, 250 mmol· $L^{-1}$ NaCl, 1 mmol· $L^{-1}$ EDTA, and 1 % Nonidet P-40. After centrifuged for 7 min at 14 000 g, the supernatant was collected and the total protein amount was determined by SPECTRAmax 250. Twelve μg/lane of proteins were boiled in a sample buffer for 1 min at 100 ℃, electrophoresed in a multigel 10/20, and then transferred to Immobilon-P membranes (Millipore). Nonspecific antibody bindings were blocked by preincubation of the membranes for 1 h with a 5 % skim milk suspension. Then the membranes were incubated for 1 h with the polyclonal rabbit anti-human p53 antibody (1:200) (Santa Cruz, Delaware, CA), followed by further incubation overnight with horseradish peroxidase conjugated anti-rabbit IgG (1:2 000) (Santa Cruz). After each antibody incubation, the membranes were washed three times by Tris-buffer saline. To visualize the protein bands, ECL Western blot detection reagents (Amersham, Buckinghamshire, UK) were used and the membranes were exposed to X-ray film.

### *Statistical analysis*

All determinations were made in triplicate, and the results were expressed as the mean ± standard deviation (S.D.). Statistical significance was determined by Student' s *t*-test. A *P* value of 0.05 or less was considered significant.

## RESULTS

### *Effect of TRAIL or doxorubicin on SW480 cells*

MTT assay demonstrated that SW480 cells were not sensitive to TRAIL. No dose-dependent cytotoxicity of TRAIL on these cells was found at the concentrations from 0 μg· $L^{-1}$, 10 μg· $L^{-1}$, 100 μg· $L^{-1}$, 500 μg· $L^{-1}$, to 1 mg· $L^{-1}$, (as shown in Figure 1). $IC_{50}$ was above 1 mg· $L^{-1}$ which was significantly higher than 0.4 μg· $L^{-1}$ of TRAIL-sensitive leukaemic cell line Jurkat. 100 μg· $L^{-1}$ TRAIL could only affect 5.8 % of these cells, a subtoxic concentration. By contrast, SW480 cells responded to doxorubicin sensitively, with obvious dose-dependent cytotoxicity and $IC_{50}$ of 65.25±3.48 μmol· $L^{-1}$. 0.86 μmol· $L^{-1}$ doxorubicin could not damage any cell, also a subtoxic concentration (as shown in Figure 2). All values by MTT assay were proved by flow cytometry assay and apoptosis applauded parallel with cytotoxicity.

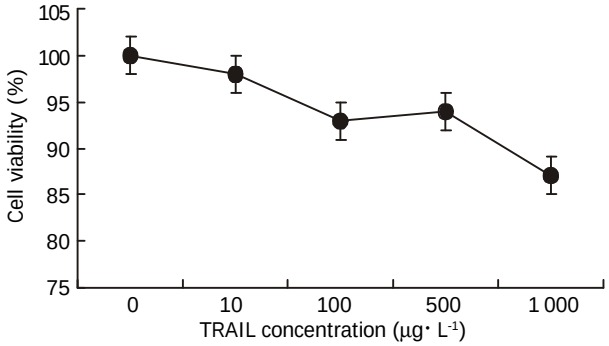


**Figure 1** Effect of TRAIL on SW480 cells. SW480 cells were treated with TRAIL at the concentrations of 0, 10, 100, 500 and 1 000 μg·$L^{-1}$ for 24 h. Cell growth inhibition was assessed by MTT assay and confirmed by flow cytometry assay. Compared with TRAIL-sensitive leukaemic cell line Jurkat ($IC_{50}$ 0.42 μg·$L^{-1}$), SW480 cells ($IC_{50}$ >1 000 μg·$L^{-1}$) were not responsive to TRAIL at concentration more than 100 times those active on Jurkat.

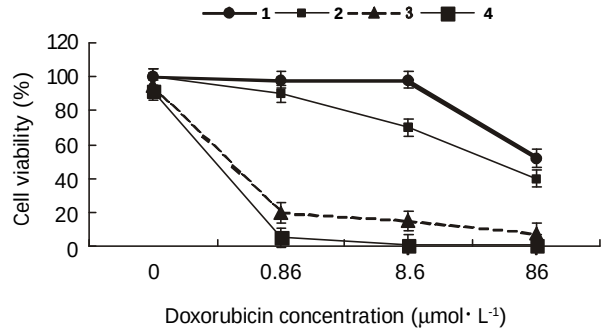


1, 2, 3, 4 was respectively doxorubicin with TRAIL 0, 10, 100, 1000 μg·$L^{-1}$.

**Figure 2** Effect of TRAIL and doxorubicin on SW480 cells SW480 cells were treated with doxorubicin alone or a combination of doxorubicin with TRAIL at different concentrations. The combination resulted in the reduction of doxorubicin $IC_{50}$ in cells ($P$<0.05). Doxo-

rubicin $IC_{50}$ was 65.25±3.48 when cells were treated by doxorubicin alone, while it was further reduced with the increased concentrations of TRAIL. Doxorubicin $IC_{50}$ was 43.17±2.54 μmol·$L^{-1}$ when it was combined with 10 μg·$L^{-1}$ of TRAIL, 0.51±0.02 μmol·$L^{-1}$ $IC_{50}$ when combined with 100 μg·$L^{-1}$ TRAIL, and 0.44±0.02 μmol·$L^{-1}$ $IC_{50}$ when combined with 1 000 μg·$L^{-1}$ TRAIL.

### *Effect of TRAIL and doxorubicin on SW480 cells*

SW480 cells were treated by doxorubicin alone, TRAIL alone, and a combination of doxorubicin and TRAIL, and cell viability after each treatment was determined by MTT assay. The cell growth inhibitory effects of the combined treatment were synergistic and more significant in proportion to the increasing concentrations of TRAIL as compared with doxorubicin alone. Furthermore, TRAIL could cause a decrease in doxorubicin $IC_{50}$ (as shown in Figure 2).

### *Effect of subtoxic TRAIL with subtoxic doxorubicin on SW480 cells*

Subtoxic concentration TRAIL of 100 μg· $L^{-1}$, with subtoxic concentration doxorubicin of 0.86 μmol· $L^{-1}$ was capable of killing 80.12±2.67 % cells by MTT assay. Much more apoptotic cells were observed under phase-contrast microscope in the group treated by this combination compared with those treated by TRAIL or doxorubicin alone. Flow cytometry assay also measured apoptosis rate of 76.82±1.93 % and obvious pre-$G_1$ apoptotic DNA peak among the cells (as shown in Figure 3). And electron microscopy observed a large number of apoptosis cells in them (as shown in Figure 4).

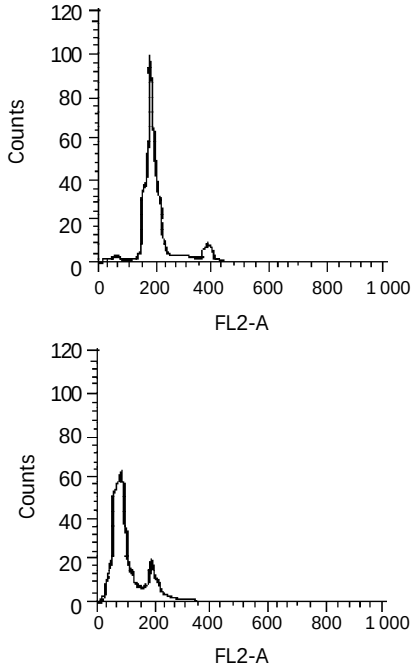


**Figure 3** Apoptosis assay by flow cytometry. SW480 cells were treated with doxorubicin (0.86 μmol·$L^{-1}$) alone, TRAIL (100 μg·$L^{-1}$) alone or a combination of them for 24 h. The apoptosis-inducing effect was quantified by PI stain flow cytometry assay. A: There was no hypodiploid DNA peak before $G_1$ phase which was similar to normal cells when treated with TRAIL (100 μg·$L^{-1}$) or doxorubicin (0.86 μmol·$L^{-1}$) alone. B: There was an obvious hyperdiploid DNA peak before $G_1$ phase in combination treatment, with apoptotic rate of 76.82±1.93 %. It was in accordance with cytotoxicity by MTT assay.

### *Protein level of mutant p53 before and after treatment of TRAIL and/or doxorubicin*

SW480 cells were treated with 100 μg· $L^{-1}$ TRAIL alone, 0.86 μmol· $L^{-1}$ doxorubicin alone, and their combination or complete control medium for 24 h. The protein level of mutant p53 was not different among them, with $P>0.05$ (as shown in Figure5). Variation of agent concentration turned out similar result.

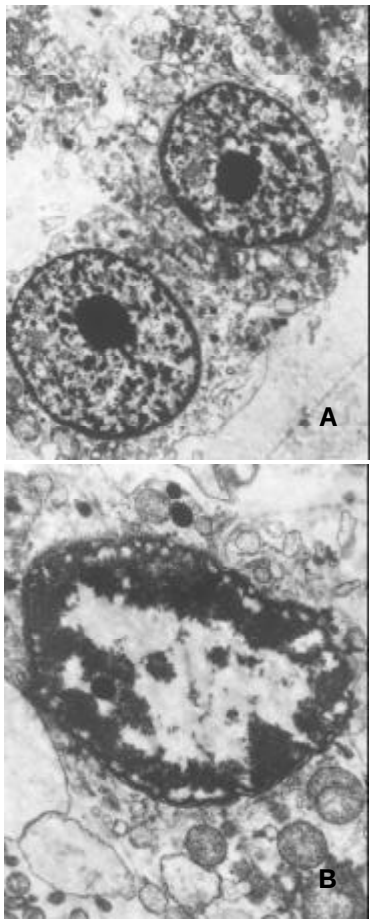


**Figure 4** Subcellular morphology of SW480 cells under treatment of TRAIL (100 μg·$L^{-1}$), doxorubicin (0.86 μmol·$L^{-1}$), or the combination of them. The electron microscopic morphology was observed after 24 hours treatment at the given concentration. A: TRAIL (100 μg·$L^{-1}$) or doxorubicin (0.86 μmol·$L^{-1}$) alone didn't affect the morphology of cells, with complete construction and evenly distributed chromatin (×5 000). B: The combination of TRAIL (100 μg·$L^{-1}$) and doxorubicin (0.86 μmol·$L^{-1}$) induced apoptosis in many cells, presented as condensed chromatin, distributing along nuclear perimeter (×15 000).

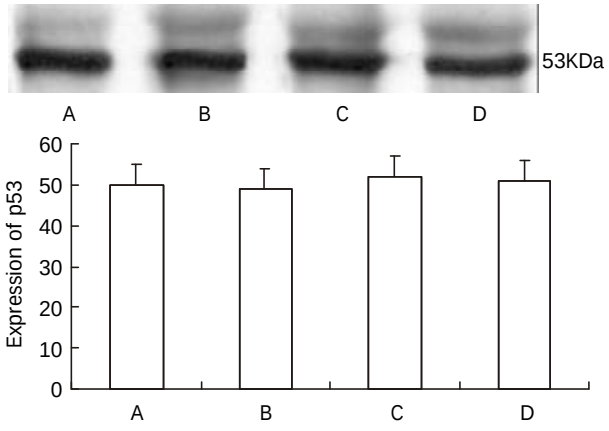


**Figure 5** p53 protein level by Western blot assay. They were detected after 24 hours of treatment. A, B, C, D were respectively normal control, TRAIL (100 μg·$L^{-1}$), doxorubicin (0.86 μmol·$L^{-1}$) and TRAIL (100 μg·$L^{-1}$) + doxorubicin (0.86 μmol·$L^{-1}$) groups. There was no difference in p53 protein expression among these four groups ($P>0.05$).

## DISCUSSION

TRAIL, also named Apo-2L, is a new member of the TNF cytokine family. It resembles Fas/Apo-2L in its amino acid sequence, as well as in its ability to induce apoptosis. It conducts or regulates the activities via a set of receptors on the surface of various cells[15-24]. TRAIL has attracted much interest for a profound feature since its discovery in 1995. That is the selectivity of killing cells, namely, TRAIL only induces apoptosis in transformed or tumor cells, but does not damage the normal ones[1,2]. There was a proposal for its clinical use after a series of *in vitro* experimentations. But a variety of cancer cells of breast, lung, prostate, colon and bladder were reported resistant to the effect of TRAIL[5-7].

Results in this study demonstrated that colon cancer cell line SW480 was relatively resistant to TRAIL, compared with TRAIL-sensitive leukaemic cell line Jurkat. The mechanisms of the underlying resistance was not clear update[7-9]. The conditions of decoy receptors, caspase-inhibition protein (FLIP), caspases and some apoptosis-related genes might attribute to the different responses[25-34]. It' s necessary to find a way to reverse the resistance if it is used in clinic in the future. Previous articles indicated some chemotherapeutic drugs could sensitize the cancer cells to TRAIL-mediated apoptosis[10-15]. Doxorubicin is a member of antibiotics, specifically for cancer cells. It belongs to the classical chemotherapeutic agents, with high anti-cancer efficacy. However, severe cardiac toxicity limits its broad use in clinic. Reducing concentration and maintaining efficacy of doxorubicin should be necessary for continuing its work. This study also demonstrated the sensitivity of SW480 cells to doxorubicin and its synergistic effect with TRAIL when percentage of cell viabilities were significantly decreased by the combined treatment at any dose as compared with those treated by doxorubicin or TRAIL alone. The degrees of growth inhibition were greater accompanied by the increased concentrations of TRAIL. Furthermore, augmentation of the cytotoxic effect of doxorubicin with TRAIL was significant even at low Doxorubicin (0.86 $\mu mol \cdot L^{-1}$) and low TRAIL (100 $\mu g \cdot L^{-1}$) concentrations in SW480 cells. It presented the evidence that TRAIL could reduce the dose of doxorubicin against tumor cells, which ultimately resulted in minimizing risks for systemic side effects while increasing the efficacy of doxorubicin, suggesting the clinical applicability of this combination for colon cancers.

Concentrations of TRAIL that were completely inactive on their own, boosted the activity of doxorubicin in the SW480 cells. This correlated well with the increased ability of this drug when combined with TRAIL to induce apoptosis and it did not correlate with the status of p53. Mutant-type p53 was said to contribute to drug-resistance of most cancer cells[27, 28]. The precise mechanisms enabling TRAIL to augment the cytotoxicity of chemotherapeutic agents in the p53 mutant-type cells have not been extensively investigated; however, recent evidence has suggested several possibilities: First, the augmentation of TRAIL-induced apoptosis by adriamycin or 5FU in p53 wild- and mutant-type breast cancer cell lines was mediated through a selective activation of caspases by these agents[28]. Subsequent investigations demonstrated that caspase activation, which was not observed with TRAIL or doxorubicin alone, became more evident after the combined treatment in p53 mutant-type cell lines. These findings implied that the up-regulation of intracellular apoptotic signaling events contributed to overcome resistance to TRAIL alone even in p53 mutant-type cells. Second, the increase of KILLER/DR5 expression by certain genotoxic stresses, which resulted in the enhancement of TRAIL, is regulated in a p53-dependent and -independent manner[29, 30]. Finally, another TRAIL receptor, DR4, which transmitted a death signal through its binding with TRAIL, is regulated in a p53-independent manner[31-34].

The finding that TRAIL could boost the activity of doxorubicin against colorectal carcinoma cells should have important therapeutic implications. Since TRAIL itself is thought to have no apparent toxicity to normal cells and to be safe in systemic administration, the combination of doxorubicin and TRAIL will result in minimization of the toxicity and maximization of the antitumor activity.

## REFERENCES


1 **Ashkenazi A**, Pai RC, Fong S, Leung S, Lawrence DA, Marsters SA, Blackie C, Chang L, McMurtrey AE, Hebert A, De Forge L, Koumenis IL, Lewis D, Harris L, Bussiere J, Koeppen H, Shahrokh Z, Schwall RH. Safety and antitumor activity of recombinant soluble Apo2 ligand. *J Clin Invest* 1999; **104**: 155-162

2 **Lin T,** Huang X, Gu J, Zhang L, Roth JA, Xiong M, Curley SA, Yu Y, Hunt KK, Fang B. Long-term tumor-free survival from treatment with the GFP-TRAIL fusion gene expressed from the hTERT promoter in breast cancer cells. *Oncogene* 2002; **21**: 8020-8028

3 **Jang YJ**, Park KS, Chung HY, Kim HI. Analysis of the phenotypes of Jurkat clones with different TRAIL-sensitivity. *Cancer Lett* 2003; **194**: 107-117

4 **Naumann U**, Waltereit R, Schulz JB, Weller M. Adenoviral (full-length) Apo2L/TRAIL gene transfer is an ineffective treatment strategy for malignant glioma. *J Neurooncol* 2003; **61**: 7-15

5 **Gliniak B**, Le T. Tumor necrosis factor-related apoptosis-inducing ligand's antitumor activity in vivo is enhanced by the chemotherapeutic agent CPT-11. *Cancer Res* 1999; **59**: 6153-6158

6 **Jin Z**, Dicker DT, El-Deiry WS. Enhanced sensitivity of G1 arrested human cancer cells suggests a novel therapeutic strategy using a combination of simvastatin and TRAIL. *Cell Cycle* 2002; **1**: 82-89

7 **Hernandez A**, Wang QD, Schwartz SA, Evers BM. Sensitization of human colon cancer cells to TRAIL-mediated apoptosis. *J Gastrointesti Surg* 2001; **5:** 56-65

8 **Hietakangas V**, Poukkula M, Heiskanen KM, Karvinen JT, Sistonen L, Eriksson JE. Erythroid differentiation sensitizes K562 leukemia cells to TRAIL-induced apoptosis by downregulation of c-FLIP. *Mol Cell Biol* 2003; **23**: 1278-1291

9 **Keane MM**, Ettenberg SA, Nau MM, Russell EK, Lipkowitz S. Chemotherapy augments TRAIL-induced apoptosis in breast cell lines. *Cancer Res* 1999; **59**: 734-741

10 **Vignati S**, Codegoni A, Polato F, Broggini M. Trail activity in human ovarian cancer cells: potentiation of the action of cytotoxic drugs. *Eur J Cancer* 2002; **38**: 177-183

11 **Mizutani Y,** Nakanishi H, Yoshida O, Fukushima M, Bonavida B, Miki T. Potentiation of the sensitivity of renal cell carcinoma cells to TRAIL-mediated apoptosis by subtoxic concentrations of 5-fluorouracil. *Eur J Cancer* 2002; **38:** 167-176

12 **Shimoyama S,** Mochizuki Y, Kusada O, Kaminishi M. Supra-additive antitumor activity of 5FU with tumor necrosis factor-related apoptosis-inducing ligand on gastric and colon cancers *in vitro*. *Int J Oncol* 2002; **21**: 643-648

13 **Wei XC,** Wang XJ, Chen K, Zhang L, Liang Y, Lin XL. Killing effect of TNF-related apoptosis inducing ligand regulated by tetracycline on gastric cancer cell line NCI-N87. *World J Gastroenterol* 2001; **7**: 559-562

14 **Chen XX**, Lai MD, Zhang YL, Huang Q. Less cytotoxicity to combination therapy of 5-fluorouracil and cisplatin than 5-fluorouracil alone in human colon cancer cell lines. *World J Gastroenterol* 2002; **8**: 841-846

15 **Sheridan JP**, Marsters SA, Pitti RM, Gurney A, Skubtch M, Baldwin D, Ramakrishnan L, Gray CL, Baker K, Wood WL, Goddard AD, Godowski P, Ashkenazi A. Control of TRAIL-induced apoptosis by a family of signaling and decoy receptors. *Science*1997; **277**: 818-821

16 **Schneider P**, Thome M, Burns K, Bodmer JL, Hofmann K, Kataoka T, Holler N, Tschopp J. TRAIL receptors 1 (DR4) and 2 (DR5) signal FADD-dependent apoptosis and activate NF-κB. *Immunity* 1997; **7**: 831-836

17 **Walczak H,** Degli-Esposti MA, Johnson RS, Smolak PJ, Waugh JY, Boiani N, Timour MS, Gerhart MJ, Schooley KA, Smith CA,

Goodwin RG, Rauch CT. TRAIL-R2: a novel apoptosis-mediating receptor for TRAIL. *EMBO J* 1997; **16**: 5386-5397

18 **Strater J**, Hinz U, Walczak H, Mechtersheimer G, Koretz K, Herfarth C, Moller P, Lehnert T. Expression of TRAIL and TRAIL receptors in colon carcinoma: TRAIL-R1 is an independent prognostic parameter. *Clin Cancer Res* 2002; **8**: 3734-3740

19 **Degli-Esposti MA,** Smolak PJ, Walczak H., Waugh J, Huang CP, Dubose RF, Goodwin RG, Smith CA. Cloning and characterization of TRAIL-R3, a novel member of the emerging TRAIL receptor family. *J Exp Med* 1997; **186**: 1165-1170

20 **Degli-Esposti MA**, Dougall WC, Smolak PJ, Waugh JY, Smith CA, Goodwin RG. The novel receptor TRAIL-R4 induces NF-κB and protects against TRAIL-mediated apoptosis, yet retains an incomplete death domain. *Immunity* 1997; **7**: 813-820

21 **Marsters SA,** Sheridan JP, Pitti RM, Huang A, Skubtch M, Baldwin D, Yuan J, Gurney A, Goddard AD, Godowski P, Ashkenazi A. A novel receptor for Apo2L / TRAIL contains a truncated death domain. *Curr Biol* 1997; **7**: 1003-1006

22 **Pan G,** Ni J, Yu G, Wei YF, Dixit VM. TRUNDD, a new member of the TRAIL receptor family that antagonizes TRAIL signaling. *FEBS Lett* 1998; **424**: 41-45

23 **Emery JG,** McDonnell P, Burke MB, Deen KC, Lyn S, Silverman C, Dul E, Appelbaum ER, Eichman C, DiPrinzio R, Dodds RA, James IE, Rosenberg M, Lee JC, Young PR. Osteoprotegerin is a receptor for the cytotoxic ligand TRAIL. *J Biol Chem* 1998; **273**: 14363-14367

24 **Shipman CM**, Croucher PI. Osteoprotegerin is a soluble decoy receptor for tumor necrosis factor-related apoptosis-inducing ligand / apo2 ligand and can function as a paracrine survival Factor for human myeloma cells. *Cancer Res* 2003; **63**: 912-916

25 **Griffith TS,** Lynch DH. TRAIL: a molecule with multiple receptors and control mechanisms. *Curr. Opin Immunol* 1998; **10**: 559-563

26 **Grotzer MA**, Eggert A, Zuzak TJ, Janss AJ, Marwaha S, Wiewrodt BR, Ikegakin, Brodeur GM, Phillips PC. Resistance to TRAIL-induced apoptosis in primitive neuroectodermal brain tumor cells correlates with a loss of caspase-8 expression. *Oncogene* 2000; **19**: 4604-4610

27 **Xu SQ**, El-Deiry WS. $P21^{WAF1/CIP1}$ inhibits initiator caspase cleavage by TRAIL death receptor DR4. *Biochem Biophys Res Commun* 2000; **269**: 179-190

28 **Xu M,** Jin YL, Fu J, Huang H, Chen SZ, Qu P, Tian HM, Liu ZY, Zhang W. The abnormal expression of retinoic acid receptor-β, p53 and Ki67 protein in normal, premalignant and malignant esophageal tissues. *World J Gastroenterol* 2002; **8**: 200-202

29 **Siervo-Sassi RR**, Marrangoni AM, Feng X, Naoumova N, Winans M, Edwards RP, Lokshin A. Physiological and molecular effects of Apo2L / TRAIL and cisplatin in ovarian carcinoma cell lines. *Cancer Lett* 2003; **190:** 61-72

30 **Ng CP,** Zisman A, Bonavida B. Synergy is achieved by complementation with Apo2L / TRAIL and actinomycin D in Apo2L / TRAIL-mediated apoptosis of prostate cancer cells: role of XIAP in resistance. *Prostate* 2002; **53:** 286-299

31 **Lee KY,** Park JS, Jee YK, Rosen GD. Triptolide sensitizes lung cancer cells to TNF-related apoptosis-inducing ligand (TRAIL)-induced apoptosis by inhibition of NF-kappaB activation. *Exp Mol Med* 2002; **34**: 462-468

32 **Kelly MM**, Hoel BD, Voelkel-Johnson C. Doxorubicin pretreatment sensitizes prostate cancer cell Lines to TRAIL induced apoptosis which correlates with the loss of c-FLIP expression. *Cancer Biol Ther* 2002; **1**: 520-527

33 **Thomas RP**, Farrow BJ, Kim S, May MJ, Hellmich MR, Evers BM. Selective targeting of the nuclear factor-kappaB pathway enhances tumor necrosis factor-related apoptosis-inducing ligand-mediated pancreatic cancer cell death. *Surgery* 2002; **132**: 127-134

34 **Shetty S,** Gladden JB, Henson ES, Hu X, Villanueva J, Haney N, Gibson SB. Tumor necrosis factor-related apoptosis inducing ligand (TRAIL) up-regulates death receptor 5 (DR5) mediated by NFkappaB activation in epithelial derived cell lines. *Apoptosis* 2002; **7**: 413-420

**Edited by** Wu XN

P.O.Box 2345, Beijing 100023,China
Fax: +86-10-85381893
E-mail: wjg@wjgnet.com www.wjgnet.com

World J Gastroenterol 2003;9(6):1246-1250
World Journal of Gastroenterology
Copyright ©2003 by The WJG Press ISSN 1007-9327

• COLORECTAL CANCER •

# Role of inducible nitric oxide synthase expression in aberrant crypt foci-adenoma-carcinoma sequence

Mei-Hua Xu, Chang-Sheng Deng, You-Qing Zhu, Jun Lin

**Mei-Hua Xu, Chang-Sheng Deng, You-Qing Zhu, Jun Lin,** Department of Gastroenterology, Zhongnan Hospital, Wuhan University, Wuhan 430071, Hubei Province China
**Correspondence to:** Mei-Hua Xu, Zhongnan Hospital, Wuhan University,Wuhan 430071 Hubei Province, China. xmh-11@163.com
**Telephone:** +86-27-87330404
**Received:** 2002-07-18 **Accepted:** 2002-09-12

## Abstract

**AIM:** To investigate the expression of inducible nitric oxide synthase (iNOS) in aberrant crypt foci (ACF) -adenoma-carcinoma sequence and its relation with tumor cell apoptosis, proliferation and angiogenesis.

**METHODS:** The expression of iNOS, proliferating cell nuclear antigen (PCNA) and microvessel density (MVD) in different stages of colorectal cancer were studied by immunohistochemical method from 30 normal tissues, 30 nonhyperplastic ACF, 30 hyperplastic ACF, 30 dysplastic ACF, 30 adenomas and 60 carcinomas. The apoptotic cells were detected by terminal deoxynucleotidyl transferase-mediated dUTP-biotin nick end labeling (TUNEL) method using an Apop Tag *in situ* detection kit.

**RESULTS:** The immunoreactivity of iNOS significantly increased in the transition from hyperplastic ACF to dysplastic ACF. This transition was associated with a significant decrease in the apoptotic index (AI) (0.73±0.37 *vs* 0.61±0.35, $P<0.05$) and significant increases in the PCNA labeling index (LI) (27.3±2.80 *vs* 40.3±3.11, $P<0.01$) and microvessel density (MVD) (55±11.5 *vs* 70±13.2, $P<0.01$). The expression of iNOS was in low levels and positively correlated with PCNA-LI ($r=0.812$, $P<0.01$) and MVD ($r=0.863$, $P<0.01$) during transition from normal mucosa to nonhyperplastic ACF and hyperplastic ACF. The expression of iNOS was in high levels and positively correlated with AI ($r=0.901$, $P<0.01$) after transition from hyperplastic ACF to dysplastic ACF, adenoma and carcinoma.

**CONCLUSION:** The results suggest that the transition from hyperplastic ACF to dysplastic ACF may be a crucial step in the ACF-adenoma-carcinoma sequence, in which iNOS plays an important role by regulating tumor cell apoptosis, proliferation and angiogenesis.

Xu MH, Deng CS, Zhu YQ, Lin J. Role of inducible nitric oxide synthase expression in aberrant crypt foci-adenoma-carcinoma sequence. *World J Gastroenterol* 2003; 9(6): 1246-1250
http://www.wjgnet.com/1007-9327/9/1246.asp

## INTRODUCTION

Aberrant crypt foci (ACF) are recently described colorectal lesions that might be related to the earliest steps in multistage colorectal carcinogenesis[1]. Nitric oxide (NO) is an important bioactive agent and signaling molecule that mediates a variety of physical actions and may contribute to the pathogenesis of a variety of disorders including cancer[2-6]. Several studies implicate iNOS in colorectal tumorigenesis[7-9], but none has evaluated the expression of iNOS in ACF-adenoma-carcinoma sequence. In this study, TUNEL technique and immunohistochemical staining were used to detect biologic parameters of tumor and compare the state of apoptosis, proliferation, MVD and iNOS expression in ACF-adenoma-carcinoma sequence. The purpose was to find out the relationship between aberrant expression of iNOS and colorectal carcinogenesis and the possible mechanism.

## MATERIALS AND METHODS

### *Tissue specimens*

Human colorectal tissues were obtained from Zhongnan Hospital and the People' s Hospital of Wuhan University and Hubei Cancer Hospital. We collected 90 ACF and their adjacent normal mucosa from 32 colorectal carcinomas (CRC) (19 males and 13 females; mean age, 54±7.5 years). 30 adenomas (18 males and 12 females; mean age, 51±7.3 years) and 60 carcinomas were included in this study. The cancer patients included 32 males and 28 females that had 7 Dukes' stage A, 24 stage B, 12 stage C, and 17 stage D. There were 22 well-differentiated CRCs, 26 moderately differentiated and 12 poorly differentiated CRCs. All specimens were routinely fixed in 10 % buffered formalin, embedded in paraffin, and cut into 5 μm sections. Each of the 5 sections was stained with hematoxylin and eosin for classification.

### *Sampling of ACF*

Immediately after bowel resection, freshly resected colorectal segments were opened longitudinally, and the mucosa from macroscopically normal segments were dissected from the underlying layers, spread over on a piece of filter paper, and fixed in 10 % buffered formalin solution.24 hours later, the fixed mucosal strips were immersed in 0.2 % methylene blue solution for 5 to 10 minutes and screened under 40× magnification for ACF. Methylene blue-stained ACF were easily distinguished from normal crypts by their deeper blue color, larger diameter, and the shape of their crypt orifices (oval, serrated, or slit-like)[10]. Randomly selected ACF were microdissected with a rim of normal surrounding mucosa, paraffin embedded, and serially cut perpendicular to the surface.

### *Histochemical detection of apoptosis and determination of apoptotic index*

Apoptotic cell tissue sections were detected by terminal deoxynucleotidyl transferase-mediated dUTP-biotin nick end labeling (TUNEL) method using an Apop Tag *in situ* detection kit according to the manufacturer' s instructions. Morphologic characteristics of apoptosis were chromatin condensation, nuclear disintegration, and formation of crescent caps of condensed chromatin at the nuclear periphery. The apoptotic index (AI) was expressed as the ratio of positively stained cells

to total cells evaluated for each tissue section after counting 1 000 cells at 5 areas randomly selected for counting less than 400-fold magnification.

### *Immunohistochemical staining and evaluation of the sections*

SP kit was used. The primary antibodies were iNOS polyclonal antibody (ready to use, Boster, Wuhan), PCNA monoclonal antibody (ready to use, Maxin, Fujian) and CD34 monoclonal antibody (ready to use, Maxin, Fujian), respectively. Before staining, the sections were heated in microwave heated in 0.01 mol/L citric acid solution for antigen retrieval. PBS was substituted for primary antibodies as negative control. The stained sections were reviewed and scored independently by two investigators using an Olympus microscope. The extent and intensity of immunoreactivity for iNOS of all specimens were recorded. The following scale was used to express the extent of positivity: 0,≤5 %; 1,>5-25 %; 2,>25-50 %; 3,>50-75 %; 4,>75 %. The intensity of iNOS expression was scored as follows: 0, negative; 1, weak; 2, moderate; 3, strong. The final score, obtained by multiplying the intensity and extent of positivity scores, ranged from 0-12. Scores of 0- 4 were defined as "markedly reduced" or "no expression"; Scores 5-8 were defined as "intermediate expression"; and scores of 9-12 were defined as "strong expression"[11]. The PCNA labeling index (LI) was expressed as the ratio of cells positively stained for PCNA to all epithelial cells in at least 5 areas randomly selected for counting less than 200-fold magnification. For microvessel density (MVD) determination, 5 areas were randomly selected and counted less than 200-fold magnification. The average count was recorded and expressed as the absolute number of vessels per 0.74 $mm^2$ (per × 200 field) for each case.

### *Statistical analysis*

*T* test was used for comparison of the means. The positivity of iNOS protein was analyzed by Fisher exact probability method. For the tendency of AI, LI and MVD in the ACF-adenoma-carcinoma sequence analysis of variance was performed based on the trend test. *P* value less than 0.05 was regarded as statistically significant.

## RESULTS

### *Expression of iNOS in ACF-adenoma-carcinoma sequence*

Although most cases of normal mucosa, nonhyperplastic ACF and hyperplastic ACF showed intermediate, weak or absent iNOS expression, the expression of iNOS increased markedly during transition from hyperplastic ACF to dysplastic ACF ($P<0.01$) (Table 1, Figure 1). Greater than 70 % of cases of dysplastic ACF, adenoma or carcinoma showed strong expression of iNOS. We found no relationship between expression of iNOS and the Ducks' classification and the differentiation of cancer.

**Table 1** iNOS expression in normal mucosa-ACF-adenoma-carcinoma sequence

| | iNOS expression | | | Total |
|---|---|---|---|---|
| | Strong | Intermediate | Weak or absent | |
| Normal mucosa | 3 | 6 | 21 | 30 |
| Nonhyperplastic ACF | 6 | 8 | 16 | 30 |
| Hyperplastic ACF | 8 | 10 | 12 | 30 |
| Dysplastic ACF | 26 | 2 | 2 | 30 |
| Adenoma | 24 | 4 | 2 | 30 |
| Carcinoma | 41 | 10 | 9 | 60 |

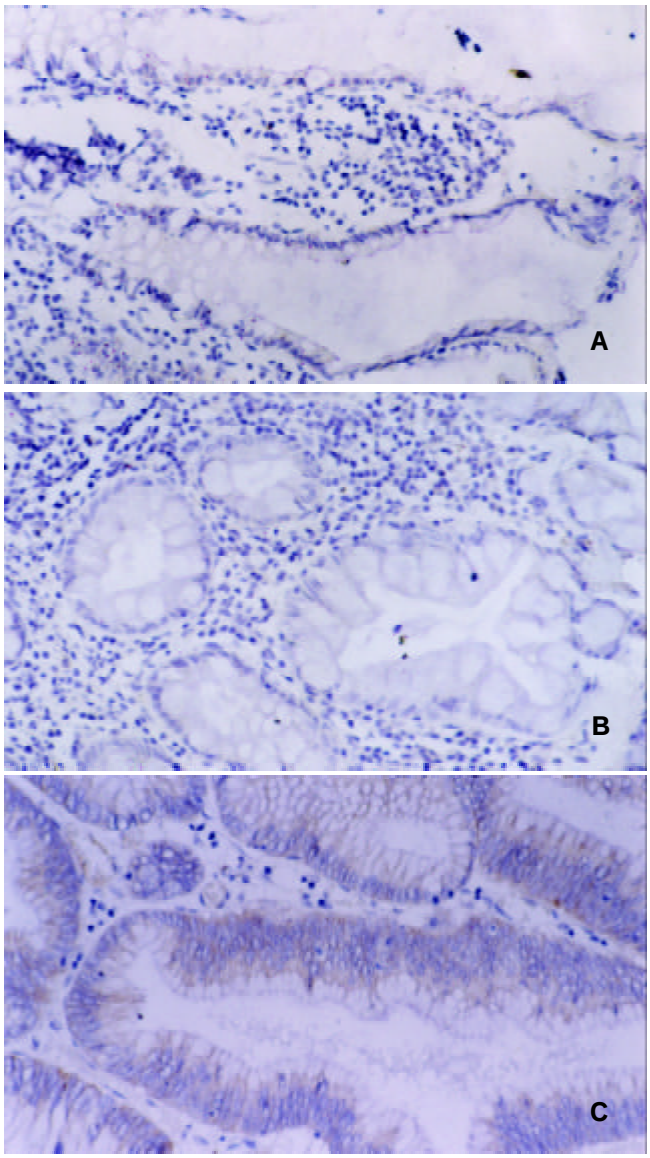


**Figure 1** Immunohistochemical analysis for iNOS protein in ACF. (A) weak staining was observed in the cytoplasm of nonhyperplastic ACF. (SP method, ×200). (B) weak staining was observed in the cytoplasm of hyperplastic ACF. (SP method, ×200). (C) strong staining was observed in the cytoplasm of dysplastic ACF. (SP method, ×200).

**Table 2** Changes in AI, PCNA-LI, and MVD in ACF-adenoma-carcinoma sequence ($\bar{x}\pm s$)

| | *n* | AI (%) | PCNA-LI (%) | MVD (MVD /0.74$mm^2$) |
|---|---|---|---|---|
| Normal mucosa | 30 | 0.21±0.13 | 12.1±2.48 | 50±10.3 |
| Nonhyperplastic ACF | 30 | 0.28±0.16 | 14.7±2.47 | 52±10.6 |
| Hyperplastic ACF | 30 | 0.73±0.37[ab] | 27.3±2.80[ab] | 55±11.5 |
| Dysplastic ACF | 30 | 0.61±0.35[abc] | 40.3±3.11[abd] | 70±13.2[abd] |
| Adenoma | 30 | 0.58±0.25[abc] | 45.4±3.24[abd] | 80±14.7[abde] |
| Carcinoma | 60 | 0.49±0.43[abde] | 52.2±3.17[abdf] | 95±13.3[abdf] |

[a]$P<0.01$, *vs* normal mucosa; [b]$P<0.01$, *vs* nonhyperplastic ACF; [c]$P<0.05$, *vs* hyperplastic ACF; [d]$P<0.01$, *vs* Hyperplastic ACF; [e]$P<0.05$, *vs* dysplastic ACF; [f]$P<0.01$, *vs* dysplastic ACF.

### *Changes in AI, PCNA-LI, and MVD in ACF-adenoma-carcinoma sequence*

Apoptotic index was highest in hyperplastic ACF, whereas it significantly decreased after transition to dysplastic ACF

(Figure 2), adenoma and carcinoma ($P<0.05$). Conversely, the proliferative activity as determined by PCNA-LI gradually increased during ACF (Figure 3)-adenoma-carcinoma sequence ($P<0.01$). Microvessel density significantly increased after the transition to dysplastic ACF (Figure 4), and further elevated in adenoma and carcinoma ($P<0.01$) (Table 2).

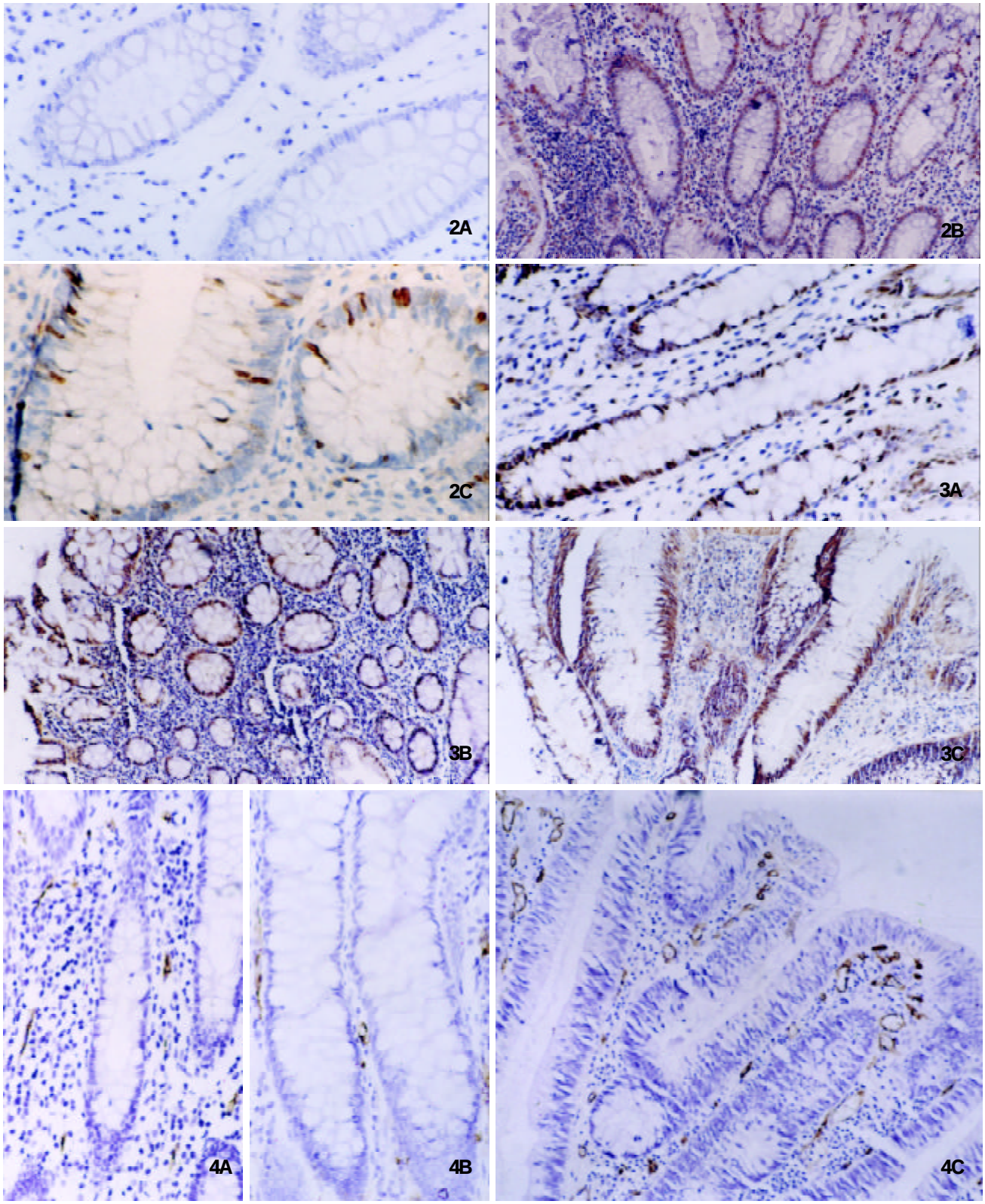


**Figure 2** Histochemical detection of apoptosis by TUNEL in ACF. Few apoptotic cells were detected in nonhyperplastic ACF (PanelA, original magnification ×200), and more apoptotic cells were detected in hyperplastic ACF (Panel B, original magnification ×100) whereas they decreased significantly after transition to dysplastic ACF (Panel C, original magnification ×200).

**Figure 3** Immunohistochemistry of PCNA protein in ACF. PCNA expression was gradually increased from nonhyperplastic ACF (Panel A, original magnification ×200), hyperplastic ACF (PanelB, original magnification ×100) to dysplastic ACF (Panel C, original magnification ×100).

**Figure 4** Immunohistochemistry of CD34 protein in ACF. MVD determined by anti-CD34 antibody was low in nonhyperplastic ACF (Panel A, original magnification ×200) and hyperplastic ACF (Panel B, original magnification ×200) whereas significantly increased in dysplastic ACF (Panel C, original magnification ×200).

***Correlations between iNOS expression and biologic parameters***

The expression of iNOS was in low level and positively correlated with PCNA-LI ($r$=0.812, $P$<0.01) and MVD ($r$=0.863, $P$<0.01) during transition from normal mucosa to nonhyperplastic ACF and hyperplastic ACF. The expression of iNOS was in high level and positively correlated with AI ($r$=0.901, $P$<0.01) after transition to dysplastic ACF, adenoma and carcinoma.

## DISCUSSION

The development of colorectal carcinoma usually occurs via the adenoma-carcinoma sequence[12,13]. The search for the earliest morphological precursors led to the description of ACF. Currently, there is a tendency to consider ACF as putative preneoplastic lesions that could represent one of the earliest stages of the multistep colorectal carcinogenesis[1,14]. Alteration of enzymes, specifically hexosaminidase, and carcinoembryonic antigen expression have been identified in ACF. Genetic mutations that include APC suppressor gene and k-ras gene as well as beta-catenin gene have been found in ACF[15,16]. Genomic instability, manifested as altered lengths of microsatellites and oligo A sequences similar to alterations that occur in neoplasm, has been identified in some ACF[17]. Morphological alterations from nonhyperplasia to hyperplasia to varying degrees of dysplasia have been found in ACF[18]. One study suggested that some hyperplastic ACF can develop into the adenomatous type[19]. In a carcinogen-induced colonic tumorigenesis model, these lesions may show dysplastic morphology and precede formation of adenomas and adenocarcinomas. Phenotypic and genetic abnormalities in ACF have been postulated as evidence that ACF are preneoplastic and the smallest lesions preceding adenoma and carcinoma. Recently, there was a direct evidence of the existence of an ACF-adenoma-carcinoma sequence[20].

A disturbance in the balance between cell proliferation and cell loss, or apoptosis may underlie neoplastic development[21-27]. In this study, we noticed that in normal mucosa the apoptotic cells were identified in colorectal surface epithelium and formed "an apoptotic zone". Proliferative cells were seen in the basal region of the mucosa glands and formed "a proliferating zone". However in colorectal carcinoma, apoptotic cells and proliferative cells clustered all over the tumor tissue. This phenomenon elucidated that the regulation of apoptosis and proliferation had already been beyond control. Angiogenesis also played a crucial role in tumorigenesis[28-32]. In this study, we demonstrated that MVD increased gradually in ACF-adenoma-carcinoma sequence. This change indicated that the regulation of growth of vessel was also disordered.

We investigated iNOS expression in human colorectal cancer with respect to tumor staging. Only low levels were found in the surrounding normal tissue, nonhyperplastic ACF and hyperplastic ACF. However, we found markedly increased iNOS in dysplastic ACF, adenoma and carcinoma. After transition to dysplastic ACF, adenoma and carcinoma, iNOS activity decreased with increasing staging. The markedly increased iNOS expression during hyperplastic ACF-dysplastic ACF transition suggested that the increase of iNOS expression might be an early event in the development of colorectal tumor. The different expression of iNOS in the epithelial cells in ACF-adenoma-carcinoma sequence may provide important clues that host factor regulates iNOS differently in different tumor stages.

During transition from normal mucosa to nonhyperplastic ACF and hyperplastic ACF, the expression of iNOS was at low levels. This transition was associated with a gradual increase in the AI, PCNA-LI and MVD. Several reports suggest that low concentrations of NO and iNOS induce angiogenesis and enhance the growth rate of tumor[33]. Increased proliferation might result in a state of lacking of nutrients, competition for growth factors or oxygen starvation and then in turn induce apoptosis[34]. Our results demonstrated that the initial neoplastic transformation was associated with a remarkable increase in rates of both proliferation and apoptosis, which suggested the increased instability of colorectal mucosa in this process. The immunoreactivity of iNOS significantly increased during the transition from hyperplastic ACF to dysplastic ACF. The perturbation of tissue homeostasis derived from the increased proliferation and decreased apoptosis detected at this transition. Microvessel density (MVD) was found markedly increased at this transition. These results suggested that the transition from hyperplastic ACF to dysplastic ACF might be a crucial step in the ACF-adenoma-carcinoma sequence, in which iNOS might play an important role. The expression of iNOS was in high level and associated with a significant increase in the PCNA-LI, MVD and marked decrease in the AI after transition to dysplastic ACF, adenoma and carcinoma. With the decreased expression of iNOS, AI decreased gradually and was lowest in carcinoma in this process. Several reports suggest that high concentrations of NO and iNOS are cytotoxic and can induce apoptosis[33]. Because the increased instability of colorectal mucosa in former stages led to the formation of "supper clone" and the micro-environmental changes such as expression of EGF and TGF-a in the tumor tissues[35,36], epithelial cells maintained at hyperproliferation and increased angiogenesis was present after transition to dysplastic ACF, adenoma and carcinoma. These results elucidate that iNOS might be an important factor of colorectal carcinogenesis by regulating tumor cell apoptosis, proliferation and angiogenesis. What may cause the overexpression of iNOS after transition to dysplastic ACF, adenoma and carcinoma remains unclarified and awaits further study.

## REFERENCES


1 **Bird RP**. Role of aberrant crypt foci in understanding the pathogenesis of colon cancer. *Cancer lett* 1995; **93**: 55-71

2 **Holian O**, Wahid S, Atten MJ, Attar BM. Inhibition of gastric cancer cell proliferation by resveratrol: role of nitric oxide. *Am J Physiol Gastrointest Liver Physiol* 2002; **282**: G809-816

3 **Zhang K**, Deng CS, Zhu YQ, Yang YP, Zhang YM. Significance of nuclear factor-κB, cyclooxgenase 2 and inducible nitric oxide synthase expression in human ulcerative colitis tissues. *Shijie Huaren XiaoHua Zazhi* 2002; **10**: 575-578

4 **Diao TJ**, Yuan TY, Li YL. Immunologic role of nitric oxide in acute rejection of golden hamster to rat liver xenotransplantation. *World J Gastroenterol* 2002; **8**: 746-751

5 **Bing RJ**, Miyataka M, Rich KA, Hanson N, Wang X, Slosser HD, Shi SR. Nitric oxide, prostanoids, cyclooxygenase, and angiogenesis in colon and breast cancer. *Clin Cancer Res* 2001; **7**: 3385-3392

6 **Song ZJ**, Gong P, Wu YE. Relationship between the expression of iNOS,VEGF,tumor angiogenesis and gastric cancer. *World J Gastroenterol* 2002; **8**: 591-595

7 **Ambs S**, Merriam WG, Bennett WP, Felley-Bosco E, Ogunfusika MO, Oser SM, Klein S, Shields PG, Billiar TR, Harris CC. Frequent nitric oxide synthase-2 expression in human colon adenomas: implication for tumor angiogenesis and colon cancer progression. *Cancer Res* 1998; **58**: 334-341

8 **Rao CV**, Kawamori T, Hamid R, Reddy BS. Chemoprevention of colonic aberrant crypt foci by an inducible nitric oxide synthase-selective inhibitor. *Carcinogenesis* 1999; **20**: 641-644

9 **Nozoe T**, Yasuda M, Honda M, Inutsuka S, Korenaga D. Immunohistochemical expression of cytokine induced nitric oxide synthase in colorectal carcinoma. *Oncol Rep* 2002; **9**: 521-524

10 **Nucci MR**, Robinson CR, Longo P, Campbell P, Hamilton SR. Phenotypic and genotypic characteristics of aberrant crypt foci in human colorectal mucosa. *Hum pathol* 1997; **28**: 1396-1407

11 **Hao XP**, Willis JE, Pretlow TG, Rao JS, MacLennan GT, Talbot IC, Pretlow TP. Loss of fragile histidine triad expression in

colorectal carcinomas and premalignant lesions. *Cancer Res* 2000; **60**: 18-21

12 **Li A**, Yonezawa S, Matsukita S, Hasui K, Goto M, Tanaka S, Imai K, Sato E. Comparative study for histology, proliferative activity, glycoproteins, and p53 protein between old and recent colorectal adenomas in Japan. *Cancer Lett* 2001; **170**: 45-52

13 **Luo MJ**, Lai MD. Identification of differentially expressed genes in normal mucosa, adenoma and adenocarcinoma of colon by SSH. *World J Gastroenterol* 2001; **7**: 726-731

14 **Bird RP**, Good CK. The significance of aberrant crypt foci in understanding the pathogenesis of colon cancer. *Toxicol lett* 2000; **112-113**: 395-402

15 **Yuan P**, Sun MH, Zhang JS, Zhu XZ, Shi DR. APC and K-ras gene mutation in aberrant cryot foci of human colon. *World J Gastroenterol* 2001; **7**: 352-356

16 **Takahashi M**, Mutoh M, Kawamori T, Sugimura T, Wakabayashi K. Altered expression of beta-catenin, inducible nitric oxide synthase and cyclooxygenase-2 in azoxymethane-induced rat colon carcinogenesis. *Carcinogenesis* 2000; **21**: 1319-1327

17 **Pedroni M**, Sala E, Scarselli A, Borghi F, Menigatti M, Benatti P, Percesepe A, Rossi G, Foroni M, Losi L, Di Gregorio C, De Pol A, Nascimbeni R, Di Betta E, Salerni B, de Leon MP, Roncucci L. Microsatellite instability and mismatch-repair protein expression in hereditary and sporadic colorectal carcinogenesis. *Cancer Res* 2001; **61**: 896-899

18 **Bouzourene H**, Chaubert P, Seelentag W, Bosman FT, Saraga E. Aberrant crypt foci in patients with neoplastic and nonneoplastic colonic disease. *Hum pathol* 1999; **30**: 66-71

19 **Otori K**, Sugiyama K, Hasebe T, Fukushima S, Esumi H. Emergence of adenomatous aberrant crypt foci (ACF) from hyperplastic ACF with concomitant increase in cell proliferation. *Cancer res* 1995; **55**: 4743-4746

20 **Shpitz B**, Hay K, Medline A, Bruce WR, Bull SB, Gallinger S, Stern H. Natural history of aberrant crypt foci. A surgical approach. *Dis Colon Rectum* 1996; 3**9**: 763-767

21 **Wang LD**, Zhou Q, Wei JP, Yang WC, Zhao X, Wang LX, Zou JX, Gao SS, Li YX, Yang CS. Apoptosis and its relationship with cell proliferation, p53, Waf1p21, bcl-2 and c-myc in esophageal carcinogenesis studied with a high-risk population in northern China. *World J Gastroenterol* 1998; **4**: 287-293

22 **Liu HF,** Liu WW, Fang DC, Men RP. Expression and significance of proapoptotic gene Bax in gastric carcinoma. *World J Gastroenterol* 1999; **5**: 15-17

23 **Sun BH**, Zhao XP, Wang BJ, Yang DL, Hao LJ. FADD and TRADD expression and apoptosis in primary human hepatocellular carcinoma. *World J Gastroenterol* 2000; **6**: 223-227

24 **Jia XD,** Han C. Chemoprevention of tea on colorectal cancer induced by dimethylhydrazine in Wistar rats. *World J Gastroenterol* 2000; **6**: 699-703

25 **Zhang Z**, Yuan Y, Gao H, Dong M, Wang L, Gong YH. Apoptosis, proliferation and p53 gene expression of *H. pylori* associated gastric epithelial lesions. *World J Gastroenterol* 2001; **7**: 779-782

26 **Oda T**, Takahashi A, Miyao N, Yanase M, Masumori N, Itoh N, Sato MA, Kon SI, Tsukamoto T. Cell proliferation, apoptosis, angiogenesis and growth rate of incidentally found renal cell carcinoma. *Int J Urol* 2003; **10**: 13-18

27 **Hao X**, Du M, Bishop AE, Talbot IC. Imbalance between proliferation and apoptosis in the development of colorectal carcinoma. *Virchows Arch* 1998; **433:** 523-527

28 **Tanigawa N**, Amaya H, Matsumura M, Lu C, Kitaoka A, Matsuyama K, Muraoka R. Tumor angiogenesis and mode of metastasis in patients with colorectal cancer. *Cancer Res* 1997; **57**: 1043-1046

29 **Xiong B**, Gong LL, Zhang F, Hu MB, Yuan HY. TGFβ1 expression and angiogenesis in colorectal cancer tissue. *World J Gastroenterol* 2002; **8**: 496-498

30 **Minagawa N**, Nakayama Y, Hirata K, Onitsuka K, Inoue Y, Nagata N, Itoh H. Correlation of plasma level and immunohistochemical expression of vascular endothelial growth factor in patients with advanced colorectal cancer. *Anticancer Res* 2002; **22**: 2957-2963

31 **Fan YF**, Huang ZH. Angiogenesis inhibitor TNP-470 suppresses growth of peritoneal disseminating foci of human colon cancer line Lovo. *World J Gastroenterol* 2002; **8**: 853-856

32 **Tao HQ**, Lin YZ, Wang RN. Significance of vascular endothelial growth factor messenger RNA expression in gastric cancer. *World J Gastroenterol* 1998; **4**: 10-13

33 **Thomsen LL**, Miles DW. Role of nitric oxide in tumour progression: lessons from human tumours. *Cancer Metastasis Rev* 1998; **17**: 107-118

34 **Sinicrope FA**, Roddey G, McDonnell TJ, Shen Y, Cleary KR, Stephens LC. Increased apoptosis accompanies neoplastic development in the human colorectum. *Clin Cancer Res* 1996; **2**: 1999-2006

35 **Wang Q**, Wu JS, Gao DM, Lai DL, Ma QJ. Significance of EGF receptor and TGF-á messenger RNA expression in colorectal carcinoma. *Shijie Huaren Xiaohua Zazhi* 1999; **7**: 590-592

36 **Xia L**, Yuan YZ, Xu CD, Zhang YP, Qiao MM, Xu JX. Effects of epidermal growth factor on the growth of human gastric cancer cell and the implanted tumor of nude mice. *World J Gastroenterol* 2002; **8**: 455-458

**Edited by** Wu XN

P.O.Box 2345, Beijing 100023,China
Fax: +86-10-85381893
E-mail: wjg@wjgnet.com www.wjgnet.com

World J Gastroenterol 2003;9(6):1251-1255
World Journal of Gastroenterology
Copyright ©2003 by The WJG Press ISSN 1007-9327

• VIRAL HEPATITIS •

# Distribution and anti-HBV effects of antisense oligodeoxynu-cleotides conjugated to galactosylated poly-L-lysine

Su-Jun Zheng, Sen Zhong, Jian-Jun Zhang, Feng Chen, Hong Ren, Cun-Liang Deng

**Su-Jun Zheng, Jian-Jun Zhang, Hong Ren,** Institute of Viral Hepatitis, Chongqing University of Medical Sciences, Chongqing 400016, China
**Sen Zhong, Feng Chen, Cun-Liang Deng,** Department of Infectious Diseases, Luzhou Medical College Hospital, Luzhou 646000, Sichuan Province, China
**Supported by** the Natural Science Foundation of China, No. 39370648
**Correspondence to:** Sen Zhong, Department of Infectious Diseases, Luzhou Medical College Hospital, Luzhou 646000, China. zhongsenz@yahoo.com.cn
**Telephone:** +86-830-2392712-5419
**Received:** 2002-12-08 **Accepted:** 2003-01-08

## Abstract

**AIM:** To describe distribution of the phosphorothioated antisense oligodeoxynucleotides (PS-asODNs) conjugated to galactosylated poly-L-lysine (Gal-PLL) in mice, and to observe their effects on expression of HBV gene in the 2.2. 15 cells and transgenic mice.

**METHODS:** According to the result of direct sequencing of PCR amplified products, a 16 mer phosphorothioate analogue of the antisense oligodeoxynucleotides (PS-asODNs) directed against the HBV $U_5$-like region was conjugated to the hepatotropic Gal-PLL molecules. Its distribution was demonstrated using asODNs labeled with $^{32}P$ at the 5' terminus with a T4-polynucleotide Kinase. Its inhibition effect on HBV expression was observed in the transfected 2.2.15 cells and transgenic mice.

**RESULTS:** The Gal-PLL and asODNs could form stable complex at a molar ratio of 2:1. As shown in the HBV-transfected 2.2.15 cells, the inhibition effects of asODNs alone and asODNs conjugated to Gal-PLL, at 10 μmol/L for both, on HBsAg and HBeAg production were different,the former being 70 % and 58 %, respectively, and the latter being 96 % and 82 %, respectively. A more pronounced reduction was also observed in viral DNA load in the culture supernatant for the test with Gal-PLL-asODNs. Among many mouse organs, livers retained more asODNs molecules after administration. The preferential concentration in liver was found to be 52.14 % for Gal-PLL-asODNs, as high as 2.38-fold of that for asODNs (21.9 %). Both elements decreased gradually in liver, with 2.9 % of the former, 5.99 % of the latter retained 24 hours after the administration. The injection interval, therefore, was recommended to be 24 hours. In the transgenic mice, serum HBsAg decreased significantly ($P<0.01$) at the 12th day after administrating Gal-PLL- asODNs, the serum HBV DNA turned negative in 4 of the 6 mice.

**CONCLUSION:** Antisense oligodeoxynucleotides conjugated to Gal-PLL can be concentrated in liver and intaked by hepatocytic cells. This may result in specific inhibition of expression and replication of HBV *in vitro* and *in vivo*.

Zheng SJ, Zhong S, Zhang JJ, Chen F, Ren H, Deng CL. Distribution and anti-HBV effects of antisense oligodeoxynucleotides conjugated to galactosylated poly-L-lysine. *World J Gastroenterol* 2003; 9(6): 1251-1255
http://www.wjgnet.com/1007-9327/9/1251.asp

## INTRODUCTION

The antisense oligodeoxynucleotides (asODNs) have been demonstrated previously to be effective for inhibition of HBV gene expression and viral replication *in vitro* and *in vivo*, being potential new agents for anti-HBV therapy[1-4]. However, there are still some hinders for their potential application. First, their molecules must be water soluble and can penetrate the lipophilic cell membrane. Second, they must be resistant enough to enzymatic degradation to allow their concentration in liver. Third, They must be bound specifically to the target HBV sequence. In the present study, a 16-mer phosphorothioate analogue of the antisense oligonucleotides (PS-asODNs) directed against the HBV $U_5$-like region was synthesized and then conjugated to hepa totropic galactosyted poly-L-lysine (Gal-PLL). The anti-HBV effects of asODNs and Gal-PLL-asODNs were demonstrated in the 2.2.15 cells and transgenic mice. In addition, distribution of asODNs was studied in mice.

## MATERIALS AND METHODS

### *PCR product sequencing*

PCR was conducted using the primer pair $P_1$/ $P_2$ in a 50 μl system with the initial denaturation temperature at 94 ℃ for 4 min, followed by 30 cycles at 94 ℃ for 30 s, at 55 ℃ for 30 s and at 72 ℃ for 40 s. The reaction was for the pre-C and C genes of HBV (ayw1 subtype). The sequence of the PCR primers pair was as follows: $P_1$: 5' -AAGGTCTTTGTACTAGGAGGC-3' (1 761-1 781); $P_2$: 5' -TTCCCGATACAGAGCTGAGGC-3' (2 000-2 020). The PCR products were as long as 260 bp and were sequenced using the method given by the Pharmacia $T_7$ kit.

### *Cells and cell culture*

2.2.15 cell line, human hepatoblastoma Hep G2 cell line stably transfected by HBV genome[5-7], were cultured in PRMI1640 medium at 37 ℃ under 5 % $CO_2$, pH: 7.2-7.4, which contained 15 % fetal calf serum, 2 mmol/L glutamine, 0.1 mu/L penicillin and streptomycin, and 380 mg/L G418 (Sigma).

### *Preparation of targeting antisense ODNs*

A targeting water soluble DNA carrier was prepared by coupling galactose and poly-L-lysine using the method of Schwartz and Gray[8], with their molar ratio being 10:1. A 16-mer phosphorothioated antisense oligodeoxynucleotide (5' -CATGCCCCAAAGCCAC-3' ), corresponding to the nucleotides 1 980-1 905, and complementary to preC/C regions of HBV genome (ayw1 subtype), was synthesized. As a reference molecule, another 16-mer phosphorothioated oligodeoxynucleotide (5' -AGTCACTCAGTCAGTC-3' ),

unrelated to the HBV sequence, was prepared. By agarose gel (2.5 %) electrophoresis, conjunctive ratio of Gal-PLL to PS-asODNs was identified[9].

### *Anti-viral effect of PS-asODNs in vitro*

The 2.2.15 cells were incubated for 60 h, and then were transferred to the medium containing asODNs, HBV-specific Gal-PLL-asODNs, HBV-unrelated Gal-PLL-ODNs, or the medium without any oligodeoxynucleotides. The concentration of ODNs in the media was 10 μmol/L. 72 h later, the 2.2.15 cells were transferred to the ordinary medium for 72 h, then 200 ul of supernatant was used for the ELISA reaction for HBsAg and HBeAg, HBV DNA was detected by dot hybridization.

### *Animals*

Kunming mice, (weighing 20 g in average) were used to describe the distribution of asODNs. HBV transgenic mice, were provided by 458 Hospital of PLA in Guangzhou, China, whose expression of HBsAg (126-930 ng/ml) was well documented in the previous studies[10,11].

### *Radiolabeling of asODNs*

The $^{32}$P-labelling of asODNs was at 5' terminus with T4-polynucleotide kinase (Amersham) in the reaction mixture containing asODNs 6.6 ug/20 μl, [γ-$^{32}$P] ATP 90 μl (10 mCi/ml), 10×buffer 18 μl,T4-polynucleotide kinase 9 μl and deionized water 43 μl for 1.5 h. The reaction was stopped by adding 9 μl 0.5M EDTA (pH 8.0). The product was extracted by chloroform and separated using Sephadex-G50. Using the same method, the reaction was carried out twice.

### *Distribution of as ODNs in Kunming mice*

A total number of 24 Kunming mice were equally divided randomly into two groups, one for asODNs and the other for Gal-PLL-asODNs. The labeled asODNs were equally divided into 25 pieces,each piece for 200 μl, with the radioactivity of $9.42\times10^6$ cpm. Twelve pieces of asODNs were mixed with Gal-PLL at a molar ratio of 1:2, and were incubated at room temperature for 60 min. Twenty-four pieces of asODNs were administered intravenously via tail vein to 24 mice, respectively. At 2 min, 30 min, 1 h, 4 h, 13 h, 24 h following intravenous administration, 2 animals were sacrificed for each group at each time point, their blood and organs were collected for determination of total radioactivity using liquid scintillation counter.

### *Anti-HBV effects of Gal-PLL-asODNs in the transgenic mice*

Twelve mice, strongly positive for HBsAg and carrying HBV DNA in serum were equally divided into Gal-PLL-asODNs and control groups. Gal-PLL was then mixed with asODNs in a molar ratio of 2:1 at room temperature. The mixture was then administered intravenously via the tail vein in a dose of 15 μg/g. weight/d of asODNs for successive 12 days. The same volume of saline was used for the control mice by the same means. Blood samples were collected at the venous plexus behind orbital cavity before, or 12 days after the treatment. Sera were separated by incubating at 37 ℃ for 30 min and contrifuged, and stored at -20 ℃ for use. Being diluted at 1:100 with normal saline, the sera were subjected to the ELISA for HBsAg and nested PCR (TakaRa Biotechnology Co.) for viral DNA, with its product being 230 bp in size.

## RESULTS

### *PCR and sequencing of PCR products*

Figure 1 shows that the band of PCR product was between the size of 221-298bp. The sequence of the 132bp product was: 5' -CCAGCACCATGCAACTTTTTCACCTCTGCC-TAATCATCTCTTGTTCATGTCCTACTGTTCAAGCCTCCAA-GCTGTGCCTTGGGTGGCTTTGGGGCATGGACATC-GACCCTTATAAAGAATTTGGAGCTACTG-3' . This was in accordance with the corresponding sequence of HBV genome (ayw1 subtype) which contained the preC region (1 816-1 902), $U_5$-like sequence (1 857-1 918) and partial poly-A addition signal sequence (1 919-1 962)[12,13].

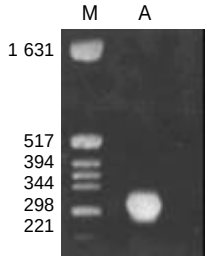


**Figure 1** Amplification of HBV DNA in the 2.2.15 cells with PCR. The PCR products were resolved on 1.5 % agarose gel. M: Molecule weight marker; A: HBV DNA in 2.2.15 cells.

### *The complexion of Gal-PLL and asODNs*

Gal-PLL at different concentrations was incubated with asODNs, and the proper molar ratio for their binding was assessed by agarose gel electrophoresis. The binding was detectable at the molar ratio of 1:1, and complete at the molar ratio of 2:1 or more (Figure 2).

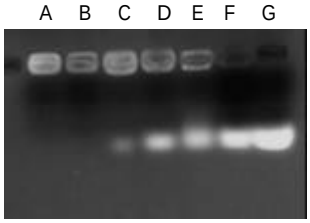


**Figure 2** Analysis of Gal-PLL/asODNs complex formation at different molar ratios. A: Gal-PLL/asODNs=3:1; B: Gal-PLL/asODNs=2:1; C: Gal-PLL/asODNs=1.75:1; D: Gal-PLL/asODNs=1.5:1; E: Gal-PLL/asODNs=1:1; F: Gal-PLL/asODNs=0. 5:1; G: Gal-PLL/asODNs=0:1.

### *Effects of antisense ODNs on HBV gene expression in vitro*

As shown in Table 1, after incubation of 2.2.15 cells with asODNs for 8.5 days, the inhibition rates of HBsAg, HbeAg were 70 % and 50 %, respectively, while those with Gal-PLL-asODNs were 96 % and 82 %, respectively. Only slightly negative effects were observed for the reference agent Gal-PLL-ODNs on expression of HBsAg (19 %) and HBeAg (10 %). The Gal-PLL-asODNs treatment was shown to markedly reduce the amount of HBVDNA in the 2.2.15 cells and the culture medium, compared with free asODNs and conjugated HBV-unrelated Gal-PLL-ODNs.

**Table 1** Inhibition of asODNs on HBsAg and HBeAg secretion in 2.2.15 cells (P/N values $\bar{x}\pm s$)

| Groups | HBsAg | Inhibitory rate (%) | HBeAg | Inhibitory rate (%) |
|---|---|---|---|---|
| Cell control | 9.4±0.16 | | 15.10±0.15 | |
| PS-asODNs | 4.30±0.25 | 70 | 7.60±1.10 | 58 |
| Gal-PLL:PS-asODNs | 2.40±0.26 | 96 | 4.50±0.42 | 82 |
| Gal-PLL:PS-ODNs | 8.10±0.13 | 19 | 13.80±0.76 | 10 |

### *Distribution of asODNs in mice*

Plasma level of asODNs declined rapidly after intravenous administration, with its half-life being approximately 1-2 min, and 7.6 % of asODNs was left in circulation one hour later. Among organs examined, liver retained more asODNs (21.9 %) 30 min after the administration, and the retained molecules decreased gradually, with 2.93 % of them detected 24 hours later. At the time point of 30 min, the retained radioactivity listed in the order of intensity was as following: liver> kidney > lung> heart > spleen> brain (Figure 3).

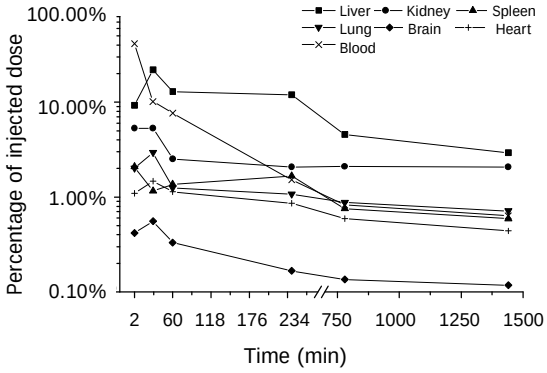


**Figure 3** Distribution of asODNs in Kunming mice ($n$=2).

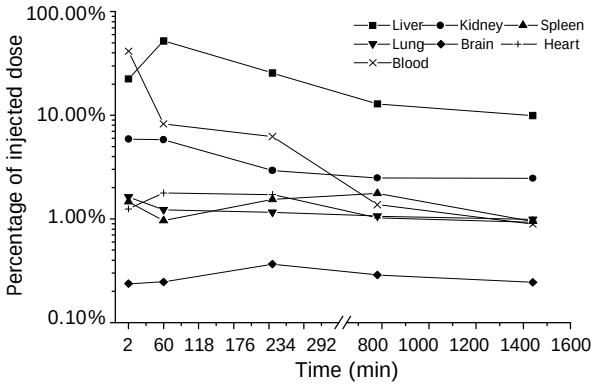


**Figure 4** Distribution of Gal-PLL-asODNs in Kunming mice ($n$=2).

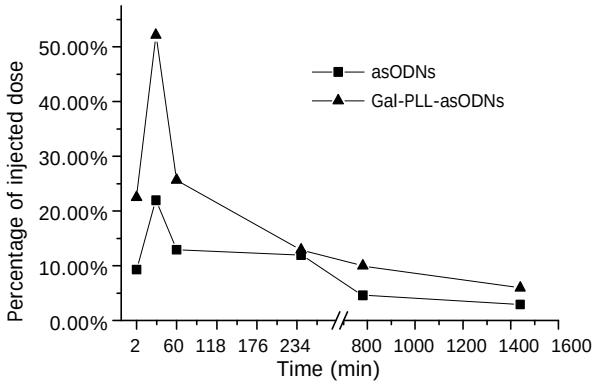


**Figure 5** Comparision of the amount retained in liver between asODNs and Gal-PLL-asODNs ($n$=2).

### *Distribution of Gal-PLL-asODNs in mice*

The elimination process of Gal-PLL-asODNs from bloodstream was similar to that of asODNs, with its half-life being 1-2 minutes. Less Gal-PLL-asODNs was shown to be retained in the circulation at the time points of 30 min (8.26 %), 60 min (6.24 %) than asODNs (10.17 % for 30 min, 7.65 % for 60 min) at the corresponding time points. Up to 52.14 % of Gal-PLL-asODNs was shown to be in liver at the time point of 30 min, and only 5.99 % of the activity was retained in liver 24 hours after its administration. Kidney was the second radioactivity concentrating organ, retaining 5.89 % of injected Gal-PLL-asODNs at the time point of 2 min. The amount in the brain was the smallest (Figure 4). In comparison to that for asODNs, more radioactivity for Gal-PLL-asODNs was retained in liver at each time points (Figure 5). Evidently, Gal-PLL had prompted hepatic intake of asODNs. It might enhance the preferential concentration of agent in liver, with a factor of 8.98-fold to kidney, 42.66-fold to lung, 54.24-fold to spleen. However, there were only few asODNs in liver for both groups 24 hours later (5.99 % and 2.93 %, respectively).

### *Inhibition of viral protein expression by antisense oligonucleotides in vivo*

After treatment for 12 days, serum HBsAg decreased significantly in the Gal-PLL-PSODNs treated group ($P$<0.01); in contrast, no apparent change was detected after treatment with HBV-unrelated Gal-PLL-ODNs (Table 2). In serum HBsAg level, as shown in Figure 6, serum HBV DNA turned negative in 4 of the 6 (66.7 %) Gal-PLL-asODNs treated transgenic mice, but it remained unchanged in the control mice.

**Table 2** Change of serum HBsAg (the value of OD) between pretreatment and posttreatment in HBV transgenic mice

| Groups | Pieces ($n$) | Days of therapy | |
|---|---|---|---|
| | | Pretreatment | The 12th day |
| Normal saline | 6 | 1.335±0.769 | 1.262±0.765[a] |
| Gal- PLL–asODNs | 6 | 1.608±0.658 | 0.733±0.547[b] |

Note: Matched $t$ test analysis showed that, compared with pretreatment, [a]$P$>0.05; [b]$P$<0.01.

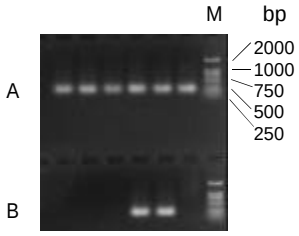


**Figure 6** Products of HBV DNA nested-PCR in the mice serum after 12 days treatment. Lane A: Products of HBVDNA nested-PCR in serum after normal saline treatment; Lane B: Products of HBVDNA nested-PCR in serum after asODNs treatment. M: Molecule weight marker.

## DISCUSSION

The 2.2.15 cells were shown to carry HBVDNA, being a useful model for screening of HBV-specific asODNs. Exonucleases and endonucleases were identified in serum, cells, and other body fluid, both being able to degrade ODNs. Nucleoside modifications may enhance the resistance of ODNs to nuclease digestion. Among them, phosphorothioate oligodeoxynucleotides were found to be more stable in cell culture medium, cells, the cell extraction, serum, tissue and urine. PSODNs, therefore, were used as a drug in this study.

Foreign DNA can be introduced into cells by transfection using several protocols, including electroporation, liposome and calcium phosphate-mediated procedure. In addition, some DNA delivery systems have been designed for binding foreign gene to target cells[14,15]. The DNA-carrier system consisting

of an asialoglycoprotein (asialoorosomucoid, ASOR) covalently linked to poly-L-lysine has been used as a hepatotropic ligand to bring a foreign gene preferentially to hepatocytes via asialoglycoprotein receptors[16-23].

For this purpose, Gal-PLL was prepared in this laboratory previously. Its selective affinity to hepatocytes was demonstrated *in vitro*, proposed to be mediated by asialoglycoprotein receptors on hepatocytes membrane[24-30]. In this study, the optimized molar ratio 2:1 between Gal-PLL and ODNs was estimated to be 2:1, being in agreement with the reported data (17). Gal-PLL was also suggested to be useful as a liver-targeting plasmid DNA carrier *in vivo*[27, 28, 30, 31]. This was approved in this study.

The distribution of different ODNs in *vivo* may vary with their length and sequence[32], and this shoud be clarified before gene therapy. More than a half of asODNs conjugated to Gal-PLL was shown to be retained in liver, being 2.38-fold of that to free asODNs. In order to avoid the possible interference by plasma HBV DNA in HBV infected animal, normal Kunming mice were used to explore the distribution of asODNs *in vivo*.

According to the data presented, Gal-PLL appears to be a more favorable hepatotropic ligand for gene delivery in *vivo* regarding its convenient preparation and stability, as compared to other compounds such as the well characterized tetra-antennary cluster galactoside $L_3G_4$[33].

Considering the dynamic of asODNs, free or conjugated to Gal-PLL, asODNs in liver were 2.97 % and 5.99 %, respectively, 24 hrs after administration, the recommended drug injection interval was 24 hours.

In the same condition of experiment, the inhibition rates of HBsAg and HBeAg by asODNs were 70 % and 58 %, respectively, while those of HBsAg and HBeAg by Gal-PLL-asODNs were 96 % and 82 %, These data indicate that asODNs conjugated to Gal-PLL can block HBV gene expression more efficiently i*n vitro*.

HBV transgenic mice were proved to be the suitable animal model for screening anti-HBV drugs[10,11,34,35,36]. In the present study, a pronounced inhibition was observed by Gal-PLL-asODNs treatment. In addition, serum HBVDNA turned negative in 4 of the 6 transgenic mice. These data show the potential application significance of Gal-PLL-asODNs as an anti-HBV agent.

## REFERENCES


1 **Jensen KD,** Kopeckova P, Kopecek J. Antisense oligonucleotides delivered to the lysosome escape and actively inhibit the hepatitis B virus. B*ioconjug Chem* 2002; **13**: 975-984

2 **Liu S,** Sun W, Cao Y. Study on anti-HBV effects by antisense oligodeoxynucleotides *in vitro. Zhonghua Yufang Yixue Zazhi* 2001; **35**: 338-340

3 **Robaczewska M,** Guerret S, Remy JS, Chemin I, Offensperger WB, Chevallier M, Behr JP, Podhajska AJ, Blum HE, Trepo C, Cova L. Inhibition of hepadnaviral replication by polyethylenimine-based intravenous delivery of antisense phosphodiester oligodeoxynucleotides to the liver. *Gene Ther* 2001; **8**: 874-881

4 **Soni PN,** Brown D, Saffie R, Savage K, Moore D, Gregoriadis G, Dusheiko GM. Biodistribution, stability, and antiviral efficacy of liposome-entrapped phosphorothioate antisense oligodeoxynucleotides in ducks for the treatment of chronic duck hepatitis B virus infection. *Hepatology* 1998; **28**: 1402-1410

5 **Sells MA,** Chen ML, Acs G. Production of hepatitis B virus particles in Hep G2 cells transfected with cloned hepatitis B virus DNA. *Proc Natl Acad Sci USA* 1987; **84**: 1005-1009

6 **Acs G,** Sells MA, Purcell RH, Price P, Engle R, Shapiro M, Popper H. Hepatitis B virus produced by transfected Hep G2 cells causes hepatitis in chimpanzees. *Proc Natl Acad Sci USA* 1987; **84**: 4641-4644

7 **Sells MA,** Zelent AZ, Shvartsman M, Acs G. Replicative intermediates of hepatitis B virus in Hep G2 cells that produce infectious virions. *J Virol* 1988; **62**: 2836-2844

8 **Schwartz BA,** Gray GR. Proteins containing reductively aminated disaccharides. Synthesis and chemical characterization. *Arch Biochem Biophys* 1977; **181**: 542-549

9 **Zhong S,** Zhang D, Wen S. Inhibition of hepatitis B viral gene expression and replication *in vitro* by targeted antisense oligonucleotides. *Zhonghua Yixue Zazhi* 1995; **75:** 392-395, 444

10 **Xiong Y,** Jia Y, Wang H, Liu G, Ren H, Zhuo Z, Zhang D. Hepatitis B virus transgenic mice for the model of anti-hepatitis B virus drug study. *Zhonghua Ganzangbing Zazhi* 2001; **9**: 19-21

11 **Xiong YL**, Jia YZ, Wang HM, Liu GZ, Zhang YJ. High-level hepatitis B virus expression in transgenic mice. *Chuanranbing Xinxi* 2000; **13**: 164-165

12 **Miller RH,** Kaneko S, Chung CT, Girones R, Purcell RH. Compact organization of the hepatitis B virus genome. *Hepatology* 1989; **9**: 322-327

13 **Galibert F,** Mandart E, Fitoussi F, Tiollais P, Charnay P. Nucleotide sequence of the hepatitis B virus genome (subtype ayw) cloned in *E. coli*. *Nature* 1979; **281**: 646-650

14 **Wu CH,** Wilson JM, Wu GY. Targeting genes: delivery and persistent expression of a foreign gene driven by mammalian regulatory elements *in vivo*. *J Biol Chem* 1989; **264**: 16985-16987

15 **Lu XM,** Fischman AJ, Jyawook SL, Hendricks K, Tompkins RG, Yarmush ML. Antisense DNA delivery in vivo: liver targeting by receptor mediated uptake. *J Nucl Med* 1994; **35**: 269-275

16 **Nakazono K,** Ito Y, Wu CH, Wu GY. Inhibition of hepatitis B virus replication by targeted pretreatment of complexed antisense DNA *in vitro*. *Hepatology* 1996; **23**: 1297-1303

17 **Wu GY,** Walton CM, Wu CH. Targeted polynucleotides for inhibition of hepatitis B and C viruses. *Croat Med J* 2001; **42**: 463-466

18 **Wu GY,** Wu CH. Specific inhibition of hepatitis B viral gene expression in vitro by targeted antisense oligonucleotides. *J Biol Chem* 1992; **267**: 12436-12439

19 **Martinez** Fong D, Mullersman JE, Purchio AF, Armendariz Borunda J, Martin ezHernanddez A. Nonenzymatic glycosylation of poly-L-lysine: a new tool for targeted gene delivery. *Hepatology* 1994; **20**: 1602-1608

20 **Guo J,** Zhou YX, Yao ZQ, Wang SQ, Weng SM, Wang BC. Specific delivery to liver cells by asialoglycoprotein modified antisense oligodeoxynucleotides *in vitro* and *in vivo*. *Zhonghua Chuanranbing Zazhi* 1997; **15**: 16-19

21 **Dini L,** Falasca L, Lentini A, Mattioli P, Piacentini M, Piredda L, Autuo ri F. Galactose specific receptor modulation related to the onset of apoptosis in rat liver. *Eur J Cell Biol* 1993; **61**: 329-337

22 **Anderson WF.** Human gene therapy. *Science* 1992; **256**: 808-813

23 **Walton CM,** Wu CH, Wu GY. A DNA delivering system containing listeriolysin O results in enhanced hepatocyte directed gene expression. *World J Gastroenterol* 1999; **5**: 465-469

24 **Zhang J,** Chen F, Zhong S, Tang K, Shi X, Wang M, Peng J. Anti-HBV effect of targeted antisense RNA against HBV C gene. *Zhonghua Ganzangbing Zazhi* 2000; **8**: 169-170

25 **Zhong S,** Wen S, Zhang D, Wang Q, Wang S, Ren H. Inhibition of HBV gene expression by antisense oligonucleotides using galactosyted poly(l-lysine)as a hepatotropic carrier. *Zhonghua Shiyan He Linchuang Bingduxue Zazhi* 2001; **15**: 150-153

26 **Zhoug S,** Wen SM, Zhang DF, Wang QL, Wang SQ, Ren H. Sequencing of PCR amplified HBV DNA pre-c and c regions in the 2.2.15 cells and antiviral action by targeted antisense oligonucleotide directed against sequence. *World J Gastroenterol* 1998; **4**: 434-436

27 **Yang CQ,** Wang JY, He BM, Liu JJ, Guo JS. Glyco-poly-L-lysine is better than liposomal delivery of exogenous genes to rat of liver. *World J Gastroenterol* 2000; **6**: 526-531

28 **Yang CQ,** Wang JY, Fang GT, Liu JJ, Guo JS. A comparison between intravenous and peritoneal route on liver targeted uptake and expression of plasmid delivered by Glyco-poly-L-lysine. *World J Gastroenterol* 2000; **6**: 508-512

29 **Chen YP,** Zhang L, Lu QS, Feng XR, Luo KX. Lactosamination of liposomes and hepatotropic targeting research. *World J Gastroenterol* 2000; **6**: 593-596

30 **Yang C,** Wang J, Wen S, Liu J, Guo J. Comparative studies of different carriers and introducing routes on the effects of liver targeted uptake of exogenous gene. *Zhonghua Ganzangbing Zazhi* 2000; **8**: 227-229

31 **Mani SA,** Harish S, Vathsala PG, Rangarajan PN, Padmanaban G. Receptor –mediated gene delivery approach demonstrates the role of 5'-proximal DNA region in conferring phenobarbitone responsiveness to CYP2B2 gene in rat liver *in vivo*. *Biochem Biophys Res Commun* 2000; **268**: 734-739

32 **Biessen EA,** Vietsch H, Kuiper J, Bijsterbosch MK, Berkel TJ. Liver uptake of phosphodiester oligodeoxynucleotides is mediated by scavenger receptors. *Mol Pharmacol* 1998; **53**: 262-269

33 **Biessen EA,** Vietsch H, Rump ET, Fluiter K, Kuiper J, Bijsterbosch MK, van Berkel TJ. Targeted delivery of oligodeoxynucleotides to parenchymal liver cells *in vivo*. *Biochem J* 1999; **340**: 783-792

34 **Morrey JD,** Korba BE, Sidwell RW. Transgenic mice as a chemotherapeutic model for hepatitis B virus infection. *Antivir Ther* 1998; **3**(Suppl 3):59-68

35 **Morrey JD,** Bailey KW, Korba BE, Sidwell RW. Utilization of transgenic mice replicating high levels of hepatitis B virus for antiviral evaluation of lamivudine. *Antiviral Res* 1999; **42**: 97-108

36 **Julander JG,** Sidwell RW, Morrey JD. Characterizing antiviral activity of adefovir dipivoxil in transgenic mice expressing hepatitis B virus. *Antiviral Res* 2002; **55**: 27-40

**Edited by** SuQ

P.O.Box 2345, Beijing 100023,China
Fax: +86-10-85381893
E-mail: wjg@wjgnet.com www.wjgnet.com

World J Gastroenterol 2003;9(6):1256-1260
World Journal of Gastroenterology
Copyright © 2003 by The WJG Press ISSN 1007-9327

• VIRAL HEPATITIS •

# Cross-reactivity of hypervariable region 1 chimera of hepatitis C virus

Bing-Shui Xiu, Shi-Gan Ling, Xiao-Guo Song, He-Qiu Zhang, Kun Chen, Cui-Xia Zhu

**Bing-Shui Xiu, Shi-Gan Ling, Xiao-Guo Song, He-Qiu Zhang, Kun Chen, Cui-Xia Zhu,** Laboratory of Molecular Virology, Institute of Basic Medical Sciences, Academy of Military Medical Sciences, Beijing 100850, China
**Supported by** National 10th Five-Year Plan of Science and Technology Brainstorm Project, No. 2001BA708B06 and a grant from Natural Science Foundation of Beijing, No.7002031
**Correspondence to:** Professor Shi-Gan Ling, Laboratory of Molecular Virology, Institute of Basic Medical Sciences, Academy of Military Medical Sciences, Beijing 100850, P.R.China. lingsg@nic.bmi.ac.cn
**Telephone:** 010-66932308 **Fax:** +86-10-68285718
**Received:** 2003-01-04 **Accepted:** 2003-02-16

## Abstract

**AIM:** To analyze the amino acid sequences of hypervariable region 1 (HVR1) of HCV isolates in China and to construct a combinatorial chimeric HVR1 protein having a very broad high cross-reactivity.

**METHODS:** All of the published HVR1 sequences from China were collected and processed with a computer program. Several representative HVR1's sequences were formulated based on a consensus profile and homology within certain subdivision. A few reported HVR1 mimotope sequences were also included for a broader representation. All of them were cloned and expressed in *E.coli.* The cross-reactivity of the purified recombinant HVR1 antigens was tested by ELISA with a panel of sera from HCV infected patients in China. Some of them were further ligated together to form a combinatorial HVR1 chimera.

**RESULTS:** Altogether 12 HVR1$_s$ were selected and expressed in *E.coli* and purified to homogeneity. All of these purified antigens showed some cross-reactivity with sera in a 27 HCV positive panel. Recombinant HVR1s of No. 1, 2, 4, and 8# showing broad cross-reactivities and complementarity with each other, were selected for the ligation elements. The chimera containing these 4 HVR1s was highly expressed in *E.coli*. The purified chimeric antigen could react not only with all the HCV antibody positive sera in the panel but also with 90/91 sera of HCV -infected patients.

**CONCLUSION:** The chimeric antigen was shown to have a broad cross-reactivity. It may be helpful for solving the problem caused by high variability of HCV, and in the efforts for a novel vaccine against the virus.

Xiu BS, Ling SG, Song XG, Zhang HQ, Chen K, Zhu CX. Cross-reactivity of hypervariable region 1 chimera of hepatitis C virus. *World J Gastroenterol* 2003; 9(6): 1256-1260
http://www.wjgnet.com/1007-9327/9/1256.asp

## INTRODUCTION

Hepatitis C virus (HCV) is a major etiological agent of non-A, non-B hepatitis worldwide[1-3], and HVR1, the N-terminal 27 amino acid residues of the putative HCV envelope protein E2, is known as the principal neutralization epitopes up to date[4-7]. Antibodies to HVR1 in human sera have been shown to block viral attachment to human cell lines *in vitro* and to protect chimpanzees from HCV infection *in vivo*[8-10]. The HVR1 sequence is highly variable, and is the greatest obstacle for the vaccine development and immune therapy[11,12]. However, the highly variable HVR1s have been shown to have some cross-reactivities with each other, indicating that a broadly cross-reactive HVR1 peptide or their cocktails are helpful to solving the problem[13]. Data were accumulated in this study all over the world[14-17].

In China, HVR1 sequences of different HCV isolates have been reported by many authors, but few studies were on HVR1 cross-reactivity. Integrating the HVR1 sequences reported in China together with some published mimotopes, 12 representative HVR1 sequences were selected using bioinformatics technology. All of the representative HVR1 sequences were cloned and expressed, and their cross-reactivity was studied with a panel of 27 HCV positive sera. Finally we obtained an HVR1 fusion antigen broadly cross-reactive with the HCV-infected sera.

## MATERIALS AND METHODS

### *Human sera*

Samples of HCV-infected sera were obtained from blood donor applicants in Beijing Red Cross Blood Center and from chronic HCV-infected patients from 302 Hospital of PLA. All were positive for HCV antibodies using the 2nd-generation ELISA kit. (Ortho Diagnostics, Raritan N.J).

### *Selection of representative HVR1 sequences*

All of the HVR1 sequences published in China were loaded into database and their consensus sequence was obtained by BASIC program according to the frequency of amino acid residues. All of these HVR1 sequences were divided into several groups according to their alignment, and one sequence was chosen as the representative from each group. All of the work above was operated on Goldkey (a molecular biology software developed by our institute). Some HVR1 sequences or mimotopes published were chosen as representative ones for their high cross-reactivity with sera of HCV infected patients from other countries.

### *Construction of expression plasmid HVR1-1 # to 12*

The representative HVR1 sequences were modified considering the Escherischia coli's favorable codon usage. The coding genes were synthesized chemically and to facilitate further ligation, two linkers with a specially designed restriction endonuclease site were incorporated into their N- and C-terminals respectively. The N terminal arm is F1 (5'- gc ctc gag ggt ggt gga tct -3'), The C terminal arm is R1 (5'-gc tct aga acc tcc acc act -3'). The fragments were digested with XhoI and XbaI enzymes and inserted into the expressing plasmid pBVIL1 digested by the same restrictive enzymes. In

the same way, 12 different pBVIL1-HVR1 constructs were prepared and the HVR1 genes were expressed as fusion protein with IL1β in *E. coli*.

### *Construction of the chimeric plasmid*

According to the cross-reactivity with the HCV antibodies positive sera panel, several HVR1s were chosen to ligate together one by one as illustrated in Figure 1. The plasmid pBVIL1-HVR1-1# (pHVR1#) was chosen as a vector digested by Xba I and BamH I, while the plasmid pBVIL1-HVR1-2#, was chosen as the donor of pattern, amplified using constant primer F2 (5' gc act agt ggt ggt gga tct 3') and R2 (5'cg gga tcc tta gga aga cac aaa 3') which annealed to C-terminal of IL1β. The PCR product was digested with *Spe* I and *BamH* I, and inserted into the digested vector, pBVIL1-HVR1-1#. Owe to the same cohesive end of the endonuclease *Xba* I and *Spe* I, the digested PCR fragment could accurately linked to the digested plasmid and the new ligated site could be digested by neither of them.

The pBVIL1-HVR1-1+2# had the same enzyme sites with pHVR1# and so it could be used as a new vector and connected with other HVR1 gene fragments. In this way, the pBVIL1-chimeric-HVR1 was constructed to contain four HVR1 genes, HVR1-1#, HVR1-4#, HVR1-6# and HVR1-8#.

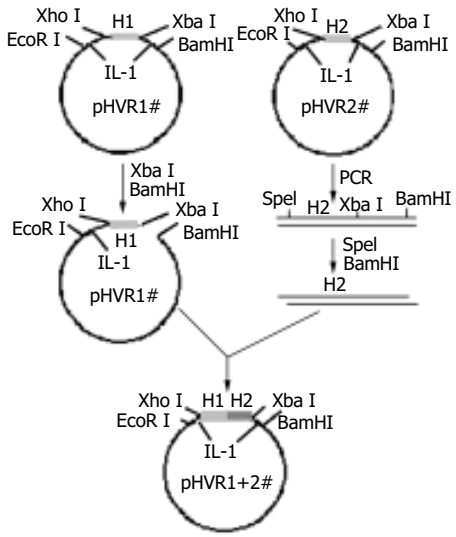


**Figure 1** Four different HVR1 gene fragments were cloned on pBVIL-1. HVR1-2 gene fragment was ligated with pBVIL-1-HVR1-1 (pHVR1#). The new pHVR1+2 had the same site with pHVR1#, and the HVR1-4# gene fragments could be ligated by the same way. After 3 cycles, the chimera HVR1 plamid was constructed.

### *Purification of representative HVR1-1-12# and the chimeric antigen*

The plasmids carrying HVR1 fragments were transformed into HB101 as routine, and were examined for their orientation and nucleic acid sequences. The transformed HB101 was grown overnight, diluted 1:20 with fresh LB-medium and further incubated at 37 ¡æto an $OD_{600}$ of 0.6. After induction for 4 h at 42 ¡æ, the bacteria were harvested by centrifugation, and lysed by sonication. All of the recombinant proteins existed in inclusion bodies, and could be dissolved in a solution containing 8 M urea. The recombinant proteins were isolated and purified consecutively by Q-Sepharose-FF and Sephadex G50 chromatography.

### *ELISA*

Microplates were coated with 0.3 μg recombinant HVR1 peptide in 100 mM phosphate buffer (pH7.4) by incubation overnight at 4 ¡æ The plates were then blocked with the phosphate buffer containing 0.2 % BSA at 4 ¡æfor 3 h, and then incubated with 100 μl of the serum sample 1:10 diluted with a sample buffer (100 mM sodium phosphate buffer, pH7.5 containing 10 % goat serum and 0.05 % Tween) at 37 ¡æfor 1 h. After being washed for five times with 100 mM phosphate buffer (pH7.5) containing 0.05 % Tween, the plates were then incubated for 30 min at 37 ¡æwith 1:25 000 diluted HRP-conjugated monoclonal antibody against human IgG. After washing, the reaction was visualized in the substrate buffer (50 mM sodium phosphate-citric acid buffer, pH5.0 containing 0.4 mg/ml TMB and 0.4 μl/ml of 30 % hydrogen peroxide). The reaction was stopped by adding 50 μl of 2 M sulfuric acid, and the absorbance was measured in a microplates ELISA reader at 450 nm.

## RESULTS

### *Determination of 12 representative peptides*

A total number of 123 sequences on HVR1 were reported in China, and the derived consensus profile of them is shown in Figure 2A. Some amino acid residues of HVR1 were shown to be hypervariable, while those at position 385, 389, 406, 409 were conserved. The sequence on first line was defined as CCS (Chinese consensus sequence), whose amino acid residues emerged most frequently. CCS was chosen as the first representative sequence, named HVR1-1#, being different at some positions from Puntoriero's consensus sequence[13] (Figure 2B). The homology of the 123 sequences was analyzed using the Goldkey software, and divided into 6 groups, HVR1-2 to 7# according to their alignment to CCS. In this way 6 sequences named were obtained. HVR1-8# 9# were from GenBank (L19383, S24080), both being broadly cross-reactive with mice sera induced by mimotopes. HVR1-10# and 11# were sequences for the mimotope R9 and M122 respectively (Puntoriero *et al*, 1998), and HVR1-12# reported by Watanabe[14].

A

```
1     5     10    15    20    25  27
STHVTGGAAGRTTSGFTSLFTPGPSQK
GHYTSAAVQAHSLRSLAGFLSSAAAKN
DSRAVTRTTSQAIQAIVNISALSSK N
N QII SSVHYNAHRVMRMKNF R  I
E TLM  KSTAGVYTKGTVTRR Q  T
Q KSH  QEKNVMGIMIA YQT T
R V L  DHQIDHAHYKK  KH N
T F W  EGRDIPLK S   MA
A L    MR KK N Y   N
H S       FQ T     Q
I C       GR F     V
K D       SY K     Y
L I         W
Y
```

B

```
STHVTGGAAGRTTSGFTSLFTPGPSQK
E------S-A-----L----S--A---
```

**Figure 2** Derivation of the Chinese consensus sequence. (A) Consensus pattern of the 123 natural variants of the HCV HVR1 sequence used in this work. Shaded residues accounted alone for 80 % of the observed frequency. Residues were listed in decreasing order of observed frequency from top to bottom. The first line was Chinese consensus sequence (CCS). (B) The Chinese consensus sequence (upper) was different with Puntoriero's (lower). Dashes indicate residues identical to the upper line.

### *Reactivity of representative peptide with sera of panel I*

Twelve representative HVR1 gene as shown in Figure 3, were expressed in *E.coil* fused with human IL-1β. The HVR1/IL-1β fusion protein migrated at the expected position of about 21 kD (Figure 4). Twenty-seven HCV patients' sera were used as panel I to show the cross-reactivities of 12 representative HVR1 by ELISA. As shown in Figure 5, all of the HVR1 peptide reacted with more than one serum. No reactivity was detected to IL-1β in sera of panel I, and none of the anti-HCV negative sera reacted with the 12 recombinant peptides. The most broadly cross-reactive HVR1 was HVR1-11#, and the Chinese consensus sequence (CCS) which showed a higher cross-reactivity too.

We took HVR1-1,2,4,8# as components for the best cocktail, because these 4 HVR1 peptides showed complementary reactivities to the sera in panel I, as showed in Figure 5. There overall cross-reactivity was found to be 25/27.

| | |
|---|---|
| 1# | STHVTGGAAGRTTSGFTSLFTPGPSQK |
| 2# | STHVTGGVQGHSLRGLTSLFTSGPAQK |
| 3# | ITRVTGGVQGHSLRSLTSLFTPGPAQK |
| 4# | STHVTGAVQGRSLQSFTSFLSPGPSQK |
| 5# | DTHVTGGAAARGASGLANLFTSGPAQK |
| 6# | GTYVTGGATAHTASGFASLFTTGSKQN |
| 7# | TTHVTAGTAAHATSSFTKLFAPGAKQN |
| 8# | NTYVTGGSAAHTTSRFTSLFSPGPQQN |
| 9# | ETHTSGGSVARAAFGLTSIFSPGKSQN |
| 10# | TTTTTGGVQGHTTRGLVRLFSLGSKQN |
| 11# | DTTVTGGQAARTTQSFTSLFPPGPSQK |
| 12# | DTTVTGGQAARTTQSFTSLFTPGPSQK |

**Figure 3** The amino acid sequence of 12 representative HVR1 sequences. Amino acid residues were indicated by standard single-letter codes.

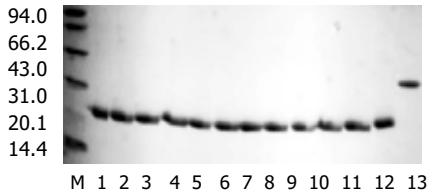


**Figure 4** The Coomassic stain after SDS-PAGE of 12 purified representative and chimera HVR1 antigen. M. marker; 1-12. 12 purified representative HVR1 antigen; 13. chimera HVR1 antigen.

### *Reactivity of chimera HVR1 antigen with panel I and panel II*

HVR1-1#, 2#, 4# and 8# were ligated one by one in tandem within plasmid pBVIL1. The chimeric protein was expressed in HB101 and further purified (Figure 4).

As expected, a broader reactive spectrum was observed for the chimeric HVR1 antigen. It was shown to be reactive with all of the sera of panel I, including sera 73# and 39# which were not reactive with any single HVR1 (Figure 5). For more data 91 sera from HCV-infected patients were also used for the assay as panel II, with 90 reactive with chimera antigen (Table 1). The data indicated that application of the chimera protein helped to acquire a higher cross-reactivity.

**Table 1** Reactivity of F4HVR1 with another panel (91 sera of HCV infected patient)

| OD difference between sera and co | No. of reactive sera | The adding up percent of total sera |
|---|---|---|
| >2.0 | 56 | 61.5 |
| 1.5~2.0 | 14 | 76.9 |
| 1.0~1.5 | 13 | 91.2 |
| 0.5~1.0 | 6 | 97.8 |
| 0.371 | 1 | 98 |
| 0.065 | 1 | |

The cutoff of the ELISA was as defined in Figure 5.

## DISCUSSION

HVR1, which contains a principal neutralization epitope in HCV, is important for the development of HCV vaccine[4-7]. Due to the high mutation rate of HVR1, there are now hundreds of HVR1 isolates reported, presenting a great obstacle for HCV vaccine development[18-21]. It was suggested that to select a highly cross-reactive HVR1 antigen could solve the variability problem[22-27], thus highlighted the importance to study the cross-reactivity of HVR1.

Most of the work about the cross-reactivity of HVR1 focused on single HVR1 antigen. However we think the cross-reactivity of single HVR1 is limited. Recently, multi-epitope chimeric antigen was used to improve the sensitivity of HCV immunoassay reagents[28,29]. Here we provided evidence for enhancing the cross-reactivity by constructing a chimeric antigen that incorporates several representative HVR1 peptides.

Considering geographical variation of HVR1[30-33], we gave

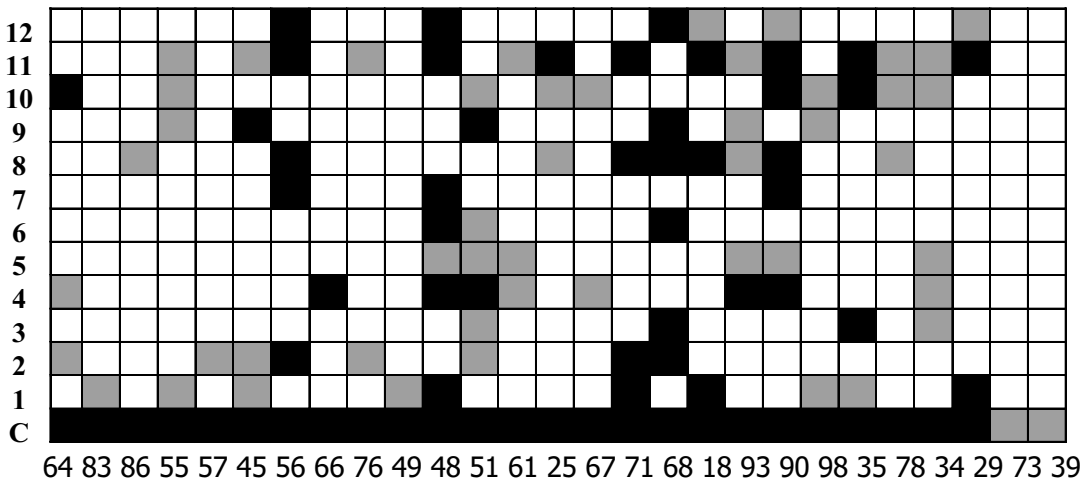


**Figure 5** Reaction of the 12 representative HVR1$_s$ and chimera HVR1antigen (C) with 27 sera from HCV-infected patients. HVR1 names are indicated at the left of each column. For each serum (indicated on the bottom of each column) average values (A450) have been determined from two independent experiments. The mean of 10 sera from non-infected individuals plus 4SD defined the cutoff (co). Results were expressed as the difference between the average value of the HCV antibody positive sera and co. Strong positive values (>0.5) are indicated in black. And weak positive values are indicated in grey (0.15-0.5).

priority to Chinese sequence when we selected representative HVR1 sequences. The differences between CCS and Puntoriero's suggest the HVR1 variant found in China differs to a certain extent from what occurred elsewhere[14]. The chimeric antigen contains 3 representative HVR1 sequences coming from China, and showed broad cross-reactivity with sera of the HCV-infected patients.

The reported HVR1 antigen or mimotope could cross-react with no more than 80 % of sera containing HCV antibodies[22-27]. Chimeric HVR1 antigen could cross-react with 90/91 (98 %) of tested sera. The results also suggested that most of HCV infected patients could generate some antibodies against HVR1. The possible association between HVR1 antibody and the self-limiting course of HCV infection and a more favorable response to interferon[34-40], remains to be evaluated in the following study.

Evidently, the reaction spectrum of the chimera HVR1 antigen include the total cross-reactivity of the representative HVR1 antigen contained. Interestingly, the chimera HVR1 antigen could react with sera 73# and 39#, which are not definitely reactive with any of the four representative HVR1. In our consideration, those samples might react with some of the representative HVR1 used for ligation, but reactions are too weak to be detected. The OD value would be elevated when 4 HVR1 is added up together.

In this study, we used a prepared chimeric antigen instead of synthetic peptides[41-43]. The antigen may also be used in the study for the HCV vaccine. In addition, the chimeric antigen is fused with IL-1β. The latter part contains a nano-peptide sequence. It may act as an immune adjuvant[44-46], promoting a strong immune response when injected.

In summary, the chimeric HVR1 antigen, containing several representative HVR1 fragments, can show very high cross-reactivity, which may be helpful to overcome the variability of HCV. The chimeric HVR1 antigen is of potential application for HCV vaccination and immune therapy.

## REFERENCES


1 **Alter HJ**. To C or not to C. these are the questions.*Blood* 1995; **85:** 1681-1695

2 **Choo QL,** Kuo G, Weiner AJ, Overby LR, Bradley DW, Houghton M. Isolation of a cDNA clone derived from a blood-borne non-A, non-B viral hepatitis genome. *Science* 1989; **244:** 359-362

3 **Sela B.** New approaches to immune against hepatitis C virus *Harefuah* 2002; **141:** 1076-1080

4 **Esumi M,** Rikihisa T, Nishimura S, Goto J, Mizuno K, Zhou YH, Shikata T. Experimental vaccine activities of recombinant E1 and E2 glycoproteins and hypervariable region 1 peptides of hepatitis C virus in chimpanzees. *Arch Virol* 1999; **144:** 973-980

5 **Farci P,** Alter HJ, Wong DC, Miller RH, Govindarajan S, Engle R, Shapiro M, Purcell RH. Prevention of hepatitis C virus infection in chimpanzees after antibody-mediated in vitro neutralization. *Proc Natl Acad Sci U S A* 1994; **91:** 7792-7796

6 **Cerino A,** Meola A, Segagni L, Furione M, Marciano S, Triyatni M, Liang TJ, Nicosia A, Mondelli MU. Monoclonal antibodies with broad specificity for hepatitis C virus hypervariable region 1 variants can recognize viral particles. *J Immunol* 2001; **167:** 3878-3886

7 **Farci P,** Shimoda A, Wong D, Cabezon T, De Gioannis D, Strazzera A, Shimizu Y, Shapiro M, Alter HJ, Purcell RH. Prevention of hepatitis C virus infection in chimpanzees by hyperimmune serum against the hypervariable region 1 of the envelope 2 protein. *Proc Natl Acad Sci U S A* 1996; **93:** 15394-15399

8 **Zhou YH,** Takekoshi M, Maeda F, Ihara S, Esumi M. Recombinant antibody Fab against the hypervariable region 1 of hepatitis C virus blocks the virus adsorption to susceptible cells *in vitro*. *Antiviral Res* 2002; **56:** 51-59

9 **Goto J,** Nishimura S, Esumi M, Makizumi K, Rikihisa T, Nishihara T, Mizuno K, Zhou Y, Shikata T, Fujiyama S, Tomita K. Prevention of hepatitis C virus infection in a chimpanzee by vaccination and epitope mapping of antiserum directed against hypervariable region 1. *Hepatol Res* 2001; **19:** 270-283

10 **Zibert A,** Schreier E, Roggendorf M. Antibodies in human sera specific to hypervariable region 1 of hepatitis C virus can block viral attachment. *Virology* 1995; **208:** 653-661

11 **Korenaga M,** Hino K, Katoh Y, Yamaguchi Y, Okuda M, Yoshioka K, Okita K. A possible role of hypervariable region 1 quasispecies in escape of hepatitis C virus particles from neutralization. *J Viral Hepat* 2001; **8:** 331-340

12 **Gao G,** Buskell Z, Seeff L, Tabor E. Drift in the hypervariable region of the hepatitis C virus during 27 years in two patients. *J Med Virol* 2002; **68:** 60-67

13 **Scarselli E,** Cerino A, Esposito G, Silini E, Mondelli MU, Traboni C. Occurrence of antibodies reactive with more than one variant of the putative envelope glycoprotein (gp70) hypervariable region 1 in viremic hepatitis C virus-infected patients. *J Virol* 1995; **69:** 4407-4412

14 **Puntoriero G,** Meola A, Lahm A, Zucchelli S, Ercole BB, Tafi R, Pezzanera M, Mondelli MU, Cortese R, Tramontano A, Galfre' G, Nicosia A. Towards a solution for hepatitis C virus hypervariability: mimotopes of the hypervariable region 1 can induce antibodies cross-reacting with a large number of viral variants. *EMBO J* 1998; **17:** 3521-3533

15 **Watanabe K,** Yoshioka K, Ito H, Ishigami M, Takagi K, Utsunomiya S, Kobayashi M, Kishimoto H, Yano M, Kakumu S. The hypervariable region 1 protein of hepatitis C virus broadly reactive with sera of patients with chronic hepatitis C has a similar amino acid sequence with the consensus sequence. *Virology* 1999; **264:** 153-158

16 **Mondelli MU,** Cerino A, Segagni L, Meola A, Cividini A, Silini E, Nicosia A. Hypervariable region 1 of hepatitis C virus: immunological decoy or biologically relevant domain? *Antiviral Res* 2001; **52:** 153-159

17 **Rispeter K,** Lu M, Behrens SE, Fumiko C, Yoshida T, Roggendorf M. Hepatitis C virus variability: sequence analysis of an isolate after 10 years of chronic infection. *Virus Genes* 2000; **21:** 179-188

18 **Fan X,** Di Bisceglie AM. Genetic characterization of hypervariable region 1 in patients chronically infected with hepatitis C virus genotype 2. *J Med Virol* 2001; **64:** 325-333

19 **Lin HJ,** Seeff LB, Barbosa L, Hollinger FB. Occurrence of identical hypervariable region 1 sequences of hepatitis C virus in transfusion recipients and their respective blood donors: divergence over time. *Hepatology* 2001; **34:** 424-429

20 **Lu L,** Nakano T, Orito E, Mizokami M, Robertson BH. Evaluation of accumulation of hepatitis C virus mutations in a chronically infected chimpanzee: comparison of the core, E1, HVR1, and NS5b regions. *J Virol* 2001; **75:** 3004-3009

21 **Ray SC,** Wang YM, Laeyendecker O, Ticehurst JR, Villano SA, Thomas DL. Acute hepatitis C virus structural gene sequences as predictors of persistent viremia: hypervariable region 1 as a decoy. *J Virol* 1999; **73:** 2938-2946

22 **Zucchelli S,** Roccasecca R, Meola A, Ercole BB, Tafi R, Dubuisson J, Galfre G, Cortese R, Nicosia A. Mimotopes of the hepatitis C virus hypervariable region 1, but not the natural sequences, induce cross-reactive antibody response by genetic immunization. *Hepatology* 2001; **33:** 692-703

23 **Roccasecca R,** Folgori A, Ercole BB, Puntoriero G, Lahm A, Zucchelli S, Tafi R, Pezzanera M, Galfre G, Tramontano A, Mondelli MU, Pessi A, Nicosia A, Cortese R, Meola A. Induction of cross-reactive humoral immune response by immunization with mimotopes of the hypervariable region 1 of the hepatitis C virus. *Int Rev Immunol* 2001; **20:** 289-300

24 **Roccasecca R,** Folgori A, Ercole BB, Puntoriero G, Lahm A, Zucchelli S, Tafi R, Pezzanera M, Galfre G, Tramontano A, Mondelli MU, Pessi A, Nicosia A, Cortese R, Meola A. Mimotopes of the hyper variable region 1 of the hepatitis C virus induce cross-reactive antibodies directed against discontinuous epitopes. *Mol Immunol* 2001; **38:** 485-492

25 **Li C,** Candotti D, Allain JP. Production and characterization of monoclonal antibodies specific for a conserved epitope within hepatitis C virus hypervariable region 1. *J Virol* 2001; **75:** 12412-12420

26 **Shang D,** Zhai W, Allain JP. Broadly cross-reactive, high-affinity antibody to hypervariable region 1 of the hepatitis C virus in rabbits. *Virology* 1999; **258:** 396-405

27 **Zhou YH,** Moriyama M, Esumi M. Multiple sequence-reactive antibodies induced by a single peptide immunization with hypervariable region 1 of hepatitis C virus. *Virology* 1999; **256:** 360-370

28 **Yagi S,** Kashiwakuma T, Yamaguchi K, Chiba Y, Ohtsuka E, Hasegawa A. An epitope chimeric antigen for the hepatitis C virus serological screening test. *Biol Pharm Bull* 1996; **19:** 1254-1260

29 **Paolini R,** Marson P, Vicarioto M, Ongaro G, Viero M, Girolami A. Anti-hepatitis C virus serology in patients affected with congenital coagulation defects: a comparative study using three second generation ELISA tests. *Transfus Sci* 1994; **15:** 303-311

30 **Bosch FX,** Ribes J. Epidemiology of liver cancer in Europe. *Can J Gastroenterol* 2000; **14:** 621-630

31 **Simmonds P.** Viral heterogeneity of the hepatitis C virus. *J Hepatol* 1999; **31**(Suppl 31): 54-60

32 **Cai Q,** Zhang X, Tian L, Yuan M, Jin G, Lu Z. Variant analysis and immunogenicity prediction of envelope gene of HCV strains from China. *J Med Virol* 2002; **67:** 490-500

33 **Oliveira ML,** Bastos FI, Sabino RR, Paetzold U, Schreier E, Pauli G, Yoshida CF. Distribution of HCV genotypes among different exposure categories in Brazil. *Braz J Med Biol Res* 1999; **32:** 279-282

34 **Zibert A,** Meisel H, Kraas W, Schulz A, Jung G, Roggendorf M. Early antibody response against hypervariable region 1 is associated with acute self-limiting infections of hepatitis C virus. *Hepatology* 1997; **25:** 1245-1249

35 **Lechner S,** Rispeter K, Meisel H, Kraas W, Jung G, Roggendorf M, Zibert A. Antibodies directed to envelope proteins of hepatitis C virus outside of hypervariable region 1. *Virology* 1998; **243:** 313-321

36 **Isaguliants MG,** Widell A, Zhang SM, Sidorchuk A, Levi M, Smirnov VD, Santantonio T, Diepolder HM, Pape GR, Nordenfelt E. Antibody responses against B-cell epitopes of the hypervariable region 1 of hepatitis C virus in self-limiting and chronic human hepatitis C followed-up using consensus peptides.*J Med Virol* 2002; **66:** 204-217

37 **Del Porto P,** Puntoriero G, Scotta C, Nicosia A, Piccolella E. High prevalence of hypervariable region 1-specific and -cross-reactive CD4(+) T cells in HCV-infected individuals responsive to IFN-alpha treatment. *Virology* 2000; **269:** 313-324

38 **Hjalmarsson S,** Blomberg J, Grillner L, Pipkorn R, Allander T. Sequence evolution and cross-reactive antibody responses to hypervariable region 1 in acute hepatitis C virus infection. *J Med Virol* 2001; **64:** 117-124

39 **Hattori M,** Yoshioka K, Aiyama T, Iwata K, Terazawa Y, Ishigami M, Yano M, Kakumu S. Broadly reactive antibodies to hypervariable region 1 in hepatitis C virus-infected patient sera: relation to viral loads and response to interferon. *Hepatology* 1998; **27:** 1703-1710

40 **Pawlotsky JM,** Germanidis G, Frainais PO, Bouvier M, Soulier A, Pellerin M, Dhumeaux D. Evolution of the hepatitis C virus second envelope protein hypervariable region in chronically infected patients receiving alpha interferon therapy. *J Virol* 1999; **73:** 6490-6499

41 **Zhou YH,** Sugitani M, Esumi M. Sequences in the hypervariable region 1 of hepatitis C virus show only minimal variability in the presence of antibodies against hypervariable region 1 during acute infection in chimpanzees. *Arch Virol* 2002; **147:** 1955-1962

42 **Wang Y,** Hao F, Huang Y. Molecular design and immunoreactivity studies of multiple antigen peptide corresponding to hypervariable region 1 sequence of hepatitis C virus. *Zhonghua Ganzangbing Zazhi* 2000; **8:** 48-50

43 **Duenas-Carrera S,** Vina A, Garay HE, Reyes O, Alvarez-Lajonchere L, Guerra I, Gonzalez LJ, Morales J. Immunological evaluation of Escherichia coli-derived hepatitis C virus second envelope protein (E2) variants. *J Pept Res* 2001; **58:** 221-228

44 **Bockmann S,** Mohrdieck K, Paegelow I. Influence of interleukin-1 beta on bradykinin-induced responses in guinea pig peritoneal macrophages. *Inflamm Res* 1999; **48:** 56-62

45 **Akasu T,** Tsurusaki M. Effects of interleukin-1 beta on neurons in mammalian pelvic ganglia. *Kurume Med J* 1999; **46:** 143-150

46 **Boraschi D,** Tagliabue A. Interleukin-1 and interleukin-1 fragments as vaccine adjuvants. *Methods* 1999; **19:** 108-113


**Edited by** Su Q and Wang XL

P.O.Box 2345, Beijing 100023,China
Fax: +86-10-85381893
E-mail: wjg@wjgnet.com www.wjgnet.com

World J Gastroenterol 2003;9(6):1261-1264
World Journal of Gastroenterology
Copyright ©2003 by The WJG Press ISSN 1007-9327



# TT virus infection in patients with chronic hepatitis B and response of TTV to lamivudine

Javier Moreno Garcia, Rafael Barcena Marugan, Gloria Moraleda Garcia, M Luisa Mateos Lindeman, Jesus Fortun Abete, Santos del Campo Terron

**Javier Moreno Garcia, Rafael Barcena Marugan, Gloria Moraleda Garcia, Santos del Campo Terron**, Department of Gastroenterology, Hospital Ramony Cajal, Madrid, Spain
**M Luisa Mateos Lindeman**, Department of Microbiology, Hospital Ramony Cajal, Madrid, Spain
**Jesus Fortun Abete**, Department of Infectious Diseases, Hospital Ramony Cajal, Madrid, Spain
**Supported by** Fundacion Manchega de Investigaciony Docencia en Gastroenterologia
**Correspondence to:** Dr. Rafael Barcena Marugan, Department of Gastroenterology, Hospital Ramony Cajal, Ctra. Colmenar, Km 9.1, 28034 Madrid, Spain. rbarcena.hrc@salud.madrid.org
**Telephone:** +34-91-3368093 **Fax:** +34-91-7291456
**Received:** 2003-02-25 **Accepted:** 2003-03-16

## Abstract

**AIM:** To investigate the responses of TT virus (TTV) and hepatitis B virus (HBV) to a long-term lamivudine therapy.

**METHODS:** Sixteen patients infected with both TTV and HBV were treated with lamivudine 100 mg daily for 30 months. Blood samples were drawn at the beginning of the therapy and subsequently at month 3, 6, 9, 12 and 30. Serum TTV was quantified by real time PCR and serum HBV was detected by hybridization assay and nested polymerase chain reaction.

**RESULTS:** TTV infection was detected in 100 % of HBV-infected patients. Loss of serum TTV DNA after one year of treatment occurred in 1/16 (6 %) patients. At the end of therapy, TTV DNA was positive in 94 % of them. The decline of HBV viremia was evident at 3 months after therapy and the response rate was 31 %, 44 %, 63 %, 50 % and 50 % at month 3, 6, 9, 12 and 30, respectively.

**CONCLUSION:** TTV replication is not sensitive to lamivudine and is highly prevalent in HBV-infected patients.

Garcia JM, Marugan RB, Garcia GM, Lindeman MLM, Abete JF, Terron SC. TT virus infection in patients with chronic hepatitis B and response of TTV to lamivudine. *World J Gastroenterol* 2003; 9(6): 1261-1264
http://www.wjgnet.com/1007-9327/9/1261.asp

## INTRODUCTION

TT virus (TTV) was recently discovered in a patient with post-transfusional hepatitis of unknown etiology[1]. Its genome is a circular, single-stranded DNA of negative polarity, which shares similarities with the members of the Circoviridae family[2]. In contrast to DNA viruses, TTV isolates exhibit a high level of genetic heterogeneity[3]. TTV presents an extreme diffusion of active infection throughout the world[4]. Its presence in blood products could indicate that TTV can be transmitted through transfusion[5]. Although it has been proposed that TT virus might be responsible for the small proportion of acute and chronic forms of hepatitis that still remain unsolved, no other illness has yet been attributed to the virus.

Hepatitis B virus (HBV) causes transient and chronic infections of the liver, which may progress to cirrhosis and eventually to hepatocellular carcinoma (HCC)[6]. Interferon (IFN)-alpha is the only approved drug for the treatment of chronic HBV infection, but the recent registration of lamivudine, a dideoxycytidine analogue that inhibits both the HIV and HBV reverse transcriptases, has provided new perspectives for the treatment of chronic HBV infection[7, 8]. Coinfection of TTV and HBV is commonly seen because both viruses share the same transmission routes such as blood transfusion[9]. In previous studies, IFN therapy has been reported effective against TTV[10], but the possible susceptibility of the virus to lamivudine treatment has not yet been investigated. Thus, the aims of this study were: (1) to know the impact of TTV in patients with chronic hepatitis B; (2) to investigate the response of TTV to lamivudine therapy; and (3) to evaluate whether the outcome of long term lamivudine therapy in chronic hepatitis B is influenced by a TTV coinfection.

## MATERIALS AND METHODS

### *Patients*

The study group consisted of 16 patients (12 males and 4 females; mean age: 52.62 years; range: 33 and 66 years) with chronic dual HBV and TTV infection. The diagnosis of chronic hepatitis was made on the basis of clinical and histological results. Patients included 15 cases of liver cirrhosis and 1 hepatocarcinoma. In 9 patients the transmission route was unknown, 2 had a history of blood transfusion, 2 developed HBV infection after liver transplantation, 1 had primary biliary cirrhosis and 2 were addicts to alcohol. At the beginning of the therapy, all patients were positive to HBV DNA by solution hybridization assay and had elevated alanine aminotransferase (ALT) levels that were 3 times of the upper normal limit (normal range: 5-45 IU/L). Nine patients were hepatitis B e antigen (HBeAg) positive, 5 had antibodies against HBeAg (anti-HBe) and 2 patients were negative to both HBeAg and anti-HBe.

Ten patients underwent liver transplantation; 8 of them for HBV-related liver cirrhosis. The remaining 2 patients without evidence of HBV infection before allograft developed a *de novo* post-transplant HBV infection.

Lamivudine (Glaxo Wellcome, UK) was given orally to all patients at a dose of 100 mg daily for 30 months. Blood samples were taken at the baseline time and subsequently were obtained at month 3, 6, 9, 12 and 30. To evaluate the effects of lamivudine, levels of ALT, TTV DNA and HBV DNA and viral serological markers were evaluated at each time. HBV complete responders to lamivudine therapy were defined as patients showing clearance of serum HBV DNA by nested polymerase chain reaction (PCR) and normal ALT levels at 30 months of treatment. All patients gave written informed consent before the enrollment in the study, which was approved by the ethics committees of the hospital.

### *Detection and quantification of TTV DNA*

TTV DNA quantification was carried out with a real time PCR by the SYBR Green approach using primers targeting the untranslated region (UTR) of the viral genome: forward primer T801: 5' -GCTACGTCACTAACCACG-3' , position 6 to 25; reverse primer T935: 5' -CTGCGGTGTGTAAACTCACC-3' , position 185 to 204[11]. Total DNA was purified from 200 μl of serum using the High Pure Viral Nucleic Acid Kit (Roche Diagnostic, Mannheim, Germany) and eluted in a final volume of 50 μl. Real time PCR was done using 2 μl of the eluted DNA with 0.2 μM of each primer in 23 μl 2×SYBR Green PCR mix (Qiagen). The cycling conditions were: 95 ℃ for 10 min to activate the DNA polymerase followed by 45 cycles of amplification: 95 ℃ for 15 sec, 62 ℃ for 30 sec and 72 ℃ for 30 sec.

### *HBV markers*

Hepatitis B surface antigen (HBsAg), hepatitis B e antigen (HBeAg) and antibodies to HBsAg, HBeAg and hepatitis B c antigen (HBcAg) were determined by immunoassay (EIA; Abbott Laboratories, N Chicago, IL). Serum HBV DNA levels at the beginning of lamivudine therapy were quantified using Abbott hybridization assay. Viral DNA during the following time points was detected by nested PCR[12].

### *Statistical analysis*

Statistical analysis was performed using Student' s *t* test. Data were analyzed with the computer program SPSS (SPSS Inc., Chicago, IL, USA). A probability (*P*) value of less than 0.05 was considered statistically significant.

## RESULTS

### *Detection and response of TTV to lamivudine therapy*

Sixteen patients doubly infected with TTV and HBV were monitored for levels of both viruses in serum, at selected time points, during the lamivudine treatment by real time and nested PCR methodology, respectively. Of the 16 patients, serum TTV DNA could be detected in all of them by real time PCR at the beginning of lamivudine therapy, with TTV values that ranged between $8.7\times10^3$ to $1.9\times10^8$ genomes per ml of serum (mean: $5.7\times10^8$ genomes/ml). After 30 months of lamivudine treatment, 15/16 patients (94 %) still had TTV DNA in serum and TTV values ranged between $3\times10^4$ to $4.2\times10^8$ genomes per ml of serum (mean: $4.3\times10^7$ genomes/ml). The patient who became negative to TTV DNA lost this marker after 12 months of treatment and he still remained TTV DNA negative until the end of therapy. The TTV DNA value of this patient at baseline time point was $8\times10^4$ viral genomes per ml of serum. However, this patient did not respond to the lamivudine therapy and he was serum HBV DNA positive at each time point. With respect to the 15 positive TTV DNA patients, at the end of the treatment and relative to baseline levels, 1 patient (7 %) showed unchanged serum TTV DNA levels, 6 patients (40 %) had 6 times of reduction of serum TTV load and 8 cases (53 %) presented 8 times of increase of the levels of TTV DNA in serum.

Changes in serum TTV DNA concentration with respect to HBV non-responsive and responsive patients to lamivudine treatment were also analyzed. It was found that there was no statistically significant difference when basal and final serum samples were compared between both groups (Table 1) or when basal and final serum samples were compared in the same group (Table 2).

Finally, serum TTV DNA values in patients with or without liver transplants were evaluated as well. Once again, there were not significant differences when baseline and final serum samples were compared between non-transplanted and transplanted patients (Table 3) or when baseline and final serum samples were compared between non-transplanted or transplanted patients (Table 4).

**Table 1** Comparison of serum TTV DNA concentration changes before treatment and at the end of treatment

| | Non-responders (*n*=7) | Responders (*n*=8) | *P*[a] |
|---|---|---|---|
| Before treatment | $4.6\times10^7$ | $8.0\times10^7$ | 0.66 |
| End of treatment | $1.1\times10^8$ | $3.4\times10^7$ | 0.29 |

TTV DNA concentration was expressed as viral genomes / ml of serum. [a]Student's *t*-test, HBV non-responsive patients *vs.* responsive patients to lamivudine therapy.

**Table 2** Changes of TTV DNA concentration in HBV non-responsive and responsive patients to lamivudine therapy

| | Before treatment | End of treatment | *P*[a] |
|---|---|---|---|
| Non-responders (*n*=7) | $4.6\times10^7$ | $1.1\times10^8$ | 0.60 |
| Responders (*n*=8) | $8.0\times10^7$ | $3.4\times10^7$ | 0.55 |

TTV DNA concentration was expressed as viral genomes / ml of serum. [a]Student's *t*-test, before *vs* at the end of treatment.

**Table 3** Comparison of serum TTV DNA concentration changes before treatment and at the end of treatment

| | Non-transplanted (*n*=5) | Transplanted (*n*=10) | *P*[a] |
|---|---|---|---|
| Before treatment | $1.2\times10^7$ | $8.9\times10^7$ | 0.22 |
| End of treatment | $8.8\times10^6$ | $1.0\times10^8$ | 0.07 |

TTV DNA concentration was expressed as viral genomes / ml of serum. [a]Student´s *t*-test, non-transplanted *vs.* transplanted patients.

**Table 4** Changes in TTV DNA concentration in non-transplanted and transplanted patients

| | Before treatment | End of treatment | *P*[a] |
|---|---|---|---|
| Non-transplanted (*n*=5) | $1.2\times10^7$ | $8.8\times10^6$ | 0.59 |
| Transplanted (*n*=10) | $8.9\times10^7$ | $1.0\times10^8$ | 0.87 |

TTV DNA concentration was expressed as viral genomes / ml of serum. [a]Student´s *t*-test, before *vs* at the end of treatment.

### *HBV response to lamivudine treatment*

At the baseline time point, HBV DNA values ranged between $4.2\times10^9$ and $8.4\times10^{11}$ DNA genomes per ml of serum (mean: $1.2\times10^{11}$ genomes/ml). The decline of HBV viremia was clearly evident at month 3 after therapy and the response rate was 31 %, 44 %, 63 %, 50 % and 50 % at month 3, 6, 9, 12 and 30, respectively. When compared between responsive and non-responsive patients, the vesponders had almost 4 times the value of the non-responder ones but the difference was not significant ($2.6\times10^{11}$ *vs* $7\times10^{10}$ genomes per ml of serum, respectively). Also, there was no significant difference in baseline of ALT levels between responsive and non-responsive patients (117 IU/L *vs.* 123 IU/L, respectively). However, differences were statistically significant in post-treatment ALT levels between responsive and non-responsive patients (37 IU/L *vs* 128 IU/L, respectively; *P*=0.03). Of the 5 HBeAg positive patients, 2 seroconverted to anti-HBe by month 12. The other 3 patients still remained HBeAg positive after 30 months of lamivudine therapy. In the 2 HBeAg and anti-HBe negative patients, they

developed anti-HBe by month 3.

With respect to the 10 liver transplant recipients, 4 patients (40 %) started to receive lamivudine treatment after recurrent allograft re-infection. In these cases, serum HBV DNA was still detectable after 30 months of therapy. However, in those 6 patients who started lamivudine administration before liver transplantation as a prophylaxis regimen, 5 (50 %) lost viral DNA at month 3 of treatment, and then they underwent liver allograft and remained HBV DNA negative throughout the therapy. By contrast, the remaining patient developed a recurrent HBV infection at month 6 of post-transplant.

## DISCUSSION

Since TTV was discovered a few years ago, many studies have been done trying to assess whether it causes liver disease; however, there is still a poor understanding of its molecular properties and pathogenic potential.

This study shows, in agreement with other groups, that TTV infection is chronic and characterized by the continued presence of high virus loads in serum with wide variations ranging between $10^3$ and $10^8$ genomes per ml[13, 14]. Over a period of 30 months, 96 % of the patients presented high TTV DNA levels; however, in some individuals, viremia levels fluctuated extensively while they remained essentially constant in others.

Different epidemiological studies have clearly indicated that TTV can behave as a transmissible blood-borne virus sharing common transmission routes with the hepatitis viruses. Then, coinfection of TTV is frequently observed in patients with chronic hepatitis B[9]. One important finding in our study is that 100 % of patients infected with HBV were TTV DNA-positive by real-time PCR. These results suggest that the prevalence of TTV infection is very high in the HBV-infected population. However, our results are in disagreement with other studies that reported TTV DNA rates between 15 % and 36 %[15-17]. One explanation for this result might be due to the different primers used for the detection of TTV DNA; we used a set of primers that already showed 92 % positivity to TTV in healthy adults in Japan[11]. Another possible explanation why these patients were TTV positive is their histological status: 94 % of them presented cirrhosis. A TTV well-recognized feature is that TTV infection is chronic and tends to last many years, so it could be that TTV infection is more prevalent in patients with advanced HBV-associated liver disease than in those with stable disease.

However, the most novel and interesting information that emerged from this study is that lamivudine treatment in a regimen of 100 mg daily and for a period of 30 months did not inhibit TTV replication in patients coinfected with HBV and TTV. Only one individual (6 %) of the 16 patients enrolled in the study became serum TTV DNA negative after 12 months of therapy. This observation could suggest that this patient lost TTV in a spontaneous way and not by effect of lamivudine on TTV replication.

With respect to the effect of lamivudine treatment of chronic hepatitis B, this study confirms earlier reports where HBV infection responded positively to lamivudine treatment[18-20]. The response of HBV to lamivudine treatment was not affected with the concurrent TTV infection. This observation can be explained by two reasons. Firstly, the changes observed in ALT values during the lamivudine treatment period were correlated with the change of HBV DNA in chronic hepatitis B; it seemed that ALT dynamic was unrelated to TTV viremia. Secondly, TTV viremia was not related to different HBV DNA levels, so TTV did not seem to interfere with HBV replication. Thus, in agreement with many other published studies, TTV may lack clinical association with liver disease in these patients[21, 22].

Finally, it has been suggested a relationship between an increased TTV viral load and host immunological disorders[23]. In immunosuppressed patients, such as recipients of liver transplants, TTV viremia could be higher than that in individuals without liver allografts. However, we did not find any significant difference in TTV viral load when both groups were compared, even if transplanted patients had always higher TTV titers. Based on our results it seems that immune system is not involved in elevated TTV viremia in HBV patients, although more extensive studies need to be performed to prove this hypothesis.

In conclusion, during the lamivudine therapy for chronic hepatitis B, disappearance of TTV does not occur in the majority of the HBV-infected patients which supports the interpretation that lamivudine does not inhibit TTV replication. Moreover, this study shows the highly prevalence of TTV infection in patients with chronic hepatitis B, but without any effect on the course of HBV infection.

## REFERENCES


1 **Nishizawa T**, Okamoto H, Konishi K, Yoshizawa H, Miyakawa Y, Mayumi M. A novel DNA virus (TTV) associated with elevated transaminase levels in posttransfusion hepatitis of unknown etiology. *Biochem Biophys Res Commun* 1997; **241**: 92-97

2 **Miyata H**, Tsunoda H, Kazi A, Yamada A, Khan MA, Murakami J, Kamahora T, Shiraki K, Hino S. Identification of a novel GC-rich 113-nucleotide region to complete the circular, single-stranded DNA genome of TT virus, the first human circovirus. *J Virol* 1999; **73**: 3582-3586

3 **Hijikata M**, Takahashi K, Mishiro S. Complete circular DNA genome of a TT virus variant (isolate name SANBAN) and 44 partial ORF2 sequences implicating a great degree of diversity beyond genotypes. *Virology* 1999; **260**: 17-22

4 **Abe K**, Inami T, Asano K, Miyoshi C, Masaki N, Hayashi S, Ishikawa K, Takebe Y, Win KM, El Zayadi AR, Han KH, Zhang DY. TT virus infection is widespread in the general populations from different geographic regions. *J Clin Microbiol* 1999; **37**: 2703-2705

5 **Matsumoto A**, Yeo AE, Shih JW, Tanaka E, Kiyosawa K, Alter HJ. Transfusion-associated TT virus infection and its relationship to liver disease. *Hepatology* 1999; **30**: 283-288

6 **Lee WM**. Hepatitis B virus infection. *N Engl J Med* 1997; **337**: 1733-1745

7 **Eron JJ**, Benoit SL, Jemsek J, MacArthur RD, Santana J, Quinn JB, Kuritzkes DR, Fallon MA, Rubin M. Treatment with lamivudine, zidovudine, or both in HIV-positive patients with 200 to 500 CD4+ cells per cubic millimeter. North American HIV Working Party. *N Engl J Med* 1995; **333**: 1662-1669

8 **Dienstag JL**, Perrillo RP, Schiff ER, Bartholomew M, Vicary C, Rubin M. A preliminary trial of lamivudine for chronic hepatitis B infection. *N Engl J Med* 1995; **333**: 1657-1661

9 **Kao JH**, Chen W, Chen PJ, Lai MY, Chen DS. TT virus infection in patients with chronic hepatitis B or C: influence on clinical, histological and virological features. *J Med Virol* 2000; **60**: 387-392

10 **Nishizawa Y**, Tanaka E, Orii K, Rokuhara A, Ichijo T, Yoshizawa K, Kiyosawa K. Clinical impact of genotype 1 TT virus infection in patients with chronic hepatitis C and response of TT virus to alpha-interferon. *J Gastroenterol Hepatol* 2000; **15**: 1292-1297

11 **Takahashi K**, Hoshino H, Ohta Y, Yoshida N, Mishiro S. Very high prevalence of TT virus (TTV) infection in general population of Japan revealed by a new set of PCR primers. *Hepatol Res* 1998; **12**: 233-239

12 **Lindh M**, Gonzalez JE, Norkrans G, Horal P. Genotyping of hepatitis B virus by restriction pattern analysis of a pre-S amplicon. *J Virol Methods* 1998; **72**: 163-174

13 **Lefrere JJ**, Roudot-Thoraval F, Lefrere F, Kanfer A, Mariotti M, Lerable J, Thauvin M, Lefevre G, Rouger P, Girot R. Natural history of the TT virus infection through follow-up of TTV DNA-positive multiple-transfused patients. *Blood* 2000; **95**: 347-351

14 **Oguchi T**, Tanaka E, Orii K, Kobayashi M, Hora K, Kiyosawa K. Transmission of and liver injury by TT virus in patients on maintenance hemodialysis. *J Gastroenterol* 1999; **34**: 234-240

15 **Lai YC**, Hu RT, Yang SS, Wu CH. Coinfection of TT virus and response to interferon therapy in patients with chronic hepatitis B or C. *World J Gastroenterol* 2002; **8**: 567-570
16 **Naoumov NV**, Petrova EP, Thomas MG, Williams R. Presence of a newly described human DNA virus (TTV) in patients with liver disease. *Lancet* 1998; **352**: 195-197
17 **Tanaka H**, Okamoto H, Luengrojanakul P, Chainuvati T, Tsuda F, Tanaka T, Miyakawa Y, Mayumi M. Infection with an unenveloped DNA virus (TTV) associated with posttransfusion non-A to G hepatitis in hepatitis patients and healthy blood donors in Thailand. *J Med Virol* 1998; **56**: 234-238
18 **Lai CL**, Chien RN, Leung NW, Chang TT, Guan R, Tai DI, Ng KY, Wu PC, Dent JC, Barber J, Stephenson SL, Gray DF. A one-year trial of lamivudine for chronic hepatitis B. Asia Hepatitis Lamivudine Study Group. *N Engl J Med* 1998; **339**: 61-68
19 **Leung NW**, Lai CL, Chang TT, Guan R, Lee CM, Ng KY, Lim SG, Wu PC, Dent JC, Edmundson S, Condreay LD, Chien RN. Extended lamivudine treatment in patients with chronic hepatitis B enhances hepatitis B e antigen seroconversion rates: results after 3 years of therapy. *Hepatology* 2001; **33**: 1527-1532
20 **Leung N**. Liver disease-significant improvement with lamivudine. *J Med Virol* 2000; **61**: 380-385
21 **Gimenez-Barcons M**, Forns X, Ampurdanes S, Guilera M, Soler M, Soguero C, Sanchez-Fueyo A, Mas A, Bruix J, Sanchez-Tapias JM, Rodes J, Saiz JC. Infection with a novel human DNA virus (TTV) has no pathogenic significance in patients with liver diseases. *J Hepatol* 1999; **30**: 1028-1034
22 **Forns X**, Hegerich P, Darnell A, Emerson SU, Purcell RH, Bukh J. High prevalence of TT virus (TTV) infection in patients on maintenance hemodialysis: frequent mixed infections with different genotypes and lack of evidence of associated liver disease. *J Med Virol* 1999; **59**: 313-317
23 **Touinssi M**, Gallian P, Biagini P, Attoui H, Vialettes B, Berland Y, Tamalet C, Dhiver C, Ravaux I, De Micco P, De Lamballerie X. TT virus infection: prevalence of elevated viremia and arguments for the immune control of viral load. *J Clin Virol* 2002; **21**: 135-141

**Edited by** Xu XQ and Zhu LH

P.O.Box 2345, Beijing 100023,China
Fax: +86-10-85381893
E-mail: wjg@wjgnet.com www.wjgnet.com

World J Gastroenterol 2003;9(6):1265-1269
World Journal of Gastroenterology
Copyright ©2003 by The WJG Press ISSN 1007-9327



# Antralization at the edge of proximal gastric ulcers: Does *Helicobacter pylori* infection play a role?

Harry Hua-Xinag Xia, Shiu Kum Lam, Wai Man Wong, Wayne Hsing Cheng Hu, Kam Chuen Lai, Sau Hing Wong, Suet Yi Leung, Siu Tsan Yuen, Nicholas A. Wright, Benjamin Chun-Yu Wong

**Harry Hua-Xinag Xia, Shiu Kum Lam, Wai Man Wong, Wayne Hsing Cheng Hu, Kam Chuen Lai, Sau Hing Wong, Benjamin Chun-Yu Wong,** Department of Medicine, The University of Hong Kong, Hong Kong SAR, China
**Suet Yi Leung, Siu Tsan Yuen,** Department of Pathology, The University of Hong Kong, Hong Kong SAR, China
**Nicholas A. Wright,** Histopathology Unit, London Research Institute, Cancer Research, UK
**Supported by** the Seed Funding for Basic Research 2001 (301/01), The University of Hong Kong, and a competitive earmarked research grant from the Research Grants Council of Hong Kong Special Administrative Region, China (HKU7318/01M) to HH-X Xia
**Correspondence to:** Dr Benjamin CY Wong, Department of Medicine, The University of Hong Kong, Queen Mary Hospital, Hong Kong, China. bcywong@hku.hk
**Telephone:** +852-28554541 **Fax:** +852-28725828
**Received:** 2003-03-04 **Accepted:** 2003-03-08

## Abstract

**AIM:** To determine the prevalence of antralization at the edge of proximal gastric ulcers, and the effect of *H. pylori* eradication on the mucosal appearances.

**METHODS:** Biopsies were taken from the antrum, body and the ulcer edge of patients with benign proximal gastric ulcers before and one year after treatment. Gastric mucosa was classified as antral, transitional or body type. *H. pylori* positive patients received either triple therapy, or omeprazole.

**RESULTS:** Patients with index ulcers in the incisura, body or fundus ($n$=116) were analyzed. Antral-type mucosa was more prevalent at the ulcer edge in *H. pylori*-positive patients than *H. pylori*-negative patients (93 % *vs* 60 %, OR=8.95, 95 %CI: 2.47-32.4, $P$=0.001). At one year, there was a significant reduction in the prevalence of antralization (from 93 % to 61 %, $P$=0.004) at the ulcer edge in patients with *H. pylori* being eradicated. However, there was no difference in the prevalence of antralization at the ulcer edge in those with persistent infection.

**CONCLUSION:** *H. pylori* infection is associated with antralization at the edge of proximal gastric ulcers, which may be reversible in some patients after eradication of the infection.

Xia HHX, Lam SK, Wong WM, Hu WHC, Lai KC, Wong SH, Leung SY, Yuen ST, Wright NA, Wong BCY. Antralization at the edge of proximal gastric ulcers: Does *Helicobacter pylori* infection play a role? *World J Gastroenterol* 2003; 9(6): 1265-1269
http://www.wjgnet.com/1007-9327/9/1265.asp

## INTRODUCTION

Peptic ulcer disease is common, and is associated with considerable mortality due to complications such as bleeding and perforation[1]. *H. pylori* infection is now recognized to be a major cause for peptic ulcer, accounting for up to 90 % of duodenal ulcer cases and 80 % of gastric ulcer cases, with the use of non-steroidal anti-inflammatory drugs being another major cause[2-4]. While gastric metaplasia in duodenum has been identified to be an important morphopathological change in the development of *H. pylori*-associated duodenal and prepyloric ulcer[5-7], the mucosal morpho-pathogenesis of gastric ulcer, which occurs predominantly along the body-antrum transitional zone (particularly at the gastric incisura), remains unclear. Previous studies have observed a stem-cell-derived "ulcer-associated cell lineage" (UACL) at the sites of chronic gastrointestinal ulceration, commonly found in the borders of Crohn' s ulcers in small bowel, and in gastroduodenal ulceration[8-11]. In the literature, UACL was usually described as pseudopyloric (or pyloric) metaplasia, because it has morphological similarities to pyloric glands[8, 9], and similar changes can occur in other tissues, such as gall bladder, bile ducts, and pancreatic ducts, often associated with malignant transformation of these tissues[12-16]. In the stomach, pseudopyloric metaplasia is specifically defined as a replacement of specialized glands by mucous-secreting glands in the gastric body or at the body-antrum junction[17], a concept identical to "antralization" as described in our previous studies[18, 19].

In a previous study, we have demonstrated that in the absence of *H. pylori* infection, the gastric incisura mucosa belongs to either body-type or transitional type in most (82 %) individuals, suggesting that normal incisura mucosa is histologically distinct from the antral mucosa, but more homologous to the body and fundus mucosa[18]. However, *H. pylori* infection is associated with the presence of antral (pyloric)-type mucosa in the proximal stomach (i.e. gastric incisura, body and fundus), indicating that *H. pylori* infection may be a causal factor for antralization of the proximal stomach[18]. Thus, it is conceivable that *H. pylori*-induced antralization may play an important pathogenic role in proximal gastric ulceration, and eradication of *H. pylori* infection may reverse antralization to normal transitional or body type mucosa, and thus reduce the risk for ulcer relapse. Therefore, the present study was carried out to determine the prevalence of antralization at the edge of proximal gastric ulcer in relation to *H. pylori* infection, and the effect of *H. pylori* eradication on the mucosal appearances.

## MATERIALS AND METHODS

### *Patients*

One hundred and sixteen patients with newly diagnosed uncomplicated benign-looking proximal gastric ulcers (>5 mm in diameter and >1 mm in depth) at the Endoscopy Unit of Department of Medicine, Queen Mary Hospital were included in the study. The location of gastric ulcers and demographic and clinical characteristics of these patients were summarized in Table 1. Exclusion criteria at entry included patients who had been taking aspirin or non-steroidal anti-inflammatory drugs (NSAIDs) over the past year, or taking antibiotics, $H_2$ receptor blockers, bismuth or proton pump inhibitors in the

preceding 4 weeks, patients with previous gastric surgery, and those with a histological diagnosis of gastric carcinoma or lymphoma.

Informed written consent was obtained from all patients who participated in the trial. This project was approved by the Ethics Committee of the University of Hong Kong.

**Table 1** The demographic clinical characteristics of the patients initially recruited, according to the location of gastric ulcers ($n$=116)

| | Ulcer location | | |
|---|---|---|---|
| | Incisura ($n$=91) | Body ($n$=23) | Fundus ($n$=2) |
| Age (mean ±SD) | 59.5±13.3 | 69.3±10.2 | 51.0±11.2 |
| Gender (male/female) | 60/31 | 17/6 | 2/0 |
| Smoking (yes/no) | 44/46 | 11/12 | 1/1 |
| *H.pylori* status (positive/negative) | 81/10 | 19/4 | 1/1 |

### Diagnosis of H. pylori infection

During the first endoscopy, three biopsies were taken at the gastric antrum within 3 cm of the pylorus at the lesser curvature, two at the midway between the pylorus and cardioesophageal junction at the greater curvature, and four from the edge of gastric ulcer. When the ulcer was present in the body, the body biopsies were taken at least 3 cm apart from the ulcer. One antral biopsy was used for a rapid urease test (RUT) and the rest were sent for the detection of *H. pylori* infection and histological examination after haematoxylin & eosin (H&E) staining. All patients then received a $^{13}$C-urea breath test following a standard protocol measured by an isotope ratio mass spectrometer[20]. The definition of *H. pylori* infection in this study required that at least two of the three tests (the RUT, histology and $^{13}$C-urea breath test) were positive. The absence of *H. pylori* infection required all three tests to be negative. This definition was used as the "gold standard" in this study.

### Histological examination

Slides were read by experienced pathologists who were blinded to all clinical and endoscopic information, including the RUT results. The mucosa of gastric biopsies taken from different sites was classified as antral (mucous-secreting or pyloric) type, body (acid-secreting or oxyntic) type or transitional (junctional) type according to the definitions set out in the updated Sydney system[21]. The characteristic feature of antral-type mucosa was the presence of coiled and branching antral glands, which were lined by mucus cells that were interspersed with endocrine cells (chiefly G and D types), and a few parietal cells. The glands in body-type mucosa were straight tubes that constituted acid-producing parietal cells along with scattered mucus cells in their upper portion and mainly chief cells in their lower portion, with scattered argyrophilic endocrine cells. Transitional type mucosa was a mixture of the architectural features and cell types found in the antral and body type mucosae[21].

### Treatment and endoscopy at one year

One hundred and one patients received triple therapy consisting of clarithromycin 250 mg, metronidazole 300 mg each given 4 times daily for 2 weeks and sucralfate 1 gm 4 times daily for 4 weeks ($n$=54), or acid suppression therapy consisting of omeprazole 20 mg daily for one year ($n$=47). Successful eradication was indicated if the rapid urease test, histological examination by H&E and Giemsa staining and $^{13}$C-urea breath test were all negative at week 6 after treatment. 65 patients (male/female 44/21, age (mean±SD) 61.9±11.0 years) received either triple therapy ($n$=28), or omeprazole ($n$=37), with ulcers completely healed at 12 weeks. Upper endoscopy and $^{13}$C-urea breath test were repeated at month 12. Gastric biopsies were obtained from the antrum, body and ulcer site (visible scar area in 47 of 53 (90.6 %) cases with a healed ulcer) or the edge of ulcer in 12 patients with relapsed ulcers, and assessed as described above. Successful eradication was indicated if the rapid urease test, histological examination by H&E and Giemsa staining and $^{13}$C-urea breath test were all negative at week 6 or month 12 after treatment. The histological characteristics of these biopsies were compared with those biopsies taken at the first endoscopy. Histological improvement of gastric mucosa over the period of one year was defined as changes from antral to transitional or body, or from transitional to body-type, whereas worsening of gastric mucosa was defined as changes from body to transitional or antral, or from transitional to antral-type. An upper endoscopy and a $^{13}$C-urea breath test were repeated at month 12 for 65 patients (male/female 44/21, age (mean±SD) 61.9±11.0 years) who had their ulcers completely healed 12 weeks after treatment. Gastric biopsies were obtained from the antrum, body and ulcer site (visible scar area) in 47 of 53 (90.6 %) cases with a healed ulcer or the edge of ulcer in 12 patients with relapsed ulcers, and assessed as described above. The histological characteristics of these biopsies were compared with those biopsies taken at the first endoscopy. Histological improvement of gastric mucosa over the period of one year was defined as changes from antral to transitional or body, or from transitional to body-type, whereas worsening of gastric mucosa was defined as changes from body to transitional or antral, or from transitional to antral-type.

### Statistical analysis

The Chi-squared test (with Yates' correction if required), the Fisher's exact test or McNemar test was used for categorical variables, and odds ratios (OR) and 95 % confidence interval (CI) were estimated where appropriate. All tests were carried out using the SPSS system (version 10.0, SPSS Inc. Chicago, Illinois, USA). All $P$ values calculated were two-tailed. The alpha level of significance was set at $P$<0.05.

## RESULTS

### The presence of antral-type mucosa in the gastric body and at the edge of proximal gastric ulcers

Of the 116 patients, 91 had the index ulcers at the incisura, 23 in the body and 2 in the fundus. Of these, 101 were *H. pylori*-positive and 15 were *H. pylori*-negative. All biopsies taken from the antrum showed antral-type mucosa. Overall, antral-type mucosa was present in the gastric body in 6 (5.2 %) patients and at the edge of proximal gastric ulcers in 103 (88.8 %) patients. Of *H. pylori*-positive patients 6 (5.9 %) had antral-type mucosa and 4 (4 %) had transitional type mucosa whereas all (100 %) of *H. pylori*-negative patients had body-type mucosa at the gastric body. Antral-type mucosa was present at the edge of proximal gastric ulcers in 93.1 % (94/101) of *H. pylori*-positive patients and 60 % (9/15) of *H. pylori*-negative patients (OR=8.95, 95 % CI: 2.47-32.4, $\chi^2$=14.35, $P$=0.001) (Figure 1). In *H. pylori*-positive patients, 81 had ulcers at the incisura, 19 at the body and one at the fundus. In the presence of *H. pylori* infection, there was no difference in the prevalence of antral-type mucosa at the ulcer edge at different gastric sites: 92.6 % (75/81) at the incisura, 94.7 % (18/19) at the body and 100 % (1/1) at the fundus. In *H. pylori*-negative patients, antral-type mucosa was present at the edges of ulcers in 70 % (7/10), 50 % (2/4) and 0 % (0/1) of patients when the ulcer occurred at the incisura, body and fundus, respectively.

### *Changes of gastric mucosa in the gastric body and at the edge of proximal gastric ulcers at one year*

Of the 65 patients who were followed up for one year, 28 had *H. pylori* infection eradicated and 27 had persistent infection. Of the 12 patients with ulcers relapse, one (3.6 %) was from patients in whom *H. pylori* infection was eradicated and 11 (29.7 %) were from those with persistent infection (OR=11.4, 95 % CI: 1.38-94.9, $\chi^2$=5.61, *P*=0.018).

There was a significant reduction in the prevalence of antral-type mucosa at both the gastric body (from 7.1 % to 0 %) and the gastric ulcer sites (from 92.9 % to 60.7 %, *P*=0.004, McNemar test) in patients in whom *H. pylori* infection was eradicated. However, there was no difference in the prevalence of antral-type mucosa when *H. pylori* infection was persistent (Figure 2).

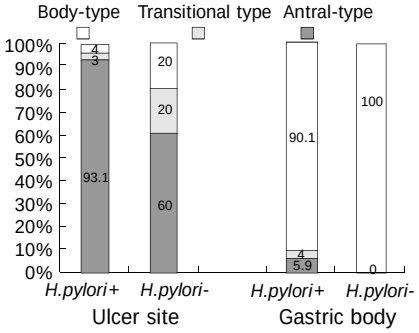


**Figure 1** Prevalence of antral-type mucosa at the edge of proximal gastric ulcers and non-ulcerated gastric body in *H. pylori*-positive patients (*H. pylori*+, *n*=101) and those without *H. pylori* infection (*H. pylori*-, *n*=15).

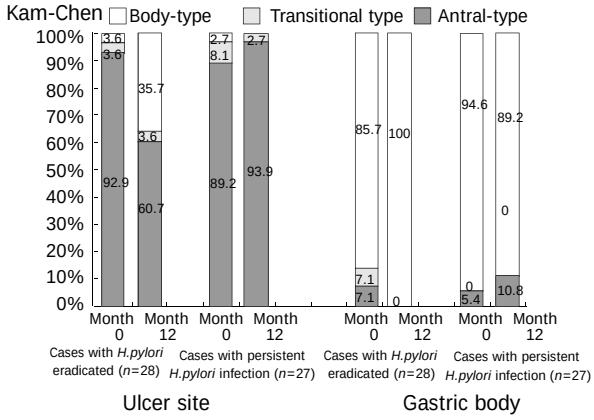


**Figure 2** Presence of antral-type mucosa at the edge of proximal gastric ulcers and non-ulcerated gastric body in patients with *H. pylori* eradicated (*n*=28) and in those with persistent infection (*n*=37) before (month 0) and 12 months after treatment.

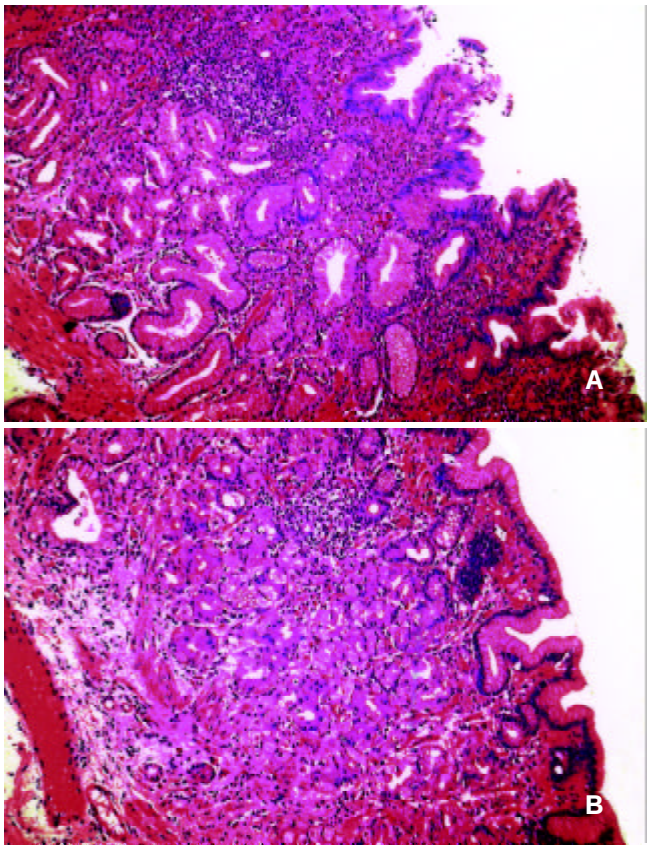


**Figure 3** Gastric mucosa at the ulcer edge before and after eradication of *H. pylori* infection in the same patient. A, biopsy of the ulcer edge before *H. pylori* eradication showing antral-type gastric mucosa with severe active chronic inflammation; B, biopsy of the healed ulcer site after *H. pylori* eradication showing body-type gastric mucosa with presence of parietal and chief cells in the gastric glands and mild residual chronic inflammation. Haematoxylin & eosin (H&E) staining ×250.

Histological improvement of gastric mucosa was observed in 14 (21.5 %) patients; 3 at the gastric body, 9 at the ulcer site and 2 at both sites (Figure 3). Histological improvement of gastric mucosa at the ulcer sites was more common in patients in whom *H. pylori* was eradicated than those with persistent infection (35.7 % *vs* 2.7 %, OR=20.0, 95 % CI: 2.37-168.6, $\chi^2$=12.35, *P*<0.001) (Table 2). When patients with relapsed ulcers were excluded, the association remained unchanged (37.0 % *vs* 3.8 %, OR=14.71, 95 % CI: 1.72-125.7, $\chi^2$=8.87, *P*=0.003). Similarly, triple therapy was associated with a higher rate of histological improvement at the ulcer site, compared to omeprazole treatment (31.0 % *vs* 5.6 %, OR=7.65, 95 % CI: 1.50-39.0, $\chi^2$=5.72, *P*=0.017). Gastric mucosa at the ulcer site was improved in more patients with cured ulcers than those

**Table 2** Changes of gastric mucosa at the edge of proximal gastric ulcers and gastric body one year after treatment, in relation to post-treatment *H. pylori* status, treatment regimens, ulcer relapse and ulcer location (*n*=65)

| | Mucosal type change (%) | | | | | |
|---|---|---|---|---|---|---|
| | Ulcer edge | | | Gastric body | | |
| | Improvement[a] (*n*=11) | No change[b] (*n*=49) | Worsening[c] (*n*=5) | Improvement (*n*=5) | No change (*n*=58) | Worsening (*n*=2) |
| *H. pylori* infection | | | | | | |
| Eradicated (*n*=28) | 35.7[d] | 64.3 | 0 | 14.3 | 85.7 | 0 |
| Persistent (*n*=37) | 2.7 | 83.8 | 13.5 | 2.7 | 91.9 | 5.4 |
| Ulcer location | | | | | | |
| Incisura (*n*=52) | 15.4 | 76.9 | 7.7 | 5.8 | 90.4 | 3.8 |
| Body (*n*=13) | 23.1 | 69.2 | 7.7 | 15.4 | 84.6 | 0 |

[a], Improvement, antral-type (A)→transitional type (T), A→body-type (B), or T→B; [b], No change, A→A, T→T or B→B; [c], Worsening, T→A, B→A or B→T. [d], *P*<0.001, compared with persistent infection.

with relapsed ulcers, although the difference did not reach statistical significance (20.8 % *vs* 0 %, *P*=0.109). There was no difference in histological improvement between patients with ulcers at the body/fundus and those with ulcers at the incisura (23.1 % *vs* 15.4 %, OR=1.65, 95 % CI: 0.37-7.35, *P*=0.804) (Table 2). Age and gender were not associated with histological improvement (data not shown).

Overall, 7 (10.8 %) patients had worsened histology after treatment; 5 at the ulcer edge and the other 2 at the gastric body (Table 2). All of these patients had persistent *H. pylori* infection; 6 were treated with omeprazole and one with triple therapy. 3 (75 %) of these patients had ulcer relapsed.

## DISCUSSION

In the present study, approximately 90 % of patients with proximal gastric ulcers had antral-type mucosa at the ulcer edge, and *H. pylori* infection was associated with a higher prevalence of antralization in the proximal gastric ulceration. Moreover, eradication of *H. pylori* infection resulted in histological improvement at the ulcer edge of 36 % of patients in 12 months, whereas the persistence of the infection was accompanied by worsening of histology (14 %). These findings suggest that *H. pylori* infection contributes to antralization, which may, in turn, play an important role in gastric ulceration.

*H. pylori*-associated antralization is believed to be a consequence of direct insults of chronic *H. pylori* infection, as a host defense and reparative response to the mucosal damage caused by organisms. As demonstrated in our previous study and in the present study, *H. pylori* infection is associated with antralization (or pseudopyloric metaplasia) at the gastric incisura and less frequently at the body and fundus[18]. It has been established that *H. pylori* infection induces apoptosis of gastric epithelial cells, and subsequently stimulates cell proliferation in the gastric mucosa[22]. Hanby *et al* reported that mucous neck cells formed an important cell lineage which secretes a series of peptides including the spasmolytic polypeptide, or trefoil family factor 2 (TFF-2) with luminal protective functions[23]. It has been suggested that pseudopyloric metaplasia occurs in the body glands as a result of hyperplasia of mucous neck cells, and represents a mucosal response to damage associated with *H. pylori* infection[18, 23]. Indeed, Schmidt *et al* reported that the spasmolytic polypeptide-expressing metaplastic (SPEM) lineage was closely associated with fundic *H. pylori* infection[24]. Thus, we propose that the hyperplastic mucous neck cells move both upwards and particularly downwards in the oxyntic tubule, replace the specialized parietal and chief cells, and create a mucous cell lineage. This process can occur focally, occupying a single oxyntic tubule, groups of tubules, or on a fairly massive scale with many tubules involved[25]. Eventually a mucous gland, which resembles pyloric glands, is formed, and thus antralization of proximal gastric mucosa follows. It is most likely that the weakened antralized mucosa in the proximal stomach is prone to be further damaged by *H. pylori*, resulting in ulceration even in the presence of subnormal acid production[26] Therefore, in the presence of persistent chronic infection with *H. pylori*, this defense and reparative mechanism probably facilitates rather than prevents the development of ulceration.

In the present study, eradication of *H. pylori* infection led to histological improvement, and persistent infection was associated with the development of antralization in the proximal stomach. These observations may have implications for the prevention of the development of gastric cancer, as we have previously reported that antralization of gastric incisura is strongly associated with precancerous lesions such as gastric atrophy and intestinal metaplasia[18]. It has been shown that the time-dependent progression of gastritis in grade (development of atrophy and intestinal metaplasia) and in extent (spreading of gastritis by pyloro-cardial extension) is correlated with the development of gastric cancer in the distal and angular stomach[27], and that atrophic gastritis and intestinal metaplasia progress and exhibit a cephaloid shift (i.e. pyloro-cardial extension) in chronic *H. pylori* infection[28]. Therefore, it is hypothesized that the initial events in gastric carcinogenesis occur at the junction of the oxyntic and antral mucosae, and it is the antral type mucosa that is prone to gastric atrophy and intestinal metaplasia, and expansion of antral mucosa towards the proximal stomach (either by pyloro-cardial extension or by differentiation) may be associated with an increased risk of developing intestinal metaplasia[29]. However, gastric atrophy and intestinal metaplasia are unlikely to regress after eradication of *H. pylori* infection although this is controversial[30-33]. On the other hand, the reversibility of antralization at the proximal gastric mucosa may provide a new hallmark in the chemoprevention of gastric cancer, although further studies on the role of antralization in gastric carcinogenesis are required. If the proposals of Schmidt *et al*[24] are confirmed, the prevention or reversal of SPEM might be critical.

Sampling error might account for the difference in improvement of gastric mucosa between patients with *H. pylori* eradication and those with persistent infection. For example, biopsies may be more correctly taken at the edge of active ulcers than healed ulcers. In most cases, ulcer scars are visible, which helps to improve the accuracy of the biopsy site.

Notably, the rate of antralization reached 60 % (9/15) for patients with proximal ulcers but without *H. pylori* infection, suggesting that certain other factors that result in gastric mucosal damage also lead to antralization and gastric ulceration. In the present study, there were no documented records on the causes of *H. pylori*-negative gastric ulcers, and thus we were unable to identify the potential factors that may lead to antralization. Some NSAID users who were unaware of NSAID use at entry might have been included. Previously, Lanas *et al* demonstrated that between 13 % and 22 % of patients with gastrointestinal bleeding and perforation who claimed not to have used aspirin had objective evidence of current aspirin intake[34, 35]. If this were the case in the present study, then NSAID use would account for proximal gastric ulcer in up to 3 of the 15 patients. Nevertheless, the significance of NSAID use and other factors in antralization of proximal stomach remains to be clarified.

In conclusion, *H. pylori* infection is associated with antralization at the edge of proximal gastric ulcers, which may be reversible in a proportion of patients after eradication of *H. pylori* infection. Antralization in the proximal stomach may play an important role in the pathogenesis of gastric ulceration.

## REFERENCES

1 **Westbrook JI**, Rushworth RL. The epidemiology of peptic ulcer mortality 1953-1989: a birth cohort analysis. *Int J Epidemiol* 1993; **22:** 1085-1092

2 **Anonymous.** NIH Consensus Conference. *Helicobacter pylori* in peptic ulcer disease. NIH consensus development panel on *Helicobacter pylori* in peptic ulcer disease. *Helicobacter pylori* in peptic ulcer disease. *JAMA* 1994; **272:** 65-69

3 **Xia HHX**, Wong BCY, Wong KW, Wong KW, Wong SY, Wong WM, Lai KC, Hu WHC, Chan CK, Lam SK. Clinical and endoscopic characteristics of non-*Helicobacter pylori*, non-NSAID duodenal ulcers: a long-term prospective study. *Aliment Pharmacol Ther* 2001; **15**: 1875-1882

4 **Xia HHX**, Phung N, Kalantar JS, Talley NJ. Demographic and endoscopic characteristics of *Helicobacter pylori-positive* and negative peptic ulcer disease. *Med J Aust* 2000; **173:** 515-519

5 **Carrick J**, Lee A, Hazell S, Ralston M, Daskalopoulos G.

*Campylobacter pylori*, duodenal ulcer, and gastric metaplasia: possible role of functional heterotopic tissue in ulcerogenesis. *Gut* 1989; **30:** 790-797

6 **Taha AS**, Dahill S, Nakshabendi I, Lee FD, Sturrock RD, Russell RI. Duodenal histology, ulceration, and *Helicobacter pylori* in the presence or absence of non-steroidal anti-inflammatory drugs. *Gut* 1993; **34:** 1162-1166

7 **Olbe L**, Fandriks L, Hamlet A, Svennerholm AM. Conceivable mechanisms by which *Helicobacter pylori* provokes duodenal ulcer disease. *Best Pract Res Clin Gastroenterol* 2000; **14:** 1-12

8 **Longman RJ,** Douthwaite J, Sylvester PA, Poulsom R, Corfield AP, Thomas MG, Wright NA. Coordinated localisation of mucins and trefoil peptides in the ulcer associated cell lineage and the gastrointestinal mucosa. *Gut* 2000; **47:** 792-800

9 **Pera M,** Heppell J, Poulsom R, Teixeira FV, Williams J. Ulcer associated cell lineage glands expressing trefoil peptide genes are induced by chronic ulceration in ileal pouch mucosa. *Gut* 2001; **48:** 792-796

10 **Hanby AM,** Jankowski JA, Elia G, Poulsom R, Wright NA. Expression of the trefoil peptides pS2 and human spasmolytic polypeptide (hSP) in Barrett's metaplasia and the native oesophageal epithelium: delineation of epithelial phenotype. *J Pathol* 1994; **173:** 213-219

11 **Wright NA**, Poulsom R, Stamp GW, Hall PA, Jeffery RE, Longcroft JM, Rio MC, Tomasetto C, Chambon P. Epidermal growth factor (EGF/URO) induces expression of regulatory peptides in damaged human gastrointestinal tissues. *J Pathol* 1990; **162:** 279-284

12 **Roberts IS,** Stoddart RW. Ulcer-associated cell lineage ('pylori metaplasia') in Crohn's disease: a lectin histochemical study. *J Pathol* 1993; **171:** 13-19

13 **Callea F**, Sergi C, Fabbretti G, Brisigotti M, Cozzutto C, Medicina D. Precancerous lesions of the biliary tree. *J Surg Oncol* 1993; **3 (Suppl):** 131-133

14 **Sasaki M,** Yamato T, Nakanuma Y, Ho SB, Kim YS. Expression of MUC2, MUC5AC and MUC6 apomucins in carcinoma, dysplasia and non-dysplastic epithelia of the gallbladder. *Pathol Inter* 1999; **49:** 38-44

15 **Yamagiwa H**. Mucosal dysplasia of gallbladder: isolated and adjacent lesions to carcinoma. *Jpn J Cancer Res* 1989; **80:** 238-243

16 **Bakotic BW,** Robinson MJ, Sturm PD, Hruban RH, Offerhaus GJ, Albores-Saavedra J. Pylori gland adenoma of the main pancreatic duct. *Am J Surg Pathol* 1999; **23:** 227-231

17 **Dixon MF.** Atrophy, metaplasia and dysplasia – a risk for gastric cancer: are they reversible? In: Hunt R, Tytgat G, editors. *Helicobacter pylori.* Basic Mechanisms to Clinical Cure. Lancaster: Kluwer 1998; pp336-353

18 **Xia HHX,** Kalantar J, Talley NJ, Ma Wyatt J, Adams S, Cheung K. Antral-type mucosa in the gastric incisura (antralization) - a link between *Helicobacter pylori* infection and intestinal metaplasia? *Am J Gastroenterol* 2000; **95:** 114-121

19 **Xia HHX**, Zhang G-S, Talley NJ, Wong BC, Yang Y, Henwood C, Wyatt JM, Adams S, Cheung K, **Xia** B, Zhu YQ, Lam SK. Topographic association of gastric epithelial expression of Ki-67, Bax and Bcl-2 expression with antralization in the gastric incisura, body and fundus. *Am J Gastroenterol* 2002; **97:** 3123-3131

20 **Wong BCY**, Wong WM, Wang WH, Wang WH, Tang VSY, Young J, Lai KC, Yuen ST, Leung SY, Hu WHC, Chan CK, Hui WM, Lam SK. An evaluation of invasive and non-invasive tests for the diagnosis of *Helicobacter pylori* infection in Chinese. *Aliment Pharmacol Ther* 2001; **15:** 505-511

21 **Dixon MF,** Genta RM, Yardley JH, Correa P. And the participants in the International Workshop on the Histopathology of Gastritis, Houston 1994. Classification and grading of gastritis. The updated Sydney System. *Am J Surg Pathol* 1996; **20:** 1161-1181

22 **Xia HHX**, Talley NJ. Apoptosis in gastric epithelium induced by *Helicobacter pylori* infection: implications in gastric carcinogenesis. *Am J Gastroenterol* 2001; **96:** 16-26

23 **Hanby AM**, Poulsom R, Playford RJ, Wright NA. The mucous neck cell in the human gastric corpus: a distinctive, functional cell lineage. *J Pathol* 1999; **187:** 331-337

24 **Schmidt PH**, Lee JR, Joshi V, Playford RJ, Poulsom R, Wright NA, Goldenring JR. Identification of a metaplastic cell lineage associated with human gastric adenocarcinoma. *Lab Invest* 1999; **79:** 639-646

25 **Wright NA**. Mechanisms involved in gastric atrophy. In: Hunt R, Tytgat G, editors. *Helicobacter pylori.* Basic Mechanisms to Clinical Cure 2000. *Dordrecht: Kluwer* 2000: pp239-247

26 **Dixon MF**. Patterns of inflammation linked to ulcer disease. *Best Pract Res Clin Gastroenterol* 2000; **14:** 27-40

27 **Sipponen P**, Kimura K. Intestinal metaplasia, atrophic gastritis and stomach cancer: trends over time. *Eur J Gastroenterol Hepatol* 1994; **6** (Suppl 1)**:** S79-S83

28 **Sakaki N**, Kozawa H, Egawa N, Tu Y, Sanaka M. Ten-year prospective follow-up study on the relationship between Helicobacter pylori infection and progression of atrophic gastritis, particularly assessed by endoscopic findings. *Aliment Pharmacol Ther* 2002; **16**(Suppl 2): 198-203

29 **Seery JP**. A reinterpretation of the events in gastric carcinogenesis. *Med Hypoth* 1991; **35:** 179-181

30 **Genta RM**. Atrophy, metaplasia and dysplasia: are they reversible? *Ital J Gastroenterol Hepatol* 1998; **30**(Suppl 3): S324-S325

31 **Satoh K**. Does eradication of *Helicobacter pylori* reverse atrophic gastritis or intestinal metaplasia? Data from Japan. *Gastroenterol Clin North Am* 2000; **29:** 829-835

32 **Dixon MF**. Prospects for intervention in gastric carcinogenesis: reversibility of gastric atrophy and intestinal metaplasia. *Gut* 2001; **49:** 2-4

33 **Xia HHX**, Wong BCY, Lam SK. *Helicobacter pylori* infection and gastric cancer. *Asian J Surg* 2001; **24:** 217-221

34 **Lanas A**, Sekar C, Hirschowitz BI. Objective evidence of aspirin use in both ulcer and nonulcer upper and lower gastrointestinal bleeding. *Gastroenterology* 1992; **103**: 862-869

35 **Lanas A**, Serano P, Bajador E, Esteva F, Benito R, Sainz R. Evidence of aspirin use in both upper and lower gastrointestinal perforation. *Gastroenterology* 1997; **112:** 683-689

**Edited by** Zhang JZ

P.O.Box 2345, Beijing 100023,China
Fax: +86-10-85381893
E-mail: wjg@wjgnet.com www.wjgnet.com

World J Gastroenterol 2003;9(6):1270-1272
World Journal of Gastroenterology
Copyright ©2003 by The WJG Press ISSN 1007-9327



# Clinicopathologic study of mucosa-associated lymphoid tissue lymphoma in gastroscopic biopsy

Hong Cheng, Jun Wang, Chuan-Shan Zhang, Pei-Song Yan, Xiao-Hui Zhang, Pei-Zhen Hu, Fu-Cheng Ma

**Hong Cheng, Chuan-Shan Zhang, Pei-Song Yan, Xiao-Hui Zhang, Pei-Zhen Hu, Fu-Cheng Ma,** Department of Pathology, Xijing Hospital, Fourth Military Medical University, Xi' an 710033, Shaanxi Province, China
**Jun Wang,** Department of Pathology, Shaanxi Traditional Chinese Medicine College, Xianyang 712083, Shaanxi Province, China
**Correspondence to:** Dr Hong Cheng, Department of Pathology, Xijing Hospital, Fourth Military Medical University, Xi' an 710033, Shaanxi Province, China. nelson@fmmu.edu.cn
**Telephone:** +86-29-3375497
**Received:** 2003-01-15 **Accepted:** 2003-02-22

## Abstract

**AIM:** To explore and discuss the clinicopathologic characteristics of mucosa-associated lymphoid tissue (MALT) lymphoma in gastroscopic biopsy specimen.

**METHODS:** A retrospective study of 26 cases of lymphoma diagnosed by gastroscopic biopsy during 1999 to 2001 from gastroscopy files of Xijing Hospital was made. The diagnostic criteria were adopted according to the new classification of non-Hodgkin's lymphoma.

**RESULTS:** Twenty-six cases of primary gastric lymphoma consisting of 15 men and 11 women, aged between 23 to 76 years were recruited from 6 225 cases who received gastroscopy. All of them were diagnosed by both endoscopic findings and histological examinations. Histologically, 23 cases were MALToma (low grade) and 3 cases lymphoblastic lymphoma (high grade). Immunohistochemically, all cases were CD20 positive, while CK and EMA were negative.

**CONCLUSION:** The majority of the cases of primary low-grade gastric lymphoma have morphologic and clinical features that justify their inclusion in the category of low-grade lymphoma of mucosa associated lymphoid tissue.

Cheng H, Wang J, Zhang CS, Yan PS, Zhang XH, Hu PZ, Ma FC. Clinicopathologic study of mucosa-associated lymphoid tissue lymphoma in gastroscopic biopsy. *World J Gastroenterol* 2003; 9(6): 1270-1272
http://www.wjgnet.com/1007-9327/9/1270.asp

## INTRODUCTION

Primary gastric lymphoma is the most common extra nodal lymphoma, and the vast majority of them are of B cell origin. Most of the low-grade gastric lymphomas are of the mucosa-associated lymphoid tissue (MALT) type[1-4]. The concept of MALT lymphoma was first proposed in 1983 by Isaacson and Wright[1]. Histologically it is characterized by centrocyte-like cells, often with plasmacytic differentiation, and accompanied by lymphoepithelial lesions. The histopathological criteria for the diagnosis of gastric MALToma have largely been based on analysis of partial gastrectomy specimens. From routine biopsy diagnosis by gastroscopy, it is very difficult to distinguish MALToma from reactive lymphoid hyperplasia on small pieces of tissue. In this article, twenty-six cases were retrospectively analyzed with regard to criteria of diagnosis and clinicopathologic characteristics.

## MATERIALS AND METHODS

### *Materials*

During the period of 1999-2001, 6 225 cases received gastroscopy in Xijing Hospital and 26 cases of gastric lymphoma were diagnosed according to the new classification of lymphoid neoplasms. The patients (11 women and 15 men) ranged in age from 23 to 76 years. According to the new classification of lymphoid neoplasms[2], all the histology of MALToma was established if the following criteria were met: (1) invasion of epithelial structures resulting in "lymphoepithelial lesions"; (2) small lymphocytes, marginal zone cells and/or monocytoid B cells; (3) infiltration of diffuse, perifollicular, interfollicular, or even follicular type due to colonization of reactive follicles. Tissue specimens were embedded in paraffin, sectioned and stained with haematoxylin-eosin and immunohistochemical method.

### *Immunohistochemical analysis*

Immunohistochemical staining of CD20, CD45, CD45RO, Keratin and EMA were performed on paraffin-embedded sections by using the monoclonal antibody (Dako, Copenhagen, Denmark). For antigen retrieval, the deparaffinized slides were microwaved in 0.01 mol/L sodium citrate buffer (pH 6.0) for 10 minutes. Endogenous peroxidase activity was inhibited by hydrogen peroxidase. The sections were incubated with the monoclonal antibody (1:100) overnight at room temperature, and then the detection was performed by the avidin-biotin peroxidase complex method. The sections were counterstained with hematoxylin. PBS buffer solution was substituted for the first antibodies as the negative control, whereas the lymphoma cases were used as positive control.

## RESULTS

### *Clinical data*

There were 26 cases of MALToma, of them 15 were males and 11 females, with age ranging from 23 to 76 years. Clinical manifestations were epigastric discomfort, abdominal pain, dyspepsia, fever, melena and mucous stool. Endoscopic evaluation showed the location of 5 cases in gastric body, 4 in gastric antrum, 15 in gastric body and antrum, 1 in gastric angulus and 1 in gastric fundus. By endoscopic diagnosis, 9 cases were gastric cancer and 17 cases were gastric ulcer.

### *Pathological data*

Based on the appearance of biopsy specimens, all 26 cases were gastric lymphomas, of them 23 were MALToma (low grade) and 3 lymphoblastic lymphoma (high grade).

Macroscopically, MALToma could be categorized into erosion and ulcerative types; the size of tumor varied from millet to rice. The lymphomatous cells infiltrated into the

mucosa, sub-mucosa and muscular layer diffusely or locally. Typical features of a low-grade mucosa-associated lymphoma with an organized architectural arrangement including lymphoid follicles, centrocyte-like cells and classical lymphoepithelial lesions were seen. Lymphoid follicles were seen and the germinal centers were partly or entirely replaced by lymphoma cells. Dendritic cells and macrophages with chromophilic bodies disappeared. This phenomenon is called follicular colonization. Lymphoepithelial lesion was shown in which there were clusters of pleomorphic, mitotically active lymphomatous cells infiltration locally and gastric glands destroyed (Figure 1). The neoplastic cells presented a serial cell lineage of small lymphocyte, centrocyte-like cell, monocyte-like B cell, lymphoplasma cell, and also centroblast like cells. In all these cells, several kinds were in a mixed distribution, but usually one kind was predominant. Immunohistochemically, all cases of MALTomas were CD20 positive (Figure 2) and CD45 positive. CK and EMA were negative in all cases.

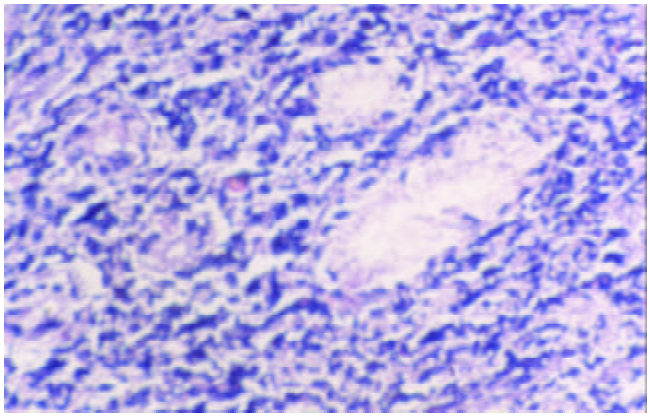

**Figure 1** Neoplastic lymphocytes infiltrated into and destroyed glands forming lymphoepithial lesion. HE ×200.

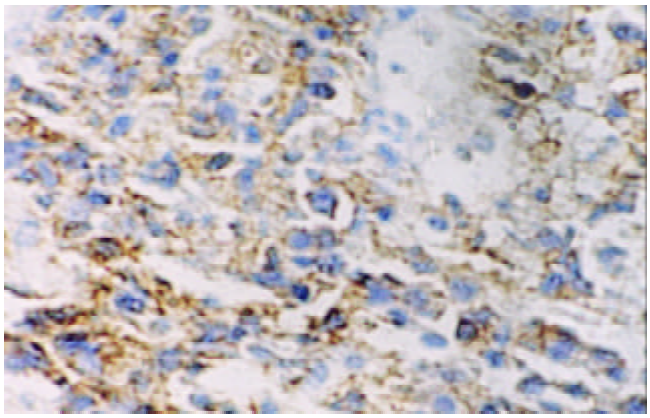

**Figure 2** Neoplastic lymphocytes infiltrated into mucosa membrane, with positive CD20. Envision method. ×400.

## DISCUSSION

The gastrointestinal tract is the most frequently involved extranodal site of origin for non-Hodgkin's lymphoma, accounting for 12-15 % of all non-Hodgkin's lymphomas and 30-40 % of all extranodal lymphomas[1,5]. The lymphomas in the stomach arise from MALT. Usually they are not present in the stomach but acquired following *H. pylori* infection of the gastric mucosa. *H. pylori*, a microaerophilic Gram-negative rod, has been proposed as the causative agent for low-grade primary gastric lymphoma of MALT[6-10]. Presenting features of primary gastric lymphomas are nonspecific, with dyspepsia, vague epigastric pain, nausea and vomiting[11-15]. Fever with night sweats and elevated lactate dehydrogenase levels are very uncommon. By endoscopy, diffuse gastritis, thickened gastric folds, erosions and occasionally ulcers are more common findings. Although any region of the stomach may be involved, most MALTomas arise in the antrum or the distal body, the sites commonly colonized by *H. pylori*. Histologically, the prominent lymphoepithelial lesion on endoscopic biopsy specimens is one of the most important features for the diagnosis of MALToma of the stomach[2, 16-18]. They are seen in 100 % of the biopsy specimens. It is a key point for the diagnosis of MALToma that the infiltrating lymphocytes showed homogeneity in marginal zone cells, small lymphocytes, or monocytoid B cells[2, 16-18]. All of the three types of cells comprise low-grade lymphomas with a dense infiltrate of a superficial and peripheral plasma cell component. Cytologically, neoplastic lymphocytes are characterized by cellular heterogeneity, including centrocyte like cells (small, atypical cells, but with more abundant cytoplasm), monocytoid B cells, small lymphocytes, and plasma cells. Occasionally large cells (centroblast or immunoblast like) are present in most cases. If reactive follicles are present, neoplastic cells will occupy the marginal zone and/or the interfollicular region. When neoplastic lymphocytes take on a follicular pattern, it is called follicular colonization.

Therefore, the diagnosis of gastric MALToma is based on (1) prominent lymphoepithelial lesions; (2) dense lymphoid infiltrate with marginal zone cells, small lymphocytes, or monocytoid B cells. Lymphoepithelial lesions are considered as the characteristic features of MALToma. Nest formation could also be found in the inflammatory and reactive status, it might be difficult to distinguish them from the real lymphoepithelial lesions. In such cases, immunohistochemistry may be helpful. The former is several leukocytes of polyclone and the latter is the lymphocytes of mono-clone. Follicular colonization is easy to be misjudged as reactive follicles. The following morphological characteristics and immunophenotype may be helpful for the differentiation[14-18]: (1) Follicular colonization has no dendritic cells or macrophages with chromophilic bodies. (2) Centrocyte like cell is the immunophenotype of B cells in the marginal area, rather than at the germinal center. Both lymphoepithelial lesion and follicular colonization are characteristic features for diagnosis, but they could only be seen in some of the cases. If one case is highly suspected for MALToma of the stomach, repeated biopsy should be performed if clinically indicated and then, immunohistochemistry and molecular biology technique should be done.

Understanding primary gastric lymphomas is undergoing rapid and significant transformation from both clinicopathological and therapeutic standpoints. The most important new developments in therapy are the use of *H. pylori* eradication as the initial treatment for localized low-grade primary gastric lymphomas, and the use of chemoradiation over a surgical approach for localized high-grade primary gastric lymphoma[19-30]. Patients with low-grade primary gastric lymphoma should be treated with *H. pylori* eradication therapy as most patients respond with prompt amelioration of dyspeptic symptoms, although histological regression may take several months. Patients need to be followed-up with serial endoscopies. If no histologically proven lymphoma regression occurs, then biopsy should be done to rule out the presence of co-existing high-grade primary gastric lymphoma. The finding of high-grade primary gastric lymphoma usually indicates the need for more aggressive treatment with chemotherapy and radiotherapy. Surgery is an option in cases of significant

hemorrhage or perforation. With appropriate treatment, the long-term survival is 70-80 % for limited-stage disease and 50-60 % for advanced stage disease.

## REFERENCES


1 **Stolte M**, Bayerdorffer E, Morgner A, Alpen B, Wundisch T, Thiede C, Neubauer A. *Helicobacter* and gastric MALT lymphoma. *Gut* 2002; **50**(Suppl 3): III 19-24

2 **Isaacson PG**, Muller-Hermelink HK, Paris MA, Berger F, Nathwani BN, Swerdlow SH, Harris NL. Extranodal marginal zone B-cell lymphoma of mucosa-associated lymphoid tissue (MALT lymphoma). In Jaffe ES, Harris NL, Stein H, Vardiman JW eds. World Health Organization Classification of Tumours. Pathology and genetics of tumours of haematopoietic and lymphoid tissues. *Lyon: IARC Press* 2001: 157-160

3 **Zhou Q**, Xu TR, Fan QH, Zhen ZX. Clinicopathologic study of primary intestinal B cell malignant lymphoma. *World J Gastroenterol* 1999; **5**: 538-540

4 **Salam I**, Durai D, Murphy JK, Sundaram B. Regression of primary high-grade gastric B-cell lymphoma following *Helicobacter pylori* eradication. *Eur J Gastroenterol Hepatol* 2001; **13**: 1375-1378

5 **Delchier JC**, Lamarque D, Levy M, Tkoub EM, Copie-Bergman C, Deforges L, Chaumette MT, Haioun C. *Helicobacter pylori* and gastric lymphoma: high seroprevalence of CagA in diffuse large B-cell lymphoma but not in low-grade lymphoma of mucosa-associated lymphoid tissue type. *Am J Gastroenterol* 2001; **96**: 2324-2328

6 **Go MF**, Smoot DT. *Helicobacter pylori*, gastric MALT lymphoma, and adenocarcinoma of the stomach. *Semin Gastrointest Dis* 2000; **11**: 134-141

7 **Wotherspoon AC**, Doglioni C, Diss TC, Pan L, Moschini A, de Boni M, Isaacson PG. Regression of primary low-grade B-cell gastric lymphoma of mucosa-associated lymphoid tissue type after eradication of *Helicobacter pylori*. *Lancet* 1993; **342**: 575-577

8 **Furusyo N**, Kanamoto K, Nakamura S, Yao T, Suekane H, Yano Y, Ariyama I, Hayashi J, Kashiwagi S. Rapidly growing primary gastric B-cell lymphoma after eradication of *Helicobacter pylori*. *Intern Med* 1999; **38**: 796-799

9 **Montalban C**, Santon A, Boixeda D, Bellas C. Regression of gastric high grade mucosa associated lymphoid tissue (MALT) lymphoma after *Helicobacter pylori* eradication. *Gut* 2001; **49**: 584-587

10 **Miki H**, Kobayashi S, Harada H, Yamanoi Y, Uraoka T, Sotozono M, Ohmori M. Early stage gastric MALT lymphoma with high-grade component cured by *Helicobacter pylori* eradication. *J Gastroenterol* 2001; **36**: 121-124

11 **Gretschel S**, Hunerbein M, Foss HD, Krause M, Schlag PM. Regression of high-grade gastric B-cell lymphoma after eradication of *Helicobacter pylori*. *Endoscopy* 2001; **33**: 805-807

12 **Morgner A**, Miehlke S, Fischbach W, Schmitt W, Muller-Hermelink H, Greiner A, Thiede C, Schetelig J, Neubauer A, Stolte M, Ehninger G, Bayerdorffer E. Development of early gastric cancer 4 and 5 years after complete remission of *Helicobacter pylori* associated gastric low grade marginal zone B cell lymphoma of MALT type. *World J Gastroenterol* 2001; **7**: 248-253

13 **Morgner A**, Miehlke S, Fischbach W, Schmitt W, Muller-Hermelink H, Greiner A, Thiede C, Schetelig J, Neubauer A, Stolte M, Ehninger G, Bayerdorffer E. Complete remission of primary high-grade B-cell gastric lymphoma after cure of *Helicobacter pylori* infection. *J Clin Oncol* 2001; **19**: 2041-2048

14 **Bouzourene H**, Haefliger T, Delacretaz F, Saraga E. The role of *Helicobacter pylori* in primary gastric MALT lymphoma. *Histopathology* 1999; **34**: 118-123

15 **Morgner A**, Lehn N, Andersen LP, Thiede C, Bennedsen M, Trebesius K, Neubauer B, Neubauer A, Stolte M, Bayerdorffer E. *Helicobacter* heilmannii-associated primary gastric low-grade MALT lymphoma: complete remission after curing the infection. *Gastroenterology* 2000; **118**: 821-828

16 **Hiyama T**, Haruma K, Kitadai Y, Masuda H, Miyamoto M, Ito M, Kamada T, Tanaka S, Uemura N, Yoshihara M, Sumii K, Shimamoto F, Chayama K. Clinicopathological features of gastric mucosa-associated lymphoid tissue lymphoma: a comparison with diffuse large B-cell lymphoma without a mucosa-associated lymphoid tissue lymphoma component. *J Gastroenterol Hepatol* 2001; **16**: 734-773

17 **Tang CC**, Shih LY, Chen PC, Chen TC. Simultaneous occurrence of gastric adenocarcinoma and low-grade gastric lymphoma of mucosa-associated lymphoid tissue. *Chang Gung Med J* 2002; **25**: 115-121

18 **Papa A**, Cammarota G, Tursi A, Gasbarrini A, Gasbarrini G. *Helicobacter pylori* eradication and remission of low-grade gastric mucosa-associated lymphoid tissue lymphoma: a long-term follow-up study. *J Clin Gastroenterol* 2000; **31**: 169-171

19 **Xue FB**, Xu YY, Wan Y, Pan BR, Ren J, Fan DM. Association of *H. pylori* infection with gastric carcinoma:a Meta analysis. *World J Gastroenterol* 2001; **7**: 801-804

20 **Wang RT**, Wang T, Chen K, Wang JY, Zhang JP, Lin SR, Zhu YM, Zhang WM, Cao YX, Zhu CW, Yu H, Cong YJ, Zheng S, Wu BQ. *Helicobacter pylori* infection and gastric cancer: evidence from a retrospective cohort study and nested case-control study in China. *World J Gastroenterol* 2002; **8**: 1103-1107

21 **Lu XL**, Qian KD, Tang XQ, Zhu YL, Du Q. Detection of *H. pylori* DNA in gastric epithelial cells by *in situ* hybridization. *World J Gastroenterol* 2002; **8**: 305-307

22 **Vandenplas Y**. *Helicobacter pylori* infection. *World J Gastroenterol* 2000; **6**: 20-31

23 **Hu PJ**. *Hp* and gastric cancer: challenge in the research. *Shijie Huaren Xiaohua Zazhi* 1999; **7**: 1-2

24 **Quan J**, Fan XG. Progress in experimental research of *Helicobacter pylori* infection and gastric carcinoma. *Shijie Huaren Xiaohua Zazhi* 1999; **7**: 1068-1069

25 **Guo CQ**, Wang YP, Ma SW, Ding GY, Li LC. Study on *Helicobacter pylori* infection and p53, c-erbB-2 gene expression in carcinogenesis of gastric mucosa. *Shijie Huaren Xiaohua Zazhi* 1999; **7**: 313-315

26 **Xiao SD**, Liu WZ. Current status in treatment of *Hp* infection. *Shijie Huaren Xiaohua Zazhi* 1999; **7**: 3-4

27 **Begum S**, Sano T, Endo H, Kawamata H, Urakami Y. Mucosal change of the stomach with low-grade mucosa-associated lymphoid tissue lymphoma after eradication of *Helicobacter pylori*: follow-up study of 48 cases. *J Med Invest* 2000; **47**: 36-46

28 **Yamashita H**, Watanabe H, Ajioka Y, Nishikura K, Maruta K, Fujino MA. When can complete regression of low-grade gastric lymphoma of mucosa-associated lymphoid tissue be predicted after *Helicobacter pylori* eradication? *Histopathology* 2000; **37**: 131-140

29 **Urakami Y**, Sano T, Begum S, Endo H, Kawamata H, Oki Y. Endoscopic characteristics of low-grade gastric mucosa-associated lymphoid tissue lymphoma after eradication of *Helicobacter pylori*. *J Gastroenterol Hepatol* 2000; **15**: 1113-1119

30 **Alpen B**, Thiede C, Wundisch T, Bayerdorffer E, Stolte M, Neubauer A. Molecular diagnostics in low-grade gastric marginal zone B-cell lymphoma of mucosa-associated lymphoid tissue type after *Helicobacter pylori* eradication therapy. *Clin Lymphoma* 2001; **2**: 103-108


**Edited by** Xu JY

P.O.Box 2345, Beijing 100023,China
Fax: +86-10-85381893
E-mail: wjg@wjgnet.com www.wjgnet.com

World J Gastroenterol 2003;9(6):1273-1277
World Journal of Gastroenterology
Copyright ©2003 by The WJG Press ISSN 1007-9327

• BASIC RESEARCH •

# Expression and cell-specific localization of cholecystokinin receptors in rat lung

Bin Cong, Shu-Jin Li, Yi-Ling Ling, Yu-Xia Yao, Zhen-Yong Gu, Jun-Xia Wang, Hong-Yu You

**Bin Cong, Shu-Jin Li, Yi-Ling Ling, Yu-Xia Yao, Zhen-Yong Gu,** Department of Pathophysiology, Hebei Medical University, Shijiazhuang 050017, Hebei Province, China
**Jun-Xia Wang, Hong-Yu You,** Molecular Biological Laboratory, Hebei Medical University, Shijiazhuang 050017, Hebei Province, China
**Supported by** National Natural Science Foundation of China, No. 39570304
**Correspondence to:** Professor Yi-Ling Ling, Department of Pathophysiology, Hebei Medical University, Shijiazhuang 050017, Hebei Province, China. lingyiling@163.net
**Telephone:** +86-311-6265645
**Received:** 2003-01-04 **Accepted:** 2003-02-11

## Abstract

**AIM:** To elucidate whether CCK receptors exist in lung tissues and their precise cellular localization in the lung.

**METHODS:** CCK-AR and CCK-BR mRNA expression and cellular distribution in the rat lung were detected by highly sensitive method of *in situ* reverse transcription-polymerase chain reaction (RT-PCR) and conventional *in situ* hybridization.

**RESULTS:** CCK-AR and CCK-BR gene positive signals were observed in bronchial epithelial cells, alveolar epithelial cells, pulmonary macrophages and vascular endothelial cells of the rats' lung by *in situ* RT-PCR. The hybridization signals of CCK-AR were relatively faint. By *in situ* hybridization, however, only the signals of CCK-BR but not CCK-AR were detected in the lung, and the positive staining was only found in vascular endothelial cells and macrophages.

**CONCLUSION:** CCK-AR and CCK-BR gene were present in pulmonary vascular endothelial cells, macrophages, bronchial epithelial cells and alveolar epithelial cells, which play an important role in mediating the regulatory actions of CCK-8 on these cells.

Cong B, Li SJ, Ling YL, Yao YX, Gu ZY, Wang JX, You HY. Expression and cell-specific localization of cholecystokinin receptors in rat lung. *World J Gastroenterol* 2003; 9(6): 1273-1277
http://www.wjgnet.com/1007-9327/9/1273.asp

## INTRODUCTION

Cholecystokinin (CCK) is a gut-brain peptide that exerts a variety of physiological actions in the gastrointestinal tract and central nervous system (CNS) through cell surface CCK receptors[1]. CCK receptors have been pharmacologically classified into two subtypes CCK-A receptor (CCK-AR) and CCK-B receptor (CCK-BR) according to their affinity for the peptide agonists CCK and gastrin, which share the same COOH-terminal pentrapeptide amide sequence but differ in sulfation at the sixth (gastrin) and seventh (CCK) tyrosyl residues[2]. CCK-AR is highly selective to sulfated analogues of CCK and the antagonist L-364 718, whereas CCK-BR has similarly high affinity to both sulfated and nonsulfated peptide analogues of CCK/gastrin peptides and the antagonist L-365 260[2]. CCK-AR is found principally in the gastrointestinal tract and selective areas of the CNS, while CCK-BR is found principally in the CNS and selective areas of the gastrointestinal tract, on pancreatic acinar cells and parietal cells[3,4]. CCK binds to CCK-AR present on a variety of gastrointestinal target tissues including pancreatic acini, islets, gastric mucosa and gallbladder to induce pancreatic enzyme secretion, insulin secretion, release of pepsinogen and gallbladder contraction[5]. CCK-BR in the CNS regulates feeding, anxiety and memory, etc[3]. CCK-AR and CCK-BR are also expressed in the neoplastic cells such as pancreatic cancer cells[6,7], gastric cancer cells[8,9], colonic cancer cells[10] and small cell lung cancer cells[11-13] where they may stimulate cell growth. In addition, CCK-BR is also present on T lymphocytes[14,15] to regulate lymphocytes proliferation[16,17]. These data suggested that CCK receptors were widely distributed around various kinds of tissues and their presence provided the structural basis for CCK to exert a broad array of physiological action.

Our previous data demonstrated that CCK-8, as an intestinal neuropeptide, not only protected gastric mucosa against alcohol-induced injury[18-20], but also was a potent protective agent against acute lung injury by LPS[21,22]. It obviously reduced the pulmonary artery hypertention (PAH) and lessened the inflammatory lesion in lung tissues of endotoxin shock (ES) rats[21,22]. Moreover, CCK-8 could inhibit the reduction of endothelial-dependent relaxation of isolated pulmonary artery to acetylcholine (ACh) induced by LPS[23]. Stretton and Barnes reported that CCK-8 produced a concentration-dependent contractile response in guinea-pig trachea and this effect was antagonized by the CCK receptor antagonists dibutyryl cyclic guanosine monophosphate and L-364 718[24]. These data indicated that there might be CCK receptors in the lung tissues to mediate the action of CCK-8. However, whether CCK receptors are present in lung tissues and their precise cellular localization remains unclear. In the present study, we detected the cellular localization of CCK receptors in the rats' lung using highly sensitive method of *in situ* RT-PCR.

## MATERIALS AND METHODS

### *Animal model and tissue preparation*

Healthy Sprague-Dawley rats (weighing 180-220 g BW) were anaesthetized with urethane (1 g/kg). Lung tissues were dissected from the rats. The inferior lobe of right lung was fixed in 4 % paraformaldehyde for 1 h and embedded in paraffin for *in situ* hybridization and *in situ* RT-PCR.

### *Primers and probe*

The primers and probe of CCK receptor were designed according to Mostein' s report[25]. The sequences of CCK-AR primers were 5' -CTC GCT CGC CCA GAA CTC TAC CAA GGA ATC AAA TTT GAT GC-3' (sense) and 5' -CTG GTT CGG CCC ATG GAG CAG AGG TGC TCA TGT GGC TGT AG-3' (antisense). The sequences of CCK-BR primers were

5' -CTC GCT CGC CCA GAA CTC TAC CTA GGA CTC CAC TTT GA-3' (sense) and 5' -CTG GTT CGG CCC ACG CAC CAC CCG CTT CTT AGC CAG CA-3' (antisense). The sequences of CCK-AR and CCK-BR probes were respectively 5' -CGG GGG CCG GGG ACT TCT GCA AGT AAC AGC CAT CAC TAT CCT CAT A-3' and 5' -AGC TAC GCT GGT TAC AGG CCG GCA GCC CCC GTT-3' . The oligonucleotide probes were labeled with alkaline phosphatase (Boehringer Mannheim). All the primers and probes were synthesized by Sangon Corporation (Shanghai).

### *In situ RT-PCR*

The sections (5 μm) were baked and deparaffinized to water, and then treated with 0.2 mol/L HCl and EDTA. The slides were pretreated with 0.1 % proteinase K at 37 ℃ for 12 min to prevent background staining and inactivate endogenous enzyme. Then the tissues were treated overnight in a Rnase-free DNAase solution (Boehringer Mannheim) at 37 ℃. The *in situ* reverse trancription step was performed in 30 μl solution containing 2 μmol/L CCK-AR or CCK-BR primers and 1 U/μl AMV-RT at 42 ℃ for 1.5 h. Then the slides were overlain with 50 μl *in situ* PCR reaction mixture containing 1×PCR buffer, 4.5 mmol/L $MgCl_2$, 0.2 μmol/L dNTPs, 1 μmol/L each of primers, and 10 U Taq polymerase (Perkin Elmer). The PCR was performed at conditions of initial denaturation at 94 ℃ for 2 min, followed by 30 cycles of denaturation at 94 ℃ for 1.5 min, annealing at 55 ℃ for 1 min, and extension at 72 ℃ for 1 min. PCR-amplified products were detected with alkaline phosphatase (AP)-labeled CCK-AR and CCK-BR oligonucleotide probes (2 pmol/ml) at 37 ℃ for 24 h. The slides were then developed in NBT/BCIP solutions at room temperature for 48 h. To stop the color reaction, the slides were washed in distilled water and mounted with glycergel.

### *Controls*

The brain sections were used as positive control. A series of negative controls were performed to guarantee the specificity of the method of *in situ* RT-PCR. Samples pretreated with RNase were used as negative control. Other five negative controls were samples treated without AMV-RT, or Taq polymerase, or primers, or probes specified or unspecified.

### *In situ hybridization*

The procedure was carried out the same way as *in situ* RT-PCR, but without the RT-PCR steps.

## RESULTS

### *The positive and negative controls of in situ RT-PCR*

The rat brain sections expressed both CCK-AR and CCK-BR. The hybridization signal was present in the neuron. There was no positive signal in RNase-pretreated samples. Omission of AMV-RT, or Taq polymerase, or primers, or probes prevented specific staining (Figure 1, Table 1).

**Table 1** Negative controls for in situ RT-PCR

| Reagent | a | b | c | d | e | f |
|---|---|---|---|---|---|---|
| AMV-RT | √ | √ | √ | √ | × | √ |
| Taq polymerase | √ | √ | √ | × | √ | √ |
| Primers | √ | √ | × | √ | √ | √ |
| Probes | √ | × | √ | √ | √ | √ |
| RNase | √ | × | × | × | × | × |
| Probes (Unspecified) | × | √ | × | × | × | × |
| Signal | - | - | ± | - | - | - |

### *In situ expression of CCK-BR gene in rat lungs*

By *in situ* RT-PCR, CCK-BR mRNA stainings (dark blue color) were found in bronchial mucosal epithelial cells, endothelial cells, alveolar epithelial cells and macrophages (Figure 2). By *in situ* hybridization, however, CCK-BR mRNA staining was only seen in endothelial cells and macrophages (Figure 3).

### *In situ expression of CCK-AR gene in rat lungs*

By *in situ* RT-PCR, the hybridization signals of CCK-AR mRNA were also found in bronchial mucosal epithelial cells, endothelial cells, alveolar epithelial cells and macrophages, and the hybridization signals of CCK-AR were weaker than those of CCK-BR (Figure 4). By *in situ* hybridization, however, no expression of CCK-AR mRNA was detected (Figure 5).

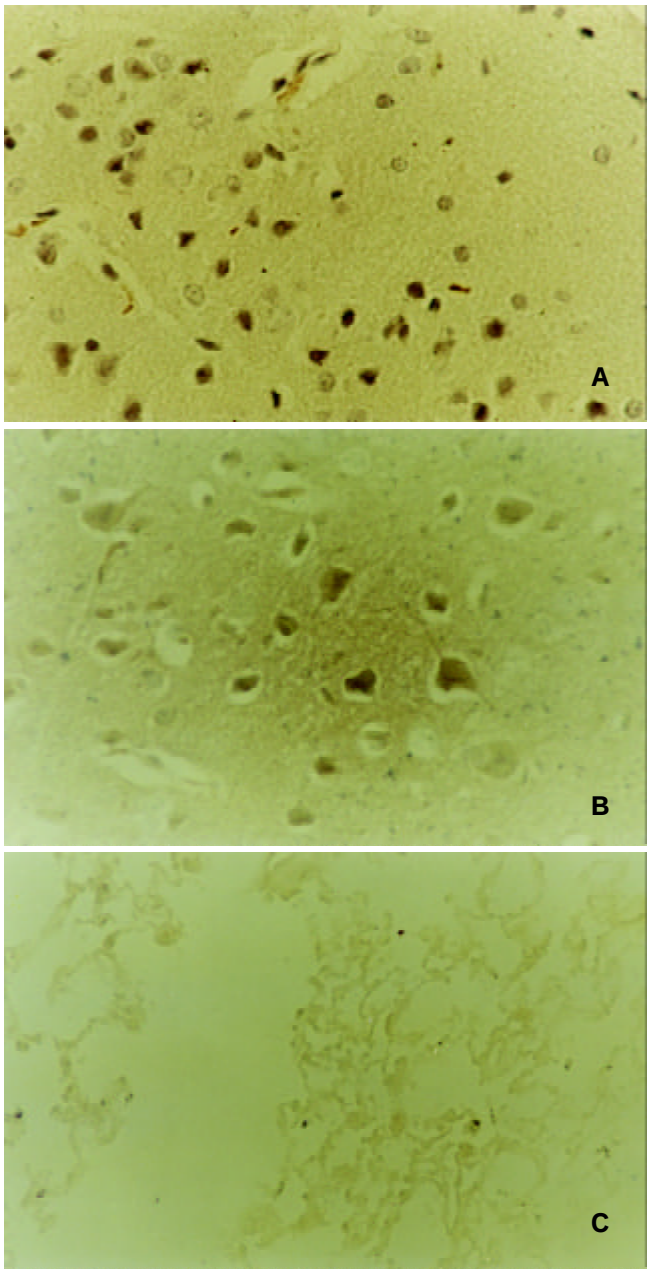


**Figure 1** Appearance of positive and negative control tissue section for detecting *in situ* expression of CCK-AR and CCK-BR gene by *in situ* RT-PCR. (A) *In situ* expression of CCK-BR gene in the brain of SD rats (×400). (B) *In situ* expression of CCK-AR gene in the brain of SD rats (×400). (C) Negative control section from the lung tissue of SD rats (×200).

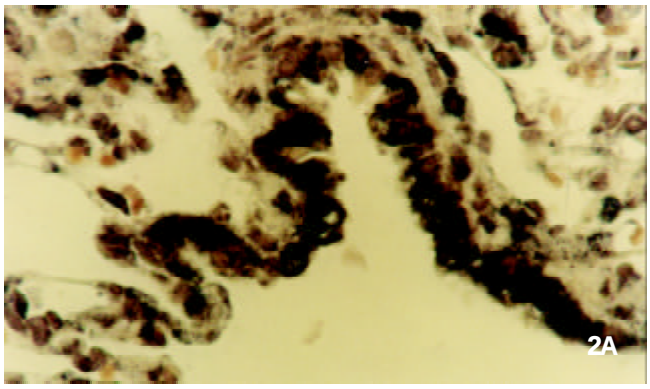


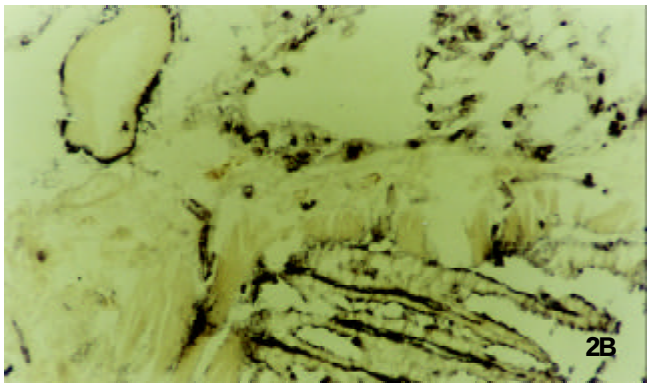


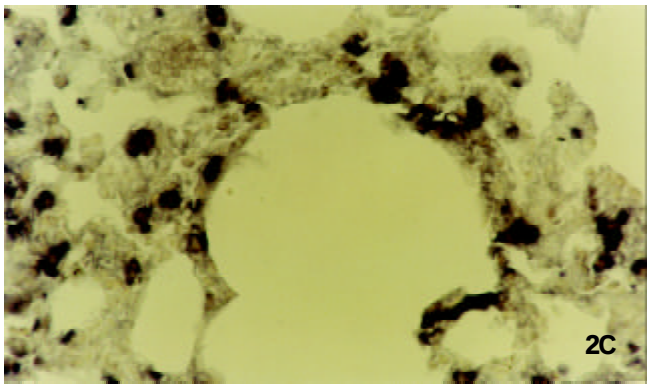


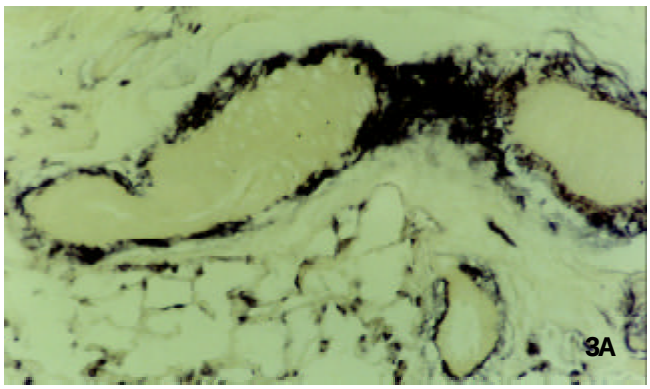


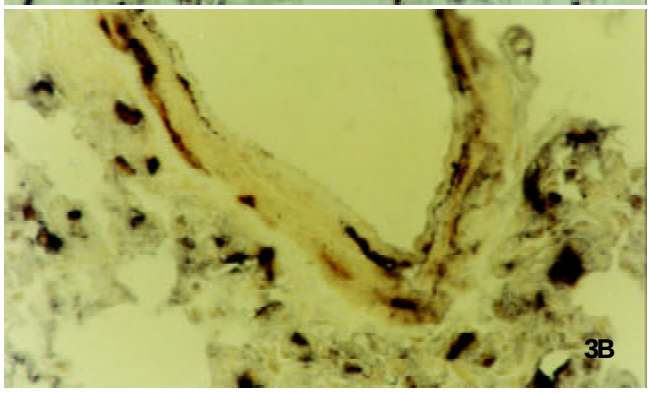


**Figure 2** Localization of CCK-BR gene in the lung tissues of SD rats by *in situ* RT-PCR (×400). (A) Expression of CCK-BR gene in bronchial mucosal cells. (B) Expression of CCK-BR gene in vascular endothelial cells. (C) Expression of CCK-BR gene in macrophages and alveolar epithelial cells.

**Figure 3** Localization of CCK-BR mRNA in rat lung tissues by *in situ* hybridization. (A) Expression of CCK-BR gene in vascular endothelial cells (×100). (B) Expression of CCK-BR gene in vascular endothelial cells and macrophages (×400).

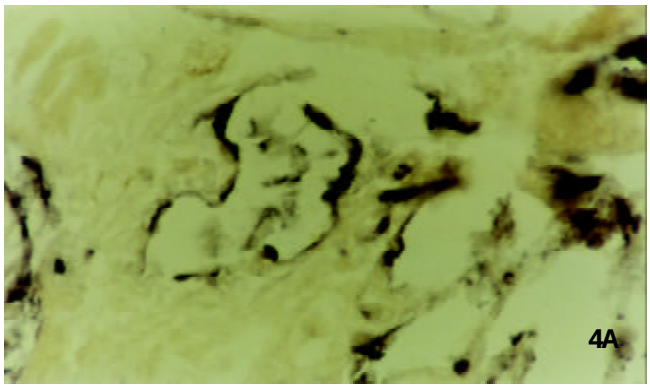


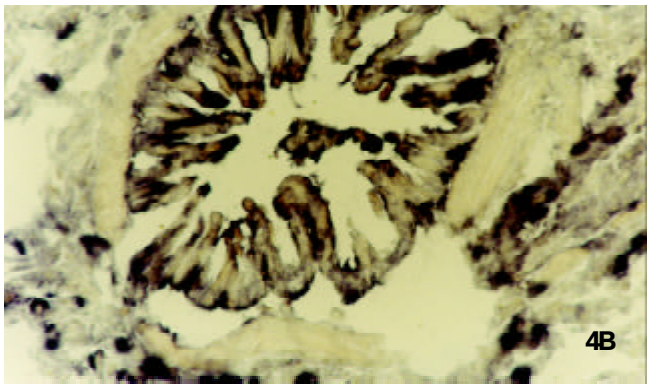


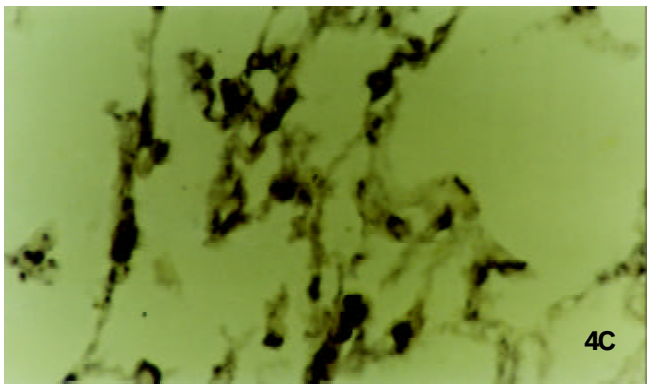


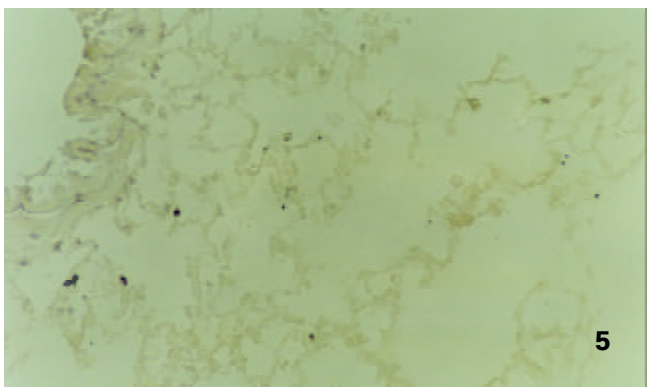


**Figure 4** *In situ* expression of CCK-AR gene in the lung tissues of SD rats, detected by *in situ* RT-PCR (×400). (A) Expression of CCK-AR gene in vascular endothelial cells. (B) Expression of CCK-AR gene in bronchial mucosal cells and macrophages. (C) Expression of CCK-AR gene in alveolar epithelial cells.

**Figure 5** No positive signal of CCK-AR gene was detected in lung tissues by *in situ* hybridization (×200).

## DISCUSSION

*In situ* RT-PCR is a novel molecular biological technique that combines the high sensitivity of RT-PCR for generating a cDNA from small amounts of mRNA with cellular localization of *in situ* hybridization. The sensitivity of *in situ* hybridization is 10-20 copies per cell when detecting the single-copy and low-copy (less than 10 copies) target DNA or RNA in tissues, while using *in situ* RT-PCR could significantly enhance the sensitivity for detecting the target DNA or RNA[26]. In the present study, we detected the *in situ* expression of CCK receptors by two methods of in situ hybridization and *in situ* RT-PCR. By *in situ* hybridization, only little amount of CCK-BR gene staining was found in vascular endothelial cells and macrophages, whereas by *in situ* RT-PCR, both CCK-AR and CCK-BR mRNA expressions were detected in bronchial mucosal cells and alveolar epithelial cells other than endothelial cells and macrophages. Our results also demonstrated that the sensitivity of *in situ* RT-PCR was obviously higher than that of *in situ* hybridization. Large amounts of cDNA were amplified by specially designed target-specific primers and followed by hybridization with highly specific probes[27]. So the specific binding of nucleotide on the basis of base complementation was performed twice, which increased the specificity of *in situ* RT-PCR. High sensitivity and specificity made *in situ* RT-PCR a favorable technique to study the *in situ* expression and cellular distribution of target gene in tissues. To further ensure the specific results, we designed six negative controls: First, omission of AMV-RT prevented the positive staining, indicating that genome DNA was completely digested. Second, omission of Taq polymerase produced negative results, suggesting endogenous polymerase was inactive. Third, omission of primers produced weak positive reaction which was the results of little amounts of cDNA binding with specific probes, and it confirmed the specificity of the primers. Fourth, addition of RNase produced negative results, confirming that mRNA was detected during RT-PCR. Fifth, omission of specific probes and addition of nonspecific probes produced negative reaction, confirming the specificity of the probes. Sixth, addition of unlabeled specific probes prevented the positive staining, indicating that endogenous alkaline phosphatase was inactive.

Using *in situ* RT-PCR, we found that CCK-AR and CCK-BR were present in the rats' lungs. It is the first report about the distribution of CCK receptors in lung tissues. The results of *in situ* RT-PCR also demonstrated the cellular localization of CCK receptors in lung tissues: vascular endothelial cells, macrophages, bronchial epithelial cells and alveolar epithelial cells. Our previous study showed that exposure of rabbit pulmonary artery to LPS or TNF-α led to significant reduction of endothelial-dependent relaxation to ACh and enhancement of contractile response to phenylephrine, which could be reversed by CCK-8[23,28]. This may be the mechanisms of CCK-8 to abolish PAH during endotoxin shock. The present study showed that pulmonary vascular endothelial cells expressed both CCK-AR and CCK-BR gene. So CCK-8 may bind to CCK receptors on pulmonary vascular endothelial cells to mediate its effects on isolated pulmonary artery. Gu *et al*[29] reported that CCK-8 protected cultured bovine pulmonary artery endothelial cells (BPAEC) against the detrimental effect of LPS such as lipoperoxide damages and cell apoptosis as well as LPS-induced peroxynitrite formation, which might be in part reversed by proglumide, a nonspecific CCK receptor antagonist. These data suggested that there might be CCK receptors on BPAEC. Therefore, CCK receptors on pulmonary endothelial cells may mediate effects of CCK-8 on pulmonary vascular such as regulating the reactivity of pulmonary vascular to vasoactive agents and protecting the endothelial cells against damages.

Our present study also demonstrated existence of CCK-AR and CCK-BR gene expression in pulmonary macrophages. It is well known that activation of macrophages plays a critical role in inducing the inflammatory response[30]. Macrophages stimulated by LPS or other inflammatory factors produce and release large quantities of various proinflammatory cytokines including TNF-α, IL-1β, IL-6 etc. Overproduction of these cytokines can result in systemic inflammatory response syndrome (SIRS) and multiple organ dysfunction syndrome (MODS), which might lead to death[31]. So controlling the overactivation of macrophages may be an effective measure in preventing the generation and development of SIRS and MODS. In another study, we found that CCK-8 could inhibit LPS-induced TNF-α release and gene expression in rat pulmonary interstitial macrophages (PIMs) *in vitro*[32,33]. The study about its upstream signalling mechanisms demonstrated that CCK-8 inhibited LPS-induced NF-κB activity and IκB degradation in PIMs, which was abrogated by proglumide[33]. Furthermore, LPS-induced expression of LPS receptor CD14 on PIMs could be downregulated by CCK-8 *in vitro*[32]. These data suggested that CCK-8 might bind to CCK receptors on pulmonary macrophages to interfere with the activation of macrophages during inflammation. But the cellular signal transduction mechanisms through which CCK receptors mediated in macrophages were not fully clarified. Other than pulmonary macrophages, several functions of murine peritoneal macrophages were negatively modulated by CCK-8 including the production of superoxide anion, phagocytosis and mobility[34,35]. Therefore, CCK receptors on macrophages provide the structural basis for CCK-8 to regulate the functions and activation of macrophages, which may be beneficial to the control of inflammatory responses.

In addition, CCK-AR and CCK-BR mRNA expressions were observed on bronchial epithelial cells and alveolar epithelial cells in this study. Stretton and Barnes reported that CCK-8 produced a concentration-dependent contractile response in guinea-pig trachea and this effect was antagonized by the CCK receptor antagonists dibutyryl cyclic guanosine monophosphate and L-364 718[24]. So the CCK receptors present on bronchial epithelial cells may mediate the regulatory effect of CCK-8 on the tonus of bronchus. The functions of CCK receptors on alveolar epithelial cells remain unclear.

In summary, we successfully detected CCK-AR and CCK-BR mRNA expression in rats' lung tissues and clarified their cellular localization using *in situ* RT-PCR. To our knowledge, this is the first report about the CCK receptors gene expression in lung tissues. CCK receptors present on pulmonary endothelial cells, macrophages, bronchial epithelial cells and alveolar epithelial cells play an important role in mediating effects of CCK-8 such as protecting endothelial cells against damages, inhibiting the overactivation of macrophage and regulating the pulmonary vascular tonus and bronchial tonus.

## REFERENCES

1 **Crawley JN**, Corwin RL. Biological actions of cholecystokinin. *Peptides* 1994; **15**: 731-755
2 **Wank SA.** Chokecystokinin receptors. *Am J Physiol* 1995; **269**: G628-G646
3 **Noble F**, Roques BP. CCK-B receptor: chemistry, molecular biology, biochemistry and pharmacology. *Progress in Neurobiol* 1999; **58**: 349-379
4 **Kulaksiz H**, Arnold R, Goke B, Maronde E, Meyer M, Fahrenholz F, Forssmann WG, Eissele R. Expression and cell-specific localization of the cholecystokinin B/gastrin receptor in the human stomach. *Cell Tissue Res* 2000; **299**: 289-298
5 **Wank SA**. G protein-coupled receptors in gastrointestinal physiology I. CCK receptors: an exemplary family. *Am J Physiol* 1998; **274**: G607-G613

6 **Smith JP**, Verderame MF, McLaughlin P, Martenis M, Ballard E, Zagon IS. Characterization of the CCK-C (cancer) receptor in human pancreatic cancer. *Int J Mol Med* 2002; **10**: 689-694

7 **Clerc P,** Leung-Theung-Long S, Wang TC, Dockray GJ, Bouisson M, Delisle MB, Vaysse N, Pradayrol L, Fourmy D, Dufresne M. Expression of CCK2 receptors in the murine pancreas: proliferation, transdifferentiation of acinar cells, and neoplasia. *Gastroenterology* 2002; **122**: 428-437

8 **Pagliocca A**, Wroblewski LE, Ashcroft FJ, Noble PJ, Dockray GJ, Varro A. Stimulation of the gastrin-cholecystokinin(B) receptor promotes branching morphogenesis in gastric AGS cells. *Am J Physiol Gastrointest Liver Physiol* 2002; **283**: G292-G299

9 **Henwood M**, Clarke PA, Smith AM, Watson SA. Expression of gastrin in developing gastric adenocarcinoma. *Br J Surg* 2001; **88**: 564-568

10 **Fontana MG**, Moneghini D, Villanacci V, Donato F, Rindi G. Effect of cholecystokinin-B gastrin receptor blockade on chemically induced colon carcinogenesis in mice: follow-up at 52 weeks. *Digestion* 2002; **65**: 35-40

11 **Reubi JC**, Schaer JC, Waser B. Cholecystokinin(CCK)-A and CCK-B / gastrin receptors in human tumors. *Cancer Res* 1997; **57**: 1377-1386

12 **Matsumori Y**, Katakami N, Ito M, Taniguchi T, Iwata N, Takaishi T, Chihara K, Matsui T. Cholecystokinin-B / gastrin receptor: a novel molecular probe for human small cell lung cancer. *Cancer Res* 1995; **55**: 276-279

13 **Behr TM**, Jenner N, Radetzky S, Behe M, Gratz S, Yucekent S, Raue F, Becker W. Targeting of cholecystokinin-B / gastrin receptors in vivo: preclinical and initial clinical evaluation of the diagnostic and therapeutic potential of radiolabelled gastrin. *Eur J Nucl Med* 1998; **25**: 424-430

14 **Dornand J**, Roche S, Michel F, Bali JP, Cabane S, Favero J, Magous R. Gastrin-CCK-B type receptors on human T lymphoblastoid Jurkat cells. *Am J Physiol* 1995; **268**: G522-529

15 **Oiry C**, Gagne D, Cottin E, Bernad N, Galleyrand JC, Berge G, Lignon MF, Eldin P, Le Cunff M, Leger J, Clerc P, Fourmy D, Martinez J. CholecystokininB receptor from human Jurkat lymphoblastic T cells is involved in activator protein-1-responsive gene activation. *Mol Pharmacol* 1997; **52**: 292-299

16 **Medina S**, Rio MD, Cuadra BD, Guayerbas N, Fuente MD. Age-related changes in the modulatory action of gastrin-releasing peptide, neuropeptide Y and sulfated cholecystokinin octapeptide in the proliferation of murine lymphocytes. *Neuropeptides* 1999; **33**: 173-179

17 **De la Fuente M**, Carrasco M, Del Rio M, Hernanz A. Modulation of murine lymphocyte functions by sulfated cholecystokinin octapeptide. *Neuropeptides* 1998; **32**: 225-33

18 **Mercer DW**, Cross JM, Smith GS, Miller TA. Protective action of gastrin-17 against alcohol-induced gastric injury in the rat: role in mucosal defense. *Am J Physiol* 1997; **273**: G365-G373

19 **Mercer DW**, Cross JM, Chang L, Lichtenberger LM. Bombesin prevents gastric injury in the rat: role of gastrin. *Dig Dis Sci* 1998; **43**: 826-833

20 **Mercer DW**, Smith GS, Miller TA. Cyclooxygenase inhibition attenuates cholecystokinin-induced gastroprotection. *Dig Dis Sci* 1998; **43**: 468-475

21 **Ling YL**, Huang SS, Wang LF, Zhang JL, Wan M, Hao RL. Cholecystokinin octapeptide reverses experimental endotoxin shock. *Shengli Xuebao* 1996; **48**: 390-394

22 **Ling YL**, Cong B, Gu ZY, Li SJ, Zhou XH. Inhibitory effect of cholecystokinin octapeptide on pulmonary arterial hypertension during endotoxic shock. *Zhongguo Xueshu Qikan Wenzhai* 2000; **6**: 890-892

23 **Gu ZY**, Ling YL, Meng AH, Cong B, Hung SS. Effects of cholecystokinin-octapeptide on the response of rabbit pulmonary artery induced by LPS *in vitro*. *Zhongguo Bingli Shengli Zazhi* 1999; **15**: 484-487

24 **Stretton CD**, Barnes PJ. Cholecystokinin–octapeptide constricts guinea-pig and human airways. *Br J Pharmacol* 1989; **97**: 675-682

25 **Monstein HJ**, Nylander AG, Salehi A, Chen D, Lundquist I, Hakanson R. Cholecystokinin-A and cholecystokinin-B / gastrin receptor mRNA expression in the gastrointestinal tract and pancreas of the rat and man. *Scand J Gastroenterol* 1996; **31**: 383-390

26 **Bartlett JM**. Approaches to the analysis of gene expression using mRNA: a technical overview. *Mol Biotechnol* 2002; **21**: 149-160

27 **Peters J,** Krams M, Wacker HH, Carstens A, Weisner D, Hamann K, Menke M, Harms D, Parwaresch R. Detection of rare RNA sequences by single-enzyme in situ reverse transcription-polymerase chain reaction. *Am J Pathol* 1997; **150**: 469-476

28 **Meng AH**, Ling YL, Wang DH, Gu ZY, Li SJ, Zhu TN. Role of nitric oxide in cholecystokinin-octapeptide alleviation of tumor necrosis factor-alpha induced changes in rabbit pulmonary arterial reactivity. *Shengli Xuebao* 2001; **53**: 478-482

29 **Gu ZY.** Peroxynitrite-mediated pulmonary vascular injury induced by endotoxin and the protective role of cholecystokinin. *Shengli Kexue Jinzhan* 2001; **32**: 135-137

30 **Tobias PS**, Tapping RI, Gegner JA. Endotoxin interactions with lipopolysaccharide-responsive cells. *Clin Infec Dis* 1999; **28**: 476-481

31 **Salomao R**, Rigato O, Pignatari AC, Freudenberg MA, Galanos C. Bloodstream infections: epidemiology, pathophysiology and therapeutic perspectives. *Infection* 1999; **27**: 1-11

32 **Li SJ**, Cong B, Yan YL, Yao YX, Ma CL, Ling YL. Cholecystokinin octapeptide inhibits the in vitro expression of CD14 in rat pulmonary interstitial macrophages induced by lipopolysaccharide. *Chin Med J (English Issue)* 2002; **115**: 276-279

33 **Cong B**, Li SJ, Yao YX, Zhu GJ, Ling YL. Effect of cholecystokinin octapeptide on tumor necrosis factor α transcription and nuclear factor-κB activity induced by lipopolysaccharide in rat pulmonary interstitial macrophages. *World J Gastroenterol* 2002; **8**: 718-723

34 **De la Fuente M**, Campos M, Del Rio M, Hernanz A. Inhibition of murine peritoneal macrophage functions by sulfated cholecystokinin octapeptide. *Regul Pept* 1995; **55**: 47-56

35 **De la Fuente M**, Medina S, Del Rio M, Ferrandez MD, Hernanz A. Effect of aging on the modulation of macrophage functions by neuropeptides. *Life Sci* 2000; **67**: 2125-2135


**Edited by** Wu XN

P.O.Box 2345, Beijing 100023,China
Fax: +86-10-85381893
E-mail: wjg@wjgnet.com www.wjgnet.com

World J Gastroenterol 2003;9(6):1278-1281
World Journal of Gastroenterology
Copyright ©2003 by The WJG Press ISSN 1007-9327

• BASIC RESEARCH •

# Effect of caffeic acid phenethyl ester on proliferation and apoptosis of hepatic stellate cells *in vitro*

Wen-Xing Zhao, Jing Zhao, Chong-Li Liang, Bing Zhao, Rong-Qing Pang, Xing-Hua Pan

**Wen-Xing Zhao, Jing Zhao, Chong-Li Liang, Bing Zhao, Rong-Qing Pang, Xing-Hua Pan,** Medical Laboratory of Kunming General Hospital, Chengdu Command, Kunming 650032, Yunnan Province, China
**Supported by** Natural Science Foundation of Yunnan Province for Younth, No. 1999C0034Q, No. 2000C0031Q
**Correspondence to:** Dr. Wen-Xing Zhao, Medical Laboratory of Kunming General Hospital, Chengdu Command, 212 Daguan Road, Kunming 650032, Yunnan Province, China. zwx-zzh@sohu.com
**Telephone:** +86-871-4074771 **Fax:** +86-871-4074771
**Received:** 2002-12-07 **Accepted:** 2003-01-08

## Abstract

**AIM:** To investigate the role of nuclear factor-κB (NF-κB) inhibitor caffeic acid phenethy1 ester (CAPE) in the proliferation, collagen synthesis and apoptosis of hepatic stellate cells (HSCs) of rats.

**METHODS:** The HSCs from rats were isolated and cultured in Dulbecco's Modified Eagle's Medium (DMEM) and treated with CAPE. The proliferation and collagen synthesis of HSCs were determined by $^3$H-TdR and $^3$H-proline incorporation respectively, and the expression of type I, III procollagen genes was further explored by *in situ* hybridization. Apoptosis cell indices (AIs) were examined using terminal deoxynucleotidyl transferase- mediated DIG-dUTP nick end labeling (TUNEL).

**RESULTS:** In activated HSC in culture, CAPE significantly inhibited $^3$H-TdR and $^3$H-proline incorporation by HSCs at concentrations of 5 μmol/L and 10 μmol/L respectively. CAPE also reduced the type I procollagen gene expression ($P$<0.05) at higher concentration. Apoptosis of HSC was induced by CAPE and the AIs were time-and dose-dependently increased from 2.82±0.73 % to 7.66±1.25 % at 12 h ($P$<0.01) and from 3.15±0.88 % to 10.61±2.88 % at 24 h ($P$<0.01).

**CONCLUSION:** CAPE inhibits proliferation and collagen synthesis of HSC at lower concentration and induces HSC apoptosis at higher concentration.

Zhao WX, Zhao J , Liang CL, Zhao B, Pang RQ, Pan XH. Effect of caffeic acid phenethyl ester on proliferation and apoptosis of hepatic stellate cells *in vitro*. *World J Gastroenterol* 2003; 9 (6): 1278-1281
http://www.wjgnet.com/1007-9327/9/1278.asp

## INTRODUCTION

Liver fibrosis is a progressive pathological process involving multi-cellular and molecular events that ultimately lead to deposition of excess matrix proteins in the extracellular space. It is generally accepted that HSC is the most pathogenetically relevant cell type for the development of liver fibrosis[1-5]. During liver injury and inflammation, quiescent HSCs transdifferentiate into activated-type HSCs, also termed myofibroblasts (MFBs), which result in accumulation of a cell type that provides main collagenous and non-collagenous components of the extracellular fibrotic matrix, contribute to diminished degradation of extracellular matrix by the expression of tissue inhibitors of metalloproteinases (TIMPs) and also produce an array of proinflammatory cytokines and chemokines involving the development of liver fibrosis[3-11].

It has recently been shown that the recovery from established experimental fibrosis can occur through the apoptosis of HSC, which is associated with reduction of collagen and expression of TIMPs in liver. Apoptosis, therefore, plays an important role in the resolution of fibrosis by eliminating the sources of both the neomatrix and TIMPs, and thereby facilitates net matrix degradation[12-15]. Activation and apoptosis of HSCs could play a central role in turnover of liver fibrosis.

Recent research showed that cultured HSC underwent a rapid and persistent induction of a high-mobity NF-κB DNA binding complex, and the activation of NF-κB in cultured HSC was required for activated phenotype of HSCs and might be anti-apoptotic for HSCs[16-19]. In this study, we investigated the effect of NF-κB inhibitor CAPE on the proliferation, collagen synthesis and apoptosis of HSCs.

## MATERIALS AND METHODS

### *Materials*

Wistar rats, male, 450-500 g of body mass, were provided by the Center for Laboratory Animal of Kunming General Hospital. DMEM and FBS were obtained from GIBCO. CAPE and collagenase were purchased from SIGMA, $^3$H-TdR and $^3$H-proline were provided by Beijing Institute of Atomic Energy, RNA Mimi Kit and DIG DNA Labeling and Detecting Kit were respectively obtained from Gene and Boehringer Mannherm.

### *Methods*

**Isolation and culture of HSCs** HSCs were isolated from normal liver by sequential *in situ* perfusion with collagenase, as previously described[20,21]. Briefly, the livers were perfused first with $Ca^{2+}$- and $mg^{2+}$- free solution for 10 min at 37 ℃, and next with 0.05 % (w/v) collagenase solution for 30 min at 37 ℃, the digested liver were excised, dispersed in D-Hanks, and filtered through gauze. The residual hepatocytes were removed by two low-speed centrifugation (50 g, 4 ℃, 2 min). The stellate-cell enriched fraction was obtained by centrifugation with a triple-layered (9, 11, and 17 %) Nycodenz cushion (1 400×g, 4 ℃ 20 min). The cells in the upper-layer were washed and seeded onto uncoated plastic tissue culture plate in DMEM supplemented with 10 % FBS and grown for 14 days. Purity and viability of freshly isolated HSC were determined by Desmin immunohistochemistry and trypan-blue stain respectively.

**$^3$H-TdR and $^3$H-proline uptake by HSC** Passaged HSCs were cultured in 24-well plates for 48 h and then treated with CAPE at concentrations of 0.0, 1.0, 2.5, 5.0, 10.0, 20.0, and 40.0 μol/L for 24 h. CAPE was dissolved in DMSO. The cells were then labeled with 1 μci/ml $^3$H-TdR or 1 μci/ml $^3$H-proline

respectively. After washed with D-Hanks, the HSCs were digested with trypsin and absorbed on glass fiber filter paper. The cells were then washed once with 10 % trichloroacetic acid and three times with saline and dried overnight at 80 ℃, the radioactivity (CPM) of each sample was counted using liquid-scintillation analyzer.

**Expression of procollagen gene in HSC** Type I and III procollagen gene sequences were enquired from GeneBank of National Center of Biotechnology Information, and primers that amplified the procollagen genes were designed with OLIGO microsoft according to the gene sequences and synthesized by Sangon Company. The primers were 5' -CGA TGG ATT CCC GTT CGA GTA C-3' and 5' -GTC CAC AAC CCT GTA GGT G-3' for type I procollagen gene, 5' -GGA AAC AGC AAA TTC ACT TAC A-3' and 5' -TCA CTT GCA CTG GTT GAT AAG A-3' for type III procollagen gene. The RNA was extracted from the skin of newborn ICR mice by RNA mini kit, the genes were amplified by RT-PCR and procollagen gene probes were labeled with PCR and DIG-dUTP. HSCs cultured in 24-well plates were treated with 20 μmol/L CAPE for 24 h and the procollagen gene expression was detected according to the previously described procedure[22].

**Apoptosis assay** Passaged HSCs were cultured for 48 h and then cultured in 5 % FBS DMEM and treated with CAPE at predetermined concentrations of 0.0, 20.0, and 40.0 μmol/L for 12 h and 24 h, the cells were fixed in formaldehyde solution and stained with TUNEL reaction solution containing DIG-dUTP and terminal deoxynucleotide transferase for 60 min at 37 ℃. DIG was detected by anti-DIG-AP conjugate and colorimetric substrate NBT/BCIT. Positive cells were counted under microscope.

## RESULTS

### *Characteristics of HSCs*

Freshly isolated HSCs were round-shaped with many yellow-coloured droplets in cytoplasm, after 2-3 days in culture on uncoated plastic surface, the cells had spread and showed a typical ' star' -like configuration. More than 80 % of freshly isolated cells were desmin-positive, and the cell viability was about 90 % according to trypan-blue staining.

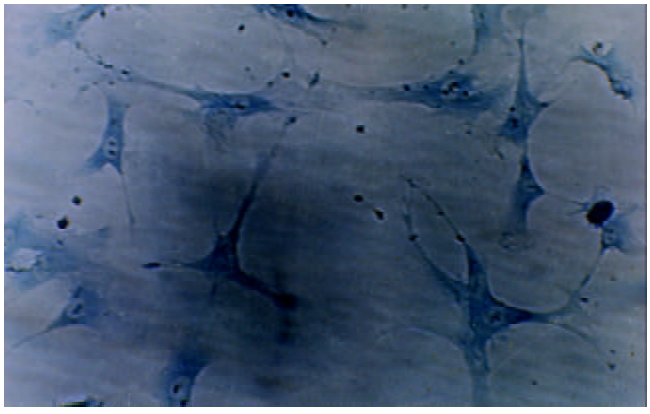

**Figure 1** The hepatic stellate cells stained with toluidine after cultured for 10 days after isolation (×66).

### *Effect of CAPE on $^3$H-TdR and $^3$H-proline incorporation by HSC*

We observed the effect of CAPE on $^3$H-TdR and $^3$H-proline incorporation by cultured HSCs. As shown in Figure 2, CAPE significantly and dose-dependently suppressed the incorporation of $^3$H-TdR and $^3$H-proline by HSCs. The median inhibitory concentrations were 5 and 10 μmol/L respectively for $^3$H-TdR and $^3$H-proline. These concentrations were lower, especially for the inhibition of HSCs proliferation, indicating that CAPE was a potent inhibitor for proliferation, and collagen synthesis.

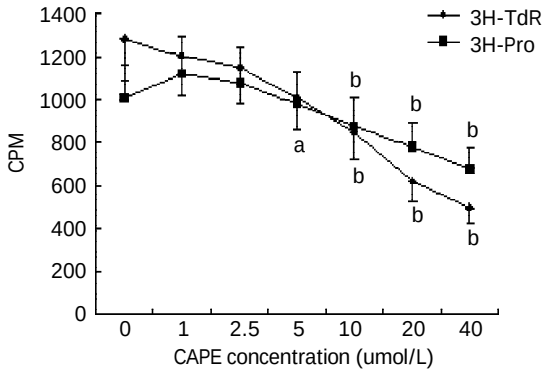


**Figure 2** Effects of CAPE on $^3$H-TdR and $^3$H-proline uptake by HSCs. $^aP<0.05$; $^bP<0.01$ *vs* groups without CAPE treatment.

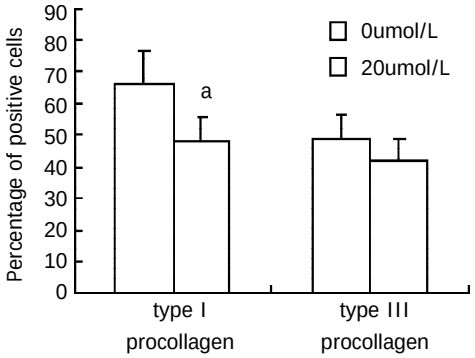


**Figure 3** Effect of CAPE on type I and III procollagen gene expression. $^aP<0.05$ *vs* the group without CAPE treatment.

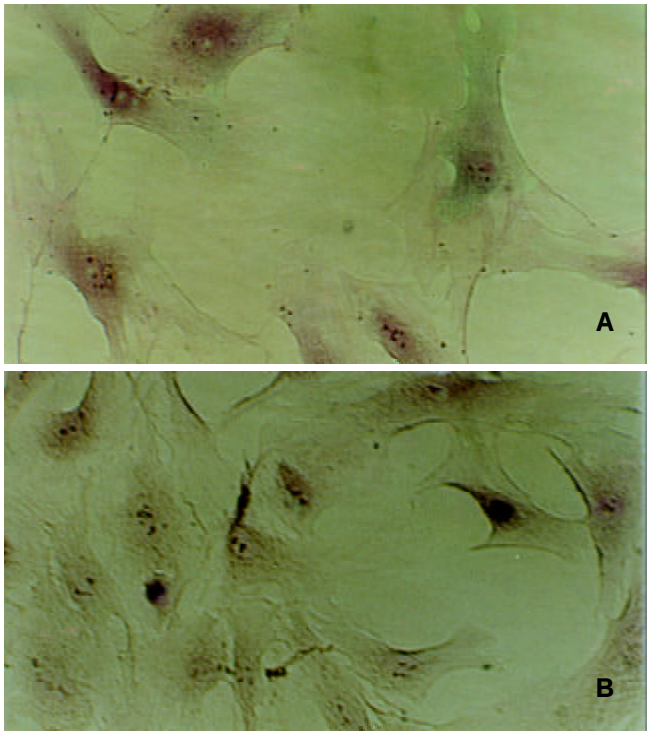


**Figure 4** Apoptotic HSCs detected by TUNEL without (A) or with 40 μmol/L CAPE treatment (B).

### *Effects of CAPE on procollagen gene expression*

Type I and III collagens are the main components of extracellular matrix in liver fibrosis. *In situ* hybridization

analysis of type I and III procollagen genes showed that positive HSCs were reduced by CAPE at the concentration of 20 μmol/L. And the reduction of type I procollagen gene expression was statistically significant, indicating that CAPE suppressed the procollagen gene expression.

### *Apoptosis of HSC induced by CAPE*

Apoptosis of HSC was demonstrated by TUNEL, the nucleus of apoptotic HSCs were stained with violet blue (Figure 4). After treatment with CAPE, AIs were time- and dose-dependently increased from 2.82±0.73 % to 7.66±1.25 % at 12h and from 3.15±0.88 % to 10.61±2.88 % at 24 h. The data indicated that CAPE induced HSC apoptosis at higher concentrations (Figure 5).

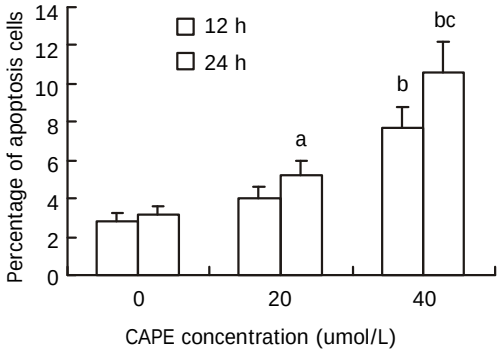


**Figure 5** Effects of CAPE on HSC apoptosis. [a]$P<0.05$; [b]$P<0.01$ *vs* the groups without CAPE treatment; [c]$P<0.01$ *vs* the group with 40 μmol/L CAPE treated for 12 h.

## DISCUSSION

HSCs, previously termed as fat or vitamin A-storing cells or Ito cells, localized in close proximity to sinusoidal endothelial cell and hepatocyte in the space of Disse, are the most pathogenetically relevant cell type for development of liver fibrosis[2-5]. Activated HSCs in liver tissue provide virtually most main components of ECM, contribute to diminished degradation of ECM by expressing TIMPs, and produce an array of proinflammatory cytokines and chemokines involving the development of liver fibrosis[3-11]. It is generally accepted that HSCs are important target cells for the treatment of liver fibrosis[5,23].

In our study, we observed that the NF-κB inhibitor CAPE inhibited the proliferation and collagen synthesis of HSCs. CAPE dose-dependently suppressed the incorporation of $^3$H-TdR and $^3$H-proline by HSCs. This indicated CAPE inhibited the proliferation of HSCs. Because the reduction of either total cell number or collagen synthesis may contribute to the reduction of $^3$H-proline incorportion by HSCs, the expressions of type I and type III procollagen genes were further explored in HSCs. Our data showed that the procollagen gene expressions were reduced by CAPE, and the reduction of $^3$H-proline uptake partially indicated that CAPE inhibited collagen synthesis, in addition to the reduction of HSC number.

CAPE, a structural relative of flavonoids that is an active component of propolis from honeybee hives, has been shown to inhibit the growth of different types of cells including endothelial cells, keratinocyte and tumor cells, which involves in nuclear factor, protein kinase C and cytokine signal transduction[24-29]. CAPE inhibited the proliferation and collagen synthesis of HSCs, properly by reducing the reactive oxygen intermediates, this is consistent with the antioxidant property of CAPE[30,31]. Previous studies showed that reactive oxidant species induced HSCs activation and collagen gene expression *in vivo* and *in vitro*[32-35]. The antioxidant phenolic compounds reduced the proliferation and collagen synthesis by suppressing inositol phosphate metabolism, tyrosine and protein kinase activation[33,36]. Since CAPE is a structural relative of flavonoids, CAPE probably inhibits the proliferation and collagen synthesis of HSCs similarly. Other mechanisms might include inhibition of the expression of COX2 and activation of NF-κB by CAPE, which are associated with the phenotype of activated HSCs[37,38].

Activated HSCs undergo auto-apoptosis in serum-deprived DMEM and in experimental fibrosis induced by $CCl_4$. $P^{75}$ and Fas have already been identified as molecules associated with the apoptosis of HSCs, which were expressed in HSCs. Apoptosis of HSCs can be induced by nerve growth factor and soluble Fas-ligand[39,40]. The recovery from established experimental fibrosis is relevant to the apoptosis of HSCs, which contributes to the reduction of neomatrix synthesis and expression of TIMPs. Recent reports showed the persistent activation of NF-κB was induced in activated but not in quiescent HSCs, which is required for activated phenotype of HSCs and may be antiapoptotic for HSCs[16-18]. CAPE is a potent and specific inhibitor of NF-κB, CAPE inhibits the activation of NF-κB induced by TNF and other inflammatory agents including phorbol ester, ceramide, hydrogen peroxide, *etc*[41]. Our data showed the AIs of HSCs were increased by CAPE, the inhibition of NF-κB activation by CAPE probably played a key role in HSC apoptosis. CAPE inhibited the activation of NF-κB and the expression of proinflammatory cytokines TNF-α and IL-1β; CAPE also induced apoptosis in macrophages[42], similar results were observed in leucocytes as well[43]. However, CAPE induced apoptosis of tumor cells by regulating the expression of caspas-3, bcl-2, bax and $P^{53}$[44-46]. For HSCs, the mechanism of apoptosis induced by CAPE needs further investigation.

CAPE has been shown to be a pharmacologically safe compound with known antiinflammatory, antimitogenic, anticarcinogenic, antioxidant, and immunomodulatory effects[37,47]. Therefore, CAPE might have a therapeutic role in liver fibrosis by inhibiting the proliferation or inducing the apoptosis of HSCs.

## REFERENCES

1 **Brenner DA,** Waterboer T, Choi SK, Lindquist JN, Stefanovic B, Burchardt E, Yamauchi M, Gillan A, Rippe RA. New aspects of hepatic fibrosis. *J Hepatol* 2000; **32**(Suppl 1): 32-38
2 **Benyon RC**, Iredale JP. Is liver fibrosis reversible. *Gut* 2000; **46**: 443-446
3 **Rockey DC**. The cell and molecular biology of hepatic fibrogenesis. Clinical and therapeutic implications. *Clin Liver Dis* 2000; **4**: 319-355
4 **Arthur MJ**. Fibrogenesis II. Metalloproteinases and their inhibitors in liver fibrosis. *Am J physiol Gastrointest liver Physiol* 2000; **279**: G245-249
5 **Bataller R**, Brenner DA. Hepatic stellate cells as a target for the treatment of liver fibrosis. *Semin Liver Dis* 2001; **21**: 437-451
6 **Yao XX**, Tang YW, Yao DM, Xiu HM. Effects of Yigan Decoction on proliferation and apoptosis of hepatic stellate cells. *World J Gastroenterol* 2002; **8**: 511-514
7 **Reeves HL**, Friedman SL. Activation of hepatic stellate cells-a key issue in liver fibrosis. *Front Biosci* 2002; **7**: d808-826
8 **Gressner AM**. The up and down of hepatic stellat cells in tissue injury: apoptosis restore cellular homeostasis. *Gastroenterology* 2001;**120**: 1285-1287
9 **Wang JY**, Zhang QS, Guo JS, Hu MY. Effects of glycyrrhetinic acid on collagen metabolism of hepatic stellate cells at different stages of liver fibrosis in rats. *World J Gastroenterol* 2001; **7**: 115-119
10 **Marra F.** Chemokines in liver inflammation and fibrosis. *Front Biosci* 2002; **7**: d1899-1914
11 **Gressner AM**. The cell biollgy of liver fibrosis-an imbalance of proliferation, growth arrest and apoptosis of myofibroblasts. *Cell Tissue Res* 1998; **292**: 447-454

12 **Benyon RC**, Arthur MJ. Extracellular matrix degradation and the role of hepatic stellate cells. *Semin Liver Dis* 2001; **21**: 373-384

13 **Issa R**, Williams E, Trim N, Kendall T, Arthur MJ, Reichen J, Benyon RC, Iredale JP. Apoptosis of hepatic stellate cells: involvement in resolution of biliary fibrosis and regulation by soluble growth factors. *Gut* 2001; **48**: 548-557

14 **Wright MC**, Issa R, Smart DE, Trim N, Murray GI, Primrose JN, Arthur MJ, Iredale JP, Mann DA. Gliotoxin stimulates the apoptosis of human and rat hepatic stellate cells and enhances the resolution of liver fibrosis in rats. *Gastroenterology* 2001; **121**: 685-698

15 **Liu XJ**, Yang L, Mao YQ, Wang Q, Huang MH, Wang YP, Wu HB. Effects of the tyrosine protein kinase inhibitor genistein on the proliferation,activation of cultured rat hepatic stellate cells. *World J Gastroenterol* 2002; **8**: 739-745

16 **Hellerbrand C**, Jobin C, Licato LL, Sartor RB, Brenner DA. Cytokines induced NF-κB in activated but not in quiescent rat hepatic stellate cells. *Am J physiol* 1998; 275: G269-278

17 **Saile B,** Matthes N, El Armouche H, Neubauer K, Ramadori G. The bcl, NFkappaB and p53/p21WAF1 systems are involved in spontaneous apoptosis and in the anti-apoptotic effect of TGF-beta or TNF-alpha on activated hepatic stellate cells. *Eur J Cell Biol* 2001; **80**: 554-561

18 **Elsharkawy AM**, Wright MC, Hay RT, Arthur MJ, Hughes T, Bahr MJ, Degitz K, Mann DA. Persistent activation of nuclear factor-κB in cultured rat hepatic stellate cells involves the induction of potentially novel Rel-like factors and prolonged changes in the expression of IkB family proteins. *Hepatol* 1999; **30**: 761-769

19 **Murphy FR**, Issa R, Zhou X, Ratnarajah S, Nagase H, Arthur MJ, Benyon C, Iredale JP. Inhibition of apoptosis of activated hepatic stellate cells by tissue inhibitor of metalloproteinase-1 is mediated via effects on matrix metalloproteinase inhibition: implications for reversibility of liver fibrosis. *J Biol Chem* 2002; **277**: 11069-11076

20 **Kawada N**, Klein H, Decker K. Eicosanoid-mediated contractility of hepatic stellate cells. *Biochem J* 1992; **285**: 367-371

21 **Zhou Y**, Shimizu I, Lu G, Itonaga M, Okamura Y, Shono M, Honda H, Inoue S, Muramatsu M, Ito S. Hepatic stellate cells contain the functional estrogen receptor beta but not the estrogen receptor alpha in male and female rats. *Biochem Biophys Res Commun* 2001; **286**: 1059-1065

22 **Zhao W**, Liang C, Chen Z, Pang R, Zhao B, Chen Z. Luteolin inhibits proliferation and collagen synthesis of hepatic stellate cells. *Zhonghua Ganzangbing Zazhi* 2002; **10**: 204-206

23 **Beljaars L**, Meijer DK, Poelstra K. Targeting hepatic stellate cells for cell-specific treatment of liver fibrosis. *Front Biosci* 2002; **7**: e214-222

24 **Song YS**, Park EH, Jung KJ, Jin C. Inhibition of angiogenesis by propolis. *Arch Pharm Res* 2002; **25**: 500-504

25 **Maffia P**, Ianaro A, Pisano B, Borrelli F, Capasso F, Pinto A, Ialenti A. Beneficial effects of caffeic acid phenethyl ester in a rat model of vascular injury. *Br J Pharmacol* 2002; **136**: 353-360

26 **Mahmoud NN**, Carothers AM, Grunberger D, Bilinski RT, Churchill MR, Martucci C, Newmark HL, Bertagnolli MM. Plant phenolics decrease intestinal tumors in an animal model of familial adenomatous polyposis. *Carcinogenesis* 2000; **21**: 921-927

27 **Zheng ZS,** Xue GZ, Grunberger D, Prystowsky JH. Caffeic acid phenethyl ester inhibits proliferation of human keratinocytes and interferes with the EGF regulation of ornithine decarboxylase. *Oncol Res* 1995; **7**: 445-452

28 **Usia T**, Banskota AH, Tezuka Y, Midorikawa K, Matsushige K, Kadota S. Constituents of Chinese propolis and their antiproliferative activities. *J Nat Prod* 2002; **65**: 673-676

29 **Huleihel M,** Ishano V. Effect of propolis extract on malignant cell transformation by moloney murine sarcoma virus. *Arch Virol* 2001; **146**: 1517-1526

30 **Uz E**, Sogut S, Sahin S, Var A, Ozyurt H, Gulec M, Akyol O. The protective role of caffeic acid phenethyl ester (CAPE) on testicular tissue after testicular torsion and detorsion. *World J Urol* 2002; **20**: 264-270

31 **Son S,** Lewis BA. Free radical scavenging and antioxidative activity of caffeic acid amide and ester analogues: structure-activity relationship. *J Agric Food Chem* 2002; **50**: 468-472

32 **Greenwel P,** Dominguez-Rosales JA, Mavi G, Rivas-Estilla AM, Rojkind M. Hydrogen peroxide: a link between acetaldehyde-elicited alpha1(I) collagen gene up-regulation and oxidative stress in mouse hepatic stellate cells. *Hepatology* 2000; **31**:109-116

33 **Kawada N,** Seki S, Inoue M, Kuroki T. Effect of antioxidants, reveratrol. quercetin and N-acetylcysteine, on the functions of cutured rat hepatic stellate cells and kupffer cells. *Hepatol* 1998; **27**: 1265-1274

34 **Svegliati-Baroni G,** Saccomanno S, van Goor H, Jansen P, Benedetti A, Moshage H. Involvement of reactive oxygen species and nitric oxide radicals in activation and proliferation of rat hepatic stellate cells. *Liver* 2001; **21**: 1-12

35 **Poli G**. Pathogenesis of liver fibrosis: role of oxidative stress. *Mol Aspects Med* 2000; 21: 49-98

36 **Nagaoka T,** Banskota AH, Tezuka Y, Saiki I, Kadota S. Selective antiproliferative activity of caffeic acid phenethyl ester analogues on highly liver-metastatic murine colon 26-L5 carcinoma cell line. *Bioorg Med Chem* 2002; **10**: 3351-3359

37 **Gallois C**, Habib A, Tao J, Moulin S, Maclouf J, Mallat A, Lotersztajn S. Role of NF-KB in the antiprliferative effect of endothelin-1 and tumor necrosis factor-α in human hepatic stellate cells. *J Biol Chem* 1998; **273**: 23183-23190

38 **Cheng J**, Imanishi H, Liu W, Iwasaki A, Ueki N, Nakamura H, Hada T. Inhibition of the expression of alpha-smooth muscle actin in human hepatic stellate cell line, LI90, by a selective cyclooxygenase 2 inhibitor, NS-398. *Biochem Biophys Res Commun* 2002; **297**: 1128-1134

39 **Trim N,** Morgan S, Evans M, Issa R, Fine D, Afford S, Wilkins B, Iredale J. Hepatic stellate cells express the low affinity nerve growth factor receptor p75 and undergo apoptosis in response to nerve growth factor stimulation. *Am J Pathol* 2000; **156**: 1235-1243

40 **Gong W,** Pecci A, Roth S, Lahme B, Beato M, Gressner AM. Transformation-dependent susceptibility of rat hepatic stellate cells to apoptosis induced by soluble Fas ligand. *Hepatol* 1998; 28: 492-502

41 **Natarajan K**, Singh S, Burke TR Jr, Grunberger D, Aggarwal BB. Caffeic acid phenethyl ester is a potent and specific inhibitor of activation of nuclear transcription factor NF-κB. *Pro Natl Acad Sci USA* 1996; **93**: 9090-9095

42 **Lu B,** Wang L, Medan D, Toledo D, Huang C, Chen F, Shi X, Rojanasakul Y. Regulation of Fas (CD95)-induced apoptosis by nuclear factor-kappaB and tumor necrosis factor-alpha in macrophages. *Am J Physiol Cell Physiol* 2002; **283**: C831-838

43 **Orban Z**, Mitsiades N, Burke TR Jr, Tsokos M, Chrousos GP. Caffeic acid phenethyl ester induces leukocyte apoptosis, modulates nuclear factor-kappa B and suppresses acute inflammation. *Neuroimmunomodulation* 2000; **7**: 99-105

44 **Nomura M**, Kaji A, Ma W, Miyamoto K, Dong Z. Suppression of cell transformation and induction of apoptosis by caffeic acid phenethyl ester. *Mol Carcinog* 2001; **31**: 83-89

45 **Chen YJ**, Shiao MS, Hsu ML, Tsai TH, Wang SY. Effect of caffeic acid phenethyl ester, an antioxidant from propolis, oninducing apoptosis in human leukemic HL-60 cells. *J Agric Food Chem* 2001; **49**: 5615-5619

46 **Chen YJ,** Shiao MS, Wang SY. The antioxidant caffeic acid phenethyl ester induces apoptosis associated with selective scavenging of hydrogen peroxide in human leukemic HL-60 cells. *Anticancer Drugs* 2001; **12**: 143-149

47 **Isla MI**, Nieva-Moreno MI, Sampietro AR, Vattuone MA. Antioxidant activity of argentine propolis extracts. *J Ethnophormacol* 2001; **76**:165-170


**Edited by** Yuan HT

P.O.Box 2345, Beijing 100023,China
Fax: +86-10-85381893
E-mail: wjg@wjgnet.com www.wjgnet.com

World J Gastroenterol 2003;9(6):1282-1286
World Journal of Gastroenterology
Copyright © 2003 by The WJG Press ISSN 1007-9327

• BASIC RESEARCH •

# Isolation and analysis of a novel gene over-expressed during liver regeneration

Yu-Chang Li, Cun-Shuan Xu, Wu-Lin Zhu, Wen-Qiang Li

**Yu-Chang Li, Cun-Shuan Xu, Wen-Qiang Li,** College of Life Science, Henan Normal University, Xinxiang 453002, Henan Province, China
**Wu-Lin Zhu,** Xinxiang Medical College, Xinxiang 453002, Henan Province, China
**Supported by** a grant from Key Scientific and Technical Problem of Henan Province No.0122031900
**Correspondence to:** Dr. Yu-Chang Li, College of Life Science, Henan Normal University, Xinxiang 453002, Henan Province, China. ycli_us@yahoo.com
**Telephone:** +86-373-3328084 **Fax:** +86-373-3326609
**Received:** 2002-12-05 **Accepted:** 2003-03-03

## Abstract

**AIM:** To isolate and analyze a novel gene over-expressed during liver regeneration.

**METHODS:** Total RNA of regenerating liver was extracted from liver tissue after 0-4-36-36-36 hr short interval successive partial hepatectomy (SISPH). Reverse transcription-polymerase chain reaction was used to synthesize double strand cDNA, after the tissue was digested by proteinase K and Sfi A/B. The double-strand cDNA was ligated to λTriplEx2. λphage packaging reaction was performed and *E. coli* XL1-Blue was infected for titering and amplifying. One expressed sequence tag was probed by Dig and phage *in situ* hybridization was carried out to isolate positive clones. Positive recombinant λTriplEx2 was converted to the corresponding pTriplEx2, and bioinformatics was used to analyze full-length cDNA.

**RESULTS:** We isolated a novel full-length cDNA during liver regeneration following SISPH.

**CONCLUSION:** We have succeeded in cloning a novel gene, based on bioinformatics. We postulate that this gene may function in complicated network in liver regeneration. On the one hand, it may exert initiation of liver regeneration via regulating nitric oxide synthesis. On the other hand, it may protect damaged residue lobus following SISPH.

Li YC, Xu CS, Zhu WL, Li WQ. Isolation and analysis of a novel gene over-expressed during liver regeneration. *World J Gastroenterol* 2003; 9(6): 1282-1286
http://www.wjgnet.com/1007-9327/9/1282.asp

## INTRODUCTION

Liver regeneration is a system suitable for investigating normally regulated growth[1-4]. After surgical removal of 70 % of the mass of a healthy liver (two-thirds hepatectomy), residual tissue enlarges to make up for the mass of removed substance in entirety, in small animals, this process usually lasts 5 to 7 days[5-7].

The growth response after partial hepatectomy is governed by priming and progression through the cell cycle[2,6,8]. The priming phase coincides with loss of growth inhibition and represents the $G_0$ to $G_1$ transition, whereas the progression phase acts on promoting cell replication and represents the $G_1$ to S transition. Priming involves the activation of a group of non-specific factors, which are necessary, but not sufficient for the S phase completion; they comprise the nuclear factor for kappa chains (NF-κ) in B cells, signal transducer and activator of transcription-3 (STAT3), activator protein-1 (AP-1), CCAAT enhancer binding protein, and several immediate early genes like epithelial growth factor (EGF), tumor necrosis factor-alpha (TNF-α, IL-6), insulin, and matrix changes[9-15]. The priming step is reversible until the cells have crossed the so-called $G_1$ checkpoint, the cells thereupon being irreversibly committed for replication. Moreover, the initiation of the growth response depends on complex interactions among hepatocytes and nonparenchymal cells, the extracellular matrix (ECM), endocrine, autocrine, paracrine, and neuroregulatory factors, oxygen free radicals, metabolites, and nutrients[2,6,9,16]. Progression signals include hepatocyte growth factor (HGF), transforming growth factor-alpha (TGF-α), EGF and insulin. The regulation of hepatic regenerative process depends on a number of myriad factors that ultimately modulate immediate-early, delayed-early, and liver-specific gene expression[2,6,9,17-20].

The termination of hepatic regeneration still remains an enigma. A variety of factors have been touted as growth inhibitors/terminators during the regenerative response once recovery of the liver mass has been achieved.TGF-β and activins are regarded as potent inhibitors involved in the termination response[21,22]. TGF-β is a fibrogenic cytokine secreted by hepatic stellate cells, TGF-β mRNA, almost undetectable in normal liver, increases within 3-4 h after partial hepatectomy, and attains a plateau after 48-72 h. TGF-β1 overexpression in transgenic mice inhibits the abundance of the cyclin-dependent kinase activating tyrosine phosphatase cdc25A protein, and is associated with increased binding of histone deacetylase 1 to p130 in the liver[23]. Activin A (the homodimer of the inhibin β A chain) inhibits but follistatin (anactivin-binding protein) promotes hepatocyte proliferation. Whereas activin A is a negative regulator of hepatocyte proliferation, mice deficient in both activin βC and activin βE, are not different from wild-type mice with respect to liver development and the regenerative response after partial hepatectomy. The activin system also plays a significant role in the dynamics of the ECM, in particular fibronectin; ECM components are reconstructed during desinualization and hepatocyte cluster formation. After rat liver injury and partial hepatectomy, hepatocyte activin A receptors are down-regulated at 24 hr and normalized at 72 hr. This phenomenon may be involved in rendering hepatocytes responsive to mitogenic stimuli, whereas increased activin A levels stimulate stellate cell production of fibronectin, important for the growth and proper placement of regenerating hepatocytes[24].

Despite the research efforts, our knowledge on the regulatory mechanisms of cell growth, differentiation and tissue organization is limited. There may be some unknown factors that may play important roles in the process of liver regeneration. To acquire a better understanding on the

mechanisms involved, some researchers have established a series of successive partial hepatectomy (SPH) models. These mainly include the long interval successive partial hepatectomy (LISPH) in which an interval of more than three weeks is applied as described by Wu et al, the SPH model where a one-third hepatectomy 2 weeks after a two-thirds hepatectomy is performed as described by Takeshi *et al*[25], and the short interval successive partial hepatectomy (SISPH) model (0-4-40-76-112 hr) which has an interval of 4 and/or 36 h because the cells would re-enter into dedifferentiation stage after 4 hr and reach the peak of cell division after 36 hr following partial hepatectomy as described by Xu *et al*[26]. Studies have demonstrated that SISPH could provide more useful materials for analyzing the mechanism of liver regeneration[27]. We have begun identifying and characterizing some genes that are strongly expressed in liver regeneration. We took 0 h and 112 hr as driver and tester respectively in 0-4-36-36-36hr SISPH model and a suppression subtracted hybridization (SSH ) method was performed[28-30]. Then we constructed a forward-subtractive cDNA library from which we have cloned 53 up-regulated expressed sequence tags (ESTs). Among these, nine ESTs were 100 % homologous to GenBank and 44 ESTs were homologous to GenBank. one of these ESTs was found to be a novel gene in GenBank. In the present study, we have used one subtracted probe from suppression subtracted library in liver regeneration and isolated its full-length cDNA from cDNA library by the phage *in situ* hybridization method. Based on bioinformatics, we suggest that it might play important roles in the regulation of initiation of liver regeneration.

## MATERIALS AND METHODS

### *Establishment of the SISPH model*

Adult Spargue-Dawfey rats (weighing 200-250 g) were provided by the Experimental Animal House of Henan Normal University, and the 0-4-36-36-36 hr SISPH model was made according to the method described by Xu *et al*[26]. Lobus external sinister and lobus centralis sinister, lobus centralis, lobus dexter and lobus candatus were removed one by one at four different time points, i.e. at 4, 36, 36 and 36 hr (total time: 4 hr, 40 hr, 76 hr, 112 hr), respectively. The fourth resected liver lobus was washed with precooled phosphate- buffered saline (PBS) thoroughly, then the sample was frozen in liquid nitrogen and transferred to the -80 ¡æfreezer for storage.

### *Primers*

A1: 5'-ATTCTAGAGGCCGAGGCGGCCGACATG-d $(T)_{30}$ N-3'
A2: 5'-AAGCAGTFFTATCAACGCAGAGT-3'
A3: 5'-TCGAGCGGCCGCCCGGGCAGGT-3'
A4: 5'-AGCGTGGTCGCGGCCGAGGT-3'
A5: 5'-TCCGAGATCTGGACGAGC-3'
A6: 5'-TAATACGACTCACTATAGGG-3'

Among these primers, A1 was used for synthesis of first cDNA strand, A1/A2 were used to amplify dscDNA, A3/A4 were used to probe expressed sequence tag with Dig, A5/A6 were used to detect full length cDNA.

### *RNA Isolation*

Total RNA was isolated from 112 h liver tissue samples following SISPH by the method described by Chomczynski and Sacchi[31]. Tissues were homogenized and extracted twice with acidic guanidinium isothiocyanate-phenol-chloroform. The poly(A)+ RNA fraction was isolated by oligo-dT cellulose chromatography (Pharmacia Diagnostics AB, Uppsala, Sweden). The purity and integrity of total RNA were monitored by absorbance of ultraviolet spectrometer at 260/280 nm, and electrophoresis was carried out on a denaturing formaldehyde agarose gel and the gel was stained with ethidium bromide.

### *RT-PCR*

300 ng mRNA was reversely transcripted to single-stranded cDNA by Powerscriptase at 42 ¡æfor 1hr. First-strand cDNA was synthesized with a Sfi IB-oligo(dT) adapter-primer (A1). The resulting single strand cDNA was amplified by PCR using CDSIII/3'primer (A1) and 5'primer (A2) following parameters: 94 ¡æfor 45 s, 68 ¡æfor 6 min.

### *cDNA library construction*

The double strand cDNA synthesis and library construction were carried out mainly according to the manual of SMART cDNA Library Construction Kit (Clontech, Heidelberg, Germany). After second-strand synthesis and ligation of Sfi IA adapters, cDNA was digested by Sfi IA/Sfi IB, generating cDNA flanked by Sfi IA sites at 5' ends and /Sfi IB sites at the 3' ends. Digested cDNAs were size-fractionated with Sephacryl S-500 spin columns and ligated into the λTriplEx2 express vector predigested by Sfi IA/Sfi IB. The resulting concatomers were packaged by using Gigapack Gold packaging extracts. After titration, aliquots of primary packaging mixture were stored in 7 % DMSO at -80 ¡æas primary library stocks. At the same time, the ratio of white (recombinant) to total (white + blue (nonrecombinant)) assay was determined[32]. The remainder was amplified to establish stable library stocks.

### *Probe labeling and Phage in situ hybridization*

A novel EST related to liver regeneration was probed with A3/A4 primers according to the user manual of Dig Probe Synthesis kit (Roche Diagnostics, Mannheim,Germany). Thermal cycle parameters were 94 ¡æfor 2 min, 25 cycles including a denaturation step at 94 ¡æfor 15sec, an annealing step at 68 ¡æfor 30sec, extension at 72 ¡æfor 1 min and 30sec, and a final extension step at 72 ¡æfor 7 min. The amplified phage cDNA library was diluted in 1×lamda dilution buffer to obtain a concentration of 104 pfu/ml and then to infect *E. coli* XL1-Blue. Host bacterial cells were absorbed by phage at 37 ¡æfor 15 min and the indicated volume of melted LB top agarose/$MgSO_4$ was added. The mixture was inverted once and poured onto a prewarmed, dry LB/$MgSO_4$ plate. The plate was inverted and incubated at 37 ¡æuntil plaques became distinctly visible. A nylon filter was numbered and placed onto the LB soft top agarose, then the filter was marked in three asymmetric locations. After 2 min, the filter was peeled off carefully. The filter was placed in petri dishes orderly containing DNA denaturing solution for 5 min, neutralizing solution for 5 min, or 2×SSC for 5 min. Hybridization and wash procedures were performed according to Sambrook[33]. When positive signal appeared the process was performed as above for the secondary and tertiary screening until single clone was obtained. Then recombinant λTriplEx2 was converted to the corresponding pTriplEx2. Plasmid was extracted and sent to TaKaRa (Dalian,China) for sequencing analysis.

## RESULTS

### *RT-PCR*

The mRNA was isolated from the 112 h liver tissue following SISPH. A modified oligo (dT) primer (A1 primer) primed the first-strand synthesis reaction. The resulting single strand cDNA was amplified by PCR using CDSIII/3'primer (A1) and 5'primer (A2) derived from SMART oligonucleotide (Figure 1).

### *Determination of cDNA library*

The unamplified library and amplified library were titered when *E.coli* XL1-Blue was infected by λphage. The plaques were counted and cDNA library was calculated respectively as

follows: pfu/ml=number of plaques ×dilution ×$10^3$ μl/ml/μl of diluted phage plated. Results showed that umamplified cDNA library and amplified library were $6\times10^6$ pfu/ml and $6\times10^{10}$ pfu/ml respectively. X-gal/IPTG was used to assess recombination efficiency. Among 500-1 000 plaques, the ratio of white (recombinant) to total (recombinant and blue (nonrecombinant)) was 99.52 %. These data suggest that the cDNA library was successfully established.

### *Screening result and bioinformatics*

Figure 2 shows the tertiary positive clone screened by phage *in situ* hybridization. After conversion of a recombinant λTriplEx2 to the corresponding pTriplEx2, the tertiary positive clones were analyzed by PCR with the sequencing primers A5/A6.The length detected by electrophoresis was consistent with the sequencing result and its full length cDNA was 1 354 bp (Figure 3). We identified that its ORF region encodes 344 amino acids, its start codon AUG was in 47-49 nucleotide and its termination codon TAG was in 1 079-1 081 nucleotides, and the sequence followed by TAG was polyA (Figure 4). It was compared with other sequences in the GenBank through Internet by BLAST and found to be 98.8 % homologous to mouse arginase. The sequence has been deposited in the GenBank database (accession No. AF508019).

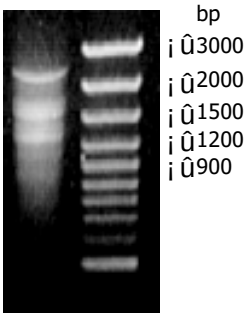


**Figure 1** Gel electrophoresis of double strand cDNA. Lane 1: Double strand cDNA; lane 2: DNA mass marker.

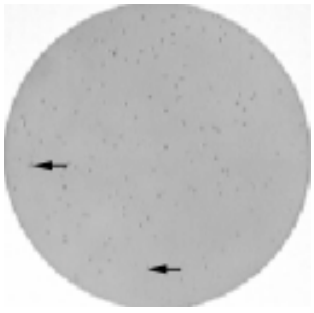

**Figure 2** Tertiary screening result of positive clones. Arrows point the positive clones.

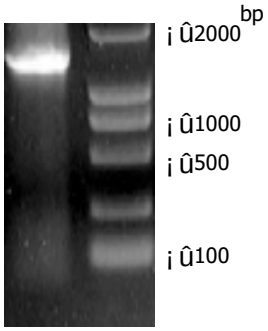


**Figure 3** Detection of cDNA full length gel electrophoresis. Lane 1: 1 354bp; lane 2: DNA mass maker.

```
   1 gttgcaccgagccggttctcctagggtaatcccctcctgccaatc
  47 atgttcctgaggagcagcgcctcccgtctcctccacgggcaaatt
       M  F  L  R  S  S  A  S  R  L  L  H  G  Q  I
  92 ccttgcgtcctgacgagatccgtccactctgtagctatagtcgga
       P  C  V  L  T  R  S  V  H  S  V  A  I  V  G
 137 gccccctctcggggacagaagaagctaggagtggaatatggtcca
       A  P  S  R  G  Q  K  K  L  G  V  E  Y  G  P
 182 gctgccattcgagaagctggcttgctgaagaggctctccaggttg
       A  A  I  R  E  A  G  L  L  K  R  L  S  R  L
 227 ggatgccacctaaaagactttggagacttgagttttactaatgtc
       G  C  H  L  K  D  F  G  D  L  S  F  T  N  V
 272 ccacaagataatccctacaataatctggttgtgtatcctcgttca
       P  Q  D  N  P  Y  N  N  L  V  V  Y  P  R  S
 317 gtgggccttgccaaccaggaactggctgaagtggttagtagagct
       V  G  L  A  N  Q  E  L  A  E  V  V  S  R  A
 362 gtgtcaggtggctacagctgtgtcaccatgggaggagaccacagc
       V  S  G  G  Y  S  C  V  T  M  G  G  D  H  S
 407 ctggcaataggtaccattatcggtcacgcccggcaccgcccagac
       L  A  I  G  T  I  I  G  H  A  R  H  R  P  D
 452 tgtgtcatctgggttgatgctcatgcggacattaatacacctctc
       C  V  I  W  V  D  A  H  A  D  I  N  T  P  L
 497 gtatctggaaatatacatggacagccactttcctttctcatcaaa
       V  S  G  N  I  H  G  Q  P  L  S  F  L  I  K
 542 gaactacaagacaaggtaccacaactgccaggattttcctggatc
       E  L  Q  D  K  V  P  Q  L  P  G  F  S  W  I
 587 aaaccttgcctctctcccccaaatattgtgtacattggcctgaga
       K  P  C  L  S  P  P  N  I  V  Y  I  G  L  R
 632 gatgtggagcctcctgaacattttatttttttatgacatccagtat
       D  V  E  P  P  E  H  F  I  F  Y  D  I  Q  Y
 677 ttttccatgagagagattgatcgacttgggatccagaaggtgatg
       F  S  M  R  E  I  D  R  L  G  I  Q  K  V  M
 722 gaacagacatttgatcggctgattggcaaaaggcagaggccaatc
       E  Q  T  F  D  R  L  I  G  K  R  Q  R  P  I
 767 cacctgagttttgatattgatgcatttgaccctaaattggctcca
       H  L  S  F  D  I  D  A  F  D  P  K  L  A  P
 812 gccacaggaacccctgttgtaggggattaacctacagagaagga
       A  T  G  T  P  V  V  G  G  L  T  Y  R  E  G
 857 gtgtatattactgaagaaatacataatacagggttgctgtcagct
       V  Y  I  T  E  E  I  H  N  T  G  L  L  S  A
 902 ctggatgaagtcaatcctcatttggccacttctgaggaagaggcc
       L  D  E  V  N  P  H  L  A  T  S  E  E  E  A
 947 aaggcaacagccagactagcagtggatgtgattgcttcaagtttt
       K  A  T  A  R  L  A  V  D  V  I  A  S  S  F
 992 ggtcagacaagagaaggcattgtctatgaccaccttcctactcct
       G  Q  T  R  E  G  I  V  Y  D  H  L  P  T  P
1037 agttcaccacacgaatcagaaaatgaagaatgtgtgagaatttag
       S  S  P  H  E  S  E  N  E  E  C  V  R  I  *
1081 GAAATACTGTACTCTGGCACCTTTCACAACAGCATTCCAGAGTTGCAAGGCAGGGACAG
1141 ATATGAAATGGCTGTCTGGATCAATATTGCCTTAATGAGAACATCTGTGCACTCTCACAA
1201 CTGTAAAACTCCCTTCTCTATTTTGGTCACCAACACTGTAAATGTATTTTTTGTTGTTTT
1261 TGAAGTTTACAAGCTATTAATGTTATACATGTAAGTTTGAAGGAGTCATAAACAACATTT
1321 ATTACCTTAGTATATCATAAAAAAAAAAAAAAAA
```

**Figure 4** The full length of cDNA and its amino acid sequence.

## DISCUSSION

To understand and elucidate the mechanism of liver regeneraion, we established short interval successive partial hepatectomy, and attached great importance to seeking some novel differential display genes responsible for cell differentiation and dedifferentiation by suppression subtracted hybridization (SSH) to obtain a bulk of up-regulated and down-

regulated expressed sequence tags (ESTs) in liver regeneration. In the 0-4-36-36-36h SISPH model, we took 0h and 112 hr as driver and tester respectively, and performed the SSH method. Then we constructed a forward-subtractive cDNA library from which we cloned 53 up-regulated ESTs. The 53 up-regulated ESTs may be classified as following: (1) Related to positive/ negative major acute phase protein (MAPP) mRNA genes, such as serum amyloid A, transferrin, haptoglobin, alpha acid glyprotein and fibrinogen like factor; (2) Related to mitochondrial oxidative phosphorylation genes such as ankyrin protein and mitochondrial cytochrome oxidase subunits I, II, III genes; (3)Related to protein synthesis genes such as mitochondrial ribosomal protein 63 (Mrp63); (4) Related to cell division genes, such as microtubulin associated protein (MAP); and (5) Related to signal transduction genes; for example, arginase gene may be related to NO signal pathway and regulate hepatic regeneration together with NO synthase l.

5'end cDNA is not completely reversely transcripted in constructing traditional cDNA library, which leads to some defaults in cloning full-length cDNA. In our study, we adopted a switching mechanism at 5'end of RNA transcript and successfully resolved this shortcoming. Morover, the cDNA library we constructed may simultaneously express three open reading frames, and thus enables us to study from nucleic acid and protein aspects[34].

Arginase is an important enzyme in ornithine cycle[35]. In liver regeneration this enzyme is expressed highly, which may regulate the process of generating NO. Recent work has suggested that NO synthase (NOS) is necessary for liver regeneration[36-38]. Aginase and NOS require the same substrate amino acid L-arginine, thereby they compete for the same substrate in liver regeneration[38,39]. In our study, arginase was up-regulated, suggesting the involvement of arginase in regulating NO signal pathway.

Lepoivre *et al* proved that inducible NO could inhibit mouse DNA synthesis in hepatocellular carcinoma (HCC) *in vitro*. TA3 cell may stimulate L-arginine to produce nitrite in condition of adding IFN-γ or not adding LPS. NO affects nucleotide reductase activity by binding unferrohemoglobin, therefore, to inhibit DNA synthesis[40]. NO may trigger phagocyte into G1 but negatively correlate with DNA synthesis of hepatocytes.

The increase of NO concentration in residue lobus following partial hepatectomy depends on gradual recovery of hepatocyte function. NO may expand vascular smooth muscle in liver to inhibit leukocyte adhesion and platelet aggregation, to improve microcirculation and reduce fat accumulation and deposition in liver accordingly. In normal state, arginine granted may enhance arginine transportation and NO synthesis by hepatocytes[41,42]. Thereby up-regulated arginine will protect damaged liver, to some extent, following SISPH.

In conclusion, we succeeded in cloning a novel gene, based on bioinformatics. We postulate that this gene may function in complicated network in liver regeneration. On the one hand, it may exert initiation of liver regeneration via regulating NO synthesis. On the other hand, it may protect damaged residue lobus following SISPH. More detailed studies are required to clarify the biological functions of this gene in liver regeneration.

## REFERENCES


1 **Stolz DB**, Mars WM, Petersen BE, Kim TH, Michalopoulos GK. Growth factor signal transduction immediately after two-thirds partial hepatectomy in the rat. *Cancer Res* 1999; **59**: 3954-3960

2 **Michalopoulos GK**, DeFrances MC. Liver regeneration. *Science* 1997; **276**: 60-66

3 **Fausto N**, Webber EM. Control of liver growth. *Crit Rev Eukaryot Gene Expr* 1993; **3**: 117-135

4 **Diehl AM**, Rai RM. Liver regeneration 3: Regulation of signal transduction during liver regeneration. *FASEB J* 1996; **10**: 215-227

5 **Zimmermann A**. Liver regeneration: the emergence of new pathways. *Med Sci Monit* 2002; **8**: RA53-63

6 **Ankoma-Sey V**. Hepatic regeneration-revisiting the myth of Prometheus. *News Physiol Sci* 1999; **14**: 149-155

7 **Xu CS**, Xia M, Lu AL, Li XY, Li YH, Zhao XY, Hu YH. Changes in the content and activity of HSC70/HSP68, proteinase and phosphatases during liver regeneration. *Sheng Li Xue Bao* 1999; **51**: 548-556

8 **Cressman DE**, Greenbaum LE, DeAngelis RA, Ciliberto G, Furth EE, Poli V, Taub R. Liver failure and defective hepatocyte regeneration in interleukin-6-deficient mice. *Science* 1996; **274**: 1379-1383

9 **Xia M**, Xue SB, Xu CS. Shedding of TNFR1 in regenerative liver can be induced with TNF alpha and PMA. *World J Gastroenterol* 2002; **8**: 1129-1133

10 **Mohn KL**, Laz TM, Melby AE, Taub R. Immediate-early gene expression differs between regenerating liver, insulin-stimulated H-35 cells, and mitogen-stimulated Balb/c 3T3 cells. Liver-specific induction patterns of gene 33, phosphoenolpyruvate carboxykinase, and the jun, fos, and egr families. *J Biol Chem* 1990; **265**: 21914-21921

11 **Cressman DE**, Diamond RH, Taub R. Rapid activation of the Stat3 transcri Ption Complex in liver regeneration. *Hepatology* 1995; **21**: 1443-1449

12 **Cressman DE**, Greenbaum LE, Haber BA, Taub R. Rapid activation of post-hepatectomy factor/nuclear factor kappa B in hepatocytes, a primary response in the regenerating liver. *J Biol Chem* 1994; **269**: 30429-30435

13 **Hsu JC**, Laz T, Mohn KL, Taub R. Identification of LRF-1, a leucine-zipper protein that is rapidly and highly induced in regenerating liver. *Proc Natl Acad Sci USA* 1991; **88**: 3511-3515

14 **Taub R**. Liver regeneration 4: transcriptional control of liver regeneration. *FASEB J* 1996; **10**: 413-427

15 **Block GD**, Locker J, Bowen WC, Petersen BE, Katyal S, Strom SC, Riley T, Howard TA, Michalopoulos GK. Population expansion, clonal growth, and specific differentiation patterns in primary cultures of hepatocytes induced by HGF/SF, EGF and TGF alpha in a chemically defined (HGM) medium. *J Cell Biol* 1996; **132**: 1133-1149

16 **Bonney RJ**, Hopkins HA, Walker PR, Potter VR. Glycolytic isoenzymes and glycogen metabolism in regenerating liver from rats on controlled feeding schedules. *Biochem J* 1973; **136**: 115-124

17 **Walker PR**, Potter VR. Isozyme studies on adult, regenerating, precancerous and developing liver in relation to findings in hepatomas. *Adv Enzyme Regu* 1972; **10**: 339-364

18 **Tsanev R**, Sendov B. A model of the regulatory mechanism of cellular multiplication. *J Theor Biol* 1966; **12**: 327-341

19 **Loyer P**, Glaise D, Cariou S, Baffet G, Meijer L, Guguen-Guillouzo C. Expression and activation of cdks (1 and 2) and cyclins in the cell cycle progression during liver regeneration. *J Biol Chem* 1994; **269**: 2491-2500

20 **Fausto N**. Liver regeneration. *J Hepatol* 2000; **32**(Suppl 1): 19-31

21 **Bouzahzah B**, Fu M, Iavarone A, Factor VM, Thorgeirsson SS, Pestell RG. Transforming growth factor-beta1 recruits histone deacetylase 1 to a p130 repressor complex in transgenic mice *in vivo*. *Cancer Res* 2000; **60**: 4531-4537

22 **Webber EM**, FitzGerald MJ, Brown PI, Bartlett MH, Fausto N. Transforming growth factor-alpha expression during liver regeneration after partial hepatectomy and toxic injury, and potential interactions between transforming growth factor-alpha and hepatocyte growth factor. *Hepatology* 1993; **18**: 1422-1431

23 **Nakamura T**, Sakata R, Ueno T, Sata M, Ueno H. Inhibition of transforming growth factor beta prevents progression of liver fibrosis and enhances hepatocyte regeneration in dimethylnitrosamine-treated rats. *Hepatology* 2000; **32**: 247-255

24 **Lau AL**, Kumar TR, Nishimori K, Bonadio J, Matzuk MM. Activin betaC and betaE genes are not essential for mouse liver growth, differentiation, and regeneration. *Mol Cell Biol* 2000; **20**: 6127-6137

25 **Aoki T**, Murakami M, Niiya T, Murai N, Shimizu Y, Kato H, Kusano M. Capacity of hepatic regeneration following a second partial hepatectomy in rats. *Hepatol Res* 2001; **21**: 228-241

26 **Xu CS**, Li YC, Lin JT, Zhang HY, Zhang YH. Cloning and analysizing the up-regulated expression of transthyretin-related gene (LR(1)) in rat liver regeneration following short interval successive partial hepatectomy. *World J Gastroenterol* 2003; **9**: 148-151

27 **Lu AL**, Xu CS. Effect of heat shock on change of HSC70/ HSP68, acid and alkaline phosphatases before and after rat partial hepatectomy on HSC/ HSP68, acid and alkaline phosphatases. *World J Gastroenterol* 2000; **6**: 730-733

28 **Diatchenko L**, Lau YF, Campbell AP, Chenchik A, Moqadam F, Huang B, Lukyanov S, Lukyanov K, Gurskaya N, Sverdlov ED, Siebert PD. Suppression subtractive hybridization: a method for generating differentially regulated or tissue-specific cDNA probes and libraries. *Proc Natl Acad Sci USA* 1996; **93**: 6025-6030

29 **Nishizuka S**, Tsujimoto H, Stanbridge EJ. Detection of differentially expressed genes in HeLa x fibroblast hybrids using subtractive suppression hybridization. *Cancer Res* 2001; **61**: 4536-4540

30 **Shridhar V**, Sen A, Chien J, Staub J, Avula R, Kovats S, Lee J, Lillie J, Smith DI. Identification of underexpressed genes in early- and late-stage primary ovarian tumors by suppression subtraction hybridization. *Cancer Res* 2002; **62**: 262-270

31 **Chomczynski P**, Sacchi N. Single-step method of RNA isolation by acid guanidinium thiocyanate- phenol-chloroform extraction. *Anal Biochem* 1987; **162**: 156-159

32 **Hagen FS**, Gray CL, Kuijper JL. Assaying the quality of cDNA libraries. *Biotechniques* 1988; **6**: 340-345

33 **Sambrook J**, Fritsch EF, Maniatis T. Molecular Cloning: A laboratory Manual. 2nd ed. *New York: Cold Spring Harbor* 1989: 18-24

34 **Young RA**, Davis RW. Efficient isolation of genes by using antibody probes. *Proc Natl Acad Sci USA* 1983; **80**: 1194-1198

35 **Brebnor LD**, Balinsky JB. Changes in activities of urea cycle enzymes in early stages of liver regeneration after partial hepatectomy in rats. *Life Sci* 1983; **32**: 1391-1400

36 **Rai RM**, Lee FY, Rosen A, Yang SQ, Lin HZ, Koteish A, Liew FY, Zaragoza C, Lowenstein C, Diehl AM. Impaired liver regeneration in inducible nitric oxide synthase-deficient mice. *Proc Natl Sci USA* 1998; **95**: 13829-13834

37 **Hortelano S**, Dewez B, Genaro AM, Diaz-Guerra MJ, Bosca L. Nitric oxide is released in regenerating liver after partial hepatectomy. *Hepatology* 1995; **21**: 776-786

38 **Tenu JP**, Lepoivre M, Moali C, Brollo M, Mansuy D, Boucher JL. Effects of the new arginase inhibitor N (omega)-hydroxy-nor-L-arginine on NO synthase activity in murine macrophage. *Nirtic Oxide* 1999; **3**: 427-438

39 **Liu ZW**, Zhao MJ, Li ZP. Identification of up-regulated genes in rat regenerating liver tissue by suppression subtractive hybridization. *Shengwu Huaxue Yu Shengwu Wuli Xuebao (Shanghai)* 2001; **33**: 191-197

40 **Lepoivre M**, Flaman JM, Bobe P, Lemaire G, Henry Y. Quenching of the tyrosyl free radical of ribonucleotide reductase by nitric oxide. Relationship to cytostasis induced in tumor cells by cytotoxic macrophages. *J Biol Chem* 1994; **269**: 21891-21897

41 **Obolenskaya M**, Schulze-Specking A, Plaumann B, Frenzer K, Freudenberg N, Decker K. Nitric oxide production by cells isolated from regenerating rat liver. *Biochem Biophys Res Commun* 1994; **204**: 1305-1311

42 **Obolenskaya M**, Vanin AF, Mordvintcev PI, Mulsch A, Decker K. Epr evidence of nitric oxide production by the regenerating rat liver. *Biochem Biophys Res Commun* 1994; **202**: 571-576


**Edited by** Xia HHX

P.O.Box 2345, Beijing 100023,China
Fax: +86-10-85381893
E-mail: wjg@wjgnet.com www.wjgnet.com

World J Gastroenterol 2003;9(6):1287-1291
World Journal of Gastroenterology
Copyright ©2003 by The WJG Press ISSN 1007-9327

• BASIC RESEARCH •

# Expression of insulin-like growth factor 1 and insulin-like growth factor 1 receptor and its intervention by interleukin-10 in experimental hepatic fibrosis

Xiao-Zhong Wang, Zhi-Xin Chen, Li-Juan Zhang, Yun-Xin Chen, Dan Li, Feng-Lin Chen, Yue-Hong Huang

**Xiao-Zhong Wang, Zhi-Xin Chen, Li-Juan Zhang, Yun-Xin Chen, Dan Li, Feng-Lin Chen, Yue-Hong Huang,** Department of Gastroenterology, Affiliated Union Hospital, Fujian Medical University, Fuzhou, 350001, Fujian Province, China
**Supported by** Science and Technology fund of Fujian Province, No. 2003D05
**Correspondence to:** Xiao-Zhong Wang, Department of Gastroenterology, Affiliated Union Hospital, Fujian Medical University, Fuzhou, 350001, Fujian Province, China. drwangxz@pub6.fz.fj.cn
**Telephone:** +86-591-3322384
**Received:** 2002-12-28 **Accepted:** 2003-02-11

## Abstract

**AIM:** To study the expression of IGF-1 and IGF-1R and its intervention by interleukin-10 in the course of experimental hepatic fibrosis.

**METHODS:** Hepatic fibrosis was induced in rats by carbon tetrachloride intoxication and liver specimens were taken from the rats administered $CCl_4$ with or without IL-10 treatment and the animals of the control group. Immunoreactivities for insulin-like growth factor-1 (IGF-1) and IGF-1 receptor(IGF-1R) were demonstrated by immunohistochemistry, and their intensities were evaluated in different animal groups.

**RESULTS:** The positive levels for IGF-1 and IGF-1R were increased with the development of hepatic fibrosis, with the positive signals localized in cytoplasm and/or at the plasmic membrane of hepatocytes. The positive signals of IGF-1 and IGF-1R were observed more frequently ($P<0.01$) in the $CCl_4$-treated group (92.0 % and 90.0 %) compared to those in the control group. The positive signals decreased significantly ($P<0.05$) in IL-10-treated group. The responses in IGF-1 and IGF-1R expression correlated with the time of IL-10 treatment.

**CONCLUSION:** The expression of IGF-1 and IGF-1R immunoreactivities in liver tissue seems to be up-regulated during development of hepatic fibrosis induced by $CCl_4$, and exogenic IL-10 inhibits the responses.

Wang XZ, Chen ZX, Zhang LJ, Chen YX, Li D, Chen FL, Huang YH. Expression of insulin-like growth factor 1 and insulin-like growth factor 1 receptor and its intervention by interleukin-10 in experimental hepatic fibrosis. *World J Gastroenterol* 2003; 9 (6): 1287-1291

http://www.wjgnet.com/1007-9327/9/1287.asp

## INTRODUCTION

Hepatic fibrosis is a common pathological change resulted from various chronic hepatic injuries, which is characterized by an increase of extracelluar matrix (ECM) deposition in the Disse' s space and the imbalance between synthesis and degeneration of ECM. It is a change before cirrhosis[1-6]. Many studies suggested that cytokines play important roles during hepatic fibrosis with different mechanisms[1,7-16]. There is a contrary effect of insulin-like growth factor-1 (IGF-1) on rat hepatic stellate cells (HSC) *in vivo* and *in vitro*. IGF-1 and its receptor (IGF-1R) may play a significant role in hepatic fibrosis. The rat hepatic fibrosis model was established and the immunoreactivities for IGF-1 and IGF-1R in rat liver tissues were assessed to show the possible involvement of IGF-1 and IGF-1R in the process of hepatic fibrosis and the effect of interleukin-10 on this change.

## MATERIALS AND METHODS

### *Materials*

One hundred clean male Sprague-Dawley rats weighing 140-180 g (Provided by Shanghai Experimental Animal Center) were divided randomly into 3 groups. The control group (group C) included 24 rats; the model group (group M) included 40 rats and the IL-10 treated group (group T) included 36 rats. All the rats were bred under routine conditions.

### *Methods*

**Preparation of rats** The rats of group C were injected intraperitoneally with saline 2 $ml\cdot kg^{-1}$ twice a week. The rats of group M and group T were injected intraperitoneally with 50 % $CCl_4$ (dissolved in castor oil) 2 $ml\cdot kg^{-1}$ twice a week. From the third week, the rats of group T were injected intraperitoneally with IL-10 4 $ug\cdot kg^{-1}$ (dissolved in saline) 20 minutes before they were injected with $CCl_4$. All injections were given on Monday and Thursday. To the fifth week, 3 rats in group M and 2 rats in group T died; to the seventh week, 8 rats in group M and 4 rats in group T died; to the ninth week, 10 rats in group M, 6 rats in group T and 3 rats in group C died. In the 5,7,9 week, 10 rats of groups M and T and 7 rats of control group were sacrificed and their livers were taken. The specimens were fixed in 10 % formalin and embedded with paraffin. Sections were stained by hematoxylin and eosin and evaluated by pathologists.

**Immunohistochemistry and data evaluation** The rat liver tissues were sectioned at a thickness of 4 μm. The sections were deparaffinized with xylene, dehydrated with graded ethanol, incubated in PBS containing 3 % $H_2O_2$ to block endogenous perxoidase activity and then incubated in PBS containing 0.1M citrate to saturate nonspecific binding sites. After incubation with rabbit anti-rat IGF-1 or IGF-1R monoclonal antibody (American Neomarkers Company), the recations were with the instance S-P immunohistochemistry reagents (American Zymed Company). And then, the sections were incubated in a buffer containing 3, 3-diaminobenzidine tetrahydrochloride (DAB) and $H_2O_2$ to produce a brown reaction product, then were dehydrated and coverslipped. The reactions were graded according to their intensities and percentage of the positive cell as follows: negative=0, stained yellowish=1, stained with deep yellows or brown=2; the percentage of stained cell: <5 %=0, 6 % to

25 %=1, 26 % to 50 %=2, >50 % =3. Then the eventual result was by these two scores according to the following predefined definitions: 0 to 1= negative (-), 2 to 3=positive (+), 4 and above 4=strongly positive (++). Ridit analysis described the difference between groups.

## RESULTS

### *Expression of IGF-1 and IGF-1R in the liver tissues of the three groups*

The positive rates of IGF-1 in the control group, the $CCl_4$-treated group and the $CCl_4$-and IL-10-treated group were 38.1 %, 92. 0 % and 71.4 %, respectively. Those of IGF-1R were 33.3 %, 80. 0 % and 64.3 %, respectively. The granular positive products were localized in the cytoplasm and/or at the membrane, but not in the nuclei. In group C, IGF-1 and IGF-1R signals were weak, mainly located in the perivenular area (Figure 1,2). In group M, the expression increased obviously with the development of hepatic fibrosis, and the positive cells distributed throughout the hepatic lobule (Figure 3,4). In group T, the changes were less pronounced than in group M (Figure 5,6).

### *Intensities of IGF-1 and IGF-1R immunoreactivities*

The comparasion of IGF-1 and IGF-1R system expression levels in groups C, M and T is listed in Table 1. Ridit analysis showed a significant difference among the three groups ($P<0.01$). Expression levels of the IGF-1 and IGF-1R in group M were found to be higher than that in group C ($P<0.01$). In group T, after the treatment with IL-10, the immunoreactivities for IGF-1 and IGF-1R decreased ($P<0.01$ and $P<0.05$, respectively). The data for IGF-1 and IGF-1R reactivities in different stages of hepatic fibrosis are listed in Table 2. With the development of hepatic fibrosis, intensities of IGF-1 and IGF-1R immunoreactivities increased significantly ($P<0.05$). The data for IGF-1 and IGF-1R immunoreactivities in different stages of hepatic fibrosis in group T are listed in Table 3. A significant decrease was observed in IGF-1 and IGF-1R expression with the IL-10 treatment ($P<0.05$).

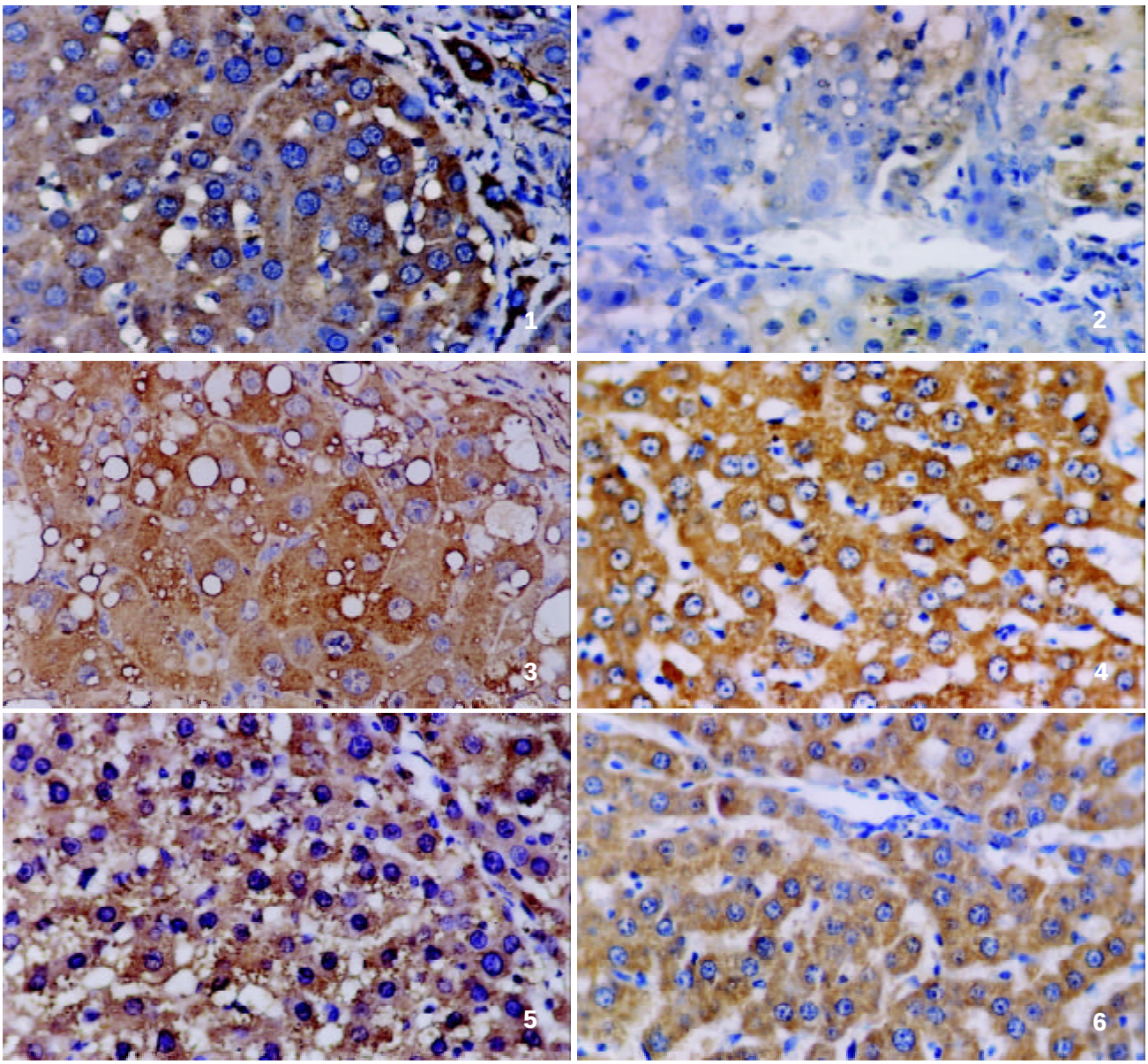


**Figure 1** IGF-1 positively expressed cell in group C S-P method ×400.
**Figure 2** IGF-1R positively expressed cell in group C S-P method ×400.
**Figure 3** IGF-1 positively expressed cell in group M S-P method ×400.
**Figure 4** IGF-1R positively expressed cell in group M S-P method ×400.
**Figure 5** IGF-1 positively expressed cell in group T S-P method ×400.
**Figure 6** IGF-1R positively expressed cell in group T S-P method ×400.

**Table 1** Intensities for IGF-1/IGF-1R immunoreactivities in groups C, M and T

| Group | *n* | IGF-1 | | | | IGF-1R | | | |
|---|---|---|---|---|---|---|---|---|---|
| | | - | + | ++ | Ridit value | - | + | ++ | Ridit value |
| C | 21 | 13 | 8 | 0 | 0.302[acf] | 14 | 7 | 0 | 0.331[ac] |
| M | 25 | 2 | 10 | 13 | 0.689[acd] | 5 | 8 | 12 | 0.666[ace] |
| T | 28 | 8 | 16 | 4 | 0.480[adf] | 10 | 16 | 2 | 0.478[ae] |

[a]$P<0.01$ *vs* among three groups, [c]$P<0.01$ group M *vs* group C [d]$P<0.01$, [e]$P<0.05$ group M *vs* group T, [f]$P<0.05$ group C *vs* group T.

**Table 2** Intensities for IGF-1 and IGF-1R immunoreactivities in different time points of hepatic fibrosis induced by $CCl_4$

| Week | *n* | IGF-1 | | | | IGF-1R | | | |
|---|---|---|---|---|---|---|---|---|---|
| | | - | + | ++ | Ridit value | - | + | ++ | Ridit value |
| 5 wk | 8 | 0 | 1 | 7 | 0.683[ab] | 0 | 1 | 7 | 0.710[ab] |
| 7 wk | 8 | 0 | 4 | 4 | 0.510[a] | 2 | 3 | 3 | 0.445[a] |
| 9 wk | 9 | 2 | 5 | 2 | 0.329[ab] | 3 | 4 | 2 | 0.362[ab] |

[a]$P<0.05$ *vs* among three groups, [b]$P<0.05$, 5 wk *vs* 9 wk.

**Table 3** Intensities for IGF-1 and IGF-1R immunoreactivities in different periods of hepatic fibrosis in group T

| Week | *n* | IGF-1 | | | | IGF-1R | | | |
|---|---|---|---|---|---|---|---|---|---|
| | | - | + | ++ | Ridit value | - | + | ++ | Ridit value |
| 5 wk | 10 | 0 | 7 | 3 | 0.678[ab] | 1 | 7 | 2 | 0.661[ab] |
| 7 wk | 9 | 3 | 5 | 1 | 0.468[ab] | 3 | 6 | 0 | 0.488[a] |
| 9 wk | 9 | 5 | 4 | 0 | 0.333[ab] | 6 | 3 | 0 | 0.334[ab] |

[a]$P<0.05$ *vs* among three groups, [b]$P<0.05$, 5 wk *vs* 9 wk.

## DISCUSSION

Hepatic fibrosis is the early stage of hepatic cirrhosis, characterized by accumulation of excessive extracellular matrix, necrosis, nodular regeneration of hepatocytes and formation of fibrous septum[1-6]. Cytokines play important roles in the formation and regression of hepatic fibrosis[1,7-16].

In the present study, up-regulated expression of IGF-1 and IGF-1R was observed in liver tissues injured by $CCl_4$-intoxication, and was positively correlated with the development of hepatic fibrosis. However, the response was less pronounced in IL-10- treated group.

Insulin-like growth factors (IGFs) include two related homologous polypeptides: IGF-1 and IGF-2, which have similar structure and activity *in vitro*, but different biological effect *in vivo*. Activation of mitosis and induction or acceleration of differentiation are their major functions, which are mediated through IGF-1R by means of autocrine, paracrine and endocrine mechanisms. IGF-1R is a transmembrane tyrosine kinase receptor. After binding with its ligand, intracellular transcription and synthesis of proteins are activated and regulated through a series of signal transduction. This gives rise to insulin-like metabolic effects and promotes proliferation and differentiation of cells. It is also involved in the maintenance of transformed cell phenotypes. Its expression is essential for the transforming function of cell cycle-related protocogenes and viral oncogenes[17,18]. In addition, IGF-1 and IGF-1R have an anti-apoptosis effect on different cells[13]. Liver is the main organ of IGF-1, but the function of IGF-1 and IGF-1R in hepatic fibrosis still remains controversial. Many authors have observed a decreased serum concentration of IGF-1 and insulin-like growth factor-binding protein 3 (IGFBP3) in patients with hepatic cirrhosis, this change is correlative with cirrhosis progression. With the treatment of recombinant somatotropin, the serum concentration increased along with the improvement of protein synthesis and liver metabolism. For these patients, the IGF-1 concentration below 10 nmol/L was considered an unfavored response to the treatment and poor prognosis[19-31]. Castilla *et al* and Myguerza *et al* reported that the histological parameters in hepatic fibrosis animals were improved after being treated with exogenous IGF-1. So IGF-1 might act as an antifibrogenic factor[32,33]. On the contrary, other researches speculated IGF-1 had a great influence on hepatic stellate cell (HSC), which was the main producer of ECM, such as activating proliferation, inhibiting apoptosis, accelerating the secretion of collagen type I, etc[13,34]. The function of IGF-1 also seems to be regulated by IGF-BP, IGF-1R and other cytokines[22-30].

The present study observed and evaluated IGF-1 expression with the fibrosis progression, which might be a compensatory reaction to the continuous loss of hepatocytes in the $CCl_4$-treated animals. We consider that IGF-1 may stimulate the replication of hepatocytes and interfere with fibrosis. The discordance was observed between the IGF-1 level in liver tissue and that in serum, with the former higher and the latter lower, this is likely due to the decrease of IGF-1 released from hepatocytes to blood circulation. In other words, the hepatocytic secretion of IGF-1 maybe regulated by means of autocrine under such a situation. The positive correlation between the expression of IGF-1 and IGF-1R and the fibrosis progression may be helpful for fibrosis staging.

IL-10 is an antifibrogenic cytokine produced by Th2 cells, macrophages, stellate cells and hepatocytes[35-47]. It has been reported the deficiency of IL-10 prompted fibrosis probably by its failure in inhibiting the overproduction of TGF-$\beta_1$ and TNF-$\alpha$. The latter two cytokines are secreted by macrophages and can enhance synthesis of collagen type I[48]. The knock-out experiments (IL-10-/-mice) indicated that endogenous IL-10 actually relieved $CCl_4$-induced fibrosis[49-51]. In our previous study, exogenous IL-10 was found to be able to inhibit the progress of fibrosis and might be used for treatment. Similar results were also reported by Nelson, but its mechanism remains obscure[52,53]. The present study showed that IGF-1 and IGF-1R expression decreased with the improvement of fibrosis after treatment with IL-10. It seems that antifibrogenic effect of IL-10 is associated with down-regulation of IGF-1/IGF-1R. More works are demanded to clarify whether this action is regulated by IGF-1 and IGF-1R or the decrease of IGF-1R expression is only a phenomenon of hepatic cirrhosis remission.

## REFERENCES


1 **Friedman SL.** Cytokines and fibrogenesis. *Semi Liver Dis* 1999; **19**: 129-140

2 **Liu HL,** Li XH, Wang DY, Yang SP. Matrix metalloproteinase-2 and tissue inhibitor of metalloproteinase-1 expression in fibrotic rat liver. *World J Gastroenterol* 2000; **6**: 881-884

3 **Du WD,** Zhang YE, Zhai WR, Zhou XM. Dynamic changes of type I, III and IV collagen synthesis and distribution of collagen-producing cells in carbon tetrachloride-induced rat liver fibrosis. *World J Gastroenterol* 1999; **5**: 397-403

4 **Wang JY,** Guo JS, Yang CQ. Expression of exogenous rat collagenase *in vitro* and in a rat model of liver fibrosis. *World J Gastroenterol* 2002; **8**: 901-907

5 **Nie QH,** Cheng YQ, Xie YM, Zhou YX, Cao YZ. Inhibiting effect of antisense oligonucleotides phosphorthioate on gene expression of TIMP-1 in rat liver fibrosis. *World J Gastroenterol* 2001; **7**: 363-369

6 **Vaillant B,** Chiaramonte MG, Cheever AW, Soloway PD, Wynn TA. Regulation of hepatic fibrosis and extracellular matrix genes

by the th response: new insight into the role of tissue inhibitors of matrix metalloproteinases. *J Immunol* 2001; **167**: 7017-7026

7 **Zhang GL,** Wang YH, Teng HL, Lin ZB. Effects of aminoguanidine on nitric oxide production induced by inflammatory cytokines and endotoxin in cultured rat hepatocytes. *World J Gastroenterol* 2001; **7**: 331-334

8 **Daniluk J,** Szuster-Ciesielska A, Drabko J, Kandefer-Szerszen M. Serum cytokine levels in alcohol-related liver cirrhosis. *Alcohol* 2001; **23**: 29-34

9 **Von Baehr V,** Docke WD, Plauth M, Liebenthal C, Kupferling S, Lochs H, Baumgarten R, Volk HD. Mechanisms of endotoxin tolerance in patients with alcoholic liver cirrhosis: role of interleukin 10, interleukin 1 receptor antagonist, and soluble tumour necrosis factor receptors as well as effector cell desensitisation. *Gut* 2000; **47**: 281-287

10 **Si XH,** Yang LJ. Extraction and purification of TGFβ and its effect on the induction of apoptosis of hepatocytes. *World J Gastroenterol* 2001; **7**: 527-531

11 **Weng HL,** Cai WM, Liu RH. Animal experiment and clinical study of effect of gamma2interferon on hepatic fibrosis. *World J Gastroenterol* 2001; **7**: 42-48

12 **Li D,** Zhang LJ, Chen ZX, Huang YH, Wang XZ. Effects of TNFα, IL-6 and IL-10 on the development of experimental rat liver fibrosis. *Shijie Huaren Xiaohua Zazhi* 2001; **9**: 1242-1245

13 **Issa R,** Williams E, Trim N, Kendall T, Arthur MJP, Reichen J, Benyon RC, Iredale JP. Apoptosis of hepatic stellate cells: involvement in resolution of biliary fibrosis and regulation by soluble growth factors. *Gut* 2001; **48**: 548-557

14 **Gong JP,** Dai LL, Liu CA, Wu CX, Shi YJ, Li SW, Li XH. Expression of CD14 protein and its gene in liver sinusoidal endothelial cells during endotoxemia. *World J Gastroenterol* 2002; **8**: 551-554

15 **Wang JY,** Wang XL, Liu P. Detection of serum TNF-α, IFN-β, IL-6 and IL-8 in patients with hepatitis B. *World J Gastroenterol* 1999; **5**: 38-40

16 **Assy N,** Paizi M, Gaitini D, Baruch Y,Spira G. Clinical implication of VEGF serum levels in cirrhotic patients with or without potal hypertension. *World J Gastroenterol* 1999; **5**: 296-300

17 **Kalebic T,** Tsokos M, Helman LJ. *In vivo* treatment with antibody against IGF-1 receptor supresses growth of human rhabdomyosarcoma and down-regulates $p34^{cdc2}$. *Cancer Res* 1994; **54**: 5531-5534

18 **Zhou P,** Zhou ZC, Chen WS, Liu WW, Fang DC, Yang JM. Effect of IGF-1R antisense gene on the morphology of hepatoma cell line SMMC-7721. *Shijie Huaren Xiaohua Zazhi* 2002; **10**: 279-282

19 **Gayan-Ramirez G,** van de Casteele M, Rollier H, Fevery J, Vanderhoydonc F, Verhoeven G, Decramer M. Biliary cirrhosis induces type IIx/b fiber a atrophy in rat diaphragm and skeletal muscle, and decreases IGF-I mRNA in the liver but not in muscle. *J Hepatol* 1998; **29**: 241-249

20 **Donaghy A,** Ross R, Wicks C, Hughes SC, Holly J, Gimson A, Williams R. Growth hormone therapy in patients with cirrhosis: a pilot study of efficacy and safety. *Gastroenterology* 1997; **113**: 1617-1622

21 **Moller S,** Juul A, Becker U, Henriksen JH. The acid-labile subunit of the ternary insulin-like growth factor complex in cirrhosis: relation to liver dysfunction. *J Hepatol* 2000; **32**: 441-446

22 **Ormarsdottir S,** Ljunggren O, Mallmin H, Olofsson H, Blum WF, Loof L. Circulating levels of insulin-like growth factors and their binding proteins in patients with chronic liver disease: lack of correlation with bone mineral density. *Liver* 2001; **21**: 123-128

23 **Assy N,** Hochberg Z, Amit T, Shen-Orr Z, Enat R, Baruch Y. Growth hormone-stimulated insulin-like growth factor (IGF) I and IGF-binding protein-3 in liver cirrhosis. *J Hepatol* 1997; **27**: 796-802

24 **Assy N,** Hochberg Z, Enat R, Baruch Y. Prognostic value of generation of growth hormone-stimulated insulin-like growth factor-I (IGF-I) and its binding protein-3 in patients with compensated and decompensated liver cirrhosis. *Dig Dis Sci* 1998; **43**: 1317-1321

25 **Shmueli E,** Miell JP, Stewart M, Alberti KG, Record CO. High insulin-like growth factor binding protein 1 levels in cirrhosis: link with insulin resistance. *Hepatology* 1996; **24**: 127-133

26 **Moller S,** Gronbaek M, Main K, Becker U, Skakkebaek NE. Urinary growth hormone (U-GH) excretion and serum insulin-like growth factor 1 (IGF-1) in patients with alcoholic cirrhosis. *J Hepatol* 1993; **17**: 315-320

27 **Donaghy A,** Ross R, Gimson A, Hughes SC, Holly J, Williams R. Growth hormone, insulinlike growth factor-1, and insulinlike growth factor binding proteins 1 and 3 in chronic liver disease. *Hepatology* 1995; **21**: 680-688

28 **Moller S,** Juul A, Becker U, Flyvbjerg A, Skakkebaek NE, Henriksen JH. Concentrations, release, and disposal of insulin-like growth factor (IGF)-binding proteins (IGFBP), IGF-I, and growth hormone in different vascular beds in patients with cirrhosis. *J Clin Endocrinol Metab* 1995; **80**: 1148-1157

29 **Kratzsch J,** Blum WF, Schenker E, Keller E. Regulation of growth hormone (GH), insulin-like growth factor (IGF)I, IGF binding proteins -1, -2, -3 and GH binding protein during progression of liver cirrhosis. *Exp Clin Endocrinol Diabetes* 1995; **103**: 285-291

30 **Ottesen LH,** Bendtsen F, Flyvbjerg A. The insulin-like growth factor binding protein 3 ternary complex is reduced in cirrhosis. *Liver* 2001; **21**: 350-356

31 **Santolaria F,** Gonzalez- Gonzalez G, Gonzalez –Reimers E, Martinez-Riera A, Milena A, Rodgiguez-Moreno F, Gonzalez-Garcia C. Effects of alcohol and liver cirrhosis on the GH-IGF-I axis. *Alcohol Alcohol* 1995; **30**: 703-708

32 **Muguerza B,** Castilla-Cortazar I, Garcia M, Quiroga J, Santidrian S, Prieto J. Antifibrogenic effect *in vivo* of low doses of insulin-like growth factor-I in cirrhotic rats. *Biochim Biophys Acta* 2001; **1536**: 185-195

33 **Castilla-Cortazar I,** Garcia M, Muguerza B, Quiroga J, Perez R, Santidrian S, Prieto J. Hepatoprotective effects of insulin-like growth factor 1 in rats with carbon tetrachloride-induced cirrhosis. *Gastroenterology* 1997; **113**: 1682-1691

34 **Svegliati-Baroni G,** Ridolfi F, Di Sario A, Casini A, Marucci L, Gaggiotti G, Orlandoni P, Macarri G, Peregon L, Benedetti A, Folli F. Insulin and insulin-like growth factor 1 stimulate proliferation and type I collagen accumulation by human hepatic stellate cells: differential effects on signal transduction pathways. *Hepatology* 1999; **29**: 1743-1751

35 **Di Marco R,** Xiang M, Zaccone P, Leonardi C, France S, Meroni P, Nicoletti F. Concanavalin A-induced hepatitis in mice is prevented by interleukin (IL)-10 and exacerbated by endogenous IL-10 deficiency. *Autoimmunity* 1999; **31**: 75-83

36 **Louis H,** Le Moine O, Peny MO, Gulbis B, Nisol F, Goldman M, Deviere J. Hepatoprotective role of interleukin 10 in galactosamine/lipopolysaccharide mouse liver injury. *Gastroenterology* 1997; **112**: 935-942

37 **Louis H,** Le Moine O, Peny MO, Quertinmont E, Fokan D, Goldman M, Deviere J. Production and role of interleukin-10 in concanavalin A-induced hepatitis in mice. *Hepatology* 1997; **25**: 1382-1389

38 **Hill DB,** D'Souza NB, Lee EY, Burikhanov R, Deaciuc IV, de Villiers WJ. A role for interleukin-10 in alcohol-induced liver sensitization to bacterial lipopolysaccharide. *Alcohol Clin Exp Res* 2002; **26**: 74-82

39 **Santucci L,** Fiorucci S, Chiorean M, Brunori PM, Di Matteo FM, Sidoni A, Migliorati G, Morelli A. Interleukin 10 reduces lethality and hepatic injury induced by lipopolysaccharide in galactosamine-sensitized mice. *Gastroenterology* 1996; **111**: 736-744

40 **Howard M,** O'Garra A. Biological properties of interleukin 10. *Immunol Today* 1992; **13**:198-200

41 **De Vries JE**. Immunosuppressive and anti-inflammatory properties of interleukin 10. *Ann Med* 1995; **27**: 537-541

42 **Wakkach A,** Cottrez F, Groux H. Can interleukin-10 be used as a true immunoregulatory cytokine? *Eur Cytokine Netw* 2000; **11**: 153-160

43 **Oberholzer A,** Oberholzer C, Moldawer LL. Interleukin-10: a complex role in the pathogenesis of sepsis syndromes and its potential as an anti-inflammatory drug. *Crit Care Med* 2002; **30**: S58-63

44 **Weng S,** Leng X, Wei Y. Interleukin-10 inhibits the activation of cultured rat hepatic stellate cells induced by Kupffer cells. *Zhonghua Yixue Zazhi* 2002; **82**: 104-107

45 **Louis H,** Le Moine A, Quertinmont E, Peny MO, Geerts A, Goldman M, Le Moine O, Deviere J. Repeated concanavalin A challenge in mice induces an interleukin 10-producing phenotype and liver fibrosis. *Hepatology* 2000; **31**: 381-390

46 **Nagano T,** Yamamoto K, Matsumoto S, Okamoto R, Tagashira

M, Ibuki N, Matsumura S, Yabushita K, Okano N, Tsuji T. Cytokine profile in the liver of primary biliary cirrhosis. *J Clin Immunol* 1999; **19**: 422-427

47 **Wang XZ,** ZhangLJ, Li D, Huang YH, Chen ZX, Li B. Effects of transmitters and interleukin-10 on rat hepatic fibrosis induced by CCl4. *World J Gastroenterol* 2003; **9**: 539-543

48 **Nagaki M,**Tanaka M, Sugiyama A, Ohnishi H, Moriwaki H. Interleukin-10 inhibits hepatic injury and tumor necrosis factor-alpha and interferon-gamma mRNA expression induced by staphylococcal enterotoxin B or lipopolysaccharide in galactosamine-sensitized mice. *J Hepatol* 1999; **31**: 815-824

49 **Thompson K,** Maltby J, Fallowfield J, Mcaulay M, Millward-Sadler H, Sheron N. Interleukin-10 expression and function in experimevtal murine liver inflammation and fibrosis. *Hepatology* 1998; **28**: 1597-1606

50 **Louis H,** Van Laethem JL, Wu W, Quertinmont E, Degraef C, Van den Berg K, Demols A, Goldman M, Le Moine O, Geerts A, Deviere J. Interleukin-10 controls neutrophilic infitration, hepatocyte proliferation, and liver fibrosis induced by carbon tetrachloride in mice. *Hepatology* 1998; **28**: 1607-1615

51 **Demols A,** Van Laethem JL, Quertinmont E, Degraef C, Delhaye M, Geerts A, Deviere J. Endogenous interleukin-10 modulates fibrosis and regeneration in experimental chronic pancreatitis. *Am J Physiol Gastrointest Liver Physiol* 2002; **282**: G1105-1112

52 **Zhang LJ,** Wang XZ, Huang YH. Effect of interneukin-10 on experimental liver fibrosis. *Zhonghua Xiaohuu Zazhi* 2002; **22**: 179-180

53 **Nelson DR,** Lauwers GY, Lau JY, Davis GL. Interneukin-10 treatment reduces fibrosis in patients with chronic hepatitis C: a pilot trail of interferon nonresponders. *Gastroenterology* 2000; **118**: 655-660

**Edited by** Su Q

P.O.Box 2345, Beijing 100023,China
Fax: +86-10-85381893
E-mail: wjg@wjgnet.com www.wjgnet.com

World J Gastroenterol 2003;9(6):1292-1295
World Journal of Gastroenterology
Copyright © 2003 by The WJG Press ISSN 1007-9327

• BASIC RESEARCH •

# Experimental study of effect of Ganyanping on fibrosis in rat livers

Wang-Xian Tang, Zi-Li Dan, Hong-Mei Yan, Cui-Huan Wu, Guo Zhang, Mei Liu, Qin Li, Shao-Bai Li

**Wang-Xian Tang, Zi-Li Dan, Guo Zhang, Mei Liu, Qin Li, Shao-Bai Li,** Institute of Liver Diseases, Tongji Hospital, Tongji Medical College, Huazhong University of Science and Technology, Wuhan 430030, Hubei Province, China
**Hong-Mei Yan,** The 7th Hospital of Wuhan, Wuhan 430071, Hubei Province, China
**Cui-Huan Wu,** Department of Pathology, Tongji Medical College, Huazhong University of Science and Technology, Wuhan 430030, Hubei Province, China
**Supported by** the Natural Science Foundation of Hubei Province, No. 1999 J151
**Correspondence to:** Professor Wang-Xian Tang, Institute of Liver Diseases, Tongji Hospital, Tongji Medical College, Huazhong University of Science and Technology, Wuhan 430030, Hubei Province, China. tangwx@tjh.tjmu.edu.cn
**Telephone:** +86-27-83662873 **Fax:** +86-27-83615970
**Received:** 2002-11-06 **Accepted:** 2003-02-11

## Abstract

**AIM:** To observe the effects of Ganyanping on $CCl_4$-induced hepatic fibrosis in rats.

**METHODS:** The rats were separated randomly into five groups. Groups A to group D, each consisting of 15 rats, were for different tests, while 8 rats were used as normal controls (N). For group D, $CCl_4$ was injected subcutaneously, at a dosage of 3 ml/kg for 9 weeks. For group A, Ganyanping was administered via gastric tube at a dosage of 10 ml/kg. For group B, the treatment with Ganyanping was started 4 weeks after $CCl_4$ administration. In group C, Ganyanping was administered 8 weeks after the intoxication, and treatment lasted for 4 weeks. Liver tissues were fixed in 10 % formalin and embedded in paraffin. Pathologic changes, particularly fibrosis, were evaluated on the HE and V-G-stained sections. Ten middle-power fields were randomly selected for assessment of collagen deposition.

**RESULTS:** Loss of normal hepatic architecture, some with pseudo-lobule formation, was observed in group D, while hepatocytes steatosis and fibrosis were less pronounced in the animals treated with Ganyanping. Pseudo-lobule formation was not evident in the latter groups. The total collagen area and ratio were 840.23±81.65 and 7.0±0.9, respectively in group D, the ratio being reduced greatly in the Ganyanping-treated groups (148.73±45.89 and 1.16±0.33, respectively). The activities of MAO and ACP were elevated and that of SDH in group D decreased in the hepatic tissue as compared to the control group. The treatment with Ganyanping abrogated these enzymatic changes.

**CONCLUSION:** Our data approved that Ganyanping could improve the microcirculation in the liver, reduce oxygen-derived free radicals, and enhance the cellular metabolism and immune function, all resulting in an anti-fibrotic effect. Hence, Ganyanping can protect the liver from fibrosis. It may be a safe and effective preparation for patient with fibrosis.

Tang WX, Dan ZL, Yan HM, Wu CH, Zhang G, Liu M, Li Q, Li SB. Experimental study of effect of Ganyanping on fibrosis in rat livers. *World J Gastroenterol* 2003; 9(6): 1292-1295
http://www.wjgnet.com/1007-9327/9/1292.asp

## INTRODUCTION

Ganyanping, a preparation of Chinese herbs proposed by Li Shaobai *et al*[1] has been used in clinical and experimental fields for many years. It has been shown to be protective for the animal liver against injury by D-GalN and cirrhosis caused by $CCl_4$ intoxication[2-6]. In this study, the effects of Ganyanping on liver fibrosis used a $CCl_4$- intoxication model. The V-G and enzyme histochemistry techniques were employed to observe the effects of Ganyanping.

## MATERIALS AND METHODS

### *Reagents*

$CCl_4$ (Beijing Chemical Factory, Lot No. 20000225) was diluted to 40 % in vegetable oil (Southseas Oils & Fats Industrial (CHI Wan) Limited, Grade One, Lot No. KO'SOF Ts88). Ganyanping tablet preparation (Lot No.20001110) was provided by the Institute of Liver Disease, Tongji Hospital, Tongji Medical College, consisting of Radix Astragali seu Hedysari, Radix Salviae Miltiorrhizae, Rhizoma polygoni Cuspidati and other herbs. The tablets were prepared in the Chinese Medicine Pharmacy of Tongji Hospital. The powder of Ganyanping was dissolved into water (1.2 g/ml) before use.

### *Animals*

68 Wistar rats (¡â & ¡á, 38 for ¡â and 30 for ¡â), weighing between 170 and 250 g, were provided by the Laboratory Animal Center of Tongji Medical College. The rats were separated randomly into five groups. Group N, normal control, consisted of 8 rats. For group A to group D, rats (15 for each) were treated with $CCl_4$ by subcutaneous injection at a dosage of 3 ml/kg for 9 weeks. For group A, Ganyanping (10 ml/kg) was also administered via gastric tube along with the $CCl_4$ intoxication. For group B, Ganyanping treatment was started 4 weeks later and lasted for the remaining 5 weeks. For group C, Ganyanping was given after 8 weeks of $CCl_4$ administration, and the treatment lasted for 4 weeks. Ganyanping was administrated in the form of an aqueous suspension (2 g/ml). After 9 weeks, the overnight fasting animals were anesthetized with sodium pentobarbital (30 mg/kg, per injection). Blood was taken from inferior vena cava for the estimation of biochemical parameters including values of ALT, AST, and concentrations of protein and albumin.

### *Pathological observations*

Hepatic tissues were fixed with formalin and embedded with paraffin. The sections were stained with hematoxylin and eosin.

Samples for electron microscopy were fixed in 25 g/L glutaraldehyde buffer for two hours, then with osmium acid, dehydrated in acetone, and embedded with epoxy resin. The sections were observed under an electron microscope (OPTON EM10C, Carl Zelss Company, Made in Germany, No.5166, voltage is 60KV).

### *V-G staining and enzymatic reactions*

Van Gieson's method was used to demonstrate collagen fibers[7]. HPIAS-1000 auto medical image analyzing system was used for quantitative assessment of collagen fibers in liver. Ten middle power fields were selected randomly for the total area occupied by collagen fibers and its ratio against the total area observed. Activity of monoamine oxidase (MAO) was demonstrated using 15 μm-thick frozen sections with the chayen method, that of succinic dehydrogenase (SDH) was visualized using lojda method, that of ALP with culling method, and that of ACP with Bancroft method[8]. NOS was shown using NADPH method[9].

### *Statistics*

Statistical analysis with ANOVA: Data were presented as $\bar{x}\pm s$. Significant differences were determined by using ANOVA in statistical software SPSS11.0. Results were considered significant when $P<0.05$.

## RESULTS

### *Histologic and ultrastructural findings*

Liver sample from group D showed loss of normal lobular architecture. The parenchyma showed steatosis, cellular swelling, necrosis, and was divided into rounded nodules, separated by bands of fibrous tissues, while in groups A, B and C, the steatosis was not severe and the fibrosis was not so pronounced, without any pseudo-lobule observed (Figures 1, 2). Hepatocellular degeneration was frequently seen in the intoxicated animals under electron microscope, characterized by marked swelling of mitochondria, loss of rough endoplasmic reticulum structures and distention of them. Glycogen particles were greatly reduced and more lipid droplets were found in the cytoplasmic compartment. In some hepatocytes, nuclear irregularity was noted, lipid droplets and some components resembling rough endoplasmic reticulum (nuclear or pseudo-nuclear inclusions) were also found within the nuclei. A few lipid droplets were found in the cytoplasm in the Ganyanping-treated groups (Figures 3, 4).

### *VG staining*

Fibrosis was shown in group D by VG staining, with hepatic parenchyma separated by the rough, red-stained fibrotic septa. The change was less pronounced in the Ganyanping-treated groups. The total collagen-deposited area and ratio in group D, but not in the Ganyanping-treated groups ($P<0.05$), were increased compared to those in the control group ($P<0.001$) (Table1, Figures 5, 6).

**Table 1** Area occupied by fibrotic septa and its ratio to the total area examined

| Groups | *n* | Area covered by fibrotic septa ($um^2$) | Ratio (%) |
|---|---|---|---|
| N | 8 | 35.30±13.86[b] | 0.32±0.18[b] |
| A | 15 | 200.74±33.84[a] | 1.63±0.45[a] |
| B | 15 | 148.73±45.89[a] | 1.16±0.33[a] |
| C | 15 | 158.73±40.89[a] | 1.12±0.28[a] |
| D | 15 | 840.23±81.65 | 7.00±0.90 |

[a]$P<0.05$ *vs* Group D, [b]$P<0.001$ *vs* Group D.

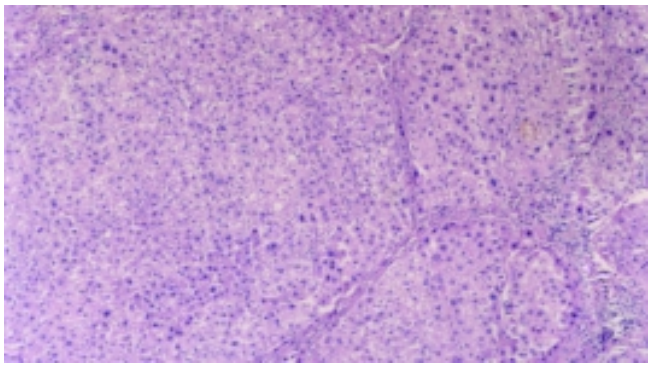

**Figure 1** Loss of normal lobular architecture,some had pseudo lobule formation in the $CCl_4$ intoxicated groups. HE×100.

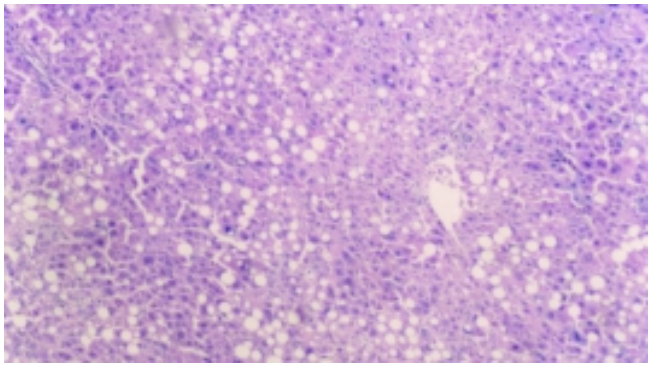

**Figure 2** Steatosis was not severe and fibrosis was not so pronounced, without any pseudo -lobule formation in the Ganyanping-treated groups. HE×100.

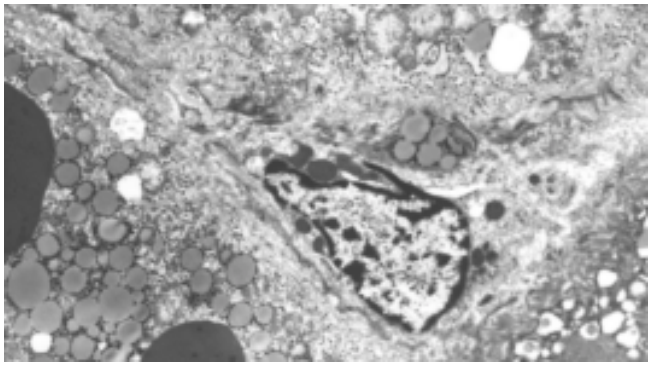

**Figure 3** The numbers of hepatic stellate cells and collagen fibrils increased in Disse's space and hepatocellular degeneration were frequently seen in the $CCl_4$ intoxicated groups.×4 000.

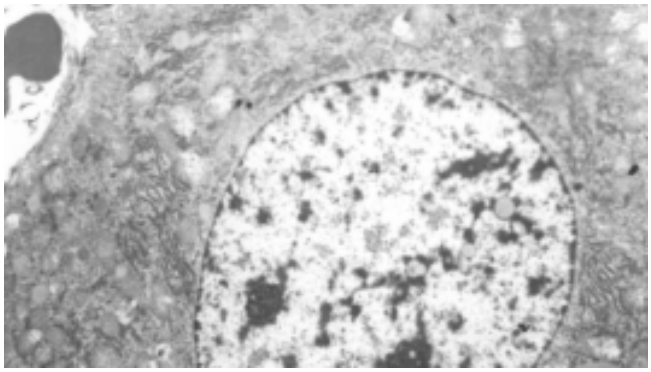

**Figure 4** Most of hepatocytes showed basically normal ultra-structure and a few lipid droplets were found in the cytoplasm in the Ganyanping-treated groups. ×4 000.

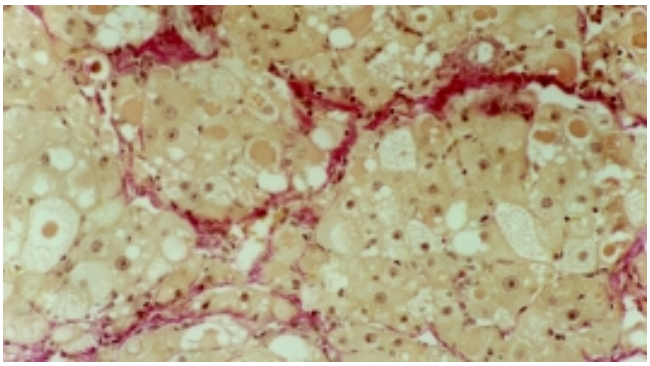

**Figure 5** Hepatic parenchyma separated by the rough, red-stained fibrotic septa in the $CCl_4$ intoxicated groups. VG×200.

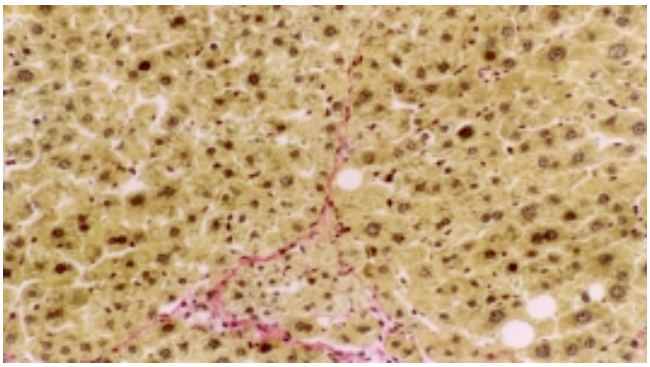

**Figure 6** Collagen fibrosis was less pronounced in the Ganyanping-treated groups. VG×200.

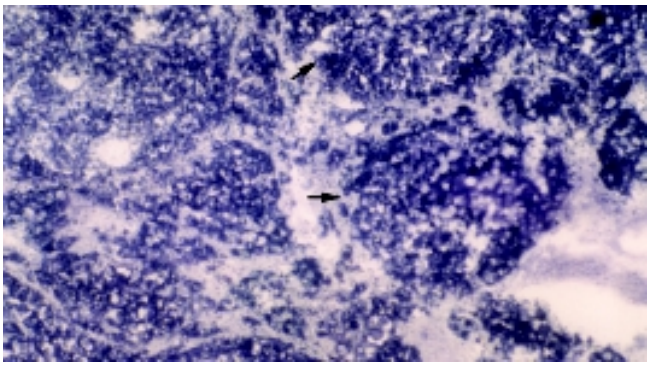

**Figure 7** Increase in the activities of MAO(+++) in the $CCl_4$ intoxicated groups. ×75.

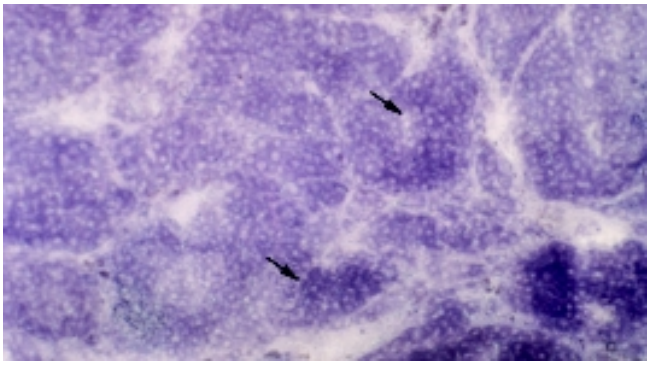

**Figure 8** Decrease in the activities of MAO in the Ganyanping-treated groups (++). ×75.

### *Enzymatical reactions*

Activities of MAO, SDH, ALP and NOS were demonstrated in frozen sections with the procedures described above. Those for MAO and ACP were found to be elevated and that of SDH was reduced in group D compared to those in the control group. The changes were not so marked in any of the Ganyanping-treated groups (Tables 2, 3; Figures 7, 8).

**Table 2** Semiquantitative assessment of enzymatic activities in different liver samples

| Groups | *n* | MAO | SDH | ACP | LDH | NOS | ALP |
|---|---|---|---|---|---|---|---|
| N | 8 | ++ | +++ | + | ++ | ++ | ++ |
| A | 15 | ++ | +++ | ++ | +¡ý | ++ | ++ |
| B | 15 | ++ | +++ | + | ++ | ++ | ++ |
| C | 15 | ++ | +++ | + | ++ | ++ | ++ |
| D | 15 | +++¡ü | ++¡ý | +++¡ü | +¡ý | ++ | ++ |

+: positive; ++: moderately positive; +++: strongly positive; ¡ü: activity enhancement; ¡ý: activity weakened.

**Table 3** Quantitative observation of the liver enzymatic activities (mean absorbance)

| Groups | *n* | MAO | SDH | ACP | LDH |
|---|---|---|---|---|---|
| N | 8 | 0.2042±0.041[a] | 0.4057±0.030[a] | 0.1160±0.0338[a] | 0.1685±0.0103 |
| A | 15 | 0.3201±0.066[a] | 0.2917±0.045[a] | 0.1623±0.0246[a] | 0.1948±0.0319 |
| B | 15 | 0.3308±0.079[a] | 0.3380±0.103[a] | 0.2101±0.0342[a] | 0.1331±0.0071 |
| C | 15 | 0.1835±0.060[a] | 0.3939±0.0434[a] | 0.1884±0.0542[a] | 0.1757±0.0216 |
| D | 15 | 0.5022±0.149 | 0.1819±0.1049 | 0.4235±0.0727 | 0.1656±0.0145 |

[a]$P<0.05$ *vs* group D.

## DISCUSSION

It remains a problem to prevent cirrhosis or to control its progression in patients with a chronic liver disease[10,11]. Great efforts have been made to find safe and effective drugs. Recent clinical and experimental observations have demonstrated that Chinese medicines might be of some preventive and therapeutic values against fibrosis[12-20]. Ganyanping, prepared according to the regime of Li Shaobai *et al*[21], has been used for many years for this purpose. However, its effect and associated mechanism need further experimental evidence. For this reason, we used $CCl_4$ to induce liver fibrosis and investigated herein the effects of Ganyanping on fibrosis.

Liver fibrosis is a pathologic process associated with over production and deposition of collagen fibers[22, 23] and other extracellular matrix (ECM) components[24-27] resulted from various hepatic diseases. It is considered a necessary intermediate step between liver parenchyma injury and cirrhosis[28]. Activation of hepatic stellate cells (HSCs) has been shown to be one of the critical steps during hepatic fibrosis[29-34]. It is associated to a number of pathological factors, resulting in ECM deposition and hepatic fibrosis. This was also observed in the fibrosis caused by $CCl_4$ intoxication, and this process could be effectively controlled by treatment with Ganyanping. The preparation was found to be inhibitory in the collagen production.

MAO is used as a marker for evaluating hepatic function in cirrhosis, its elevation indicating liver damage[35]. An increase in MAO activity was observed in the intoxication group. Ganyanping was found to be able to abrogate this change. Thus, Ganyanping is considered to have some anti-cirrhotic effect. SDH is a rate-limiting enzyme in the tricarboxylic acid cycle[36,37]. The elevation of its activities reflects more active metabolism. Our data indicate the treatment with Ganyanping might be helpful for liver parenchyma cells to

maintain this SDH activity through the intoxication. The treatment was also shown to be helpful for stabilizing the lysosome membrane in chronic hepatic injury, reflected by its interference to ACP values of the animals received intoxication. In the present study, activity of NOS was shown to be reduced in the $CCl_4$-intoxicated group, but the effect was partially abrogated by the treatment with Ganyanping, indicating that the treatment might help the liver to recover its function through the stress caused by $CCl_4$ administration.

In summary, Ganyanping was found to play some anti-fibrotic role. According to the theory of traditional Chinese medicine, Ganyanping may possess multiple pharmaceutical effects, such as invigorating "qi" and activating "blood", dispersing stagnated hepatic "qi" and facilitating the discharge of "bile", delivering "heat" and "toxins", and eliminating "dampness" in view of its composition. Our experimental data have proved that Ganyanping could reduce oxygen-derived free radicals, and enhance the cellular metabolism and immune function, all resulting in an anti-fibrotic effect. Ganyanping may be used as a safe and effective preparation for patients with fibrosis.

## REFERENCES


1 **Li XG,** Li SB, Wang TC, Tang WX, Du LJ, Zhang WY. Protective Effect of Gan Yanping on Con A induced liver injury. *Zhonghua Ganzangbing Zazi* 1996; **4**: 243-244

2 **Tang WX**, Yu DX, Dan ZL, Zhang WY, Du LJ, Li SB. Study on protective effect of Traditional Chinese herbs (Gan Yanping) on acute liver injury induced by D-GalN in rats. *Tongji Yike Daxue Xuebao* 1998; **27**: 56-58

3 **Tang WX**, Yu DX, Dan ZL, Du LJ, Zhang WY, Li SB. An experimental study on the effect of Gan Yanping on Collagen Fiber in rat Chronic Liver Induced by $CCl_4$. *Weichang Bingxue He Ganbingxue Zazhi* 1998; **7**: 167-169

4 **Du LJ**, Tang WX, Dan ZL, Zhang WY, Li SB. Protective effect of gan yanping on $CCl_4$ induced liver fibrosis in rats. *Shijie Huaren Xiaohua Zazhi* 1998; **6**: 22-23

5 **Du LJ**, Tang WX, Dan ZL, Zhang WY, Li SB. Study of protective effect of GanYanping in acute liver injury model. *Tongji Yike Daxue Xuebao* 1997; **26**: 149-151

6 **Tang WX**, Du LJ, Zhang WY, Xiong XK, Zhang Y. Histochemistry study on the protective effect of Gan Yanping from liver injury induced by D-GalN in rats. *Zhongguo Zuzhi Huaxue He Xibao Huaxue Zazhi* 1996; **5**: 397-340

7 **Wei HS**, Li DG, Lu HM, Zhan YT, Wang ZR, Huang X, Zhang J, Chang JL, Xu OF. Effects of AT1 receptor antagonist, losartan, on rat hepatic induced by $CCl_4$. *World J Gastroenterol* 2000; **6**: 540-545

8 **Pen CN**, Wang Y, Niu JZ, Weng JG, Shi SS, Shun PW, Piao YJ, Li SG, She Y, Guo SG, Peng JY, Ge ZH, Xie JY, Xiong XK. Histochemistry.1. Beijing: People's Medical Publishing Company 2001: 392-528

9 **Punkt K**, Zaitsev S, Vwllner M, Schreiter T, Fitzl G, Buchwalow LB. Myopathy-dependent changes in activity of ATPase SDH and GPDH and NOS expression in the different fibre types of hamster muscles. *Acta histochem* 2002; **104**: 15-22

10 **Zeng MD**. Treatment of liver fibrosis. *Zhonghua Ganzhangbing Zazhi* 2001; **9**: 68-69

11 **Dai WJ**, Jiang HC. Advances in gene therapy of liver cirrhosis: a review. *World J Gastroenterol* 2001; **7**: 1-8

12 **Zheng LN**, Han T, Wang BE, Ma XM, Jia JD, Qian SC, Gao YT. Effect of Bupleurum on collagen content in hepatic stellate cell media *in vitro*. *Tianjing YiKe Daxue Xuebao* 2001; **7**: 502-504

13 **Cheng ML**, Wu YY, Huang KF, Luo TY, Ding YS, Lu YY, Liu RC, Wu J. Clinical study on the treatment of liver fibrosis due to hepatitis B by IFN-$\alpha$1 and traditional medicine preparation. *World J Gastroenterol* 1999; **5**: 267-269

14 **Liu P**, Liu C, Xu LM, Xue HM, Liu CH, Zhang ZQ. Effects of Fuzheng Huayu 319 recipe on liver fibrosis in chronic hepatitis B. *World J Gastroenterol* 1998; **4**: 348-353

15 **Li JM**. Recent condition of traditional chinese herb on treatment of fibrosis. *Tianjing Zhongyi Xueyuan Xuebao* 2002; **21**: 37-38

16 **Cai DY**, Zhao G, Chen JC, Ye GM, Bing FH, Fan BW. Therapeutic effect of Zijin capsule in liver fibrosis in rats. *World J Gastroenterol* 1998; **4**: 260-263

17 **Li JC**, Ding SP, Xu J. Regulating effect of Chinese herbal medicine on the peritoneal lymphatic stomata in enhancing ascites absorption of experimental hepatofibrotic mice. *World J Gastroenterol* 2002; **8**: 333-337

18 **Liu P**, Hu YY, Liu C, Zhu DY, Xue HM, Xu ZQ, Xu LM, Liu CH, Gu HT, Zhang ZQ. Clinical observation of salvianolic acid B in treatment of liver fibrosis in chronic hepatitis B. *World J Gastroenterol* 2002; **8**: 679-685

19 **Shen BS**, Wong XG, Qiao HC, Lu ZH, Han Q, Wang W, Guan HL. Preventive effect of Sanjia Yigan granule in hepatofibrosis in rats. *Shijie Huaren Xiaohua Zazhi* 1998; **6**: 386-388

20 **Liu CH**, Hu YY, Wang XL, Liu P, Xu LM. Effects of salvianolic acid-A on NIH/3T3 fibroblast proliferation, collagen synthesis and gene expression. *World J Gastroenterol* 2000; **6**: 361-364

21 **Du LJ,** Tang WX, Zhang WY, Li SB. Effect of Gan Yanping on Cytokines in acute liver injury induced by D-GalN in rats. *Zhongxiyi Jiehe Ganbingxue Zazhi* 1998; **8**: 28-30

22 **Wang AM**, Wang BE, Yang YW, Zhang B, Jiang LA, Du SC. Interstitial collagenase gene expression in patients with liver disease. *Linchuang Gandanbing Zazhi* 2000; **16**: 90-91

23 **Nie QH**, Cheng YQ, Xie YM, Zhou YX, Cao YZ. Inhibiting effect of antisense oligonucleotides phosphorthioate on gene expression of TIMP-1 in rat liver fibrosis. *World J Gastroenterol* 2001; **7**: 363-369

24 **Wang TL**, Wang BE, Zhang HH, Liu X, Dan ZP, Zhang J, Ma H, Li XM, Li NZ. Pathology study of the therapeutic effect on HBV-related liver fibrosis with herbal compound 861. *Zhongguo Weichang Bingxue He Ganbingxue Zazhi* 1998; **7**: 148-150

25 **Wang TL**, Zhang B, Jie J. Effect of anti-fibrosis compound on collagen expression of hepatic cells in experimental liver fibrosis of rats. *World J Gastroenterol* 2000; **6**: 877-880

26 **George J**, Rao KR, Stem R, Chandrakasan G. Dimethylnitrosamine-induced liver injuryin rats: the early deposition of collagen. *Toxicology* 2001; **156**: 129-138

27 **Wang BE**. Heptic stellate cell and Fibrosis. *Zhonghua Ganzhangbing Zazhi* 2000; **8**: 197-199

28 **Wang GY**, Cai WM, Wang JQ, Weng HR, Cheng F. An experimental study of histological quantitative method in the diagnosis of hepatic fibrosis. *Zhonghua Ganzhangbing Zazhi* 1998; **6**: 201-202

29 **Cheng ML**, Wu J, Wang HQ, Xue LM, Tan YZ, Ping L, Li CX, Huang NH, Yao YM, Ren LZ, Ye L, Li L, Jia ML. Effect of Maotai liquor in inducing metallothioneins and on hepatic stellate cells. *World J Gastroenterol* 2002; **8**: 520-523

30 **Wei HS**, Lu HM, Li DG, Zhan YT, Wang ZR, Huang X, Cheng JL, Xu QF. The regulatory role of AT 1 receptor on activated HSCs in hepatic fibrogenesis: effects of RAS inhibitors on hepatic fibrosis induced by CCl4. *World J Gastroenterol* 2000; **6**: 824-828

31 **Zhan YT**, Zhan CY, Chen YW, Li DG. Heptic stellate cell and Fibrosis. *Linchuang Gandanbing Zazhi* 2000; **16**: 71-73

32 **Lou Y**, Dai LL, Shen DM. Research progress of hepatic stellate cell and fibrosis. *Zhonghua Ganzhangbing Zazhi* 2000; **8**: 251-252

33 **Liu J**, Zhao FD, Jia SJ, Han QR. The study of VG staining for liver fibrosis of chrionic liver diseases. *Jilin Yixueyuan Xuebao* 1998; **18**: 21-22

34 **Ma H**, Wang BE, Ma XM, Jia JD. Effect of compound 861 on rat hepatic cell collagen synthesis and degradation *in vitro*. *Zhonghua Ganzhangbing Zazhi* 1999; **7**: 30-32

35 **Wang W**, Liu HL. Significance and change of HA, LN and MAO of hepatitis B patients' serum. *Bao Tou Yixue Zazhi* 2001; **17**: 41-42

36 **Shah V,** Toruner M, Haddad F, Cadelina G, Papapetropoulos A, Choo K, Sessa WC, Groszmann RJ. Impaired endothelial nitric oxide synthase activity associated with enhanced caveolin binding in experimental cirrhosis in the rat. *Gastroenterology* 1999; **117**: 1222-1228

37 **Song BC**, Yin SY, Tang WX, Xiong XK. Study on enzyme histochemistry of experimental cirrhosis liver. *Zhongguo Zuzhi Huaxue he Xibao Huaxue Zazhi* 1999; **8**: 47-50


**Edited by** Su Q

P.O.Box 2345, Beijing 100023,China
Fax: +86-10-85381893
E-mail: wjg@wjgnet.com www.wjgnet.com

World J Gastroenterol 2003;9(6):1296-1301
World Journal of Gastroenterology
Copyright ©2003 by The WJG Press ISSN 1007-9327

• BASIC RESEARCH •

# NF-κB activation and zinc finger protein A20 expression in mature dendritic cells derived from liver allografts undergoing acute rejection

Ming-Qing Xu, Wei Wang, Lan Xue, Lv-Nan Yan

**Ming-Qing Xu, Wei Wang, Lv-Nan Yan,** Department of General Surgery, West China (Huaxi) Hospital, Sichuan University, Chengdu 610041, Sichuan Province, China
**Lan Xue,** 208 PLA Hospital, Changchun 130021, Jilin Province, China
**Correspondence to:** Dr Ming-Qing Xu, Department of General Surgery, West China Hospital, Sichuan University, Chengdu 610041, Sichuan Province, China. xumingqing@hotmail.com
**Telephone:** +86-28-85582968
**Received:** 2002-12-22 **Accepted:** 2003-02-16

## Abstract

**AIM:** To investigate the role of NF-κB activation and zinc finger protein A20 expression in the regulation of maturation of dendritic cells (DCs) derived from liver allografts undergoing acute rejection.

**METHODS:** Sixty donor male SD rats and sixty recipient male LEW rats weighing 220-300 g were randomly divided into whole liver transplantation group and partial liver transplantation group. Allogeneic (SD rat to LEW rat) whole and 50 % partial liver transplantation were performed. DCs from liver grafts 0 hour and 4 days after transplantation were isolated and propagated in the presence of GM-CSF *in vitro*. Morphological characteristics and phenotypical features of DCs propagated for 10 days were analyzed by electron microscopy and flow cytometry, respectively. NF-κB binding activity, IL-12p70 protein and zinc finger protein A20 expression in these DCs were measured by EMSA and Western blotting, respectively. Histological grading of rejection was determined.

**RESULTS:** Allogeneic whole liver grafts showed no signs of rejection on day 4 after the transplantation. In contrast, allogeneic partial liver grafts demonstrated moderate to severe rejection on day 4 after the transplantation. After propagation for 10 days in the presence of GM-CSF *in vitro*, DCs from allogeneic whole liver grafts exhibited features of immature DC with absence of CD40 surface expression, these DCs were found to exhibit detectable but very low level of NF-κB activity, IL-12 p70 protein and zinc finger protein A20 expression. Whereas, DCs from allogeneic partial liver graft 4 days after transplantation displayed features of mature DC, with high level of CD40 surface expression, and as a consequence, higher expression of IL-12p70 protein, higher activities of NF-κB and higher expression of zinc finger protein A20 compared with those of DCs from whole liver grafts ($P<0.001$).

**CONCLUSION:** These results suggest that A20 expression is up-regulated in response to NF-κB activation in mature DCs derived from allogeneic liver grafts undergoing acute rejection. Given the NF-κB inhibition function of this gene, it is suggested that their expression survives to limit NF-κB activation and maturation of DCs, and consequently inhibits the acute rejection and induces acceptance of liver graft.

Xu MQ, Wang W, Xue L, Yan LN. NF-κB activation and zinc finger protein A20 expression in mature dendritic cells derived from liver allografts undergoing acute rejection. *World J Gastroenterol* 2003; 9(6): 1296-1301
http://www.wjgnet.com/1007-9327/9/1296.asp

## INTRODUCTION

Dendritic cells (DCs) are specialized antigen-presenting cells (APCs) that play an essential role in the activation of lymphocytes[1-10]. Among APCs, which also include macrophages and B cells, only DCs are believed to be capable of activating naive T cells. DC function is regulated by their state of maturation. Immature DCs resident in nonlymphoid tissues such as normal liver are deficient at antigen capture and progressing processing[11, 12]. "Maturation" of DC can be induced by microbial stimuli, proinflammatory cytokines, as well as through interaction with CD40L-CD40 cross-linking[13-20]. The control of DC maturation and activation plays an important role in regulating their T cell priming functions[21]. Significantly, engagement of CD40 expressed on DCs with CD40L expressed on T cells not only stimulates maturation and cytokine production but also enhances DC survival and activation[19, 22, 23]. Mature DCs are highly immunogenic due to high levels of expression of MHC I and II, costimulatory and adhesion molecules, including B7-1, B7-2, CD40, and ICAM-1[11-19]. In the case of experimental skin, heart, or kidney allografts, mature dendritic cells resident in donor tissue have been implicated as the principal instigators of rejection. Whereas, DCs derived from normal liver display an immature phenotype with absence of costimulatory molecules (CD40, CD80 and CD86) surface expression, low levels of MHC class I and II, and as a consequence, low stimulatory capacity for naive allogeneic T cells. Unlike mature DC, these liver-derived immature DCs do not induce detectable levels of intracytoplasmic IFN-γ in allogeneic $CD4^+$ cells in 72-h MLR, and elicite very low levels of CTLs *in vitro*[11, 12]. It has been observed that liver-derived[11, 24] or bone marrow-derived immature DCs[25], propagated *in vitro* and lacking surface costimulatory molecules, can prolong heart or pancreatic islet allograft survival. Whereas, marked augmentation of DCs numbers and maturation of DCs in liver allografts by donor treatment with the hematopoietic growth factor fms-like tyrosine kinase 3 (Flt3) ligand (FL) results in acute liver graft rejection[26, 27].

Although the significance of DCs as regulators of transplantation immunity is beyond doubt, little is known about intracellular mechanisms specifically responsible for regulation of DC activation and maturation. Previous studies have suggested that NF-κB may play a key role in DC maturation[20, 28-30], and NF-κB inhibition could impair the maturation and function of DC[28, 29].

A20 is a zinc finger protein originally identified as a TNF-

inducible gene product in endothelial cells (EC), and has been shown to be dependent upon NF-κB for its expression. A20 is expressed in a variety of cell types including fibroblasts, B, T, and β-cells in response to different stimuli including LPS, IL-1 and CD40 cross-linking[31-36]. A20 is itself a NF-κB-dependent gene and is part of a negative regulatory loop critical for modulation of cell activation[37, 38]. A20 serves a broad cytoprotective function in EC by protecting EC from apoptosis and down-regulating inflammatory responses via NF-κB inhibition[39]. $A20^{-/-}$ knock-out mice are born cachectic and die within 3 weeks from severe and uncontrolled inflammation that further confirms the potent anti-inflammatory function of A20[40]. A20 is also part of the physiologic NF-κB-dependent survival response of hepatocytes to injury, limited expression of A20 in hepatocytes drastically improves the fate of mice in the D-gal/LPS model of toxic FHF where A20 protects hepatocytes from apoptosis and promotes the liver regeneration [37]. In addition, investigation has shown that A20 expression is up-regulated in human renal allografts in response to immune injury inferred by acute rejection, and the result suggests that A20 could limit graft injury[41].

Although A20 is a very effective inhibitor of NF-κB activation induced by LPS, IL-1 and CD40 cross-linking, little is known about the role of A20 in the regulation of maturation of DCs derived from allogeneic liver grafts accompanied by acute rejection.

The purpose of the present study was to investigate the binding activity of NF-κB DNA and A20 expression in mature DCs derived from allogeneic partial liver grafts undergoing acute rejection in rats. Attempts were made also to correlate A20 expression in DCs derived from liver grafts with the acceptance of allogeneic liver grafts.

## MATERIALS AND METHODS

### *Animals*

Sixty donor male SD rats and sixty recipient male LEW rats weighing 220-300 g were randomly divided into whole liver transplantation group and partial liver transplantation group. Allogeneic whole and 50 % partial liver transplantation were performed using a SD to LEW combination. The animals were purchased from Chinese Academy of Sciences and Sichuan University. They were maintained with a 12-hour light/dark cycle in a conventional animal facility with water and commercial chow provided ad libitum, with no fasting before the transplantation.

### *Liver transplantation*

All operations were performed under ether anesthesia in clean but not sterile conditions. All surgical procedures were performed from 8 a.m to 5 p.m . Donors and recipients of similar weight (±10 g) were chosen. Liver reduction was achieved by removing the left lateral lobe and the two caudate lobes, which resulted in a 50 % reduction of the liver mass. Whole liver transplantation (WLT) and partial liver transplantation (PLT) were performed according to the method described in our previous study[42].

### *Histology*

Part of liver tissues was sectioned and preserved in 10 % formalin, embedded in paraffin, cut with microtome, and stained with hematoxylin and eosin. The histological grading of rejection was determined according to the criteria described by Williams.

### *Propagation and purification of liver graft-derived DC populations*

DCs from liver graft 0 hour and 4 days after the transplantation were propagated in GM-CSF from nonparenchymal cells (NPC) isolated from collagenase-digested liver graft tissue, as described by Lu *et al*[24]. Nonadherent cells, released spontaneously from proliferating cell clusters, were collected after culture for 10 days, and purified by centrifugation 500 ×g, for 10 minutes at room temperature on a 16 % w/v metrizamide gradient (DC purity 80-85 %).

### *Morphological and phenotypical features of DCs*

Morphological characteristics of DCs derived from liver graft were observed by electron microscopy. Expression of cell surface molecules was quantitated by flow cytometry as described in our previous study[42]. Aliquots of $2\times10^5$ DCs propagated for 10 days *in vitro* were incubated with the following primary mouse anti - rat mAbs against OX62, CD40 (Serotec, USA), or rat IgG as an isotype control for 60 minutes on ice (1 μg/ml diluted in PBS/1.0 % FCS). The cells were washed with PBS/1.0 % FCS and labeled with FITC-conjugated goat anti-mouse IgG, diluted 1/50 in PBS/1.0 % FCS for 30 minutes on ice. At the end of this incubation, cells were washed, propidium iodide/PBS were added, and the cells were subsequently analyzed in an FACS-4200 flow cytometer (Becton-Dikison, USA).

### *Isolation of nuclear proteins*

Nuclear proteins were isolated from DCs extract by placing the sample in 0.9 ml of ice-cold hypotonic buffer [10 mM· $L^{-1}$ HEPES (pH7.9), 10 mM· $L^{-1}$ KCl, 0.1 mM· $L^{-1}$ EDTA, 0.1 mM· $L^{-1}$ ethylene glycol tetraacetic acid, 1 mM· $L^{-1}$ DTT; Protease inhibitors (aprotinin, pepstatin, and leupeptin, 10 mg· $L^{-1}$ each)]. The homogenates were incubated on ice for 20 minutes, vortexed for 20 seconds after adding 50 μl of 10 % Nonide-P40, and then centrifuged for 1 minutes at 4 ℃ in an Eppendorf centrifuge. Supernatants were decanted, the nuclear pellets after a single wash with hypotonic buffer without Nonide-P40 were suspended in an ice-cold hypertonic buffer [20 mM· $L^{-1}$ HEPES(pH7.9), 0.4 M· $L^{-1}$ NaCl, 1 mM· $L^{-1}$ EDTA,1 mM· $L^{-1}$ DTT; Protease inhibitors], incubated on ice for 30 minutes at 4 ℃, mixed frequently, and centrifuged for 15 minutes at 4 ℃. The supernatants were collected as nuclear extracts and stored at -70 ℃. Concentrations of total proteins in the samples were determined according to the method of Bradford.

### *Electrophoretic mobility shift assay (EMSA) for NF-kB activation of DCs*

NF-κB binding activity was performed in a 10-μl binding reaction mixture containing 1×binding buffer [50 mg· $L^{-1}$ of double-stranded poly (dI-dC), 10 mM· $L^{-1}$ Tris-HCl (pH7.5), 50 mM· $L^{-1}$ NaCl, 0.5 mM· $L^{-1}$ EDTA, 0.5 mM· $L^{-1}$DTT, 1 mM· $L^{-1}$ $MgCl_2$, and 100 ml· $L^{-1}$ glycerol], 5 μg of nuclear protein, and 35 fmol of double-stranded NF-κB consensus oligonucleotide (5' -AGT TGA GGG GAC TTT CCC AGG-3' ) that was endly labeled with γ-$^{32}$P (111TBq $mM^{-1}$ at 370 $GBq^{-1}$) using T4 polynucleotide kinase. The binding reaction mixture was incubated at room temperature for 20 minutes and analyzed by electrophoresis on 7 % nondenaturing polyacrylamide gels. After electrophoresis, the gels were dried by Gel-Drier (Biol-Rad Laboratories, Hercules, CA) and exposed to Kodak X-ray films at -70 ℃.

### *Western blotting for IL-12 p70 and zinc finger protein A20 expression in DCs*

DCs cultured for 10 days *in vitro* were starved in serum-free medium for 4 hours at 37 ℃. These cells were washed twice in cold PBS, resuspended in 100 μl lysis buffer (1 % Nonidet -P40, 20 mM Tris-HCl, pH8.0, 137 mM NaCl, 10 % glycerol,

2 mM EDTA, 10 μg· $mL^{-1}$ leupeptin, 10 μg· $mL^{-1}$ aprotinin, 1mM PMSF, and 1 mM sodium orthovanadate), and total cell lysates were obtained. The homogenates were centrifuged at 10 000×g for 10 minutes at 4 ℃. Cell lysates (20 μg) were electrophoresed on SDS-PAGE gels, and transferred to PVDC membranes for Western blot analysis. Briefly, PVDC membranes were incubated in a blocking buffer for 1 hour at room temperature, then incubated for 2 hours with Abs raised against IL-12 p70 and A20 (Santa Cruz, CA). The membranes were washed and incubated for 1 hour with HRP-labeled IgG. Immunoreactive bands were visualized by ECL detection reagent. The binding bands were quantified by scanning densitometer of a Bio-Image Analysis System. The results were expressed as relative optical density.

### *Statistics analysis*

Statistic analysis of data was performed using the Student' s *t*-test; $P<0.05$ was considered statistically significant.

## RESULTS

### *Histological rejection*

Histological rejection features of allografted livers were compared between the whole and partial groups on day 4 after the transplantation, allogeneic whole liver grafts demonstrated no rejection. In contrast, partial liver grafts demonstrated moderate to severe rejection, including inflammatory cellular infiltration in the portal tract, endotheliitis, bile duct damage and hepatocytes necrosis.

### *Phenotypic characteristics of liver graft-derived DCs propagated in vitro*

As shown in our previous study[42], after cultured for 10 days in the presence of GM-CSF, DCs both from whole and partial liver grafts displayed typical morphological features of DC, including anomalous shape, bigger body, and numerous longer dendrites. Flow cytometry showed 80-85 % of these DCs strongly expressed rat DC - specific OX62 antigen molecule, which suggested that high purity DCs were obtained. Flow cytometric analysis showed that DCs from whole liver grafts and from partial liver grafts 0 hour after the transplantation were negative for the costimulatory molecule CD40 expression, which was an immature phenotype ($CD40^-$), whereas DCs from partial liver graft 4 days after the transplantation showed high level of CD40 expression, which was a mature phenotype($CD40^+$). These results suggested maturation of DCs resident in allogeneic partial liver graft undergoing acute rejection.

### *IL-12 p70 protein expression in DCs derived from allogeneic partial liver grafts*

Our previous study showed that IL-12 p35 and IL-12 p40 subunit expressions were significantly up-regulated in mature DCs derived from allogeneic partial liver grafts undergoing acute rejection[42]. In the present study, we evaluated IL-12 p70 expression in DCs from allogeneic liver grafts. As shown in Figure 1, DCs derived from both whole and partial liver grafts 0 hour after the transplantation expressed detectable but very low level of IL-12 p70, and expression level of IL-12 p70 in DCs from whole liver graft 4 days after transplantation was not elevated compared with those of DCs from whole liver graft 0 hour after the transplantation ($P>0.05$). However, expression of IL-12 p70 in DCs from partial liver graft 4 days after transplantation was markedly increased, and their expression levels were significantly higher than those of DCs both from partial liver graft 0 hour and whole liver graft 4 days after transplantation ($P<0.001$).

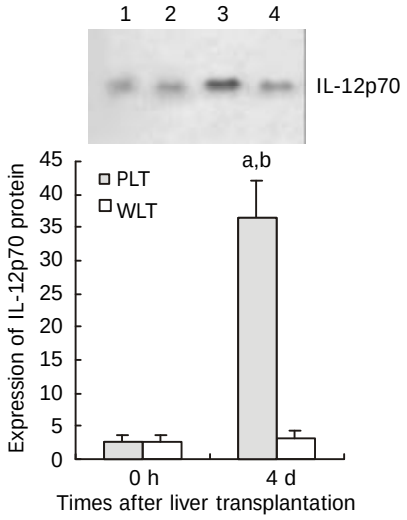


**Figure 1** Expression of IL-12 p70 in liver graft - derived DCs by Western blotting. Lanes 1, 2: Expression of IL-12 p70 in DCs from partial liver graft and whole liver graft 0 hour after transplantation. Lanes 3, 4: Expression of IL-12 p70 in DCs from partial liver graft and whole liver graft 4 days after transplantation. [a]$P<0.001$ *vs* 4d WLT group ; [b]$P<0.001$ *vs* 0 hour PLT group.

### *Electrophoretic mobility shift assay (EMSA) for NF-κB activation of DCs*

As shown in Figure 2, EMSA analysis showed detectable but very low level of NF-κB activity of DCs derived from both whole and partial liver grafts 0 hour after transplantation, and NF-κB activity of DCs from whole liver graft 4 days after transplantation was not increased compared with those of DCs from liver graft 0 hour after transplantation ($P>0.05$). However, NF-κB activity of DCs from partial liver graft 4 days after transplantation was significantly elevated compared with those of DCs from partial liver graft 0 hour and whole liver graft 4 days after transplantation ($P<0.001$).

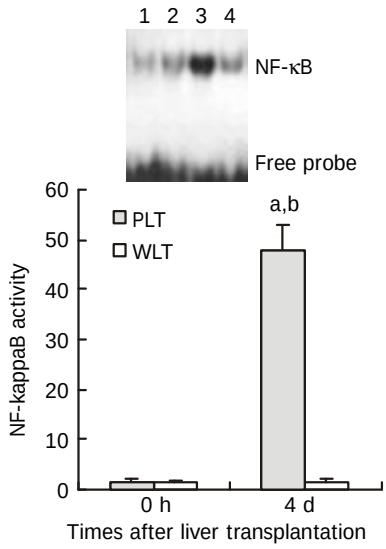


**Figure 2** NF-κB activation of DCs derived from allogeneic liver grafts. Lanes 1, 2: NF-κB activation of DCs from partial liver graft and whole liver graft 0 hour after transplantation. Lanes 3, 4: NF-κB activation of DCs from partial liver graft and whole liver graft 4 days after transplantation. [a]$P<0.001$ *vs* 4 d WLT group; [b]$P<0.001$ *vs* 0 hour PLT group.

### *A20 protein expression in DCs derived from partial liver allografts*

In order to investigate the intracellular mechanisms specifically

responsible for regulation of DC activation and maturation, we evaluated NF-κB inhibitor zinc finger protein A20 expression in DCs derived from allogeneic liver grafts. As shown in Figure 3, DCs from both whole and partial liver grafts 0 hour after the transplantation expressed detectable but very low level of A20, and expression level of A20 in DCs derived from whole liver graft 4 days after transplantation was not increased compared with those of DCs from whole liver graft 0 hour after transplantation ($P$>0.05). However, expression of A20 in DCs from partial liver graft 4 days after transplantation was markedly up-regulated, and its expression level was significantly higher than those of DCs both from partial liver graft 0 hour and whole liver graft 4 days after transplantation ($P$<0.001).

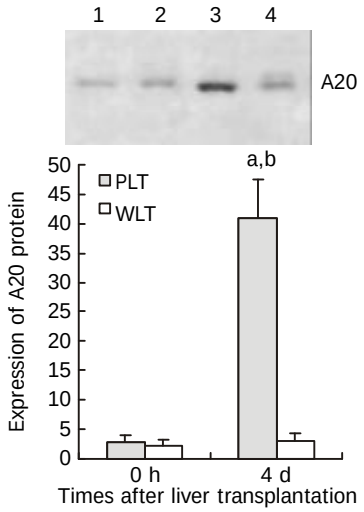


**Figure 3** Expression of A20 protein in DCs derived from allogeneic liver grafts. Lanes 1, 2: Expression of A20 protein in DCs from partial liver graft and whole liver graft 0 hour after transplantation. Lanes 3, 4: Expression of A20 protein in DCs from partial liver graft and whole liver graft 4days after transplantation. [a]$P$<0.001 *vs* 4 d WLT group; [b]$P$<0.001 *vs* 0 hour PLT group.

## DISCUSSION

Despite the emergence of DCs as key cellular players in the immune system, the signal transduction events that regulate DC maturation and function have been poorly understood. This study was conducted to explore whether NF-κB activation and its inducible expression gene of A20 could be detected in mature DCs derived from liver allograft undergoing acute rejection. Our aim was to determine whether A20 gene is involved in NF-κB inhibition of these mature DCs. In the present study, it has been shown that engagement of CD40 on DCs derived from allogeneic partial liver grafts undergoing acute rejection leads to a powerful NF-κB activation of these mature DCs, and as a consequence, leads to high level expression of the protective gene A20 in these DCs. Expression of this gene in mature DCs derived from liver graft undergoing acute rejection is consistent with their known potential to be induced in response to NF-κB activation.

It has been shown that DCs derived from allogeneic partial liver grafts undergoing acute rejection displayed mature phenotypic high level CD40 expression and NF-κB activation. Although resting DCs residing in normal liver tissues display only low levels of CD40, B7, and MHC class II molecule expression[11, 12, 24]. The ischemia/reperfusion injury which is consecutive to the transplantation procedure will rapidly activate them. In addition, partial hepatectomy has been reported to induce the expression of MHC II on Kupffer cell. Interstitial dendritic cells and sinusoidal endothelium in rats, together with the up-regulated TNF-α production after partial hepatectomy would induce the expression of B7 and CD40 molecules on DCs[16]. These factors could stimulate maturation of DCs derived from partial liver grafts. These mature DCs may contribute to the allogeneic liver graft rejection induction. Previously other studies showed that mature DC could provide signals able to trigger T cell proliferation after TCR engagement[43, 44]. These accessory, or "costimulatory" signals, are consecutive to interactions between costimulatory molecules present on activated DC such as B7, CD40, and OX40-ligand and their respective counter-receptors, CD28, CD40-ligand, and OX40, on T cell membranes. Several intracellular signals follow the engagement of costimulatory molecules. Interactions of CD40L, CD28, and OX40 with their ligands on DCs activate the transcription factor NF-κB in both T cells and DCs[29, 30]. In turn, NF-κB initiates the transcription of numerous genes involved in immune activation, such as chemokines and cytokines[20, 30], and also of costimulatory molecules themselves. For instance, CD40 ligation on the APC will up-regulate its expression of B7 molecules. This initiates positive feedback loops ultimately contributing to T cell expansion[45]. Among the costimulatory molecules, CD40 and B7 seem to play a crucial role in alloreactive responses. Indeed, blockade of both CD40 and B7 molecules at the time of transplantation prevents allograft rejection and induces alloreactive T cell anergy[46, 47]. In the present study, DCs derived from allogeneic partial liver grafts undergoing acute rejection demonstrated high level expression of CD40, which could interact with the CD40-ligand on T cells, leading to a powerful NF-κB activation and high level of IL-12p70 expression in these mature DCs. Given an essential role for NF-κB transcription in LPS- and CD40L - induced expression of IL-12 (IL-12 p35, p40 and p70) in DCs[20], IL-12 is a key inducer of liver graft rejection[26], together with high level of IL-12 p35 and IL-12 p40 protein expression in the mature DCs derived from allogeneic liver grafts undergoing acute rejection[42]. Our results suggest that NF-κB may play a key role in the maturation of DCs derived from allogeneic liver grafts undergoing acute rejection.

To provide further insights into potential intracellular mechanisms responsible for maturation regulation of DCs derived from allogeneic liver grafts undergoing acute rejection, we measured the protective A20 gene expression in these DCs. Zinc finger protein A20 is a potent inhibitor of NF-κB[31], and although other studies have shown A20 is mainly expressed in endothelial and infiltrating mononuclear cells of human renal allografts undergoing acute rejection[41], little is known about whether it is also involved in the regulation of DC maturation and activation. Our results first demonstrate that high level A20 expression is detected in the mature DCs (which presente significant NF-κB activation) derived from acute rejecting liver allografts, but few A20 is detected in the immature DCs (which present few NF-κB activation) derived from nonrejecting liver allografts. Given A20 is itself a NF-κB - dependent gene and is part of a negative regulatory loop critical for modulation of cell activation[37, 38], together with NF-κB which may play a key role in the maturation of DCs derived from liver allografts undergoing acute rejection, it is suggested that A20 expression in these mature DCs derived from liver allografts undergoing acute rejection survives to inhibit NF-κB activation and to limit maturation of these DCs, and as a consequence to limit the graft rejection.

In summary, we demonstrate for the first time an association between NF-κB activation and expression of the protective gene A20 and maturation of DCs derived from liver allografts undergoing acute rejection. NF-κB binding activity and A20 expression in these mature DCs are strongly up-regulated in

response to acute rejection. NF-κB may play a key role in the maturation of DCs derived from allogeneic liver grafts undergoing acute rejection, and A20 expression in these mature DCs derived from liver allografts undergoing acute rejection survives to inhibit NF-κB activation and to limit maturation of these DCs.

## REFERENCES


1 **Zhang JK**, Chen HB, Sun JL, Zhou YQ. Effect of dendritic cells on LPAK cells induced at different times in killing hepatoma cells. *Shijie Huaren Xiaohua Zazhi* 1999; **7**: 673-675
2 **Li MS**, Yuan AL, Zhang WD, Chen XQ, Tian XH, Piao YT. Immune response induced by dendritic cells induce apoptosis and inhibit proliferation of tumor cells. *Shijie Huaren Xiaohua Zazhi* 2000; **8**: 56-58
3 **Luo ZB**, Luo YH, Lu R, Jin HY, Zhang BP, Xu CP. Immunohistochemical study on dendritic cells in gastric mucosa of patients with gastric cancer and precancerous lesions. *Shijie Huaren Xiaohua Zazhi* 2000; **8**: 400-402
4 **Li MS**, Yuan AL, Zhang WD, Liu SD, Lu AM, Zhou DY. Dendritic cells *in vitro* induce efficient and special anti-tumor immune response. *Shijie Huaren Xiaohua Zazhi* 1999; **7**: 161-163
5 **Wang FS**, Xing LH, Liu MX, Zhu CL, Liu HG, Wang HF, Lei ZY. Dysfunction of peripheral blood dendritic cells from patients with chronic hepatitis B virus infection. *World J Gastroenterol* 2001; **7**: 537-541
6 **Zhang JK**, Li J, Chen HB, Sun JL, Qu YJ, Lu JJ. Antitumor activities of human dendritic cells derived from peripheral and cord blood. *World J Gastroenterol* 2002; **8**: 87-90
7 **Tang ZH**, Qiu WH, Wu GS, Yang XP, Zou SQ, Qiu FZ. The immunotherapeutic effect of dendritic cells vaccine modified with interleukin-18 gene and tumor cell lysate on mice with pancreatic carcinoma. *World J Gastroenterol* 2002; **8**: 908-912
8 **Zhang J**, Zhang JK, Zhuo SH, Chen HB. Effect of a cancer vaccine prepared by fusions of hepatocarcinoma cells with dendritic cells. *World J Gastroenterol* 2001; **7**: 690-694
9 **Banchereau J**, Briere F, Caux C, Davoust J, Lebecque S, Liu YJ, Pulendran B, Palucka K. Immunobiology of dendritic cells. *Annu Rev Immunol* 2000; **18**: 767-811
10 **Banchereau J**, Steinman RM. Dendritic cells and the control of immunity. *Nature* 1998; **392**: 245-252
11 **Khanna A**, Morelli AE, Zhong CP, Takayama T, Lu LN, Thomson AW. Effects of liver-derived dendritic cell progenitors on Th1- and Th2-like cytokine responses *in vitro* and *in vivo*. *J Immunol* 2000; **164**: 1346-1354
12 **Morelli AE**, O'Connell PJ, Khanna A, Logar AJ, Lu LN,Thomson AW. Preferential induction of Th1 responses by functionally mature hepatic ($CD8\alpha^-$ and $CD8\alpha^+$) dendritic cells: association with conversion from liver transplant tolerance to acute rejection. *Transplantation* 2000; **69**: 2647-2657
13 **Hertz CJ**, Kiertscher SM, Godowski PJ, Bouis DA, Norgard MV, Roth MD, Modlin RL. Microbial lipopeptides stimulate dendritic cell maturation via Toll-like receptor 2. *J Immunol* 2001; **166**: 2444-2450
14 **Thoma-Uszynski S**, Kiertscher SM, Ochoa MT, Bouis DA, Norgard MV, Miyake K, Godowski PJ, Roth MD, Modlin RL. Activation of toll-like receptor 2 on human dendritic cells triggers induction of IL-12, but not IL-10. *J Immunol* 2000; **165**: 3804-3810
15 **Kaisho T**, Takeuchi O, Kawai T, Hoshino K, Akira S. Endotoxin-induced maturation of MyD- 88 deficient dendritic cells. *J Immunol* 2001; **166**: 5688-5694
16 **Kitamura H**, Iwakabe K, Yahata T, Nishimura S, Ohta A, Ohmi Y, Sato M, Takeda K, Okumura K, Van Kaer L, Kawano T, Taniguchi M, Nishimura T. The natural killer T (NKT) cell ligand alpha-galactosylceramide demonstrates its immunopotentiating effect by inducing interleukin (IL)-12 production by dendritic cells and IL-12 receptor expression on NKT cells. *J Exp Med* 1999; **189**: 1121-1128
17 **Nagayama H**, Sato K, Kawasaki H, Enomoto M, Morimoto C, Tadokoro K, Juji T, Asano S, Takahashi TA. IL-12 responsiveness and expression of IL-12 receptor in human peripheral blood monocyte-derived dendritic cells. *J Immunol* 2000; **165**: 59-66
18 **Visintin A**, Mazzoni A, Spitzer JH, Wyllie DH, Dower SK, Segal DM. Regulation of Toll-like receptor in human monocytes and dendritic cells. *J Immunol* 2001; **166**: 249-255
19 **Corinti S**, Albanesi C, la Sala A, Pastore S, Girolomoni G. Regulatory activity of autocrine IL-10 on dendritic cell functions. *J Immunol* 2001; **166**: 4312-4318
20 **Ouaaz F**, Arron J, Zheng Y, Choi Y, Beg AA. Dendritic cell development and survival require distinct NF-κB subunits. *Immunity* 2002; **16**: 257-270
21 **Josien R**, Li HL, Ingulli E, Sarma S, Wong BR, Vologodskaia M, Steinman RM, Choi Y. TRANCE, a tumor necrosis factor family member, enhances the longevity and adjuvant properties of dendritic cells *in vivo*. *J Exp Med* 2000; **191**: 495-502
22 **Miga AJ**, Masters SR, Durell BG, Gonzalez M, Jenkins MK, Maliszewski C, Kikutani H, Wade WF, Noelle RJ. Dendritic cell longevity and T cell persistence is controlled by CD154-CD40 interactions. *Eur J Immunol* 2001; **31**: 959-965
23 **Cella M**, Scheidegger D, Palmer-Lehmann K, Lane P, Lanzavecchia A, Alber G. Ligation of CD40 on dendritic cells triggers production of high levels of interleukin-12 and enhances T cell stimulatory capacity: T-T help via APC activation. *J Exp Med* 1996; **184**: 747-752
24 **Lu L**, Woo J, Rao AS, Li Y, Watkins SC, Qian S, Starzl TE, Demetris AJ, Thomson AW. Propagation of dendritic cell progenitors from normal mouse liver using granulocyte / macrophage colony-stimulating factor and their maturational development in the presence of type-1 collagen. *J Exp Med* 1994; **179**: 1823-1834
25 **Khanna A**, Steptoe RJ, Antonysamy MA, Li W, Thomson AW. Donor bone marrow potentiates the effect of tacrolimus on nonvascularized heart allograft survival: association with microchimerism and growth of donor dendritic cell progenitors from recipient bone marrow. *Transplantation* 1998; **65**: 479-485
26 **Li W**, Lu L, Wang Z, Wang L, Fung JJ, Thomson AW, Qian S. IL-12 antagonism enhances apoptotic death of T cells within hepatic allografts from Flt3 ligand-treated donors and promotes graft acceptance. *J Immunol* 2001; **166**: 5619-5628
27 **Steptoe RJ**, Fu F, Li W, Drakes ML, Lu L, Demetris AJ, Qian S, McKenna HJ, Thomson AW. Augmentation of dendritic cells in murine organ donors by Flt3 ligand alters the balance between transplant tolerance and immunity. *J Immunol* 1997; **159**: 5483-5491
28 **Rescigno M**, Martino M, Sutherland CL, Gold MR, Ricciardi-Castagnoli P. Dendritic cell survival and maturation are regulated by different signaling pathways. *J Exp Med* 1998; **188**: 2175-2180
29 **Verhasselt V**, Vanden Berghe W, Vanderheyde N, Willems F, Haegeman G, Goldman M. N-acetyl-L-cysteine inhibits primary human T cell responses at the dendritic cell level: association with NF-κB inhibition. *J Immunol* 1999; **162**: 2569-2574
30 **Mann J**, Oakley F, Johnson PW, Mann DA. CD40 induces interleukin-6 gene transcription in dendritic cells. *J Biol Chem* 2002; **277**: 17125-17138
31 **Zetoune FS**, Murthy AR, Shao Z, Hlaing T, Zeidler MG, Li Y, Vincenz C. A20 inhibits NF-kappa B activation downstream of multiple Map3 kinases and interacts with the I kappa B signalosome. *Cytokine* 2001; **15**: 282-298
32 **Klinkenberg M**, Van-Huffel S, Heyninck K, Beyaert R. Functional redundancy of the zinc fingers of A20 for inhibition of NF-kappaB activation and protein-protein interactions. *FEBS Lett* 2001; **498**: 93-97
33 **Hofer-Warbinek R**, Schmid JA, Stehlik C, Binder BR, Lipp J, de-Martin R. Activation of NF-kappa B by XIAP, the X chromosome-linked inhibitor of apoptosis, in endothelial cells involves TAK1. *J Biol Chem* 2000; **275**: 22064-22068
34 **Beyaert R**, Heyninck K, Van-Huffel S. A20 and A20-binding proteins as cellular inhibitors of nuclear factor-kappa B-dependent gene expression and apoptosis. *Biochem Pharmacol* 2000; **60**: 1143-1151
35 **Sarma V**, Lin Z, Clark L, Rust BM, Tewari M, Noelle RJ, Dixit VM. Activation of the B-cell surface receptor CD40 induces A20, a novel zinc finger protein that inhibits apoptosis. *J Biol Chem* 1995; **270**: 12343-12346
36 **Kupfner JG**, Arcaroli JJ, Yum HK , Nadler SG, Yang KY, Abraham E. Role of NF-kappaB in endotoxemia-induced alterations of lung

neutrophil apoptosis. *J Immunol* 2001; **167**: 7044-7051

37 **Heyninck K**, De Valck D, Vanden Berghe W, Van Criekinge W, Contreras R, Fiers W, Haegeman G, Beyaert R. The zinc finger protein A20 inhibits TNF-induced NF-κB-dependent gene expression by interfering with an RIP- or TRAF2-mediated transactivation signal and directly binds to a novel NF-κB-inhibiting protein ABIN. *J Cell Biol* 1999; **145**: 1471-1482

38 **Arvelo MB**, Cooper JT, Longo C, Daniel S, Grey ST, Mahiou J, Czismadia E, Abu-Jawdeh G, Ferran C. A20 protects mice from D-galactosamine/LPS acute toxic lethal hepatitis. *Hepatology* 2002; **35**: 535-543

39 **Ferran C**, Stroka DM, Badrichani AZ, Cooper JT, Wrighton CJ, Soares M, Grey ST, Bach FH. A20 inhibits NF-κB activation in endothelial cells without sensitizing to tumor necrosis factor-mediated apoptosis. *Blood* 1998; **91**: 2249-2258

40 **Lee EG**, Boone DL, Chai S, Libby SL, Chien M, Lodolce JP, Ma A. Failure to regulate TNF-induced NF-kappaB and cell death responses in A20-deficient mice. *Science* 2000; **289**: 2350-2354

41 **Avihingsanon Y**, Ma N, Csizmadia E, Wang C, Pavlakis M, Giraldo M, Strom TB, Soares MP, Ferran C. Expression of protective genes in human renal allografts: a regulatory response to injury associated with graft rejection. *Transplantation* 2002; **73**:1079-1085

42 **Xu MQ**, Yao ZX. Functional changes of dendritic cells derived from allogeneic partial liver graft undergoing acute rejection in rats. *World J Gastroenterol* 2003; **9**: 141-147

43 **Lechler R**, Ng WF, Steinman RM. Dendritic cells in transplantation: friend or foe? *Immunity* 2001; **14**: 357-368

44 **Matzinger P**. Graft tolerance: a duel of two signals. *Nat Med* 1999; **5**: 616-617

45 **Stout RD**, Suttles J. The many roles of CD40 in cell-mediated inflammatory responses. *Immunol Today* 1996; **17**: 487- 492

46 **Larsen CP**, Elwood ET, Alexander DZ, Ritchie SC, Hendrix R, Tucker-Burden C, Cho HR, Aruffo A, Hollenbaugh O, Linsley PS, Winn KJ, Pearson TC. Long-term acceptance of skin and cardiac allografts after blocking CD40 and CD28 pathways. *Nature* 1996; **381**: 434-438

47 **Kirk AD**, Harlan DM, Armstrong NN, Davis TA, Dong Y, Grag GS, Hong X, Thomas D, Fechner JH Jr, Knechtle SJ. CTLA4-Ig and anti-CD40 ligand prevent renal allograft rejection in primates. *Proc Natl Acad Sci USA* 1997; **94**: 8789-8794

**Edited by** Xu XQ

P.O.Box 2345, Beijing 100023,China
Fax: +86-10-85381893
E-mail: wjg@wjgnet.com www.wjgnet.com

World J Gastroenterol 2003;9(6):1302-1306
World Journal of Gastroenterology
Copyright ©2003 by The WJG Press ISSN 1007-9327

• BASIC RESEARCH •

# Celecoxib inhibits proliferation and induces apoptosis via prostaglandin $E_2$ pathway in human cholangiocarcinoma cell lines

Gao-Song Wu, Sheng-Quan Zou, Zheng-Ren Liu, Zhao-Hui Tang, Ju-Hua Wang

**Gao-Song Wu, Sheng-Quan Zou, Zheng-Ren Liu, Zhao-Hui Tang, Ju-Hua Wang,** Department of General Surgery, Tongji Hospital, Tongji Medical College, Huazhong University of Science and Technology, Wuhan, 430030, Hubei Province, China
**Correspondence to:** Gao-Song Wu, Department of General Surgery, Tongji Hospital, 1095 Jiefang Road, Wuhan, 430030, Hubei Province, China. wugaosong9172@sina.com
**Telephone:** +86-27-83662851 **Fax:** +86-27-83662851
**Received:** 2002-04-26 **Accepted:** 2002-06-11

## Abstract

**AIM:** To evaluate the roles and mechanisms of celecoxib in inducing proliferation inhibition and apoptosis of human cholangiocarcinoma cell lines.

**METHODS:** Cyclooxygenase-2-overexpressing human cholangiocarcinoma cell line QBC939 and cyclooxygenase-2-deficient human cholangiocarcinoma cell line SK-CHA-1 were used in the present study. The anti-proliferative effect was measured by methabenzthiazuron (MTT) assay; apoptosis was determined by transferase-mediated dUTP nick end labeling (TUNEL) detection and transmission electron microscopy (TEM). Cell cycle was analyzed by flow cytometry (FCM). The $PGE_2$ levels in the supernatant of cultured cholangiocarcinoma cells were quantitated by enzyme-linked immunoabsordent assay (ELISA).

**RESULTS:** Celecoxib suppressed the production of $PGE_2$ and inhibited the growth of QBC939 cells. Celecoxib at 10, 20, and 40 μmol/L inhibited $PGE_2$ production by 26 %, 58 %, and 74 % in QBC939 cells. The $PGE_2$ level was much lower constitutively in SK-CHA-1 cells (18.6±3.2) compared with that in QBC939 (121.9±5.6) cells ($P<0.01$) and celecoxib had no significant influence on $PGE_2$ level in the SK-CHA-1 cells. The $PGE_2$ concentration in SK-CHA-1 cells also reduced but not significantly after treatment with celecoxib. The $PGE_2$ concentration in SK-CHA-1 cells was (16.5±2.9) ng/well, (14.8±3.4) ng/well, (13.2±2.0) ng/well and (12.6±3.1) ng/well respectively, when pre-treated with 1 μmol/L, 10 μmol/L, 20 μmol/L and 40 μmol/L of celecoxib for 48 h ($P>0.05$, *vs* control). The anti-proliferation effect of celecoxib (20 μmol/L) on QBC939 cells was time-dependent, it was noticeable on day 2 (OD490=0.23±0.04) and became obvious on day 3 (OD490=0.31±0.07) to day 4 (OD490=0.25±0.06), and the OD490 in the control group (day 1) was 0.12±0.03 ($P<0.01$, *vs* control). The anti-proliferation effect of celecoxib could be abolished by the addition of 200 pg/mL $PGE_2$. The proliferation of SK-CHA-1 cells was inhibited slightly by celecoxib, the cell density OD490 in the presence of celecoxib and in control group was 0.31±0.04 and 0.42±0.03 respectively on day 2 ($P>0.05$), 0.58±0.07 and 0.67±0.09 respectively on day 3 ($P>0.05$), and 0.71±0.08 and 0.78±0.06 respectively on day 4 ($P>0.05$). Celecoxib induced proliferation inhibition and apoptosis by $G_1$-S cell cycle arrest: the percentage of QBC939 cells in $G_0$-$G_1$ phase after treatment with 40 μmol/L (74.66±6.21) and 20 μmol/L (68.63±4.36) celecoxib increased significantly compared with control cells (54.41±5.12, $P<0.01$). The percentage of SK-CHA-1 cells in $G_0$-$G_1$ phase after treatment with various concentrations of celecoxib didn't change significantly compared with control cells. The TUNEL index was much higher in QBC939 cells treated with 20 μmol/L celecoxib for 2 d (0.063±0.018) and for 4 d (0.102±0.037) compared with control cells (0.017±0.004, $P<0.01$).

**CONCLUSION:** The current *in vitro* study indicates that inhibition of proliferation and induction of apoptosis in human cholangiocarcinoma cells by cyclooxygenase-2 specific inhibitor celecoxib may involve in COX-dependent mechanisms and $PGE_2$ pathway. Celecoxib as a chemopreventive and chemotherapeutic agent might be effective primarily on COX-2-expressing cholangiocarcinoma.

Wu GS, Zou SQ, Liu ZR, Tang ZH, Wang JH. Celecoxib inhibits proliferation and induces apoptosis via prostaglandin $E_2$ pathway in human cholangiocarcinoma cell lines. *World J Gastroenterol* 2003; 9(6): 1302-1306
http://www.wjgnet.com/1007-9327/9/1302.asp

## INTRODUCTION

Prostaglandins (PGs) are important in the proliferation of various types of cancer cells[1-13]. PGs are synthesized by two isoforms of cyclooxygenase (COX) enzymes, COX-1 and COX-2, each of which displays distinct physiological profile. Inducible isozyme COX-2 has been shown to be important in carcinogenesis[14-26]. $PGE_2$ is the major metabolite of arachidonic acid in many human cells[27,28]. The selective COX-2 inhibitors are currently being evaluated for their effectiveness as chemopreventive and chemotherapeutic agents[29-32]. However, the effects of specific inhibitor of COX-2 on the proliferation of human carcinoma cells remain to be investigated. There are many controversies on whether or not these effects are mediated predominantly through the inhibition of COX-2 activity and prostaglandin synthesis[33]. Our previous studies have demonstrated that overexpression of COX-2 may play a crucial role in the carcinogenesis and development of extra-hepatic cholangiocarcinoma. In this study we aimed to explore the effects and mechanism of celecoxib and the role of $PGE_2$ in inducing proliferation inhibition and apoptosis of COX-2 overexpressing human cholangiocarcinoma cell line QBC939 and COX-2-deficient human cholangiocarcinoma cell line SK-CHA-1.

## MATERIALS AND METHODS

### *Materials*

Human extra-hepatic cholangiocarcinoma cells SK-CHA-1 were a gift from Professor A. Knuth (Frankfurt, Germany)[35]; and human cholangiocarcinoma cell line QBC939 was established by Professor Wang SG in the Third Military Medical University, China, and was offered to us as a gift[34]. Both cells were maintained as mono-layers in Dulbecco's modified Eagle's medium (DMEM) supplemented with 10 %

fetal bovine serum (FBS, Gibco. USA.), 100 units/ml penicillin and 100 mg/ml streptomycin in a humidified atmosphere of 95 % air and 5 % $CO_2$ at 37 ℃. They were subcultivated every 3-5 d and given fresh medium every other day. Cholangiocarcinoma cells at 70-80 % subconfluent were employed in all experiments. $PGE_2$ ELISA detection kit was purchased from Jingmei Biotech Co., Wuhan, China. TUNEL kit was purchased from Boster Co., Wuhan, China. $PGE_2$ was purchased from Sigma, USA. Celecoxib was synthesized by Dr. Mei ZN (Wuhan University, China) and given to us as a gift[36]. Stock solution was prepared in dimethylsulfoxide (DMSO) and stored at -20 ℃. In all experiments DMSO final concentration in the medium was ≤0.1 %.

### Methods

**MTT assay** The human cholangiocarcinoma cells QBC939 and SK-CHA-1 proliferation status were determined by MTT assay. Cholangiocarcinoma cells were seeded at a density of $1\times10^4$ cells per well in flat-bottomed 96-well microplates. 12 h after incubation, cells were treated with celecoxib (40, 20, 10, or 0 μmol/L respectively). In some experiments 200 pg/mL $PGE_2$ was added to cells prior to addition of celecoxib. After 1, 2, 3, or 4 days' incubation, 20 μl MTT (5 g/L) was added to each well and incubated for 4 h. Supernatant was then removed and 150 μl DMSO was added. It was shaken for 5 min until the crystal was dissolved. OD490nm value was measured by an enzyme-linked immunoabsorbent assay reader. The negative control well had no cells and was used as zero point of absorbance. Each well was read three times in triplicate.

**TUNEL** Preparation of specimens: cholangiocarcinoma cells QBC939 were subcultured on coverslips in 6-well culture plates. After 12 h, cells were treated with 20 μmol/L celecoxib. Every day medium and celecoxib were changed. After 2 and 4 d the coverslips were taken out and fixed with 4 % fresh polyformaldehyde in PBS (pH 7.4-7.6) for 30 min at room temperature. Cell apoptosis was measured by TUNEL method according to the instruction of the kit. Cells were washed with PBS for 2 min, 3 times, followed by washing with distilled water for 2 min, 3 times. Cells were soaked in fresh 3 % $H_2O_2$ for 10 min, and then rinsed with distilled water for 2 min, 3 times. Cells were digested with proteinase K (diluted 1:100 by TBS) for 5 min at 37 ℃, and were rinsed with distilled water for 2 min, 3 times. Labelling buffer (20 μl/sample) was added to keep the slides wet. TDT and DIG-d-UTP (1 μl each) were mixed in 18 μl labelling buffer. The redundant liquid was removed and labelling reagent (20 μl/sample) was added. The slides were put in a humidified box and incubated for 2 h at 37 ℃. The slides were washed with TBS for 2 min, 3 times. Blocking solution (50 μl /sample) was added to the slides for 30 min at room temperature. The blocking solution was removed from the slides. The biotin-DIG antibody was diluted with a blocking solution at a ratio of 1:100, and 50 μl/sample of it was added to the slides. The slides were kept in a humidified box, incubated at 37 ℃ for 30 min, and followed by washing with TBS for 5 min, 3 times. SABC was diluted to 1:100 with TBS and added to the slides. They were incubated at 37 ℃ for 30 min and washed with TBS for 5 min, 3 times. BCIP/NBT was diluted to 1:20 with TBS, and added to the slides. They were incubated at 37 ℃ for 10-30 min. The reaction was monitored under microscope: when purplish red was developed, the slides were washed with distilled water. After being stained with nuclear fast red, the slides were sealed with glycerite. Substitution of PBS for TUNEL staining solution was used as negative control. Three hundred cells were counted, and the TUNEL index was expressed as the number of positive cells/the total number of cells.

**ELISA** The $PGE_2$ levels in the supernatant of cultured human cholangiocarcinoma cells QBC939 and SK-CHA-1 were quantitated by ELISA. Cells were seeded into $4.0\times10^5$/well microplates and allowed to adhere overnight. The cells were then incubated in the presence or absence of celecoxib for 24 h. The supernatants were aspirated and centrifuged to prepare for the detection of $PGE_2$. Supernatant (0.5 ml) was added into 1 N HCl (0.1 ml) and centrifuged for 10 min at room temperature, then 1.2 N NaOH (0.1 ml) was used to neutralize the acidified samples. Standard solution (200 μl per well) or activated samples were added into the microplates. Then the steps for ELISA were performed as instructed. The value of OD of each well was measured at 450nm. The supernatants were harvested in triplicates and the experiment was performed twice.

**FCM** Human cholangiocarcinoma cells QBC939 and SK-CHA-1 were trypsinized and plated in 6-well culture dishes in the presence of celecoxib (40, 20, 10, 0 μmol/L respectively). After 48 h, cells were harvested, centrifuged at low speed and fixed in 70 % ethanol. After overnight incubation at 4 ℃, cells were stained with 50 μg/ml propidium iodide in the presence of RNAse A (10 μg/ml) and 0.1 % Triton X-100 and measured with a flow cytometer. The experiments were repeated three times.

**TEM** After treatment with celecoxib for 3 d cholangiocarcinoma cells QBC939 were digested by 0.25 % trypsin and collected. Cells were rinsed with PBS and fixed with 3 % glutaraldehyde for 30 min. After routine embedding and sectioning, cells were examined under electron microscope.

### Statistical analysis

Data were expressed as mean ± standard deviation. Student's *t*-test was used for statistical analysis. $P<0.05$ indicates significant difference.

## RESULTS

### $PGE_2$ production

The concentration of $PGE_2$ in culture medium of each cell line treated with or without celecoxib is shown in Figure 1. Celecoxib at 10 μmol/L inhibited $PGE_2$ production in QBC939 cells by 26 %. With 20 μmol/L and 40 μmol/L of celecoxib, $PGE_2$ production was further inhibited by 58 % and 74 %, which were statistically significant ($P<0.01$, *vs* control). The $PGE_2$ level was much lower constitutively in SK-CHA-1 cells (18.6±3.2) compared with that in QBC939 (121.9±5.6) cells (*t* test, $P<0.01$). The $PGE_2$ concentration in SK-CHA-1 cells was also reduced, but not significantly after treatment with celecoxib. The $PGE_2$ concentration in SK-CHA-1 cells was (16.5±2.9) ng/well, (14.8±3.4) ng/well, (13.2±2.0) ng/well and (12.6±3.1) ng/well respectively, when pre-treated with 1 μmol/L, 10 μmol/L, 20 μmol/L and 40 μmol/L of celecoxib for 48 h ($P>0.05$, *vs* control).

### Celecoxib inhibition on cholangiocarcinoma cells growth

QBC939 and SK-CHA-1 cells were incubated in the presence or absence of celecoxib (20 μmol/L) and the cell density OD490 was measured. As shown in Figure 2, proliferation inhibition of QBC939 by celecoxib was time-dependent: it was noticeable on day 2 (OD490=0.23±0.04) and became obvious on day 3 (OD490=0.31±0.07) to day 4 (OD490=0.25±0.06), and the OD490 in the control group (day 1) was 0.12±0.03 ($P<0.01$, *vs* control). The proliferation of SK-CHA-1 cells was inhibited slightly by celecoxib, but the effect was not statistically significant (Figure 3). The cell density OD490 in the presence of celecoxib and in control group was 0.31±0.04 and 0.42±0.03 respectively on day 2 ($P>0.05$), 0.58±0.07 and 0.67±0.09 respectively on day 3 ($P>0.05$), and 0.71±0.08 and 0.78±0.06 respectively on day 4 ($P>0.05$).

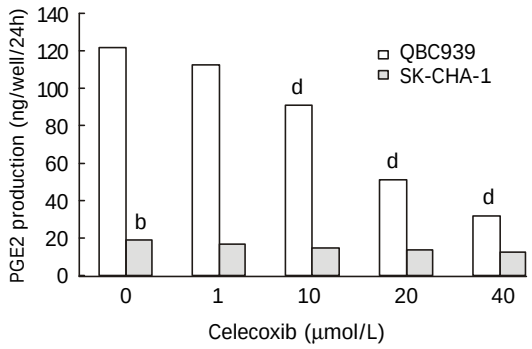


**Figure 1** ELISA for $PGE_2$ detection using supernatants from QBC939 and SK-CHA-1 cells pre-treated with celecoxib at various concentrations for 48 h. Celecoxib at 10 μmol/L inhibited $PGE_2$ production in QBC939 cells by 26 %. With 20 μmol/L and 40 μmol/L of celecoxib, $PGE_2$ production was further inhibited by 58 % and 74 %, which were statistically significant ($^dP<0.01$, *vs* control). The $PGE_2$ level was much lower constitutively in SK-CHA-1 cells (18.6±3.2) compared with that in QBC939 (121.9±5.6) cells (*t* test, $^bP<0.01$). The $PGE_2$ concentration in SK-CHA-1 cells was also reduced, but not significantly after treatment with celecoxib. The $PGE_2$ concentration in SK-CHA-1 cells was (16.5±2.9) ng/well, (14.8±3.4) ng/well, (13.2±2.0) ng/well and (12.6±3.1) ng/well respectively, when pre-treated with 1 μmol/L, 10 μmol/L, 20 μmol/L and 40 μmol/L of celecoxib for 48 h ($P>0.05$, *vs* control).

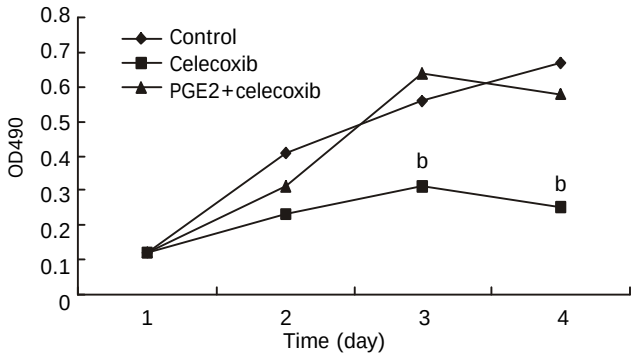


**Figure 2** Growth curves of QBC939 cells in the presence of celecoxib, celecoxib + $PGE_2$ and control group. Proliferation inhibition of QBC939 by celecoxib (20 μmol/L) was time-dependent: it was noticeable on day 2 and became significant on day 3 to 4 ($^bP<0.01$, *vs* control). The anti-proliferation effect of celecoxib on QBC939 cells was abolished by pre-added $PGE_2$ (200 pg/mL).

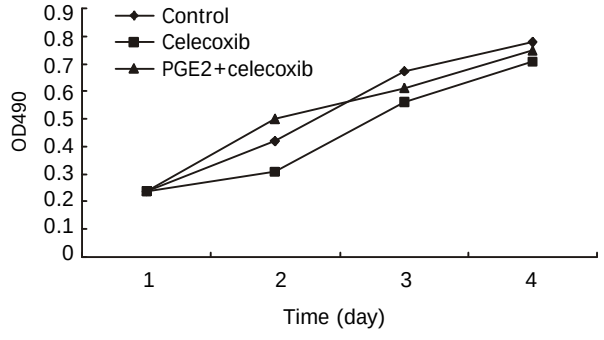


**Figure 3** Growth curves of SK-CHA-1 cells in the presence of celecoxib, celecoxib + $PGE_2$ and control group. The proliferation of SK-CHA-1 cells was inhibited slightly by celecoxib, the cell density OD490 in the presence of celecoxib and in control group was 0.31±0.04 and 0.42±0.03 respectively on day 2 ($P>0.05$), 0.58±0.07 and 0.67±0.09 respectively on day 3 ($P>0.05$), and 0.71±0.08 and 0.78±0.06 respectively on day 4 ($P>0.05$).

### *$PGE_2$ abolished the anti-proliferation effect of celecoxib on QBC939 cells*

To investigate whether the anti-proliferation effect of celecoxib on QBC939 cells was due to suppression of $PGE_2$ production by QBC939 cells, 200 pg/mL $PGE_2$ was added to QBC939 cells prior to the addition of celecoxib, and MTT assay was performed (Figure 2). The anti-proliferation effect of celecoxib on QBC939 cells was abolished by $PGE_2$. However, addition of 200 pg/mL $PGE_2$ had no significant influence on the proliferation of SK-CHA-1 cells when pre-treated with 20 μmol/L celecoxib (Figure 3).

### *Apoptosis induction and detection*

The TUNEL index of QBC939 cells treated with 20 μmol/L celecoxib for 2 d (0.063±0.018) and 4 d (0.102±0.037) was much higher compared with control cells (0.017±0.004, $P<0.01$).

### *Celecoxib induces $G_1$-S cell cycle arrest*

Cell cycle analysis by flow cytometry showed that the percentage of QBC939 cells in $G_0$-$G_1$ phase after treatment with 40 μmol/L (74.66±6.21) and 20 μmol/L (68.63±4.36) increased significantly compared with control cells (54.41±5.12, $P<0.01$, Figure 4). The percentage of SK-CHA-1 cells in $G_0$-$G_1$ phase after treatment with various concentrations of celecoxib did not change significantly compared with control cells.

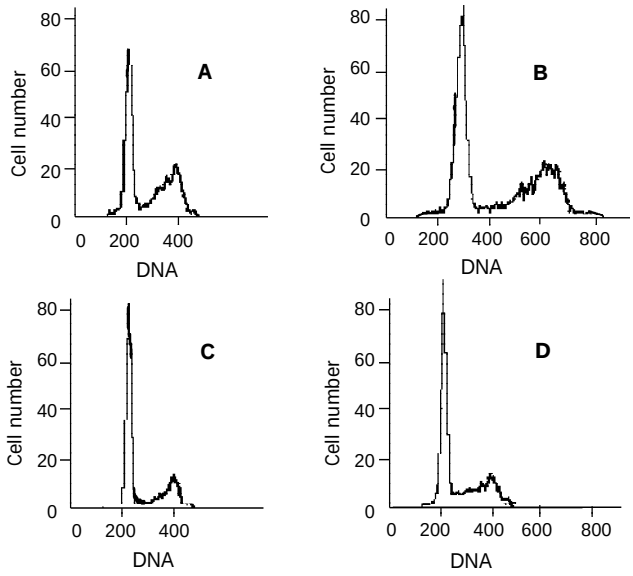


**Figure 4** Cell cycle analysis. Representative flow cytometry data from QBC939 cells after 48 h in the presence of various concentration of celecoxib: 0 μmol/L (A), 10 μmol/L (B), 20 μmol/L (C) and 40 μmol/L (D). The percentage of QBC939 cells in $G_0$-$G_1$ phase after treatment with 40 μmol/L (74.66±6.21) and 20 μmol/L (68.63±4.36) of celecoxib increased significantly compared with control cells (*t* test, $P<0.01$).

### *Electron micrography of apoptosis of cholangiocarcinoma cells*

QBC939 cells were treated for 3 d with 20 μmol/L of celecoxib. The chromatin became condensed and attached to the inner surface of nuclear membrane.

## DISCUSSION

A substantial body of evidence indicates that COX and PGs are important in carcinogenesis. COX catalyzes the synthesis of PGs from arachidonic acid. Several PGs, most notably $PGE_2$, can promote tumorigenesis by stimulating angiogenesis, inhibiting immune surveillance[37-40], modulating several signal

transduction pathways[41-44]. Several studies have demonstrated that COX-2 selective inhibitor celecoxib has significant efficacy in animal cancer models: celecoxib inhibited intestinal tumor multiplicity by up to 71 % compared with controls in the Min mouse model and inhibited colorectal tumor burden in the rat azoxymethane (AOM) model[45-48]. Recently celecoxib has been approved by FDA to reduce the number of adenomatous colorectal polyps in patients with familial adenomatous polyposis (FAP). However, the exact mechanisms that account for the anti-proliferative effects of celecoxib are still not fully understood. It is still controversial that whether or not these effects are mediated predominantly through the inhibition of COX-2 activity and prostaglandin synthesis. Several studies have shown both COX-dependent and COX-independent mechanisms are involved in non-steroidal anti-inflammatory drug (NSAIDs) induced growth in human colorectal tumor cells[49].

Our previous studies have demonstrated that overexpression of COX-2 may play a crucial role in the carcinogenesis and development of extra-hepatic cholangiocarcinoma. In the present study we found the $PGE_2$ level was much lower constitutively in COX-2-deficient human cholangiocarcinoma cell line SK-CHA-1 cells than that in COX-2 overexpressing human cholangiocarcinoma cell line QBC939. In this study we have shown that the proliferation of QBC939 cells was inhibited by celecoxib in a time- and dose-dependent manner. Our study also showed celecoxib had no significant influence on the SK-CHA-1 cells. These findings indicate that COX-2 inhibitor might be an effective anti-proliferative agent, especially against cancer cells that express COX-2 and produce high-level $PGE_2$. Our data demonstrated that celecoxib suppressed the production of $PGE_2$ in QBC939 cells, and the anti-proliferative effect of celecoxib could be abolished by addition of $PGE_2$. These results suggest that COX-2 might play a central role in production of $PGE_2$ and the specific inhibition of COX-2 inhibits proliferation and induces apoptosis of QBC939 cells via suppression of $PGE_2$ production. Our data also indicate that celecoxib inhibits proliferation and induces apoptosis of human cholangiocarcinoma QBC939 cells by an accumulation of cells in the $G_0/G_1$ phase and the inhibition of $G_0/G_1$ phase transition to S phase.

In summary, our results in the present study demonstrate that inhibition of proliferation and induction of apoptosis by celecoxib in human cholangiocarcinoma cells may involve in COX-dependent mechanisms and $PGE_2$ pathway and these findings also suggest that celecoxib, as a chemopreventive and chemotherapeutic agent may be effective primarily on COX-2-expressing cholangiocarcinoma.

## REFERENCES


1 **Bostrom PJ,** Aaltonen V, Soderstrom KO, Uotila P, Laato M. Expression of cyclooxygenase-1 and -2 in urinary bladder carcinomas in vivo and in vitro and prostaglandin E2 synthesis in cultured bladder cancer cells. *Pathology* 2001; **33:** 469-474

2 **Fan XM,** Wong BC, Lin MC, Cho CH, Wang WP, Kung HF, Lam SK. Interleukin-1beta induces cyclo-oxygenase-2 expression in gastric cancer cells by the p38 and p44/42 mitogen-activated protein kinase signaling pathways. *J Gastroenterol Hepatol* 2001; **16**: 1098-1104

3 **Wu GS**, Zou SQ, Luo XW, Wu JH, Liu ZR. Proliferative activity of bile from congenital choledochal cyst patients. *World J Gastroenterol* 2003; **9**: 184-187

4 **Chasseing NA,** Hofer E, Bordenave RH, Shanley C, Rumi LS. Bone marrow fibroblasts in patients with advanced lung cancer. *Braz J Med Biol Res* 2001; **34:** 1457-1463

5 **Berger S,** Siegert A, Denkert C, Kobel M, Hauptmann S. Interleukin-10 in serous ovarian carcinoma cell lines. *Cancer Immunol Immunother* 2001; **50:** 328-333

6 **Venza I,** Giordano L, Piraino G, Medici N, Ceci G, Teti D. Prostaglandin E2 signalling pathway in human T lymphocytes from healthy and conjunctiva basal cell carcinoma-bearing subjects. *Immunol Cell Biol* 2001; **79:** 482-489

7 **Chen X,** Yang CS. Esophageal adenocarcinoma: a review and perspectives on the mechanism of carcinogenesis and chemoprevention. *Carcinogenesis* 2001; **22:** 1119-1129

8 **McHowat J,** Creer MH, Rickard A. Stimulation of protease activated receptors on RT4 cells mediates arachidonic acid release via Ca2+ independent phospholipase A2. *J Urol* 2001; **165**: 2063-2067

9 **Krishnan K,** Ruffin MT, Normolle D, Shureiqi I, Burney K, Bailey J, Peters-Golden M, Rock CL, Boland CR, Brenner DE. Colonic mucosal prostaglandin E2 and cyclooxygenase expression before and after low aspirin doses in subjects at high risk or at normal risk for colorectal cancer. *Cancer Epidemiol Biomarkers Prev* 2001; **10:** 447-453

10 **Lim JW,** Kim H, Kim KH. Nuclear factor-kappaB regulates cyclooxygenase-2 expression and cell proliferation in human gastric cancer cells. *Lab Invest* 2001; **81:** 349-360

11 **Akhtar M,** Cheng Y, Magno RM, Ashktorab H, Smoot DT, Meltzer SJ, Wilson KT. Promoter methylation regulates *Helicobacter pylori*-stimulated cyclooxygenase-2 expression in gastric epithelial cells. *Cancer Res* 2001; **61:** 2399-2403

12 **Sheng H,** Shao J, Washington MK, DuBois RN. Prostaglandin E2 increases growth and motility of colorectal carcinoma cells. *J Biol Chem* 2001; **276:** 18075-18081

13 **Faas FH,** Dang AQ, White J, Schaefer R, Johnson D. Increased prostatic lysophosphatidylcholine acyltransferase activity in human prostate cancer: a marker for malignancy. *J Urol* 2001; **165:** 463-468

14 **Tian G,** Yu JP, Luo HS, Yu BP, Yue H, Li JY, Mei Q. Effect of Nimesulide on proliferation and apoptosis of human hepatoma SMMC-7721 cells. *World J Gastroenterol* 2002; **8:** 483-487

15 **Wu YL,** Sun B, Zhang XJ, Wang SN, He HY, Qiao MM, Zhong J, Xu JY. Growth inhibition and apoptosis induction of Sulindac on Human gastric cancer cells. *World J Gastroenterol* 2001; **7:** 796-800

16 **Cheng J,** Imanishi H, Iijima H, Shimomura S, Yamamoto T, Amuro Y, Kubota A, Hada T. Expression of cyclooxygenase 2 and cytosolic phospholipase A(2) in the liver tissue of patients with chronic hepatitis and liver cirrhosis. *Hepatol Res* 2002; **23:** 185-195

17 **Davies G,** Martin LA, Sacks N, Dowsett M. Cyclooxygenase-2 (COX-2), aromatase and breast cancer: a possible role for COX-2 inhibitors in breast cancer chemoprevention. *Ann Oncol* 2002; **13:** 669-678

18 **Seno H,** Oshima M, Ishikawa TO, Oshima H, Takaku K, Chiba T, Narumiya S, Taketo MM. Cyclooxygenase 2- and prostaglandin E(2) receptor EP(2)-dependent angiogenesis in Apc (Delta716) mouse intestinal polyps. *Cancer Res* 2002; **62:** 506-511

19 **Zimmermann KC,** Sarbia M, Weber AA, Borchard F, Gabbert HE, Schror K. Cyclooxygenase-2 expression in human esophageal carcinoma. *Cancer Res* 1999; **59:** 198-204

20 **Gupta S,** Srivastava M, Ahmad N, Sakamoto K, Bostwick DG, Mukhtar H. Lipoxygenase-5 is overexpressed in prostate adenocarcinoma. *Cancer* 2001; **91:** 737-743

21 **Weddle DL,** Tithoff P, Williams M, Schuller HM. Beta-adrenergic growth regulation of human cancer cell lines derived from pancreatic ductal carcinomas. *Carcinogenesis* 2001; **22:** 473-479

22 **Ristimaki A,** Nieminen O, Saukkonen K, Hotakainen K, Nordling S, Haglund C. Expression of cyclooxygenase-2 in human transitional cell carcinoma of the urinary bladder. *Am J Pathol* 2001; **158:** 849-853

23 **Kulkarni S,** Rader JS, Zhang F, Liapis H, Koki AT, Masferrer JL, Subbaramaiah K, Dannenberg AJ. Cyclooxygenase-2 is overexpressed in human cervical cancer. *Clin Cancer Res* 2001; **7:** 429-434

24 **Tong BJ,** Tan J, Tajeda L, Das SK, Chapman JA, DuBois RN, Dey SK. Heightened expression of cyclooxygenase-2 and peroxisome proliferator-activated receptor-delta in human endometrial adenocarcinoma. *Neoplasia* 2000; **2:** 483-490

25 **Uefuji K,** Ichikura T, Mochizuki H. Expression of cyclooxygenase-2 in human gastric adenomas and adenocarcinomas. *J Surg Oncol* 2001; **76:** 26-30

26 **Kokawa A,** Kondo H, Gotoda T, Ono H, Saito D, Nakadaira S, Kosuge T, Yoshida S. Increased expression of cyclooxygenase-2 in human pancreatic neoplasms and potential for chemoprevention by cyclooxygenase inhibitors. *Cancer* 2001; **91:** 333-338

27 **Kakiuchi Y,** Tsuji S, Tsujii M, Murata H, Kawai N, Yasumaru M, Kimura A, Komori M, Irie T, Miyoshi E, Sasaki Y, Hayashi N, Kawano S, Hori M. Cyclooxygenase-2 activity altered the cell-surface carbohydrate antigens on colon cancer cells and enhanced liver metastasis. *Cancer Res* 2002; **62:** 1567-1572

28 **Sumitani K,** Kamijo R, Toyoshima T, Nakanishi Y, Takizawa K, Hatori M, Nagumo M. Specific inhibition of cyclooxygenase-2 results in inhibition of proliferation of oral cancer cell lines via suppression of prostaglandin E2 production. *J Oral Pathol Med* 2001; **30:** 41-47

29 **Hosomi Y,** Yokose T, Hirose Y, Nakajima R, Nagai K, Nishiwaki Y, Ochiai A. Increased cyclooxygenase 2 (COX-2) expression occurs frequently in precursor lesions of human adenocarcinoma of the lung. *Lung Cancer* 2000; **30:** 73-81

30 **Tsubouchi Y,** Mukai S, Kawahito Y, Yamada R, Kohno M, Inoue K, Sano H. Meloxicam inhibits the growth of non-small cell lung cancer. *Anticancer Res* 2000; **20:** 2867-2872

31 **Souza RF,** Shewmake K, Beer DG, Cryer B, Spechler SJ. Selective inhibition of cyclooxygenase-2 suppresses growth and induces apoptosis in human esophageal adenocarcinoma cells. *Cancer Res* 2000; **60:** 5767-5772

32 **Grubbs CJ,** Lubet RA, Koki AT, Leahy KM, Masferrer JL, Steele VE, Kelloff GJ, Hill DL, Seibert K. Celecoxib inhibits N-butyl-N-(4-hydroxybutyl)-nitrosamine-induced urinary bladder cancers in male B6D2F1 mice and female Fischer-344 rats. *Cancer Res* 2000; **60:** 5599-5602

33 **Sabine G,** Irmgard T, Elien N, Lutz B, Gerd G. COX-2 independent induction of cell cycle arrest and apoptosis in colon cancer cells by the selective COX-2 inhibitor of celecoxib. *FASEB* 2001; **15:** 2742-2744

34 **Knuth A,** Gabbert H, Dippold W, Klein O, Sachsse W, Bitter-Suermann D, Prellwitz W. Biliary adenocarcinoma. Characterisation of three new human tumor cell lines. *J Hepatol* 1985; **1:** 579-596

35 **Wang SG,** Han BL, Duan HC, Chen YS, Peng ZM. Establishment of the extrahepatic cholangiocarcinoma cell line. *Zhonghua Shiyan Waike Zazhi* 1997; **14:** 67-68

36 **Mei ZY,** Shi Z, Wang XH, Luo XD. Synthesis of COX-2 Inhibitor Celecoxib. *Zhongguo Yiyao Gongye Zazhi* 2000; **31:** 433-434

37 **Soslow RA,** Dannenberg AJ, Rush D, Woerner BM, Khan KN, Masferrer J, Koki AT. COX-2 is expressed in human pulmonary, colonic, and mammary tumors. *Cancer* 2000; **89:** 2637-2645

38 **Vanaja DK,** Grossmann ME, Celis E, Young CY. Tumor prevention and antitumor immunity with heat shock protein 70 induced by 15-deoxy-delta12,14-prostaglandin J2 in transgenic adenocarcinoma of mouse prostate cells. *Cancer Res* 2000; **60:** 4714-4718

39 **O'Byrne KJ,** Dalgleish AG, Browning MJ, Steward WP, Harris AL. The relationship between angiogenesis and the immune response in carcinogenesis and the progression of malignant disease. *Eur J Cancer* 2000; **36:** 151-169

40 **Morecki S,** Yacovlev E, Gelfand Y, Trembovler V, Shohami E, Slavin S. Induction of antitumor immunity by indomethacin. *Cancer Immunol Immunother* 2000; **48:** 613-620

41 **Jang BC,** Sanchez T, Schaefers HJ, Trifan OC, Liu CH, Creminon C, Huang CK, Hla T. Serum withdrawal-induced post-transcriptional stabilization of cyclooxygenase-2 mRNA in MDA-MB-231 mammary carcinoma cells requires the activity of the p38 stress-activated protein kinase. *Biol Chem* 2000; **275:** 39507-39515

42 **Paik JH,** Ju JH, Lee JY, Boudreau MD, Hwang DH. Two opposing effects of non-steroidal anti-inflammatory drugs on the expression of the inducible cyclooxygenase. Mediation through different signaling pathways. *J Biol Chem* 2000; **275:** 28173-28179

43 **Subbaramaiah K,** Michaluart P, Sporn MB, Dannenberg AJ. Ursolic acid inhibits cyclooxygenase-2 transcription in human mammary epithelial cells. *Cancer Res* 2000; **60:** 2399-2404

44 **Higashi Y,** Kanekura T, Kanzaki T. Enhanced expression of cyclooxygenase (COX)-2 in human skin epidermal cancer cells: evidence for growth suppression by inhibiting COX-2 expression. *Int J Cancer* 2000; **86:** 667-671

45 **Takahashi M,** Mutoh M, Kawamori T, Sugimura T, Wakabayashi K. Altered expression of beta-catenin, inducible nitric oxide synthase and cyclooxygenase-2 in azoxymethane-induced rat colon carcinogenesis. *Carcinogenesis* 2000; **21:** 1319-1327

46 **Jacoby RF,** Cole CE, Tutsch K, Newton MA, Kelloff G, Hawk ET, Lubet RA. Chemopreventive efficacy of combined piroxicam and difluoromethylornithine treatment of Apc mutant Min mouse adenomas, and selective toxicity against Apc mutant embryos. *Cancer Research* 2000; **60:** 1864-1870

47 **Reddy BS,** Rao CV, Seibert K. Evaluation of cyclooxygenase-2 inhibitor for potential chemopreventive properties in colon carcinogenesis. *Cancer Research* 1996; **56:** 4566-4569

48 **Kawamori T,** Rao CV, SeibertK, Reddy BS. Chemopreventive activity of celecoxib, a selective cyclooxygenase -2 inhibitor, against colon carcinogenesis. *Cancer Research* 1998; **58:** 409-412

49 **Richter M,** Weiss M, Weinberger I, Furstenberger G, Marian B. Growth inhibition and induction of apoptosis in colorectal tumor cells by cyclooxygenase inhibitors. *Carcinogenesis* 2001; **22:** 17-25


**Edited by** Zhu L and Bo XN

P.O.Box 2345, Beijing 100023,China
Fax: +86-10-85381893
E-mail: wjg@wjgnet.com www.wjgnet.com

World J Gastroenterol 2003;9(6):1307-1311
World Journal of Gastroenterology
Copyright ©2003 by The WJG Press ISSN 1007-9327

• BASIC RESEARCH •

# Effects of melatonin on the expression of iNOS and COX-2 in rat models of colitis

Wei-Guo Dong, Qiao Mei, Jie-Ping Yu, Jian-Ming Xu, Li Xiang, Yu Xu

**Wei-Guo Dong, Jie-Ping Yu, Yu Xu,** Department of Gastroenterology, Renmin Hospital, Wuhan University, Wuhan 430060, Hubei Province, China
**Qiao Mei, Jian-Ming Xu, Li Xiang,** Department of Gastroenterology, the First Affiliated Hospital, Anhui Medical University, Hefei 230032, Anhui Province, China
**Correspondence to:** Wei-Guo Dong, Department of Gastroenterology, Renmin Hospital, Wuhan University, Wuhan 430060, China. dongwg@public.wh.hb.cn
**Telephone:** +86-27-88041911 Ext 7737
**Received:** 2002-11-26 **Accepted:** 2003-01-13

## Abstract

**AIM:** To investigate the effects of melatonin (MT) on the expression of inducible nitric oxide synthase (iNOS) and cyclooxygenase-2 (COX-2) in rat models of colitis.

**METHODS:** Healthy adult Sprague-Dawlay (SD) rats of both sexes, weighing 280±30 g, were employed in the present study. The rat models of colitis were induced by either acetic acid or 2,4,6-trinitrobenzene sulfonic acid (TNBS) enemas. The experimental animals were randomly divided into melatonin treatment and model control group that were intracolicly treated daily with melatonin at doses of 2.5, 5.0, 10.0 $mg \cdot kg^{-1}$ and equal amount of saline respectively from 24 h following induction of colitis in rats inflicted with acetic acid enema and the seventh day in rats with TNBS to the end of study. A normal control group of rats treated with neither acetic acid nor TNBS but saline enema was also included in the study. On the 28th day of the experiment, the rat colon mucosal damage index (CDMI) was calculated, and the colonic prostaglandin $E_2$ ($PGE_2$), nitric oxide (NO), as well as the iNOS and COX-2 expression were also determined biochemically or immunohistochemically.

**RESULTS:** CDMI increased to 2.87±0.64 and 3.12±1.12 respectively in rats treated with acetic acid and TNBS enema, which was in accordance with the significantly elevated colonic NO and $PGE_2$ contents, as well as the up-regulated colonic iNOS and COX-2 expression in both of the two rat models of colitis. With treatment by melatonin at the doses of 5.0 and 10.0 $mg \cdot kg^{-1}$, CDMI in both models of rat colitis was significantly decreased ($P$<0.05-0.01), which accorded synchronously and unanimously with the reduced colonic NO and $PGE_2$ content, as well as the down-regulated expression of colonic iNOS and COX-2.

**CONCLUSION:** Melatonin has a protective effect on colonic injury induced by both acetic acid and TNBS enemas, which is probably via a mechanism of local inhibition of iNOS and COX-2 expression in colonic mucosa.

Dong WG, Mei Q, Yu JP, Xu JM, Xiang L, Xu Y. Effects of melatonin on the expression of iNOS and COX-2 in rat models of colitis. *World J Gastroenterol* 2003; 9(6): 1307-1311
http://www.wjgnet.com/1007-9327/9/1307.asp

## INTRODUCTION

Inflammatory bowel disease (IBD) consists of a group of illnesses with chronic inflammation of the gastrointestinal tract, which causes life-impairing symptoms, necessitates long-term dependence on powerful drugs, and often results in debilitating surgery and even death. Although the etiology remains unclear, IBD appears to result from a dysregulated immune response. In recent years, plenty of studies have shown that nitric oxide (NO) and prostaglandin (PG) as the main inflammatory mediators take part in the pathogenesis of inflammatory bowel disease, with enhanced expression of inducible nitric oxide synthase (iNOS) and cyclooxygenase-2 (COX-2) in the morbid colonic mucosa[1,2]. Meanwhile, it has been noted melatonin (MT) normally produced mainly in the gastrointestinal tract besides the pineal gland bears a number of beneficial properties including anti-oxidation, anti-inflammation and immunoregulation[3-15], and could alleviate colonic injury caused by both dextran sulfate sodium[16] and dinitrobenzene sulfonic acid[17] in rats. It is reasonable to extrapolate that the protective roles of melatonin might be related to its effect on the expression of iNOS and COX-2 in local tissue. We therefore performed the present study in an attempt to confirm this hypothesis.

## MATERIALS AND METHODS

### Animals

Healthy adult Sprague-Dawlay (SD) rats of both sexes, weighing 280±30 g, were employed in the study. They were purchased from the Experimental Animal Center, Anhui Medical University, housed in a temperature conditioned room (22-24 ℃) with a 12 h light-dark cycle, allowed access to standard rat chow and water ad libium, and acclimatized to the surroundings for one week prior to the experiments. The study protocol was in accordance with the guideline for animal research and was approved by the Ethical and Research Committee of the hospital.

### Reagents

Melatonin, TNBS, and N-1-naphthylenediamine hydrochloride came from Sigma Corp. Acetic acid was purchased from Bangbu Chemical Corp. $PGE_2$ assay kit was from Radio-immunity Institute of PLA General Hospital. Immunohistochemical assay kits for iNOS and COX-2 were provided by Beijing Zhongshan Reagent Corp. Other reagents used in the present study were all with a quality of analytical grade.

### Experimental protocol

Rat model of colitis induced with either acetic acid or TNBS enema was described in the literature[18, 19]. According to different treatment regimens, the experimental animals were randomly divided into melatonin treatment and model control group that were intracolicly treated under anesthesia with melatonin at doses of 2.5, 5.0, 10.0 $mg \cdot kg^{-1}$ and equal amount of saline respectively and daily (8:00 am) from 24

h following induction of colitis in rats inflicted with acetic acid enema and the seventh day in rats after TNBS treatment to the end of the experiment. A normal control group of rats treated with neither acetic acid nor TNBS but saline enema was also included in the study. On the 28th day of the experiment, the animals were killed and the colon mucosal damage index (CDMI) was evaluated with the methods reported elsewhere[19, 20]. At the same time, colon tissue prostaglandin $E_2$ ($PGE_2$) and nitric oxide (NO), as well as the expression of iNOS and COX-2 were determined biochemically or immunohistochemically.

### Determination of NO and $PGE_2$

Colonic specimen was prepared to a concentration of 20 g·$L^{-1}$ by adding dehydrated alcohol-saline (1:4), and then centrifuged at 4 000 g for 30 min, 4 ℃. Two milliliters of the supernatant were added into 0.1 ml of HCL (0.1 mol·$L^{-1}$) and further adjusted pH to 3.5 by 0.05 mol·$L^{-1}$ of NaOH. After mixed with ethyl acetate 5 ml for 2 min, they were centrifuged at 1 500 g for 15 min. Repeat the procedures above and the sample solution was evaporated to dryness by $N_2$ and stored at -20 ℃ until analysis. The samples was dissolved to 1 ml of phosphate buffered saline, from which 0.1 ml of specimen was taken to perform the $PGE_2$ measurement following the manufacturer's instruction of the assay kit[21]. The colonic tissue NO was detected as described in the literature[22].

### Immunohistochemistry detection

The expression of iNOS and COX-2 in colon tissue was exhibited immunohistochemically as reported before[23], in which the employed first polyclonal antibody was 1:80 rabbit-anti-rat-iNOS and 1:50 goat-anti-rat-COX-2, and the second antibody was biotinylation goat-anti-rabbit IgG and biotinylation rabbit-anti-goat IgG respectively. The iNOS or COX-2 negatively expressed cells were manifested as blue-stained nuclei and the positive cell was with brown-yellow cytoplasma or nuclear membrane. The expression of target protein was further semiquantitated according to the percentage of positively-stained cells, in which positive cells appeared less than 5 %, from 6 % to 30 %, from 31 % to 70 % and morn than 71 % were scored as 0, 1, 2 and 3 respectively.

### Statistical analysis

Experimental results were analyzed by ANOVA and *t*-tests for multiple comparisons between groups. Data were finally expressed as mean ± standard error of the mean. *P* value less than 0.05 was considered statistically significant.

## RESULTS

### Protective effects of melatonin on rat colonic lesion

Pronounced pathological changes of colonic mucosa similar to that in human IBD were observed in rats with colitis induced by both acetic acid and TNBS enema, which were in accordance with the colon mucosal damage index that was significantly increased in these experimental animals compared with normal controls ($P<0.01$). Local treatment with different doses of melatonin by enema could effectively reduce the severity of gut injury and the CMDI was significantly decreased in a dose dependent manner in rats treated by melatonin compared with that in model control animals ($P<0.05$-$0.01$, Table 1).

### Effects of MT on NO content and iNOS expression

In normal controls, colonic iNOS expression was mainly observed on histocytes, neutrophils and smooth muscle cells with a sparse distribution in epithelial cells. The NO content and the expression of iNOS in colonic tissue were synchronously and significantly increased in rats inflicted with both acetic acid and TNBS enema compared with that of the normal controls ($P<0.01$), which were significantly inhibited by different doses of melatonin employed in the present study ($P<0.05$-$0.01$ *vs.* Model control, Table 2, 3, Figure 1).

**Table 1** Effects of MT on CMDI in rats with experimental colitis ($\bar{x}$±s, $n$=8)

| Group | Doses (mg · $kg^{-1}$) | CMDI | |
|---|---|---|---|
| | | Acetic acid | TNBS |
| Normal control | | 0.0±0.0 | 0.0±0.0 |
| Model control | | 2.87±0.64[a] | 3.12±1.12[a] |
| Melatonin | 2.5 | 2.12±0.83[b] | 2.33±0.51 |
| Melatonin | 5.0 | 1.75±0.88[c] | 1.66±0.81[b] |
| Melatonin | 10.0 | 1.12±0.35[c] | 1.75±0.88[b] |

[a]$P<0.01$ *vs.* Normal control; [b]$P<0.05$, [c]$P<0.01$ *vs.* Model control.

**Table 2** Effects of MT on the colonic NO and $PGE_2$ levels in rats with experimental colitis ($\bar{x}$±s, $n$=8)

| Group | Doses (mg·$kg^{-1}$) | NO (μmol·$g^{-1}$ tissue) | | $PGE_2$ (ng·$g^{-1}$ tissue) | |
|---|---|---|---|---|---|
| | | Acetic acid | TNBS | Acetic acid | TNBS |
| Normal control | | 0.174±0.044 | 0.287±0.069 | 43.1±32.1 | 43.1±32.1 |
| Model control | | 0.327±0.090[b] | 0.533±0.068[b] | 184.5±96.3[b] | 181.3±51.7[b] |
| Melatonin | 2.5 | 0.230±0.017[d] | 0.403±0.042[d] | 89.1±59.1[c] | 109.0±33.3[d] |
| Melatonin | 5.0 | 0.218±0.018[d] | 0.380±0.029[d] | 76.4±23.6[c] | 89.8±37.7[d] |
| Melatonin | 10.0 | 0.189±0.029[d] | 0.340±0.019[d] | 57.1±23.2[d] | 85.9±39.2[d] |

[a]$P<0.05$, [b]$P<0.01$, *vs.* normal control; [c]$P<0.05$, [d]$P<0.01$ *vs.* model control.

### Effects of melatonin on $PGE_2$ content and COX-2 expression

Compared with normal group, the content of $PGE_2$ and the expression of COX-2 in rat colitis, the number of positive granules and the degree of staining were enhanced significantly. The content of $PGE_2$ was decreased after different doses of melatonin were given by enema. The expression of COX-2 was inhibited by melatonin, which proved that melatonin decreased the synthesis of $PGE_2$ and it might be related with inhibition of the expression of COX-2 (Figure 2, Table 2, 3).

**Table 3** Effects of MT on the colonic expression of iNOS and COX-2 semi-quantitated in rats with experimental colitis ($\bar{x}$±s, $n$=6)

| Group | Doses (mg·$kg^{-1}$) | iNOS | | COX-2 | |
|---|---|---|---|---|---|
| | | Acetic acid | TNBS | Acetic acid | TNBS |
| Normal control | | 0.3±0.5 | 0.3±0.5 | 0.2±0.4 | 0.2±0.4 |
| Model control | | 2.2±0.9[b] | 2.3±0.8[b] | 1.8±0.9[b] | 2.2±0.9[b] |
| Melatonin | 2.5 | 1.3±0.5[c] | 1.5±0.5[c] | 1.2±0.4 | 1.7±0.8 |
| Melatonin | 5.0 | 0.5±0.5[d] | 1.2±0.8[c] | 1.0±0.6 | 1.3±0.8 |
| Melatonin | 10.0 | 0.3±0.5[d] | 0.7±0.8[d] | 0.5±0.5[c] | 0.8±0.8[c] |

[a]$P<0.05$, [b]$P<0.01$ *vs.* Normal control; [c]$P<0.05$, [d]$P<0.01$ *vs.* Model control.

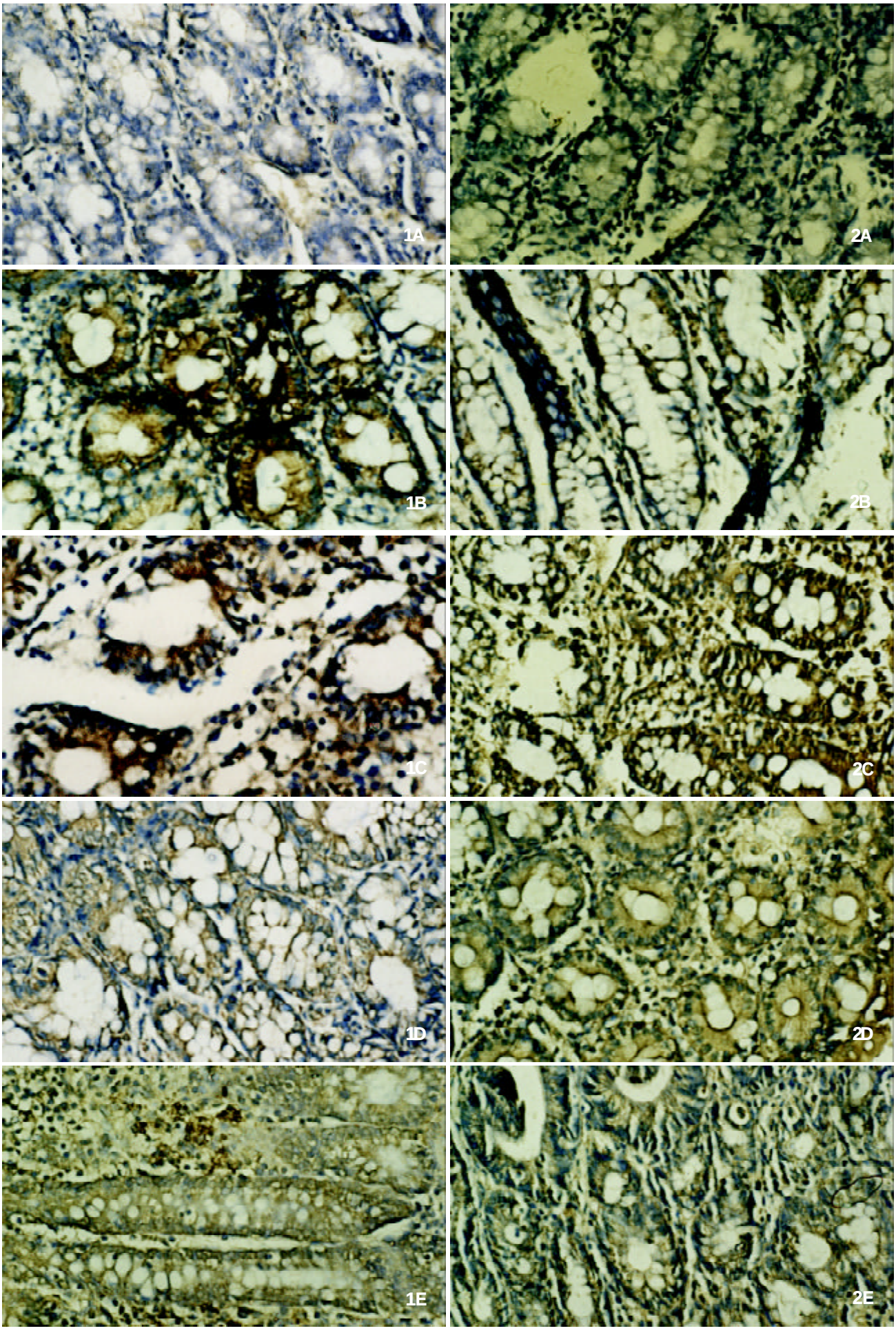


**Figure 1** Abnormal expression of iNOS in colonic tissue of rats with cloitis induced by both acetic acid and TNBS enemas and its

improvement by melatonin. A. Immunohistochemical localization of iNOS in normal control, which was manifested as fine brown granules distributed mainly in the cytoplasm of histocytes, neutrophils and smooth muscle cells. B. Positively stained granules for iNOS were significantly increased in both number and intensity in colonic tissue of model control rats. (a) Acetic acid treated rats; (b) TNBS treated rats. C. The colonic iNOS expression was significantly reduced in both acetic acid (a) and TNBS (b) treated rats after intervened with 10.0 $mg \cdot kg^{-1}$ of melatonin.

**Figure 2** Abnormal expression of COX-2 in colonic tissue of rats with colitis induced by acetic acid or TNBS enema and its improvement by melatonin, which was in accordance with the observation in clonic iNOS expression. A. Positively stained COX-2 granules in colonic tissue of normal control rats. B. iNOS expression was significantly increased as manifested by the augmented and intensified positively stained granules in colonic tissue of model control rats. (a) Acetic acid treated rats; (b) TNBS treated rats. C. The colonic COX-2 expression was significantly reduced in both acetic acid (a) and TNBS (b) treated rats after intervened with 10.0 $mg \cdot kg^{-1}$ of melatonin.

## DISCUSSION

Although the etiology of IBD remains unclear, dysregulated immune response has been widely accepted as a possible mechanism in the pathogenesis of inflammatory bowel disease. Numerous reports have revealed that certain local bioactive agents including NO and $PGE_2$ are involved in colonic injury by various inducers[1, 2]. Meddleton and other authors[24, 25] found NO concentration was rather higher in ulcerative colitis patients with obviously strengthened iNOS activity. As an important inflammatory mediator, NO could react with superoxide anion to form more poisonous nitrite anion, which then disturbs the function of inflammatory cells and further impairs the colonic mucosa[26, 27]. $PGE_2$, another major local inflammatory mediator that might come from activated eosinophils and monocytes[28], is also considered as a marker of colitis. In the two rat models of colitis respectively induced by acetic acid and TNBS in the present study, the mucosal NO and $PGE_2$ contents in the morbid colon were significantly increased with enhanced expression of iNOS and COX-2, which was in accordance with the previous reports.

Melatonin, a major hormone produced in pineal gland, was also found in recent years to be secreted for a certain amount from gastrointestinal tract and played an important role in the adjustment of gastrointestinal function[7-14]. As a potent antioxidant agent that could clear oxygen-derived free radicals, inhibit the activation of NF-κB and reduce inflammatory response, melatonin has been widely used to treat inflammatory bowel diseases[29, 30]. Pentney and his coworker[16] have shown melatonin could reduce the severity of dextran-induced colitis in mice. Protective effects of melatonin on dinitrobenzene sulfonic acid induced colitis have been proved by Cuzzocrea and his colleagues[17]. In the present investigation, melatonin was demonstrated to reduce colonic lesions induced by acetic acid and TNBS enemas, which combined with the reports above, suggested that the protective effect of melatonin on the induced colitis might be universal. The present study also revealed the improvement of colonic lesions by melatonin accorded synchronously and unanimously with the decrease of colonic NO and $PGE_2$ content, as well as the down-regulated expression of colonic iNOS and COX-2, which indicates the improvement is probably via a mechanism of local inhibition of iNOS and COX-2 expression in the colonic mucosa. Further studies are needed to explore other mechanisms involved in the protection of colonic mucosa by melatonin.

## REFERENCES


1 **Sakamoto C**. Roles of COX-1 and COX-2 in gastrointestinal pathophysiology. *J Gastroenterol* 1998; **33**: 618-624

2 **Kankuri E**, Asmawi MZ, Korpela R, Vapaatalo H, Moilanen E. Induction of iNOS in a rat model of acute colitis. *Inflammation* 1999; **23**: 141-152

3 **Vural H**, Sabuncu T, Arslan SO, Aksoy N. Melatonin inhibits lipid peroxidation and stimulates the antioxidant status of diabetic rats. *J Pineal Res* 2001; **31**: 193-198

4 **Cuzzocrea S**, Reiter RJ. Pharmacological action of melatonin in shock, inflammation and ischemial-reperfusion injury. *Eur J Pharmacol* 2001; **426**: 1-10

5 **Bubenik GA**. Gastrointestinal melatonin: localization, function, and clinical relevance. *Dig Dis Sci* 2002; **47**: 2336-2348

6 **Maestroni GJ**. The immunotherapeutic potential of melatonin. *Expert Opin Investig Drug* 2001; **10**: 467-476

7 **Sjoblom M**, Jedstedt G, Flemstrom G. Peripheral melatonin mediates neural stimulation of duodenal mucosal bicarbonate secretion. *J Clin Invest* 2001; **108**: 625-633

8 **Sener-Muratoglu G**, Paskaloglu K, Arbak S, Hurdag C, Ayanoglu-Dulger G. Protective effect of famotidine, omeprazole, and melatonin against acetylsalicylic acid-induced gastric damage in rats. *Dig Dis Sci* 2001; **46**: 318-330

9 **Otsuka M**, Kato K, Murai I, Asai S, Iwasaki A, Arakawa Y. Roles of nocturnal melatonin and the pineal gland in modulation of water-immersion restraint stress-induced gastric mucosal lesions in rats. *J Pineal Res* 2001; **30**: 82-86

10 **Bubenik GA**. Localization, physiological significance and possible clinical implication of gastrointestinal melatonin. *Biol Signals Recept* 2001; **10**: 350-366

11 **Cabeza J**, Motilva V, Martin MJ, de la Lastra CA. Mechanisms involved in gastric protection of melatonin against oxidant stress by ischemia-reperfusion in rats. *Life Sci* 2001; **68**: 1405-1415

12 **Bandyo Padhyay D**, Biswas K, Bandyopadhyay U, Reiter RJ, Banerjee RK. Melatonin protects against stress-induced gastric lesion by scavenging the hydroxyl radical. *J Pineal Res* 2000; **29**: 143-151

13 **Messner M**, Huether G, Lorf T, Ramadori G, Schworer H. Presence of melatonin in the human hepatobiliary-gastrointestinal tract. *Life Sci* 2001; **69**: 543-551

14 **Ustundag B**, Kazez A, Demirbag M, Canatan H, Halifeoglu I, Ozercan IH. Protective effect of melatonin on antioxidative system in experimental ischemia-reperfusion of rat small intestine. *Cell Physiol Biochem* 2000; **10**: 229-236

15 **Poon AM**, Mak AS, Luk HT. Melatonin and 2[$^{125}$I] iodomelatonin binding sites in the human colon. *Endocr Res* 1996; **22**: 77-94

16 **Pentney PT**, Bubenik GA. Melatonin reduces the severity of dextran-induced colitis in mice. *J Pineal Res* 1995; **19**: 31-39

17 **Cuzzocrea S**, Mazzon E, Serraino I, Lepore V, Terranova ML, Ciccolo A. Melatonin reduces dinitrobenzene sulfonic acid-induced colitis. *J Pineal Res* 2001; **30**: 1-12

18 **Morris GP**, Beck PL, Herridge MS. Hapten-induced model of chronic inflammation and ulceration in the rat colon. *Gastroenterol* 1989; **96**: 795-803

19 **Mei Q**, Yu JP, Xu JM, Wei W, Xiang L, Yue L. Melatonin reduces colon immunological injury in rats by regulating activity of macrophages. *Acta Pharmacol Sin* 2002; **23**: 882-886

20 **Millar AD**, Rampton DS, Chander CL, Claxson AW, Blades S, Coumbe A. Evaluating the antioxidant potential of new treatments for inflammatory bowel disease using a rat model of colitis. *Gut* 1996; **39**: 407-415

21 **Raab Y**, Sundberg C. Mucosal synthesis and release of prostaglandin E2 from activated eosinophils and macrophages in ulcerative colitis. *Am J Gastroentrol* 1995; **90**: 614-620

22 **Shechter H**, Gruener N, Shuval HI. A micromethod for the determination of nitrite in blood. *Anal Chim Acta* 1972; **60**: 93-99

23 **Luo YQ**, Wu KC, Sun AH, Pan BR, Zhang XY, Fan DM. Significance of COX-1, COX-2 and iNOS expression in superficial gastritis, gastric mucosa atypical hyperplasia and gastric carcinoma. *Zhonghua Xiaohua Zazhi* 2000; **20**: 223-226

24 **Southey A**, Tanaka S, Murakami T. Pathophysiological role of nitric oxide in rat experimental colitis. *Int J Immunopharmacol* 1997; **19**: 669-676

25 **Middleton SJ**, Shorthouse M, Hunter JO. Increased nitric oxide synthesis in ulcerative colitis. *Lancet* 1993; **341**: 465-469
26 **Dijkstra G**, Moshage H, van Dullemen HM, de Jager-Krikken A, Tiebosch AT, Kleibeuker JH, Jansen PL, van Goor H. Expression of nitric oxide synthases and formation of nitrotyrosine and reactive oxygen species in inflammatory bowel disease. *J Pathol* 1998; **186**: 416-421
27 **El-Shenawy SM**, Abdel-Salam OM, Baiuomy AR, El-Batran S, Arbid MS. Studies on the anti-inflammatory and anti-nociceptive effects of melatonin in the rat. *Pharmacol Res* 2002; **46**: 235-243
28 **Schmidt C**, Baumeister B, Kipnowski J. Alteration of prostaglandin $E_2$ and leukotriene $B_4$ synthesis in chronic inflammatory bowel disease. *Hepatogastroenterology* 1996; **43**: 1508-1512
29 **Reiter RJ**, Melchiorri D, Sewerynek E, Poeggeler B, Barlow-Walden L, Chuang J. A review of the evidence supporting Melatonin's role as an antioxidant. *J Pineal Res* 1995; **18**: 1-11
30 **Bubenik GA**, Blask DE, Brown GM, Maestroni GJ. Prospects of the clinical utilization of melatonin. *Biol Signals Recept* 1998; **7**: 195-219

**Edited by** Zhu L

P.O.Box 2345, Beijing 100023,China
Fax: +86-10-85381893
E-mail: wjg@wjgnet.com www.wjgnet.com

World J Gastroenterol 2003;9(6):1312-1317
World Journal of Gastroenterology
Copyright ©2003 by The WJG Press ISSN 1007-9327

• BASIC RESEARCH •

# Rapid mitogen-activated protein kinase by basic fibroblast growth factor in rat intestine after ischemia/reperfusion injury

Xiao-Bing Fu, Yin-Hui Yang, Tong-Zhu Sun, Wei Chen, Jun-You Li, Zhi-Yong Sheng

**Xiao-Bing Fu, Yin-Hui Yang, Tong-Zhu Sun, Wei Chen, Jun-You Li, Zhi-Yong Sheng,** Wound Healing and Cell Biology Laboratory, Burns Institute, 304 Hospital, Trauma Center of Postgraduate Medical College, Beijing 100037, China
**Supported in part by** the National Basic Science and Development Programme (973 Programme, No.G1999054204), Grant for National Distinguished Young Scientists No. 39525024, Grant for National Natural Science Foundation of China, No. 39900054, 30170966
**Correspondence to:** Professor Xiao-Bing Fu, Wound Healing and Cell Biology Laboratory, 304 Hospital, Burns Institute, Trauma Center of Postgraduate Medical College, 51 Fu Cheng Road, Beijing 100037, China. fuxb@cgw.net.cn
**Telephone:** +86-10-66867396 **Fax:** +86-10-88416390
**Received:** 2003-03-04 **Accepted:** 2003-04-01

## Abstract

**AIM:** Previous studies showed that exogenous basic fibroblast growth factor (bFGF or FGF-2) could improve physiological dysfunction after intestinal ischemia/reperfusion (I/R) injury. However, the mechanisms of this protective effect of bFGF are still unclear. The present study was to detect the effect of bFGF on the activities of mitogen-activated protein kinase (MAPK) signaling pathway in rat intestine after I/R injury, and to investigate the protective mechanisms of bFGF on intestinal ischemia injury.

**METHODS:** Rat intestinal I/R injury was produced by clamping the superior mesenteric artery (SMA) for 45 minutes and followed by reperfusion for 48 hours. Seventy-eight Wistar rats were used and divided randomly into sham-operated group (A), normal saline control group (B), bFGF antibody pre-treated group (C), and bFGF treated group (D). In group A, SMA was separated without occlusion. In groups B, C and D, SMA was separated and occluded for 45 minutes, then, released for reperfusion for 48 hours. After the animals were sacrificed, blood and tissue samples were taken from the intestine 45 minutes after ischemia in group A and 2, 6, 24, and 48 hours after reperfusion in the other groups. Phosphorylated forms of p42/p44 MAPK, p38 MAPK and stress activated protein kinase/C-Jun N-terminal kinase (SAPK/JNK) were measured by immunohistochemistry. Plasma levels of D-lactate were examined and histological changes were observed under the light microscope.

**RESULTS:** Intestinal I/R injury induced the expression of p42/p44 MAPK, p38 MAPK, and SAPK/JNK pathways and exogenous bFGF stimulated the early activation of p42/p44 MAPK and p38 MAPK pathways. The expression of phosphorylated forms of p42/p44 MAPK was primarily localized in the nuclei of crypt cells and in the cytoplasm and nuclei of villus cells. The positive expression of p38 MAPK was localized mainly in the nuclei of crypt cells, very few in villus cells. The activities of p42/p44 MAPK and p38 MAPK peaked 6 hours after reperfusion in groups B and C, while SAPK/JNK peaked 24 hours after reperfusion. The activities of p42/p44 MAPK and p38 MAPK peaked 2 hours after reperfusion in group D and those of SAPK/JNK were not changed in group B. D-lactate levels and HE staining showed that the intestinal barrier was damaged severely 6 hours after reperfusion; however, histological structures were much improved 48 hours after reperfusion in group D than in the other groups.

**CONCLUSION:** The results indicate that intestinal I/R injury stimulates the activities of MAPK pathways, and that p42/p44 MAPK and p38MAPK activities are necessary for the protective effect of exogenous bFGF on intestinal I/R injury. The protective effect of bFGF on intestinal dysfunction may be mediated by the early activation of p42/p44 MAPK and p38 MAPK signaling pathways.

Fu XB, Yang YH, Sun TZ, Chen W, Li JY, Sheng ZY. Rapid mitogen-activated protein kinase by basic fibroblast growth factor in rat intestine after ischemia/reperfusion injury. *World J Gastroenterol* 2003; 9(6): 1312-1317
http://www.wjgnet.com/1007-9327/9/1312.asp

## INTRODUCTION

Previous studies have shown that intestinal ischemia/reperfusion (I/R) injury reduce the expression of endogenous basic fibroblast growth factor (bFGF) in rats, and the intravenous administration of exogenous bFGF could induce the expression of endogenous bFGF and improve the physiological functions of the intestine, lung, kidney, and other internal organs after I/R injury[1-6]. However, the protective mechanisms of bFGF on intestinal I/R injury remain unknown.

Mitogen-activated protein kinase (MAPK) cascade, a cytoplasmic protein kinase that requires dual phosphorylation on specific threonine and tyrosine residues for their activation, can transmit mitogen or differentiation signals from the cell surface into the nucleus, thus regulating the gene expression[7-10]. P42/p44 MAPK, p38MAPK and stress activated protein kinase/C-Jun N-terminal kinase (SAPK/JNK) are three important members of the MAPK family. The purpose of the present study was to detect the activities of mitogen-activated protein kinase (MAPK) signaling pathway in rat intestine after administration of bFGF, and to investigate the protective mechanisms of bFGF on intestinal (I/R) injury.

Rat intestinal I/R injury was produced by clamping the superior mesenteric artery (SMA) for 45 minutes and by different durations of reperfusion[11]. The activities of p42/p44 MAPK, p38 MAPK, and SAPK/JNK were measured after administration of bFGF or bFGF monoclonal antibody. The results indicate that the early activation of p42/p44 MAPK and p38 MAPK is necessary for the protective effect of bFGF on intestinal I/R injury.

## MATERIALS AND METHODS

### *Animal model*

Seventy-eight healthy Wistar rats weighing 220±20 g (Animal Center, Academy of Military Medical Sciences, Beijing) were used. All animals were housed in the laboratory and given free access to food and water for 1 week before being used. The animal was under anesthesia by 3 % sodium pentobarbital (40 mg/kg), a middle incision was made. The superior mesenteric artery (SMA) was identified and freed by blunt dissection. A microvascular clamp was placed at the root of SMA to cause complete cessation of blood flow for 45 minutes, and thereafter the clamp was loosened to form reperfusion injury[1, 11].After 2, 6, 24 and 48 hours reperfusion, the animals were sacrificed and blood samples and intestinal tissue biopsies were taken. Blood samples were centrifuged and serum was frozen to measure plasma D-lactate. Tissue biopsies were fixed with 4 % paraformaldehyde.

In this study, all operations were performed under aseptic conditions. The animal experiments were approved by the local animal management committee.

### *Experimental design*

The animals were randomly divided into four groups: sham-operated (A), normal saline control (B), bFGF monoclonal antibody (Sigma, St. Louis, MO, USA) pre-treated (C) and bFGF (Sigma, St. Louis, MO, USA) treated groups (D). In group A, SMA was freed but without occlusion and blood samples and tissue biopsies were taken 45 minutes after exposure of the SMA. In groups B and D, 0.15 ml saline or 0.15 ml saline plus bFGF (2 μg/rat) was injected immediately 45 minutes after SMA occlusion from the tail vein. In group C, 0.15 ml saline plus bFGF monoclonal antibody (25 μg/rat) was injected right before SMA occlusion from tail vein for pre-treatment.

### *Measurement of phosphorylated forms of p42/p44 MAPK, p38 MAPK and SAPK/JNK*

Formalin-fixed, paraffin-embedded small intestinal tissues were used to measure the expression of phosphorylated forms of p42/p44 MAPK, p38 MAPK, and SAPK/JNK by immunohistochemistry. Immunohistochemical staining was performed according to the instructions of the PowerVision™ kit (Santa Cruze, USA). Briefly, sections (5 μm) were dewaxed and rehydrated in graded alcohols. Endogenous peroxidase activity was quenched, and antigen retrieval was performed by heating for 20 minutes at 100 ℃ in 0.01 mol/L sodium citrate. The primary monoclonal antibodies for p42/p44 MAPK, p38 MAPK and SAPK/JNK (Cell Signaling Technology, Inc., USA) were diluted to 1:100 in buffer and incubated for 40 minutes at 37 ℃. The sections were then incubated with HRP-conjugated secondary antibodies (Santa Cruz, USA) for 20 minutes at 37 ℃. Positive expression was detected with diaminobenzidine (DAB) (Sigma, St. Louis, MO, USA). The sections were lightly counterstained with hematoxylin, dehydrated in graded alcohol, and mounted. For negative control, the sections were processed similarly but PBS was used as primary antibodies instead of the MAPKs monoclonal antibodies.

The result of positive staining was semi-quantitatively defined as -, +, ++ and +++. This was observed under microscope with 10 times eyepiece and 40 times objective. "-" represents no visible positive staining, "+" less than 10 stained cells and "++" 10-30 stained cells, while "+++" represents more than 30 positively stained cells within one high power field.

### *Measurement of plasma D-lactate*

The levels of plasma D-lactate were measured with modified Brandt' s method[12]. Briefly, heparinized blood was centrifuged at 3 200 rpm for 10 min and 2 ml of the plasma was deproteinized with 0.2 ml perchloric acid (PCA) (1/10 vol), mixed and kept in an ice bath for 10 min. The denatured protein solution was centrifuged at 3 200 rpm for 10 min and the supernatant solution was removed. To 1.4 ml of supernatant solution, 0.12 ml KON was added and they were mixed for 20 s. Precipitant $KClO_4$ was removed by centrifugation at 3 200 rpm for 10 min. The supernatant solution and neutralized-protein-free plasma were used to measure the absorbency at 340 nm. Plasma D-lactate concentration was expressed as mmol/L.

### *Histological observation*

Paraformaldehyde fixed, paraffin embedded small intestine samples were also cut 5 μm in thickness, deparaffinized in xylene, rehydrated in graded ethanol, and then stained with haematoxylin-eosin (HE) for histological observation under light microscope (Olympus, Japan).

### *Statistical analysis*

Data were expressed as mean ± standard error. Comparisons between groups of data were analyzed by Student' s *t*-test. *P* values <0.05 were considered statistically significant.

## RESULTS

### *Activities of p42/p44 MAPK and p38 MAPK*

Quantitative immunohistochemical results for phosphorylated forms of p42/p44 MAPK and p38 MAPK were evaluated (Tables 1 and 2). The expression of activated p42/p44 MAPK was localized in the cytoplasm and nuclei of villus cells and in the nuclei of crypt cells, mainly in the epithelium and villus cells (Figure 1). Activated p38 MAPK was localized primarily in the nuclei of crypt cells, very few in villus cells (Figure 2). There was a consistent correlation between positive expression levels and the intensity of p42/p44 MAPK and p38 MAPK. The positive expression of p42/p44 MAPK and p38 MAPK was weak in the sham-operated intestinal tissues and ischemic tissues. However, the number of positive staining cells increased with high staining intensity after reperfusion injury. In the normal saline and bFGF antibody pre-treated groups, the number of positive staining cells of p42/p44 MAPK (Figures 1B and C) and p38 MAPK (Figures 2B and C) increased 2 hours after reperfusion, peaked at 6th hours, and decreased from 24 to 48 hours. In the bFGF treated group, however, the number of positive staining cells and the intensity of p42/p44 MAPK and p38 MAPK peaked 2 hours after reperfusion (Figures 1D and 2D) and decreased afterwards, but they were still higher than those in the sham-operated control at 48 hours. Compared with the normal saline and bFGF treated groups, the intensity of p42/p44 MAPK and p38 MAPK positive staining in the bFGF antibody pretreated group was weaker from 2 hours to 48 hours after reperfusion.

### *Activities of SAPK/JNK*

Weak staining of SAPK/JNK was observed in small intestine after I/R injury. Positive staining was localized in the nuclei and cytoplasm of villus and crypt cells. The staining, however, was weak without much difference among the groups (Table 3). The positive staining of SAPK/JNK in bFGF treated group was slightly higher only at 24 hours after reperfusion. Among all the groups, the positive staining of SAPK/JNK was weaker than that of p42/p44 MAPK and p38 MAPK.

### *Changes of plasma D-lacate levels*

Plasma D-lactate levels were measured 2, 6, 24, and 48 hours after reperfusion in all groups. They were elevated 2 hours after reperfusion in all groups, peaked at 6th hour, and decreased to nearly normal 48 hours later (Table 4). The levels at 45 min after ischemia in the sham-operated group were served as controls.

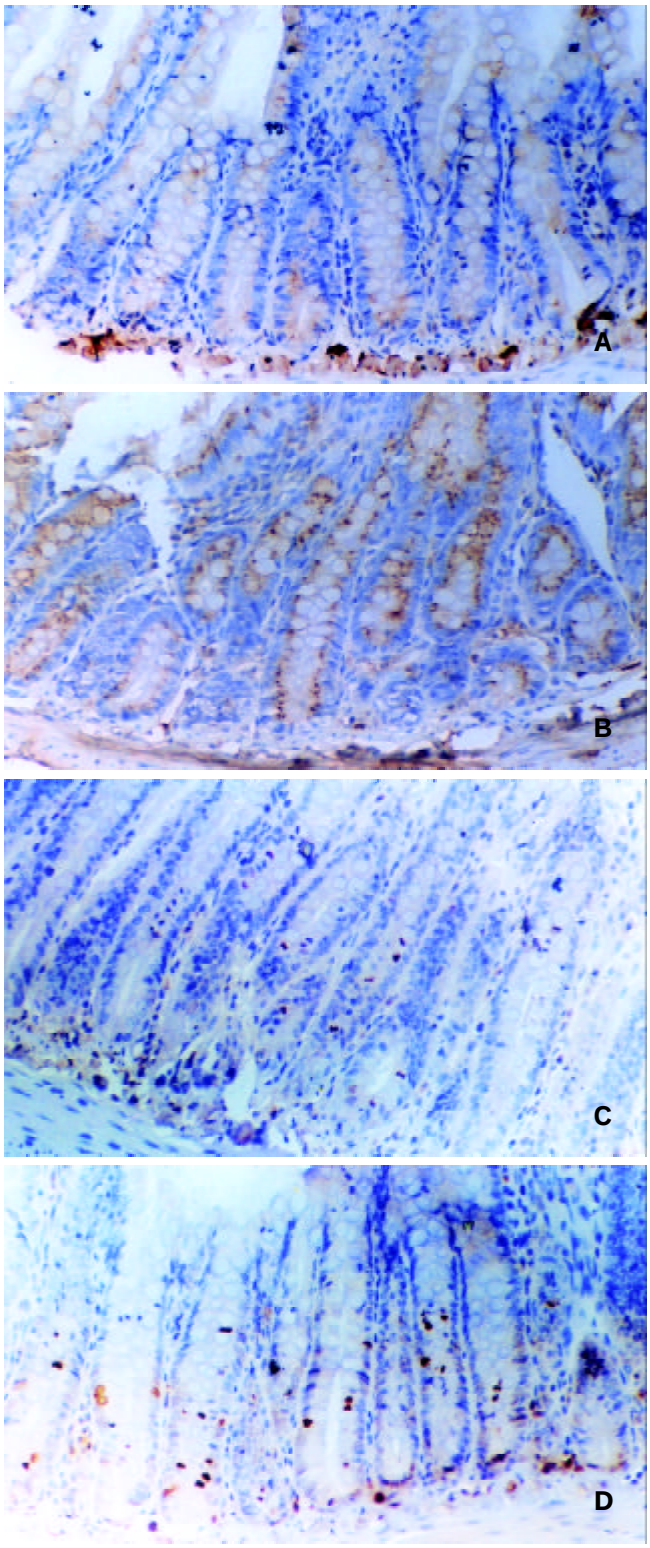


**Figure 1** Immunohistochemical staining of phosphorylated p42/p44 MAPK in intestinal biopsies in rats after ischemia/reperfusion injury (SP×200). A: Negative control of p42/p44 MAPK staining. There was no positive expression signal in this group. B: The expression of phosphorylated p42/p44 in intestinal biopsies in the saline control group 2 hours after reperfusion. The activated p42/p44 MAPK expression was localized in the cytoplasm and nuclei of villus cells and in the nuclei of crypt cells, mainly in the epithelium and villus cells. C: Phosphorylated p42/p44 staining in the bFGF antibody pre-treated group. The number of positive cells and intensity in this group were weaker compared with those in the saline control and bFGF treated groups. D: The expression of phosphorylated p42/p44 in the bFGF treated group 2 hours after reperfusion. The activated p42/p44 MAPK expression was localized in the cytoplasm and nuclei of villus cells and in the nuclei of crypt cells, mainly in the epithelium and villus cells. The number of positive cells in this group was more than that in the bFGF antibody pre-treated group. ISH×400.

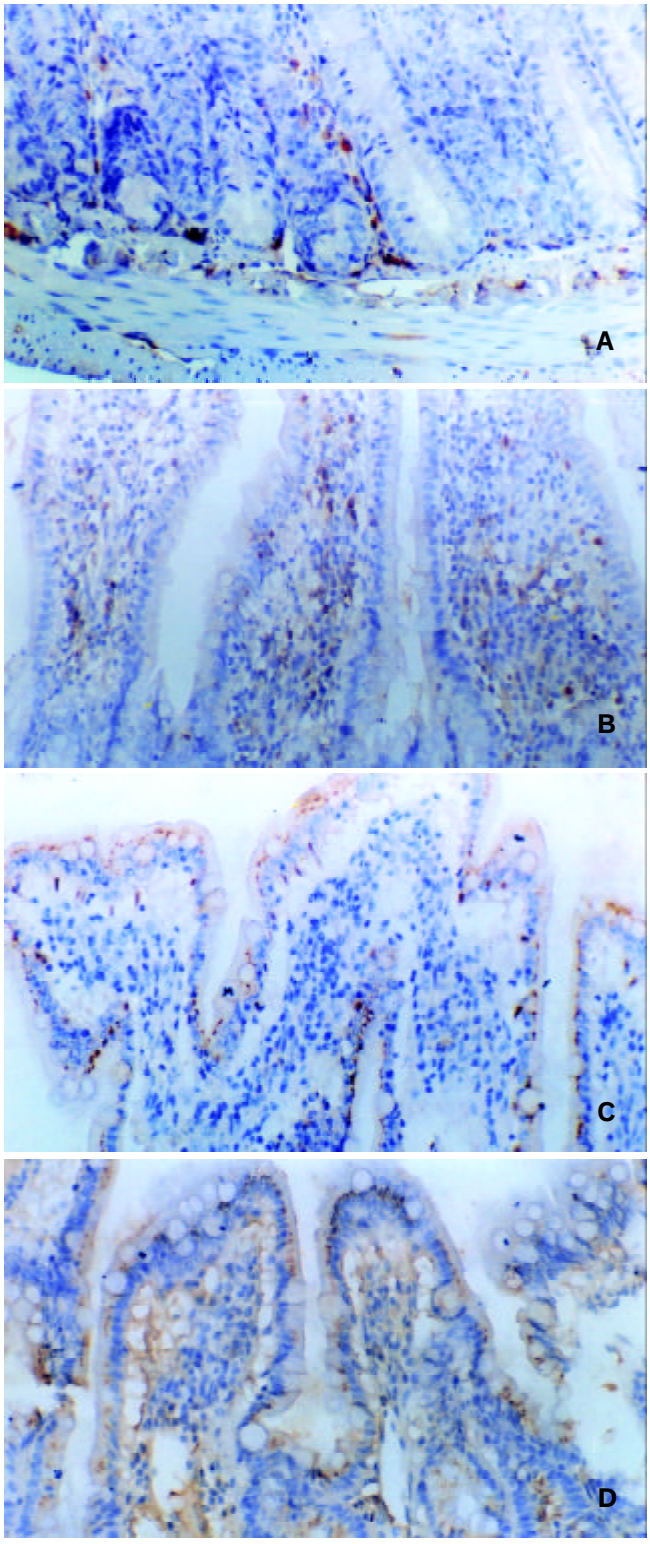


**Figure 2** Immunohistochemical staining of phosphorylated p38 MAPK in intestinal biopsies in rats after ischemia/reperfusion injury (SP×200). A: Negative control of p38 MAPK staining. There was no positive expression signal in this group. B: Phosphorylated p38 MAPK staining in the saline control group 2 hours after reperfusion. Few p38 MAPK positive expression were localized in the cytoplasm and nuclei of villus cells and in the nuclei of crypt cells, mainly in the

**Table 1** Semi-quantitative results of immunohistochemical staining for phosphorylated forms of p42/p44 MAPK in different groups

| Groups | Pre-injury | 2 hrs post-injury | 6 hrs post-injury | 24 hrs post-injury | 48 hrs post-injury |
|---|---|---|---|---|---|
| Group B | - | ++ | ++ | + | ++ |
| Group C | - | + | ++ | + | + |
| Group D | - | +++ | +++ | + | + |

"-" represents no visible positive staining, "+" less than 10 stained cells and "++" 10-30 stained cells, while "+++" represents more than 30 positively stained cells within one high power field.

**Table 2** Semi-quantitative results of immunohistochemical staining for phosphorylated forms of p38 MAPK in different groups

| Groups | Pre-injury | 2 hrs post-injury | 6 hrs post-injury | 24 hrs post-injury | 48 hrs post-injury |
|---|---|---|---|---|---|
| Group B | - | ++ | ++ | + | ++ |
| Group C | - | + | ++ | + | + |
| Group D | - | +++ | ++ | + | + |

"-" represents no visible positive staining, "+" less than 10 stained cells and "++" 10-30 stained cells, while "+++" represents more than 30 positively stained cells within one high power field.

**Table 3** Semi-quantitative results of immunohistochemical staining for phosphorylated forms of SAPK/JNK in different groups

| Groups | Pre-injury | 2 hrs post-injury | 6 hrs post-injury | 24 hrs post-injury | 48 hrs post-injury |
|---|---|---|---|---|---|
| Group B | - | + | + | ++ | + |
| Group C | - | + | + | + | + |
| Group D | - | + | + | ++ | + |

"-" represents no visible positive staining, "+" less than 10 stained cells and "++" 10-30 stained cells, while "+++" represents more than 30 positively stained cells within one high power field.

**Table 4** The changes of plasma D-lactate levels at different time points in three groups (mmol/L) ($\bar{x}\pm s$)

| Groups | Animal numbers | Control | 2 hours | 6 hours | 24 hours | 48 hours |
|---|---|---|---|---|---|---|
| Group B | 24 | 0.332±0.132 | 0.372±0.090 | 0.397±0.096 | 0.463±0.147 | 0.511±0.179 |
| Group C | 24 | 0.332±0.132 | 0.309±0.079 | 0.327±0.098 | 0.415±0.177[a] | 0.425±0.208[a] |
| Group D | 24 | 0.332±0.132 | 0.369±0.124 | 0.407±0.089 | 0.475±0.128 | 0.537±0.098 |

[a]$P<0.05$ *vs* compared with control.

epithelium and villus cells. C: P38 MAPK staining in the bFGF antibody pre-treated group. The number of positive cells and localization of p38 MAPK positive cells were similar with those in the saline group. D: Phosphorylated p38 staining in the bFGF treated group 2 hours after reperfusion. Activated p38 MAPK was localized primarily in the nuclei of crypt cells, few in villus cells. The number of positive cells was more than that in the saline control and bFGF antibody pre-treated groups. In the bFGF treated group, the number of positive expression cells of p38 MAPK as well as its intensity peaked 2 hours after reperfusion.

### *Histological evaluation*

Intestinal I/R injury resulted in the damage of intestinal barrier and the increase of mucosal permeability. HE staining showed partial loss of the mucosa 2 hours after reperfusion. 6 hours after reperfusion, however, the damage of intestinal epithelial cells, hemorrhage and necrosis were observed and accompanied by inflammatory cell infiltration into the intestinal wall. Histological structure of the intestinal mucosa was markedly improved after administration of bFGF.

## DISCUSSION

Intestinal I/R injury causes release of bacteria and toxin from the gut into the host blood circulation and changes of inflammatory factors, cytokines and growth factors, resulting in damage to the intestinal barrier and other internal organs[1-3,13-17]. We found that administration of exogenous basic fibroblast growth factor (bFGF) could reduce the intestinal injury caused by I/R insult. However, the mechanisms of this protective effect of bFGF are not elucidated. BFGF is expressed in many normal adult tissues and has mitogenic activity in a wide variety of cells of mesenchymal, neuronal, and epithelial origins, and regulates events in normal embryonic development, angiogenesis, wound repair, and neoplasia[18-20]. Also, it can regulate migration and replication of intestinal epithelial cells in culture[21]. Recent studies have shown that L-glutamine, tumor necrosis factor-$\alpha$ and epidermal growth factor (EGF) stimulate proliferation of intestinal crypt cells by activating the MAPK pathway, and that p42/p44 MAPK activities are necessary for both cell cycle progression and differentiation of the intestinal cells[22-25]. In many other cell types, growth factor controls proliferation and differentiation

via the MAPK pathway. MAPK is a common signal pathway to transmit the mitogen or the differentiating signals from the cell surface to the nucleus, and thus ultimately regulates different gene expression[26-28]. Hence, we hypothesized that MAPK activation might be involved in the regulation of bFGF signals in the process of intestinal barrier repair.

To investigate this hypothesis, we evaluated changes of the activated MAPK signal pathway after administration of bFGF and bFGF antibodies. We found that intestinal I/R injury stimulated the activities of phosphorylated forms of the p42/p44 MAPK and p38MAPK pathways, and increased the SAPK/JNK activity slightly. p42/p44 MAPK and p38MAPK activities were increased 2 hours after reperfusion, and peaked at 6 hours. At the same time, the levels of SAPK/JNK increased slightly 24 hours after reperfusion compared with those of the normal control. Phosphorylated forms of p42/p44 MAPK were mainly localized in the nuclei of crypt cells and in the cytoplasm and nuclei of villus cells, whereas those of p38MAPK were primarily localized in the nuclei of crypt cells, few in villus cells. After administration of bFGF, the expression of both p42/p44 MAPK and p38MAPK was quickly stimulated, and the activation of both p42/p44 MAPK and p38MAPK peaked 2 hours after reperfusion, declined gradually to normal at 48 hours. A coherence was noted between the changes of p42/p44 MAPK and p38MAPK and histological findings. These results indicate that intestinal I/R injury induces the activities of the MAPK pathways, and p42/p44 MAPK and p38MAPK activities are necessary for the protective effects of exogenous bFGF on intestinal I/R injury. The early stimulation of the p42/p44 MAPK and p38MAPK signal pathways may mediate the protective effects of bFGF on intestinal dysfunction.

MAPK family is composed of "extracellular signal regulated" p42/p44 MAPK, "stress-regulated" MAPK (SR-MAPKs), stress-activated protein kinases (SAPKs)/c-Jun N-terminal kinases (JNKs) and p38-MAPKs. On stimulation, MAPKs are translated into the nucleus where they may phosphorylate nuclear transcription factors and thus regulate gene expression. The four principal differentiated cell lineages of intestinal epithelium are derived from common multipotent stem cells located near the base of each crypt. These crypt stem cells divide to produce daughter stem cells as well as more rapidly replicating transit cells, which in turn undergo 4-6 rapid cell divisions in the proliferative zone located in the lower half of each crypt[29,30]. Factors determining whether cells continue to proliferate, cease dividing, and begin to differentiate, appear to operate during the first gap phase (G1) of the cell cycle. P42/p44 is activated during G0 to G1 transition, and the activity remains elevated up to S phase entry, implicating this family of protein quinces in the control of G1 progression[31,32]. Activation of p42/p44 MAPK is also necessary for growth factor-dependent proliferation of some cell lines.

We propose the possible mechanisms of the protective effects of bFGF on intestinal I/R injury be involved in the activation of MAPK pathway. First, to protect the survival of intestinal stem cells within crypt and mediate the proliferation and differentiation of these cells. Intestinal epithelium is maintained by continuous and rapid replacement of differentiated epithelial cells by replication of undifferentiated epithelial cells. Exogenous bFGF markedly enhances the survival of crypt stem cells before and after irradiation injury[33]. Microvascular endothelial apoptosis is the primary lesion leading to stem cell dysfunction, while endothelial apoptosis could be inhibited by intravenous bFGF[34]. Second, to regulate the inflammation reactions after I/R injury. The TNF translation by IL-10 is inhibited mainly by inhibiting the activation of the p38 MAPK pathway[35]. This is necessary for maintenance of immune homeostasis in the gut.

In the perfused heart, ischemia/reperfusion activates stress-regulated MAPKs, direct pharmacological activation of p38 triggers delayed preconditioning of the heart, and there is minimal activation of the p42/p44 MAPK subfamily by heart I/R injury[35-37]. Yet phosphorylation of p42/p44 MAPK occurs consistently in the grey matter penumbra of brain tissue after ischemic stroke, and may be associated with neuronal survival and/or angiogenic activity in the recovering brain tissue[38]. The results indicate that the MAPK pathways respond differently to ischemic injury in different sites.

The changes of serum D (-)-lactate were used as a predictor of intestinal I/R injury in this study. D (-)-lactate is the stereoisomer of mammalian L (+)-lactate. Mammalian tissue does not produce D (-)-lactate and only slowly metabolizes it. It is a strict product of bacterial fermentation. Since mammals do not possess the enzyme systems to rapidly metabolize D (-)-lactate[11, 39,40], the released D (-)-lactate will pass through the gut barrier and liver in an unchanged form and appear in the peripheral blood. As intestinal ischemia injury causes mucosal injury and subsequent bacterial proliferation, D (-)-lactate is released from gut into the circulation. In this study, the serum D (-)-lactate level was increased after injury, but in the bFGF treated group, it was not significantly increased as in the control group, indicating that bFGF exerts a positive protective effect on the mucosal barrier and decreases the intestinal permeability.

In summary, intestinal I/R injury induces the activities of the MAPK pathways, and p42/p44 MAPK and p38MAPK activities are necessary for the protective effect of exogenous bFGF on intestinal I/R injury. The protective effect of bFGF on intestinal dysfunction may be mediated by the early stimulation of the p42/p44 MAPK and p38 MAPK signaling pathways.

## REFERENCES


1 **Fu XB**, Sheng ZY, Wang YP, Ye YX, Xu MH, Sun TZ, Zhou BT. Basic fibroblast growth factor reduces the gut and liver morphologic and functional injuries after ischemia and reperfusion. *J Trauma* 1997; **42:** 1080-1085

2 **Yang YH,** Fu XB, Sun TZ, Jiang LX, Gu XM. bFGF and TGFβ expression in rat kidneys after ischemic / reperfusional gut injury and its relationship with tissue repair. *World J Gastroenterol* 2000; **6**: 147-149

3 **Fu XB,** Yang YH, Sun XQ, Sun TZ, Gu XM, Sheng ZY. Protective effects of endogenous basic fibroblast growth factor activated by 2, 3 butanedion monocime on functional changes of ischemic intestine, liver and kidney in rats. *Zhongguo Weizhongbing Jijiu Yixue* 2000; **12**: 69-72

4 **Yang YH,** Fu XB, Sun TZ, Jiang LX, Gu XM. The effect of exogenous basic fibroblast growth factor on hepatic endogenous basic fibroblast growth factor and fibroblast growth factor receptor expression after intestinal ischemia-reperfusion injury. *Zhongguo Weizhongbing Jijiu Yixue* 1999; **11**: 734-736

5 **Fu XB,** Yang YH, Sun TZ, Sun XQ, Gu XM, Chang GY, Sheng ZY. Effect of inhibition or anti-endogenous basic fibroblast growth factor on functional changes in intestine, liver and kidneys in rats after gut ischemia-reperfusion injury. *Zhongguo Weizhongbing Jijiu Yixue* 2000; **12**: 465-468

6 **Yang YH,** Fu XB, Sun TZ, Jiang LX, Gu XM. Renal endogenous expression of basic fibroblast growth factor and transforming growth factor β after intestinal ischemia-reperfusion injury. *Zhongguo Weizhongbing Jijiu Yixue* 1999; **11**: 203- 205

7 **Marshall CJ.** Specificity of receptor tyrosine kinase signaling: transient versus sustained extracellular signal-regulated kinase activation. *Cell* 1995; **80**: 179-185

8 **Seger R,** Krebs EG. The MAPK signaling cascade. *FASEB J* 1995; **9:** 726-735

9 **Marais R,** Wynne J, Treisman R. The SRF accessory protein Elk-1 contains a growth factor-regulated transcriptional activation domain. *Cell* 1993; **73:** 381-393

10 **Nishida E,** Gotoh Y. The MAP kinase cascade is essential for diverse signal transduction pathways. *Trends Biochem Sci* 1993; **18**: 128-131

11 **Sun XQ,** Fu XB, Zhang R, Lu Y, Deng Q, Jiang XG, Sheng ZY. Relationship between plasma D(-)-lactate and intestinal damage after severe injuries in rats. *World J Gastroenterol* 2001; **7:** 555-558

12 **Qin RY,** Zou SQ, Wu ZD, Qiu FZ. Influence of splanchnic vascular infusion on the content of endotoxins in plasma and the translocation of intestinal bacteria in rats with acute hemorrhage necrosis pancreatitis. *World J Gastroenterol* 2000; **6**: 577-580

13 **Wang XJ,** Luo XD, Luo Q, Yang ZC. Effects of sera from burn patients on human hepatocytic viscoelasticity. *World J Gastroenterol* 1998; **4**: 60

14 **Zhang P,** Yang WM, Shui WX, Du YG, Jin GY. Effect of Chinese herb mixture, shock decoction on bacterial translocation from the gut. *World J Gastroenterol* 2000; **6**(Suppl 3): 74

15 **Zhu L,** Yang ZC, Li A, Cheng DC. Protective effect of early enteral feeding on postburn impairment of liver function and its mechanism in rats. *World J Gastroenterol* 2000; **6**: 79-83

16 **Li YS,** Li JS, Li N, Jiang ZW, Zhao YZ, Li NY, Liu FN. Evaluation of various solutions for small bowel graft preservation. *World J Gastroenterol* 1998; **4**: 140-143

17 **Zhang GL,** Wang YH, Ni W, Teng HJ, Lin ZB. Hepatoprotective role of ganoderma lucidum polysaccharide against BCG in duced immue liver injury in mice. *World J Gastroenterol* 2002; **8:** 728-733

18 **Liu XJ,** Yang L, Mao YQ, Wang Q, Huang MH, Wang YP, Wu HB. Effects of the tyrosine protein kinase inhibitior genistein on the proliferation, activation of cultured rat hepatic stellate cells. *World J Gastroenterol* 2002; **8**: 739-745

19 **Brandt RB,** Siegel SA, Waters MG, Bloch MH. Spectrophotometric assay for D-(-)-Lactate in plasma. *Anal Biochem* 1980; **102**: 39-46

20 **Basilico C,** Moscatelli D. The FGF family of growth factors and oncogenes. *Adv Cancer Res* 1992; **59:** 115-165

21 **Dignass AU,** Tsunekawa S, Podolsky DK. Fibroblast growth factors modulate intestinal epithelial cell growth and migration. *Gastroenterology* 1994; **106:** 1254-1262

22 **Estival A**, Monzat V, Miquel K, Gaubert F, Hollande E, Korc M, Vaysse N, Clemente F. Differential regulation of fibroblast growth factor receptor-1 mRNA and protein by two molecular forms of basic FGF. *J Biol Chem* 1996; **271**: 5663-5670

23 **Nice EC,** Fabri L, Whitehead RH, James R, Simpson RJ, Burgess AW. The major colonic cell mitogen extractable from colonic mucosa ia an N-terminally extended form of basic fibroblast growth factor. *J Biol Chem* 1991; **266**: 14425-14430

24 **Rhoads JM,** Argenzio RA, Chen W, Rippe RA, Westwick JK, Cox AD, Berschneider HM, Brenner DA. L-glutamine stimulates intestinal cell proliferation and activates mitogen-activated protein kinases. *Am J Physiol* 1997; **272:** G943-G953

25 **Oliver BL,** Sha'afi RI, Hajjar JJ. Transforming growth factor-alpha and epidermal growth factor activate mitogen-activated protein kinase and its substrates in intestinal epithelial cells. *Proc Soc Exp Biol Med* 1995; **210**: 162-170

26 **Goke M,** Kanai M, Lgnch-Devaney K, Podolsky DK. Rapid mitogen-activated protein kinase activation by transforming growth factor alpha in wounded rat intestinal epithelial cells. *Gastroenterology* 1998; **114**: 697-705

27 **Aliaga JC,** Deschenes C, Beaulieu JF, Calvo EL, Rivard N. Requirement of the MAP kinase cascade for cell cycle progression and differentiation of human intestinal cells. *Am J Physiol* 1999; **277**:G631-G641

28 **Gordon JI,** Hermiston ML. Differentiation and self-renewal in the mouse gastrointestinal epithelium. *Curr Opin Cell Biol* 1994; **6**: 795-803

29 **Potten CS,** Booth C, Pritchard DM. The intestinal epithelial stem cell: the mucosal governor. *Int J Exp Pathol.* 1997; **78:** 219-243

30 **Brondello JM,** McKenzie FR, Sun H, Tonks NK, Pouyssegur J. Constitutive MAP kinase phosphatase (MKP-1) expression blocks G1 specific gene transcription and S-phase entry in fibroblasts. *Oncogene* 1995; **10:** 1895-1904

31 **Meloche S,** Seuwen K**,** Pages G, Pouyssegur J. Biphasic and synergistic activation of p44MAPK (ERK1) by growth factors: correlation between late phase activation and mitogenicity. *Mol Endocrinol* 1992; **6**: 845-854

32 **Houchen CW,** George RJ, Sturmoski MA, Cohn SM. FGF-2 enhances intestinal stem cell survival and its expression is induced after radiation injury. *Am J Physio* 1999; **276**: G249-G258

33 **Paris F,** Fuks Z, Kang A, Capodieci P, Juan G, Ehleiter D, Haimovitz-Friedman A, Cordon-Cardo C, Kolesnick R. Endothelial apoptosis as the primary lesion initiating intestinal radiation damage in mice. *Science* 2001; **293:** 293-297

34 **Kontoyiannis D,** Kotlyarov A, Carballo E, Alexopoulou L, Blackshear PJ, Gaestel M, Davis R, Flavell R, Kollias G. Interleukin-10 targets p38 MAPK to modulate ARE-dependant TNF mRNA translation and limit intestinal pathology. *EMBO J* 2001; **20:** 3760-3770

35 **Clerk A,** Fuller SJ, Michael A, Sugden PH. Stimulation of "stress-regulated" mitogen-activated protein kinases (stress-activated protein kinases/c-Jun N-terminal kinases and p38-mitogen-activated protein kinases) in perfused rat hearts by oxidative and other stresses. *J Biol Chem* 1998; **273**: 7228-7234

36 **Zhao TC**, Taher MM, Valerie KC, Kukreja RC. p38 triggers late preconditioning elicited by anisomycin in heart: involvement of NF-KB and iNOS. *Circ Res* 2001; **89**: 915-922

37 **Tong H**, Chen W, London RE, Murphy E, Steenbergen C. Preconditioning enhances glucose uptake is mediated by p38 MAP kinase not by phophatidylinositol 3-kinase. *J Biol Chem* 2000; **275**: 11981-11986

38 **Slevin M,** Krupinski J, Slowik A, Rubio F, Szczudlik A, Gaffney J. Activation of MAP kinase (ERK-1/ERK-2), tyrosine kinase and VEGF in the human brain following acute ischaemic stroke. *Neuroreport* 2000; **11:** 2759-2764

39 **Murray MJ,** Barbose JJ, Cobb CF. Serum D (-)-lactate levels as a predictor of acute intestinal ischemia in a rat model. *J Surg Res* 1993; **54:** 507-509

40 **Murray MJ,** Gonze MD, Nowak LR, Cobb CF. Serum D (-)-lactate levels as an aid to diagnosing acute intestinal ischemia. *Am J Surg* 1994; **167:** 575-578


**Edited by** Zhang JZ and Zhu LH

P.O.Box 2345, Beijing 100023,China
Fax: +86-10-85381893
E-mail: wjg@wjgnet.com www.wjgnet.com

World J Gastroenterol 2003;9(6):1318-1322
World Journal of Gastroenterology
Copyright ©2003 by The WJG Press ISSN 1007-9327

• BASIC RESEARCH •

# Role of nitric oxide and peroxynitrite anion in lung injury induced by intestinal ischemia-reperfusion in rats

Jun-Lin Zhou, Guo-Hua Jin, Yi-Ling Yi, Jun-Lan Zhang, Xin-Li Huang

**Jun-Lin Zhou,** Department of Hand Surgery, Third Affiliated Hospital, Hebei Medical University, Shijiazhuang 050051, Hebei Province, China
**Guo-Hua Jin,** Department of Liver Medicine, Third Affiliated Hospital, Hebei Medical University, Shijiazhuang 050051, Hebei Province, China
**Yi-Ling Yi, Jun-Lan Zhang, Xin-Li Huang,** Department of Pathophysiology, Hebei Medical University, Shijiazhuang 050017, Hebei Province, China
**Correspondence to:** Dr. Jun-Lin Zhou, Department of Hand Surgery, Third Affiliated Hospital, Hebei Medical University, Shijiazhuang 050051, Hebei Province, China. zhjunlin@yahoo.com
**Telephone:** +86+311-7027951 Ext 3117
**Received:** 2003-01-18 **Accepted:** 2003-03-10

## Abstract

**AIM:** To evaluate effects of nitric oxide (NO) and peroxynitrite anion ($ONOO^-$) on lung injury following intestinal ischemia-reperfusion (IR) in rats.

**METHODS:** A rat model of intestinal ischemia was made by clamping superior mesenteric artery and lung injury was resulted from reperfusion. The animals were randomly divided into 3 groups: sham operation (Sham), 2 h ischemia followed by 2 h reperfusion (IR) and IR pretreated with aminoguanidine (AG) - an inhibitor of inducible NO synthase (iNOS) 15 minutes before reperfusion (IR+AG). The lung malondialdehyde (MDA) and nitrate/nitrite ($NO_2^-$ /$NO_3^-$) contents and morphological changes were examined. Western blot was used to detect the iNOS protein expression. Immunohistochemical staining was used to determine the change of nitrotyrosine (NT)- a specific "footprint" of $ONOO^-$.

**RESULTS:** The morphology revealed evidence for lung edema, hemorrhage and polymorphonuclear sequestration after intestinal IR. Compared with sham group, lung contents of MDA and $NO_2^-$/$NO_3^-$ in IR group were significantly increased (12.00±2.18 *vs* 23.44±1.25 and 76.39±6.08 *vs* 140.40±4.34, $P<0.01$) and the positive signals of iNOS and NT were also increased in the lung. Compared with IR group, the contents of MDA and $NO_2^-$/$NO_3^-$ in IR+AG group were significantly decreased (23.44±1.25 *vs* 14.66±1.66 and 140.40±4.34 *vs* 80.00±8.56, $P<0.01$) and NT staining was also decreased.

**CONCLUSION:** Intestinal IR increases NO and $ONOO^-$ production in the lung, which may be involved in intestinal IR-mediated lung injury.

Zhou JL, Jin GH, Yi YL, Zhang JL, Huang XL. Role of nitric oxide and peroxynitrite anion in lung injury induced by intestinal ischemia-reperfusion in rats. *World J Gastroenterol* 2003; 9 (6): 1318-1322
http://www.wjgnet.com/1007-9327/9/1318.asp

## INTRODUCTION

A devastating consequence of tissue reperfusion is the damage in organs uninvolved in the initial ischemic insult[1]. Multiple organ dysfunction syndrome (MODS), as it is known, is the leading cause of death in critically ill patients and is a documented consequence of gut reperfusion[2-5]. Although systemic inflammatory characteristic of MODS can result in damage to any organ, onset of the syndrome is usually heralded by the development of respiratory insufficiency[2-9]. The pathophysiology of lung injury associated with intestinal ischemia-reperfusion (IIR) probably involves a variety of inflammatory and vasoactive mediators. Recently, the production of large amounts of nitric oxide (NO), a free radical produced by the inducible isoform of NO synthase (iNOS) has been implicated as a cytotoxic factor in a variety of pathophysiological processes, including various forms of inflammation and circulatory shock[10-14]. The cytotoxic effects of NO are in part, mediated by peroxynitrite anion ($ONOO^-$), a reactive oxidant species formed from NO and superoxide at an almost diffusion-controlled rate[15-18]. The production of $ONOO^-$ has been demonstrated in various lung injury[19-21]. However, no evidence exists about its change and role in the lung injury following IIR. The major aim of the present study, therefore, was to determine the change and role of iNOS and peroxynitrite in lung injury induced by IIR.

## MATERIALS AND METHODS

### *Animal model*[22]

Male healthy Sprague-Dawley rats (250-300 g) were anesthetized with intraperitoneal administration of sodium pentobarbital (40 mg· $kg^{-1}$) and secured in a supine position on a heated restraining board at 37 ℃ after being shaved. Following midline laparotomy, a microvascular clip was placed across the superior mesenteric artery (SMA) for 120 minutes. Removal of the clip allowed reperfusion for120 minutes. This degree of IIR is consistently associated with intestinal, hepatic and pulmonary injury with a 12-hour mortality rate of 100 %.

### *Experimental protocols*

To determine the effect of iNOS induction on the peroxynitrite formation and the lung injury, aminoguanidine (AG), an inhibitor of iNOS[23], was used. The rats were randomly divided into 3 groups ($n$=8 in each): Sham, IR and IR+AG. The surgical sham group underwent full surgical preparation including isolation of the SMA without occlusion. After that they were followed for the same aggregate period of time. The IR group received 2 h of ischemia and 2 h of reperfusion. The IR + AG group was given AG (10 mg· $kg^{-1}$ intravenously, Sigma, USA) 15 min before reperfusion. The animals in IR group and sham group were treated with equal volume of the vehicle (normal saline solution, NS; 1 ml· $kg^{-1}$). All animals were killed by exsanguination at designated time. Both lungs were harvested immediately for the following detection.

### *Lung histology*

The right middle lung lobe was harvested and fixed in 10 % formalin. After embedded in paraffin, sections of 8 μm were stained with hematoxylin and eosin for light microscopy.

### *Assessments of lung malondialdehyde (MDA) content*

The right base of lung was harvested and immediately homogenized on ice in 9 volumes saline. The homogenates were centrifuged at 4 000 r· min$^{-1}$ at 4 ℃ for 10 min. The MDA content in the supernatants was measured using MDA assay kit (Nanjing Jiancheng Corp. China).

### Lung nitrite/nitrate ($NO_2^-$ /$NO_3^-$) detection

$NO_2^-$/$NO_3^-$ production, an indicator of NO synthesis, was measured in the lung homogenate with a NO assay kit (Nanjing Jiancheng Corp. China) following the manufacturer' s instruction.

### *Western blotting analysis for iNOS*

The left lung was homogenized with PBS (pH 7.2) and centrifuged at 4 ℃, 18 000 r· min$^{-1}$ for 10 min. After precipitated unsolubilized fraction was discarded, the protein concentration in the supernatant was determined by Coomassie blue dye-binding assay (Nanjing Jiancheng Corp. China). Aliquots (30 μg) of protein from each sample were electrophoresed on a 120 g· L$^{-1}$ SDS-polyacrylamide gel for 4 hour at 100V. The protein samples were transferred onto a nitrocellulose membrane (Amersham, USA). The membrane was then probed with polyclonal rabbit anti-rat iNOS antibody (1:50 dilution, Santa Cruz Co., USA) for 2 hours at 37 ℃. After 3 washes with TPBS, blots were visualized with the use of an amplified HRP kit (Wuhan Boshide, China). The presence of iNOS was indicated by the development of brown color.

### *Immunohistochemical analysis of NT*

Tyrosine nitration, a specific "footprint" of peroxynitrite formation[16], was detected in the left lung by immunohistochemical technique. The left lung was harvested and fixed in 10 % formalin. Sections of 8 μm thickness of lung tissue were treated with 0.3 % $H_2O_2$ in methanol to block endogenous peroxide activity. Immunohistochemical staining was performed using rabbit polyclonal antibody against NT (1:50 dilution, Cayman Chemical, USA) by indirect streptavidin/peroxidase technique (SP kit, Zymed Co., USA). Experiments were performed following the manufacturer' s instruction. Paraffin-embedded sections were incubated with polyclonal anti-rat NT antibody for 12 hours at 4 ℃ after antigen retrieval. Biotinylated IgG was added as second antibody. Horseradish peroxidase labeled streptomycin-avidin complex was used to detect second antibody. Slides were stained with diaminnobenzidine, and examined under light microscope. The brown or dark brown stained cytoplasm was considered as positive.

### *Statistical analysis*

Values were expressed as mean ±SD ($\bar{x}$±*s*). Statistical analyses were performed using paired Student' s *t* test. $P<0.05$ was considered significant.

## RESULTS

### *Pathological alternations of lung tissue*

The histological structure of alveolar and mesenchymal cells was normal in the lungs of sham group, while the lung tissues from the IR group were significantly damaged, with pulmonary edema, hemorrhage and inflammatory cell infiltration. Administrating AG before reperfusion could attenuate significantly the lung injury as showed by light microscope (Figure 1).

### *Change of MDA content*

The lung MDA content was increased significantly in IR group when compared with the sham control ($P<0.05$). Compared with the IR group, the MDA content was decreased markedly in IR +AG group ($P<0.05$) (Table 1).

**Table 1** Changes of MDA and $NO^-_2$ / $NO^-_3$ contents in lung tissue after IIR with pretreatment of AG in rats ($\bar{x}$±*s*, *n*=8)

| Groups | MDA (nmol.ml$^{-1}$) | $NO^-_2$ / $NO^-_3$ (umol.L$^{-1}$) |
|---|---|---|
| Sham | 12.00±2.18 | 76.39±6.08 |
| IR | 23.44±1.25[a] | 140.40±4.34[a] |
| IR+AG | 14.66±1.66[c] | 80.00±8.56[c] |

[a]$P<0.05$ *vs* Sham group. [c]$P<0.05$ *vs* IR group.

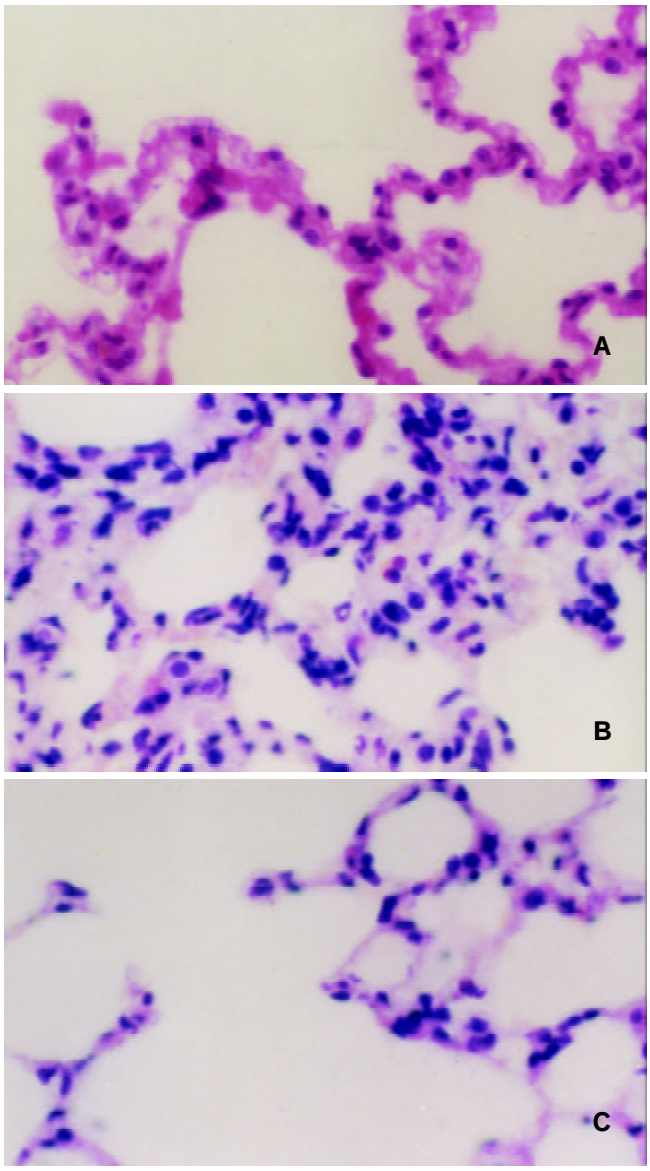


**Figure 1** Light microscopic observation on the lung after IIR with pretreatment of AG in rats (HE×400). A. The normal lung tissue structure was found in sham group. B. Lung edema, hemorrhage and inflammatory cells sequestration were found in the IR group. C. Decreased morphological changes induced by the intestinal IR were found in the IR+AG group.

### *Change of nitrite/nitrate*

Compared with the sham group, the lung content of nitrite/ nitrate in IR group was increased significantly ($P<0.05$). Compared with the IR group, the content of nitrite/nitrate in IR+AG group was decreased significantly ($P<0.05$) (Table 1).

### *Change of iNOS expression*

Western blotting showed that weak positive signal was found in the lung in sham group. In contrast, marked increase of iNOS protein expression was found in the IR group. There was still notable positive signal in the IR+AG group (Figure 2).

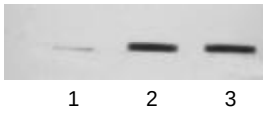


**Figure 2** Western blotting analysis of iNOS in rat lung after IIR with pretreatment of AG in rats. 1. Sham; 2. IR; 3. IR+AG.

### *Change of NT formation*

The formation of peroxynitrite in the lung sections was demonstrated by immunohistochemical staining with monoclonal anti-NT antibodies. In the sham group, no brown deposits were present in lung sections. In contrast, very strong staining was observed in lung tissue sections from the IR group. Compared with the IR group, the immunostaining for NT in the IR+AG group decreased significantly, indicating that inhibition of iNOS activity and decrease of NO production could reduce the peroxynitrite formation (Figure 3).

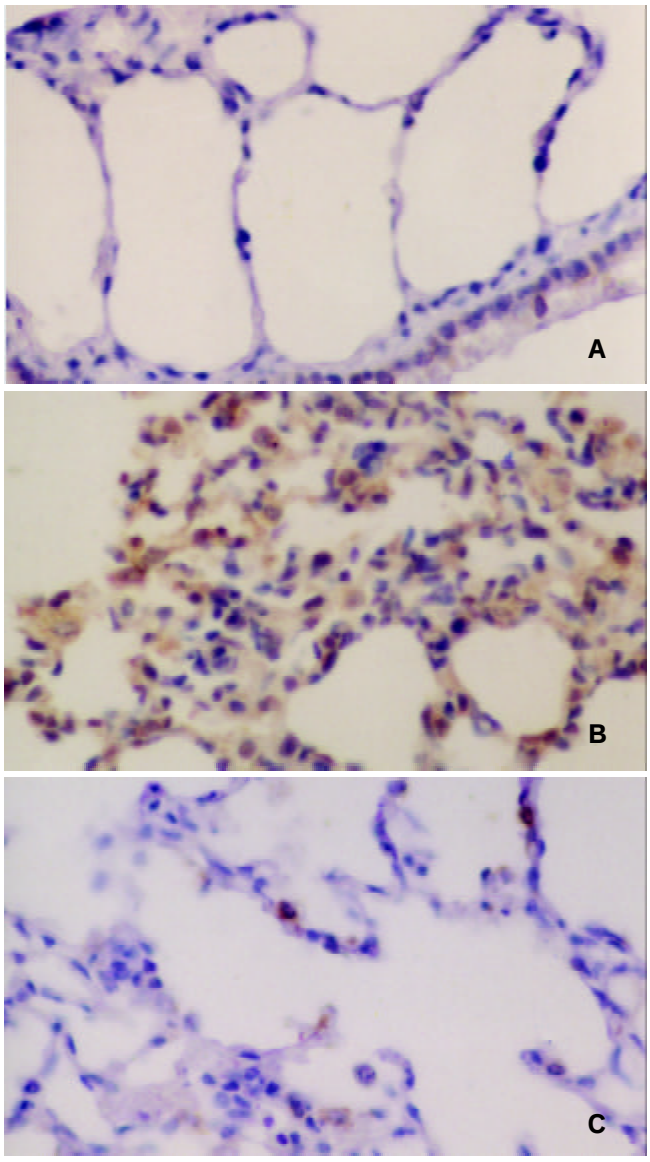


**Figure 3** Immunohistochemical analysis of NT in the lung after IIR with pretreatment of AG in rats. SP stain ×400. A. No positive signal was found in the lung in sham group. B. Intense positive NT staining was found in the IR group. C. Positive NT staining decreased in the IR+AG group.

## DISCUSSION

The lung is one of the very important target organs in multiple organ dysfunction syndrome (MODS) or multiple system organ failure (MOSF) caused by severe injury[1-9]. It has been found that in addition to the direct trauma, the lung could also be damaged by indirect injury such as gut, liver and skeletal muscle reperfusion, as well as aortic occulation-reperfusion and circulatory shock[1-9]. The present results showed that 2 h of intestinal ischemia followed by 2 h of reperfusion induced lung injury, manifested as the histological evidence of lung edema, hemorrhage and PMN infiltration. Moreover, the IIR mediated lung injury was oxygen-dependent, as indicated by the increase in the levels of MDA, an established marker of oxidative stress.

The mechanism of respiratory failure after intestinal I/R is complex and poorly understood. Under the condition of an inadequate mucosal blood flow, the gut barrier function can be progressively impaired and invaded by bacteria or endogenous endotoxin[24-26]. This process is associated with activation of systemic inflammatory mediators including bacteriotoxin, inflammatory mediators, such as tumor necrosis factor (TNF) and interleukin (IL) and immunocytokines[26-31]. In addition, several recent observations implicate that NO may be an important participant in the pulmonary response to IIR[32]. It has been suggested that nitric oxide (NO), produced from endothelial constitutive nitric oxide synthase (ecNOS), may be an important protective molecule at the onset of the IR of the small bowel. In this regard, inhibitors of endogenous NO production greatly exacerbate the increase in epithelial permeability and cardiovascular dysfunction in the reperfused post-ischemia intestine[32-34], while administration of NO donors prevents the early rise in epithelial permeability and tissue dysfunction[35,36]. Excess NO production has been attributed to a second NOS (induced NOS, iNOS) that is not present under normal condition but can be induced in response to systemic inflammatory states, including IR. The induction of iNOS has been implicated in the pathogenesis of IIR and it was reported that inhibition of iNOS activity and nitric oxide production could attenuate the intestinal ischemia/reperfusion injury[37-40]. In the present experiment, we studied the contribution of iNOS to the IIR-induced lung injury. The results demonstrated that 2 h of intestinal ischemia followed by 2 h of reperfusion up-regulated significantly the lung iNOS expression, accompanied by the elevation of pulmonary nitrate/nitrite (stable metabolites of NO) level. This is consistent with the findings of Virlos IT, *et al*[34] who demonstrated that pulmonary iNOS activity in rats subjected to IIR was significantly increased. The effect of increased iNOS expression on IIR-induced lung injury was indirectly assessed by administration of AG, a selective inhibitor of iNOS. The results that *in vivo* treatment with AG reduced markedly the nitrate/nitrite levels and the lung injury demonstrated that the induction of iNOS and the excessive NO production in the lung following intestinal IR involved in the IIR-induced lung injury.

Though the cytotoxic actions of the excessive NO production may be involved in several potential mechanisms, recent studies suggested that peroxynitrite, may be a key mediator for cytotoxicity of excess NO generation and is involved in many pathological processes[15-18]. The cytotoxic processes triggered by peroxynitrite include initiation of lipid peroxidation, inhibition of mitochondrial respiration, inhibition of membrane pumps, depletion of glutathione, and damage to DNA with subsequent activation of poly (ADP-ribose) synthetase and

concomitant cellular energy depletion[19-21, 41, 42]. Peroxynitrite is now generally considered an oxidant more toxic than either NO or superoxide anion alone. Furthermore, it has been shown that a major product of the reaction of peroxynitrite with protein is the addition of a nitro group in the ortho position of tyrosine to form NT which could be detected by antibodies specific to protein NT[16]. The present results of immunohistochemical staining with monoclonal anti-NT antibodies demonstrated that peroxynitrite formation occurred in the reperfusion phase of ischemic intestine. The results also suggested that the formation of peroxynitrite was correlated with iNOS expression and involved in the IIR-induced lung injury, because inhibiting iNOS activity with AG reduced significantly the NT immunoreactivity and attenuated the IIR-induced lung injury. The cytotoxic actions of iNOS-NO and peroxynitrite may be associated with their damages to the endothelial barrier, their oxidant to the membrane lipid and the triggering of the PMN sequestration in the lung, manifested as the detection of lung MDA content and the observation of the lung pathological changes.

In summary, the present results demonstrate that the systemic inflammatory response and lung injury occur following IIR with an increase of NO, iNOS expression and the formation of peroxynitrite in the lung. Inhibition of iNOS prevented the lung injury and the formation of NT, suggesting that excessive NO production and peroxynitrite formation are cytotoxic to the cell and tissue and are involved in the secondary lung injury induced by the IIR. These results may partially explain the mechanism of MOF and suggest that inhibiting peroxynitrite may be a novel pharmacological approach to prevent cell injury and MOF.

## REFERENCES


1 **Carden DL,** Granger DN. Pathophysiology of ischemia-reperfusion injury. *J Pathol* 2000; **190**: 255-266

2 **Rotstein OD**. Pathogenesis of multiple organ dysfunction syndrome: gut origin, protection, and decontamination. *Surg Infect (Larchmt)* 2000; **1**: 217-225

3 **Fu XB**, Yang YH, Sun TZ, Gu XM, Jiang LX, Sun X Q, Sheng ZY. Effect of intestinal ischemia-reperfusion on expression of endogenous basic fibroblast growth factor and transforming growth factor betain lung and its relation with lung repair. *World J Gastroenterol* 2000; **6**: 353-355

4 **Wu XT**, Li JS, Zhao XF, Zhuang W, Feng XL. Modified techniques of heterotopic total small intestinal transplantation in rats. *World J Gastroenterol* 2002; **8**: 758-762

5 **Mitsuoka H**, Schmid-Schonbein GW. Mechanisms for blockade of in vivo activator production in the ischemic intestine and multiorgan failure. *Shock* 2000; **14**: 522-527

6 **Yassin MM**, Harkin DW, Barros D'Sa AA, Halliday MI, Rowlands BJ. Lower limb ischemia-reperfusion injury triggers a systemic inflammatory response and multiple organ dysfunction. *World J Surg* 2002; **26**: 115-121

7 **Zhou JL,** Zhu XG, Ling T, Zhang JQ, Chang JY. Effect of endogenous carbon monoxide on oxidant-mediated multiple organ injury following limb ischemia-reperfusion in rats. *Zhongguo Xiufu Chongjian Waie Zazhi* 2002; **16**: 273-276

8 **Rezende-Neto JB**, Moore EE, Melo de Andrade MV, Teixeira MM, Lisboa FA, Arantes RM, de Souza DG, da Cunha-Melo JR. Systemic inflammatory response secondary to abdominal compartment syndrome: stage for multiple organ failure. *J Trauma* 2002; **53**: 1121-1128

9 **Weinbroum AA**, Shapira I, Abraham RB, Szold A. Mannitol dose-dependently attenuates lung reperfusion injury following liver ischemia reperfusion: a dose-response study in an isolated perfused double-organ model. *Lung* 2002; **180**: 327-338

10 **Tavaf-Motamen H**, Miner TJ, Starnes BW, Shea-Donohue T. Nitric oxide mediates acute lung injury by modulation of inflammation. *J Surg Res* 1998; **78**: 137-142

11 **Wangle F**, Patel M, Razavi HM, Weicker S, Joseph MG, McCormack DG, Mehta S. Role of inducible nitric oxide synthase in pulmonary microvascular protein leak in murine sepsis. *Am J Respir Crit Care Med* 2002; **165**: 1634-1639

12 **Li H**, Forstermann U. Nitric oxide in the pathogenesis of vascular disease. *J Pathol* 2000; **190**: 244-254

13 **Hofseth LJ**, Saito S, Hussain SP, Espey MG, Miranda KM, Araki Y, Jhappan C, Higashimoto Y, He P, Linke SP, Quezado MM, Zurer I, Rotter V, Wink DA, Appella E, Harris CC. Nitric oxide-induced cellular stress and p53 activation in chronic inflammation. *Proc Natl Acad Sci U S A* 2003; **100**: 143-148

14 **Qin JM**, Zhang YD. Intestinal expressions of eNOSmRNA and iNOSmRNA in rats with acute liver failure. *World J Gastroenterol* 2001; **7**: 652-656

15 **Cuzzocrea S**, Zingarelli B, Caputi AP. Role of constitutive nitric oxide synthase and peroxynitrite production in a rat model of splanchnic artery occlusion shock. *Life Sci* 1998; **63**: 789-799

16 **Pryor WA**, Squadrito GL. The chemistry of peroxynitrite: a product from the reaction of nitric oxide with superoxide. *Am J Physiol* 1995; **268**: L699-L722

17 **Szabo C**. The pathophysiological role of peroxynitrite in shock, inflammation, and ischemia-reperfusion injury. *Shock* 1996; **6**: 79-88

18 **Zhao KS**, Liu J, Yang GY, Jin C, Huang Q, Huang X. Peroxynitrite leads to arteriolar smooth muscle cell membrane hyperpolarization and low vasoreactivity in severe shock. *Clin Hemorheol Microcirc* 2000; **23**: 259-267

19 **Gu ZY**, Ling Y, Cong B. Peroxynitrite mediated acute lung injury induced by lipopolysaccharides in rats. *Zhonghua Yixue Zazhi* 2000; **80**: 58-61

20 **Laskin DL**, Fakhrzadeh L, Laskin JD. Nitric oxide and peroxynitrite in ozone-induced lung injury. *Adv Exp Med Biol* 2001; **500**: 183-190

21 **Gu ZY**. Peroxynitrite-mediated pulmonary vascular injury induced by endotoxin and the protective role of cholecystokinin. *Shengli Kexue Jinzhan* 2001; **32**: 135-137

22 **Turnage RH**, Kadesky KM, Bartula L, Myers SI. Intestinal reperfusion up regulates inducible nitric oxide synthase activity within the lung. *Surgery* 1995; **118**: 288-293

23 **Zhang GL**, Wang YH, Teng HL, Lin ZB. Effects of aminoguanidine on nitric oxide production induced by inflammatory cytokines and endotoxin in cultured rat hepatocytes. *World J Gastroenterol* 2001; **7**: 331-334

24 **Turnage RH**, Guice KS, Oldham KT. Endotoxemia and remote organ injury following intestinal reperfusion. *J Surg Res* 1994; **56**: 571-578

25 **Olanders K**, Sun Z, Borjesson A, Dib M, Andersson E, Lasson A, Ohlsson T, Andersson R.The effect of intestinal ischemia and reperfusion injury on ICAM-1 expression, endothelial barrier function, neutrophil tissue influx, and protease inhibitor levels in rats. *Shock* 2002; **18**: 86-92

26 **Yao Y**, Yu Y, Chen J. The effect of intestinal ischemia / reperfusion on increased sensitivity to endotoxin and its potential mechanism. *Zhonghua Zhengxing Shaoshang Waike Zazhi* 1999; **15**: 301-304

27 **Ishii H**, Ishibashi M, Takayama M, Nishida T, Yoshida M. The role of cytokine-induced neutrophil chemoattractant-1 in neutrophil-mediated remote lung injury after intestinal ischaemia / reperfusion in rats. *Respirology* 2000; **5**: 325-331

28 **Yan GT,** Hao XH, Xue H, Wang LH, Li YL, Shi LP. Interleukin-1beta expression and phospholipase A(2) activation after intestinal ischemia / reperfusion injury. *Shengli Xuebao* 2002; **54**: 28-32

29 **Souza DG**, Cassali GD, Poole S, Teixeira MM. Effects of inhibition of PDE4 and TNF-alpha on local and remote injuries following ischaemia and reperfusion injury. *Br J Pharmacol* 2001; **134**: 985-994

30 **Wada K**, Montalto MC, Stahl GL. Inhibition of complement C5 reduces local and remote organ injury after intestinal ischemia / reperfusion in the rat. *Gastroenterology* 2001; **120**: 126-133

31 **Zhao H**, Montalto MC, Pfeiffer KJ, Hao L, Stahl GL. Murine model of gastrointestinal ischemia associated with complement-dependent injury. *J Appl Physiol* 2002; **93**: 338-345

32 **Khanna A**, Rossman JE, Fung HL, Caty MG. Attenuated nitric oxide synthase activity and protein expression accompany intestinal ischemia / reperfusion injury in rats. *Biochem Biophys Res Commun* 2000; **269**: 160-164

33 **Tavaf-Motamen H**, Miner TJ, Starnes BW, Shea-Donohue T. Nitric oxide mediates acute lung injury by modulation of inflammation. *J Surg Res* 1998; **78**: 137-142
34 **Virlos IT**, Inglott FS, Williamson RC, Mathie RT. Differential expression of pulmonary nitric oxide synthase isoforms after intestinal ischemia-reperfusion. *Hepatogastroenterol* 2003; **50**: 31-36
35 **Kalia N,** Brown NJ, Hopkinson K, Stephenson TJ, Wood RF, Pockley AG. FK409 inhibits both local and remote organ damage after intestinal ischaemia. *J Pathol* 2002; **197**: 595-602
36 **Ward DT**, Lawson SA, Gallagher CM, Conner WC, Shea-Donohue T. Sustained nitric oxide production via l-arginine administration ameliorates effects of intestinal ischemia-reperfusion. *J Surg Res* 2000; **89**: 13-19
37 **Turnage RH**, Wright JK, Iglesias J, LaNoue JL, Nguyen H, Kim L, Myers S. Intestinal reperfusion-induced pulmonary edema is related to increased pulmonary inducible nitric oxide synthase activity. *Surgery* 1998; **124**: 457-462
38 **Xia G**, Lara-Marquez M, Luquette MH, Glenn S, Haque A, Besner GE. Heparin-binding EGF-like growth factor decreases inducible nitric oxide synthase and nitric oxide production after intestinal ischemia / reperfusion injury. *Antioxid Redox Signal* 2001; **3**: 919-930
39 **Takada K**, Yamashita K, Sakurai-Yamashita Y, Shigematsu K, Hamada Y, Hioki K, Taniyama K. Participation of nitric oxide in the mucosal injury of rat intestine induced by ischemia-reperfusion. *J Pharmacol Exp Ther* 1998; **287**: 403-407
40 **Suzuki Y**, Deitch EA, Mishima S, Lu Q, Xu D. Inducible nitric oxide synthase gene knockout mice have increased resistance to gut injury and bacterial translocation after an intestinal ischemia-reperfusion injury. *Crit Care Med* 2000; **28**: 3692-3696
41 **Jagtap P**, Soriano FG, Virag L, Liaudet L, Mabley J, Szabo E, Hasko G, Marton A, Lorigados CB, Gallyas F Jr, Sumegi B, Hoyt DG, Baloglu E, VanDuzer J, Salzman AL, Southan GJ, Szabo C. Novel phenanthridinone inhibitors of poly (adenosine 5'-diphosphate-ribose) synthetase: potent cytoprotective and antishock agents. *Crit Care Med* 2002; **30**: 1071-1082
42 **Cuzzocrea S**, McDonald MC, Mazzon E, Dugo L, Serraino I, Threadgill M, Caputi AP, Thiemermann C. Effects of 5-aminoisoquinolinone, a water-soluble, potent inhibitor of the activity of poly (ADP-ribose) polymerase, in a rodent model of lung injury. *Biochem Pharmacol* 2002; **63**: 293-304

**Edited by** Zhang JZ

P.O.Box 2345, Beijing 100023,China
Fax: +86-10-85381893
E-mail: wjg@wjgnet.com www.wjgnet.com

World J Gastroenterol 2003;9(6):1323-1326
World Journal of Gastroenterology
Copyright ©2003 by The WJG Press ISSN 1007-9327

• BASIC RESEARCH •

# Effects of n-3 fatty acid, fructose-1,6-diphosphate and glutamine on mucosal cell proliferation and apoptosis of small bowel graft after transplantation in rats

Xiao-Ting Wu, Jie-Shou Li, Xiao-Fei Zhao, Ning Li, Yu-Kui Ma, Wen Zhuang, Yong Zhou, Gang Yang

**Xiao-Ting Wu, Yu-Kui Ma, Wen Zhuang, Yong Zhou, Gang Yang,** Department of General Surgery, West China Hospital, Sichuan University, Chengdu 610041, Sichuan Province, China
**Jie-Shou Li, Ning Li,** Research Institute of General Surgery, Nanjing General Hospital of PLA, Clinical School of Medical College, Nanjing University, Nanjing 210002, Jiangsu Province, China
**Xiao-Fei Zhao,** Sichuan Reproductive Health Institute, Chengdu 610041, Sichuan Province, China
**Supported by** the State Education Commission Research Foundation for Returned Overseas Chinese Scholars Abroad (1997) 436
**Correspondence to:** Professor Xiao-Ting Wu, Department of General Surgery, West China Hospital, Sichuan University, 37 Guo Xue Rd., Chengdu 610041, Sichuan Province, China. wxt1@medmail.com.cn
**Telephone:** +86-28-85422480 **Fax**: +86-28-85422411
**Received:** 2002-09-13 **Accepted:** 2002-11-21

## Abstract

**AIM:** To evaluate the effects of n-3 fatty acids (n-3FA), fructose-1,6-diphosphate (FDP) and glutamine (GLN) on mucosal cell proliferation and apoptosis of small bowel graft.

**METHODS:** One hundred and ninety-six inbred strain Wistar rats were grouped as donors and recipients, and underwent heterotopic small bowel transplantation (SBT). n-3FA, FDP and GLN were administered via gastric tube as well as venous infusion for 10 days before and after surgery, respectively. The proliferation and apoptosis of mucosal cells were analyzed with flow cytometry and *in situ* cell death detection kits.

**RESULTS:** Apparent apoptosis and minor proliferation of mucosal cells of small bowel graft after transplantation were observed. A higher mucosal cell proliferative index and lower apoptotic index were found in all small bowel grafts after supplying with n-3FA, FDP and GLN.

**CONCLUSION:** Nutritional support with n-3FA, FDP and GLN promotes mucosal cell proliferation significantly, and prevents mucosal cell from undergoing apoptosis with different degrees. These regulatory effects on the apoptosis alter the structure and absorption function of transplanted small bowel favorably.

Wu XT, Li JS, Zhao XF, Li N, Ma YK, Zhuang W, Zhou Y, Yang G. Effects of n-3 fatty acid, fructose-1,6-diphosphate and glutamine on mucosal cell proliferation and apoptosis of small bowel graft after transplantation in rats. *World J Gastroenterol* 2003; 9(6): 1323-1326
http://www.wjgnet.com/1007-9327/9/1323.asp

## INTRODUCTION

The atrophy and malabsorption of transplanted small intestine are the main obstacles to small bowel transplantation (SBT). The effects of n-3 fatty acids (n-3FA), fructose-1, 6-diphosphate (FDP) and glutamine (GLN) on mucosal cell proliferation and apoptosis of small bowel graft were evaluated. The mechanisms of mucosal atrophy and malabsorption of small bowel graft were studied at cellular and molecular levels.

## MATERIALS AND METHODS

### *Animals*

One hundred and ninety-six inbred male Wistar rats (180-310 g) purchased from Shanghai Animal Center of Chinese Academy of Medical Scienees were housed in laminar-flow cabinets under specific pathogen-free (SPF) condition. All studies on rats were conducted in accordance with the "Guideline for the Care and Use of Laboratory Animals" by National Institute of Health. The protocol approved by Shanghai Medical Experimental Animal Care Committee was followed during study. The rats were divided into 5 groups with 10 rats in each group. Group (1) was treated with non-essential amino acids. Group (2) was treated with FDP, group (3) with n-3FA, group (4) with GLN and group (5) with n-3FA+FDP+GLN. A modified heterotopic SBT was utilized[1]. End to side anastomosis between graft abdominal aorta and recipient abdominal aorta was performed. The left kidney of recipient was resected. The portal vein of graft was anastomosed to the left renal vein of the recipient. Fistulizations of the distal and proximal ends of graft were performed through left abdominal wall.

### *Administration of special nutrition*

In group (3) and (5), n-3FA (Sigma Company, USA), 1 $mL \cdot d^{-1}$, was given via gastric tube to both donor and recipient 10 days before and after operation, respectively. All animals received TPN. The dosage of FDP was 1 $g \cdot kg^{-1} \cdot d^{-1}$ (Foscama Company, Italy). The nutritional solution in group (4) contained 2 % GLN (Ajinomoto company, Japan). L-alanine, glycine, L-proline and L-serine were applied to the nutritional solution of group (1), (2) and (3). The nitrogen and calorie in the nutritional solution were equal in each group.

### *Specimen collection*

Prior to transplantation, 5 cm of jejunum distal to the treitz ligament of graft was resected as baseline samples. Ten days postoperative TPN support, 5 cm of proximal jejunum of the graft in the recipient was resected for examination.

### *Preparation of specimen*

**Flow cytometry** The mucosae of the specimen were scissored into tiny pieces in saline and filtered to get cell suspension. The nucleus was stained by hypotonic propidium iodide at 4 ℃ over night.

**TdT-mediated X-dUTP nick end labeling (TUNEL method)** The specimen was sectioned in 3 μm-thick and dehydrated through 70-90 % ethanol in series. After digestion with proteinase K (20 $\mu g \cdot mL^{-1}$), the work solution of TUNEL was added. The reaction was terminated with $ddH_2O$. The positive nucleus was stained with brownish yellow. Ten fields were selected randomly from each section under light microscope.

Two thousand mucosal cells were examined from each section. The apoptotic index (AI) was calculated with the formula: AI = (number of positive cells/total number of cells examined)×100 %.

### *Flow cytometry analysis*

Epics XL flow cytometer (Coulter Company, USA) was used in the analysis. The proportions of cells in stage $G_1$, S and $G_2$ were calculated in 10 000 cells examined. The proliferative index (PI) indicating the proliferation of mucosal cells was calculated using the formula: PI =[(S+$G_2$)/($G_1$+S+$G_2$)]×100 %.

### *Statistical analysis*

Newman-Keuls' s *q* test and Student' s *t* test were used. The statistical analysis software package stata 5.0 was used for the tests, and $P<0.05$ was considered statistically significant.

## RESULTS

### *Flow cytometry*

All the data from flow cytometry study are showed in Table 1.

**Table 1** Changes of proliferation of graft mucosal cells in each group ten days before and after SBT and TPN ($\bar{x}\pm s$)

| Group | Stage of cell cycle | Before SBT and TPN (%) | After SBT and TPN (%) | *P* |
|---|---|---|---|---|
| (1) | $G_1$ | 94.73±2.33 | 94.08±2.15 | 0.7440 |
| | $G_2$ | 0.38±0.31 | 1.38±1.44 | 0.3296 |
| | S | 4.88±2.42 | 4.55±0.92 | 0.8480 |
| | PI | 5.25±2.29 | 5.85±2.26 | 0.7682 |
| (2) | $G_1$ | 96.22±2.96[b] | 86.14±4.08[b] | 0.0011[b] |
| | $G_2$ | 0.88±1.20[a] | 3.06±1.12 | 0.0140[a] |
| | S | 2.90±1.78[b] | 10.78±3.06[b] | 0.0007[b] |
| | PI | 3.78±2.96[b] | 13.84±4.05[b] | 0.0011[b] |
| (3) | $G_1$ | 90.94±4.37[b] | 83.12±2.59[b] | 0.0069[b] |
| | $G_2$ | 1.96±1.12[a] | 3.86±0.96[a] | 0.0497[a] |
| | S | 7.10±3.98[a] | 13.02±3.39[a] | 0.0211[a] |
| | PI | 9.06±4.39[b] | 16.88±2.59[b] | 0.0071[b] |
| (4) | $G_1$ | 95.52±1.57[b] | 81.03±4.98[b] | 0.0002[b] |
| | $G_2$ | 0.63±0.60[b] | 5.93±1.62[b] | 0.0016[b] |
| | S | 4.02±1.57[b] | 13.52±4.70[b] | 0.0011[b] |
| | PI | 4.65±1.48[b] | 18.97±5.01[b] | 0.0002[b] |
| (5) | $G_1$ | 90.48±3.21[b] | 80.52±0.95[b] | 0.0053[b] |
| | $G_2$ | 2.52±2.06 | 5.02±1.43 | 0.0674 |
| | S | 6.96±2.96[a] | 14.22±1.77 | 0.0148[a] |
| | PI | 9.48±3.24[b] | 19.24±0.94[b] | 0.0057[b] |

[a]$P<0.05$, [b]$P<0.01$ *vs* before SBT.

**$G_1$ stage** No change of the proportion of graft mucosal cells in $G_1$ stage in group (1) was observed after transplantation. Most cells remained at $G_1$ stage. However, the proportions of graft mucosal cells in $G_1$ stage in the rest groups after transplantation decreased significantly.

**$G_2$ stage** Changes of proportion of graft mucosal cells in $G_2$ stage of group (1) and (5) after transplantation were not obvious. The proportions of graft mucosal cells in $G_2$ stage in the rest groups increased with great statistical significance.

**S stage** Following transplantation the change of proportion of graft mucosal cells in S stage was increased significantly in all groups except group (1).

**PI** Compared with the baseline before transplantation, the PI of graft mucosal cells changed significantly in all groups except group (1).

### *Apoptosis in situ*

**Group (1)** After SBT, the number of graft mucosal cells with apoptosis was increased. The AI was increased significantly after transplantation (Table 2). The AI in group (1) was significantly higher than those in other groups.

**Group (2)** The AI of graft mucosal cells increased after SBT and TPN with significant difference (Table 2). The AI in group (2) was higher than those in other groups with significance.

**Group (3)** The AI of graft mucosal cells after transplantation increased slightly without significance compared with baseline (Table 2). The AI was similar among groups (3), (4) and (5) without any significant difference.

**Group (4)** The AI of graft mucosal cells in group (4) was similar to that in group (5), decreased slightly after SBT without significant difference (Table 2).

**Group (5)** No change of the AI of graft mucosal cells was observed after SBT (Table 2).

**Table 2** Change of AI of graft mucosal cells in each group ten days before and after SBT and TPN ($\bar{x}\pm s$)

| Group | Before SBT and TPN (%) | After SBT and TPN (%) | *P* |
|---|---|---|---|
| (1) | 25.50±5.43[b] | 40.50±3.24[b] | 0.0041[b] |
| (2) | 24.63±1.70[a] | 30.88±2.50[a] | 0.0447[a] |
| (3) | 24.25±1.32 | 25.63±1.38 | 0.2141 |
| (4) | 25.00±2.68 | 23.63±0.85 | 0.4863 |
| (5) | 23.75±0.87 | 24.00±1.68 | 0.8130 |

[a]$P<0.05$, [b]$P<0.01$ *vs* before SBT.

## DISCUSSION

Rejection of graft will not occur in organ transplantation between two individuals from same strain of inbred animals. Thus, the effect of special nutrition on the transplanted small intestine could be observed in our research without the influence of transplant immunological factors.

Our results indicated that the proliferation of graft mucosal cells after SBT in group (1) was obviously less active than that before SBT. Most cells were rested in stage $G_1$. The ratios of cells in stage S over stage $G_2$ decreased, which suggested that DNA synthesis in graft mucosal cells after SBT reduced, and that mucosal cells were at rest stage instead of active proliferation. These changes in cytodynamics might be the underling cause of cytopathy of graft with the characteritics of atrophy and malabsorption.

Compared with the results of group (1), after SBT the proliferation of graft mucosal cells in rest groups was more active. The ratios of cells in stage S over stage $G_2$ increased, which suggested that n-3FA, FDP and GLN contributed to the proliferation and repair of graft mucosal cells, and were helpful in preventing atrophy and maintaining the normal structure and function of intestinal mucus.

The number of apoptotic cells and AI of graft mucosal cells in groups (1) and (2) after SBT and TPN increased significantly compared with those before SBT and TPN. On the contrary, those of groups (3), (4) and (5) did not change obviously. The AI in groups (2), (3), (4) and (5) after SBT and TPN decreased significantly in comparison with that in group (1). The result suggested that n-3FA, FDP and GLN could inhibit the apoptosis of graft mucus after SBT to a certain degree.

GLN might influence the graft in several ways, in which it promotes the proliferation of graft mucosal cells and inhibits the cell apoptosis. (1) GLN offers the energy and metabolic substrate which are necessary to the proliferation of intestine mucosal cells[2-15], including carbon chains for energy releasing

(30 mol ATP/mol) and nitrogen for synthesis of amino acid, protein and nuclear acid. (2) GLN also participates in the synthesis of glutathione (GSH). Administration of exogenous GLN will result in high level of GSH. It is indicated in some experiments that GSH could antagonize the oxidation injury to the biomembrane caused by oxygen-derived free radicals, and improve the survival of cells[16-19]. (3) GLN may indirectly stimulate the secretion of hormones which are beneficial to the nutrition of intestine, and improve the hormone environment of intestinal mucosal cells. This may help establish normal physiological metabolism and the balanced proliferation and apoptosis of intestinal mucosal cells[20]. (4) The apoptosis of host cells could be induced by bacterial and viral infections[21]. GLN may improve the structure and function of the transplanted intestine and reduce bacterial translocation, which could prevent infection and reduce apoptosis[22-32].

It is not clear why FDP could promote proliferation of mucosal cells of intestinal graft and inhibit apoptosis. The possible reasons might include: (1) As a kind of potent energy substrate, FDP can offer plenty of ATP quickly whether it is on normal or stress occasion, such as ischemia or anoxia[33,34]. So, FDP can meet the energy need of proliferation of intestinal mucosal cells with quick metabolism. (2) As a promoter of energy synthesis, FDP may activate pyruvate kinase and phosphofructokinase on stress occasion, such as ischemia or anoxia. These enzymes may promote the metabolism of carbohydrate to offer adequate energy[33], which is helpful to cell proliferation. The products of zymolysis could be decomposed in the energy-producing process[35]. Thus tissue damage caused by these products could be avoided and the inducing factors of apoptosis were reduced. (3) FDP could reduce the retention of intracellular calcium at stress, and inhibit endogenous calcium dependent endonuclease which is important to nuclear changes in apoptosis[36]. (4) The cell injuries during ischemia/reperfusion and cold storage of graft are associated with apoptosis[37-39]. FDP could inhibit the production of toxic oxygen group by activated polymorphonuclear leukocyte and scavange the hypoxanthine accumulated in the tissues during ischemia and reperfusion[40]. Thus, the apoptosis caused by these factors could be reduced[41].

The mechanism of n-3FA in improving the proliferation of mucosal cell of intestinal graft and inhibiting apoptosis is not clear. It may involve the following factors: (1) As a kind of energy substrate, n-3FA could offer energy for the proliferation of mucosal cells. (2) n-3FA could be esterified into phospholipid and neutral lipid which are essential to neogenetic mucosal cells as important component of structure membrane[42-45]. (3) n-3FA could inhibit the production of IL-1$\alpha$, IL-1$\beta$ and TNF secreted by monocytes. It is indicated that IL-1$\beta$ and TNF can promote apoptosis[46]. (4) Apoptosis might be one of the ways of cell death in rejection after allogeneic transplantation[47,48]. As a kind of immunosuppressant[49-51], n-3FA could inhibit the apoptosis of graft cells through immunosuppression.

In conclusion, special nutrition with n-3FA, FDP and GLN after SBT can promote the proliferation of graft mucosal cells and inhibit apoptosis. Our results may provide new ways to treat intestinal atrophy and malabsorption after SBT.

## REFERENCES


1 **Wu XT**, Li JS, Zhao XF, Zhuang W, Feng XL. Modified techniques of heterotopic total small intestinal transplantation in rats. *World J Gastroenterol* 2002; **8**: 758-762

2 **Windmueller HG,** Spaeth AE. Uptake and metabolism of plasma glutamine by the small intestine. *J Biol Chem* 1974; **249**: 5070-5079

3 **Zhang W,** Bain A, Rombeau JL. Insulin-like growth factor-I (IGF-I) and glutamine improve structure and function in the small bowel allograft. *J Surg Res* 1995; **59**: 6-12

4 **Klimberg VS,** Souba WW, Salloum RM, Holley DT, Hautamaki RD, Dolson DJ, Copeland EM 3rd. Intestinal glutamine metabolism after massive small bowel resection. *Am J Surg* 1990; **159**: 27-32

5 **Marks SL,** Cook AK, Reader R, Kass PH, Theon AP, Greve C, Rogers QR. Effects of glutamine supplementation of an amino acid-based purified diet on intestinal mucosal integrity in cats with methotrexate-induced enteritis. *Am J Vet Res* 1999; **60**: 755-763

6 **Fox AD,** Kripke SA, De Paula J, Berman JM, Settle RG, Rombeau JL. Effect of aglutamine supplemented enteral diet on methotrexate induced enteritis. *JPEN* 1988; **12**: 325-331

7 **Gu Y**, Wu ZH. The anabolic effects of recombinant human growth hormone and glutamine on parenterally fed, short bowel rats. *World J Gastroenterol* 2002; **8**: 752-757

8 **Colomb V,** Darcy-Vrillon B, Jobert A, Guihot G, Morel MT, Corriol O, Ricour C, Duee PH. Parenteral nutrition modifies glucose and glutamine metabolism in rat isolated enterocytes. *Gastroenterology* 1997; **112**: 429-436

9 **Cherbuy C,** Darcy-Vrillon B, Morel MT, Pegorier JP, Duee PH. Effect of germfree state on the capacities of isolated rat colonocytes to metabolize n-butyrate, glucose, and glutamine. *Gastroenterology* 1995; **109**: 1890-1899

10 **Wilmore DW**. Glutamine and the gut. *Gastroenterology* 1994; **107**: 1885-1901

11 **Minami H,** Morse EL, Adibi SA. Characteristics and mechanism of glutamine-dipeptide absorption in human intestine. *Gastroenterology* 1992; **103**: 3-11

12 **Dejong CH,** Kampman MT, Deutz NE, Soeters PB. Altered glutamine metabolism in rat portal drained viscera and hindquarter during hyperammonemia. *Gastroenterology* 1992; **102**: 936-948

13 **Rhoads JM,** Keku EO, Quinn J, Woosely J, Lecce JG. L-glutamine stimulates jejunal sodium and chloride absorption in pig rotavirus enteritis. *Gastroenterology* 1991; **100**: 683-691

14 **Klein S.** Glutamine: an essential nonessential amino acid for the gut. *Gastroenterology* 1990; **99**: 279-281

15 **Firmansyah A,** Penn D, Lebenthal E. Isolated colonocyte metabolism of glucose, glutamine, n-butyrate, and beta-hydroxybutyrate in malnutrition. *Gastroenterology* 1989; **97**: 622-629

16 **Yu JC**, Jiang ZM, Li DM. Glutamine: a precursor of glutathione and its effect on liver. *World J Gastroenterol* 1999; **5**: 143-146

17 **Yagi M,** Sakamoto K, Inoue T, Fukushima W, Muraoka K, Ii T, Iyobe T, Iwasa K, Hashimoto T, Shimizu K, Izumi R, Miyazaki I. Effect of a glutamine-enriched elemental diet on regeneration of the small bowel mucosa following isotransplantation of small intestine. *Transplant Proc* 1994; **26**: 2297-2298

18 **Scheppach W,** Dusel G, Kuhn T, Loges C, Karch H, Bartram HP, Richter F, Christl SU, Kasper H. Effect of L-glutamine and n-butyrate on the restitution of rat colonic mucosa after acid induced injury. *Gut* 1996; **38**: 878-885

19 **Xu Y,** Nguyen Q, Lo DC, Czaja MJ. c-myc-Dependent hepatoma cell apoptosis results from oxidative stress and not a deficiency of growth factors. *J Cell Physiol* 1997; **170**: 192-199

20 **Petronini PG,** Urbani S, Alfieri R, Borghetti AF, Guidotti GG. Cell susceptibility to apoptosis by glutamine deprivation and rescue: survival and apoptotic death in cultured lymphoma-leukemia cell lines. *J Cell Physiol* 1996; **169**: 175-185

21 **Thompson CB.** Apoptosis in the pathogenesis and treatment of disease. *Science* 1995; **267**: 1456-1462

22 **Schroeder P,** Schweizer E, Blomer A, Deltz E. Glutamine prevents mucosal injury after small bowel transplantation. *Transplant Proc* 1992; **24**: 1104

23 **Klimberg VS,** Souba WW, Dolson DJ, Salloum RM, Hautamaki RD, Plumley DA, Mendenhall WM, Bova FJ, Khan SR, Hackett RL, Bland KI, Copeland III EM. Prophylactic glutamine protects the intestinal mucosa from radiation injury. *Cancer* 1990; **66**: 62-68

24 **Zhang W,** Frankel WL, Singh A, Laitin E, Klurfeld D, Rombeau JL. Improvement of structure and function in orthotopic small bowel transplantation in the rat by glutamine. *Transplantation* 1993; **56**: 512-517

25 **Li JY**, Lu Y, Hu S, Sun D, Yao YM. Preventive effect of glutamine on intestinal barrier dysfunction induced by severe trauma. *World J Gastroenterol* 2002; **8**: 168-171

26 **Yoshida S,** Matsui M, Shirouzu Y, Fujita H, Yamana H, Shirouzu K. Effects of glutamine supplements and radiochemotherapy on

systemic immune and gut barrier function in patients with advanced esophageal cancer. *Ann Surg* 1998; **227**: 485-491

27 **Yoshida S,** Leskiw MJ, Schluter MD, Bush KT, Nagele RG, Lanza-Jacoby S, Stein TP. Effect of total parenteral nutrition, systemic sepsis, and glutamine on gut mucosa in rats. *Am J Physiol* 1992; **263**: E368-373

28 **Burke DJ,** Alverdy JC, Aoys E, Moss GS. Glutamine-supplemented total parenteral nutrition improves gut immune function. *Arch Surg* 1989; **124**: 1396-1399

29 **Rhoads JM,** Argenzio RA, Chen W, Graves LM, Licato LL, Blikslager AT, Smith J, Gatzy J, Brenner DA. Glutamine metabolism stimulates intestinal cell MAPKs by a cAMP-inhibitable, Raf-independent mechanism. *Gastroenterology* 2000; **118**: 90-100

30 **De Blaauw I,** Deutz NE, van der Hulst RR, von Meyenfeldt MF. Glutamine depletion and increased gut permeability in nonanorectic, non-weight-losing tumor-bearing rats. *Gastroenterology* 1997; **112**: 118-126

31 **Tremel H,** Kienle B, Weilemann LS, Stehle P, Furst P. Glutamine dipeptide-supplemented parenteral nutrition maintains intestinal function in the critically ill. *Gastroenterology* 1994; **107**: 1595-1601

32 **Scheppach W,** Loges C, Bartram P, Christl SU, Richter F, Dusel G, Stehle P, Fuerst P, Kasper H. Effect of free glutamine and alanyl-glutamine dipeptide on mucosal proliferation of the human ileum and colon. *Gastroenterology* 1994; **107**: 429-434

33 **Juergens TM,** Hardin CD. Fructose-1,6-bisphosphate as a metabolic substrate in hog ileum smooth muscle during hypoxia. *Mol Cell Biochem* 1996; **154**: 83-93

34 **Trimarchi GR,** Arcadi FA, Imperatore C, Ruggeri P, Costa G. Effects of fructose-1,6-biphosphate on microsphere-induced cerebral ischemia in the rat. *Life Sci* 1997; **61**: 611-622

35 **Hassinen IE,** Nuutinen EM, Ito K, Nioka S, Lazzarino G, Giardina B, Chance B. Mechanism of the effect of exogenous fructose 1,6-bisphosphate on myocardial energy metabolism. *Circulation* 1991; **83**: 584-593

36 **Pozzilli C,** Lenzi GL, Argentino C, Carolei A, Rasura M, Signore A, Bozzao L, Pozzilli P. Imaging of leukocytic infiltration in human cerebral infarcts. *Stroke* 1985; **16**: 251-255

37 **Takeuchi K,** Cao-Danh H, Friehs I, Glynn P, D'Agostino D, Simplaceanu E, McGowan FX, del Nido PJ. Administration of fructose 1,6-diphosphate during early reperfusion significantly improves recovery of contractile function in the postischemic heart. *J Thorac Cardiovasc Surg* 1998; **116**: 335-343

38 **Sun JX,** Farias LA, Markov AK. Fructose 1-6 diphosphate prevents intestinal ischemic reperfusion injury and death in rats. *Gastroenterology* 1990; **98**: 117-126

39 **Farias LA,** Smith EE, Markov AK. Prevention of ischemic-hypoxic brain injury and death in rabbits with fructose-1,6-diphosphate. *Stroke* 1990; **21**: 606-613

40 **Chu SJ**, Chang DM, Wang D, Chen YH, Hsu CW, Hsu K. Fructose-1,6-diphosphate attenuates acute lung injury induced by ischemia-reperfusion in rats. *Crit Care Med* 2002; **30**: 1605-1609

41 **Raff MC.** Social controls on cell survival and cell death. *Nature* 1992; **356**: 397-400

42 **Teo TC,** DeMichele SJ, Selleck KM, Babayan VK, Blackburn GL, Bistrian BR. Administration of structured lipid composed of MCT and fish oil reduces net protein catabolism in enterally fed burned rats. *Ann Surg* 1989; **210**: 100-107

43 **Endres S,** Ghorbani R, Kelley VE, Georgilis K, Lonnemann G, van der Meer JW, Cannon JG, Rogers TS, Klempner MS, Weber PC, Schaefer EJ, Wolff SM, Dinarello CA. The effect of dietary supplementation with n-3 polyunsaturated fatty acids on the synthesis of interleukin-1 and tumor necrosis factor by mononuclear cells. *N Engl J Med* 1989; **320:** 265-271

44 **Dinarello CA,** Cannon JG, Wolff SM, Bernheim HA, Beutler B, Cerami A, Figari IS, Palladino MA Jr, O'Connor JV. Tumor necrosis factor (cachectin) is an endogenous pyrogen and induces production of interleukin 1. *J Exp Med* 1986; **163:** 1433-1450

45 **Thiele J,** Zirbes TK, Lorenzen J, Kvasnicka HM, Dresbach S, Manich B, Leder LD, Niederle N, Diehl V, Fischer R. Apoptosis and proliferation (PCNA labelling) in CML-a comparative immunohistological study on bone marrow biopsies following interferon and busulfan therapy. *J Pathol* 1997; **181:** 316-322

46 **Steller H.** Mechanisms and genes of cellular suicide. *Science* 1995; **267:** 1445-1449

47 **Krams SM,** Egawa H, Quinn MB, Villanueva JC, Garcia-Kennedy R, Martinez OM. Apoptosis as a mechanism of cell death in liver allograft rejection. *Transplantation* 1995; **59:** 621-625

48 **Ito H,** Kasagi N, Shomori K, Osaki M, Adachi H. Apoptosis in the human allografted kidney. Analysis by terminal deoxynucleotidyl transferase-mediated DUTP-botin nick end labeling. *Transplantation* 1995; **60:** 794-798

49 **Prickett JD,** Robinson DR, Steinberg AD. Dietary enrichment with the polyunsaturated fatty acid eicosapentaenoic acid prevents proteinuria and prolongs survival in NZB x NZW F1 mice. *J Clin Invest* 1981; **68:** 556-559

50 **Kelley VE,** Ferretti A, Izui S, Strom TB. A fish oil diet rich in eicosapentaenoic acid reduces cyclooxygenase metabolites, and suppresses lupus in MRL-lpr mice. *J Immunol* 1985; **134:** 1914-1919

51 **Kelley VE,** Kirkman RL, Bastos M, Barrett LV, Strom TB. Enhancement of immunosuppression by substitution of fish oil for olive oil as a vehicle for cyclosporine. *Transplantation* 1989; **48:** 98-102

**Edited by** Ren SY

P.O.Box 2345, Beijing 100023,China
Fax: +86-10-85381893
E-mail: wjg@wjgnet.com www.wjgnet.com

World J Gastroenterol 2003;9(6):1327-1332
World Journal of Gastroenterology
Copyright ©2003 by The WJG Press ISSN 1007-9327

• BASIC RESEARCH •

# Effects of glutamine on intestinal permeability and bacterial translocation in TPN-rats with endotoxemia

Lian-An Ding, Jie-Show Li

**Lian-An Ding, Jie-Show Li,** Clinical College of Nanjing University Medical School, 305 East Zhongshan Road, Nanjing 210002 Jiangsu Province, China
**Correspondence to:** Lian-An Ding, Associate Professor of Nanjing University Medical School, 210002 Jiangsu Province, China. dlahaolq@hotmail.com
**Telephone:** +86-25-4827110-58088 **Fax:** +86-25-4803956
**Received:** 2002-10-17 **Accepted:** 2002-12-20

## Abstract

**AIM:** To evaluate the protective effect and mechanism of glutamine on the intestinal barrier function in total parenteral nutrition (TPN) rats with trauma or endotoxemia.

**METHODS:** To perform prospective, randomized and controlled animal experimentation of rats with surgical trauma, TPN and endotoxemia, thirty-four male, adult Sprague Dawley rats were divided into four groups: control group ($n$=8), TPN group ($n$=9), trauma and endotoxemia group (LPS, $n$=8) and trauma plus endotoxemia supplemented with glutamine in TPN solution group (Gln. group, $n$=9). All groups except the control group were given TPN solutions in 7-day experimental period. For Gln group, 1 000 mg/kg/d of glutamine was added to TPN solution during day 1-6. On the 7th day all the animals were gavaged with lactulose (66 mg) and mannitol (50 mg) in 2 ml of normal saline. Then 24 h urine with preservative was collected and kept at -20 ℃. On day 8, under intraperitoneal anesthesia using 100 mg/kg ketamin, the intestine, liver, mesenteric lymph nodes and blood were taken for examination.

**RESULTS:** The body weight of LPS group decreased most among the four groups. The structure of small intestinal mucosa in TPN group, LPS group and Gln group showed impairments of different degrees, and the damage of small intestinal mucosa in Gln group was remarkably alleviated. The concentrations of interleukins in small intestine mucosa were lower (for IL-4 and IL-6) or the lowest (IL-10) in Gln group. The IgA level in the blood plasma and the mucosa of Gln group was the highest among all of the groups. The urine lactulose/mannitol test showed that the intestinal permeability in LPS group was lower than that in TPN group ($P$<0.001), but there was no difference between LPS group and Gln group. The rate of bacterial translocation in Gln group was lower than that in LPS group ($P$<0.02).

**CONCLUSION:** Prophylactic treatment with glutamine could minimize the increments of intestinal permeability and bacterial translocation caused by trauma and endotoxemia in rats treated with TPN.

Ding LA, Li JS. Effects of glutamine on intestinal permeability and bacterial translocation in TPN-rats with endotoxemia. *World J Gastroenterol* 2003; 9(6): 1327-1332
http://www.wjgnet.com/1007-9327/9/1327.asp

## INTRODUCTION

Trauma, burn, infection, surgical operations and the use of intravenous alimentation over a long period can damage the barrier function of the intestine, leading to atrophy of the intestinal mucosa, increase of mucosal permeability, decrease of immunity, and occurrence of bacterial/endotoxin translocation[1-5]. If the causes could not be removed or the stress is too severe when the intestinal barrier is protected, the damage of the intestinal mucosa would become more severe and multiple organ dysfunction syndrome (MODS) would ensue. These adverse outcomes are commonly seen clinically and methods of their prevention need to be investigated. Therefore we studied the mechanism of protective effect of glutamine on the intestinal barrier function in TPN rats with trauma and endotoxemia.

## MATERIALS AND METHODS

### *Experimental animals and grouping*

Adult, healthy male Sprague-Dawley rats, with body weight of 150-180 g (supplied by Shanghai Experimental Animal Center, the Chinese Academy of Sciences) were used. The rats were fed for over a week in our lab for their adaptation and then were put into metabolic cages for 5-7 days. The temperature in the animal rooms was 17-21 ℃ with 60 % humidity and illumination of 12 h/day (6:00-18:00). During the adaptation period all rats were fed with regular rat chow and tap water ad libitum. When the rat' s weight reached 200-300 g, thirty-four rats were chosen randomly and divided into four groups: 1. control group ($n$=8), fed rat chow and tap water freely; 2. TPN group ($n$=9), infused with a whole nutrients solution through a central venous catheter, and with drinking water ad libitum; 3. LPS group (trauma + TPN + endotoxemia, $n$=8), in which an exploratory laparotomy and central venous catheterization served as the trauma. After this, TPN was their sole nutrition source plus drinking water ad libitum. On the 7th day 5 mg/kg of lipopolysaccharide (LPS) was injected intraperitoneally; 4. Gln group, (trauma + TPN + endotoxemia + glutamine, $n$=9) in which all the treatments were the same as LPS group but on days 2-6, 1 000 mg/kg/d glutamine (Dipeptiven) was added to TPN solution. All groups except the control one received isonitrogenous, isocaloric and isovolumic TPN solution during the 7-day period. All the protocols and procedures were approved by our University Committee of Animal Experiment Administration.

### *Intravenous nutrients and other relevant chemicals*

**TPN ingredients** 11.4 % compound amino acids injection (Novamin), 20 % mid-long chain fat emulsion (Lipovenoes MCT), Dipeptiven (alanyl-glutamine dipeptide solution), multivitamin mixture (Soluvit, Vitalipid) and a trace element mixture (Addamel), all from Sino-Sweden and Fresenius Pharmaceutical Corp. LTD.

**Chemicals and reagents** Lipopolysaccharide (LPS, from *E Coli*, 055: B5) was purchased from Sigma Co.; IL-4 from Diaclone Co.of France; IL-6 and IL-10, from Biosource Co., USA; and IgA, from Bethyl Co.USA.

### *Experimental model*

**Operation procedures** Under anaesthesia of 100 mg/kg of ketamin injected into the animals intraperitoneally, the TPN model was constructed and a rotary transfusion apparatus was used for TPN infusion[6,7]. For surgical trauma, the animal' s abdomen after shaving and incision (4 cm in length) was exposed and examined from the epigastrium to the pelvic cavity. The incision was sutured in double layers with silk suture No. 1 and operation was performed aseptically.

**TPN solution** The rats were put in the metabolic cages after surgical recovery. Each rat received 230 cal/kg body wt of calories and 1.42 g nitrogen/kg each day in 50 ml of TPN solution. The ratio of glucose to lipid in this solution was 2:1, and nonprotein calorie to nitrogen (kcal/g), 137:1. Multivitamins, electrolytes, trace elements and 500 units of heparin were also included in the TPN solution. All the nutrient solutions were prepared under aseptic conditions daily and the infusion was done with an injecting micropump continuously and uniformly during 24 h each day. The TPN infusion was started immediately after recovery from the laparotomy. On the first and last days of the experiment, each rat was given half of the total calories without any changes of other TPN ingredients.

**Inducing endotoxemia** On the 7th day of the experiment, 5 mg/kg of LPS in 5 ml of sterile distilled water was injected into the animals' peritoneal cavity to cause a septic state.

**Lactulose and mannitol solution gavage** On the 7th day of the experiment, 66 mg of lactulose and 50 mg of mannitol dissolved in 2 ml of normal saline were gavaged. Twenty-four hour urine was collected, with the volume recorded and 0.2 ml of mercury salicylosulfide added. Then 5 ml of the urine specimen was stored at -20 ℃ until measured.

### *Samples preparation and measurements*

Twenty-four hours after gavaging with lactulose and mannitol and injecting endotoxin, 100 mg/kg of ketamine was injected intraperitoneally as an anesthetic. After the laparotomy was done, tissue and blood samples were collected and examinations were performed.

**Bacteriological test** 0.5 ml of blood from the portal vein was drawn for culture. One gram of anterior lobe liver tissue and about 0.5 g mesenteric lymph nodes were excised. Each sample was put in a tissue homogenizer and an equivalent amount of normal saline was added before they were homogenized. The specimens were sent to microbiological laboratory for aerobic culture and bacterial identification by morphological and biochemical examinations.

**Bacterial culture** (1) 10 μl homogenates of the lymph nodes and liver homogenates were separately taken and put on blood agar plates. Another 10 μl lymph nodes and liver homogenates were mixed with 10 ml saline for a dilution and the diluted samples were inoculated also on blood agar plates. (2) 0.5 ml of portal vein blood was inoculated into 4.5 ml of common broth for bacterial enrichment of 16 hours, then 20 μl of the enrichment solution was inoculated on blood agar plates. (3) The cultured media were put in a $CO_2$ incubator at 35 ℃ for 24-48 hours. If there was no bacterial growth, they would be regarded as negative, but if there was growth, it would be further identified.

**Identification of bacteria** First, Gram stained smears were made to determine whether they were coccus or bacillus and G+ or G-. Second, biochemical and serological identifications were made using standard and routine methods.

**Preparation and examination of small intestine specimens** The whole small intestine below the Treitz ligament was excised and immediately placed in icy 0.9 % saline. The intestine was opened longitudinally and the contents of the intestine were washed out with icy saline. Two cm of proximal jejunum and distal ileum was cut and put into 10 % neutral formalin solution promptly and sent to be examined histologically.

**Histological examination of intestinal mucosa** Specimens were embedded in paraffin, 4 μm sections made and stained with H.E., analyzed with an HPIAS-1000 Multimedia Color Analysis System. Three low power (10×10) fields in each slide were read. The length of 5 villi, the depth of 5 crypts and the thickness of the mucosa at 5 sites were read and analyzed. The average value was calculated and documented. All the manipulations were done blindly by two experienced pathologists.

**Bloodletting and animal execution** Three ml of blood from the right ventricle was drawn and 1 250 u of heparin was added. The blood was centrifuged and the serum was stored at -70 ℃. Then the animals were sacrificed by exsanguination.

**Lactulose/mannitol test** The lactulose and mannitol concentrations in the preserved urine sample were measured by a high-performance liquid chromatograph (Waters Co., USA). The ion-exchange column used was bought from Transgenomic Co., USA. The ratio between the two sugars was then calculated.

**Identification of the interleukins** About 5 cm intestine segments from the upper, middle and lower paste were resected and then the surfaces of the mucosa were dried with cotton swabs. The mucous membrane of the icy specimens was scraped, weighed and divided into two equal parts. They were immediately put into liquid nitrogen and then stored at -70 ℃. For the tests, the specimens were melted to room temperature, and 1 ml normal saline was added before homogenates were made. The homogenates were then centrifuged for 15 minutes at 4 ℃ and then IL-4, IL-6 and IL-10 in the supernatants were measured with ELISA method described by Kudsk[8]. The results were described as pg/g of mucosal tissue of the small intestine.

**Determination of IgA** The frozen samples of blood plasma and the mucosa of the small intestine were melted to room temperature and the concentration of IgA in them was measured by ELISA method. The results were shown as IgA μg/ml of blood plasma and IgA μg/g of small intestinal mucosa.

### *Statistical analysis*

All the values were expressed as the mean ±SD. One-way ANOVA was used to check the differences between them. ChiSquare test was used to check the differences of bacterial translocation rates between the groups. When $P$ was less than 0.05, the difference was considered statistically significant. The degree of correlation was described using Pearson Correlation coefficient. Software SPSS10.0 was used in all statistical analyses.

## RESULTS

### *Body weight*

The body weight changes of the animals in each group are illustrated in Figure 1. At the beginning of the experiment there was no difference in the body weight of the animals among the groups. At the end of the experiment, the body weight decrease was greatest in the animals of LPS group.

### *Morphology and morphometry of small intestinal mucous membrane*

The degree of damage of villi and crypts and the thinning of mucous membrane in jejunum and ileum were most significant in LPS group among all groups (Figure 2 and 3).

### *Interleukins of small intestinal mucosal tissue*

The concentrations of IL-4 and IL-6 in Gln group were the lowest among these groups except control group. IL-10 level in Gln

group was also the lowest among the four groups, and it was significantly lower than that in TPN group ($P$<0.01, Figure 4).

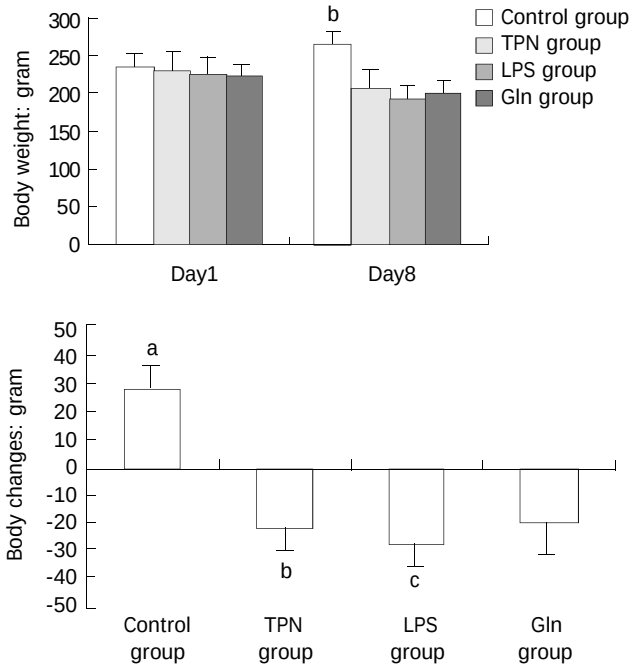


**Figure 1** Graphs of body weight changes. (a) Graphs of body weights of animals at the start and end of the experiment; Day 1 means the date when experiments started; Day 8 means the date when experiments ended; [b]$P$<0.001, *vs* control group, TPN group, and Gln group; (b) The illustration of body weight increase or decrease at the endpoint of the experiment; [a]$P$<0.001, *vs* TPN group, LPS group and Gln group; [b]$P$<0.02, *vs* LPS group; [c]$P$<0.03, *vs* Gln group.

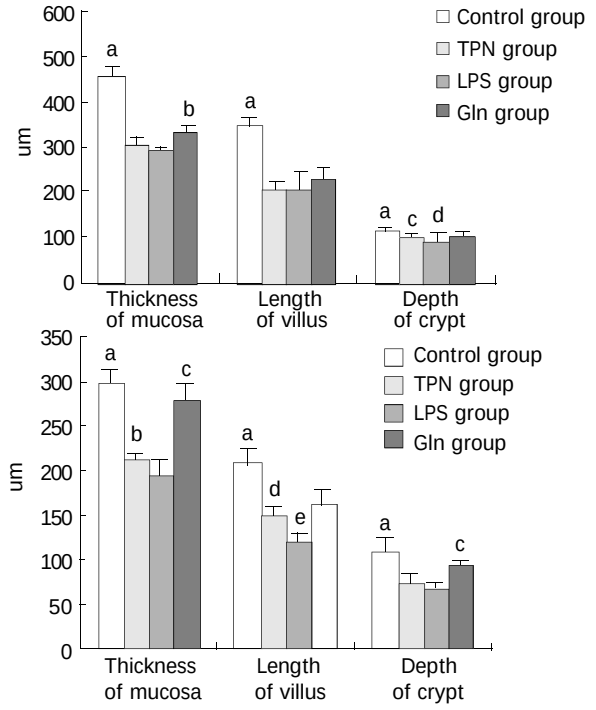


**Figure 3** Graphs of morphometry of small intestinal mucosa. (a) Morphometry of jejunal mucous membrane; [a]$P$<0.01, *vs* TPN group, LPS group and Gln group; [b]$P$<0.01, *vs* TPN group and LPS group; [c]$P$<0.02, *vs* LPS group; [d]$P$<0.04, *vs* Gln group; (b) Morphometry of ileal mucous membrane; [a]$P$<0.004, *vs* TPN group, LPS group and Gln group; [b]$P$<0.005, *vs* LPS group; [c]$P$<0.02, *vs* Gln group; [d]$P$<0.02, *vs* Gln group; [e]$P$<0.001, *vs* TPN group and Gln group.

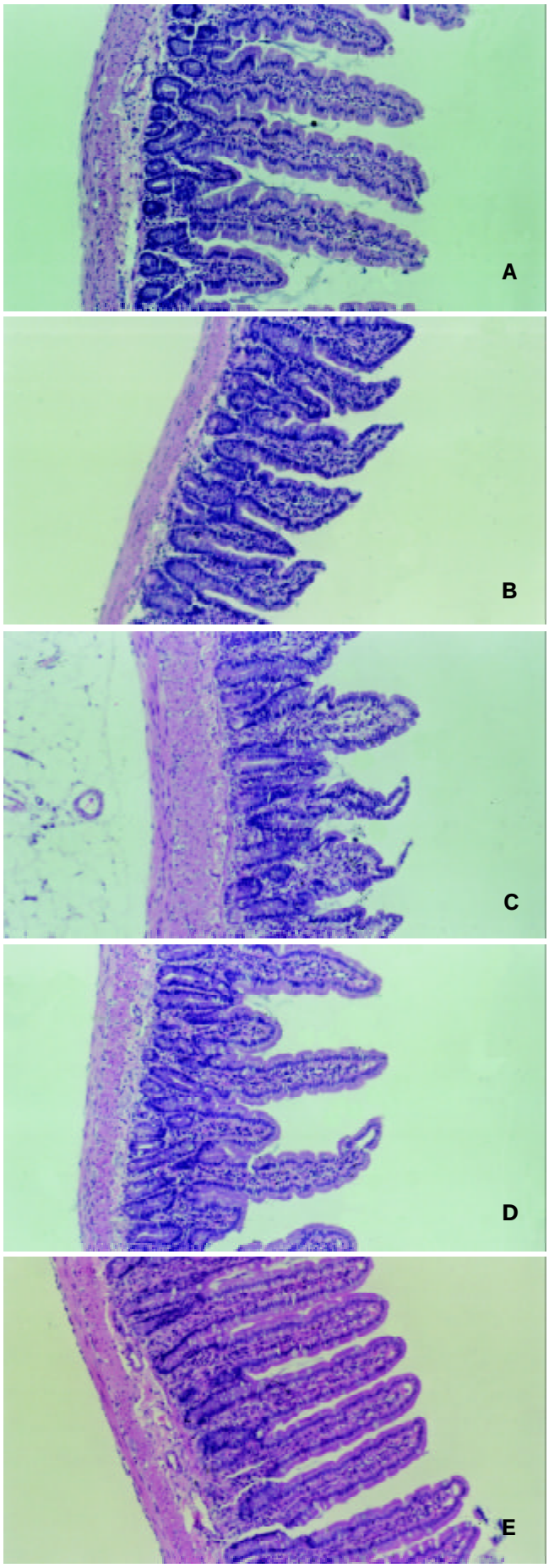


**Figure 2** Alterations of structure in mucous membrane of small intestine under microscope. A. The normal structure of jejunum mucosa in normal group rats; B. The normal structure of ileal mucosa in normal group rats; C. Slice of the structure of ileal

mucosa in TPN group. The section shows an evident damage in mucosal architecture. The villi become shorter, blunted and swollen. Infiltration of leukocytes occurs within the lamina propria. The lymphatic ducts in lamina propria reveal dilatation and edematous; D. Slice of the jejunal mucosa of LPS group. The villi are more sparse and shorter than control group. It also shows infiltration of leukocytes within lamina propria, and dilatation of lymphatic ducts in lamina propria; E. The section of ileum mucosa of Gln group. The morphology of ileal mucosa is similar to that of control group (B).

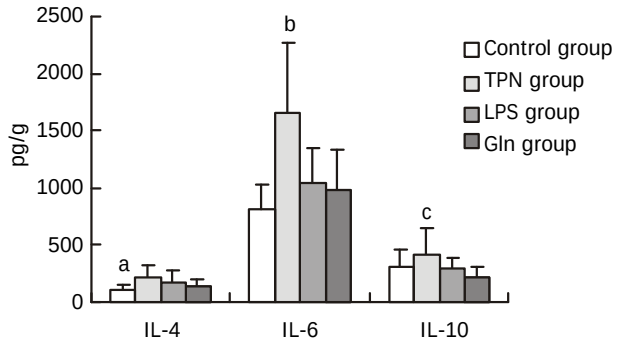


**Figure 4** Graph of interleukins in mucous membrane of small intestine. [a]*P*<0.02, *vs* TPN group; [b]*P*<0.001, *vs* Control group, LPS group, Gln group; [c]*P*<0.01, *vs* Gln group.

### *IgA levels in plasma and small intestinal mucous membrane*

IgA levels in blood plasma in Gln group were the highest among the four groups, and so was that in small intestinal mucosa. There was a positive correlation for IgAs level between those in plasma and small intestinal mucosa ($r$=0.961, $P$<0.04, Table 1).

**Table 1** IgA Levels in blood plasma and small intestinal mucous membrane

| | Blood plasma IgA (ug/ml) | Mucosal tissue IgA (ug/g) |
|---|---|---|
| Control Group | 146.73±50.98[a] | 507.48±167.39[c] |
| Group TPN | 133.94±64.41[b] | 544.62±100.78[d] |
| Group LPS | 194.52±111.18 | 611.89±171.60 |
| Group Gln | 255.13+160.59 | 827.89+279.96 |

Note: Values were expressed as mean ± SD; [a]*P*<0.02, *vs* Gln group; [b]*P*<0.04, *vs* Gln group; [c]*P*<0.01, *vs* Gln group; [d]*P*<0.02, *vs* Gln group; There ‘s a positive correlation for IgA levels in blood plasma and mucosal tissues ($r$=0.961, $P$<0.04).

### *Correlation of IgA with interleukines*

There was no significant correlation between IgA level in plasma and mucosa with the level of interleukins in mucosal tissue of small intestine (Table 2).

**Table 2** Correlation of IgAs with interleukins

| | IgA of blood plasma | | | IgA of mucous membrane | | |
|---|---|---|---|---|---|---|
| | IL-4 | IL-6 | IL-10 | IL-4 | IL-6 | IL-10 |
| *r* value | -0.562 | -0.584 | –0.744 | -0.614 | -0.373 | -0.396 |
| *P* value | 0.438 | 0.416 | 0.256 | 0.386 | 0.627 | 0.604 |
| Correlation[a] | no | no | no | no | no | no |

Note: Values were expressed as mean ± SD; [a]There was no correlations between each IgA level in plasma and mucosal tissue with that of three interleukins respectively in intestinal mucosa.

### *Lactulose and mannitol (L/M) test*

The recovery rates of lactulose and mannitol in the urine of TPN group, LPS group and Gln group were increased. The ratio of L/M was the biggest in LPS group, and the value of the ratio in LPS group was not different statistically from that in Gln group (Figure 5).

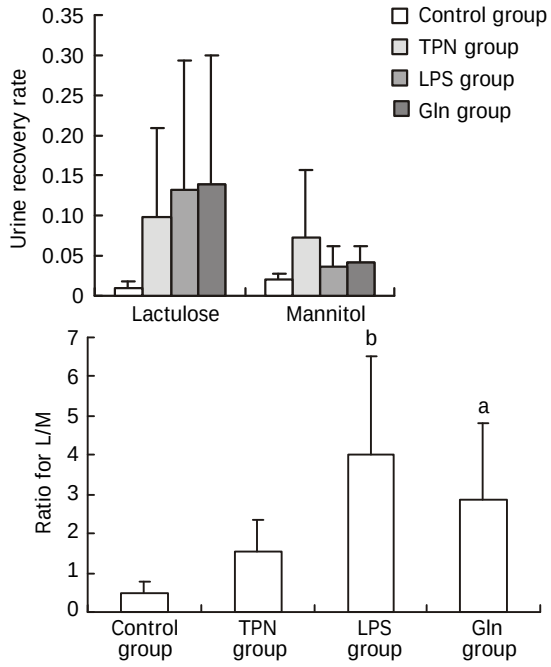


**Figure 5** Illustration of dual sugar test. (a) Recovery rate of urine for lactulose and mannitol; (b) Graphic of intestinal permeability expressed by L/M ratio. [a]*P*<0.003, *vs* control group; [b]*P*<0.001, *vs* control groups and TPN groups.

### *Bacterial identification and translocation*

The results of bacterial culture were labeled as positive when the CFU found per gram of tissue (or ml of blood) was more than or equivalent to $10^3$[9] . In LPS group the rate of bacterial translocation was the highest. The second highest rate was seen in TPN group. The logarithm of the number of translocated bacteria correlated positively with the bacterial translocation rate (Table 3). The bacteria translocated, in order of frequency, were proteus, *E. coli*, enterococcus and other Gram negative bacteria. One or two, even three bacteria were usually recovered from the same organ when translocation was present[6,9].

**Table 3** Bacteriologic tests

| | MLN | Liver | PVB | Rate of BT | Logarithm of TB |
|---|---|---|---|---|---|
| Control group | 3/8 | 0/8 | 0/8 | 12.5 % (3/24)[a] | 0.5414+1.4799[d] |
| TPN group | 4/9 | 4/9 | 4/9 | 44.4% (12/27) | 2.3279+2.3609 |
| LPS group | 5/8 | 6/8 | 7/8 | 75.0% (18/24)[b] | 3.0782±2.2824[e] |
| Gln group | 2/8 | 5/8 | 3/8 | 41.7% (10/24)[c] | 1.5845+2.3209 |

Note: Values were expressed as mean ± SD; MLN, mesenteric lymph node; PVB, portal vein blood; BT, bacterial translocation; TB, translocated bacteria; BTR, rate of BT; [a]*P*<0.01, *vs* TPN group and LPS group; [b]*P*<0.02, *vs* Gln group; [c]*P*<0.03, *vs* group control; [d]*P*<0.01, *vs* TPN group and LPS group; [e]*P*<0.01, *vs* Gln group; The rate of bacterial translocation is positively correlated to the logarithm of the number of translocated bacteria ($r$=0.978, $P$<0.022, $P$<0.03).

## DISCUSSION

Damage of intestinal barrier function and the resulting bacterial

translocation and endotoxemia caused by stress was well documented in the literature[1-4, 10-14]. How to protect this barrier function and prevent bacterial translocation and toxemia during stress are important research topics[15-17].

Animal experiments showed some good results in protecting intestinal barrier function and decreasing bacterial translocation, toxemia and enterogenous infection by various measures[6, 8, 9, 15, 17-22, 30]. Glutamine has many biological functions[23, 24]. It comprises more than 50 percent of the body' s free amino acid pool and is a precursor for synthesis of nucleic acids and glutathione. It is the main fuel for rapid proliferating and dividing cells such as enterocytes, lymphocytes, and other immunocytes etc. It can promote hyperplasia of the epithelial cells of ileum and colon[25]. The structure and function of small intestinal mucosa are maintained and the increment of intestinal permeability is reduced when glutamine is supplemented to animals fed parenterally[26-28]. Besides, glutamine could enhance body' s immunity through immune modulation[8, 24, 29]. Results from a series of experiments and clinical investigations indicate that supplementation with glutamine parenterally and/or enterally has improved the gut barrier function and body' s immunity when used in human and animals[13, 17, 23, 29-35]. It has been generally accepted that glutamine could maintain intestinal barrier function through the improvement of architecture of small intestinal mucosa. Formerly, researches along this line usually paid attention to only one aspect of the functions of the intestinal barrier. For this reason, no interrelationship among the permeability and immunity of intestinal mucosa and bacterial translocation was discussed or fully explained[6, 11, 30].

It is known that the cause of the damage of intestinal permeability in animals fed with TPN is mainly the atrophy of intestinal mucous membrane[11, 34]. The mechanism of the increase of intestinal permeability caused by endotoxin is very complicated. It may relate to many inflammation mediators such as cytokines, vasoactive amines and oxygen free radicals[16, 36]. The problem needs further investigation. Our experiment showed that injection of LPS intraperitoneally to rats indeed led to impairment of gut barrier function and an increase in bacterial translocation. Although there were no differences in body weight change when comparing that in glutamine-supplemented group with those in TPN group and LPS group, the damage of architecture of small intestinal mucosa in the former, especially in mucous membrane of ileum, was greatly alleviated than those in the latter two groups.

Glutamine has a visible effect on the secretion of interleukins in mucous membrane of small intestine. The three interleukins in small intestinal mucosa in glutamine group were lower (for IL-4 and IL-6) or lowest (IL-10) than those in other groups of our experiment. There are different opinions about the effects of interleukins on intestinal barrier function. Some authors mentioned that intestinal IL-4 and IL-10 were important in maintaining IgA concentration in the respiratory and alimentary tracts and in the blood[8]. In the present experiment, we have not found a correlation between IgA level and IL-4 and IL-10 levels in intestinal mucosa. It has been considered that type II cytokines such as IL-4 and IL-10 have an anti-inflammatory function and then it could alleviate tissue and cell damage caused inflammatory mediators and type I cytokines such as IL-6[37-39]. But there was a report that held a completely different opinion[40]. We could see from our experiment that glutamine could reduce secretion of interleukins, and it seems that the lower interleukin concentrations are beneficial in reducing the damage of intestinal permeability[40].

It is known that the digestive tract is the largest immune organ in human body and intestinal mucosal IgA is the first defense line of intestine immunity barrier. This has an important function in preventing bacterial adherence and translocation within intestinal lumen. In our experiment, the IgA levels in blood and intestinal mucosa in glutamine group were the highest among all groups. There was statistically significant difference between the mucosal IgA levels in glutamine group and those in the control and TPN groups. This result meant that the alleviation of bacterial translocation rate in animals supplemented with glutamine correlated with the increase of IgA secretion in mucous membrane of the small intestine. There was a positive correlation between IgA levels in mucous membrane and blood plasma. It confirmed that the intestine is a vital organ for IgA secretion[32].

Many changes of the immunological indicators in our experiment did not reach a statistically significant level. The reason for this might be that our experiment and observation period ended at the time when the peak of stress reaction had just passed and the animals had no sufficient recovery time[12]. In this experiment we have made a model in which the animal is injured by laparotomy and parenteral nutrition, and endotoxemia is caused by an injection with a higher dosage of LPS intraperitoneally 6 days after the injury. The protective mechanism of glutamine on gut barrier was investigated. We found that the model simulated well the conditions of the clinical infectious complications.

In summary, using 1 000 mg/kg/d glutamine parenterally can alleviate the atrophy and impairment of the mucous membrane of small intestine in rats. It can also increase the concentration of IgA and decrease concentrations of IL-4, IL-6 and IL-10 that are secreted by the mucous membrane of small intestine. Thus, the immune function of the small intestinal mucosa was modulated and the damage of gut barrier caused by trauma and endotoxemia was alleviated. The rate of bacterial translocation was also decreased. Changes of intestinal permeability measured with the dual sugar test did not completely correlated with alterations of gut barrier function[41].

## ACKNOWLEDGEMENTS

We would like to thank Prof. Shao Haifeng and Prof. Xu Genbao for their technical guidance and help; we are grateful to the staff of Animal Lab. and Institute of General Surgery for their selfless work and support in this investigation.

## REFERENCES

1 **Swank GM**, Deitch EA. Role of the gut in multiple organ failure: bacterial translocation and permeability changes. *World J Surg* 1996; **20**:411-417
2 **Berg RD**. Bacterial translocation from the gastrointestinal tract. *Trends Microbiol* 1995; **3**: 149-154
3 **Wilmore DW**, Smith RJ, O'Dwyer ST, Jacobs DO, Ziegler TR, Wang XD. The gut: A central organ after surgical stress. *Surgery* 1988; **104**: 917-923
4 **van Der Hulst RR**, von Meyenfeldt MF, van Kreel BK, Thunnissen FB, Brummer R, Arends JW, Soeters PB. Gut permeability, intestinal morphology, and nutritional depletion. *Nutrition* 1998; **14:** 1-6
5 **Carrico JC**, Meakins JL, Marshall JC, Fry D, Maier RV. Multiple-Organ-Failure Syndrome. *Arch Surg* 1986; **121**: 196-208
6 **Eizaguirre I**, Aldazabal P, Barrena MJ, Garcia-Arenzana JM, Ariz C, Candelas S, Tovar JA. Effect of growth hormone on bacterial translocation in experimental short-bowel syndrome. *Pediatr Surg Int* 1999; **15**: 160-163
7 **Zhou X**, Li YX, Li N, Li JS. Effect of bowel rehabilitative therapy on structural adaptation of remnant small intestine: animal experiment. *World J Gastroenterol* 2001; **7**: 66-73
8 **Kudsk KA**, Wu Y, Fukatsu K, Zarzaur BL, Johnson CD, Wang R, Hanna MK. Glutamine-enriched total parenteral nutrition maintains intestinal interleukin-4 and mucosal immunoglobulin A levels. *JPEN* 2000; **24**: 270-274
9 **Huang KF**, Chung DH, Herndon DN. Insulinlike growth factor

1(IGF-1) reduces gut atrophy and bacterial translocation after severe burn injury. *Arch Surg* 1993; **128**: 47-54
10 **Naaber P**, Smidt I, Tamme K, Liigant A, Tapfer H, Mikelsaar M, Talvik R. Translocation of indigenous microflora in an experimental model of sepsis. *J Med Microbiol* 2000; **49**: 431-439
11 **MacFie J**. Enteral versus parenteral nutrition: the significance of bacterial translocation and gut-barrier function. *Nutrition* 2000; **16**: 606-611
12 **Deich EA**, Ma WJ, Ma L, Berg RD, Specian RD. Protein malnutrition predisposes to inflammatory-induced gut-origin septic states. *Ann. Surg* 1990; **211**: 560-567
13 **MacFie J,** O'Boyle C, Mitchell CJ, Buckley PM, Johnstone D, Sudworth P. Gut origin of sepsis: a prospective study investigating associations between bacterial translocation, gastric microflora, and septic morbidity. *Gut* 1999; **45**: 223-228
14 **Reynolds JV**, Murchan P, Leonard N, Clarke P, Keane FB, Tanner WA. Gut barrier failure in experimental obstructive jaundice. *J Surg Res* 1996; **62**: 11-16
15 **Chen K**, Okuma T, Okamura K, Tabira Y, Kaneko H, Miyauchi Y. Insulin-like growth factor-I prevents gut atrophy and maintains intestinal integrity in septic rats. *JPEN* 1995; **19**: 119-124
16 **Mishima S**, Xu D, Deitch EA. Increase in endotoxin-induced mucosal permeability is related to increased nitric oxide synthase activity using the Ussing chamber. *Crit Care Med* 1999; **27**: 880-886
17 **Fukushima R**, Saito H, Inoue T, Fukatsu K, Inaba T, Han I, Furukawa S, Lin MT, Muto T. Prophylactic treatment with growth hormone and insulin-like growth factor 1 improve systemic bacterial clearance and survival in a murine model of burn-induced gut-derived sepsis. *Burns* 1999; **25**: 425-430
18 **Vazquez I**, Gomez-de-Segura IA, Grande AG, Escribano A, Gonzalez-Gancedo P, Gomez A, Diez R, De Miguel E. Protective effect of enriched diet plus growth hormone administration on radiation-induced intestinal injury and on its evolutionary pattern in the rat. *Deg Dis Sci* 1999; **44**: 2350-2358
19 **Ziegler TR**, Leader LM, Jonas CR, Griffith DP. Adjunctive therapies in nutritional support. *Nutrition* 1997; **13** (Suppl 9): 64S-72S
20 **Chen DL**, Wang WZ, Wang JY. Epidermal growth factor prevents gut atrophy and maintains intestinal integrity in rats with acute pancreatitis. *World J Gastroenterol* 2000; **6**: 762-765
21 **Gu Y**, Wu ZH. The anabolic effects of recombinant human growth hormone and glutamine on parenterally fed, short bowel rats. *World J Gastroenterol* 2002; **8**: 752-757
22 **Zhou X**, Li N, Li JS. Growth hormone stimulates remnant small bowel epithelial cell proliferation. *World J Gastroenterol* 2000; **6**: 909-913
23 **Heys SD,** Ashkanani F. Glutamine. *Br J Surg*1999; **86**: 289-290
24 **Pichard C**, Kudsk KA. From nutrition support to pharmacologic nutrition in the ICU. *Germany, Springer* 2000: 30-31
25 **Scheppach W**, Loges C, Bartram P, Christl SU, Richter F, Dusel G, Stehle P, Fuerst P, Kasper H. Effect of free glutamine and alanyl-glutamine dipeptide on mucosal proliferation of the human ileum and colon. *Gastroenterology* 1994; **107**: 429-434
26 **Van Der Hulst RR**, Van Kreel BK, Von Meyenfeldt MF, Brummer RJ, Arends JW, Deutz NE, Soeters PB. Glutamine and the preservation of gut integrity. *Lancet* 1993; **341**: 1363-1365
27 **Khan J**, Iiboshi Y, Cui L, Wasa M, Sando K, Takagi Y, Okada A. Alanyl-glutamine-supplemented parenteral nutrition increases luminal mucus gel and decreases permeability in the rat small intestine. *JPEN* 1999; **23**: 24-31
28 **Li JY**, Lu Y, Hu S, Sun D, Yao YM. Preventive effect of glutamine on intestinal barrier dysfunction induced by severe trauma. *World J Gastroenterol* 2002; **8**: 168-171
29 **Burke DJ**, Alverdy JC, Aoys E, Moss GS. Glutamine-supplemented total parenteral nutrition improves gut immune function. *Arch Surg* 1989; **124**: 1396-1399
30 **Scopa CD**, Koureleas S, Tsamandas AC, Spiliopoulou I, Alexandrides T, Filos KS, Vagianos CE. Beneficial effects of growth hormone and insulin-like growth factor 1 on intestinal bacterial translocation, endotoxemia, and apoptosis in experimentally jaundiced rats. *J Am Coll Surge* 2000; **190**: 423-431
31 **Juby LD**, Rothwell J, Axon AT. Lactulose / mannitol test: an ideal screen for celiac disease. *Gastroenterol* 1989; **96**: 79-85
32 **Hulsewé KW**, van Acker BA, von Meyenfeldt MF, Soeters PB. Nutritional depletion and dietary manipulation: effects on the immune response. *World J Surg* 1999; **23**: 536-544
33 **Byrne TA**, Morrissey TB, Nattakom TV, Ziegler TR, Wilmore DW. Growth hormone, glutamine, and a modified diet enhance nutrient absorption in patients with severe short bowel syndrome. *JPEN* 1995; **19**: 296-302
34 **Sugiura T**, Tashiro T, Yamamori H, Takagi K, Hayashi N, Itabashi T, Toyoda Y, Sano W, Nitta H, Hirano J, Nakajima N, Ito I. Effects of total parenteral nutrition on endotoxin translocation and extent of the stress response in burned rats. *Nutrition* 1999; **15**: 570-575
35 **Foitzik T**, Kruschewski M, Kroesen AJ, Hotz HG, Eibl G, Buhr HJ. Does glutamine reduce bacterial translocation? A study in two animal models with impaired gut barrier. *Int J Colorectal Dis* 1999; **14**: 143-149
36 **O'Dwyer ST**, Michie HR, Ziegler TR, Revhaug A, Smith RJ, Wilmore DW. A single dose of endotoxin increases intestinal permeability in healthy humans. *Arch Surg*1988; **123**: 1459-1464
37 **Welsh FK**, Farmery SM, MacLennan K, Sheridan MB, Barclay GR, Guillou PJ, Reynolds JV. Gut barrier function in malnourished patients. *Gut* 1998; **42**: 396-401
38 **Lyons A**, Kelly JL, Rodrick ML, Mannick JA, Lederer JA. Major injury induces increased production of interleukin-10 by cells of the immune system with a negative impact on resistance to infection. *Ann Surg* 1997; **226**: 450-460
39 **Rongione AJ**, Kusske AM, Ashley SW, Reber HA, McFadden DW. Interleukin-10 prevents early cytokine release in severe intraabdominal infection and sepsis. *J Surg Res* 1997; **70**: 107-112
40 **McKay DM**, Baird AW. Cytokine regulation of epithelial permeability and ion transport. *Gut* 1999; **44**: 283-289
41 **O'Boyle CJ**, Mac Fie J, Dave K, Sagar PS, Poon P, Mitchell CJ. Alterations in intestinal barrier function do not predispose to translocation of enteric bacteria in gastroenterologic patients. *Nutrition* 1998; **14**: 358-362

**Edited by** Wu XN

P.O.Box 2345, Beijing 100023,China
Fax: +86-10-85381893
E-mail: wjg@wjgnet.com www.wjgnet.com

World J Gastroenterol 2003;9(6):1333-1336
World Journal of Gastroenterology
Copyright ©2003 by The WJG Press ISSN 1007-9327

• BASIC RESEARCH •

# Establishment of transgenic mice carrying the gene of human nuclear receptor NR5A2 (hB1F)

Shui-Liang Wang, Hua Yang, You-Hua Xie, Yuan Wang, Jian-Zhong Li, Long Wang, Zhu-Gang Wang, Ji-Liang Fu

**Shui-Liang Wang, Hua Yang, Jian-Zhong Li, Ji-Liang Fu,** Department of Medical Genetics, Second Military Medical University, Shanghai 200433, China
**You-Hua Xie, Yuan Wang,** Institute of Biochemistry and Cell Biology, Shanghai Institute for Biological Sciences, Chinese Academy of Sciences, Shanghai 200031, China
**Long Wang, Zhu-Gang Wang, Ji-Liang Fu,** Shanghai Nanfang Research Center for Model Organisms, Shanghai 201203, China
**Supported by** the National Natural Science Foundation of China, No.39830360, and the National "863" High Technology Research and Development Program of China, No. 2001AA221261
**Correspondence to:** Professor. Ji-Liang Fu, Department of Medical Genetics, Second Military Medical University, 800 Xiangyin Road, Shanghai 200433, China. jlfu@guomai.sh.cn
**Telephone:** +86-21-25070027 **Fax:** +86-21-25070027
**Received:** 2002-12-05 **Accepted:** 2003-01-02

## Abstract

**AIM:** Human hepatitis B virus enhancer II B1 binding factor (hB1F) was cloned and characterized as a novel member of the Ftz-F1 (NR5A) nuclear receptor subfamily. Although progresses have recently been made, its biological function remains largely unidentified. The aim of this study was to establish an hB1F transgenic mouse model to promote the functional study of hB1F.

**METHODS:** Transgene fragments were microinjected into fertilized eggs of mice. The manipulated embryos were transferred into the oviducts of pseudopregnant female mice. The offsprings were identified by PCR and Southern blot analysis. Transgene expression was analyzed with RT-PCR and Western blot analysis. Transgenic founder mice were used to establish transgenic mouse lineages. The F1 and F2 mice were identified by PCR analysis.

**RESULTS:** Seven mice were identified as carrying copies of transgene. RT-PCR and Western blotting results showed that the transgene was expressed in heart, liver, lung, kidney and stomach in one of the transgenic mouse lineages. Genetic analysis of the transgenic mice demonstrated that the transgene was integrated into the chromosome at a single site, and was transmitted stably.

**CONCLUSION:** In this study we established an hB1F transgenic mouse model, which will facilitate the investigation of the biological function of hB1F *in vivo*.

Wang SL, Yang H, Xie YH, Wang Y, Li JZ, Wang L, Wang ZG, Fu JL. Establishment of transgenic mice carrying the gene of human nuclear receptor NR5A2 (hB1F). *World J Gastroenterol* 2003; 9(6): 1333-1336
http://www.wjgnet.com/1007-9327/9/1333.asp

## INTRODUCTION

Nuclear receptor (NR) is a superfamily of eukaryotic transcription factors that are crucial for gene regulation and development. Members of this superfamily include receptors for steroid and non-steroid hormones as well as a large number of orphan receptors whose regulatory ligands have not been identified[1,2]. *Fushi tarazu* factor 1 (Ftz-F1) is one of the six subfamilies of the NR superfamily[3], which has been nominated as NR5[4]. Members of the Ftz-F1 subfamily all possess a particular Ftz-F1 box located at the C-terminal of the DNA-binding domain (DBD) and bind to their response elements as monomer.

Human hepatitis B virus (HBV) enhancer II B1 binding factor (hB1F) has been cloned and characterized as a novel member of the Ftz-F1 subfamily[5]. hB1F (also known as NR5A2, CPF, and hFTF) binds specifically to the B1 element in the enhancer II of HBV and activates its function, thus regulating the viral gene expression and replication. RT-PCR and 3' -RACE have previously revealed that utilization of two polyadenylation signals results in the 3.8 and 5.2 kb transcripts[6,7]. hB1F is the human homologue of the mouse transcription factor mLRH-1. It has been reported that NR5A2 may play an important role in regulating the liver-specific expression of several genes[8]. Recent findings demonstrate that NR5A2 is a critical transcription factor in the bile acid biosynthesis pathway[9,10] and may also regulate the expression of bile acid and cholesterol transporters in the liver and intestine[11,12].

To facilitate the functional studies of hB1F, we reported here the establishment of transgenic mice carrying hB1F gene. 7 transgenic mice were identified by PCR and Southern blotting and used as founders to establish transgenic mouse lineages. The results of the F1 identification with PCR showed that the transgenes could be transmitted stably. RT-PCR and Western blotting analysis demonstrated that the transgenes expressed in multiple tissues of transgenic mice.

## MATERIALS AND METHODS

### *Plasmid*

pcDNA3-hB1F contains the full length hB1F cDNA under the control of CMV promoter. A Flag tag was placed upstream to the hB1F coding sequence to facilitate the characterization of the expressed protein.

### *Animals*

C57 and CBA mice were maintained by Shanghai Nanfang Research Center for Model Organisms. Transgenic mice were raised, and bred in the Laboratory Animal Centre of Second Military Medical University.

### *Generation of transgenic mice*

The 6.9 kb linearized pcDNA3-hB1F was purified from agarose gel with QIAGEN gel extraction kit (Qiagen, CA, USA), adjusted to a final concentration of 1 μg/ml in TE buffer and used as the DNA solution in microinjection. The F1 female hybrids of C57 and CBA mice were hormonally superovulated and mated with F1 male hybrids. Next morning the fertilized one-cell eggs were collected from the oviduct. The eggs were microinjected with the DNA solution under a microscope. The injected fertilized eggs were transplanted into the oviduct of pseudo-pregnant F1 hybrids of C57 and CBA mice.

### *Identification of transgenic mice*

Founder (G0) mice were identified by PCR and Southern blotting analysis. For PCR, DNA was extracted from tails with Genomic DNA MINIPREPES kit (Sangon Inc. China). PCR amplification was performed with hB1F primers (P1: 5'-CCGACAAGTGGTACATGGAA-3' P2: 5'-CTGCTGCGGGTAGTTACACA-3') and pcDNA3 primers (P3: 5'-ATGCGGTGGGCT CTATG-3' P4: 5'-CGGCTTCCATCCGAGTA-3') which would produce 300 bp and 1 353 bp fragments from mice carrying the transgene, respectively. For Southern blotting, genomic DNA was digested overnight with HindIII and subjected to electrophoresis on a 1.0 % agarose gel. DNA was transferred onto nylon membrane (MILLIPORE Co., Ltd, London, UK). Hybridization was performed under a stringent condition with a randomly-primed ($\alpha$-$^{32}$P)-labeled hB1F probe.

### *Expression of the transgene*

One of the transgenic mouse lineages was used to study the expression of transgene. Total RNA was isolated from tissues with the TRIzol reagent (Invitrogen, CA, USA), according to manufacturer's instructions. First strand cDNA was synthesized by reverse transcription (Promega, USA). Semiquantitative RT-PCR reactions were performed using primer pairs 5'-CCGACAAGTGGT ACATGGAA-3' and 5'-CTGCTGCGGGTAGTTACACA-3' for hB1F cDNA, and 5'-AACTTTGGCATTGTGGAAGG-3' and 5'-TGTGAGGGAGATGCTCAGT G-3' for mouse glyceraldehyde-3-phosphate dehydrogenase (GAPDH) cDNA, which resulted in the generation of 300 bp and 600 bp products, respectively. PCR was performed for 30 cycles at 94 ℃ for 1 min, at 57 ℃ for 1 min, and at 72 ℃ for 1 min. PCR products were electrophoresed on 1.5 % agarose gels. Signals were quantified by density analysis of the digital images using BioStar image software,version 2.

For Western blotting, protein samples from tissues were prepared according the protocols by the manufacturer (Santa Cruz Biotechnology, Inc. WA, USA). 50 μg protein of each sample was electrophoresed on 10 % SDS-polyacrylamide gel and transferred to PVDF membrane. Membranes were blocked with 5 % (w/v) non-fat milk in Tween-TBS (TBST) overnight at 4 ℃ and incubated with anti-Flag antibody (Sigma, USA) at a dilution of 1:500 in TBST for 2 h at room temperature. Membranes were washed three times with TBST and incubated with a secondary antibody (horseradish peroxidase-conjugated anti-mouse IgG) at a dilution of 1:2 000 at room temperature for 1 h. Immunodetection was carried out with an enhanced chemiluminescence kit (Amersham Pharmacia Biotech, USA).

### *Transmission of transgene*

To study the transmission of transgene in mice, transgenic founder mice were mated to normal C57 mice to produce the first generation (F1) transgenic mice which were identified by PCR analysis using hB1F primers P1 and P2, and primers P5 (5'-GTTGGAGGTCGCTGAGTA-3') and P6 (5'-AGTAGGAAAGTCCCATAAGGTC-3'), yielding 300 bp and 500 bp products, respectively, from mice carrying the transgene. The F1 mice of the same founder carrying the transgene were mated between brother and sister mice to produce the second generation (F2). The F2 transgenic mice were identified by the same methods for the F1 transgenic mice.

## RESULTS

### *Establishment of hB1F transgenic mice*

The transgene fragment containing the full length hB1F cDNA was microinjected into the male pronucleus of 653 fertilized oocytes of F1 hybrids between C57 and CBA mice. The injected eggs were implanted into the oviducts of 24 pseudo-pregnant foster mothers, of which 13 mice became pregnant and gave birth to 97 offsprings. Eleven offspring mice were identified to carry the hB1F cDNA as demonstrated by PCR analysis (Figure 1), seven out of which were further confirmed by Southern blotting analysis (Figure 2). The ratio of transgene integration was 11.3 % and 7.2 %, respectively, by PCR and Southern blotting analysis.

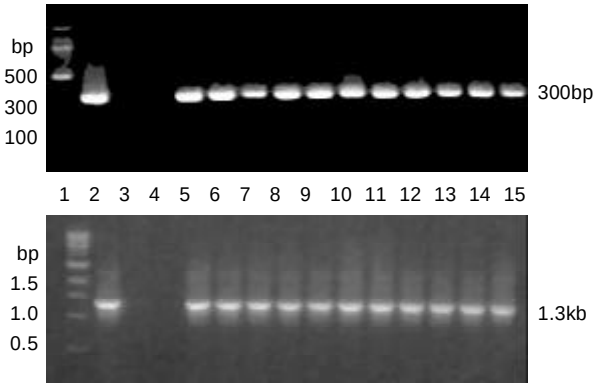


**Figure 1** PCR results of transgenic mice. 1: DNA molecular weight marker, up 100bp ladder,down 1kb ladder; 2: Positive control (pcDNA3-hB1F); 3: Negative control (normal mouse); 4: Water as template; 5-15: Transgenic founder mice; Up: P1-P2 primers amplified; Down: P3-P4 primers amplified.

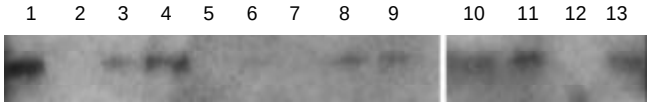


**Figure 2** Genonic DNA Southern blotting results of transgenic mice. 1: Positive control (pcDNA3-hB1F); 2: Negative control (normal mouse); 3-13: Transgenic founder mice.

### *hB1F transgene expressed in multiple tissues of transgenic mice*

As the transgene was driven by the CMV promoter, to study if it can express in multiple tissues of transgenic mice, we analysed the tissue expression profile of the hB1F transgene by RT-PCR and Western blot. The results (Figure 3, Figure 4) showed that the hB1F transgene was expressed in the heart, liver, lung, stomach and kidney, but not in intestine and encephalon.

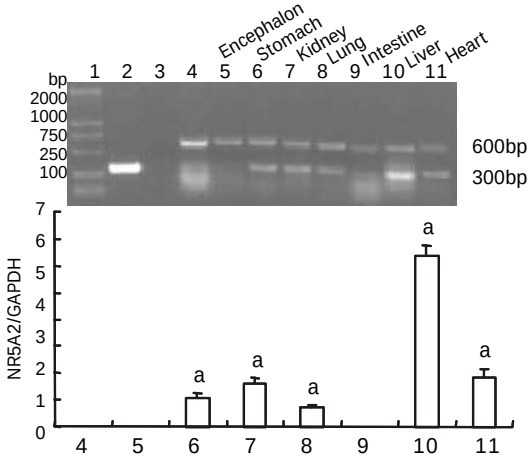


**Figure 3** RT-PCR results of transgene expression. 1: DNA molecular weight marker DL 2000; 2: Positive control (pcDNA3-hB1F); 3: Negative control (non-reversely transcribed RNA); 4: C57 mouse liver; 5-11: Transgenic mice tissues. [a]$P<0.05$.

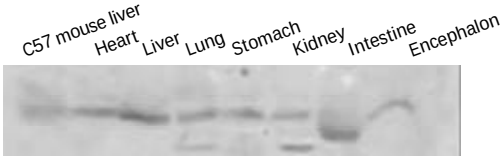


**Figure 4** Western blotting analysis of transgene expression.

### *Genetics of transgenic mice*

To establish the transgenic mouse lineages, founder mice were mated to C57 mice to produce F1 mice. Among 128 mice of the first generation, 60 were identified as carrying hB1F cDNA transgene by PCR analysis (Figure 5). The ratio of transgene transmission was 46.9 %. The F1 mice from the same founder were mated each other to produce the F2 mice. 45 out of 64 F2 mice were hB1F transgenic mice, with a ratio of transgene transmission of 70.3 %. These results showed that the inheritance of hB1F transgene was in accordance with Mendel' s laws, and the transgene was integrated into the chromosome in a single site and could be transmitted stably.

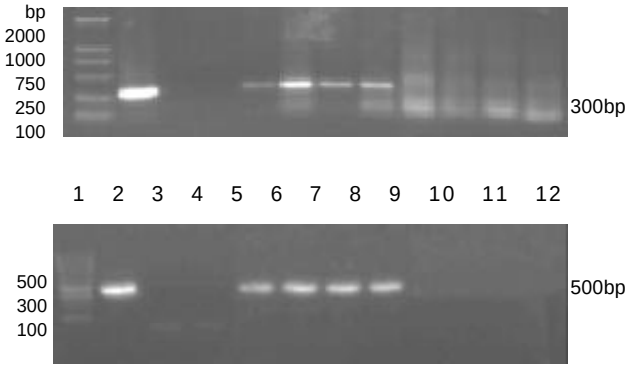


**Figure 5** Partial PCR results of F1 transgenic mice. 1: DNA molecular weight marker, up DL 2000, down 100bp ladder; 2: Positive control (pcDNA3-hB1F); 3: Negative control (normal mouse); 4: Water as control; 5-12: F1 mice; Up: P1-P2 primers amplified; Down: P5-P6 primers amplified.

## DISCUSSION

hB1F (NR5A2) is a novel member of the FTZ-F1 nuclear receptor subfamily. It was originally cloned based on its interaction with hepatitis B virus (HBV) enhancer II B1 element[5]. It has been shown to be a critical regulator of HBV gene expression and replication. Recent studies have revealed that hB1F is mainly involved in the regulation of cholesterol related gene expresssion in the hepatic-intestinal system. hB1F and its mouse homolog mLRH-1 are essential for the transcription of the gene encoding cholesterol 7a hydroxylase (CYP7A1), the first and rate limiting enzyme in bile acid biosynthesis[6,9,10]. Together with two other nuclear receptors, FXR and SHP, and hB1F/ mLRH-1 can mediate the feedback effect of bile acids on the transcription of CYP7A1. Moreover, hB1F/mLRH-1 can also regulate the expression of sterol 12α-hydrolyase (CYP8B1)[13], multidrug resistance protein-3 (MRP-3)[11], cholesterol ester transport protein (CETP)[12] and aromatases[14]. There is evidence that mLRH-1 may also regulate the expression of several critical transcritional factors, such as HNF1, HNF3β and HNF4[15]. It is possible that hB1F/mLRH-1 may exert broad influences on many genes by regulating these important factors. Since the regulation of cholesterol and bile acid homeostats is complicated, prone to be influenced by various genetic and environmental factors, it is vital to establish a transgenic or knock-out animal model for the studies of the biological role that hB1F plays in a living organism. The strategy to knock out mLRH-1 in mice has not been successful, due to early embryo lethality (personal communication), which suggests that hB1F/mLRH-1 has yet unidentified crucial functions during embryogenesis. The attempt to generate hB1F transgenic mice has not been reported either. To our knowledge, we have generated the first transgenic mice carrying and expressing the hB1F transgene.

*In vivo* hB1F/mLRH-1 is mainly expressed in the liver and pancreas. However, weak expression of hB1F has also been detected in other tissues such as heart, lung, skeletal muscle and intestine[5,6]. Recent studies have also demonstrated that hB1F is expressed abundantly in human ovary, testis[16] and preadipocytes[14], as well as in human adrenal and placenta in small amount[16], thus hB1F has a broader expression tissue profile than previously thought. In this study, the hB1F transgene was expressed in multiple tissues, most of which are capable of expressing endogenous hB1F *in vivo*. Therefore, the hB1F transgenic mice we generated in this study is an invaluable animal model, for investigating hB1F function not only in hepatic tissues, but also in other tissues, which may ultimately reveal the yet unidentified biological functions of hB1F.

In conclusion, we reported here the successful generation of a transgenic mouse model expressing the orphan nuclear receptor hB1F (NR5A2). Future studies will focus on the physiological and pathological changes in this mouse model using powerful analytic methods e.g. microarray comparisons of gene expression profiles between normal and transgenic mice.

## REFERENCES

1 **Beato M**, Herrlich P, Schutz G. Steroid hormone receptors: many actors in search of a plot. *Cell* 1995; **83**: 851-857
2 **Kastner P**, Mark M, Chambon P. Non-steroid nuclear receptors: what are genetic studies telling us about their role in real life? *Cell* 1995; **83**: 859-869
3 **Laudet V**. Evolution of the nuclear receptor superfamily: early diversification from an anceatral orphan receptor. *J Mol Endocrinol* 1997; **19**: 207-226
4 **Nuclear Receptors Nomenclature Committee**. A unified nomenclature system for the nuclear receptor superfamily. *Cell* 1999; **97**: 161-163
5 **Li M**, Xie YH, Kong YY, Wu X, Zhu L, Wang Y. Cloning and characterization of a novel human hepatocyte transcripion factor, hB1F, which binds and activates enhancer II of hepatitis B virus. *J Biol Chem* 1998; **273**: 29022-29031
6 **Nitta M**, Ku S, Brown C, Okamoto AY, Shan B. CPF: an orphan nuclear receptor that regulates liver-specific expression of the human cholesterol 7alpha-hydroxylase gene. *Proc Natl Acad Sci USA* 1999; **96**: 6660-6665
7 **Zhang CK**, Lin W, Cai YN, Xu PL, Dong H, Li M, Kong YY, Fu G, Xie YH, Huang GM, Wang Y. Characterization of the genomic structure and tissue-specific promoter of the human nuclear receptor NR5A2 (hB1F) gene. *Gene* 2001; **273**: 239-249
8 **Galarneau L**, Pare JF, Allard D, Hamel D, Levesque L, Tugwood JD, Green S, Belanger L. The alpha1-fetoprotein locus is activated by a nuclear receptor of the Drosophila FTZ-F1 family. *Mol Cell Biol* 1996; **16**: 3853-3865
9 **Goodwin B**, Jones SA, Price RR, Watson MA, McKee DD, Moore LB, Galardi C, Wilson JG, Lewis MC, Roth ME, Maloney PR, Willson TM, Kliewer SA. A regulatory cascade of the nuclear receptors FXR, SHP-1,and LRH-1 represses bile acid biosynthesis. *Mol Cell* 2000; **6**: 517-526
10 **Lu TT**, Makishima M, Repa JJ, Schoonjans K, Kerr TA, Auwerx J,Mangelsdorf DJ. Molecular basis for feedback regulation of bile acid synthesis by nuclear receptors. *Mol Cell* 2000; **6**: 507-515
11 **Inokuchi A**, Hinoshita E, Iwamoto Y, Kohno K, Kuwano M, Uchiumi T. Enhanced expression of the human multidrug resis-

tance protein 3 by bile salt in human enterocytes: A transcriptional control of a plausible bile acid transporter. *J Biol Chem* 2001; **276**: 46822-46829

12 **Luo Y**, Liang CP, Tall AR. The orphan nuclear receptor LRH-1 potentiates the sterol-mediated induction of the human CETP Gene by Liver X Receptor. *J Biol Chem* 2001; **276**: 24767-24773

13 **del Castillo-Olivares A**, Gil G. A1pha-fetoprotein transcription factor is required for the expression of sterol 12 a1pha-hydroxylase, the specific enzyme for cholic acid synthesis. Potential role in the bile acid-mediated regulation of gene transcription. *J Biol Chem* 2000; **275**: 17793-17799

14 **Clyne CD**, Speed CJ, Zhou J, Simpson ER. Liver receptor homologue-1 (LRH-1) regulates expression of aromatase in preadipocytes. *J Biol Chem* 2002; **277**: 20591-20597

15 **Pare JF**, Roy S, Galarneau L, Belanger L. The mouse fetoprotein transcription factor (FTF) gene promoter is regulated by three GATA elements with tandem E-box and Nkx motifs, and FTF in turn activates the HNF3beta, HNF4a1pha and HNF1a1pha gene promoters. *J Biol Chem* 2001; **276**: 13136-13144

16 **Sirianni R**, Seely JB, Attia G, Stocco DM, Carr BR, Pezzi V, Rainey WE. Liver receptor homologue-1 is expressed in human steroidogenic tissues and activates transcription of genes encoding steroidogenic enzymes. *J Endocrinol* 2002; **174**: R13-17

**Edited by** Xia HHX

P.O.Box 2345, Beijing 100023,China
Fax: +86-10-85381893
E-mail: wjg@wjgnet.com www.wjgnet.com

World J Gastroenterol 2003;9(6):1337-1341
World Journal of Gastroenterology
Copyright ©2003 by The WJG Press ISSN 1007-9327

• BASIC RESEARCH •

# Gene-expression analysis of single cells-nested polymerase chain reaction after laser microdissection

Xin Shi, Jörg Kleeff, Zhao-Wen Zhu, Bruno Schmied, Wen-Hao Tang, Arthur Zimmermann, Markus W. Büchler, Helmut Friess

**Xin Shi, Jörg Kleeff, Zhao-Wen Zhu, Bruno Schmied, Markus W. Büchler, Helmut Friess**, Department of General Surgery, University of Heidelberg, Im Neuenheimer Feld 110, D-69120 Heidelberg, Germany
**Xin Shi, Wen-Hao Tang,** Department of General Surgery, Zhongda Hospital, Southeast University, Nanjing 210009, Jiangsu Province, P. R. China
**Arthur Zimmermann**, Institute of Pathology, University of Bern, Inselspital, CH-3010 Bern, Switzerland
**Correspondence to:** Helmut Friess, M.D.Department of General Surgery, University of Heidelberg, Im Neuenheimer Feld 110, D-69120 Heidelberg, Germany. helmut_friess@ med.uni-heidelberg.de
**Telephone:** +49-6221-566900 **Fax:** +49-6221-566903
**Received:** 2002-12-30 **Accepted:** 2003-03-12

## Abstract

**AIM:** The structural and functional characteristics of cells are dependent on the specific gene expression profile. The ability to study and compare gene expression at the cellular level will therefore provide valuable insights into cell physiology and pathophysiology.

**METHODS:** Individual cells were isolated from frozen colon tissue sections using laser microdissection. DNA as well as RNA were extracted, and total RNA was reversely transcribed to complementary DNA (cDNA). Both DNA and cDNA were analyzed by nested polymerase chain reaction (PCR). The quality of isolated DNA and RNA was satisfactory.

**RESULTS:** Single cells were successfully microdissected using an ultraviolet laser micromanipulator. Nested PCR amplification products of DNA and cDNA of single cells could clearly be visualized by agarose gel electrophoresis.

**CONCLUSION:** The combined use of laser microdissection and nested-PCR provides an opportunity to analyze gene expression in single cells. This method allows the analysis and identification of specific genes which are involved in physiological and pathophysiological processes in a complex of variable cell phenotypes.

Shi X, Kleeff J, Zhu ZW, Schmied B, Tang WH, Zimmermann A, Büchler MW, Friess H. Gene-expression analysis of single cells-nested polymerase chain reaction after laser microdissection. *World J Gastroenterol* 2003; 9(6): 1337-1341
http://www.wjgnet.com/1007-9327/9/1337.asp

## INTRODUCTION

Techniques for isolating a specific cell population from a tissue complex for subsequent analysis of its molecular and biochemical contents have long been critical in cellular and molecular biology. To this end, various microdissection techniques have been developed to reduce contamination of surrounding cells[1-3]. Microdissection originally involved manual or micromanipulator guidance of a needle to scrape off an area of interest of a thin tissue section[4]. Selective ultraviolet radiation fractionation, which relies on negative selection and ablation of the unwanted areas of the tissue on the slide, provides a technical advancement in this field[1]. Micromanipulators and microdissection have improved the accuracy and reliability of microdissection; however, it remains an intrinsically slow, technique-dependent process of procuring pure cell populations from tissues. Modern techniques, such as flow cytometry with cell sorting and affinity-labeled magnetic beads, allow separation of cell subpopulations from heterogeneous pools of single cells in suspension. To apply these techniques to tissues, there is a requirement for the dissolution of intercellular adhesion and the formation of a suspension of individual cells, which is not generally practical in solid tissues and may change the characteristics of the isolated cells. Perhaps the biggest breakthrough in this approach and one that is rapidly gaining popularity is laser microdissection (LM)[5,6]. LM can be used to collect individual cells or specific cell populations from complex tissues without any contamination, and an individual operator can collect many samples in a single session.

The use of LM to obtain pure cell populations has so far been applied to DNA analysis[5], protein analysis[7] and mRNA analysis[8]. A variety of approaches are routinely used to assess the expression of specific genes in cells and tissues, such as Northern blot and RNase protection assay. The quantity of mRNA that can be harvested from a single cell is on the order of 1 pg at best. Thus, the techniques used to analyze gene expression are limited when applied to single cells. Nested PCR has proved to be a sensitive and specific procedure[9], and the use of nested PCR increases both the sensitivity and specificity of the standard PCR assay[10,11].

We now present an approach that allows analysis of DNA and mRNA down to the cellular level within intact tissue sections using a combination of LM and nested PCR.

## MATERIALS AND METHODS

### *Preparation of tissue sections*

Normal colon tissues were obtained from operation specimens in which a partial colon resection was performed for colon cancer. The Human Subject Committee of the University of Bern approved the studies. Immediately following surgical removal, tissues were snap-frozen in liquid nitrogen and maintained at -80 ℃ until use. Tissues were embedded in Tissue Tek OCT medium (VWR Scientific Products Corporation, San Diego, CA, USA) and sectioned at 8 μm in a cryostat, mounted on uncoated glass slides, and immediately stored at -80 ℃ once air dried. Slides containing frozen sections were fixed in 70 % ethanol for 2 min, stained with hematoxylin and eosin, then dehydrated in 70 %, 94 % and 100 % alcohol (each for 2 minutes) and finally dehydrated for 2 minutes in xylene.

### *Laser microdissection*

The ultraviolet-laser Robot-Microbeam (P.A.L.M., Wolfratshausen, Germany) used for microdissection consists

of a nitrogen laser of high-beam precision (wavelength 337nm) coupled to an inverted microscope (Axiovert 135; Zeiss, Jena, Germany) via the epifluorescence illumination path. The microscope stage and micromanipulator are digitally controlled and moved by a computer mouse. The high photon density within the laser focus catapults the material to the cap without any heating effect-a so-called cold ablation-so that DNA and RNA would not degrade during microdissection. With the combination of laser-manipulated microdissection (LMM) and the laser pressure catapulting (LPC) technique, single cells could be processed in seconds[12].

### *DNA extraction from microdissected samples*

DNA was extracted using DNA extraction solution with 100 mM Tris-HCl, pH 8.0, 400 μg/ml proteinase K (Sigma, Deisenhofen, Germany). After incubation at 37 ℃ for 3 h, the samples were boiled to inactivate proteinase K. After centrifugation, the supernatants of the DNA extraction buffer, now containing DNA from the microdissected cells, were used for nested PCR.

### *RNA isolation from microdissected samples and reverse transcription*

Total RNA was independently isolated by means of a modification of the RNA microisolation protocol, as described previously[13]. Briefly, caps were placed in Eppendorf tubes containing guanidinium isothiocyanate buffer, inverted several times, extracted with phenol/chloroform/isoamyl alcohol, and precipitated with sodium acetate and glycogen carrier (10 μg/μl) in isopropanol. After initial recovery and resuspension of the RNA pellet, a DNAse treatment was performed for 2 h at 37 ℃ using 10 units of DNAse (Roche Diagnostics, Mannheim, Germany) in the presence of 10 units of RNAse inhibitor (Roche Diagnostics, Mannheim, Germany), followed by re-extraction and precipitation. The pellet was resuspended in 24 μl of RNAse-free water. 12 μl of total RNA was reversely transcribed into complementary DNA (cDNA) using random hexamers according to the manufacturer' s instructions (Roche Diagnostics, Rotkreuz, Switzerland)[14]. For each cDNA reaction tube, an identical tube containing the same amount of RNA was prepared as a negative control (mock RT). In these tubes, the same amount of water was substituted for reverse transcriptase. After incubation, the reaction was terminated by heating to 95 ℃ for 10 min. The cDNA preparations were used immediately or stored at -20 ℃ until use.

### *Gene analysis by nested PCR*

The human beta-actin gene, a ubiquitously and constitutively expressed gene, was used as the target gene[15] for nested PCR. This approach involves the use of two pairs of PCR primers. The primers were synthesized by Amplimmun (Amplimmun AG, Madulain, Switzerland); the sequence is shown in Table 1. PCR amplification was carried out using beta-actin-outer primers in a final volume of 25 μl with a Perkin-Elmer GeneAmp System 9700 using 0.625U of Taq DNA polymerase (Roche Diagnostics GmbH, Mannheim, Germany). Cycling conditions were as follows: 35 cycles of denaturation at 94 ℃ for 1 min, annealing at 62 ℃ for 1 min, and elongation at 72 ℃ for 2.5 min. The first PCR cycle was preceded by denaturation at 94 ℃ for 3 min, and the last PCR cycle was followed by incubation at 72 ℃ for 8 min. Nested PCR was performed using 0.5 μl of the first PCR product as a template. The PCR cycling conditions for the beta-actin-inner primers were the same as above except for an annealing temperature of 60 ℃. The amplification products were analyzed by electrophoresis on 1 % agarose gels and stained with ethidium bromide.

**Table 1** β-actin primers used for nested PCR analysis

| Primer | Sequence | Primer size (bp) | Size of PCR products (bp) |
|---|---|---|---|
| β-actin-outer | | | |
| Forward primer | GGC ATC CTC ACC CTG AAG TA | 20 | 494 |
| Reverse primer | CCA TCT CTT GCT CGA AGT CC | 20 | |
| β-actin-inner | | | |
| Forward primer | AAA TCT GGC ACC ACA CCT TC | 20 | 240 |
| Reverse primer | AGG GCA TAC CCC TCG TAG AT | 20 | |

## RESULTS

### *Laser microdissection of cells from cryostat sections*

Eight-micrometer cryostat sections were prepared from normal colon tissues. Single colon mucosa cells were selected and cut with LM and catapulted by LPC under visual control (Figure 1). For LPC, the setting of laser energy was sufficiently high to catapult the microdissected cells into the microcentrifuge cap. Cell clusters of interest were also selected and laser-microdissected under visual control (Figure 2). The laser precisely circumcised a selected area or a single cell, which yielded a clear-cut gap between selected and non-selected areas.

### *DNA analysis in microdissected cells by nested PCR*

100 cells, 10 cells and 1 cell were microdissected from normal colon sections. Samples were digested by proteinase K and boiled for 10 min to denature proteinase K. After centrifugation, the supernatants were used for PCR with the beta-actin-outer primers. The amplification products were analyzed by electrophoresis on 1 % agarose gels; the results are shown in Figure 3A. The bands from a complete section, 100 cells, and 10 cells could be clearly visualized. Nested PCR was performed using 0.5 μl of the first PCR product as a template; the amplification results are shown in Figure 3B. Amplification products from single cells could be clearly visualized by agarose gel electrophoresis after nested PCR. Control amplifications without DNA templates did not yield any signal.

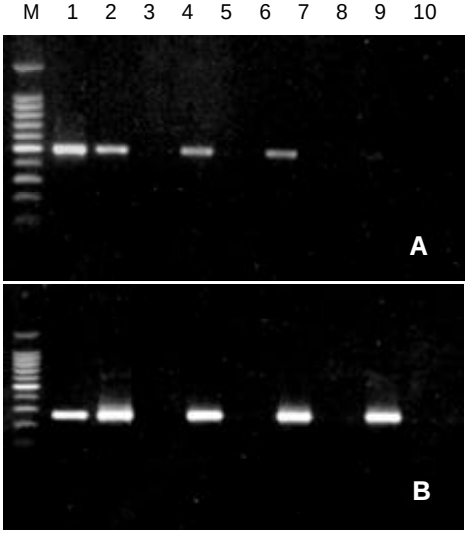


**Figure 2** Amplification results from nested PCR of colon cells after laser microdissection. Nested PCR amplification products of DNA of single cells could clearly be visualized by agarose gel electrophoresis. A: Amplification results of β-actin-outer primers. B: Amplification results of β-actin–inner primers. M: DNA markers (upper to lower: 2000, 1000, 900, 800, 700, 600, 500, 400, 300, 200, and 100 bp). 1: PCR positive control; 2: one complete section; 4, 6 and 8 are 100, 10 and 1 cell(s), respectively; 3, 5, 7 and 9 are negative controls of 2, 4, 6 and 8; 10: PCR negative control.

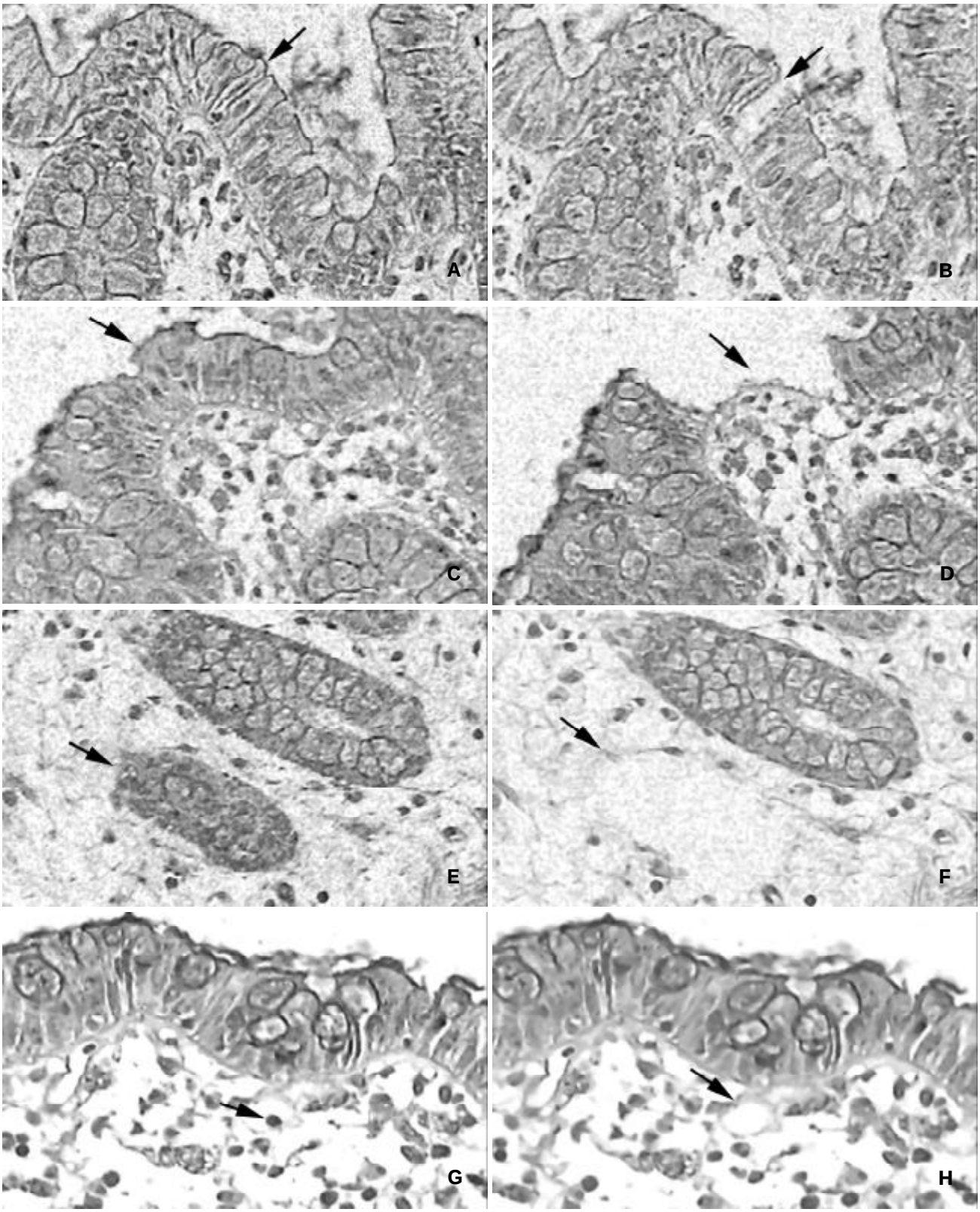


**Figure 1** Examples of laser microdissection in colon tissues (hematoxylin and eosin, magnification ×200). Single cells were picked by combination laser-manipulated microdissection (LMM) and laser pressure catapulting (LPC). A, C, E, G: Before Laser microdissection. B, D, F, H: Using LMM, the laser precisely circumcised selected cells, yielding a cut gap between selected and non-selected areas. Then the selected cells were catapulted using the LPC technique. A-F: Typical images before and after LMM and LPC. G, H: Laser microdissection could also be used to cut out the nucleus of a selected cell.

### *mRNA expression in microdissected cells by nested PCR*

Normal colon RNA was obtained from complete sections, 200 cells, 100 cells, 10 cells and single cells. cDNA was transcribed from total RNA. The amplification products were analyzed by electrophoresis on 1 % agarose gels; the results are shown in Figure 3C. Signals from complete sections could be clearly visualized. However, the signals from 200 cells and 100 cells could only be seen on the original gels, and the signals from 10 cells and single cells were below the level of detection. Nested PCR was performed using 0.5 μl of the first PCR product as a template; the amplification results are shown in Figure 3D. Amplification products of even single

cells could be clearly visualized by agarose gel electrophoresis. Control amplifications without cDNA templates did not yield any signal.

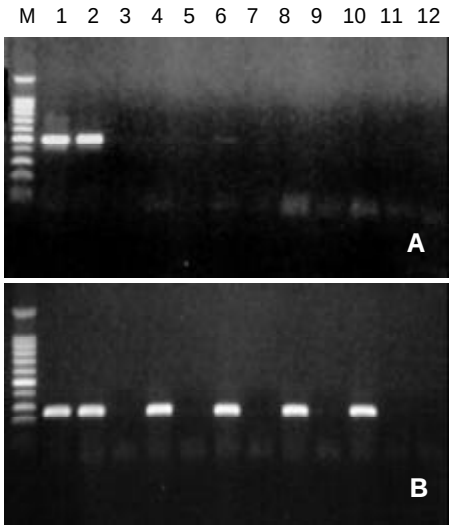


**Figure 3** Amplification results from nested RT-PCR for cDNA of single cells after laser microdissection. A: Amplification results of β-actin-outer primers. B: Amplification results of β-actin-inner primers. M: DNA markers (upper to lower: 2000, 1000, 900, 800, 700, 600, 500, 400, 300, 200, and 100 bp). 1: PCR positive control; 2: one complete section; 4, 6, 8 and 10 are 200, 100, 10 and 1 cell(s), respectively; 3, 5, 7, 9 and 11 are negative controls of 2, 4, 6, 8 and 10; 12: PCR negative control.

## DISCUSSION

In this study, single colon mucosa cells could be selectively microdissected and collected from frozen tissue sections under direct microscopic visualization using LM. Microdissected mucosa cells were used for further gene analysis using nested PCR.

Most tissues are composed of a number of different cell types, and cellular heterogeneity in most tissues is very complex. In normal or developing organs, specific cells express different genes and undergo complex molecular changes both in response to internal control signals, signals from adjacent cells, and humoral stimuli. In disease pathologies, the diseased cells of interest, such as precancerous cells or invading groups of cancer cells, are surrounded by these heterogeneous tissue elements. The percentage of non-neoplastic cells present in such specimens can be as high as 95 %[16]. This tissue heterogeneity has proved one of the major obstacles to molecular research using current methods, since varying numbers of normal cells could mask the presence of single abnormal cells when analysis of its gene expression and total DNA or RNA from heterogeneous tissue is used[17-24].

LM is a new method for performing microdissection of selected regions down to a single cell[5,6,25]. There have been other reports describing methods to collect specific regions of tissue, such as graded sieving of glomeruli or pancreatic islet cells[26,27] and isolation of suspension of proximal tubular cells[28]. These methods make it possible to obtain relatively pure and large amounts of samples; however, it is difficult to avoid possible contamination of other tissue compartments, which can cause problems with sensitive RT-PCR methods. Using LM, our study has shown that it is feasible to examine mRNA expression of single cells without the risk of contamination by neighboring cells. If more than one cell is needed, single unwanted cells can selectively be destroyed from the tissue section using LM, resulting in an area composed of a homogenous cell population. Utilizing a computer-controlled microscope stage, the cells of interest are visually selected and marked and their positions are stored electronically. The stage then automatically goes to and moves around the selected cells, while the laser fires with a preselected pulse energy and repetition rate. With a further slightly defocused laser shot, the target cells can selectively be catapulted into a microcentrifuge cap using LPC for further study. As reported in this article, this method allows gene analysis in the particular tissue region isolated from the frozen cryostat specimen, avoiding the contamination of other cells.

The quantity of mRNA that can be harvested from a single cell is approximately 1 pg at best. Therefore, to obtain meaningful gene-expression data, well-optimized or specialized amplification protocols must be applied. Using conventional PCR, the theoretical limit of detection is one copy of a single-stranded DNA molecule, and so with efficient harvesting of cytoplasm and a well-optimized PCR protocol, single-cell PCR is feasible[29]. However, this is not a trivial undertaking, and identifying the expression of rare or particularly labile transcripts would prove to be technically demanding[30].

In this study, amplification signals from DNA of single cells were only faintly present in the agarose gels, and amplification signals from cDNA could not be visualized by gel electrophoresis. Therefore, certain modifications to this approach have to be applied to provide more comprehensive single-cell expression analysis. In this study, a straightforward method of expanding the results obtained from single-cell PCR involves the use of nested PCR. Essentially, a primary conventional PCR increases the target concentration so that a second PCR reaction can be carried out to assay for the presence or absence of gene expression. The present study has shown that nested PCR is feasible for the analysis of gene expression after LM, even at the cellular level, and that this approach has the advantage of being relatively simple to apply. Further studies on the gene expression profiles of single microdissected cells will provide novel insight into different physiological and pathophysiological processes.

## REFERENCES

1 **Shibata D**, Hawes D, Li ZH, Hernandez AM, Spruck CH, Nichols PW. Specific genetic analysis of microscopic tissue after selective ultraviolet radiation fractionation and the polymerase chain reaction. *Am J Pathol* 1992; **141**: 539-543
2 **Becker I**, Becker KF, Rohrl MH, Minkus G, Schutze K, Hofler H. Single-cell mutation analysis of tumors from stained histologic slides. *Lab Invest* 1996; **75**: 801-807
3 **Whetsell L**, Maw G, Nadon N, Ringer DP, Schaefer FV. Polymerase chain reaction microanalysis of tumors from stained histological slides. *Oncogene* 1992; **7**: 2355-2361
4 **Going JJ**, Lamb RF. Practical histological microdissection for PCR analysis. *J Pathol* 1996; **179**: 121-124
5 **Emmert-Buck MR**, Bonner RF, Smith PD, Chuaqui RF, Zhuang Z, Goldstein SR, Weiss RA, Liotta LA. Laser capture microdissection. *Science* 1996; **274**: 998-1001
6 **Bonner RF**, Emmert-Buck M, Cole K, Pohida T, Chuaqui R, Goldstein S, Liotta LA. Laser capture microdissection: Molecular analysis of tissue. *Science* 1997; **278**: 1481-1483
7 **Hao J**, Jackson L, Calaluce R, McDaniel K, Dalkin BL, Nagle RB. Investigation into the mechanism of the loss of laminin 5 (alpha3beta3gamma2) expression in prostate cancer. *Am J Pathol* 2001; **158**: 1129-1135
8 **Fink L**, Seeger W, Ermert L, Hanze J, Stahl U, Grimminger F, Kummer W, Bohle RM. Real-time quantitative RT-PCR after laser-assisted cell picking. *Nat Med* 1998; **4**: 1329-1333
9 **Yan Z**, Surmeier DJ. D5 dopamine receptors enhance Zn2+-sensitive GABA(A) currents in striatal cholinergic interneurons through a PKA / PP1 cascade. *Neuron* 1997; **19**: 1115-1126
10 **Bochet P**, Audinat E, Lambolez B, Crepel F, Rossier J, Iino M,

Tsuzuki K, Ozawa S. Subunit composition at the single-cell level explains functional properties of a glutamate-gated channel. *Neuron* 1994; **12**: 383-388

11 **Massengill JL**, Smith MA, Son DI, O'Dowd DK. Differential expression of K4-AP currents and Kv3.1 potassium channel transcripts in cortical neurons that develop distinct firing phenotypes. *J Neurosci* 1997; **17**: 3136-3147

12 **Nagasawa Y**, Takenaka M, Matsuoka Y, Imai E, Hori M. Quantitation of mRNA expression in glomeruli using laser-manipulated microdissection and laser pressure catapulting. *Kidney Int* 2000; **57**: 717-723

13 **Sgroi DC**, Teng S, Robinson G, LeVangie R, Hudson JR Jr, Elkahloun AG. *In vivo* gene expression profile analysis of human breast cancer progression. *Cancer Res* 1999; **59**: 5656-5661

14 **Conejo JR**, Kleeff J, Koliopanos A, Matsuda K, Zhu ZW, Goecke H, Bicheng N, Zimmermann A, Korc M, Friess H, Buchler MW. Syndecan-1 expression is up-regulated in pancreatic but not in other gastrointestinal cancers. *Int J Cancer* 2000; **88**: 12-20

15 **Efferth T**, Fabry U, Osieka R. Leptin contributes to the protection of human leukemic cells from cisplatinum cytoxicity. *Anticancer Res* 2000; **20**: 2541-2546

16 **Becker I**, Becker KF, Rohrl MH, Hofler H. Laser-assisted preparation of single cells from stained histological slides for gene analysis. *Histochem Cell Biol* 1997; **108**: 447-451

17 **Shi X**, Gao NR, Guo QM, Yang YJ, Huo MD, Hu HL, Friess H. Relationship between overexpression of NK-1R, NK-2R and intestinal mucosal damage in acute necrotizing pancreatitis. *World J Gastroenterol* 2003; **9**: 160-164

18 **Lin JS**, Song YH, Kong XJ, Li B, Liu NZ, Wu XL, Jin YX. Preparation and identification of anti-transforming growth factor beta1 U1 small nuclear RNA chimeric ribozyme *in vitro*. *World J Gastroenterol* 2003; **9**: 572-577

19 **Yue H**, Na YL, Feng XL, Ma SR, Song FL, Yang B. Expression of p57(kip2), Rb protein and PCNA and their relationships with clinicopathology in human pancreatic cancer. *World J Gastroenterol* 2003; **9**: 377-380

20 **Wang GS**, Wang MW, Wu BY, You WD, Yang XY. A novel gene, GCRG224, is differentially expressed in human gastric mucosa. *World J Gastroenterol* 2003; **9**: 30-34

21 **Liu JW**, Tang Y, Shen Y, Zhong XY. Synergistic effect of cell differential agent-II and arsenic trioxide on induction of cell cycle arrest and apoptosis in hepatoma cells. *World J Gastroenterol* 2003;**9**: 65-68

22 **Shi M**, Wang FS, Wu ZZ. Synergetic anticancer effect of combined quercetin and recombinant adenoviral vector expressing human wild-type p53, GM-CSF and B7-1 genes on hepatocellular carcinoma cells *in vitro*. *World J Gastroenterol* 2003; **9**: 73-78

23 **Tang NH**, Chen YL, Wang XQ, Li XJ, Yin FZ, Wang XZ. Construction of IL-2 gene-modified human hepatocyte and its cultivation with microcarrier. *World J Gastroenterol* 2003; **9**: 79-83

24 **Xiong LJ**, Zhu JF, Luo DD, Zen LL, Cai SQ. Effects of pentoxifylline on the hepatic content of TGF-beta1 and collagen in Schistosomiasis japonica mice with liver fibrosis. *World J Gastroenterol* 2003; **9**: 152-154

25 **Schutze K**, Lahr G. Identification of expressed genes by laser-mediated manipulation of single cells. *Nat Biotechnol* 1998; **16**: 737-742

26 **Troyer DA**, Kreisberg JI. Isolation and study of glomerular cells. *Methods Enzymol* 1990; **191**: 141-152

27 **Figliuzzi M**, Zappella S, Morigi M, Rossi P, Marchetti P, Remuzzi A. Influence of donor age on bovine pancreatic islet isolation. *Transplantation* 2000; **70**: 1032-1037

28 **Vinay P**, Gougoux A, Lemieux G. Isolation of a pure suspension of rat proximal tubules. *Am J Physiol* 1981; **241**: F403-F411

29 **Jin L**, Thompson CA, Qian X, Kuecker SJ, Kulig E, Lloyd RV. Analysis of anterior pituitary hormone mRNA expression in immunophenotypically characterized single cells after laser capture microdissection. *Lab Invest* 1999; **79**: 511-512

30 **Dixon AK**, Richardson PJ, Pinnock RD, Lee K. Gene-expression analysis at the single-cell level. *Trends Pharmacol Sci* 2000; **21**: 65-70

**Edited by** Zhu LH

P.O.Box 2345, Beijing 100023,China
Fax: +86-10-85381893
E-mail: wjg@wjgnet.com www.wjgnet.com

World J Gastroenterol 2003;9(6):1342-1346
World Journal of Gastroenterology
Copyright ©2003 by The WJG Press ISSN 1007-9327

• BASIC RESEARCH •

# Rapid detection of the known SNPs of CYP2C9 using oligonucleotide microarray

Si-Yuan Wen, Hui Wang, Ou-Jun Sun, Sheng-Qi Wang

**Si-Yuan Wen, Hui Wang, Ou-Jun Sun, Sheng-Qi Wang,** Beijing Institute of Radiation Medicine, Beijing 100850, China
**Supported by** a grant from the State 863 High Technology Project of China, No. 2002AA2Z3411
**Correspondence to:** Professor Sheng-Qi Wang, Beijing Institute of Radiation Medicine, No. 27 Taiping Road, Beijing 100850, China. sqwang@nic.bmi.ac.cn
**Telephone:** +86-10-66932211 **Fax:** +86-10-66932211
**Received:** 2002-11-12 **Accepted:** 2002-12-18

## Abstract

**AIM:** Cytochrome P450 2C9 (CYP2C9) is a polymorphic enzyme responsible for the metabolism of a large number of clinically important drugs. Individuals with mutant enzymes may risk serious side effects under routine therapy with certain drugs metabolized by CYP2C9. In order to facilitate the detection of the known SNPs of CYP2C9, an allele-specific oligonucleotide (ASO) based microarray was made.

**METHODS:** An oligonucleotide microarray was made to facilitate the SNP (single nucleotide polymorphism) screening and was applied for the detection of CYP2C9 polymorphism in 62 high blood pressure (HBP) patients who received Irbesartan for treatment. Part of the genotyping results was confirmed by direct sequencing. And the relation between CYP2C9 polymorphism and therapeutic outcome of Irbesartan was statistically analyzed.

**RESULTS:** Heterozygous alleles of CYP2C9*1/*3 were found in 7 out of 62 subjects. No mutant alleles of CYP2C9*2, *4 and *5 and no homozygous mutant alleles were detected. The 7 heterozygous CYP2C9*1/*3 and 13 random wild type DNA samples were subjected to direct sequencing with purified PCR products and same genotyping results were obtained with the 20 DNA samples. There was no significant difference in the odds of effectiveness of Irbesartan between the wild type (normal) group and CYP2C9*1/*3 (mutant) group ($P>0.05$).

**CONCLUSION:** The oligonucleotide microarray made in this study is a reliable assay for detecting the CYP2C9 known alleles and the heterozygous CYP2C9*1/*3 has no significant effects on the therapeutic outcome of Irbesartan.

Wen SY, Wang H, Sun OJ, Wang SQ. Rapid detection of the known SNPs of CYP2C9 using oligonucleotide microarray. *World J Gastroenterol* 2003; 9(6): 1342-1346
http://www.wjgnet.com/1007-9327/9/1342.asp

## INTRODUCTION

Pharmacogenetics was established on the fact that certain genetic polymorphisms may cause significantly different responses among individuals on exposure to a particular drug[1-3]. Recent advances in the understanding of the molecular genetics of drug-metabolizing enzymes (DME), particularly cytochrome P450, have enabled the molecular basis of many polymorphisms to be elucidated and the genotyping assays to be developed[4-6].

Cytochrome P450 is one of the key enzymatic mechanisms for the metabolism of drugs, pesticides, environmental pollutants, and carcinogens[7-9]. In this superfamily, CYP2C9[10-12] is a polymorphic enzyme responsible for the metabolism of a large number of clinically important drugs such as S-warfarin, phenytoin, tolbutamide, losartan and nonsteroidal anti-inflammatory drugs. To date, 5 alleles of CYP2C9 including the wild type CYP2C9*1 and the mutants CYP2C9*2 (430C-T), CYP2C9*3 (1075A-C), CYP2C9*4 (1076T-C) and CYP2C9*5 (1080C-G) have been found (www.imm.ki.se\cypalleles). In the four mutant alleles, single nucleotide variations in the exon 3 and exon 7 cause amino acid substitutions Arg144Cys, Ile359Leu, Ile359Thr and D360E, respectively, and therefore lead to a slow metabolizing capacity of the enzymes. The altered pharmacogenetics may result in prolonged or shortened effect time. The individuals with mutant enzymes risk serious side effects under routine therapy with certain drugs metabolized by CYP2C9. So frequent variants of CYP2C9 should be analyzed in participants of clinical trials where the enzymes may play a key role.

In order to facilitate the detection of the known SNPs of CYP2C9, an ASO (allele-specific oligonucleotide) hybridization based microarray was made, which could simultaneously screen the 4 mutant alleles of CYP2C9 of 10 individuals, and was applied for the detection of CYP2C9 polymorphism in 62 hypertension patients who received Irbesartan for treatment. Irbesartan is a selective antagonist of the AT1 receptor of angiotensin II receptor (AT1R) used in the treatment of hypertension and congestive heart failure[13,14]. Previous studies indicate that Irbesartan is mainly metabolized by CYP2C9 to the inactive form[15].

## MATERIALS AND METHODS

### *DNA samples*

A total of 62 peripheral blood samples were collected from unrelated HBP patients who received Irbesartan for treatment and the therapeutic outcome was classified as outstanding (11 persons), effective (38 persons) and failed (13 persons). Genomic DNA was extracted with the Genomic DNA purification kit (Promega) and quantified by UV spectrophotometer (DU® 640, Beckman coulter).

### *Oligonucleotides synthesis*

Oligonucleotides (primers or probes) were synthesized using automatic DNA synthesizer (ABi 391A). For signal detection, the reverse primers were fluorescein (Cy3) labeled at 5' end. A probe was synthesized with the 3' end amino-modified to have a primary $NH_2$ group for immobilization onto aldehyde-coated slides, and the $NH_2$ group was linked by a polyethleneglycol spacer to a specific allele-discriminating sequence, which was 16-17 nucleotides in length with a nucleotide complimentary to either the normal or mutant allele in the middle of the sequence. A list of oligonucleotides used in this study is presented in Table 1.

**Table 1** Oligonucleotides used in this study

| ## | Sequence (5'--3') | Application |
|---|---|---|
| C1 | CAC ATG GCT GCC CAG TGT CAG CTT C | Primers used to amplify exon3 and exon7 fragments of |
| C2* | GGC CAC CCC TGA AAT GTT TCC AAG | CYP2C9 containing SNP sites. C2* and C4* were |
| C3 | ACG TGT GAT TGG CAG AAA CCG GAG C | fluorescein (Cy3) labeled at 5' end. |
| C4* | GGG ACT TCG AAA ACA TGG AGT TGC AG | |
| C1Tf | ATT GAG GAC TGT GTT CAA GAG GAA GC | Primers used to construct mutant templates. |
| C1Tr | CTT CCT CTT GAA CAC AGT CCT C | The variant bases (indicated by underlines) |
| C2Tf | CCT ACA CAG ATG CTG TGG TGC AC | were introduced when synthesized. |
| C2T1 | CTG GTG GGG AGA AGG TCA AGG TAT CTC | |
| C2T2 | CTG GTG GGG AGA AGG TCA GTG TAT CTC | |
| C2T3 | CTG GTG GGG AGA AGC TCA ATG TAT CTC | |
| P1 | TTG AGG ACC GTG TTC AA - spacer- $NH_2$ | Pairs of probes with one base difference (indicated |
| P2 | TTG AGG ACT GTG TTC AA - spacer- $NH_2$ | with underline) for SNP discrimination, immobilized |
| P3 | GAG ATA CAT TGA CCT TC - spacer- $NH_2$ | on aldehyde-coated slides surface with |
| P4 | GAG ATA CCT TGA CCT TC - spacer- $NH_2$ | 3' end primary $NH_2$ group. |
| P5 | GAG ATA CAT TGA CCT TC - spacer- $NH_2$ | |
| P6 | GAG ATA CAC TGA CCT TC - spacer- $NH_2$ | |
| P7 | TAC ATT GAC CTT CTC C - spacer- $NH_2$ | |
| P8 | TAC ATT GAG CTT CTC C - spacer- $NH_2$ | |

### *PCR amplification*

The 2 target segments containing the SNP sites to be typed were amplified by PCR in one tube. Asymmetric PCR method was used to generate single-stranded target segments. The ratio of forward primer to reverse primer (fluorescein labeled) was optimized at 1:40 in a PCR reaction (data not shown). Reaction mixtures of 20 μL contained 100 μM dNTP, 0.5 μM forward primer, 20 μM reverse primer, 100 ng of a genomic DNA or 40 ng of a plasmid DNA, 1* PCR buffer and 1 U Taq enzyme. Amplification was conducted in a thermal cycler (PTC-100™ programmable thermal controller, MJ. Research Inc) under the following conditions: initial denaturation (5 min at 94 ℃) followed by 40 cycles of denaturation (30 sec at 94 ℃), annealing (30 sec at 62 ℃) and extension (30 sec at 72 ℃). A final extension step was carried out for 5 min at 72 ℃. The PCR products were analyzed by 2 % agarose gel electrophoresis.

### *Construction of standard templates*

DNA segments of wild type or mutant CYP2C9 were subcloned to PGEM®T4-vector (Promega) according to the protocol. The plasmids were used as standard wild type or mutant templates for the optimization of hybridization conditions and establishment of signal intensity ratio of match to mismatch after verification by sequencing. The artificial heterozygous templates were constructed by mixing equal amounts of wild type and mutant plasimid DNA. To introduce a mutant nucleotide at specific position in a DNA segment, site-directed mutagenesis method[16] with mutant primers was used.

### *Preparation of DNA microarrays*

The 3' end amino-modified probes were diluted to a final concentration of 20 μmol/L in spotting solutions (3*SSC and 0.01 % SDS). The spotting solutions were transferred into 96-well plates in volumes of 10 μL and spotted to aldehyde-coated glass slides with a microarray printer (Cartisan), which deposited 0.5 nL at each spotting site, resulting in spots of 200 μm in diameter. Each probe was spotted in duplicate. The humidity during spotting was 70 % and the temperature was kept at 23 ℃. After spotting, slides were incubated for another 1 h under the same conditions and stored at room temperature for at least 1 day before use. The pattern of slide and array format are shown in Figure 3.

### *Hybridization and signal detection*

Two μL of the single-stranded Cy3-labeled target PCR products was mixed with 10 μL hybridization solution (5*SSC, 0.1 % SDS, 1 % salmon DNA), and the 12 μL final volume was transferred to the hybridization area on the glass slide. The slide was incubated in 40 ℃ water bath for 30 min in a hybridization chamber. After incubation, the slide was washed sequentially in washing solution A (1*SSC, 0.2 % SDS), washing solution B (0.2*SSC) and washing solution C (0.1 *SSC) for 1 min each.

The glass slides were scanned using the confocal Scanarray 3 000 (GSI Lumonics), with excitation at 540 nm and emission at 570 nm (Cy3). Sixteen-bit TIFF images of 10 μm resolution were analyzed. After subtraction of local background, the average signal intensity of the duplicate spots of each probe was used to calculate the signal ratios defining the genotypes.

### *Direct sequencing with PCR products*

Part of the DNA samples was subjected to direct sequencing using DNA sequencer (CEQ™ 2000XL DNA analysis system, Beckman) to confirm the results. PCR reaction was carried out in 50 μL solution and the PCR products were purified to be the sequencing templates with PCR products purification kit (Promega).

### *Statistical analysis*

Statistics was made by $\chi^2$ test.

## RESULTS

### *Determination of the signal intensity ratio of match to mismatch*

According to the hybridization result of standard wild type or mutant plasmid templates, under the optimized hybridization and stringent washing conditions, there was a great difference in signal intensities between the perfect match and the single base mismatch probes. The ratio of match to mismatch of signal pairs was above 4 at least. Detection of heterozygous alleles was a hard point for microarray. In the present study, the hybridization results of the heterozygous templates showed that the signal intensity ratio of the probe pair corresponding to heterozygous alleles was below 2.5 (the ratio was always

the stronger to the weaker). Typical results are shown in Figure 1. Repeated experiments with genomic DNA gave a statistically similar result (data not shown). So the ratio value above 4 or below 2.5 was considered sensible for genotype judgement while sample with the ratio value within 2.5-4 should be re-genotyped.

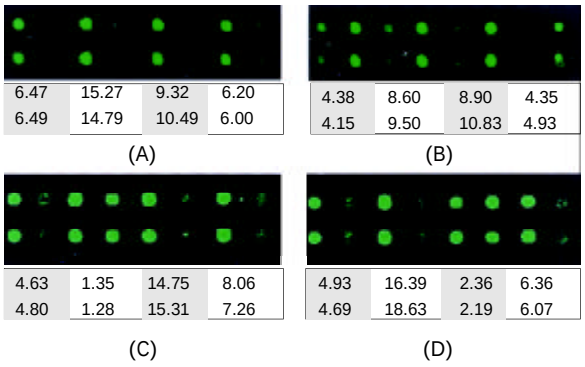


**Figure 1** The TIF image of hybridization results of (A) wildtype template, (B) mutant template, (C) heterozygous template of CYP2C9*1/CYP2C9*3, and (D) heterozygous template of CYP2C9*1/CYP2C9*4. The discriminating power of a pair of probes was represented by the ratio of match to mismatch listed below.

### *Genotype results of 62 DNA samples by DNA microarray*

In the genotype result of the 62 samples determined by the microarray, heterozygous alleles of CYP2C9*1/*3 were found in 7 out of 62 subjects. No heterozygous or homozygous mutant alleles of CYP2C9*2, *4 and *5 were detected. Repeated experiments gave the same result. A brief procedure is illustrated in Figure 2 and Figure 3.

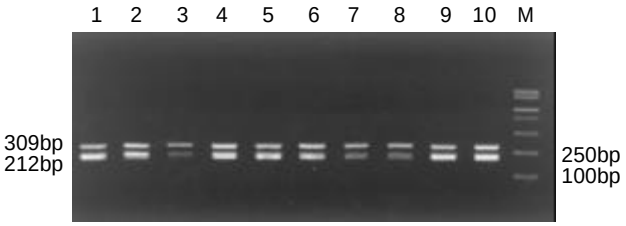


**Figure 2** 2 % agarose gel electrophoresis of the PCR products of 10 samples. 1-10: PCR products of 10 DNA samples, M: DGL2000 marker.

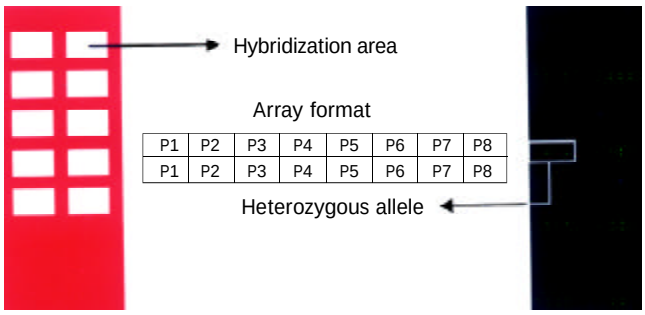


**Figure 3** Array format and microarray hybridization result of 10 samples.

### *DNA samples genotyped by direct sequencing*

To confirm the genotype result determined by microarray, the 7 heterozygous CYP2C9*1/*3 and 13 random wild type DNA samples were subjected to direct sequencing with purified PCR products. The same genotype results were obtained with the 20 DNA samples typed with two methods. The typical sequencing results of the heterozygous CYP2C9*1/*3 and wild type are compared in Figure 4.

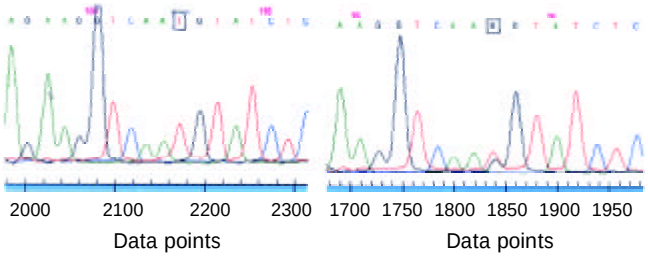


**Figure 4** Part of the sequencing results. The letters in square indicate wildtype and heterozygous of CYP2C9*1/CYP2C9*3 (1075A-C) in two samples.

### *Allele frequency and effects of CYP2C9 polymorphism on therapeutic outcome of Irbesartan*

The microarray described here is a reliable assay for detecting the CYP2C9 known alleles. The analysis of 62 HBP patients DNA samples yielded frequencies for CYP known alleles (Table 2) that were in agreement with previous study[7,17,18]. There was no significant difference in the odd of effectiveness of Irbesartan between the wild type (normal) group and the CYP2C9*1/*3 (mutant) group (Table 3, $P>0.05$).

**Table 2** CYP2C9 allele frequency in the study population

| Allele | Number of alleles | Frequency % |
|---|---|---|
| *2 | 0/124 | 0 |
| *3 | 7/124 | 5.6 |
| *4 | 0/124 | 0 |
| *5 | 0/124 | 0 |

**Table 3** Therapeutic outcome of Irbesartan in wild type group and CYP2C9*1/*3 group

| | Effective | Failed |
|---|---|---|
| Wild type | 43 | 12 |
| CYP2C9*1/*3 | 6 | 1 |

$P>1$ ($\chi^2$ test), no significant difference in the odd of effectiveness of Irbesartan between wild type group and CYP2C9*1/*3 group.

## DISCUSSION

Single nucleotide polymorphism (SNP) is the most common variation form in human genome[19-21]. The early methods to type SNPs include SSCP, RFLP, AS-PCR, etc[22-24], making genotyping judgement coupled with gel electrophoresis analysis. The methods above are unfit for a large scale screening due to the limitation of detection methods. With the advance of organic fluorescence labeling and detection technology, significant change has taken place in genotyping technology. Molecular beacon[25], TaqMan[26] probe methods, which detect fluorescence signal in homologous reaction, and DNA microarray[27-29], which is based on hybridization coupled with solid phase reaction, make genotyping easier and more accurate. In the newly developed technologies, DNA microarray is more preferable in the genetic linkage and association study between large number of genetic markers and phenotypic traits in pharmacogenomics, disease genomics etc, due to its parallel detection of a large quantity of genetic markers.

Fluorescence-labeled sample preparation is a critical step in microarray genotyping. The quality and amount of genomic DNA used as template in PCR reaction are essential to the hybridization results. In the present study, the two target segments containing the SNP sites to be typed were PCR amplified in one tube. Asymmetric PCR method was used to generate single-stranded target segments complimentary to the probes.

The fluorescence signal intensity and discriminating power (ratio of match to mismatch) of the probe pairs are the key results from microarray for genotyping judgement, which can be affected by many factors. When other conditions (the quality and amount of single stranded PCR products, the quality of aldehyde-coated slides, hybridization/washing conditions, etc) are strictly controlled, the specific sequence context of the probes is the determining factor. Because there was no simultaneous mutation reported in the CYP2C9 known alleles, the probes were designed without consideration of crosslink of SNP sites of 1075A-C, 1076T-C, 1080C-G, any two of which were assumed normal when the other one was set as SNP site to be typed. The assumption reduced the number of probe to be designed and was confirmed by the genotyping result in the present study. Four pairs of probes were designed to discriminate the normal and the four mutant alleles. However, as an improvement to probe redundancy, all possible probe patterns should be fabricated. In probe design, the probes were chosen to have a common algorithmically calculated Tm value of 50±2 ℃ with length of 16-17 nt. Under the optimized hybridization/washing conditions, the P1/P2 and P7/P8 probe pairs had a less intense signal and discriminating power than the P3/P4 and P5/P6 pairs. The signal intensity ratio value above 4 or below 2.5 is considered a critical limit for genotype judgement. When the value fell into 2.5-4, the sample should be re-genotyped.

The allele frequency of CYP2C9 determined in this study was in accordance with the published data. Yoon YR *et al*[17] showed that there were no CYP2C9*2 (430C-T) allele in Asian population. Dickmann *et al*[18] found CYP2C9*5 (1080C-G) only in Black people. In the present study, heterozygous CYP2C9*1/*3 (1075A-C) were detected in 7 out of 62 unrelated Chinese. There were marked ethnic/geographic differences in the distribution of allelic variants of many DMEs[30]. It is of obvious importance that such ethnic/geographic differences be taken into account in routine pharmacogenetic diagnosis or screening. Considering that it is challenging to optimize oligonucleotide probes to achieve global maximum discrimination of many genetic variants simultaneously, it is of importance to reduce the probe number to ensure the reproducibility and reliability of ASO hybridization based-microarray genotyping performance. For example, microarray for genotyping frequent SNP sites (>1 %) in DME-coding gene specific to Chinese should be made and applied in Chinese population.

There were no homozygous mutants detected in the studied population, and there may be other factors that affect the effectiveness of Irbesartan, such as the polymorphism in drug targets (ATIR), other potential mutation sites in CYP2C9, etc. The results of genotyping in this study suggest that there is no significant difference in the odd of effectiveness of Irbesartan between the wild type group and CYP2C9*1/*3 group. Provided that the heterozygous individuals have prolonged effective time, a better therapeutic outcome may be obtained as long as no additional side-effects occur.

## REFERENCES


1 **Nebert DW**, Mckinnon RA, Puga A. Human drug-metabolizing enzyme polymorphism: effects on risk of toxicity and cancer. *DNA Cell Biol* 1996; **15**: 273-280

2 **Shi MM,** Bleavins MR, De La Iglesia FA. Pharmacogenetic application in drug development and clinical trials. *Drug Metabolism Disposition* 2001; **29**: 591-595

3 **Krynetski EY,** Evans WE. Genetic polymorphism of thiopurine S-methyltransferase: molecular mechanism and clinical importance. *Pharmacology* 2000; **61**: 136-146

4 **Cronin MT,** Pho M, Dutta D, Frueh F, Schwarcz L, Brennan T. Utilization of new technologies in drug trials and discovery. *Drug Metabolism Disposition* 2001; **29**: 586-590

5 **Shi MM**. Enabling large-scale pharmacogenetics studies by high-throughput mutation detection and genotying technologies. *Clini Chem* 2001; **47**: 164-172

6 **Broude NE,** Woodward K, Cavallo R, Cantor CR, Englert D. DNA microarrays with stem-loop DNA probe: preparations and applications. *Nucleic Acids Research* 2001; **29**: E92

7 **Zhu GJ,** Yu YN, Li X, Qian YL. Cloning of cytochrome P-450 2C9 cDNA from human liver and its expression in CHL cells. *World J Gastroenterol* 2002; **8**: 318-322

8 **Cai L,** Yu SZ, Zhan ZF. Cytochrome P450 2E1 genetic polymorphism and gastric cancer in Changle, Fujian Province. *World J Gastroenterol* 2001; **7**: 792-795

9 **Cheng JW.** Cytochrome p450-mediated cardiovascular drug interactions. *Heart Dis* 2000; **2**: 254-258

10 **Aithal GP,** Day CP, Kesteven PJ, Daly AK. Association of polymorphisms in the cytochrome P450 CYP2C9 with warfarin dose requirement and risk of bleeding complications. *Lancet* 1999; **353:** 717-719

11 **Kidd RS,** Curry TB, Gallagher S, Edeki T, Blaisdell J, Goldstein JA. Identification of a null allele of CYP2C9 in an African-American exhibiting toxicity to phenytoin. *Pharmacogenetics* 2001; **11**: 803-808

12 **Goldstein JA.** Clinical relevance of genetic polymorphisms in the human CYP2C subfamily. *Br J Clin Pharmacol.* 2001; **52**: 349-355

13 **Timmermans PB.** Pharmacological properties of angiotension II receptor antagonists. *Can J Cardo* 1999; **15**(Suppl. F): 26F-28F

14 **Graham MR,** Allcock NM. Irbesartan substitution for valsartan or losartan in treating hypertension. *Ann Pharmacother* 2002; **36**: 1840-1844

15 **Yasar U,** Tybring G, Hidestrand M, Oscarson M, Ingelman-Sundberg M, Dahl ML, Eliasson E. Role of CYP2C9 polymorphism in losartan oxidation. *Drug Metab Dispos* 2001; **29**: 1051-1056

16 **Li T,** Liang H, Yan F, Lu S. Site-directed mutagenesis of atrial natriuretic peptide gene and effect of the mutations on its diuretic activity in nephrotic rats. *Zhonghua Yixue Zazhi* 2002; **82**: 1324-1327

17 **Yoon YR,** Shon JH, Kim MK, Lim YC, Lee HR, Park JY. Cha IJ, Shin JG. Frequency of cytochrome P450 2C9 mutant alleles in a Korean population. *Br J Clin Pharmacol* 2001; **51**: 277-280

18 **Dickmann LJ,** Rettie AE, Kneller MB, Kim RB, Wood AJ, Stein CM. Identification and functional characterization of a new CYP2C9 variant (CYP2C9*5) expressed among African American. *Mol Pharmacol* 2001; **60**: 382-387

19 **Gu HF.** Single nucleotide polymorphisms (SNPs) and SNP databases. *Zhonghua Yixue Yichuanxue Zazhi* 2001; **18**: 479-481

20 **Kwok PY.** Methods for genotyping single nucleotide polymorphisms. *Annu Rev Genomics Hum Genet* 2001; **2**: 235-258

21 **Roses AD.** Pharmacogenetics. *Hum Mol Genet* 2001; **10**: 2261-2267

22 **Hsieh KP,** Lin YY, Cheng CL, Lai ML, Lin MS, Siest JP, Huang JD. Novel mutations of CYP3A4 in Chinese. *Drug Metab Dispos* 2001; **29**: 268-273

23 **Oda Y,** Kobayashi M, Ooi A, Muroishi Y, Nakanishi I. Genotypes of glutathione S-transferase M1 and N-acetyltransferase 2 in Japanese patients with gastric cancer. *Gastric Cancer* 1999; **2**: 158-164

24 **Hersberger M,** Marti-Jaun J, Rentsch K, Hanseler E. Rapid detection of the CYP2D6*3, CYP2D6*4, and CYP2D6*6 alleles by tetra-primer PCR and of the CYP2D6*5 allele by multiplex long PCR. *Clin Chem* 2000; **46**: 1072-1077

25 **Li JJ,** Geyer R, Tan W. Using molecular beacons as a sensitive fluorescence assay for enzymatic cleavage of single-stranded DNA. *Nucleic Acids Res* 2000; **28**: E52

26 **Kleiber J,** Walter T, Haberhausen G, Tsang S, Babiel R, Rosenstraus M. Performance characteristics of a quantitative, homogeneous TaqMan RT-PCR test for HCV RNA. *J Mol Diagn* 2000; **2**: 158-166

27 **O'Meara D**, Ahmadian A, Odeberg J, Lundeberg J. SNP typing by apyrase-mediated allele-specific primer extension on DNA microarrays. *Nucleic Acids Res* 2002; **30**: e75

28 **Iwasaki H**, Ezura Y, Ishida R, Kajita M, Kodaira M, Knight J, Daniel S, Shi M, Emi M. Accuracy of genotyping for single nucleotide polymorphisms by a microarray-based single nucleotide polymorphism typing method involving hybridization of short allele-specific oligonucleotides. *DNA Res* 2002; **9**: 59-62

29 **Huber M,** Mundlein A, Dornstauder E, Schneeberger C, Tempfer CB, Mueller MW, Schmidt WM. Accessing single nucleotide polymorphisms in genomic DNA by direct multiplex polymerase chain reaction amplification on oligonucleotide microarrays. *Anal Biochem* 2002; **303**: 25-33

30 **Bertilsson L,** Geogrophical / interracial difference in polymorphic drug oxidation. *Clin. Pharmacokinet* 1995; **29**: 192-209

**Edited by** Pang LH

P.O.Box 2345, Beijing 100023,China
Fax: +86-10-85381893
E-mail: wjg@wjgnet.com www.wjgnet.com

World J Gastroenterol 2003;9(6):1347-1351
World Journal of Gastroenterology
Copyright ©2003 by The WJG Press ISSN 1007-9327

• BASIC RESEARCH •

# Identification of RanBMP interacting with *Shigella flexneri* IpaC invasin by two-hybrid system of yeast

Xiao Yao, Heng-Liang Wang, Zhao-Xing Shi, Xiao-Yu Yan, Er-Ling Feng, Bo-Lun Yang, Liu-Yu Huang

**Xiao Yao, Bo-Lun Yang,** College of Environmental and Chemical Engineering, Xi' an Jiaotong University, Xi' an 710049, Shaanxi Province, China
**Heng-Liang Wang, Zhao-Xing Shi, Xiao-Yu Yan, Er-Ling Feng, Liu-Yu Huang,** Beijing Institute of Biotechnoloy, Beijing 100071, China
**Supported by** Capital "248" Key Innovation Project (H010210360119) and State key Research and Development Project (G1999054103)
**Correspondence to:** Liu-Yu Huang, Beijing Institute of Biotechnology, 20 Dongdajie, Fengtai, Beijing 100071, China. huangly@nic.bmi.ac.cn
**Telephone:** +86-10-66948836 **Fax:** +86-10-63833521
**Received:** 2002-12-22 **Accepted:** 2003-01-14

## Abstract

**AIM:** Bacillary dysentery caused by *Shigella flexneri* is still a threat to human health. Of four invasion plasmid antigen proteins (IpaA,B,C and D), IpaC plays an important role in the pathogenicity of this pathogen. The purpose of this study was to investigate the proteins interacting with IpaC in the host cell during the pathogenic process of this disease.

**METHODS:** By applying two-hybrid system, the bait plasmid containing *ipaC* gene was constructed and designated pGBKT-ipaC. The bait plasmid was transformed AH109, and proved to express IpaC and then HeLa cDNA library plasmids were introduced into the above transformed AH109. The transformation mixture was plated on medium lacking Trp, Leu, and His in the initial screen, then restreaked on medium lacking Trp, Leu, His and Ade. Colonies growing on the selection medium were further assayed for β-galactosidase activity. BLAST was carried out in the database after sequencing the inserted cDNA of the positive library plasmid.

**RESULTS:** Among the $2\times10^6$ transformants, 64 positive clones were obtained as determined by activation of His, Ade and LacZ reporter genes. Sequence analysis revealed that cDNA inserts of two colonies were highly homologous to a known human protein, RanBPM.

**CONCLUSION:** These results provide evidence that IpaC may be involved in the invasion process of *S. flexneri* by interacting with RanBPM, and RanBPM is most likely to be the downstream target of IpaC in the cascade events of *S. flexneri* infection.

Yao X, Wang HL, Shi ZX, Yan XY, Feng EL, Yang BL, Huang LY. Identification of RanBMP interacting with *Shigella flexneri* IpaC invasin by two-hybrid system of yeast. *World J Gastroenterol* 2003; 9(6): 1347-1351
http://www.wjgnet.com/1007-9327/9/1347.asp

## INTRODUCTION

*Shigella* is a Gram-negative bacterium responsible for intestinal diseases ranging from mild watery diarrhea to bacillary dysentery in humans. The severe forms of shigellosis are due to colonization and destruction of the colonic mucosa by this invasive pathogen. The infectious potential of *Shigella* is very high, since as few as 100 microorganisms administered orally are sufficient to cause dysentery in volunteers. Each year, at least a billion cases of diarrheal diseases account for about three million deaths. In the developing world, children under 5 years of age are the most susceptible victims, with over half a million deaths occurred annually worldwide[1].

The phenotype which is essential to the pathogenicity of *S. flexneri* is encoded by a 31kb sequence[2,3] located on the 200kb large virulence plasmid[4,5]. One locus in this fragment, composed of the ipa operon (invasion plasmid antigen), is necessary to encode and secrete the effectors, the Ipa proteins or invasins. The ipa operon encodes four secreted proteins: IpaB(62kDa), IpaC(42kDa), IpaD(37kDa) and IpaA(70kDa), which elicit the formation of the entry focus via localized actin polymerization[6]. The Ipa proteins are rapidly secreted from *S. flexneri* when the bacterium comes into contact with epithelial cells[7-10]. Following their secretion, IpaB and IpaC are found as part of a protein complex and this complex is absolutely required for entry into epithelial cells[7,11,12]. Latex beads coated with anti-IpaC antibodies have been used to recover the extracellular Ipa complex containing IpaB and IpaC, and were shown to be internalized in HeLa cells through the formation of membrane ruffles similar to those induced upon bacterial entry[13]. These results have led to the proposal that IpaB and IpaC play major roles in the entry of *shigella* into epithelial cells.

Although IpaB is undoubtedly important for *S. flexneri* invasion[14-17], a great deal of foci were shifted to IpaC as a potential effector of *S. flexneri* invasion when purified IpaB was shown not to possess *in vitro* membranolytic activity[11], and purified IpaC was demonstrated to have such activities consistent with its contribution to invasion[18]. Effector-related functions that have been demonstrated for purified IpaC include: enhanced invasion of cultured cells by *S. flexneri* at nanomlar IpaC concentrations[16,19]; induced uptake of virulence plasmid-cured at micromolar IpaC concentrations[24]; association with model phospholipid membranes[16,21]; and triggering of cytoskeletal changes in cultured cells[22,27]. Additional activities associated with IpaC also include *in vitro* reconstitution into complexes with IpaB, which may promote the uptake of non-invasive strains of *Escherichia coli*[12, 19].

Shigellosis provides a model to study how a pathogenic microorganism can subvert an integrated defense barrier and interact with the host cells, which in turn facilitates invasion at the early stage of the process. A major challenge is to understand the role of Ipa proteins in entry into epithelial cells. In order to investigate the mechanism of IpaC in the entry process, two-hybrid system was exploited to identify the proteins in host cells that interacted with IpaC invasin.

## MATERIALS AND METHODS

### *Materials*

The strains and plasmids used in this study are listed in Table 1.

**Table 1** Strains and plasmids

| | Relevant characteristics | Source |
|---|---|---|
| Strains | | |
| *S. flexneri* 2a, 2 457T | Wild type, $Nal^r$ | Maurelli AT |
| *E. coli* DH5α | SupE44, ΔlacU169 (Φ80 lacZ ΔM15), hsdR17, recA1, endA1, gyrA96, thi-1, relA1, $Nal^r$ | Our lab |
| *S. cerevisiae* AH109 | MATa, trp1-901, leu2-3, ura3-52, his3-200, gal4Δ, gal80Δ, LYS2::$GAL1_{UAS}$-$GAL1_{TATA}$-HIS3, $GAL2_{UAS}$-$GAL2_{TATA}$-ADE2, URA3::$MEL1_{UAS}$-$MEL1_{TATA}$-LacZ | Clontech |
| Plasmids | | |
| pGBKT7 | GAL4 DNA-BD, TRP1, c-Myc epitope tag, $Km^r$ | Clontech |
| pGBKT-ipaC | GAL4 DNA-BD fusion of IpaC, TRP1, c-Myc epitope tag, $Km^r$ | This study |
| pACT2 | GAL4 DNA-AD, HA epitope, LEU2, $Ap^r$ | Clontech |
| pLAM5'-1 | GAL4 DNA-BD fusion of the human lamin C, TRP1, a false-positive detection plasmid, $Ap^r$ | Clontech |
| p1 | A positive library plasmid | This study |

Human HeLa MATCHMAKER cDNA library (HL4048AH), c-Myc monoclonal antibody, YPD medium, minimal SD base and DO supplement medium were purchased from Clontech. Peroxidase-conjugated goat anti-mouse IgG was from Santa Cruz. Mini- and Megapreps plasmid kits were obtained from Promega. Restriction endonucleases and T4 DNA ligase were purchased from New England Biolabs. Taq DNA polymerase, deoxyribonucleotides, and PCR fragment recovery kit were from TaKaRa. Primers for the 5' and 3' ends of *ipaC* gene, P1 and P2, were synthesized in our lab.

### Methods

Growth and maintenance of strains *Shigella flexneri* 2a was grown at 37 ℃ with constant stirring in trypticase soy broth (TSB). Prior to use, the bacteria were streaked onto trypticase soy agar (TSA) containing 0.025 % Congo red so that colonies binding the dye could be selected. Bacteria that had lost the invasion plasmid were not able to bind this dye and thus appeared white in the presence of Congo red. Yeast strain AH109 was grown at 30 ℃ with vigorous shaking in YPAD. Antibiotics were used at the following concentrations: ampicillin (Ap), 100 mg· $L^{-1}$; kanamycin (Km), 50 mg· $L^{-1}$; nalidixic acid (Nal), 40 mg· $L^{-1}$.

**Construction of bait plasmid** Isolation of plasmid and all other molecular biology procedures were carried out according to the standard published procedures[22]. *ipaC* gene was amplified by PCR in a standard 100-μl reaction containing 2.5 mM $MgCl_2$, 0.25 mM of each dNTP, 100 pmol of P1 and P2 primers, 10 μl boiled *S. flexneri*, and 5U Taq DNA polymerase. Reactions were allowed to proceed in a Perkin-Elmer 2400 thermal cycler programmed for 30 cycles (94 ℃, 30 s; 56 ℃,30 s; and 72 ℃, 90 s) with one additional cycle for 7 min at 72 ℃. PCR product was purified by agarose gel electrophoresis, digested by NcoI and SalI, then ligated into the pGBKT7 plasmid digested by NcoI and SalI. The ligation products were then transformed into *E.coli* DH5α. The insert of *ipaC* gene was then confirmed by PCR using the conditions described above. To confirm if the ipaC gene was fused in frame to the coding sequence of the GAL4 DNA-binding domain, the plasmids were subjected to double-stranded DNA sequencing with T7 sequencing primer according to the manufacturer's specifications.

**Yeast transformation** The lithium acetate (LiAc)-mediated method was performed to transform DNA into yeast as described in the reference[23]. In brief, the yeast competent cells were prepared and suspended in a LiAc solution with the plasmids DNA to be transformed, along with excess carrier DNA. Polyethylene glycol (PEG) with an appropriate amount of LiAc was then added and the mixture of DNA and yeast was incubated at 30 ℃. After incubation, DMSO was added and the cells were heat shocked at 42 ℃. The cells were then plated on the appropriate medium to select transformants. The amount of plasmids used for transformation was 0.1 μg except that 50 μg library plasmid was used.

**SDS-PAGE and western blot analysis** Extraction of yeast protein sample was carried out by using urea/SDS method as described in reference[24]. SDS-PAGE was performed using the standard procedure of Laemmli[22]. The samples were resolved on a 12 % polyacrylamide gel. The samples could be stained with Coomassie brilliant blue R250, or the proteins electroblotted to NC membranes for western blot analysis using a Bio-Rad Transbolt Semi-dry Blotter according to the manufacturer's instructions. Western blot analysis was performed as previously described[22,25]. Briefly, the membranes were blocked following protein transfer by incubation in TBS (50 mM Tris-HCl pH7.4, 5 % BSA, 500 mM NaCl) and then incubated with c-Myc monoclonal antibody diluted in TBS containing 0.1 % Tween 20 (v/v). After several rinses in the same buffer, the membrane was incubated with HRP-conjugated secondary antibody in the same buffer. The membrane was then rinsed in TBS containing 10 mM EDTA, 0.5 M NaCl , and 0.1 % Tween 20 (w/v). Blots were developed using TBS (50 mM Tris-HCl pH7.4, 5 % BSA, 500 mM NaCl) containing 0.7 mg/ml 3,3'-diaminobenzidine (DAB) and 0.003 % $H_2O_2$, finally terminated with 2M $H_2SO_4$.

**Two-hybrid strategy** Before the screening process, intrinsic activation function of the bait was tested as demonstrated by a bait-testing assay. To perform the two-hybrid screening, the bait plasmid pGBKT-ipaC was transformed into the yeast strain AH109. The HeLa cDNA libraries were extracted from *E.coli* and introduced into the AH109 transformed with the bait. Cells were first spread on plates lacking Leu, Trp and His, and containing 1mM 3-aminotriazole to select colonies by prototrophy for histidine. The $His^+$ colonies were streaked on selective plates lacking Leu, Trp, His and Ade. The $His^+$, $Ade^+$ colonies were assayed for expression of β-galactosidase by an X-Gal overlay assay, and blue colonies were streaked twice on selective plates. After that, individual $His^+$, $Ade^+$, $LacZ^+$ colonies were cultured in liquid SD synthetic medium. Yeast DNA was recovered and transformed into *E. coli* DH5α by electroporation. The insert carried by the prey plasmid in each of the selected clones was amplified by PCR and grouped. Representative plasmids from each group were retransformed back into yeast to test their interaction with IpaC. The cDNA inserts were subjected to sequencing.

## RESULTS

### Construction of bait plasmid

PCR primers for the 5' and 3' ends of *ipaC* gene were designed as follows based on its published sequences[26]: P1, 5'-

CGGCCATGGTAATAGAACTGATGTTGC-3' containing an *Nco*I restriction site and 18 bases of the 5' end of *ipaC* gene; and P2, 5' -GCGTCGACTTAAGCTCGAATGTTAC-3' containing a SalI restriction site and 18 bases of the 3' end of *ipaC* gene. After amplification of ipaC gene by PCR, there was a band of about 1.1kb by agarose gel electrophoresis (data not shown). The fragment was purified, digested by NcoI and SalI, and cloned into the NcoI and SalI sites of pGBKT7. The resulting plasmid was designated as pGBKT-ipaC (Figure 1). Sequencing revealed that the ipaC gene was fused in the correct reading frame with the coding sequence of GAL4 DNA-binding domain (data not shown).

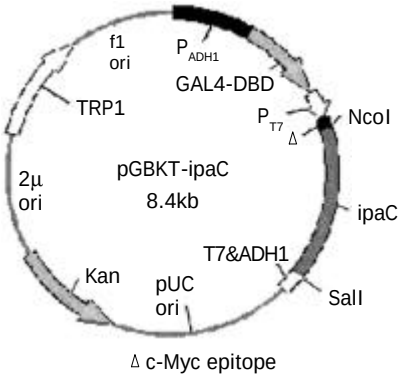


**Figure 1** Construction of recombinant plasmid expressing IpaC.

### *Expression of IpaC in yeast*

SDS-PAGE and western blotting were carried out with the protein extracted from yeast AH109, AH109 transformed with pGBKT7 and pGBKT-ipaC (Figure 2). An approximate 20kDa GAL4 DNA binding domain containing c-Myc epitope tag was expressed in AH109 transformed with pGBKT7, while a 62kDa peptide was expressed in AH109 transformed with pGBKT-ipaC. This showed that IpaC could be expressed in frame with the GAL4 DNA binding domain and the bait plasmid could be used in two-hybrid screening.

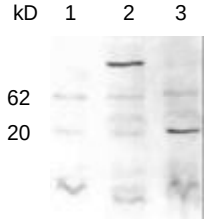


**Figure 2** Western blot analysis of the fused expression of IpaC with c-Myc monoclonal antibody as a primary antibody. Lane 1, AH109; lane 2, AH109 transformed with pGBKT-ipaC; lane 3, AH109 transformed with pGBKT7.

### *Two-hybrid screening*

In order to identify whether the fused bait protein could activate the expression of reporter genes, yeast containing the bait plasmid (pGBKT-ipaC) and yeast containing the empty vector of library (pACT2) were tested as demonstrated by a bait-testing assay (Table 2). The results indicated that IpaC was devoid of transcriptional activity and could be used as bait in a yeast two-hybrid assay.

The bait plasmid and cDNA library were sequentially transformed into yeast strain AH109. Initial screening of $2\times10^6$ colonies of a human HeLa MATCHMAKER cDNA library identified 92 clones that showed specific activation of His reporter gene. Further testing of the specificity of interaction screening on selective media lack of Trp, Leu, His, Ade and by β-galactosidase assay showed that only 64 colonies interacted specifically with the bait BD-IpaC protein, but not with fusion proteins between BD and human lamin C (Table 3).

**Table 2** Detection of transcriptional activity of bait fusion protein in AH109

| Tranformed plasmids | Growth on SD His$^-$ | X-Gal |
|---|---|---|
| pGBKT-ipaC | - | white |
| pGBKT-ipaC + pACT2 | - | white |

**Table 3** Verification of the interaction in positive clones

| | Tranformed plasmids | β-Gal activity |
|---|---|---|
| 1 | p1 | white |
| 2 | p1 + pGBKT7 | white |
| 3 | p1 + pLAM5'-1 | white |
| 4 | p1 + pGBKT-ipaC | blue |

Sequence analysis of the clones revealed that two independent colonies (p1 and p25) contained the same gene. A database search using the BLAST program showed that this gene encoded the protein which had as much as 99 % homology with RanBPM (GenBank accession number AB055311). The two library colonies isolated from the yeast-two hybrid assay contained amino acid sequences that were upstream of the BPM55 start codon, but were within the coding region of BPM90. The resulting product of p1 contained 584 C-terminal amino acids of RanBPM, which fused in the frame with the GAL4 activation domain.

## DISCUSSION

An important step in *S. flexneri* infection is bacterial invasion of colonic epithelial cells, as characterized by host cytoskeletal rearrangements at the site of bacterial contact[27]. These localized changes in the host cytoskeleton lead to the formation of filopodia that combine and trap the pathogen within a membrane-bound vacuole that is rapidly lysed, thereby providing the bacterium with access to the host cell cytoplasm[6]. Evidence indicates that IpaC is necessary and sufficient to promote the formation of filopodial extensions localized at the edge of fibroblastic cells[21]. These extensions appear within seconds after exposure of permeabilized cells to IpaC. The data presented above and those from other laboratories indicate that IpaC proteins play an important role in this process.

Current understanding of the role of *S. flexneri* Ipa proteins in epithelial cell invasion is primarily based on deletion mutagenesis, genetic complementation, and immunological analyses[12-14,28,29]. To better understand the roles of the Ipa proteins in the pathogenesis of shigellosis, it is necessary to isolate proteins that interact with Ipa proteins in host cells. The two-hybrid system is an effective genetic method to identify protein-protein interaction and has been increasingly used[30,31]. Therefore, we exploited a two-hybrid screen to identify the IpaC-interacting protein in host cells. The foci of infection of this pathogen are human colonic epithelial cells, so a library prepared from them should be used in our screening. Unfortunately, it is not commercially available. The mechanism of entry of *Shigella* into cells has been studied extensively in cultured cell lines. Of these cell lines, Hela was derived from human epithelial cells and has been frequently used in the invasion of *S. flexneri*[32-35]. Therefore a HeLa cDNA library was used instead in our screening. Two library colonies that were isolated in the yeast-two hybrid assay contained amino

acid sequences with high homology to RanBPM.

RanBPM was originally identified by its interaction with Ran, a small Ras-like GTPase. Ran shuttles between the nucleus and the cytoplasm to complete its GTPase cycle, carrying out nucleocytoplasmic transport of macromolecules and inducing microtubule self-assembly by interacting with distinct Ran binding protein[36,37]. RanBPM was initially identified as a 55kD protein (BPM55) which contains 500 amino acids[37]. A subsequent report has shown that BPM55 is a truncated protein and the full-sized RanBPM is a 90kD protein (BPM90) which contains 729 amino acids[38]. Here we demonstrated that the function domain within BPM90 was able to interact with IpaC *in vivo*. RanBPM was predominantly localized both in the nucleus and in the cytoplasmic region surrounding the centrosome[38]. When truncated RanBPM was overexpressed in green monkey kidney COS7 cells, the multiple spots which were colocalized with γ-tubulin were formed and acted as ectopic microtubule nucleation sites, resulting in a reorganization of microtubule network[37]. The function of BPM90 is still unclear, but it has recently been linked to the Ras/Erk signaling pathway[39].

Actin filaments and microtubule (MT) arrays have been regarded as constituting separate cytoskeletal systems with distinct functions. However, it has become clear that the cell' s system of cytoskeletal filaments and its network of signaling pathways are intimately linked and function cooperatively to generate a cell phenotype tailored to the immediate conditions of the cell[40]. When a signal occurs, the structural responses driven by the cytoskeleton are usually complex, such as establishing new axes of polarity, making and breaking contacts, moving or dividing, especially generating protrusions as observed in the entry process of *S. flexneri*.

Taken the data presented above together, we therefore become greatly interested in possible involvement of IpaC in the signaling cascade resulting in massive cytokeletal rearrangements (Figure 3).

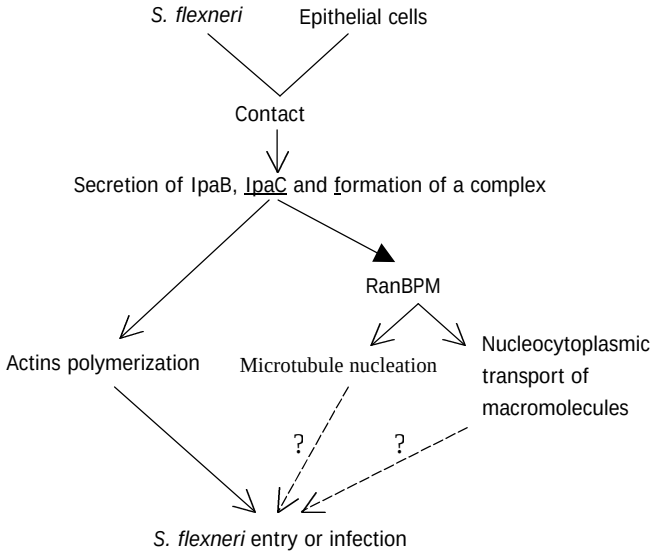


**Figure 3** A schematic diagram of possible IpaC signaling cascade in *S. flexneri* entry.

The early step of infection is the invasion of epithelial cells of the colon. As bacteria contact the cell surface, Ipa invasins are secreted through the specialized secretory apparatus, two of which (IpaB and IpaC) form a complex. IpaC has hydrophobic regions that form transmembrane helices and insert into cell membrane[41]. This complex constitutes the primary effector of *Shigella* entry and is able to activate entry via its interaction with the host cell membrane. Then IpaC stimulates localized accumulation of filamentous actin at the site of bacterial contact. Meanwhile IpaC also leads to microtubule nucleation and/or nucleocytoplasmic transport of macromolecules possibly by interacting with RanBPM. So it is likely that IpaC elicits major rearrangements of host cell cytoskeleton, and these cytoskeletal filaments function cooperatively and form bundles supporting the membrane projections which achieve bacterial entry. Both the pathogen and the host cell actively contribute to this process.

This is the first report that IpaC interacts with RanBPM identified by two-hybrid screening. This information provides an important step in studying the protein-protein interaction that occurs in the host cells during initiation of *Shigella* pathogenesis. Although our understanding of the mechanisms that govern *Shigella* entry and actin-based intracellular motility has improved at a considerable pace, many questions remain open. In particular, it will be interesting to establish various connections between signaling pathways involved in *Shigella* entry and responses linked to the ipa proteins. Understanding how these responses integrate together and act in a concerted manner to induce bacterial entry will represent another exciting field of investigations.

## ACKNOWLEDGMENTS

We would like to thank Prof. Qi-Nong Ye for his technical assistance and helpful discussions. We also thank Prof. Jian-Guang Zhou, Dr. Hao Zhang for their support in this project. We acknowledge the technical assistance of De-Hui He, Kun Hu and Zhi-Yong Gao.

## REFERENCES

1 **Lindberg AA**, Pal T. Stratregies for development of potential candidate *Shigella* vaccine. *Vaccine* 1993; **11**: 168-179
2 **Maurelli AT**, Baudry B, d'Hauteville H, Hale TL, Sansonetti PJ. Cloning of plasmid DNA sequences involved in invasion of HeLa cells by *Shigella flexneri Infect Immun* 1985; **49**: 164-171
3 **Sasakawa C**, Kamata K, Sakai T, Makino S, Yamada M, Okada N, Yoshikawa M. Virulence-associated genetic regions comprising 31 kilobases of the 230-kilobase plasmid in *Shigella flexneri* 2a. *J Bacteriol* 1988; **170**: 2480-2484
4 **Sansonetti PJ**, Kopecko DJ, Formal SB. Involvement of a large plasmid in the invasive ability of *Shigella flexneri*. *Infect Immun* 1987; **55**: 2681-2688
5 **Sansonetti PJ**, Hale TL, Dammin GJ, Kapfer C, Collins HHJr, Formal SB. Alterations in the pathogenicity of *Escherichia coli* K-12 after transfer of plasmid and chromosomal genes from *Shigella flexneri*. *Infect Immun* 1983; **39**: 1392-1402
6 **Clerc P**, Sansonetti PJ. Entry of *Shigella flexneri* into HeLa cells: evidence for directed phagocytosis involving actin polymerization and myosin accumulation. *Infect Immun* 1987; **55**: 2681-2688
7 **Parsot C**, Menard R, Gounon P, Sansonetti PJ. Enhanced secretion through the *Shigella flexneri* Mxi-Spa translocon leads to assembly of extracellular proteins into macromolecular structures. *Mol Microbiol* 1995; **16**: 291-300
8 **Watarai M**, Tobe T, Yoshikawa M, Sasakawa C. Contact of *Shigella* with host cells triggers release of Ipa invasins and is an essential function of invasiveness. *EMBO J* 1995; **14**: 2461-2470
9 **Menard R**, Sansonetti P, Parsot C. The secretion of the *Shigella flexneri* Ipa invasins is activated by epithelial cells and controlled by IpaB and IpaD. *EMBO J* 1994; **13**: 5293-5302
10 **Watarai M**, Tobe T, Yoshikawa M, Sasakawa C. Disulfide oxidoreductase activity of *Shigella flexneri* is required for release of Ipa proteins and invasion of epithelial cells. *Proc Natl Acad Sci USA* 1995; **92**: 4927-4931
11 **Menard R**, Sansonetti P, Parsot C, Vasselon T. Extracellular association and cytoplasmic partitioning of the IpaB and IpaC invasins of *S. flexneri*. *Cell* 1994; **79**: 515-525
12 **Menard R**, Prevost MC, Gounon P, Sansonetti P, Dehio C. The secreted Ipa complex of shigella flexneri promotes entry into mammalian cells. *Proc Natl Acad Sci USA* 1996; **93**: 1254-1258
13 **Menard R**, Sansonetti PJ, Parsot C. Nonpolar mutagenesis of the ipa genes defines IpaB, IpaC and IpaD as effectors of *Shigella*

*flexneri* entry into epithelial cells. *J Bacteriol* 1993; **175**: 5899-5906
14 **High N**, Mounier J, Prevost MC, Sansonetti PJ. IpaB of *Shigella flexneri* causes entry into epithelial cells and escape from the phagocytic vacuole. *EMBO J* 1992; **11**: 1991-1999
15 **Skoudy A,** Mounier J, Aruffo A, Ohayon H, Gounon P, Sansonetti P, Tran Van Nhieu G. CD44 binds to the *Shigella* IpaB protein and participates in bacterial invasion of epithelial cells. *Cell Microbiol* 2000; **2**: 19-33
16 **Tran N,** Serfis AB, Davis R, Osiecki JC, Coye L, Picking WL, Picking WD. Interaction of *Shigella flexneri* IpaC with model membranes correlate with effects on cultured cells. *Infect immun* 2000; **68**: 3710-3715
17 **Tran Van Nhieu G,** Bourdet-Sicard R, Dumenil G, Blocker A, Sansonetti PJ. Bacterial signals and cell responses during *Shigella* entry into epithelial cells. *Cell Microbiol* 2000; **2**: 187-193
18 **Marquart ME,** Picking WL, Picking WD. Soluble invasion plasmid antigen C (IpaC) from *Shigella flexneri* elicits epithelial cell responses related to pathogen invasion. *Infect Immun* 1996; **64**: 4182-4187
19 **Davis R,** Marquart ME, Lucius D, Picking WD. Protein-protein interactions in the assembly of *Shigella flexneri* invasion plasmid antigens IpaB and IpaC into protein complexes. *Biochim Biophys Acta* 1998; **1429**: 45-56
20 **De Geyter C,** Vogt B, Benjelloun-Touimi Z, Sansonetti PJ, Ruysschaert JM, Parsot C, Cabiaux V. Purification of IpaC, a protein involved in entry of *Shigella flexneri* into epithelial cells and characterization of its interaction with lipid membranes. *FEBS Lett* 1997; **400**: 149-154
21 **Tran Van Nhieu G,** Caron E, Hall A, Sansonetti PJ. IpaC induces actin polymerization and filopdia formation during *Shigella* entry into epithelial cell. *EMBO J* 1999; **18**: 3249-3262
22 **Sambrook J**, Fritsch EF, Maniatis T. Molecular cloning: a laboratory manual. 2nd ed. New York:Cold Spring Harbour Press 1989
23 **Gietz D**, St Jean A, Woods RA, Schiestl RH. Improved method for high efficiency transformation of intact yeast cells. *Nucleic Acids Res* 1992; **20**: 1425
24 **Printen JA**, Sprague GF. Jr. Protein-protein interactions in the yeast pheromone response pathway: Ste5p interacts with all members of the MAP kinase cascade. *Genetics* 1994; **138**: 609-619
25 **Burnette WN**. "West blotting": electrophoretic transfer of proteins from SDS-PAGE to unmodified nitrocellulose and radiographic detection with antibody and radioiodinated protein A. *Anal Biochem* 1981; **112**: 195-203
26 **Venkatesan MM**, Buysse JM, Kopecko DJ. Characterization of invasion plasmid antigen genes (ipaBCD) from *Shigella flexneri*. *Proc Natl Acad Sci USA* 1988; **85**: 9317-9321
27 **LaBrec EH**, Schneider H, Magnani TJ, Formal SB. Epithelial cell penetration as an essential step in the pathogenesis of bacillary dysentery. *J Bacteriol* 1988; **88**: 1503-1518
28 **Sasakakawa C,** Komatsu K, Tobe T, Suzuki T, Yoshikawa M. Eight genes in region 5 that form an operon are essential for invasion of epithelial cells by *Shigella flexneri* 2a. *J Bacteriol* 1993; **175**: 2334-2346
29 **Mills JA,** Buysse JM, Oaks EV. Shigella flexneri invasion plasmid antigens B and C: Epitope location and characterization with monoclonal antibodies. *Infect Immune* 1988; **56**: 2933-2941
30 **Fields S**, Sternglanz R. The two-hybrid system: an assay for protein-protein interactions. *Trends Genet* 1994; **10**: 286-292
31 **Li K,** Wang L, Cheng J, Zhang LX, Duan HJ, Lu YY, Yang JZ, Liu Y, Hong Y, Xia XB, Wang G, Dong J, Li L, Zhong YW, Chen JM. Screening and cloning of gene of hepatocyte protein 1 interacting with HCV core protein. *Shijie huaren xiaohua zazhi* 2001; **9**: 1379-1383
32 **Skoudy A**, Nhieu GT, Mantis N, Arpin M, Mounier J, Gounon P, Sansonetti P. A functional role for ezrin during *Shigella flexneri* entry into epithelial cells. *J Cell Sci* 1999; **112** (Pt 13): 2059-2068
33 **Tran Van Nhieu G**, Ben-Ze'ev A, Sansonetti PJ. Modulation of bacterial entry into epithelial cells by association between vinculin and the *Shigella* IpaA invasin. *EMBO J* 1997; **16**: 2717-2729
34 **Pal T**, Hale TL. Plasmid-associated adherence of *Shigella flexneri* in a HeLa cell model. *Infect Immun* 1989; **57**: 2580-2582
35 **Zhong QP**. Pathogenic effects of O-polysaccharide from *Shigella flexneri* strain. *World J Gastroenterol* 1999; **5**: 245-248
36 **Bischoff FR**, Ponstingl H. Mitotic regulator protein RCC1 is complexed with a nuclear ras-related polypeptide. *Proc Natl Acad Sci USA* 1991; **88**: 10830-10834
37 **Nakamura M**, Masuda H, Horii J, Kuma K, Yokoyama N, Ohba T, Nishitani H, Miyata T, Tanaka M, Nishimoto T. When overexpressed, a novel centrosomal protein, RanBPM, causes ectopic microtubule nucleation similar to gamma-tubulin. *J Cell Biol* 1998; **143**: 1041-1052
38 **Nishitani H**, Hirose E, Uchimura Y, Nakamura M, Umeda M, Nishii K, Mori N, Nishimoto T. Full-sized RanBPM cDNA encodes a protein possessing a long stretch of proline and glutamine within the N-terminal region, comprising a large protein complex. *Gene* 2001; **272**: 25-33
39 **Wang D**, Li Z, Messing EM, Wu G. Activation of Ras/Erk pathway by a novel MET-interaction protein RanBPM. *J Biol Chem* 2002; **277**: 36216-36222
40 **Hollenbeck P**. Cytoskeleton: microtubles get the signal. *Curr Biol* 2001; **11**: R820-823
41 **Blocker A,** Gounon P, Larquet E, Niebuhr K, Cabiaux V, Parsot C, Sansonetti P. The tripartite type III secretion of *Shigella flexneri* inserts IpaB and IpaC into host membranes. *J Cell Biol* 1999; **147**:683-693

**Edited by** Wu XN

P.O.Box 2345, Beijing 100023,China
Fax: +86-10-85381893
E-mail: wjg@wjgnet.com www.wjgnet.com

World J Gastroenterol 2003;9(6):1352-1355
World Journal of Gastroenterology
Copyright ©2003 by The WJG Press ISSN 1007-9327

• CLINICAL RESEARCH •

# Construction and expression of a humanized $M_2$ autoantigen trimer and its application in the diagnosis of primary biliary cirrhosis

Xiao-Hua Jiang, Ren-Qian Zhong, Sheng-Qian Yu, Yin Hu, Weng-Weng Li, Xian-Tao Kong

**Xiao-Hua Jiang,** Department of Laboratory Medicine, 85 Hospital the Chinese PLA, Shanghai 200052, China
**Ren-Qian Zhong, Weng-Weng Li, Xian-Tao Kong,** Clinical Immunology Center of the Chinese PLA, Changzheng Hospital, Second Military Medical University, Shanghai 200003, China
**Sheng-Qian Yu,** Department of Nephrology, Changzheng Hospital, Second Military Medical University, Shanghai 200003, China
**Yin Hu,** Department of Basic Science, Shanghai University of Engineering Science, Shanghai 200335, China
**Correspondence to:** Dr Xiao-Hua Jiang, Department of Laboratory Medicine, 85 Hospital of the Chinese PLA, Huashan Road, Shanghai 200052, China. jhlulu@citiz.net
**Telephone:** +86-21-62528805 **Fax:** +86-21-33110236
**Received:** 2002-07-18 **Accepted:** 2002-08-07

## Abstract

**AIM:** To construct and express a humanized $M_2$ autoantigen trimer designated as BPO and to apply it in the diagnosis of primary biliary cirrhosis (PBC).

**METHODS:** cDNA fragments encoding $M_2$-reactive epitopes of pyruvate dehydrogenase complex $E_2$ (PDC-$E_2$), branched chain 2-oxo-acid dehydrogenase complex $E_2$ (BCOADC-$E_2$) and 2-oxo-glutarate dehydrogenase complex $E_2$ (OGDC-$E_2$) were amplified with PCR using total RNA extracted from human peripheral mononuclear blood cells. The fragments were cloned into the plasmid vector pQE-30 and then transferred into *E. coli* M15 (pREP4) for expression, which was induced by isopropylthio-β-D-galactoside. The expressed recombinant BPO protein was demonstrated by SDS-PAGE, Western-blotting and Immunoabsorption test, its antigenic reactivity and specificity were identified with seven $M_2$-positive sera confirmed at Euroimmun Research Center (Germany). Using the purified BPO, $M_2$ antibodies in sera from patients with PBC and other liver related diseases were detected with ELISA.

**RESULTS:** The expressed BPO was observed with both antigenic reactivity and specificity of $M_2$ autoantigens. The determination of $M_2$ antibodies by BPO with ELISA was more sensitive than using the Euroimmun's kit with the coefficients of variation less than 10 % in both interassay and intraassay. With the newly established method, $M_2$ antibodies were found in 100 % (20/20) of patients with PBC. Six cases of liver disease with unknown etiology and 1 patient with drug induced liver injury had detectable levels of serum $M_2$ antibodies. There were also 2 patients with autoimmune cholangitis and 1 with autoimmune hepatitis showing $M_2$-antibody positive.

**CONCLUSION:** Compared with the routine immunofluorescence assay and commercially available assay kit using porcine heart mitochondrial protein as the antigen, the detection system established in the present study shows higher sensitivity and specificity and may be used as a powerful tool for the diagnosis of PBC.

Jiang XH, Zhong RQ, Yu SQ, Hu Y, Li WW, Kong XT. Construction and expression of a humanized $M_2$ autoantigen trimer and its application in the diagnosis of primary biliary cirrhosis. *World J Gastroenterol* 2003; 9(6): 1352-1355
http://www.wjgnet.com/1007-9327/9/1352.asp

## INTRODUCTION

Primary biliary cirrhosis (PBC) is a chronically progressive cholestatic liver disease with autoimmune basis. According to some reports, the incidence of this disease has been consistently increased in recent years[1-4]. One of the remarkable features of PBC is the appearance of high titre antimitochondrial antibodies (AMA) in the patient's sera. Generally, these antibodies are categorized into nine subgroups termed $M_1$-$M_9$ according to the antigens they recognize, in which only $M_2$ antibodies are considered specific for PBC patients that are detectable years or decades before the clinical and histological diagnosis[5-11].

The major autoantigens recognized by $M_2$ antibodies are the members of 2-oxo-acid dehydrogenase complex including pyruvate dehydrogenase complex $E_2$ (PDC-$E_2$), branched chain 2-oxo-acid dehydrogenase complex $E_2$ (BCOADC-$E_2$) and 2-oxo-glutarate dehydrogenase complex $E_2$ (OGDC-$E_2$), whose immunodominant epitopes have been mapped within lipoyl domains. Antibodies to these corresponding autoantigens have been reported in PBC patients with a positive rate of 95 %, 53-55 % and 39-88 % respectively[6,12]. However, when all of these antibodies are determined simultaneously, the patients with PBC can be diagnosed as high as 92-100 %[13-16]. These facts suggest such a possibility that if there is a constructed antigen containing the specific immunodominant epitopes and the antibodies above can be detected synchronously, the diagnosis of PBC patients would be more specific, sensitive and convenient.

Therefore, we designed and constructed a $M_2$ autoantigen trimer (BPO) expression vector, which could coexpress the immunodominant lipoyl domains of PDC-$E_2$, BCOADC-$E_2$ and OGDC-$E_2$ from human origin, in an attempt to establish a more accurate and sensitive method with BPO to detect $M_2$ antibodies in patients with PBC. Besides, because it has never been reported that $M_2$ antibodies were found in other liver related diseases other than PBC[17-20], a survey to detect $M_2$ antibodies under these circumstances with our constructed $M_2$ autoantigen trimer was also included in the present study.

## MATERIALS AND METHODS

### *Patients*

Eight groups of adult patients with both sexes who were treated in Shanghai Changzheng Hospital were enrolled in the present study. Group 1 consisted of 20 patients with PBC diagnosed on the criteria: the presence of AMA and at least one of the followings: (1) Elevation of serum alkaline phosphatase (ALP) and/or gamma glutamyl transpeptidase (γ-GT). (2) Liver biopsy with PBC characteristics[21]. Group 2 consisted of 5 patients with autoimmune hepatitis (AIH)[22]. Two patients diagnosed

as autoimmune cholangitis (AIC) were included in group 3, and group 4 was composed of 18 patients diagnosed as liver disease with unknown etiology (LDUE) that was defined as lack of obvious causes including drug use, alcohol abuse, exposure to hepatotoxic medication or chemicals and virus infection. Group 5 consisted of 8 patients with drug induced liver injury (DILI). Group 6 enrolled 201 patients with other liver diseases (Post-viral hepatitis and liver cirrhosis, *n*=153; Obstructive jaundice, *n*=25; Acute hepatitis A, *n*=15; Hepatic abscess, *n*=3; Wilson' s disease, *n*=1; Cardiac cirrhosis, *n*=4). Thirty-three patients with various autoimmune diseases (AID) (Rheumatoid arthritis, *n*=12; Systemic lupus erythmatosus, *n*=12; Polymyositis, *n*=4; Vasculitis, *n*=3; Hashimoto' s thyroiditis, *n*=2) were included in group 7 and 1 225 healthy volunteers taking a health checkup aged less than 28 served as the control. In the experiment, fasting serum from each patient was prepared with routine procedures and stored at -20 ℃ until further analysis.

### *Materials*

Reverse transcriptase and PCR amplification system were purchased from Roche Company (U.S.A). Restriction endonucleases and $T_4$ DNA ligase were from New England Biolabs (U.S.A). Plasmid vector pQE-30 and *E.coli* M15 (prep 4) were from Qiagen Company (Germany). Indirect immunofluorescence (IIF) test kit for AMA and Western-blotting kit for $M_2$ antibodies were all from Euroimmun Company (Germany).

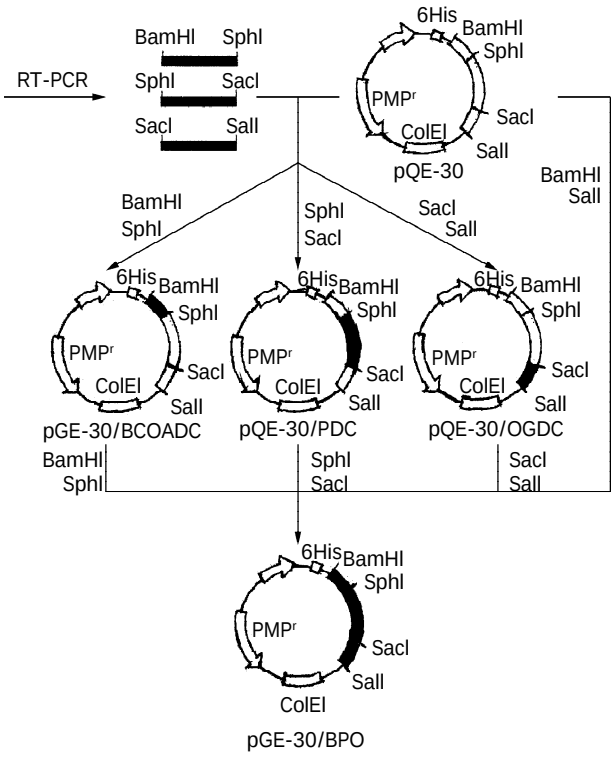


**Figure 1** Construction protocol of recombinant plasmids.

### *Expression and identification of $M_2$ autoantigen trimer*

Recombinant plasmids were constructed as illustrated in Figure 1. Briefly, total RNA was extracted from human peripheral mononuclear blood cells. The objective cDNAs were synthesized by reverse transcriptase and used as the template to amplify the immunodominant epitopes of BCOADC-$E_2$, PDC-$E_2$ and OGDC-$E_2$ with polymerase chain reaction. The PCR products were digested with relevant restriction endonuclease and purified cDNA fragments were inserted into the expression vector pQE-30 to form recombinant plasmids pQE-30/BCOADC-$E_2$, pQE-30/PDC-$E_2$, pQE-30/OGDC-$E_2$ and pQE-30/BPO respectively. The pQE-30/BPO was then transferred into *E. Coli* M15 (pREP4) and induced by isopropylthio-β-D-galactoside to express BPO protein, which was finally confirmed with SDS-PAGE, Western-blotting and Immunoabsorption test.

The antigenic reactivity and specificity of the recombinant BPO trimer were identified with seven $M_2$-positive sera confirmed at Euroimmun Research Center (Germany) by immunoblotting using beef heart mitochondrial preparations.

### *Detection of $M_2$ antibodies with BPO*

The obtained recombinant BPO protein fused with the 6×His affinity tag in the N-terminus was purified by Ni-NTA affinity chromatography under denaturing conditions. After renatured by removing denaturants slowly with dialysis, the BPO protein was used as the specific antigen to detect $M_2$ antibodies with the routine procedures of ELISA. The coefficients of variation for this assay method, the mean OD±SD for the control sera, as well as the critical OD value for the positive determination were respectively calculated or defined based on the experimental results. The measurements of $M_2$ antibodies and AMA with Euroimmun' s kits as a comparison of the present assay method were also simultaneously performed in the study.

## RESULTS

### *Identification of expressed $M_2$ autoantigen trimer*

The segment analysis by restriction endonuclease digestion confirmed that inserted cDNA sequences in the constructed plasmids were completely consistent with that of the published data (Figure 2). The molecular mass of BPO protein was examined by SDS-PAGE in 15 % polycrylamide gel, in which a specific 42 KD protein band was clearly visualized (Figure 3).

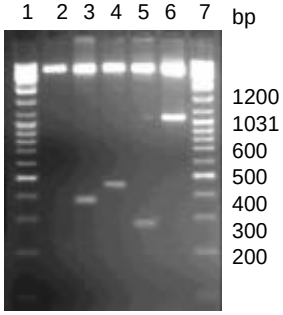


**Figure 2** Segment analysis of recombinant plasmids by restriction endonuclease digestion. 1, 7. Markers; 2. pQE-30 (Bamh1); 3. pQE-30/BCOADC-$E_2$ (Bamh1+Sph1); 4. pQE-30/PDC-$E_2$ (Sph1+Sac1); 5. p30/OGDC-$E_2$ (Sac1+Sal1); 6. pQE-30/BPO (Bamh1+Sal1).

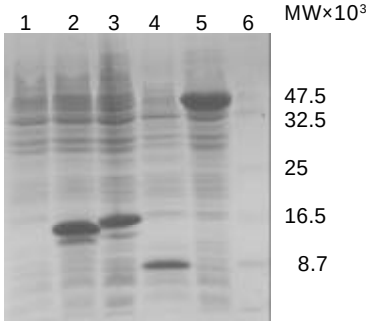


**Figure 3** Expression products of recombinant plasmids detected by SDS-PAGE stained with Coomassie Brilliant Blue R-

250. Lane 1: pQE-30 (control); Lane 2: pQE-30/BCOADC-$E_2$; Lane 3: pQE-30/PDC-$E_2$; Lane 4: pQE-30/OGDC-$E_2$; Lane 5: pQE-30/BPO; Lane 6: protein marker.

The expressed BPO protein could react with all of the seven $M_2$-positive sera confirmed at Euroimmun Research Center (Germany) by immunoblotting using beef heart mitochondrial preparations, which identified the antigenic reactivity of the recombinant BPO trimer (Figure 4). When mixed beforehand with the lysates of *E.coli* expressing BPO overnight, the sera became $M_2$-negative by Western-blotting, which confirmed the BPO specificity determined by the immunodominant epitopes of PDC-$E_2$, BCOADC-$E_2$ and OGDC-$E_2$.

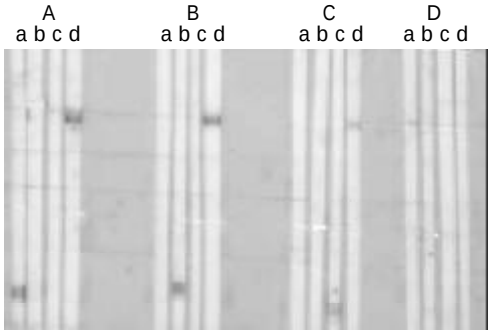


**Figure 4** Immunoreactivity of sera against recombinant proteins. Three $M_2$ antibody positive sera (A, B, C) and a $M_2$ antibody negative serum (D) were probed with SDS-PAGE-separated recombinant proteins of BCOADC-$E_2$ (lane a), PDC-$E_2$ (lane b), OGDC-$E_2$ (lane c), BPO (lane d).

### *Effectiveness of BPO in the detection of $M_2$ antibodies*

The coefficients of variation for the detection of $M_2$ antibodies by BPO with ELISA were less than 10 % in both interassay and intraassay. The mean OD ± SD for the control sera was 0.073±0.046. The critical OD value for positive was defined as ≥ 0.303 based on the mean control value + 5 SD.

### *$M_2$ antibodies in patients with PBC*

In the patients with PBC who were AMA positive determined by IIF test kit, the positive rate of $M_2$ antibodies detected by BPO with ELISA and Euroimmun's kit was 100 % (20/20) and 80 % (16/20) respectively (Table 1).

**Table 1** AMA and $M_2$ antibodies in patients with different diseases

| Group | *n* | AMA positive | $M_2$- positive | | AASLD's guideline (+) |
|---|---|---|---|---|---|
| | | | Euroimmun's kit | ELISA | |
| PBC | 20 | 20 | 16 | 20 | 20 |
| AIH | 5 | 0 | 0 | 1 | 0 |
| AIC | 2 | 0 | 1 | 2 | 0 |
| LDUE | 18 | 7 | 6 | 6 | 6 |
| DILI | 8 | 1 | 1 | 1 | 1 |
| Other liver diseases | 201 | ND | ND | 0 | ND |
| AID | 33 | 3 | 0 | 0 | 0 |
| Control | 1225 | ND | ND | 0 | ND |

PBC: primary biliary cirrhosis; AIH: autoimmune hepatitis; AIC: autoimmune cholangitis; LDUE: liver disease with unknown etiology; DILI: drug induced liver injury; AID: autoimmune disease; AMA: antimitochondrial antibodies; ND: not done.

### *$M_2$ antibodies in patients with other diseases*

Seven patients with liver disease of unknown etiology were all AMA positive; However, only one was $M_2$ antibody negative and didn't agree with the guideline by the American Association for the Study of Liver Diseases (AASLD), and his plasma ALP and γ-GT were in normal range but alanine aminotransferase was elevated (120 U/L). The other 6 patients with $M_2$ antibody positive had no specific symptoms except the unexplained elevation of serum ALP (187-1 525 U/L) and γ-GT (88-2 685 U/L).

One patient with drug induced liver injury was demonstrated as $M_2$ antibody positive by both ELISA and Euroimmun's kit, whose additional laboratory data were as follows: AMA positive, antinuclear antibodies positive, ALP 153 U/L, γ-GT 321 U/L; alanine aminotransferase 281 U/L, aspartate transaminase 225 U/L, total bilirubin 25 μmol/L (normal < 18 μmol/L). This patient suffered from lymphatic tuberculosis and had taken rifampisin for one year before the onset of liver disease. He was in agreement with the AASLD's guideline.

It was noteworthy that the sera from 1 AIH and 2 AIC patients with AMA negative had detectable $M_2$ antibody by BPO with ELISA, while they were $M_2$ antibody negative with the Euroimmun's kit. The prominent elevation of plasma ALP and γ-GT was observed in all of the three patients.

No $M_2$ antibody positive sera were found in control, other liver disease and the AID group by BPO with ELISA.

## DISCUSSION

In the guideline by AASLD in 2000 and the standards by other researchers, AMA has long been used as an important marker for the primary biliary cirrhosis[21, 23]; however, only $M_2$ antibodies are considered as specific for the PBC diagnosis. Other AMA sub-types have been found in drug-induced disorders, cardiomyopathies, systemic lupus erythmatosus, rheumatoid arthritis, tuberculosis, syphilis and hepatitis C, indicating the nonspecific nature of AMA in the diagnosis of PBC[24]. Besides, there were about 5-17 % of the patients with biochemical and histological features compatible with PBC not having detectable AMA with the IIF method[25-34]. To get better diagnostic results, approaches to detect $M_2$ antibodies by ELISA or Western-blotting using recombinant antigen of PDC-$E_2$, BCOADC-$E_2$ and OGDC-$E_2$ have been reported in several literatures[15-17].

In 2001, Miyakawa and his coworkers[35] developed a new ELISA for the detection of $M_2$ antibody using porcine heart mitochondrial protein as the antigen. The sensitivity of this method was only 78 %, despite the specificity was 100 %. In the present study, we employed BPO as the antigen to determine $M_2$ antibodies with ELISA, which was more sensitive than the Euroimmun's kit. The reason for this was partially because the antigen used in our approach was derived from human sources instead of that from porcine used in Euroimmun's kit. The antigen heterogeneity might affect the assay results[36]. Furthermore, the three major autoantigens, BCOADC-$E_2$, PDC-$E_2$ and OGDC-$E_2$, with no cross-reactivity between, were constructed together as a trimer by molecular biological techniques, which could provide more positive chance for the detection of M2 antibodies. Therefore, the use of this recombinant molecule offered a rapid, simple and sensitive ELISA for the immunodiagnosis of PBC.

According to the investigation by James and his associates[3], the incidence of PBC has been increased in recent years. In northern England, the prevalence of PBC from 201.9 per $10^6$ adults and 541.4 per $10^6$ women over 40 in 1987 rose to 334.6 and 939.8 respectively in 1994. Owing to the lack of sensitive diagnostic methods, there have no reliable data related to the epidemiology of PBC in China so far and more seriously,

clinical doctors have not yet paid appropriate attention to this disease. We checked 10 patients with liver cirrhosis hospitalized in January, February and April in 2000 whose serum immunological variables showed no signs of viral infection, and the reason for liver cirrhosis seemed unclear. However, 7 of the 10 patients were found $M_2$ antibody positive by the detailed studies at the Euroimmun Research Center (Germany). In the past six months since we detected $M_2$ antibody by BPO with ELISA for the PBC diagnosis, over 120 patients' sera have been examined, in which 69 demonstrated $M_2$ antibody positive and 30 cases with comparatively complete clinical data listed in this paper. Our recent research and the related domestic reports in 2001 indicate that PBC is probably not so rare in China as it has been thought[4, 37].

## REFERENCES


1 **James OF**, Bhopal R, Howel D, Gray J, Burt AD, Metcalf JV. Primary biliary cirrhosis once rare, now common in the United Kingdom? *Hepatology* 1999; **30**: 390-394
2 **Metcalf J**, James O. The geoepidemiology of primary biliary cirrhosis. *Semin Liver Dis* 1997; **17**: 13-22
3 **Metcalf JV**, Bhopal RS, Gray J, Howel D, James OF. Incidence and prevalence of primary biliary cirrhosis in the city of Newcastle upon Tyne, England. *Int J Epidemiol* 1997; **26**: 830-836
4 **Medina J**, Jones EA, Garcia Monzon C, Moreno Otero R. Immunopathogenesis of cholestatic autoimmune liver diseases. *Eur J Clin Invest* 2001; **31**: 64-71
5 **Heathcote EJ**. Evidence-based therapy of primary biliary cirrhosis. *Eur J Gastroenterol Hepatol* 1999; **11**: 607-615
6 **Joplin RE**, Neuberger JM. Immunopathology of primary biliary cirrhosis. *Eur J Gastroenterol Hepatol* 1999; **11**: 587-593
7 **Metcalf JV**, Mitchison HC, Palmer JM, Jones DE, Bassendine MF, James OF. Natural history of early primary biliary cirrhosis. *Lancet* 1996; **348**: 1399-1402
8 **Kisand KE**, Metskula K, Kisand KV, Kivik T, Gershwin ME, Uibo R. The follow-up of asymptomatic persons with antibodies to pyruvate dehydrogenase in adult population samples. *J Gastroenterol* 2001; **36**: 248-254
9 **Koizumi H**, Onozuka Y, Shibata M, Sano K, Ooshima Y, Morizane T, Ueno Y. Positive rate of anti-mitochondrial antibody in Japanese corporate workers. *Rinsho Byori* 2000; **48**: 966-970
10 **Turchany JM**, Uibo R, Kivik T, Van de Water J, Prindiville T, Coppel RL, Gershwin ME. A study of antimitochondrial antibodies in a random population in Estonia. *Am J Gastroenterol* 1997; **92**: 124-126
11 **Nakano T**, Inoue K, Hirohara J, Arita S, Higuchi K, Omata M, Toda G. Long-term prognosis of primary biliary cirrhosis (PBC) in Japan and analysis of the factors of stage progression in asymptomatic PBC (a-PBC). *Hepatol Res* 2002; **22**: 250-260
12 **Migliaccio C**, Van de Water J, Ansari AA, Kaplan MM, Coppel RL, Lam KS, Thompson RK, Stevenson F, Gershwin ME. Heterogeneous response of antimitochondrial autoantibodies and bile duct apical staining monoclonal antibodies to pyruvate dehydrogenase complex $E_2$: the molecule versus the mimic. *Hepatology* 2001; **33**: 792-801
13 **Kitami N**, Komada T, Ishji H, Shimizu H, Adachi H, Yamaguchi Y, Kitamura T, Oide H, Miyazaki A, Ishikawa M. Immunological study of anti-$M_2$ in antimitochondrial antibody-negative primary biliary cirrhosis. *Intern Med* 1995; **34**: 496-501
14 **Jones DE**. Autoantigens in primary biliary cirrhosis. *J Clin Pathol* 2000; **53**: 813-821
15 **Miyakawa H**, Tanaka A, Kikuchi K, Matsushita M, Kitazawa E, Kawaguchi N, Fujikawa H, Gershwin ME. Detection of antimitochondrial autoantibodies in immunofluorescent AMA-negative patients with primary biliary cirrhosis using recombinant autoantigens. *Hepatology* 2001; **34**: 243-248
16 **Kitami N**, Ishii H, Shimizu H, Adachi H, Komada T, Mikami H, Yokoi Y, Sato N. Immunoreactivity to $M_2$ proteins in antimitochondrial antibody-negative patients with primary biliary cirrhosis. *J Gastroenterol Hepatol* 1994; **9**: 7-12
17 **Jensen WA**, Jois JA, Murphy P, De Giorgio J, Brown B, Rowley MJ, Mackay IR. Automated enzymatic mitochondrial antibody assay for the diagnosis of primary biliary cirrhosis. *Clin Chem Lab Med* 2000; **38**: 753-758
18 **Leung PS**, van de Water J, Coppel RL, Nakanuma Y, Munoz S, Gershwin ME. Molecular aspects and the pathological basis of primary biliary cirrhosis. *J Autoimmun* 1996; **9**: 119-128
19 **Strassburg CP**, Manns MP. Autoimmune tests in primary biliary cirrhosis. *Baillieres Best Pract Res Clin Gastroenterol* 2000; **14**: 585-599
20 **Quaranta S**, Shulman H, Ahmed A, Shoenfeld Y, Peter J, McDonald GB, Van de Water J, Coppel R, Ostlund C, Worman HJ, Rizzetto M, Tsuneyama K, Nakanuma Y, Ansari A, Locatelli F, Paganin S, Rosina F, Manns M, Gershwin ME. Autoantibodies in human chronic graft-versus-host disease after hematopoietic cell transplantation. *Clin Immunol* 1999; **91**: 106-116
21 **Parikh Patel A**, Gold EB, Worman H, Krivy KE, Gershwin ME. Risk factors for primary biliary cirrhosis in a cohort of patients from the United States. *Hepatology* 2001; **33**: 16-21
22 **Ma X**, Qiu DK. Relationship between autoimmune hepatitis and HLA-DR4 and DR β allelic sequences in the third hypervariable region in Chinese. *World J Gastroenterol* 2001; **7**: 718-721
23 **Heathcote EJ**. Management of primary biliary cirrhosis. The american association for the study of liver diseases practice guidelines. *Hepatology* 2000; **31**: 1005-1013
24 **Strassburg CP**, Jaeckel E, Manns MP. Anti-mitochondrial antibodies and other immunological tests in primary biliary cirrhosis. *Eur J Gastroenterol Hepatol* 1999; **11**: 595-601
25 **Michieletti P**, Wanless IR, Katz A, Scheuer PJ, Yeaman SJ, Bassendine MF, Palmer JM, Heathcote EJ. Antimitochondrial antibody negative primary biliary cirrhosis: a distinct syndrome of autoimmune cholangitis. *Gut* 1994; **35**: 260-265
26 **Lacerda MA**, Ludwig J, Dickson ER, Jorgensen RA, Lindor KD. Antimitochondrial antibody-negative primary biliary cirrhosis. *Am J Gastroenerol* 1995; **90**: 247-249
27 **Heathcote J**. Autoimmune cholangitis. *Gut* 1997; **40**: 440-442
28 **Ikuno N**, Scealy M, Davies JM, Whittingham SF, Omagari K, Mackay IR, Rowley MJ. A comparative study of antibody expressions in primary biliary cirrhosis and autoimmune cholangitis using phage display. *Hepatology* 2001; **34**: 478-486
29 **Kinoshita H**, Omagari K, Whittingham S, Kato Y, Ishibashi H, Sugi K, Yano M, Kohno S, Nakanuma Y, Penner E, Wesierska Gadek J, Reynoso Paz S, Gershwin ME, Anderson J, Jois JA, Mackay IR. Autoimmune cholangitis and primary biliary cirrhosis-an autoimmune enigma. *Liver* 1999; **19**: 122-128
30 **Invernizzi P**, Crosignani A, Battezzati PM, Covini G, De Valle G, Larghi A, Zuin M, Podda M. Comparison of the clinical features and clinical course of antimitochondrial antibody-positive and -negative primary biliary cirrhosis. *Hepatology* 1997; **25**: 1090-1095
31 **Kaserer K**, Exner M, Mosberger I, Penner E, Wrba F. Characterization of the inflammatory infiltrate in autoimmune cholangitis. A morphological and immunhistochemical study. *Virchows Arch* 1998; **432**: 217-222
32 **Mayo MJ**, Lipsky PE, Miller SN, Stastny P, Combes B. Similar T-cell oligoclonality in antimitochondrial antibody-positive and -negative primary biliary cirrhosis. *Dig Dis Sci* 2001; **46**: 345-351
33 **Fujioka S**, Yamamoto K, Okamoto R, Miyake M, Ujike K, Shimada N, Terada R, Miyake Y, Nakajima H, Piao CY, Iwasaki Y, Tanimizu M, Tsuji T. Laparoscopic features of primary biliary cirrhosis in AMA-positive and AMA-negative patients. *Endoscopy* 2002; **34**: 318-321
34 **Nakajima M**, Shimizu H, Miyazaki A, Watanabe S, Kitami N, Sato N. Detection of IgA, IgM, and IgG subclasses of anti-$M_2$ antibody by immunoblotting in autoimmune cholangitis: is autoimmune cholangitis an early stage of primary biliary cirrhosis? *J Gastroenterol* 1999; **34**: 607-612
35 **Miyakawa H**, Kikuchi K, Jong Hon K, Kawaguchi N, Yajima R, Ito Y, Maekubo H. High sensitivity of a novel ELISA for anti-$M_2$ in primary biliary cirrhosis. *J Gastroenterol* 2001; **36**: 33-38
36 **Miyakawa H**, Kawaguchi N, Kikuchi K, Fujikawa H, Kitazawa E, Matsushita M. Definition of antigen specificity for antimitochondrial proteins detected by Western blotting using native mitochondrial proteins in primary biliary cirrhosis. *Hepatol Res* 2001; **21**: 101-107
37 **Zhang F**, Jia J, Wang B, Qian L, Yin S, Wang Y, Cui Y, You H, Ma H, Wang H, Zhang C. Clinical characteristics of primary biliary cirrhosis: a report of 45 cases. *Zhonghua Neike Zazhi* 2002; **41**: 163-167


**Edited by** Zhu L

P.O.Box 2345, Beijing 100023,China
Fax: +86-10-85381893
E-mail: wjg@wjgnet.com www.wjgnet.com

World J Gastroenterol 2003;9(6):1356-1360
World Journal of Gastroenterology
Copyright ©2003 by The WJG Press ISSN 1007-9327

• CLINICAL RESEARCH •

# Functional brain imaging in irritable bowel syndrome with rectal balloon-distention by using fMRI

Yao-Zong Yuan, Ran-Jun Tao, Bin Xu, Jing Sun, Ke-Min Chen, Fei Miao, Zhong-Wei Zhang, Jia-Yu Xu

**Yao-Zong Yuan, Ran-Jun Tao, Bin Xu, Jing Sun, Jia-Yu Xu,** Department of Gastroenterology, Ruijin Hospital, Shanghai Second Medical University, Shanghai 200025, China
**Ke-Min Chen, Fei Miao, Zhong-Wei Zhang,** Department of Radiology, Ruijin Hospital, Shanghai Second Medical University, Shanghai 200025, China
**Correspondence to:** Dr. Yao-Zong Yuan, Department of Gastroenterology, Ruijin Hospital, Shanghai Second Medical University, Shanghai 200025, China. yyz28@hotmail.com
**Telephone:** +86-21-64370045-665242 **Fax:** +86-21-64150773
**Received:** 2002-11-19 **Accepted:** 2003-01-02

## Abstract

**AIM:** Irritable bowel syndrome (IBS) is characterized by abdominal pain and changes in stool habits. Visceral hypersensitivity is a key factor in the pathophysiology of IBS. The aim of this study was to examine the effect of rectal balloon-distention stimulus by blood oxygenation level-dependent functional magnetic resonance imaging (BOLD-fMRI) in visceral pain center and to compare the distribution, extent, and intensity of activated areas between IBS patients and normal controls.

**METHODS:** Twenty-six patients with IBS and eleven normal controls were tested for rectal sensation, and the subjective pain intensity at 90 ml and 120 ml rectal balloon-distention was reported by using Visual Analogue Scale. Then, BOLD-fMRI was performed at 30 ml, 60 ml, 90 ml, and 120 ml rectal balloon-distention in all subjects.

**RESULTS:** Rectal distention stimulation increased the activity of anterior cingulate cortex (35/37), insular cortex (37/37), prefrontal cortex (37/37), and thalamus (35/37) in most cases. At 120 ml of rectal balloon-distention, the activation area and percentage change in MR signal intensity of the regions of interest (ROI) at IC, PFC, and THAL were significantly greater in patients with IBS than that in controls. Score of pain sensation at 90 ml and 120 ml rectal balloon-distention was significantly higher in patients with IBS than that in controls.

**CONCLUSION:** Using fMRI, some patients with IBS can be detected having visceral hypersensitivity in response to painful rectal balloon-distention. fMRI is an objective brain imaging technique to measure the change in regional cerebral activation more precisely. In this study, IC and PFC of the IBS patients were the major loci of the CNS processing of visceral perception.

Yuan YZ, Tao RJ, Xu B, Sun J, Chen KM, Miao F, Zhang ZW, Xu JY. Functional brain imaging in irritable bowel syndrome with rectal balloon-distention by using fMRI. *World J Gastroenterol* 2003; 9(6): 1356-1360
http://www.wjgnet.com/1007-9327/9/1356.asp

## INTRODUCTION

Irritable bowel syndrome (IBS) is the most common disorder seen in gastroenterological practice[1,2]. The disorder affects approximately 15 % to 20 % of the world' s population and is predominately found in women[2]. It comprises a group of functional bowel disorders in which abdominal discomfort or pain is associated with defecation or a change in bowel habit, and with features of disordered defecation[3,4]. The pathophysiology of the symptom remains unclear, and visceral hypersensitivity or decreased pain thresholds to distension of the gut is considered to be a biologic marker for IBS and is present in most patients with this gastrointestinal disorder[5]. Possibly, there are dysfunctions in the processing of sensory stimuli in the "brain-gut" axis that may cause visceral hypersensitivity and secondary motility changes[6]. The central nervous system is believed to play a strong modulatory or etiological role in the pathophysiology of the disease[7].

In animals, the perception of somatovisceral pain is derived from the expression of the immediate early gene c-fos[8-11]. Numerous positron emission tomography (PET)[12-15] or functional magnetic resonance imaging (fMRI)[16-18] studies have dealt with the central processing of somatic pain in humans. In contrast, the neural networks involved in the perception of visceral pain in humans, especially rectal pain, have been the subjects of a limited number of functional brain imaging studies[19-23].

Previous studies of somatic pain using PET scanning to measure the regional cerebral blood flow have suggested that the anterior cingulate cortex (ACC), prefrontal cortex (PFC), insular cortex (IC), and thalamus (THAL) are important loci in pain perception[12,24]. Studies of visceral pain have generally suggested that these brain centers are important in sensation. fMRI is an alternative technique to measure changes in regional cerebral activity during stimulation. Using fMRI, the cerebral loci activated by rectal distention were also characterized in healthy volunteers[22].

In this study, we examined the effect of rectal balloon-distention stimulus by blood oxygenation level-dependent functional magnetic resonance imaging (BOLD-fMRI) in the visceral pain center and to compare the distribution, extent, and intensity of activated areas between irritable bowel Syndrome (IBS) patients and normal controls.

## MATERIALS AND METHODS

### *Subjects*

Eleven normal right-handed control subjects (6 men and 5 women; age, 24-49 years; average age, 39 years) and twenty-six right-handed patients with IBS (12 men and 14 women; age, 18-61 years; average age, 47 years) participated in the study. All volunteers were free of any gastrointestinal complaint. The IBS patients were all diagnosed in Ruijin Hospital, and met the Rome II criteria for IBS[4], which include at least 12 weeks, not necessarily to be consecutive in the preceding 12 months of abdominal discomfort or pain that has two of the following three features: (1) Relieved with defecation; (2) Onset associated with a change in frequency of stool; (3) Onset associated with a change in form (appearance) of stool. Each patient underwent a basic evaluation to exclude organic disease including a history, physical examination, and colonoscopy.

### *Distention protocol*

Subjects reclined on the magnetic resonance imaging (MRI) table with head resting on a beanbag saddle that reduced head motion. A plastic balloon (Medtronic Synectics, USA) was placed in rectum at 10-15 cm from the anal margin. First, the subjects were tested for the rectal sensation, including the thresholds for sensation of gas, defecation and pain. Second, subjects reported the subjective pain intensity at 90 ml and 120 ml rectal balloon-distention by using visual analogue scale (0=no pain, 10=unbearable pain). Then, fMRI scanning was begun. Subjects were instructed to expect 4 series of rectal stimuli. Each set of distention included 3 stimuli of the same volume lasting 30 seconds each, with a 30-second rest period in between. The balloon inflation and deflation for each stimulus required an average of 6 seconds. The baseline volume during the rest periods was 0 ml. The first series of stimulus volume was 30 ml, the second 60 ml, the third 90 ml, and the last 120 ml.

### *MRI scanning*

BOLD imaging was performed on a 1.5-T GE Signa MRI system. Each scanning consisted of a T1-weighted (the parameters included TR/TE=400 ms/14 ms, matrix=256×256, NEX=1). Next, four 10-mm-thickslices aligned at an approximately 20° angle above the anterior commissure-posterior commissure line to include the ACC, IC, PFC, and THAL. A functional scan was performed using echo planar imaging, and a matrix of 64×64, NEX=1. The pulse sequence parameters included a 90° flip-angle with a TR (image repetition rate)/TE (effective echo time) of 3 000 ms/60 ms. Each run consisted of 3 repetitions of 30 seconds of rest, followed by 30 seconds of stimulus. In each 30-second period, 10 parameters were collected, 60 data during each series.

### *Data processing and analysis*

Data analysis was performed using correlation-coefficient tool in Functional software (AW3.2, SUN workstation). The confidence level was 0.05. Brain areas thought to mediate painful sensation included the ACC, the IC, the PFC, and THAL. These regions of interest (ROI) were identified and circled on the high-resolution anatomic images by a radiologist, who was blind to the identity of the patient and to the active pixels. The regional cerebral activation was evaluated by the percentage area of ROI and the percentage change in MR signal intensity of ROI. The percentage area of ROI was calculated by the formula: the percentage area of ROI = the pixels of ROI/the total pixels of selected pain center ×100 %. The percentage change in MR signal intensity of ROI = (the MR signal intensity during stimulation - the Mean baseline signal)/ the mean baseline signal ×100 %. The average percentage change in MR signal intensity was calculated for each subject at each stimulus volume in each ROI. To exclude the influence of balloon inflation and deflation, the first and the tenth MR signal intensity of the rest and stimulus phase were eliminated.

### *Statistical analysis*

The data were expressed as means ±SEM. For comparison of means, an unpaired Student' s *t* test was used. The primary comparisons were the thresholds for sensation and VAS score between IBS patients and controls. Secondary analysis included the percentage of ROI and the average percentage change in MR signal intensity of ROI comparing IBS patients with controls. Statistically significant differences by 2-tailed *t* tests were defined by $P<0.05$.

## RESULTS

### *Rectal sensation test*

In the control group, the average thresholds for sensation of gas, defecation and pain were 28 ml, 127 ml, and 208 ml. They were 24 ml, 90 ml, and 150 ml respectively in IBS group. The thresholds for sensation of defecation and pain were significantly lower in IBS group than in control group ($P<0.05$, Figure 1).

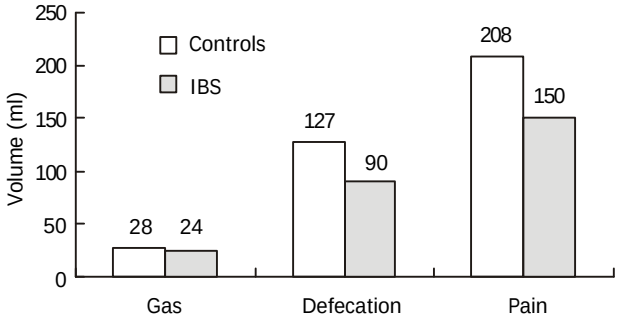


**Figure 1** Rectal sensation test (the thresholds for sensation).

### *VAS score*

At 30 ml rectal distention, subjects generally sensed a very-low-intensity stimulation, using the terms "gas", "mildly felt". At 60 ml rectal distention, some IBS patients expressed sensation of defecation. At 90 ml rectal distention, a large number of IBS patients and some normal controls expressed sensation of stool, associated with mild-moderate pain, and VAS score was 4.42±2.00 *vs* 2.71±1.78. At 120 ml rectal distention, most IBS patients reported moderate-severe painful sensation, and VAS score was 5.90±1.84 *vs* 3.95±2.04. In this study, three IBS patients could not tolerate 120 ml rectal distention. The VAS score of 90 ml and 120 ml rectal distention (painful rectal distention) was significantly higher in IBS patients than in control ($P<0.05$, Figure 2).

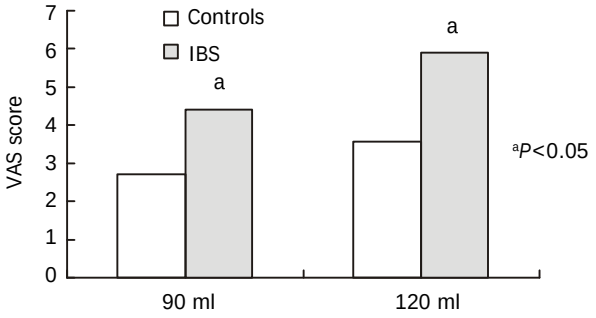


**Figure 2** Subjective pain intensity.

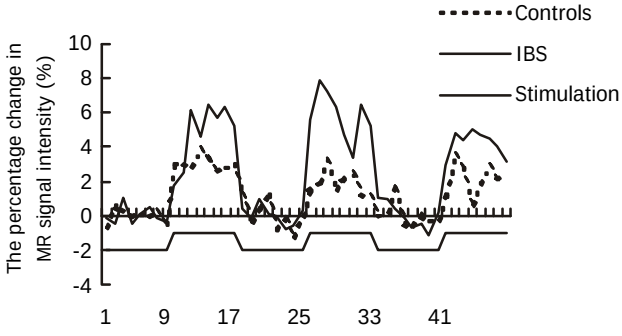


**Figure 3** The percentage change in MR signal intensity time course of PFC in response to 3 rectal distentions at 90 ml.

### *Functional brain imaging*

The time course of rectal stimulation sensation center response indicated immediate increase and rapid decline in BOLD signal

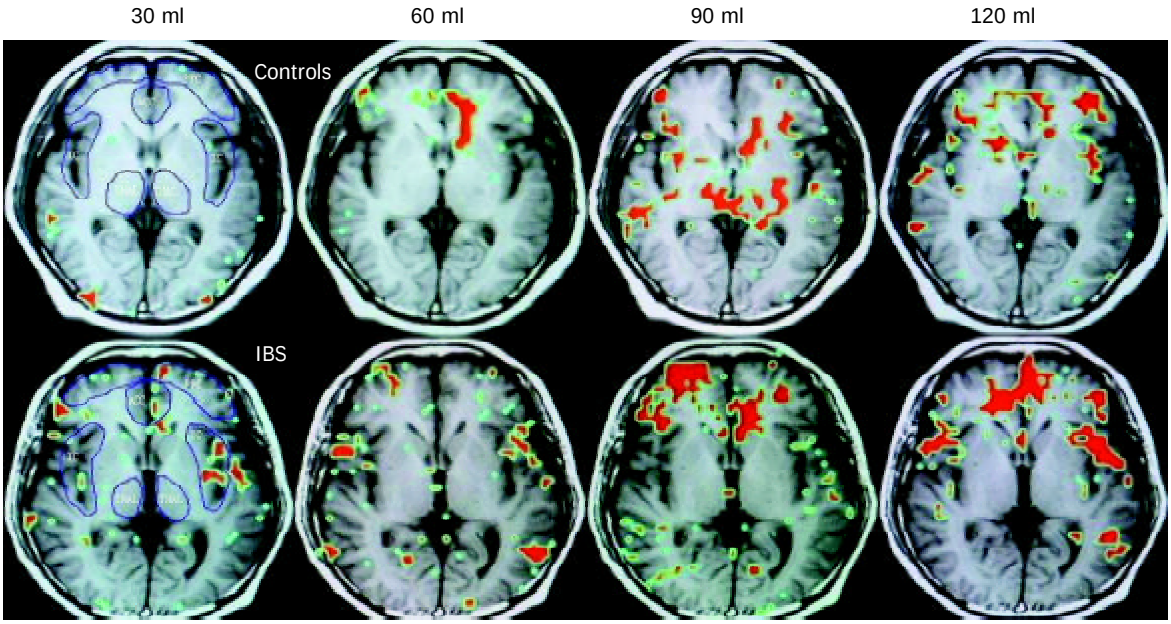


**Figure 4** Functional brain map. The red area is the ROI.

in parallel with the mechanical distending stimulus (Figure 3). For both IBS patients and control subjects, rectal distention stimulation increased the activity of anterior cingulate cortex (35/37), insular cortex (37/37), prefrontal cortex (37/37), and thalamus (35/37) in most cases.

In patients with IBS, the average percentage area of ROI increased in parallel with rectal distention volumes in the IC, PFC, and THAL, only that in PFC had statistical significance ($P$<0.05). In controls, this increasing tendency only occurred in the ACC (Figure 4). At 120 ml rectal distention, the average percentage area of ROI and the average percentage change in MR signal intensity of ROI in the IC, PFC, and THAL were significantly greater in patients with IBS than in control subjects ($P$<0.05, Figure 5 and 6).

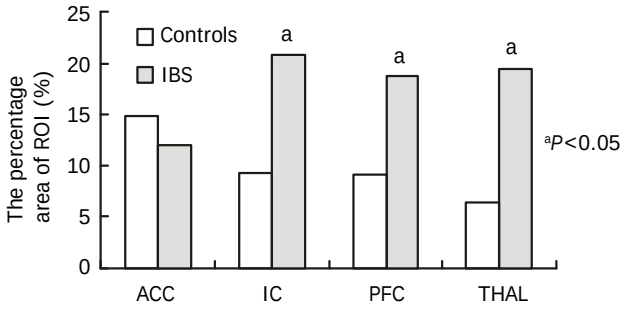


**Figure 5** The average area of ROI at 120ml rectal distention.

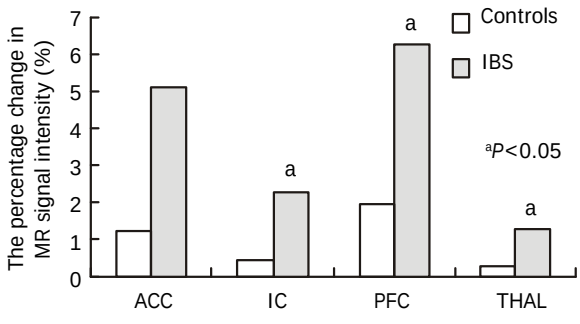


**Figure 6** The percentage change in MR signal intensity of ROI at 120 ml rectal distention.

## DISCUSSION

FMRI is a useful technology to measure changes in regional CNS blood oxygenation, which is in parallel with regional metabolic activity[25-27]. The BOLD technology detects changes in the ratio of deoxyhemoglobin to oxyhemoglobin. When brain-center neurons are metabolically active, there is an increase in local blood flow and a relative increase in the amount of oxyhemoglobin, and an increase in magnetic resonance signal[25-29]. Accordingly, the magnetic resonance signal in a given pixel will increase above baseline if the region is activated in response to stimulation. FMRI offers advantages over PET such as direct anatomic correlation, avoidance of radioisotopes, and acceptable signal-to-noise ratio that do not require large numbers of stimuli. fMRI images give similar results as PET[30,31].

It showed that fMRI has adequate sensitivity to measure regional cerebral blood flow changes in response to visceral - in this case rectal - stimulation. Activity in the 4 selected CNS pain centers, ACC, IC, PFC, and THAL, promptly increase with rectal distention stimulation. The 4 selected pain centers are components of the brain' s pain-processing system[12,24,32,33]. Current studies pointed to the THAL as a relay center, connecting afferent signals from the spinothalamic tract and spinoreticular tracts to higher centers such as the cingulate, prefrontal, and insular cortices[34,35]. The IC is believed to mediate primarily visceral sensations (taste, smell, gastric, colonic, and other visceral inputs) including rectal stimuli, whereas the ACC is thought to mediate the affective or "emotional" content of sensory information. The insular cortex neurons distributed between the taste area and the visceral area receive convergent inputs from baroreceptor, chemoreceptor, gustatory and nociceptive organs and may have roles in taste aversion or in regulation of visceral responses[36]. Using positron emission tomography (PET), Craig' s[37] group found contralateral activity correlated with graded cooling stimuli only in the dorsal margin of the middle/posterior insula in humans. Furthermore, Krushel[38] referred to the region of convergence in the agranular insular cortex as the visceral cortex, and suggested its involvement in the efficient integration of specific visceral sensory stimuli with correlated limbic or motivational consequences. The visceral cortex may help regulate the organism' s visceral response to stress.

The PFC is thought to exert higher executive functions in pain perception[39]. There are several different functional

divisions of the PFC, including the dorsolateral, ventromedial, and orbital sectors. Each of these regions plays some role in affective processing that shares the feature of representing affect in the absence of immediate rewards and punishments as well as in different aspects of emotional regulation[40].

In this study, the thresholds for sensation of defecation and pain were significantly lower in IBS group than in control group, and VAS score was significantly higher in IBS patients than in controls. The results were similar to the previous studies[41]. Normal volunteers and IBS patients had significant cerebral activation in the 4 selected brain centers (ACC, IC, PFC, and THAL) during distention stimulation at 30 ml, 60 ml, 90 ml, and 120 ml. Significant differences in cerebral activation (both the percentage area and the percentage change in MR signal intensity of ROI) were found between IBS patients and controls. In IBS patients, there was significantly greater area of ROI of the PFC with 120 ml distention than with other volume distention. Conversely, in control subjects there was no significant increase in activation of these areas with 120 ml distention compared with others. Furthermore, at 120 ml rectal distention, there was significantly greater activation of the IC, PFC, and THAL in patients with IBS than in control subjects. In summary, by a variety of measures, it is possible that IC and PFC responses to visceral pain in IBS are greater than that in controls.

There were several studies about the CNS activity in response to visceral stimulation by using PET and fMRI, but the results differed. Silverman[20] found a lack of activation within the ACC or PFC with nonpainful stimuli, and reported activation of PFC in response to rectal pain only in IBS and the ACC only in normal subjects. In contrast, more recently Mertz[23], using fMRI, observed that pain led to a greater activation of the ACC than nonpainful stimuli. In Bernstein' s[42] study, they also found that normal controls and subjects with IBD and IBS shared similar loci of activations to visceral sensations of stool and pain. A significantly higher percentage of pixels activated in the anterior cingulate gyrus over both pain and stool conditions for the control group than for the IBS group and for the IBS group than for the IBD group ($P<0.035$). In another study, Bonaz *et al* revealed significant deactivations within the right insula, the right amygdala, and the right striatum[7]. There were gender differences in cortical representation of rectal distension in healthy humans. Male subjects showed localized clusters of fMRI activity primarily in the sensory and parietooccipital regions, whereas female subjects also showed activity in the anterior cingulate and insular regions[43]. Thus, somatic and visceral sensation including pain perception can be studied noninvasively in humans with functional brain imaging techniques. Positron emission tomography and functional magnetic resonance imaging have identified a series of cerebral regions involved in the processing of somatic pain, including the anterior cingulate, insular, prefrontal, inferior parietal, primary and secondary somatosensory, and primary motor and premotor cortices, the thalamus, hypothalamus, brain stem, and cerebellum[44]. Experimental evidence supports possible specific roles for individual structures in processing the various dimensions of pain[44].

In conclusion, our data conform that fMRI is an objective brain imaging technique to measure the change in regional cerebral activation exactly. Using fMRI, some patients with IBS could be detected having visceral hypersensitivity in response to painful rectal balloon-distention. In this study, IC and PFC of IBS patients are the major loci in CNS processing of visceral perception.

## REFERENCES


1 **Olden KW**. Diagnosis of irritable bowel syndrome. *Gastroenterology* 2002; **122**: 1701-1714
2 **Foxx-Orenstein AE**, Clarida JC. Irritable bowel syndrome in women: the physician-patient relationship evolving. *J Am Osteopath Assoc* 2001; **101**: S12-16
3 **Camilleri M**, Prather CM. The irritable bowel syndrome: Mechanisms and a practical approach to management. *Ann Intern Med* 1992; **116**: 1001-1008
4 **Thompson WG**, Longstreth GF, Drossman DA, Heaton KW, Irvine EJ, Muller-Lissner SA. Functional bowel disorders and functional abdominal pain. *Gut* 1999; **45** (Suppl 2): II43-47
5 **Verne GN**, Price DD. Irritable bowel syndrome as a common precipitant of central sensitization. *Curr Rheumatol Rep* 2002; **4**: 322-328
6 **Blomhoff S**, Diseth TH, Jacobsen MB, Vatn M. Irritable bowel syndrome-a multifactorial disease in children and adults. *Tidsskr Nor Laegeforen* 2002; **122**: 1213-1217
7 **Bonaz B**, Baciu M, Papillon E, Bost R, Gueddah N, Le Bas JF, Fournet J, Segebarth C. Central processing of rectal pain in patients with irritable bowel syndrome: an fMRI study. *Am J Gastroenterol* 2002; **97**: 654-661
8 **Menetrey D**, Gannon A, Levine JD, Basbaum AI. Expression of c-fos protein in interneurons and projection neurons of the rat spinal cord in response to noxious somatic, articular, and visceral stimulation. *J Comp Neurol* 1989; **285**: 177-195
9 **Bonaz B**, Plourde V, Tache Y. Abdominal surgery induces fos immunoreactivity in the rat brain. *J Comp Neurol* 1994; **349**: 212-222
10 **Traub RJ**, Silva E, Gebhart GF, Solodkin A. Noxious colorectal distention induced c-Fos protein in limbic brain structures in the rat. *Neurosci Lett* 1996; **215**: 165-168
11 **Bonaz B**, Riviere PJ, Sinniger V, Pascaud X, Junien JL, Fournet J, Feuerstein C. Fedotozine, a kappa-opioid agonist, prevents spinal and supra-spinal Fos expression induced by a noxious visceral stimulus in the rat. *Neurogastroenterol Motil* 2000; **12**: 135-148
12 **Casey KL**, Minoshima S, Berger KL, Koeppe RA, Morrow TJ, Frey KA. Positron emission tomographic analysis of cerebral structures activated specifically by repetitive noxious heat stimuli. *J Neurosurg* 1994; **71**: 802-807
13 **Craig AD,** Reiman EM, Evans A, Bushnell MC. Functional imaging of an illusion of pain. *Nature* 1996; **384**: 258-260
14 **Rainville P**, Duncan GH, Price DD, Carrier B, Bushnell MC. Pain effect encoded in human anterior cingulate but not somatosensory cortex. *Science* 1997; **277**: 968-971
15 **Coghill RC**, Sang CN, Maisog JM, Iadarola MJ. Pain intensity processing within the human brain: A bilateral, distributed mechanism. *J Neurophysiol* 1999; **82**: 1934-1943
16 **Talbot JD**, Marrett S, Evans AC, Meyer E, Bushnell MC, Duncan GH. Multiple representations of pain in human cerebral cortex. *Science* 1991; **251**: 1355-1358
17 **Derbyshire SW**, Jones AK, Gyulai F, Clark S, Townsend D, Firestone LL. Pain processing during three levels of noxious stimulation produces differential patterns of central activity. *Pain* 1997; **73**: 431-445
18 **Apkarian AV**, Gelnar PA, Krauss BR, Szeverenyi NM. Cortical responses to thermal pain depend on stimulus size: A functional MRI study. *J Neurophysiol* 2000; **83**: 3113-3122
19 **Rothstein RD**, Stecker M, Reivich M, Alavi A, Ding XS, Jaggi J, Greenberg J, Ouyang A. Use of positron emission tomography and evoked potentials in the detection of cortical afferents from the gastrointestinal tract. *Am J Gastroenterol* 1996; **91**: 2372-2376
20 **Silverman DH**, Munakata JA, Ennes H, Mandelkern MA, Hoh CK, Mayer EA. Regional cerebral activity in normal and pathological perception of visceral pain. *Gastroenterology* 1997; **112**: 64-72
21 **Bouras EP**, O'Brien TJ, Camilleri M, O'Connor MK, Mullan BP. Cerebral topography of rectal stimulation using single photon emission computered tomography. *Am J Physiol* 1999; **277**: G687-694
22 **Baciu MV**, Bonaz BL, Papillon E, Bost RA, Le Bas JF, Fournet J, Segebarth CM. Central processing of rectal pain: A functional MR imaging study. *Am J Neuroradiol* 1999; **20**: 1920-1924
23 **Mertz H**, Morgan V, Tanner G, Pickens D, Price R, Shyr Y, Kessler R. Regional cerebral activation in irritable bowel syndrome and control subjects with painful and nonpainful rectal distention. *Gastroenterology* 2000; **118**: 842-848
24 **Derbyshire SW**, Jones AK, Devani P, Friston KJ, Feinmann C,

Harris M, Pearce S, Watson JD, Frackowiak RS. Cerebral responses to pain in patients with atypical facial pain measured by positron emission tomography. *J Neurol Neurosurg Psychiatry* 1994; **57**: 1166-1172

25 **Fox PT**, Raichle ME. Focal physiological uncoupling of cerebral blood flow and oxidative metabolism during somatosensory stimulation in human subjects. *Proc Natl Acad Sci USA* 1986; **83**: 1140-1144

26 **Le Bihan D**, Jezzard P, Haxby J, Sadato N, Rueckert L, Mattay V. Functional magnetic resonance imaging of the brain. *Ann Intern Med* 1995; **122**: 296-303

27 **Kwong KK**, Belliveau JW, Chesler DA, Goldberg IE, Weisskoff RM, Poncelet BP, Kennedy DN, Hoppel BE, Cohen MS, Turner R. Dynamic magnetic resonance imaging of human brain activity during primary sensory stimulation. *Proc Natl Acad Sci USA* 1992; **89**: 5675-5679

28 **Bandettini PA**, Wong EC, Hinks RS, Tikofsky RS, Hyde JS. Time course EPI of human brain function during task activation. *Magn Reson Med* 1992; **25**: 390-397

29 **Bandettini PA**, Jesmanowicz A, Wong EC, Hyde JS. Processing strategies for time course data sets in functional MRI of the human brain. *Magn Reson Med* 1993; **30**: 161-173

30 **Belliveau JW**, Kennedy DN Jr, McKinstry RC, Buchbinder BR, Weisskoff RM, Cohen MS, Vevea JM, Brady TJ, Rosen BR. Functional mapping of the human visual cortex by magnetic resonance imaging. *Science* 1991; **254**: 716-719

31 **Yousry TA**, Schmid UD, Jassoy AG, Schmidt D, Eisner WE, Reulen HJ, Reiser MF, Lissner J. Topography of the cortical motor hand area: prospective study with functional MR imaging and direct motor mapping at surgery. *Radiology* 1995; **195**: 23-29

32 **Rosen SD**, Paulesu E, Nihoyannopoulos P, Tousoulis D, Frackowiak RS, Frith CD, Jones T, Camici PG. Silent ischemia as a central problem: regional brain activation compared in silent and painful myocardial ischemia. *Ann Intern Med* 1996; **124**: 939-949

33 **Aziz Q**, Andersson JL, Valind S, Sundin A, Hamdy S, Jones AK, Foster ER, Langstrom B, Thompson DG. Identification of human brain local processing esophageal sensation using positron emission tomography. *Gastroenterology* 1997; **113**: 50-59

34 **Devinsky O**, Morrell MJ, Vogt BA. Contributions of anterior cingulate cortex to behaviour. *Brain* 1995; **118**: 279-306

35 **Cechetto DF**, Saper CB. Role of the cerebral cortex in autonomic function. In: Loewy AD, Spyer KM, eds. Central regulation of autonomic function. *New York: Oxford University* 1990: 208-223

36 **Hanamori T**, Kunitake T, Kato K, Kannan H. Responses of neurons in the insular cortex to gustatory, visceral, and nociceptive stimuli in rats. *J Neurophysiol* 1998; **79**: 2535-2545

37 **Craig AD**, Chen K, Bandy D, Reiman EM. Thermosensory activation of insular cortex. *Nat Neurosci* 2000; **3**: 184-190

38 **Krushel LA**, van der Kooy D. Visceral cortex: integration of the mucosal senses with limbic information in the rat agranular insular cortex. *J Comp Neurol* 1988; **270**: 39-54, 62-63

39 **Kupfermann I**. Localization of higher cognitive and affective functions: the association cortices. In Kandell E, Schwartz J, Jessell T, eds. Principles of neuroscience. 3rd ed. *East Norwalk, CT: Appleton & Lange* 1991: 823-838

40 **Davidson RJ**. Anxiety and affective style: role of prefrontal cortex and amygdala. *Biol Psychiatry* 2002; **51**: 68-80

41 **Rogers J**. Testing for and the role of anal and rectal sensation. *Bailliers Clin Gastroenterol* 1992; **6**: 179-191

42 **Bernstein CN**, Frankenstein UN, Rawsthorne P, Pitz M, Summers R, McIntyre MC. Cortical mapping of visceral pain in patients with GI disorders using functional magnetic resonance imaging. *Am J Gastroenterol* 2002; **97**: 319-327

43 **Kern MK**, Jaradeh S, Arndorfer RC, Jesmanowicz A, Hyde J, Shaker R. Gender differences in cortical representation of rectal distension in healthy humans. *Am J Physiol Gastrointest Liver Physiol* 2001; **281**: G1512-1523

44 **Ladabaum U**, Minoshima S, Owyang C. Pathobiology of visceral pain: molecular mechanisms and therapeutic implications V. Central nervous system processing of somatic and visceral sensory signals. *Am J Physiol Gastrointest Liver Physiol* 2000; **279**: G1-6

**Edited by** Wu XN

P.O.Box 2345, Beijing 100023,China
Fax: +86-10-85381893
E-mail: wjg@wjgnet.com www.wjgnet.com

World J Gastroenterol 2003;9(6):1361-1364
World Journal of Gastroenterology
Copyright ©2003 by The WJG Press ISSN 1007-9327

• CLINICAL RESEARCH •

# Tuberculosis of pancreas and peripancreatic lymph nodes in immunocompetent patients: experience from China

Feng Xia, Ronnie Tung-Ping Poon, Shu-Guang Wang, Ping Bie, Xue-Quan Huang, Jia-Hong Dong

**Feng Xia, Shu-Guang Wang, Ping Bie, Xue-Quan Huang, Jia-Hong Dong,** Institute of Hepatobiliary Surgery, Southwest Hospital, Third Military Medical University, Chongqing 400038, China
**Ronnie Tung-Ping Poon,** Center for the Study of Liver Disease and Department of Surgery, University of Hong Kong Medical Centre, Queen Mary Hospital, Hong Kong, China
**Correspondence to:** Dr. Jia-Hong Dong, Institute of Hepatobiliary Surgery, Southwest Hospital, Third Military Medical University, Chongqing 400038, China. drfxia@hotmail.com
**Telephone:** +86-23-65387419 **Fax**: +86-23-65430233
**Received:** 2002-10-04 **Accepted:** 2002-11-16

## Abstract

**AIM:** To determine the clinical, radiographic and laboratory characteristics, diagnostic methods, and therapeutic variables in immunocompetent patients with tuberculosis (TB) of the pancreas and peripancreatic lymph nodes.

**METHODS:** The records of 16 patients (6 male, 10 female; mean age 37 years, range 18-56years) with tuberculosis of the pancreas and peripancreatic lymph nodes from 1983 to 2001 in the Southwest Hospital were analyzed retrospectively. In addition, 58 similar cases published in Chinese literature were reviewed and summarized. We reviewed the clinical, radiographic and laboratory findings, diagnostic methods, therapeutic approaches, and outcome in the patients. Criteria for the diagnosis of pancreatic tuberculosis were the presence of granuloma in histological sections or the presence of *Mycobacterium tuberculosis* DNA by polymerase chain reaction (PCR).

**RESULTS:** Predominant symptoms consisted of abdominal nodule and pain (75 %), anorexia/weight loss (69 %), malaise/weakness (64 %), fever and night sweats (50 %), back pain (38 %) and jaundice (31 %). Swelling of the head of the pancreas with heterogeneous attenuation echo was detected with ultrasound in 75 % (12/16). CT scan showed pancreatic mass with heterogeneous hypodensity focus in all patients, with calcification in 56 % (9/16) patients, and peripancreatic nodules in 38 % (6/16) patients. Anemia and lymphocytopenia were seen in 50 % (8/16) patients, and pancytopenia occurred in 13 % (2/16) patients. Hypertransaminasemia, elevated alkaline phosphatase (AP) and GGT were seen in 56 % (9/16) patients. The erythrocyte sedimentation rate (ESR) was elevated in 69 % (11/16) cases. Granulomas were found in 75 % (12/16) cases, and in 38 % (6/16) cases caseous necrosis tissue was found. Laparotomy was performed in 75 % (12/16) cases, and ultrasound-guided fine needle aspiration (FNA) was done in 63 % (10 of 16). The most commonly used combinations of medications were isoniazid/rifampin/streptomycin (63 %, $n$=10) and isoniazid/rifampin pyrazinamide/streptomycin or ethambutol (38 %, $n$=6). The duration of treatment lasted for half or one year and treatment was successful in all cases. The characteristics of 58 cases from Chinese literature were also summarized.

**CONCLUSION:** Tuberculosis of the pancreas and peripancreatic lymph nodes should be considered as a diagnostic possibility in patients presenting with a pancreatic mass, and diagnosis without laparotomy is possible if only doctors are aware of its clinical features and investigate it with appropriate modalities. Pancreatic tuberculosis can be effectively cured by antituberculous drugs.

Xia F, Poon RTP, Wang SG, Bie P, Huang XQ, Dong JH. Tuberculosis of pancreas and peripancreatic lymph nodes in immunocompetent patients: experience from China. *World J Gastroenterol* 2003; 9(6): 1361-1364
http://www.wjgnet.com/1007-9327/9/1361.asp

## INTRODUCTION

Tuberculosis (TB) is a potentially systemic disease that can infect any organ and system. It was a prevalent disease in the developing countries about 50 years ago, but its incidence has been controlled with the availability of effective anti-tuberculous drugs. However, the last decade has witnessed a rise in the incidence of tuberculosis even in developed countries. In the United States, the Centers for Disease Control reported that the incidence of TB was significantly greater in 1994 than in 1985[1]. Nowadays, TB is often an acquired immune deficiency syndrome (AIDS)-defining illness in individuals found to be human immunodeficiency virus (HIV) antibody-positive; however, it can still cause a devastating disease in immunocompetent hosts[1, 2]. In China, there is a revival trend in the incidence of TB although AIDS remains uncommon nationally.

Abdominal infection with tuberculosis commonly affects the spleen, liver, and ileocecal region[2,3]. Pancreatic tuberculosis is an extremely rare disease, especially when it is isolated in the pancreas. There were a few case reports published before in literature, but its clinical characteristics remain unclear[4-6]. In this retrospective study, we reported 16 patients with TB of the pancreas and peripancreatic lymph nodes, and summarized the clinical features of 58 similar cases in the Chinese language literature where the HIV antibody status of the patients was either negative or not stated. The clinical, radiographical and laboratory findings, diagnostic methods, therapeutic approaches, and outcome in patients in an endemic area were reviewed in this study.

## MATERIALS AND METHODS

The records of 16 patients who were admitted to Hepatobiliary Surgery Center, Southwest Hospital, Third Military Medical University, Chongqing, China with TB of the pancreas and peripancreatic lymph nodes between 1983 and 2001 were reviewed. The clinical, radiographic and laboratory findings, diagnostic methods, therapeutic approaches, and outcome in these patients were summarized. Ten patients were screened for anti-HIV antibodies. Criteria for the diagnosis of pancreatic TB were (1) paraffin-embedded tissues with granuloma or (2) the presence of *Mycobacterium tuberculosis* DNA by

polymerase chain reaction (PCR). IS 6110-specific primers, which could amplify all *M. tuberculosis* complex strains, were used for amplification. In addition, all available bacteriological and histological studies were performed to confirm the diagnosis. The clinical and laboratory features of patients were collected from the casebooks. Details of follow-up were obtained from medical records. In addition, 58 similar cases published in the Chinese literature were also reviewed and summarized.

## RESULTS

A total of 16 patients with TB of the pancreas and peripancreatic lymph nodes had been documented. Six patients were male and 10 were female, with a mean age of 37 years (range 18-56 years). Eight patients had predisposing factors. Six patients had a history of pulmonary TB or TB of lymph nodes, one had diabetes mellitus, and one had connective tissue disease.

### *Presenting symptoms and physical findings*

Predominant symptoms consisted of fever, abdominal pain, abdominal nodule, back pain, jaundice, malaise/weakness, anorexia/weight loss and night sweats. In twelve patients with abdominal nodule and pain, eleven had anorexia/weight loss, ten had malaise/weakness, eight had fever and night sweats, six had back pain, and five had jaundice.

Fever, usually the intermittent type, was present in eight patients. The mean duration of fever prior to the diagnosis was 23 days (range 11-35 days).

### *Radiographic findings*

Chest X-rays revealed relic of TB focus in 8 patients, 6 with pneumonitis. All of the patients had been examined with ultrasound and computed tomography (CT) scan. Twelve patients showed swollen head of the pancreas with ultrasound image of heterogeneous attenuation echo. Four patients were demonstrated to have inner heterogeneous attenuation echo in head or body of the pancreas. CT scan showed pancreatic mass with heterogeneous hypodensity focus in all of the patients, with calcification in 9 of 16 patients, and peripancreatic nodules in 6 of 16 patients (Figures 1, 2 and 3). Endoscopic retrograde cholangiopancreatography had been performed for 12 cases, and 2 cases had pancreatic duct dilatation. Magnetic resonance imaging and digital subtraction angiogram had been done for 6 patients, and the results showed pancreatic nodules and/or peripancreatic mass.

### *Tuberculin skin test*

Tuberculin skin test was performed on 9 patients before initiation of therapy. Four in 9 were positive ($\geqslant$10 mm of induration) to 5TU of intradermally purified protein derivative (PPD).

### *Haematology and biochemistry*

In 8 patients, anemia and lymphocytopenia were seen. Pancytopenia occurred in 2 patients. Hypertransaminasemia, elevated alkaline phosphatase (AP) and GGT were seen in 9 patients, respectively. The erythrocyte sedimentation rate (ESR) was elevated in 11 cases.

### *Results of smears and mycobacterial cultures*

Secretions and body fluids were examined microscopically and cultured in 9 patients. Acid-fast bacilli were demonstrated in 1 case, and cultures for *M. tuberculosis* were positive in 4 out of 9 specimens tested. Anti-TB drug susceptibility was studied in 4 patients, and two *M. tuberculosis* strains were sensitive to the major anti-TB drugs including isoniazid (INH), rifampin (RMP), pyrazinamide (PZA), streptomycin (SM), and ethambutol (EMB). The other 2 cases were not sensitive to rifampin, isoniazid and streptomycin, respectively.

**Figure 1** Mass with heterogeneous hypodensity located in the head of pancreas. The body and tail of the pancreas appeared atrophy, and with enlarged main pancreatic duct.

**Figure 2** Pancreas appeared swollen diffusely with heterogeneous enhancement and vague margin. A circle lymph nodes showed enhancement under pancreas.

**Figure 3** Calcification of pancreatic TB occurred under the body of the pancreas and retroperitoneal lymph nodes.

### *Biopsy data*

Granuloma was found in 12 cases among specimens harvested from the pancreas and peripancreatic nodule by laparotomy (12 of 16) and ultrasound-guided fine needle aspiration (FNA) (10 of 16). Caseous necrosis tissue was found in 6 of 16 cases, and results of smears showed that there were Langhans' giant cells, epithelioid cells and lymphocytes. Seven of the 16 patients had combined TB in the liver, bile duct or spleen.

### *Initial diagnosis*

Eleven of 16 patients were initially given a diagnosis of pancreatic tumor. The diagnosis of pancreatic TB had been firstly confirmed for only three of 16 cases. Another three cases were diagnosed with retroperitoneal tumor.

### *Treatment regimen and outcome*

Biopsy and/or FNA were done for all of the patients. Twelve in 16 cases received laparotomy. In one case, cholangiojejunostomy was performed for CBD obstruction, and in another two cases splenectomy was performed for splenic tuberculosis. All 16 patients received treatment with antituberculotics for TB. The most commonly used combinations were INH/RMP/SM ($n$=10) and INH/RMP/PZA/SM or EMB ($n$=6). The therapeutic duration lasted for a half or one year.

Twelve patients received follow-up from a half to 14 years. No recurrence of TB was found in the pancreas or other organs. In 11 patients, follow-up CT scans in abdomen were available. Resolution was complete in all patients. The mean time to resolution was 132 days (range 78-186 days).

### *Literature review*

A total of 58 cases of pancreatic TB have been described in the Chinese language literature[7-17]. Fifteen of the 58 patients were stated to be HIV antibody-negative, and the HIV status of the other patients was not confirmed. All of the 58 patients were diagnosed by histological appearance being consistent with characteristics of tuberculosis, or positive organisms by acid-fast staining, culture of *Mycobacterium* tuberculosis or PCR analysis. Twenty patients were male and 36 were female, with a mean age 43.5 years (from 14 to 73). The main symptoms were epigastric pain and discomfort (37 cases), fever (31 cases), weight loss (23 cases) and anorexia (21 cases). The other unusual symptoms included malaise/ weakness (11 cases), back pain (9 cases), nausea/vomiting (8 cases), jaundice (6 cases), night sweats (6 cases), upper gastrointestinal bleeding (3 cases), cough (3 cases) and diarrhea (1 case). The duration of symptoms prior to presentation ranged from 5 days to 5 months (mean 2.6 months). Thirteen cases gave a past history of TB pneumonia (10 cases) and TB lymph nodes (3 cases). The appearance of the chest X-ray was reported in 49 cases. There was relic of TB focus in 14 patients, 9 with pneumonitis. 34 patients received tuberculin skin testing, of which 21 were positive. Single or multiple modalities of investigation were performed for the patients. Ultrasound revealed pancreatic mass in 38 cases and failed to do so in another 9 cases. Abdominal CT scan was used in 41 cases and reported pancreatic mass and/ or peripancreatic nodules in all cases. MRI was performed in 19 cases and also showed a mass in all instances. ERCP found abnormalities with CBD and pancreatic duct in 7 cases. Abdominal X-ray showed focal calcification in 6 cases and DSA located a mass in 4 cases. Ultrasound-guided fine needle aspiration was performed in 21 cases and was successful in diagnosis in 14 cases. Laparoscopic biopsy was performed in 7 cases and confirmed diagnosis in all cases. Fifteen patients had combined TB in other organs.

The initial diagnoses included pancreatic tumor (35), chronic pancreatitis (7), retroperitoneal tumor (5), acute pancreatitis (4) and pancreatic TB (3). Thirty-nine patients underwent laparotomy, 24 for biopsy, 12 for FNA, 5 for pus cavity draining, 4 for choledochojejunostomy, 2 for pancreatoduodenectomy, and 1 for celiac ganglia resection. Pathological report showed granuloma in 27 patients. Acid-fast bacilli were demonstrated in 14 of 27 cases, and cultures for M. tuberculosis were positive in 8 out of 19 specimens tested.

The treatment details were given in 41of 58 cases. The common agents were isoniazid, rifampicin, streptomycin, pyrazinamide and ethambutol. Combinations of 3 or 4 drugs were used for 36 patients. The duration of treatment was recorded in 28 cases, ranging from 3 to 12 months. 24 patients were reported to have resolution after treatment for 3 to 12 months. One death was reported among the 58 cases.

## DISCUSSION

We have presented a description of a series of 16 cases with tuberculosis of the pancreas and peripancreatic lymph nodes in immunocompetent patients. Having reviewed Chinese literature we found 58 similar cases and summarized their clinical findings. Pancreatic TB is extremely rare. Diagnosis remains difficult for most of the patients, and it is especially difficult to differentiate pancreatic TB from pancreatic tumor. Our series and review of Chinese literature revealed several clinical characteristics as follows: (1) pancreatic TB is mostly suffered by young people, with a predominance of female over male. In contrast, pancreatic tumor is common in old people; (2) some patients have a history of TB in past, and most of them come from areas with high prevalence of active tuberculosis; (3) the patients often present with epigastric pain, fever and weight loss; (4) ultrasound and CT scan show pancreatic mass and peripancreatic nodules, sometimes with focal calcification; (5) FNA and laparoscopic biopsy are the diagnostic procedures of choice for patients with a high suspicion of pancreatic TB. It can lead to confirmed diagnosis and hence avoids laparotomy. Treatment using combination of 3 or 4 antituberculous drugs is effective for most patients. However, attention should be paid to the possibility of drug resistance to some agents that have being used for a long time.

Recently, the incidence of tuberculosis is increasing[1-6]. Cases of pancreatic TB are being reported with increasing frequency, too[18-22]. The reasons may be related to evolutionary changes in the biology of the mycobacterium, drug resistance, and new populations with immunological deficits. Cases related to acquired immunodeficiencies, AIDS or immunosuppression for transplantation have been reported more frequently. Jenney *et al*. had reviewed English language literature before 1998. A total of 37 cases of pancreatic TB in patients not stated to be HIV antibody-positive was found[23]. The authors concluded that it was important to consider the diagnosis of TB when a patient presented with epigastric pain, fever and weight loss and a mass lesion in the pancreas by diagnostic imaging. Three forms of mycobacterial infection of the pancreas have been described as follows: (1) generalized (military) tuberculosis, in which *Mycobacterium tuberculosis* is the agent; (2) spread to the pancreas from celiac and other retroperitoneal lymph nodes, in which *Mycobacterium bovis* is the main agent to be considered; (3) primary localized pancreatic tuberculosis due to *Mycobacterium tuberculosis*, which may reflect a point of origin from the intestinal tract[24-32].

In conclusion, tuberculosis of the pancreas and peripancreatic lymph nodes in immunocompetent patients is rare and could present a diagnostic challenge. However, if doctors are aware of its clinical features and conduct appropriate investigations with multiple modalities including CT scan and ultrasound-guided FNA or laparoscopic biopsy, diagnosis of pancreatic tuberculosis without laparotomy is possible and the disease can be effectively treated with antituberculous drugs.

## REFERENCES

1 **Babu RD**, John V. Pancreatic tuberculosis: case report and review of the literature. *Trop Gastroenterol* 2001; **22**: 213-214

2 **Evans JD**, Hamanaka Y, Olliff SP, Neoptolemos JP. Tuberculosis of the pancreas presenting as metastatic pancreatic carcinoma. A case report and review of the literature. *Dig Surg* 2000; **17**: 183-187

3 **Turan M,** Sen M, Koyuncu A, Aydin C, Elaldi N, Arici S. Pancreatic Pseudotumor due to Peripancreatic Tuberculous Lymphadenitis. *Pancreatology* 2002; **2**: 561-564

4 **Suri S,** Gupta S, Suri R. Computed tomography in abdominal tuberculosis. *Br J Radiol* 1999; **72**: 92-98

5 **Sanabe N**, Ikematsu Y, Nishiwaki Y, Kida H, Murohisa G, Ozawa T, Hasegawa S, Okawada T, Toritsuka T, Waki S. Pancreatic tuberculosis. *J Hepatobiliary Pancreat Surg* 2002; **9**: 515-518

6 **Shan YS,** Sy ED, Lin PW. Surgical resection of isolated pancreatic tuberculosis presenting as obstructive jaundice. *Pancreas* 2000; **21**: 100-101

7 **Li XH**, Wang YL, Yao YM. A case of local portal hypertension caused by pancreatic TB. *Zhonghua Gandan Waike Zazhi* 1999; **4**: 28-28

8 **Zhao MF**, Yang JF. Analysis of 11 cases pancreatic tuberculosis *Zhonghua Putong Waike Zazhi* 2000; **15**: 292-293

9 **Tang TJ**. A case of misdiagnosis of pancreatic tuberculosis. *Chuanbei Yixueyuan Xuebao* 2000; **3**: 15-15

10 **Li GC**, Yao L. Analysis of 18 cases of pancreatic tuberculosis. *Zhongguo Shiyong Waike Zazhi* 1998; **18**: 755-756

11 **Zhao LB**, Hao F. Analysis of misdiagnosis of 4 cases pancreatic tuberculosis and a literature review. *Shiyong Yiyao Zazhi* 1998; **11**: 23-24

12 **Hou JX**, Fan YH. Diagnosis and treatment of pancreatic tuberculosis. *Zhonghua Jiehe He Huxi Zazhi* 1998; **21**: 689-689

13 **Li Z**, Wu LH, Pei SJ. A report of 3 cases of misdiagnosis of pancreatic tuberculosis. *Linchuang Wuzhen Wuzhi* 2000; **8**: 17-17

14 **Zhao JP,** Chen ZX. The diagnosis and treatment of Tuberculosis of pancreas and peripancreatic lymph nodes. *Zhongguo Jijiu Yixue* 1999; **19**: 737-737

15 **Zhong SX**, Zhao P. A report of 8 cases of pancreatic tuberculosis. *Zhonghua Waike Zazhi* 1996; **34**: 476-478

16 **Sun PL**, Chen TX. Three cases of pancreatic tuberculosis. *Xin Xiaohua Binxue Zazhi* 1997; **5**: 11-11

17 **Zhou XX,** Yin J. A report of 4 cases of pancreatic tuberculosis. *Zhonghua Chaosheng Yingxiangxue Zazhi* 1998; **7**: 373-373

18 **Ladas SD,** Vaidakis E, Lariou C, Anastasiou K, Chalevelakis G, Kintzonidis D, Raptis SA. Pancreatic tuberculosis in non-immunocompromised patients: reports of two cases, and a literature review. *Eur J Gastroenterol Hepatol* 1998; **10**: 973-976

19 **Demir K,** Kaymakoglu S, Besisik F, Durakoglu Z, Ozdil S, Kaplan Y, Boztas G, Cakaloglu Y, Okten A. Solitary pancreatic tuberculosis in immunocompetent patients mimicking pancreatic carcinoma. *J Gastroenterol Hepatol* 2001; **16**: 1071-1074

20 **Kouraklis G,** Glinavou A, Karayiannakis A, Karatzas G. Primary tuberculosis of the pancreas mimicking a pancreatic tumor. *Int J Pancreatol* 2001; **29**: 151-153

21 **Chaudhary A,** Negi SS, Sachdev AK, Gondal R. Pancreatic tuberculosis: still a histopathological diagnosis**.** *Dig Surg* 2002; **19**: 389-392

22 **Yokoyama T,** Miyagawa S, Noike T, Shimada R, Kawasaki S. Isolated pancreatic tuberculosis. *Hepatogastroenterology* 1999; **46**: 2011-2014

23 **Jenney AW**, Pickles RW, Hellard ME, Spelman DW, Fuller AJ, Spicer WJ. Tuberculosis pancreatic abscess in an HIV antibody-negative patient: case report and review. *Scand J Infect Dis.* 1998; **30**: 99-104

24 **Franco-Paredes C,** Leonard M, Jurado R, Blumberg HM, Smith RM. Tuberculosis of the pancreas: report of two cases and review of the literature. *Am J Med Sci* 2002; **323**: 54-58

25 **Riaz AA,** Singh A, Robshaw P, Isla AM. Tuberculosis of the pancreas diagnosed with needle aspiration. *Scand J Infect Dis* 2002; **34**: 303-304

26 **Echenique Elizondo M,** Amondarain Arratibel J, Compton CC, Warshaw AL. Tuberculosis of the pancreas. *Surgery* 2001; **129**: 114-116

27 **Akhan O,** Pringot J. Imaging of abdominal tuberculosis. *Eur Radiol* 2002; **12**: 312-323

28 **Ozden I,** Emre A, Demir K, Balci C, Poyanli A, Ilhan R. Solitary pancreatic tuberculosis mimicking advanced pancreatic carcinoma. *J Hepatobiliary Pancreat Surg* 2001; **8**: 279-283

29 **Kwon AH,** Inui H, Kamiyama Y. Preoperative laparoscopic examination using surgical manipulation and ultrasonography for pancreatic lesions**.** *Endoscopy* 2002; **34**: 464-468

30 **Small G,** Wilks D. Pancreatic mass caused by Mycobacterium tuberculosis with reduced drug sensitivity. *J Infect* 2001; **42**: 201-202

31 **Chen CH,** Yang CC, Yeh YH, Yang JC, Chou DA. Pancreatic tuberculosis with obstructive jaundice-a case report. *Am J Gastroenterol* 1999; **94**: 2534-2536

32 **Karia K,** Mathur SK. Tuberculous cold abscess simulating pancreatic pseudocyst. *J Postgrad Med* 2000; **46**: 33-34


**Edited by** Zhang JZ

P.O.Box 2345, Beijing 100023,China
Fax: +86-10-85381893
E-mail: wjg@wjgnet.com www.wjgnet.com

World J Gastroenterol 2003;9(6):1365-1369
World Journal of Gastroenterology
Copyright ©2003 by The WJG Press ISSN 1007-9327

• CLINICAL RESEARCH •

# Prevalence of anti-ulcer drug use in a Chinese cohort

Tzeng-Ji Chen, Li-Fang Chou, Shinn-Jang Hwang

**Tzeng-Ji Chen, Shinn-Jang Hwang,** Department of Family Medicine, Taipei Veterans General Hospital and National Yang-Ming University School of Medicine, Taipei, Taiwan, China
**Li-Fang Chou,** Department of Public Finance, National Chengchi University, Taipei, Taiwan, China
**Correspondence to:** Professor Shinn-Jang Hwang, Department of Family Medicine, Taipei Veterans General Hospital, 201, Sec. 2, Shih-Pai Road, Taipei 11217, Taiwan, China. sjhwang@vghtpe.gov.tw
**Telephone:** +86-2-28757458 **Fax:** +86-2-28737901
**Received:** 2003-02-25 **Accepted:** 2003-03-16

## Abstract

**AIM:** To estimate the age-specific prevalence of anti-ulcer drug use and to calculate the usage of different anti-ulcer drugs over 5 years within the universal health insurance program in Taiwan area.

**METHODS:** The National Health Insurance Research Database in Taipei supplied the cohort data sets of 200 000 people. The ambulatory and inpatient claims of the cohort from 1997 to 2001 were analyzed. The anti-ulcer drugs included all drug items of the group A02B (drugs for treatment of peptic ulcer) in the Anatomical Therapeutic Chemical classification system (version 2000). The amount of drug usage was measured in unit of defined daily dose.

**RESULTS:** Among the totally 13 034 393 visits with 56 672 631 ambulatory prescription items, there were 398 150 (0.7 %) prescribed items of anti-ulcer drugs in 378 855 (2.9 %) visits. Among the 107 649 admissions with 5 762 312 inpatient prescription items, there were 24 598 (0.4 %) prescribed items of anti-ulcer drugs in 11 548 (10.7 %) admissions. The annual prevalence of anti-ulcer drug use was 9.6 % in 1997, 11.6 % in 1998, 15.4 % in 1999, 14.5 % in 2000, and 15.9 % in 2001 respectively. The 5-year prevalence was 36.1 %. The age-specific prevalence among the people younger than 20 years was 9.2 % in 2001 and 23.7 % during the 5-year period. Cimetidine not only was the most popular ingredient among anti-ulcer drugs (57 634 cimetidine users in 70 729 all anti-ulcer drug users during the 5-year period) but also had the largest prescribed amount (42.3 % of DDDs for all anti-ulcer drug users during the 5-year period). The annually prescribed amount of anti-ulcer drugs had grown from 4.9 DDDs/1000 inhabitants/day in 1997 to 7.5 in 2001. This increase was largely attributed to $H_2$-receptor antagonists and the expanding number of users.

**CONCLUSION:** Prescribing of anti-ulcer drugs is indeed popular among the Chinese population in Taiwan area. The disproportionate use of anti-ulcer drugs by children demands further investigation.

Chen TJ, Chou LF, Hwang SJ. Prevalence of anti-ulcer drug use in a Chinese cohort. *World J Gastroenterol* 2003; 9(6):1365-1369
http://www.wjgnet.com/1007-9327/9/1365.asp

## INTRODUCTION

In the past three decades, the invention of several revolutionary anti-ulcer drugs, *e.g.* $H_2$-receptor antagonists, synthetic prostaglandins, proton pump inhibitors, and cytoprotective agents, has changed the physicians' treatment patterns in gastroenterology and greatly improved the ulcer-healing rate of patients with peptic ulcer disease[1-6]. In spite of effectiveness and popularity, the cost of these drugs has also aroused concern in the health care systems of developed countries[7-11]. The concern has been aggravating in recent years because of expanding use of proton pump inhibitors in treating gastroesophageal reflux disease. Although prescribing of these potent acid-suppressing drugs is popular, their patterns of utilization have been infrequently documented in national surveys[12-21].

In Taiwan area, a single and universal health insurance program started in 1995 and covered nearly all inhabitants (21 653 555 beneficiaries at the end of 2001)[22]. The prescription drug benefits are included in the insurance. Because all claims data for the reimbursement purpose are in electronic form and available to researchers, we can perform a survey of anti-ulcer drug use among the Chinese population in Taiwan area.

The aims of this study were twofold: to estimate the age-specific prevalence of anti-ulcer drug use and to calculate the usage of different anti-ulcer drugs over 5 years within the universal health insurance program in Taiwan area. The strengths of our study were to use the longitudinal data sets of a representative cohort of 200 000 people and to adopt the unit of international standards in measuring the anti-ulcer drug usage.

## MATERIALS AND METHODS

### *Data sources*

We obtained 4 cohort data sets (R01-4) from the National Health Insurance Research Database (NHIRD; http://www.nhri.org.tw/nhird/) in Taipei in November 2002. The total 200 000 people in these 4 cohort data sets had been randomly sampled from 23 753 407 people who were ever insured under the universal health insurance program in Taiwan area from March 1, 1995 to December 31, 2000. Not every person of the cohort was insured through the study period because of new birth, death, immigration, and emigration. The cohort data sets contained all insurance claims of 200 000 people from 1996 to 2001. The structure of the insurance claim files had been described in details in our previous study[23].

In the current study, we analyzed the ambulatory and inpatient files of the cohort data sets from 1997 to 2001. Totally, there were 13 034 393 visits, 56 672 631 ambulatory prescription items, 107 649 admissions, and 5 762 312 inpatient prescription items.

Besides, we obtained a complete file of 21 146 approved drug items of Western medicine in Taiwan area from the web site of the Bureau of National Health Insurance (BNHI; http://www.nhi.gov.tw/; accessed January 12, 2002). Each drug of different brand, strength and form was officially assigned a unique code for use in the claims file. The BNHI also offered a list of ATC codes (the Anatomical Therapeutic Chemical classification system, version 2000)[24] for each drug item.

### *Study design*

The anti-ulcer drugs in our study included all drug items of the group A02B (drugs for treatment of peptic ulcer, renamed to ' drugs for peptic ulcer and gastroesophageal reflux disease'

in 2002) in the ATC classification system. This group of drugs has 5 subgroups of the fourth level: A02BA ($H_2$-receptor antagonists, $H_2$RA), A02BB (prostaglandins), A02BC (proton pump inhibitors, PPI), A02BD (combinations for eradication of *Helicobacter pylori*), and A02BX (other drugs for treatment of peptic ulcer, renamed to ' other drugs for peptic ulcer and gastroesophageal reflux disease' in 2002). A total of 428 anti-ulcer drug items, including the original brands and generics, have been registered in Taiwan area since 1995. Some drugs might be no more available on the market or not reimbursable by the insurance during the study period.

In estimating the age-specific prevalence of anti-ulcer drug use, we first identified the people receiving anti-ulcer drug items in each year. Because the number of people in the cohort fluctuated during the study period, we calculated the number of the denominator in each year by excluding those people who were not insured at any time of that year. A person' s age in a year was defined as the difference between her/his birthday and the end of that year. In estimating the 5-year age-specific prevalence from 1997 to 2001, we took December 31, 2001 as the index date to calculate a person' s age.

In describing the distribution of anti-ulcer drug prescriptions among the cohort, we calculated the number of recipients and the total prescribed amount for each ingredient (ATC 5th level) in each year. Supposed that the cohort did not take anti-ulcer drugs before the base year of 1997, the number of new anti-ulcer drug users was additionally computed for each year after 1997. The prescribed amounts of anti-ulcer drugs were measured in unit of defined daily dose (DDD) by ATC classification system[24]. The original dose of each prescription was converted to a number of DDDs according to the DDD of the ingredient. Some anti-ulcer drugs (e.g. cetraxate, urogastrone, and gefarnate) lacked either ATC codes or DDDs; we used the most commonly prescribed daily doses as their DDDs. For international comparison, the numbers of DDDs per 1,000 inhabitants per day were also computed.

### *Statistical analysis*

The database software of Microsoft SQL Server 2000 was used for data linkage and processing. The regular statistics were displayed.

## RESULTS

### *General information of the cohort*

Among the 200 000-people cohort, only 195 971 people were eligible during the 5-year study period. The other 4 029 people who had dropped out of the insurance before 1997 would not be included in the following analyses. The number of eligible people varied from year to year (Table 1). There were more men than women (100 257 *vs.* 95 654), and the status of sex was unknown in 60 persons.

### *General information of anti-ulcer drug prescriptions*

During the 5-year study period, 356 distinct anti-ulcer drugs had existed in the cohort data sets. The drugs belonged to 18 ingredients of ATC 5th level. At the ambulatory sector, there were 398 150 (0.7 %) prescribed items of anti-ulcer drugs in 378 855 (2.9 %) visits; at the inpatient sector, there were 24 598 (0.4 %) prescribed items in 11 548 (10.7 %) admissions.

### *Age specific prevalence of anti-ulcer drug use*

In 1997, as high as 9.6 % (17 414/180 781) of eligible cohort received anti-ulcer drugs. The percentage increased by two-thirds to 15.9 % (29 181/183 976) in 2001. More than a third (36.1 %) of the cohort had ever received anti-ulcer drugs during the 5-year study period. Generally, the prevalence of anti-ulcer drug use increased with age. Another noteworthy finding was that anti-ulcer drugs had been prescribed to an appreciable percentage of children and adolescents (Table 1).

### *Recipients of anti-ulcer drugs by ingredient*

Cimetidine was the most popular ingredient of anti-ulcer drugs among the cohort, followed by sucralfate, ranitidine, famotidine, omeprazole, pirenzepine, and lansoprazole (Table 2). The majority of new anti-ulcer drug users in each year were also attributed to cimetidine.

**Table 1** Age distribution of patients receiving anti-ulcer drugs and age-specific prevalence of anti-ulcer drug use from 1997 to 2001

| | 1997 | 1998 | 1999 | 2000 | 2001 | 1997-2001 |
|---|---|---|---|---|---|---|
| Sampling cohort | | | | | | |
| 0 – 19 years | 57388 | 56427 | 55448 | 54684 | 51029 | 52103 |
| 20 – 39 years | 62613 | 63765 | 64848 | 65219 | 63800 | 69425 |
| 40 – 59 years | 39809 | 41420 | 42922 | 44241 | 45432 | 47663 |
| 60 years and older | 20971 | 21836 | 22489 | 23093 | 23715 | 26780 |
| Total | 180781 | 183448 | 185707 | 187237 | 183976 | 195971 |
| Patients with anti-ulcer drugs | | | | | | |
| 0 – 19 years | 2965 | 3611 | 5171 | 4634 | 4712 | 12339 |
| 20 – 39 years | 5345 | 6741 | 9249 | 8788 | 9673 | 23741 |
| 40 – 59 years | 4933 | 6213 | 8277 | 8113 | 8664 | 20166 |
| 60 years and older | 4172 | 4787 | 5905 | 5643 | 6132 | 14483 |
| Total | 17415 | 21352 | 28602 | 27178 | 29181 | 70729 |
| Prevalence of anti-ulcer drug use | | | | | | |
| 0 – 19 years | 5.2 % | 6.4 % | 9.3 % | 8.5 % | 9.2 % | 23.7 % |
| 20 – 39 years | 8.5 % | 10.6 % | 14.3 % | 13.5 % | 15.2 % | 34.2 % |
| 40 – 59 years | 12.4 % | 15.0 % | 19.3 % | 18.3 % | 19.1 % | 42.3 % |
| 60 years and older | 19.9 % | 21.9 % | 26.3 % | 24.4 % | 25.9 % | 54.1 % |
| Total | 9.6 % | 11.6 % | 15.4 % | 14.5 % | 15.9 % | 36.1 % |

**Table 2** Recipients of anti-ulcer drugs by main ingredient from 1997 to 2001 (number of new users in parentheses)

| ATC[a] coding | Group / ingredient name | 1997 | 1998 | 1999 | 2000 | 2001 | 1997-2001 |
|---|---|---|---|---|---|---|---|
| A02BA | $H_2$ RA | | | | | | |
| | 01 Cimetidine | 11538 | 15793 (11340) | 22905 (14525) | 22356 (10564) | 24305 (9667) | 57634 |
| | 02 Ranitidine | 1588 | 1852 (1482) | 2262 (1757) | 2283 (1611) | 2579 (1802) | 8240 |
| | 03 Famotidine | 974 | 1143 (953) | 1401 (1113) | 1526 (1216) | 1669 (1232) | 5488 |
| | 04 Nizatidine | 187 | 255 (221) | 295 (236) | 199 (157) | 137 (108) | 909 |
| | 06 Roxatidine | 89 | 98 (82) | 87 (76) | 83 (67) | 97 (80) | 394 |
| A02BB | Prostaglandins | | | | | | |
| | 01 Misoprostol | 128 | 145 (129) | 156 (135) | 150 (112) | 88 (68) | 572 |
| A02BC | PPIS | | | | | | |
| | 01 Omeprazole | 709 | 913 (807) | 1168 (990) | 1150 (917) | 1445 (1156) | 4579 |
| | 02 Pantoprazole | - | 1(1) | 84 (84) | 147 (133) | 273 (255) | 473 |
| | 03 Lansoprazole | 151 | 391 (365) | 531 (459) | 647 (537) | 785 (643) | 2155 |
| | 04 Rabeprazole | - | - | - | - | 31 (31) | 31 |
| A02BX | Other drugs | | | | | | |
| | 01 Carbenoxolone | 287 | 260 (219) | 337 (271) | 155 (105) | 199 (164) | 1046 |
| | 02 Sucralfate | 3463 | 3192 (2510) | 3107 (2301) | 2390 (1506) | 2173 (1390) | 11170 |
| | 03 Pirenzepine | 1177 | 1197 (937) | 1181 (857) | 731 (454) | 625 (351) | 3776 |
| | 05 Bismuth subcitrate | 329 | 299 (266) | 271 (223) | 173 (141) | 142 (111) | 1070 |
| | 06 Proglumide | 113 | 61 (53) | 36 (34) | 3 (3) | 8 (5) | 208 |
| | 07 Gefarnate | 248 | 295 (270) | 416 (363) | 326 (265) | 203 (161) | 1307 |
| | - Cetraxate | 356 | 101 (81) | 72 (59) | 48 (40) | 41 (37) | 573 |
| | - Urogastrone | 192 | 46 (34) | 42 (32) | 14 (12) | 6 (5) | 275 |
| Total | | 17415 | 21352 (14423) | 28602 (16611) | 27178 (11660) | 29181 (10622) | 70729 |

[a]ATC=Anatomical therapeutic chemical classification system.

**Table 3** Total prescribed amount of anti-ulcer drugs by main ingredient from 1997 to 2001 (unit of measurement: numbers of defined daily doses [DDDs])

| ATC[a] coding | Group / ingredient name | 1997 | 1998 | 1999 | 2000 | 2001 |
|---|---|---|---|---|---|---|
| A02BA | $H_2$ RA | | | | | |
| | 01 Cimetidine | 114145 | 151403 | 221528 | 198255 | 221836 |
| | 02 Ranitidine | 57329 | 62357 | 69780 | 69954 | 88034 |
| | 03 Famotidine | 33366 | 40063 | 51198 | 52852 | 53108 |
| | 04 Nizatidine | 8943 | 12304 | 12282 | 8269 | 5305 |
| | 06 Roxatidine | 3493 | 3057 | 3215 | 2847 | 4460 |
| A02BB | Prostaglandins | | | | | |
| | 01 Misoprostol | 2244 | 3649 | 5594 | 4534 | 1941 |
| A02BC | PPIS | | | | | |
| | 01 Omeprazole | 26635 | 33587 | 46429 | 43589 | 57193 |
| | 02 Pantoprazole | - | 14 | 2593 | 4845 | 9276 |
| | 03 Lansoprazole | 5840 | 14276 | 19624 | 24860 | 31023 |
| | 04 Rabeprazole | - | - | - | - | 864 |
| A02BX | Other drugs | | | | | |
| | 01 Carbenoxolone | 5708 | 4164 | 4768 | 1945 | 1918 |
| | 02 Sucralfate | 26172 | 20170 | 15942 | 10960 | 9898 |
| | 03 Pirenzepine | 7575 | 7378 | 5925 | 3868 | 3942 |
| | 05 Bismuth subcitrate | 7999 | 6104 | 5213 | 2686 | 2754 |
| | 06 Proglumide | 1010 | 459 | 198 | 12 | 31 |
| | 07 Gefarnate | 14379 | 17859 | 26568 | 16682 | 8972 |
| | - Cetraxate | 4072 | 1254 | 849 | 615 | 657 |
| | - Urogastrone | 5067 | 1272 | 1151 | 232 | 32 |
| Total | | 323976 | 379370 | 492856 | 447005 | 501243 |
| | Ambulatory sector | 297213 | 355837 | 465326 | 420144 | 470924 |
| | Inpatient sector | 26764 | 23532 | 27530 | 26861 | 30319 |
| DDDs / 1000 inhabitants / day | | 4.9 | 5.7 | 7.3 | 6.5 | 7.5 |

[a]ATC=Anatomical therapeutic chemical classification system.

### *Total prescribed amounts of anti-ulcer drugs*

Measured in unit of DDDs, cimetidine again had the largest prescribed amount (42.3 %) of all anti-ulcer drugs among the cohort during the 5-year study period (Table 3). It was then followed by ranitidine (16.2 %), famotidine (10.8 %), omeprazole (9.7 %), and lansoprazole (4.5 %). The majority of anti-ulcer drugs were used at the ambulatory sector (93.7 % of total DDDs).

The total prescribed amount of anti-ulcer drugs grew from 4.9 DDDs/1 000 inhabitants/day in 1997 to 7.5 in 2001 (Table 3). This increase was attributed to the expanded number of users because the average prescribed amount of anti-ulcer drugs per user in a year remained relatively stable (18.7±54.8 DDDs in 1997, 17.9±41.0 in 1998, 17.3±51.0 in 1999, 16.5±40.5 in 2000, and 17.3±40.8 in 2001).

On the other hand, $H_2$-receptor antagonists and proton pump inhibitors had contributed to the growth of the total prescribed amount of anti-ulcer drugs during the study period (Figure 1). While $H_2$-receptor antagonists had the largest share of growth, proton pump inhibitors had the highest growth rate. In the meantime, the usage of prostaglandins had remained stable, but other drugs for treatment of peptic ulcer had fewer users and smaller prescribed amount totally.

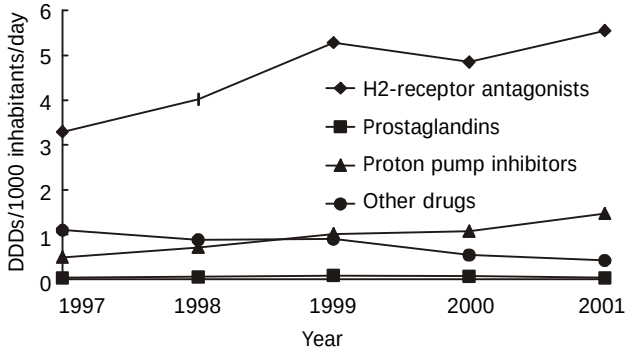


**Figure 1** Trend of total prescribed amount of anti-ulcer drugs by pharmacological subgroups from 1997 to 2001.

## DISCUSSION

To the best of our knowledge, our study might be one of the few reports that surveyed the anti-ulcer drug use in the Chinese population. Only with the computerization of insurance reimbursement, pharmacoepidemiological studies of such a large scale could be feasible. Besides, the person-based sampling in our study could estimate both the total amount and prevalence of drug use among the population.

Our study revealed that prescribing of anti-ulcer drugs was indeed popular in Taiwan. Nearly a sixth of the population received anti-ulcer drugs covered by the health insurance in 2001 and more than a third of the population had been exposed to such drugs during the 5 years. But the total usage of anti-ulcer drugs in Taiwan was not high in international comparison. According to the statistics of the OECD (Organization for Economic Co-operation and Development), 8 countries supplied their national consumption of anti-ulcer drugs in 1998: Australia (38.8 DDDs/1 000 inhabitants/day), Sweden (29.0), Iceland (28.1), Denmark (16.5), Norway (16.0), Czech Republic (13.1), Finland (12.4), and Slovakia (8.7)[25]. In contrast, Taiwan had only 5.7 DDDs/1 000 inhabitants/day of anti-ulcer drugs in the same year. However, the statistics has not been adjusted by age.

In the 1990s, the developed countries experienced a drastic increase of anti-ulcer drug consumption since the introduction of proton pump inhibitors. For example, the national consumption of anti-ulcer drugs in Sweden increased from 9.2 DDDs/1 000 inhabitants/day in 1990 to 34.4 in 2000[25]. During the 5 years of our study, a growing trend of anti-ulcer drugs was also observed in Taiwan. But the increase was largely attributed to $H_2$-receptor antagonists and expanding user group. The explanation might be that the reimbursement policy of the health insurance in Taiwan limited the use of expensive proton pump inhibitors on the one hand and loosened the regulation over the much cheaper generics of $H_2$-receptor antagonists on the other hand.

While overuse of proton pump inhibitors has become a research topic[26,27], our study found that at least the children in Taiwan might be disproportionately exposed to anti-ulcer drugs. Because children were generally not able to receive upper gastrointestinal endoscopy, their use of anti-ulcer drugs could be seldom justified. It demanded further studies to explore such a situation in Taiwan.

Our study with insurance claims in Taiwan had some limitations. At first, the drug use outside the insurance was not included in the analysis. However, the majority of anti-ulcer drugs, including the low-dose cimetidine, were prescription-only drugs in Taiwan. Besides, the compulsory health insurance covered nearly all inhabitants in Taiwan and reimbursed most prescription-only drugs. The use of anti-ulcer drugs at the private market should be of a less significant scale.

Secondly, the actual duration of drug treatment was not computed in our study because of missing dosage frequency in the inpatient files of the NHIRD data sets. Instead, we calculated the cumulated numbers of DDDs for each person as a proxy of treatment duration. But the DDD is arbitrarily set for trend and international comparisons. It does not consider the dosing at the specific conditions of children, elderly, and other risk groups. However, our data showed that the yearly amount of anti-ulcer drugs per user was low on average. It might be inferred that most people took anti-ulcer drugs only for a short term.

Thirdly, the purpose of cohort data sets in the NHIRD was to trace a cohort retrospectively and prospectively. The people of the cohort were chosen in 2000 and it was planned to follow them up continuously in the next years. Thus, the data sets of 2001 did not include anyone born after December 31, 2000. The denominator in 2001 should be smaller than the actual number of people and the prevalence correspondingly became a little overestimated.

Finally, we did not analyze the distribution of diagnoses in our study because a claims diagnosis served for the purpose of reimbursement and was seldom verified. The NHIRD data sets did provide the information whether the patients had received the endoscopic or radiological examinations of upper gastrointestinal tract. But no laboratory findings were routinely transmitted to the insurer in electronic form. Conventional epidemiological surveys are still needed to understand the prevalence of peptic ulcer and gastroesophageal reflux disease in Taiwan.

## ACKNOWLEDGMENTS

This study was based in part on data from the National Health Insurance Research Database provided by the Bureau of National Health Insurance, Department of Health and managed by National Health Research Institutes in Taiwan. The interpretation and conclusions contained herein do not represent those of Bureau of National Health Insurance, Department of Health or National Health Research Institutes.

## REFERENCES

1 **Molinder H,** Wallander MA, Svärdsudd K, Bodemar G. The introduction of $H_2$-receptor antagonists to Scandinavia: effects of expert's opinions. *Scand J Gastroenterol* 1998; **33**: 224-230

2 **Soll AH.** Medical treatment of peptic ulcer disease: practice guidelines. *JAMA* 1996; **275**: 622-629

3 **Howden CW,** Hunt RH. Guidelines for the management of *Helicobacter pylori* infection. *Am J Gastroenterol* 1998; **93**: 2330-2338

4 **DeVault KR,** Castell DO. Updated guidelines for the diagnosis and treatment of gastroesophageal reflux disease. *Am J Gastroenterol* 1999; **94**: 1434-1442

5 **Andersen IB,** Bonnevie O, Jørgensen T, Sørensen TIA. Time trends for peptic ulcer disease in Denmark, 1981-1993: analysis of hospitalization register and mortality data. *Scand J Gastroenterol* 1998; **33**: 260-266

6 **Thors H,** Svanes C, Thjodleifsson B. Trends in peptic ulcer morbidity and mortality in Iceland. *J Clin Epidemiol* 2002; **55**: 681-686

7 **McGavock H,** Webb CH, Johnston GD, Milligan E. Market penetration of new drugs in one United Kingdom region: implications for general practitioners and administrators. *BMJ* 1993; **307**: 1118-1120

8 **McManus P,** Marley J, Birkett DJ, Lindner J. Compliance with restrictions on the subsidized use of proton pump inhibitors in Australia. *Br J Clin Pharmacol* 1998; **46**: 409-411

9 **Cromwell DM,** Bass EB, Steinberg EP, Yasui Y, Ravich WJ, Hendrix TR, McLeod SF, Moore RD. Can restrictions on reimbursement for anti-ulcer drugs decrease Medicaid pharmacy costs without increasing hospitalizations? *Health Serv Res* 1999; **33**: 1593-1610

10 **O'Connor JB,** Provenzale D, Brazer S. Economic considerations in the treatment of gastroesophageal reflux disease: a review. *Am J Gastroenterol* 2000; **95**: 3356-3364

11 **Lucas LM,** Gerrity MS, Anderson T. A practice-based approach for converting from proton pump inhibitors to less costly therapy. *Eff Clin Pract* 2001; **4**: 263-270

12 **Thors H,** Sigurdsson H, Oddsson E, Thjodleifsson B. Survey of prescriptions for peptic ulcer drugs (ACT class A02B) in Iceland. *Scand J Gastroenterol* 1994; **29**: 988-994

13 **Roberts SJ,** Bateman DN. Prescribing of antacids and ulcer-healing drugs in primary care in the north of England. *Aliment Pharmacol Ther* 1995; **9**: 137-143

14 **Goudie BM,** McKenzie PE, Cipriano J, Griffin EM, Murray FE. Repeat prescribing of ulcer healing drugs in general practice-prevalence and underlying diagnosis. *Aliment Pharmacol Ther* 1996; **10**: 147-150

15 **Moride Y,** Melnychuk D, Monette J, Abenhaim L. Determinants of initiation and suboptimal use of anti-ulcer medication: a study of the Quebec older population. *J Am Geriatr Soc* 1997; **45**: 853-856

16 **Morales Suárez-Varela MM,** Pérez-Benajas MA, Girbes Pelechano VJ, Llopis-González A. Antacid (A02A) and antiulcer (A02B) drug prescription patterns: Predicting factors, dosage and treatment duration. *Eur J Epidemiol* 1998; **14**: 363-372

17 **Bashford JNR,** Norwood J, Chapman SR. Why are patients prescribed proton pump inhibitors? Retrospective analysis of link morbidity and prescribing in the General Practice Research Database. *BMJ* 1998; **317**: 452-456

18 **Martin RM,** Lim AG, Kerry SM, Hilton SR. Trends in prescribing $H_2$-receptor antagonists and proton pump inhibitors in primary care. *Aliment Pharmacol Ther* 1998; **12**: 797-805

19 **Prach AT,** McGilchrist MM, Murray FE, Johnston DA, MacDonald TM. Prescription of acid-suppressing drugs in relation to endoscopic diagnosis: a record-linkage study. *Aliment Pharmacol Ther* 1999; **13**: 397-405

20 **Boutet R,** Wilcock M, MacKenzie I. Survey on repeat prescribing for acid suppression drugs in primary care in Cornwall and the Isles of Scilly. *Aliment Pharmacol Ther* 1999; **13**: 813-817

21 **Jones MI,** Greenfield SH, Jowett S, Bradley CP, Seal R. Proton pump inhibitors: a study of GPs' prescribing. *Fam Pract* 2001; **18**: 333-338

22 **Bureau of National Health Insurance.** 2001 National Health Insurance Annual Statistical Report. Taipei: *Bureau of National Health Insurance* 2002

23 **Liu JY,** Chen TJ, Hwang SJ. Concomitant prescription of non-steroidal anti-inflammatory drugs and antacids in the outpatient setting of a medical center in Taiwan: A prescription database study. *Eur J Clin Pharmacol* 2001; **57**: 505-508

24 Guidelines for ATC Classification and DDD Assignment, 3rd ed. Oslo: *WHO Collaborating Centre for Drug Statistics Methodology* 2000

25 OECD Health Data 2001. Paris: *OECD (Organisation for Economic Co-operation and Development)* 2001

26 **Naunton M,** Peterson GM, Bleasel MD. Overuse of proton pump inhibitors. *J Clin Pharm Ther* 2000; **25**: 333-340

27 **Nardino RJ,** Vender RJ, Herbert PN. Overuse of acid-suppressive therapy in hospitalized patients. *Am J Gastroenterol* 2000; **95**: 3118-3122


**Edited by** Xu XQ

P.O.Box 2345, Beijing 100023,China
Fax: +86-10-85381893
E-mail: wjg@wjgnet.com www.wjgnet.com

World J Gastroenterol 2003;9(6):1370-1373
World Journal of Gastroenterology
Copyright ©2003 by The WJG Press ISSN 1007-9327

• BRIEF REPORTS •

# *In situ* expression and significance of B7 costimulatory molecules within tissues of human gastric carcinoma

Xiao-Li Chen, Xu-Dong Cao, An-Jing Kang, Kang-Min Wang, Bao-Shan Su, Yi-Li Wang

**Xiao-Li Chen, An-Jing Kang, Kang-Min Wang, Bao-Shan Su,** Department of Pathology, Second Hospital of Xi' an Jiaotong University, Xi' an 710004, Shaanxi Provice, China
**Xu-Dong Cao,** Medical School of Shihezi University, Shihezi 832002, Xinjiang Uygur Autonomous Region, China
**Yi-Li Wang,** Institute of Immunopathology, Medical School of Xi' an Jiaotong University, Xi' an 710061, Shaanxi Provice, China
**Correspondence to:** Dr. Xiao-Li Chen, Department of Pathology, Second Hospital of Xi' an Jiaotong University, Xi' an 710004, Shaanxi Province, China. chenxiaoli64.student@sina.com
**Telephone:** +86-29-8546322
**Received:** 2002-10-25 **Accepted:** 2002-11-16

## Abstract

**AIM:** To explore the role and significance of costimulatory molecules B7H1,B7H2 and ICOS within tissues of human gastric carcinoma and the possible mechanisms in tumor escape.

**METHODS:** mRNA expressions of costimulatory molecules including B7H1,B7H2,ICOS and B7-1 in tissues of human gastric carcinoma were investigated by *in situ* hybridization using digoxigenin-labeled oligonucleotide-probes. The tissue of chronic gastric ulcer was used as a control. All data were analyzed by SPSS statistic software.

**RESULTS:** At the site of gastric carcinoma, mRNA expression levels of B7H1, B7H2 and ICOS were much higher than that of B7-1. Their mRNA positive expression indexes were 0.512±0.333, 0.812±0.454, 0.702±0.359 and 0.293±0.253, respectively. The positively stained cells were mainly tumor infiltrating lymphocytes (TILs), and some tumor cells. The difference between them was greatly significant $P<0.005$. The mRNA expression levels of four molecules were not correlated to the pathological grade and matastasis of gastric carcinoma.

**CONCLUSION:** ICOS-B7H costimulatory pathway may be predominant at the site of gastric carcinoma. B7-1mRNA might be the basis of ICOS-B7H interaction. ICOS-B7H interaction induces the production of IL-10 which inhibits the antitumor immune responses. Therefore, it is supposed that ICOS-B7H costimulatory pathway may be involved in the negative regulation of cell-mediated immune responses.

Chen XL, Cao XD, Kang AJ, Wang KM, Su BS, Wang YL. *In situ* expression and significance of B7 costimulatory molecules within tissues of human gastric carcinoma. *World J Gastroenterol* 2003; 9(6): 1370-1373
http://www.wjgnet.com/1007-9327/9/1370.asp

## INTRODUCTION

Tumor immunity is primarily cell-mediated. The tumor antigen leads to anti-tumor immune response of the host. A body of evidences have shown that the specific activation of lymphocytes requires two signals; one is provided by T-cell receptor complex coupled to CD3/MHC peptide antigen, and the other is costimulatory signal delivered by interaction of costimulatory molecules with their ligands expressed on antigen presenting cells (APCs). In the absence of costimulatory signals, antigen-MHC complex interaction may lead to T-cell clonal anergy or deletion, and thus, the effective cellular immune response can not be induced. Furthermore, there are evidences that activation of lymphocyte subpopulation with different function needs unique costimulation factors. Therefore, investigation of costimulators on infiltrating lymphocytes and tumor cells at the tumor site and of their significance will be of great help in developing new methods of anti-tumor immunotherapy. Cell-mediated immunity is the main mechanism of anti-tumor immunity of the host. With presentation of antigen recognization and deepening of the understanding of activated T-cells, it is believed that in the presence of costimulatory signals, effective anti-tumor immune response presents tumor antigen multipeptide to T cells and stimulates T-cell immune response. B7 is an important costimulatory molecule. Most tumors lack or have a low expression of B7-1, so they do not induce effective anti-tumor immune response. The tumor cells escape from immune system of the host and continue to grow[1-15]. Although many *in vitro* experiments support this idea, *in situ* studies on human tumors have shown that most tumor tissues express the B7-1 or B7-2 molecules. So the idea meets challenges. An *in vitro* study on new members of B7 family - B7H1, B7H2 and ICOS suggested that the role of ICOS-B7H costimulatory pathway stimulated IL-10 production and induced secretion of Th2 type cytokines. The present study was to explore the role and biological significance of ICOS-B7H costimulatory signals and the possible mechanisms in tumor escape, and to provide the theoretical foundation for designing effective schemes of immunotherapy of carcinoma.

## MATERIALS AND METHODS

### *Patients*

17 patients with gastric carcinoma (10 matastatic, and 7 non-matastatic) and 6 patients with gastric ulcer were identified by pathological diagnosis at the Department of Pathology, Second Hospital of Xi' an Jiaotong University. The fresh tissue samples were instantly fixed in 10 % formalin, and embeded in paraffin according to routine procedures. Tonsil tissue served as a positive control.

### *Main reagents*

Digoxigenin (DIG)-labeling and detection kits were purchased from Boehringer Mannheim Company in Germany. Solution for *in situ* hybridization was mixed with diethyl pyrocarbonate (DEPC) water. All apparatuses were baked at 180 ℃ for four hours and DEPC water was digested with RNase.

### *Specimens*

Sections (4-5 μm) cut from the tissue block were de-paraffined in 65 ℃ oven for 24 hours and then stored at - 70 ℃ until being used.

### *Labeling of oligonucleotide probes and detection of their sensitivities*

**Labeling** On the ice, 4 μl reaction buffer (vial 1), 4 μl $CoCl_2$ solution (vial 2), 1 μl probe (100 pmol), 1 μl DIG-dUTP solution (vial 2), 1 μl dATP solution (vial 4), 1 μl terminal transferase (vial 5) and 8 μl DEPC water, were consecutively added into an eppendorf tube, and carefully mixed and incubated at 37 ℃ for 15 minutes. 2 μl stopping solution (prepared by mixing 1 μl glycogen solution (vial 9) with 200 μl 0.2 mol/L EDTA solution) was added into the tube to stop the labeling reaction. Then, 2.5 μl 4mol/L CrCl2 and 75 μl pro-cold pure alcohol were added to deposit the labeled. After the supernatants were drained out, the probe was washed with 50 μl 70 % pre-cold alcohol and dried with a frozen dry machine, and stored at - 20 ℃ until being used.

**Detection of sensitivity** Sensitivity of each probe was measured by the detection kit following the manufacturer' s instructions. The lowest concentration for positive staining was 1.25 pmol/ml. The oligonucleotide probe sequences were as follow. B7-1 5' -CAT GAA GCT GTG GTT GGT TG-3' ; B7H1 5' -TGC TTG TCC AGG TGA CTT CG-3' ; B7H2 5' -CCA TCG CTC TGA CTT CCT TC-3' ; and ICOS 5' -TTC AGC TGG CAA CAA AGT TG-3' .

### *Hybridization*

Sections stored at - 70 ℃ were recovered at room temperature, deparaffined in dimethylbenzene, and hydrated in gradient alcohol. They were digested in 0.5 μg/ml fresh proteinase K solution at room temperature for 20 minutes, and fixed in 4 % poly-formaldehyde for 20 minutes after digestion was stopped in 0.2 % glycine, and then repeatedly rinsed with 1×PBS for 10 minutes. The sections were treated in 0.2N HCl solution at room temperature for 10 minutes, rinsed with DEPC water for 3 minutes; and dehydrated in gradient alcohol. At 42 ℃ in a bio-hybridization oven, all sections were pre-hybridized for 2 hours, and then hybridized for 20 hours. After hybridization, they were rinsed with 2×SSC for two times,15 minutes each, rinsed with 1×SSC for 30 minutes and finally with buffer I solution (pH 7.5) for 6 minutes.

### *Detection*

50 μl blocking reagent (containing 8 % normal goat serum, 0.3 % Triton X-100 buffer I) was instilled onto each section. The sections were incubated at 37 ℃ for one hour and a half, and then 30 μl anti-DIG-AP conjugate (1:500) was added onto each section, and all sections were incubated at 37 ℃ for two hours and rinsed with buffer I two times, 15 minutes each, then rinsed with buffer III (100 mmol/L Tris-HCl, 100 mmol/L NaCl and 50 mmol/L $MgCl_2$, pH 9.5) for 5 minutes, and stained with NBT-BCIP at 20 ℃ for 12 hours. Finally, the reaction was stopped with buffer IV solution (10 mmol/L Tris-HCl, and 1 mmol/L EDTA, pH 8.0), and the sections were washed in running water, counterstained with methyl green, dehydrated, cleaned in xylene and coverslipped.

### *Evaluation of results*

Under a light microscope, positively hybridized signals were mainly located in the infiltrating lymphocytes and colored purple blue. Reactivity was scored using a semi-quantitative method. First, each section was randomly scored one thousand cells. The positive cell ratio in each section was calculated. Then, according to the staining intensity of positive cells, results were graded as following: intense 3+, moderate 2+,weak 1+ and negative, a score of 3, 2, 1, 0 was assigned respectively. Finally, the positive cell ratio multiplied with staining intensity score of the positive cells was regarded as positive index of mRNA expression of costimulatory molecules.

### *Control experiment*

Expression of ICOS mRNA of the chronic tonsillitis lymphocytes was regarded as a positive control. The results were negative control when no probe was used.

### *Statistical anslysis*

All data were expressed as $\bar{x}\pm s$ and analyzed by SPSS statistic software. Differences in values were considered significant if $P<0.05$.

## RESULTS

### *mRNA expression of costimulatory molecules within tissues of human gastric carcinoma*

At the site of gastric carcinoma, positive cells for B7H1, B7H2, ICOS were mainly tumor infiltrating lymphocytes (Figure 1). Some positive cells were tumor cells. Their mRNA positive expression indexes were 0.512±0.333, 0.812±0.454 and 0.702±0.359, respectively. B7-1 mRNA was expressed on tumor cells and TILs (Figure 2), with a positive expression index being 0.293±0.253. The mRNA expression levels of B7H1, B7H2 and ICOS were significantly higher than that of B7-1( all $P<0.05$).

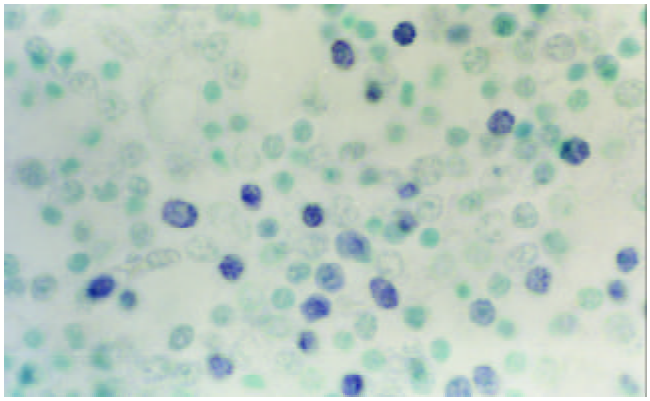

**Figure 1** B7H1 mRNA expression of tumor infiltrating lymphocytes (TILs) within tissues of human gastric carcinoma (*In situ* hybridization, NBT-BCIP Staining, counterstained with methyl green, ×1 000).

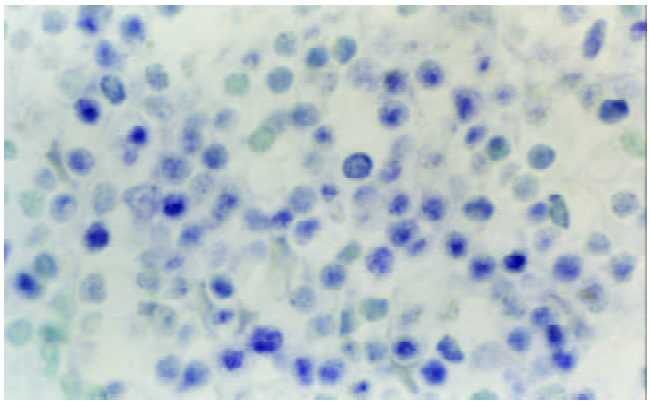

**Figure 2** B7-1 mRNA expression of tumor infiltrating lymphocytes (TILs) within tissues of human gastric carcinoma (*In situ* hybridization, NBT-BCIP Staining, counterstained with methyl green, ×1 000).

### *Expression of costimulatory molecules in relation to metastasis of gastric carcinoma*

The expression levels of B7-1, B7H1, B7H2 and ICOS had no statistical significance between metastasis and non-metastasis

of gastric carcinoma ($P$>0.05), which suggested that expressions of costimulatory molecules at tumor site were not correlated to the metastasis of tumor.

### *Expression of costimulatory molecules in relation to differentiation of gastric carcinoma*

mRNA expression levels of B7-1, B7H1 and ICOS on infiltrating lymphocytes at the tumor site was not significantly different between well-differentiated and poorly-differentiated. However, the expression level of B7H2 mRNA was significantly higher in well-differentiated than in poorly-differentiated (1.040±0.400 *vs* 0.651±0.436, $P$=0.047). mRNA expression of B7-1 was greatly lower than that of B7H1, B7H2 and ICOS in both well-differentiated and poorly-differentiated gastric carcinoma which might indicate that function of B7-1 was different from other costimulatory molecules in gastric carcinoma.

### *Expression of costimulatory molecules in comparison between gastric carcinoma and gastric ulcer*

In the tissue of gastric ulcer, the expression levels of B7-1, B7H1, B7H2 and ICOS on infiltrating lymphocytes were higher than those in gastric carcinoma. But there was no difference in the expression of B7H1, B7H2 and ICOS between the tissues of gastric carcinoma and gastric ulcer except B7-1. The effect of costimulators in the gastric ulcer was not clear.

## DISCUSSION

Cell-mediated immunity is the main mechanism of antitumor immunity of the host. With presentation of antigen identification and deepening of the understanding of T-cells activated, it is believed that in the presence of costimulatory signals, effective antitumor immune response presents tumor antigen multipeptide to T cells and stimulates T-cell immune response[16-18]. B7 is an important costimulatory molecule. Most tumors lack or have a low expression of B7-1, so they do not induce effective antitumor immune response. The tumor cells escape from immune system of the host and continue to grow. Though many *in vitro* experiments support this idea, *in situ* studies on human tumors have shown that most tumor tissues express the B7-1 or B7-2 molecules[19]. So the idea meets challenges.

The effective anti-tumor immune response requires three factors, including immunogenicity, costimulatory signals and Th1 type cytokines. In the past, it was emphasized that cytokines or/antigen essence determined the classification of immune responses. Generally, weak immunogenicity of tumor cells primarily induced Th2 response[20]. In recent years, studies on costimulatory signals *in vitro* have shown that different costimulatory signals play a determinant role in immune response type. There might be Th2 predominant costimulatory signals in human tumor site. The present study has detected mRNA expression of B7H1, B7H2 and ICOS within the tissue of human gastric carcinoma, using *in situ* hybridization with DIG-labeled oligonucleotide probes. The results suggest that tumor infiltrating lymphocytes in tissue of gastric carcinoma express high levels of recently discovered members of B7 costimulatory family, B7H1, B7H2 and ICOS[21-26]. Compared with mRNA expression level of B7-1, difference was dramatically significant. But mRNA expression levels of B7H1, B7H2 and ICOS were not correlated to the pathological grade and metastasis of gastric carcinoma. The experiments[27-35] *in vitro* have verified that the interaction between B7h and ICOS stimulates the proliferation of T-cells and production of Th2 cytokines, preferentially secretion of IL-10. This is probably the main reason that Th2 cytokines may predominate at the tumor immune- microenvironment of gastric carcinoma, and thus the type of immune response shifts from Th1 to Th2. There was an increase of Th2 cytokine-IL-10 in tumor immune-microenvironment of gastric carcinoma[36].

In this study, we have also observed the expression of B7-1 in the tissue of gastric carcinoma, and found that tumor infiltrating lymphocytes (TIL) and tumor cells expressed low gastric carcinoma levels of B7-1 mRNA. Now that there were costimulatory molecules in the tissues of gastric carcinoma, why did not the host produce the effective antitumor immune response? With the further study of immunology and tumor immunology, a new concept related to interaction between TIL and tumor cells was introduced. That is the tumor microenvironment. This theory supposes that immune system of the host cannot eliminate tumors because there are many inhibitors of tumor immunity at the site of tumor microenvironment. For example, tumor cells produce TGF-β, $PGE_2$ and so on, which are accumulated at tumor site and interfere with the activity of recruited immunocytes. Activated immunosuppressive cells further augment the immuno-depression mechanism in tumor microenvironment. In addition, a recent study[27] has shown that B7-1 costimulation also enhances the up-regulation effects of ICOS costimulation which results in the increase of Th2 cytokines, preferentially inducing the secretion of IL-10.

The present experimental results suggest that the tumor infiltrating lymphocytes in the tissues of gastric carcinoma express high levels of B7H1, B7H2 and ICOS mRNA. Some tumor cells also express them but the expression levels are low. This indicates that there are costimulatory signal pathways in the site of gastric carcinoma. Since the interaction between B7H1, B7H2 and ICOS stimulates proliferation of T cells by various ways and induces secretion of IL-10. IL-10 is known to be an immune inhibitor, which down-regulates function of Th1 type cells, and inhibits antitumor immune response of the body, and thus the body is in the state of immune inhibition. Therefore, it is supposed that although interaction between B7H1, B7H2 and ICOS delivers costimulatory signals to T-cells, promotes their activation, the effective antitumor immunity can not be induced. Tumor cells can escape from the immunosurveillance of the host and continue to grow. This is due to the fact that many inhibitors at tumor site have blocked the role of specifically activated T cells. As far as most tumors are concerned, the host' s immunoreaction can not eliminate the tumor because Th2 type response is stimulated, or it can be recognized by immune system of the body. Maybe there are other regulation mechanisms. The present study indicates that costimulatory pathways might exist at the tumor site with different functions. ICOS-B7h pathway is predominant and plays an important role in negative regulation of cell-mediated immune response. This finding might provide a new approach for designing effective immune-therapy of carcinoma.

## REFERENCES

1 **Ellis JH**, Burden MN, Vinogradov DV, Linge C, Crowe JS. Interactions of CD80 and CD86 with CD28 and CTLA4. *J Immunol* 1996; **156**: 2700-2709
2 **Guinan EC**, Gribben JG, Boussiotis VA, Freeman GJ, Nadler LM. Pivotal role of the B7:CD28 pathway in trans-plantation tolerant and tumor immunity. *Blood* 1994; 84: 3261-3282
3 **Ikemizu S**, Gilbert RJ, Fennelly JA, Collins AV, Harlos K, Jones EY, Stuart DI, Davis SJ. Structure and dimerization of a soluble form of B7-1. *Immunity* 2000; **12**: 51-60
4 **Hung K**, Hayashi R, Lafond-Walker A, Lowenstein C, Pardoll D, Levitsky H. The central role of $CD4^+$ T cells in the antitumor immune response. *J Exp Med* 1998; **188**: 2357-2368
5 **Ganss R**, Hanahan D. Tumor microenvironment can restrict the effectiveness of activated antitumor lymphocytes. *Cancer Res* 1998; **58**: 4673-4681
6 **Denfeld RW**, Dietrich A, Wuttig C, Tanczos E, Weiss JM,

Vanscheidt W, Schopf E, Simon JC. In situ expression of B7 and CD28 receptor families in human malignant melanoma: relevance for T cell-mediated anti-tumor immunity. *Int J Cancer* 1995; **62**: 259-265

7 **Salvadori S**, Martinelli G, Zier K. Resection of solid tumors reverses T cell defects and restores protective immunity. *J Immunol* 2000; **164**: 2214-2220

8 **Yu X**, Fournier S, Allison JP, Sharpe AH, Hodes RJ. The role of B7 costimulation in CD4/CD8 T cell homeostasis. *J Immunol* 2000; **164**: 3543-3553

9 **Martin-Fontecha A**, Moro M, Crosti MC, Veglia F, Casorati G, Dellabona P. Vaccination with mouse mammary adenocarcinoma cells coexpressing B7-1(CD80)and B7-2(CD86)discloses the dominant effect of B7-1 in the induction of antitumor immunity. *J Immunol* 2000; **164**: 698-704

10 **Kinoshita K**, Tesch G, Schwarting A, Maron R, Sharpe AH, Kelley VR. Costimulation by B7-1 and B7-2 is repaired for autoimmune disease in MRL-Fas mice. *J Immunol* 2000; **164**: 6046-6056

11 **Geldhof AB**, Raes G, Bakkus M, Devos S, Thielemans K, De Baetselier P. Expression of B7-1 by highly metastatic mouse T lymphomas induces optimal natural killer cell-mediated cytotoxicity. *Cancer Res* 1995; **55**: 2730-2733

12 **Huang M**, Wang J, Lee P, Sharma S, Mao JT, Meissner H, Uyemura K, Modlin R, Wollman J, Dubinett SM. Human non-small cell lung cancer cells express a type 2 cytokine pattern. *Cancer Res* 1995; **55**: 3847-3853

13 **Romagnani S**. The Th1/Th2 paradigm. *Immunol Today* 1997; **18**: 263-266

14 **Fujii H**, Inobe M, Kimura F, Murata J, Murakami M, Onishi Y, Azuma I, Uede T, Saiki I. Vaccination of tumor cells transfected with the B7-1(CD80)gene induces the antimetastatic effect and tumor immunity in mice. *Int J Cancer* 1996; **66**: 219-224

15 **Wu TC**, Huang AY, Jaffee EM, Levitsky HI, Pardoll DM. A reassessment of the role of B7-1 expression in tumor rejection. *J Exp Med* 1995; **182**: 1415-1421

16 **Judge TA**, Tang A, Turka LA. Immunosuppression through blockade of CD28:B7-mediated costimulatory signals. *Immunol Res* 1996; **15**: 38-49

17 **Hu JY**, Wang S, Zhu JG, Zhou GH, Sun QB. Expression of B7 costimulation molecules by colorectal cancer cells reducestumorigenicity and induces anti-tumor immunity. *World J Gastroenterol* 1999; **5**: 147-151

18 **Ren XF**, Luo KX. Expression of B7 and liver diseases. *Shijie Huaren Xiaohua Zazhi* 1999; **7**: 415-416

19 **Guo J,** Si L, Wang Y. An in situ study on immunostimulatory molecules in cancer cells within the cervical carcinoma tissues. *Zhonghua Yixue Zazhi* 2000; **80**: 342-345

20 **Song YJ**, Yang ZY, Dong JH. Th1/Th2 cells and immune tolerance of transplantation. *Shijie Huaren Xiaohua Zazhi* 2001; **9**: 794-796

21 **Dong H**, Zhu G, Tamada K, Chen L. B7H1, a third member of the B7 family, co-stimulates T cell proliferation and interleukin-10 secretion. *Nat Med* 1999; **5**: 1365-1369

22 **Wang S**, Zhu G, Chapoval AI, Dong H, Tamada K, Ni J, Chen L. Costimulation of T cells by B7-H2, a B7-like molecule that binds ICOS. *Blood* 2000; **96**: 2808-2813

23 **McAdam AJ**, Chang TT, Lumelsky AE, Greenfield EA, Boussiotis VA, Duke-Cohan JS, Chernova T, Malenkovich N, Jabs C, Kuchroo VK, Ling V, Collins M, Sharpe AH, Freeman GJ. Mouse inducible costimulatory molecule (ICOS) expression is enhanced by CD28 costimulation and regulate differentiation of $CD4^+$ T cells. *J Immunol* 2000; **165**: 5035-5040

24 **Dong C**, Juedes AE, Temann UA, Shresta S, Allison JP, Ruddle NH, Flavell RA. ICOS costimulatory receptor is essential for T-cell activation and function. *Nature* 2001; **409**: 97-101

25 **McAdam AJ**, Greenwald RJ, Levin MA, Chernova T, Malenkovich N, Ling V, Freeman GJ, Sharpe AH. ICOS is critical for CD40-mediated antibody class switching. *Nature* 2001; **409**: 102-105

26 **Tafuri A**, Shahinian A, Bladt F, Yoshinaga SK, Jordana M, Wakeham A, Boucher LM, Bouchard D, Chan VS, Duncan G, Odermatt B, Ho A, Itie A, Horan T, Whoriskey JS, Pawson T, Penninger JM, Ohashi PS, Mak TW. ICOS is essential for effetive T-helper-cell responses. *Nature* 2001; **409**: 105-109

27 **Hutloff A**, Dittrich AM, Beier KC, Eljaschewitsch B, Kraft R, Anagnostopoulos I, Kroczek RA. ICOS is an inducible T-cell co-stimulator structurally and functionally related to CD28. *Nature* 1999; **397**: 263-266

28 **Liu X**, Bai XF, Wen J, Gao JX, Liu J, Lu P, Wang Y, Zheng P, Liu Y. B7H costimulates clonal expansion of, and cognate destruction of tumor cells by, CD8(+) T lymphocytes *in vivo*. *J Exp Med* 2001; **194**: 1339-1348

29 **Guo J**, Stolina M, Bready JV, Yin S, Horan T, Yoshinaga SK, Senaldi G. Stimulatory effects of B7-related protein-1 on cellular and humoral immune responses in mice. *J Immunol* 2001; **166**: 5578-5584

30 **Riley JL**, Blair PJ, Musser JT, Abe R, Tezuka K, Tsuji T, June CH. ICOS costimulation requires IL-2 and can be prevented by CTLA-4 engagement. *J Immunol* 2001; **166**: 4943-4948

31 **Yoshinaga SK**, Whoriskey JS, Khare SD, Sarmiento U, Guo J, Horan T, Shih G, Zhang M, Coccia MA, Kohno T, Tafuri-Bladt A, Brankow D, Campbell P, Chang D, Chiu L, Dai T, Duncan G, Elliott GS, Hui A, McCabe SM, Scully S, Shahinian A, Shaklee CL, Van G, Mak TW. T-cell co-stimulation through B7RP-1 and ICOS. *Nature* 1999; **402**: 827-832

32 **Tamatani T**, Tezuka K, Hanzawa-Higuchi N. AILIM/ICOS: a novel lymphocyte adhesion molecule. *Int Immunol* 2000; **12**: 51-55

33 **Mages HW**, Hutloff A, Heuck C, Buchner K, Himmelbauer H, Oliveri F, Kroczek RA. Molecular cloning and characterization of murine ICOS and identification of B7h as ICOS ligand. *Eur J Immunol* 2000; **30**: 1040-1047

34 **Tamura H**, Dong H, Zhu G, Sica GL, Flies DB, Tamada K, Chen L. B7-H1 costimulation preferentially enhances CD28-independent T-helper cell function. *Blood* 2001; **97**: 1809-1816

35 **Beier KC,** Hutloff A, Dittrich AM, Heuck C, Rauch A, Buchner K, Ludewig B, Ochs HD, Mages HW, Kroczek RA. Induction, binding specificity and function of human ICOS. *Eur J Immunol* 2000; **30**: 3707-3717

36 **Liu P**, Si LS, Li R, Lai BC, Wang YL. Dynamic change of the local immune environment of human gastric carcinoma during the progress of this disease. *Xi'an Yike Daxue Xuebao* 2001; **22**: 408-410

**Edited by** Xia HHX and Wang XL

P.O.Box 2345, Beijing 100023,China
Fax: +86-10-85381893
E-mail: wjg@wjgnet.com www.wjgnet.com

World J Gastroenterol 2003;9(6):1374-1376
World Journal of Gastroenterology
Copyright ©2003 by The WJG Press ISSN 1007-9327

• BRIEF REPORTS •

# Late course accelerated hyperfractionated radiotherapy for clinical $T_{1-2}$ esophageal carcinoma

Kuai-Le Zhao, Yang Wang, Xue-Hui Shi

**Kuai-Le Zhao, Yang Wang, Xue-Hui Shi,** Department of Radiation Oncology, Cancer Hospital, Fudan University, Shanghai 200032, China
**Correspondence to:** Kuai-Le Zhao, Department of Radiation Oncology, Cancer Hospital, Fudan University, Shanghai 200032, China. kuaile_z@sina.com
**Telephone:** +86-21-64175590-3900
**Received:** 2002-11-06 **Accepted:** 2003-01-08

## Abstract

**AIM:** This retrospective study was designed to analyze the results and the failure patterns of late course accelerated hyperfractionated radiotherapy for clinical $T_{1-2}N_0M_0$ esophageal carcinoma.

**METHODS:** From Aug. 1994 to Feb. 2001, 56 patients with clinical $T_{1-2}$ esophageal carcinoma received late course accelerated hyperfractionated radiotherapy in Cancer Hospital, Fudan University. All patients had been histologically proven to have squamous cell carcinoma (SCC) and were diagnosed to be $T_{1-2}N_0M_0$ by CT scan. All patients were treated with conventional fractionation (CF) irradiation during the first two-thirds course of the treatment to a dose of about 41.4Gy/23fx/4 to 5 weeks, Which was then followed by accelerated hyperfractionation irradiation using reduced fields, twice daily at 1.5Gy per fraction, to a dose about 27Gy/18 fx. Thus the total dose was 67-70Gy/40-43fx/40-49 d.

**RESULTS:** The 1-, 3- and 5-year overall survival was 90.9 %, 54.6 %, 47.8 % respectively. The 1-, 3- and 5-year local control rate was 90.9 %, 84.5 % and 84.5 %, respectively. Twenty-five percent (14/56) patients had distant metastasis and/or lymph nodes metastasis alone. Eight point nine percent (5/56) patients had local disease alone. Another 3.6 % (2/56) patients had regional relapse and distant metastasis.

**CONCLUSION:** Late course accelerated hyperfractionated radiotherapy is effective on clinical $T_{1-2}$ esophageal carcinoma. The main failure pattern is distant metastasis.

Zhao KL, Wang Y, Shi XH. Late course accelerated hyperfractionated radiotherapy for clinical $T_{1-2}$ esophageal carcinoma. *World J Gastroenterol* 2003; 9(6): 1374-1376
http://www.wjgnet.com/1007-9327/9/1374.asp

## INTRODUCTION

Surgery has been the main treatment method for clinical $T_{1-2}$ esophageal carcinoma. But the treatment of upper thoracic esophageal carcinoma is challenging. The intimate relationship of the esophagus to the airway, arch of the aorta, and recurrent laryngeal nerve poses special technical problems. Radiotherapy is as effective as surgery, and preserves esophagus.

In 1988, Shi designed the schedule of late course accelerated hyperfractionated radiotherapy (LCAF) on SCC of the esophagus. The results were very encouraging. The 5-year survival and local control rate were markedly improved in the LCAF group. Compared with CF radiotherapy, the 5-year overall survival of 34 % versus 15 % was statistically significant, the local control rate was 55 % versus 21 %[1]. However, the outcome of clinical $T_{1-2}$ esophageal carcinoma treated with LCAF has not been investigated extensively. Therefore, we conducted a retrospective evaluation of clinical $T_{1-2}$ patients treated with LCAF.

## MATERIALS AND METHODS

### *Materials*

From August 1994 to February 2001, 56 patients with clinical $T_{1-2}N_0M_0$ SCC of esophagus were treated by LCAF radiotherapy in the Department of Radiation Oncology, Cancer Hospital, Fudan University. All patients had detailed medical records. Pretreatment evaluation generally included history and physical examination, complete blood cell count, chest radiograph, chest computed tomographic (CT) scan, esophageal barium examination, ultrasonic examination for abdomen, including liver, kidney, spleen, and retroperitoneal lymph nodes. All patients were restaged according to the TNM classification of the International Union Against Cancer (devised in 1997). The patients' eligibility for this study was as follows: (1) Primary lesion was single, and a flat plane separating the esophageal mass from the periesophageal structures was visible on all CT sections. (2) Mediastinal and upper abdominal lymph nodes were smaller than 5 mm on short-axis diameter. And (3) No supraclavicular lymph nodes and distant metastasis. The patients' clinical characteristics are listed in Table 1.

**Table 1** Pretreatment characteristics

| Characteristic | *n* | % |
|---|---|---|
| Age(years) | | |
| <65 | 30 | 53.6 |
| ≥65 | 26 | 46.4 |
| Median | 59.5 | |
| Range | 40-74 | |
| Gender | | |
| Male | 41 | 73.2 |
| Female | 15 | 26.8 |
| T stage | | |
| T1 | 2 | 3.7 |
| T2 | 54 | 96.3 |
| Site | | |
| Cervical | 2 | 3.6 |
| Upper-thoracic | 19 | 33.9 |
| Middle-thoracic | 34 | 60.7 |
| Lower-thoracic | 1 | 1.8 |
| Length (cm) | | |
| ≤5 | 25 | 44.6 |
| >5 | 31 | 55.4 |
| Median | 5.8 | |
| Range | 2.0-9.0 | |
| Thickness of wall (cm) | | |
| ≤1.5 | 42 | 75.0 |
| >1.5 | 14 | 25 |
| Median | 1.2 | |
| Range | 0.5-2.7 | |

### *Methods*

Radiation source was 6MV or 18 MV linear accelerator. The design of the radiation fields was based on the diagnosis by CT and barium examinations. For patients with lesions in cervical region, two anterior oblique fields with wedge filters were used. For patients with lesions in the thoracic a three-field approach was used: one anterior and two posterior oblique portals. The width of the fields was adjusted to cover gross tumor with 2 cm to 3 cm margins to include the subclinical lesions and the length of the field should cover clinical tumors with 3 cm to 5 cm extended margin at both ends of the lesion. All patients received 1.8Gy per fraction, five fractions a week during the first two thirds of the course of radiotherapy to a dose of about 41.4Gy/23fx/4 to 5 weeks. This was then followed by accelerated hyperfractionation using reducing fields, twice daily at 1.5Gy per fraction with a minimum interval of 6 hours between fractions. The dose contributed by the accelerated technique was about 27Gy. The total dose given to the clinical tumor was 67-70Gy/40-43fx/40-49d. No prophylactic irradiation was given to the supraclavicular region. Details of the schedule had been reported previously[1].

End-points in this analysis were overall survival and local control. Death from any cause was calculated from the date of radiotherapy until death or last follow-up evaluation. Patterns of failure were first failure (local, regional, or distant), time to any local failure, and time to any distant metastasis. If recurrences occurred within 60 days of each other, they were counted simultaneously. The time to these end points was calculated from the date of treatment until disease relapse or last follow-up.

Four patients were lost to follow-up. Median follow-up for the survival patients was 38.0 months (range 5-67 months), follow-up rate was 92.9 %.

The statistics was done by SPSS (Version 10.0). Survival rate and local control rate were estimated by the Kaplan-Meier method.

## RESULTS

### *Acute toxicities (RTOG)*

The incidence of grade 1, 2, 3 and 4 of acute radiation-induced bronchitis was 19.6 % (11/56), 17.9 % (10/56), 3.6 % (2/56), and 1.8 % (1/56), respectively. The incidence of grade 1, 2, 3 and 4 of acute radiation-induced esophagitis was 25.0 % (14/56), 46.4 % (26/56), 10.7 % (6/56), and 0 % (0 cases), respectively.

### *Late complications (SOMA)*

Three patients (53.6 %) developed grade 2 radiation-induced late esophageal stenosis, and one patient (1.8 %) developed grade 3 esophageal stenosis (the patient had required dilatation). One patient (1.8 %) developed grade 2 late pneumonary fibrosis. Two patients (3.6 %) died of late complications (1 case died of pneumonary fibrosis, 1 case died of myelitis).

### *Survival rates and local control rates*

The overall survival curve and the local control rates for all patients are shown in Figure 1, 2. The overall survival rate at 1-, 3- and 5-year was 90.9 %, 54.6 % and 47.8 %, respectively. The local control rate at 1-, 3- and 5-years was 90.9 %, 84.5 % and 84.5 %, respectively.

### *Failure patterns*

The patterns of first failure are listed in Table 2. The main first failures were local regional failure and distant metastasis (including lymph metastasis). Twenty-five percent (14/56) patients had distant metastasis and/or lymph nodes metastasis alone. Eight point nine percent (5/56) had local disease alone. Another 3.6 % (2/56) had local regional relapse and distant metastasis. The median local regional failure time was 9 months (rang: 0-18 months). The median distant metastasis time was 17.5 months (rang: 7-65 months).

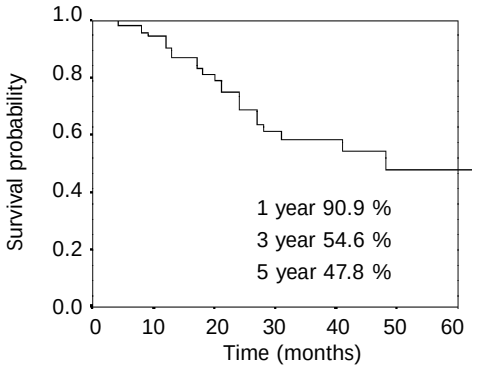


**Figure 1** The overall survival rates for clinical $T_{1-2}$ esophageal carcinoma treated with LCAF radiotherapy.

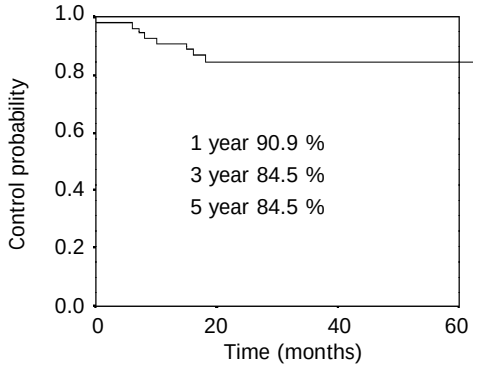


**Figure 2** The local control rates for clinical $T_{1-2}$ esophageal carcinoma treated by LCAF radiotherapy.

**Table 2** First treatment failures

| First failure | *n* | % |
|---|---|---|
| None | 31 | 55.4 |
| Local / regional only | 5 | 8.9 |
| Distant only | 14 | 25.0 |
| Local / regional / distant | 2 | 3.6 |
| Hemorrhage | 1 | 1.8 |
| Complications | 2 | 3.6 |
| Unknown | 1 | 1.8 |
| Total | 56 | 100 |

## DISCUSSION

Surgery is the main treatment for clinical $T_{1-2}$ esophageal carcinoma. In a nationwide surgical series from 1983 to 1987 in Japan[2], the survival rate of 127 patients with mucosal tumors was 92.26 % at 1 year, 81.09 % at 3 years, and 89.85 % at 5 years. A total of 533 patients with submucosal tumor had survival rate of 83.51 % at 1 year, 66.76 % at 3 years, and 59.66 % at 5 years. $T_1$ classification by UICC (1987) combines mucosal and submucosal tumors. Seven hundred forty patients with invasion to the muscularis propria, equal to $T_2$ by UICC classification, had survival rate of 69.86 % at 1 year, 41.88 % at 3 years, and 34.47 % at 5 years. Because a nearly total esophagectomy is often required, higher mortality and morbidity occur often. Orringer[3] reported 800 patients with cancer of the intrathoracic esophagus and cardia treated with transhiatal esophagectomy. Major complications included

anastomotic leaks (13 %), recurrent laryngeal nerve injury (7 %), wound infection (3 %), pulmonary complications (2 %), bleeding (1 %), and chylothorax (1 %). More than 90 % of patients were discharged within 21 days of hospitalization. Complications were more severe in the patients with carcinoma of upper thoracic esophagus. The operation of upper thoracic esophageal cancer is challenging. The intimate relationship of the esophagus to the airway, arch of the aorta, and recurrent laryngeal nerve poses special technical problems. The survival rate is often lower, and the mortality and morbidity are often higher. Vigneswaran[4] reported 49 patients treated with extended esophagectomy. There was one postoperative death (2.0 %). Fifteen patients (30.6 %) had a cervical anastomotic leak, and all occurred in patients with a gastric conduit. Leaks occurred in 5 of 10 (50 %) substernally placed stomachs and in 10 of 36 (27.7 %) transposed through the esophageal bed. Wound infection occurred in five patients. Postoperative vocal cord paralysis developed in 11 patients (22.4 %) and was unilateral in 10 and bilateral in one. Six patients developed pulmonary complications. Ten patients (20.8 %) developed mild to severe late dysphagia, which was a result of benign stenosis in eight patients and recurrent carcinoma in two. Four patients required dilatations.

Chemoradiotherapy has been widely used in Western countries. Reports on definitive chemoradiotherapy for clinical $T_{1-2}$ esophageal carcinoma are few. Zenone *et al*. concluded that the combined multimodality therapy, might be an alternative to radical surgery, based on 5-year survival of 56.3 % for $T_1$ patients and 29.8 % for $T_2$ patients[5]. Roca *et al*. also suggested the feasibility of organ preservation in a report using intensive chemoradiotherapy[7]. Murakami *et al* reported in a randomized study comparing chemoradiation with surgery that overall 1- and 3-year survival rates were 100 % and 83 % in the $T_1$/protocol group versus 82 % and 72 % in the $T_1$/surgery group ($P$=0.36), and 100 % and 51 % in the $T_2$/protocol group, versus 95 % and 68 % in the $T_2$/surgery group ($P$=0.61), respectively. There was no treatment-related mortality in either group. The rate of esophageal conservation was 92 % in the $T_1$/protocol group and 58 % in the $T_2$/protocol group[2]. These results indicate that chemoradiation for clinical $T_{1-2}$ patients is a feasible radical treatment. However, there has been no report that compares surgery and chemoradiotherapy. Although there was a significant improvement in local control and overall survival with combined multimodality therapy compared with radiation therapy alone, the combined treatment had more severe and life-threatening hematologic side effects. Grade 3-5 acute toxicity was seen in 64 % of patients treated by concurrent chemoradiotherapy, much higher than 28 % in patients treated by radiotherapy alone. Approximately 80 % of patients completed chemotherapy according to the protocol guidelines.

In China, Shi[1] modified the concomitant boost schedule designed by Anderson Cancer Center to LCAF radiotherapy on SCC of the esophagus. The results were very encouraging. The 5-year survival and local control rate were markedly improved in the LCAF group. Compared with CF radiotherapy, the 5-year overall survival was 34 % versus 15 % which was statistically significant, the local control rate was 55 % versus 21 %. Henceforth, more randomized and retrospective trials confirmed the results[7-9]. LCAF radiotherapy is the most frequently used radiotherapeutic management for localized SCC of esophageal carcinoma in some cancer hospitals in China including our department.

The survival rate and local control rate are comparable with operation and chemoradiotherapy in the patients treated with LCAF radiotherapy alone. Esophagus can be preserved, and the severe complications can be decreased. In the retrospective study, most patients were clinical stage $T_2N_0M_0$, at upper thoracic and middle thoracic. The 5-year survival rate was 47. 8 %, and the 5-year local control rate was 84.5 %. Grade 3-5 acute radiation-induced toxicities were 16.1 %. The incidence of grade 3-5 late complications was 7.0 %.

In analyzing failure patterns, there was significant difference between the patients in early-stage and advanced-stage. Local/ regional recurrence was the main reason of failure in the advanced patients treated with conventional radiotherapy. Forty-two percent patients died of local recurrence, and nineteen percent patients died of metastasis in the advanced patients treated with LCAF radiotherapy[1]. Forty-five percent patients had local regional disease as the first failure, distant metastasis as the first failure occurred in 13 % of concurrent chemoradiotherapy[2]. In our retrospective study, distant metastasis rate (28.6 %) increased significantly, and local regional recurrent rate (12.5 %) decreased markedly.

## REFERENCES


1 **Shi XH**, Yao WQ, Lui TF. Late course accelerated fractionation in radiotherapy of esophageal carcinoma. *Radiother Oncol* 1999; **51**: 21-26

2 **Murakami M**, Kuroda Y, Nakajima T, Okamoto Y, Mizowaki T, Kusumi F, Hajiro K, Nishimura S, Matsusue S, Takeda H. Comparison between chemoradiation protocol intended for organ preservation and conventional surgery for clinical T1-T2 esophageal carcinoma. *Int J Radiat Oncol Biol Phys* 1999; **45**: 277-284

3 **Orringer MB**, Marshall B, Iannettoni MD. Transhiatal esophagectomy: clinical experience and refinements. *Ann Surg* 1999; **230**: 392-400

4 **Vigneswaran WT**, Trastek VF, Pairolero PC, Deschamps C, Daly RC, Allen MS. Extended esophagectomy in the management of carcinoma of the upper thoracic esophagus. *J Thorac Cardiovascular Surg* 1994; **107**: 901-907

5 **Zenone T**, Romestaing P, Lambert R, Gerard JP. Curative non-surgical combined treatment of squamous cell carcinoma of the Oesophagus. *Eur J Cancer* 1992; **28A**: 1380–1386

6 **Roca E**, Pennella E, Sardi M, Carraro S, Barugel M, Milano C, Fiorini A, Giglio R, Gonzalez G, Kneitschel R, Aman E, Jarentchuk A, Blajman C, Nadal J, Santarelli MT, Navigante A. Combined intensive chemoradiotherapy for organ preservation in patients with resectable and non-resectable oesophageal cancer. *Eur J Cancer* 1996; **32A**: 429–432

7 **Wang WD**. Conventional radiotherapy boosted with late course hyperfractionation in patient with esophageal cancer (abstr.). *Zhonghua Fangshe Zhongliuxue Zazhi* 2001; **10**: 30

8 **Wang Y,** Shi XH, He SQ, Yao WQ, Wang Y, Guo XM, Wu GD, Zhu LX, Liu TF. Comparison between continuous accelerated hyperfractionated and late-course accelerated hyperfractionated radiotherapy for esophageal carcinoma. *Int J Radiat Oncol Biol Phys* 2002; **54**: 131-136

9 **Zhao KL**, Wang Y, Shi XH. Analysis of outcome and failure reasons of late accelerated hyperfrationation radiotherapy for esophageal carcinoma. *Zhonghua Fangshe Zhongliuxue Zazhi* 2000; **10**: 14-16


**Edited by** Wen CY

P.O.Box 2345, Beijing 100023,China
Fax: +86-10-85381893
E-mail: wjg@wjgnet.com www.wjgnet.com

World J Gastroenterol 2003;9(6):1377-1380
World Journal of Gastroenterology
Copyright ©2003 by The WJG Press ISSN 1007-9327

• CASE REPORT •

# Multiple immune disorders in unrecognized celiac disease: a case report

Giorgio La Villa, Pietro Pantaleo, Roberto Tarquini, Lino Cirami, Federico Perfetto, Francesco Mancuso, Giacomo Laffi

**Giorgio La Villa, Pietro Pantaleo, Roberto Tarquini, Federico Perfetto, Francesco Mancuso, Giacomo Laffi**, Dipartimento di Medicina Interna, Università degli Studi di Firenze, Firenze, Italia
**Lino Cirami**, Unità Operativa di Nefrologia, Dialisi e Trapianto, Azienda Ospedaliera Careggi, Firenze, Italia
**Supported by** grants from the Ministero dell' Istruzione, dell' Università e della Ricerca and the University of Florence
**Correspondence to:** Giacomo Laffi, MD, Department of Internal Medicine, University of Florence School of Medicine, viale Morgagni, 85 - 50134 Firenze, Italy. g.laffi@dmi.unifi.it
**Telephone:** +39-55-4296538 **Fax**: +39-55-417123
**Received:** 2002-11-26 **Accepted:** 2002-12-22

## Abstract

We reported a female patient with unrecognized celiac disease and multiple extra intestinal manifestations, mainly related to a deranged immune function, including macroamilasemia, macrolipasemia, IgA nephropathy, thyroiditis, and anti-b2-glicoprotein-1 antibodies, that disappeared or improved after the implementation of a gluten-free diet.

La Villa G, Pantaleo P, Tarquini R, Cirami L, Perfetto F, Mancuso F, Laffi G. Multiple immune disorders in unrecognized celiac disease: a case report. *World J Gastroenterol* 2003; 9(6): 1377-1380
http://www.wjgnet.com/1007-9327/9/1377.asp

## INTRODUCTION

Celiac disease (CD), the most common life-long food sensitive enteropathy in humans, is characterized by malabsorption, chronic inflammation of small intestine mucosa, villous atrophy and crypt hyperplasia, which occur as a consequence of the ingestion of wheat gluten or related rye and barley proteins[1, 2]. CD is strongly associated with HLA-DQ2, coded by the DQA1*0501 and DQB1*02 alleles, and/or the DQ8 (DQA1*03, DQB1*0302 alleles), but a role of non-HLA genes has also been postulated[2,3]. The current prevalence of celiac disease has increased from 1:1 000 to 1:300 inhabitants, or even more[4]. Typical symptoms include chronic diarrhea, abdominal distension, and failure to thrive[2,5]. However, only few patients with CD show clinical malabsorption, while most patients have subtle symptoms, if any[6]. Therefore, the disease is clearly under diagnosed[2,7]. The recent introduction of tests for IgA anti-endomysial antibodies and the anti-tissue transglutaminase test has proved promising with a sensitivity and specificity of over 95 %[2, 8, 9].

Celiac disease may be associated with a wide range of diseases[2, 8], including thyroid, dermatological and lympho-proliferative disorders, mainly intestinal lymphomas[2]. Furthermore, there is a greater than expected prevalence of immune disorders in CD patients[2, 10-12] as well as of CD in patients with autoimmune diseases[13-15].

The current report dealed with a female patient with unrecognized CD and recurrent miscarriage, macroamilasemia, macrolipasemia, IgA nephropathy, and thyroiditis that disappeared or improved when a correct diagnosis was made and the patient was given a gluten-free diet.

## CASE REPORT

A 34 years old, non drinker, non smoking woman, was admitted to the third Medical Clinic, Careggi University Hospital, Florence because of hyper-amilasemia and hyper-lipasemia of unknown origin. The patient had acute meningitis at the age of three. At age of 23, she was admitted to hospital because of syncope, referred to acute gastroenteritis complicated by metabolic acidosis; laboratory evaluation performed on that occasion showed iron deficient anemia, polyclonal hypergammaglobulinemia, elevated erythrocyte sedimentation rate (ESR), reduced C3 levels and circulating antinuclear antibodies (1:80), that led to suspicion of a not otherwise specified collagen disease. Iron deficiency was unresponsive to supplement of oral iron, while it improved following intravenous therapy. The patient had two spontaneous abortions when aged 30 and 31 years, respectively, both at the 16$^{th}$ week of gestation. During admission because of the second abortion, a thorough investigation was performed that was negative for potential causes of fetal demise, including fasting glucose, basal FSH, LH and estradiol levels on day 3 of a natural cycle, TSH and prolactin levels, antinuclear antibodies, antibodies against infectious agents, hysterosalpingography and genetic karyotyping of the couple. On that occasion, she was found to have hyperamilasemia and hyperlipasemia, together with the previously reported laboratory alterations; so further investigations were performed including CT, which turned out to be negative for any pancreatic disease.

At the time of admission to our hospital unit, physical examination was completely negative. Routine blood analysis showed anemia (Ht: 32.8 %, Hb: 11.2 g/dL), thrombocytosis (452 000 platelets/mL), high ESR (124 mm/h), low plasma albumin (3.05 g/dL), and high levels of IgA (1 100 mg/dL) and IgM (369 mg/dL) with no monoclonal component. The patient also had low ferritin (<9 mg/mL) and tetrahydrofolate levels (1.9 ng/ml; normal range 3-17 ng/mL). A coagulation study showed the presence of lupus anticoagulant (Table 1). Enzyme studies confirmed a remarkable increase of serum amylase (1 196 IU/L), pancreatic isoamylase fraction (798 IU/L), and serum lipase (1 650 IU/L). On the other hand, urinary amylase excretion was normal (120, normal value <1 500 IU/day), and ultrasound examination of the pancreas was normal. A chromatographic assay was therefore performed at another Institution (Ospedali Riuniti, Padova, Italy), which demonstrated the presence of macroamylasemia and macrolipasemia.

Our patient had iron-deficient anemia, which was refractory to oral iron supplementation, a well known presenting sign of CD[2, 6, 16], together with low albumin and tetrahydrofolate levels. In addition, she had macroamylasemia and macrolipasemia which could be associated with CD[17]. Therefore, a search was performed for circulating anti-gliadin, anti-endomysial and anti-transglutaminase (TTG) antibodies. Detection of these antibodies (Table 1) led us to perform upper gastrointestinal tract endoscopy and duodenal biopsy, which confirmed the diagnosis of CD. A gluten free diet was therefore introduced.

Due to the patient's clinical history of repeated abortions and the results of coagulation studies, other autoantibodies such as anti-thyreoglobulin (1:40) and anti-β2-glicoprotein-1 antibodies (24 UI/mL) were detected. Further characterization of the latter antibodies showed that IgG was 6.3 (normal range < 9) and IgM 48.7 (normal range < 5) IU/mL. All parameters of thyroid function were within the normal range.

Urinalysis showed glomerular proteinuria (0.7 g/day), microscopic hematuria, hyaline and granular casts; creatinine clearance (74 mL/min) was reduced with respect to the patient's age. These results raised the suspicion of IgA nephropathy, but the patient did not consent to undergo kidney biopsy. HLA analysis revealed the presence of HLA DQB1*-02. The main laboratory data during the first admission at our unit and the follow up are shown in Table 1.

**Table 1** Main results of laboratory studies in baseline conditions and after implementation of gluten free diet

| Parameter (normal values) | Baseline determinations | Gluten free diet | |
|---|---|---|---|
| | | 6th month | 24th month |
| Serum amylase (IU/L) (< 220) | 1196 | 146 | 132 |
| Serum lipase (UI/L) (< 200) | 1650 | 39 | ND |
| Ig A (mg/dL) (60-318) | 1100 | 119 | 155 |
| Immunocomplexes (meq/mL) (< 5) | 6.5 | ND | ND |
| Antigliadin antibodies IgA (%) (< 7) | 96.9 | 5.8 | ND |
| Antigliadin antibodies IgG (%) (< 12) | 61 | 18.5 | ND |
| Antiendomysial antibodies | Positive | Positive | ND |
| Anti-transglutaminase antibodies (UI/L) (<8) | 20.5 | ND | ND |
| Anti-thyreoglobulin antibodies (ND) | 1:40 | ND | ND |
| Total b2 GP 1 antibodies (IU/mL) (< 4 IU/mL) | 24 | ND | ND |
| Lupus anticoagulant | Positive | ND | ND |
| Creatinine clearance (mL/min) (70-120 mL/min) | 74.07 | 88.05 | 107 |
| Protein excretion rate (mg/24h) | 322 | 2268 | 320 |

IU=international units; ND=not detectable.

After six months of controlled gluten free diet, the patient's body weight increased 12 kg; laboratory investigations demonstrated normalization of serum amylase, serum lipase and immunoglobulin levels; antigliadin, anti-β2-glicoprotein-1 and anti-thyreoglobulin antibodies were no longer detectable, but antiendomysial antibodies were still present. Endoscopy showed a normal appearance of duodenal mucosa, and duodenal biopsy revealed a partial recovery of duodenal morphology. Due to the persistence of proteinuria (2.3 g/day), microscopic hematuria and hyaline and granular casts, a kidney biopsy showed that it was IgA nephropathy.

After 18 months of gluten-free diet, antiendomysial antibodies disappeared; creatinine clearance increased (Table 1), but proteinuria further worsened (2.9 g/day, Table 1), and albumin levels were still low.

After 24 months of gluten-free diet, a new duodenal biopsy showed complete recovery of villous architecture. Renal function further improved and proteinuria markedly decreased (Table 1). Amylase, lipase, and immunoglobulin levels were within the normal range. Anti-β2-glicoprotein-1, anti-thyreoglobulin, antigliadin, antiendomysial and anti-TTG antibodies were undetectable. A coagulation study was normal (Table 1).

## DISCUSSION

The increased prevalence of immune disorders in patients with CD is well recognized[2, 10-12]. The association between CD and other immune disorders may be due to the sharing of a common genetic background, such as HLA antigens. However, in a very large study, involving 909 patients with celiac disease, Ventura and his associates[12] found that the development of immune disorders in CD was clearly related to the duration of exposure to gluten. It is also interesting to note that multiple immune diseases in CD patients are uncommon. In the study of Ventura *et al.*[12], only 15/909 patients had two kinds of immune manifestations and only one patient had three kinds of immune manifestations.

In this report, we described a female patient with unrecognized CD, who developed several clinical and/or sub clinical immune diseases.

Macroamylasemia with or without macrolipasemia occurs in approximately 0.4 % of general population and about 2.5-5.9 % of patients have hyperamylasemia[18, 19]. It may be either an isolated, benign condition without pathological significance or may be associated with underlying diseases such as lymphoma, AIDS, carcinoma, liver disease and autoimmune disorders. The macroamylase complex is formed by amylase bound with serum proteins, commonly IgG and/or IgA. This molecule is too large to be filtered by the kidney and excreted in the urine, so it accumulates in plasma, whereas urinary amylase is normal or even low, a finding that should point to the correct diagnosis. Similarly, the macrolipase complex is a macroenzyme formed by association of polyclonal IgA with lipase. The incidental finding of macroamylasemia, if unrecognized, directs the diagnostic work-up to the pancreas and patients undergo unnecessary examinations and even surgery. Some case reports dealed with the occurrence of macroamylasemia with or without macrolipasemia in adult and pediatric patients with CD [20-23]; in the large study by Rabsztyn *et al.*[17], 21 out of 124 newly diagnosed CD patients (16.9 %) had macroamylasemia. Interestingly, serum macroamylase usually remained elevated despite strict gluten free diet[17], and only in few cases, macroamylasemia and macrolipasemia disappeared after gluten free diet[22, 23], as it occurred in our patient.

IgA nephropathy is the most common glomerulonephritis and is considered a relatively benign disease. However, longitudinal follow-up studies demonstrated that about 20 % of patients would progress to end stage of renal disease within 20 years from its onset. Patients with IgA nephropathy often have circulating IgA-antigliadin antibodies. However, lack of IgA-antireticulin, IgA-antiendomysium antibodies or jejunal mucosal atrophy suggests that most of these patients do not have latent CD [24-26]. On the other hand, oral immunization with gliadin can induce IgA nephropathy in mice[27]. Data on the association between CD and IgA nephropathy in humans are controversial, and only few cases of IgA nephropathy had definite CD and showed remission or improvement of renal disease after gluten withdrawal[28, 29]. In our patient, the effect of gluten free diet on proteinuria was delayed, since this parameter showed increments at the 6th and the 18th month, despite the disappearance of antigliadin antibodies and normalization of IgA levels.

Patients with insulin-dependent diabetes mellitus, autoimmune thyroid disease, Addison's disease, and alopecia aerata are at increased risk of CD. A recent study addressed whether patients

with more than one autoimmune endocrine disorder were even more susceptible to CD or had celiac-type mucosal inflammation. Seven out of the 62 patients studied (11 %) were found to have CD; in addition, 2 had minor villous deterioration and 5 had an increased density of mucosal intraepithelial gamma-delta+ T-cells. HLA-DQ2 or DQ8 alleles were found in all subjects with mucosal changes[30]. The association of CD with autoimmune thyroiditis has been proved. A study in 172 patients with autoimmune thyroiditis found a 10-fold higher prevalence of CD in this population than expected[31]. The Authors concluded that the association of CD with autoimmune thyroid disease was not surprising as they shared common immunopathogenesis and suggested that it was advisable to screen patients with autoimmune thyroid disease for CD as there might be an increased risk for gluten intolerance[31]. In our patient, anti-thyreoglobulin antibodies disappeared after six month of gluten free diet. This finding confirmed that autoimmune thyroid disease and CD may share a common pathogenetic mechanism and that the disappearance of the immunological activation due to intestinal inflammation may lead to normalization of concomitant immune disorders.

Antiphospholipid antibodies, the most commonly detected of which are lupus anticoagulant, anticardiolipin and anti-β2-glycoprotein-1 antibodies, are associated with the so-called antiphospholipid syndrome, a syndrome of arterial and venous thrombotic disease, thrombocytopenia, and fetal wastage[32, 33]. Antiphospholipid antibodies are found in young, apparently healthy subjects with a prevalence of 1-5 %. Their prevalence increases with age, especially among elderly patients with coexistent chronic diseases, and is even higher in patients with autoimmune diseases. Untreated patients with CD also have an increased prevalence (about 14 %) of anticardiolipin antibodies[34, 35], a phenomenon that Di Sabatino *et al.*[35] found that an increased susceptibility of peripheral blood lymphocytes would undergo Fas-mediated apoptosis which resulted in immunogenic exposure of phospholipids with subsequent production of autoantibodies. As we know, lupus anticoagulant was observed in one patient[36], while the female patient reported here had both lupus anticoagulant and anti-β2-glycoprotein I antibodies which disappeared within 6 months after the introduction of gluten free diet.

Untreated CD in women resulted in a 8.9-fold increase in the relative risk of pregnancy miscarriage and in an about 30 % reduction of the baby's birth weight. Both miscarriage frequency and babies' low birth weight would normalize in response to gluten free diet[37, 38]. Antiphospholipid antibodies were also associated with an unusually high proportion of pregnancy losses after the 10$^{th}$ week of gestation[32, 33]. Our patient therefore had two different risk factors for abortion, both related to untreated CD. Unfortunately, it was not possible to establish whether the gluten-free diet corrected her miscarriage tendency, since until now the patient did not wish to plan a new pregnancy.

In conclusion, we found a high prevalence of immune diseases and a large number of organ-specific autoantibodies in a patient with CD. Although both CD and the other manifestations of a deranged immunity might be explained on the basis of a common genetic predisposition to this kind of disorders, some findings suggest that CD itself is responsible for the initiation of the immunological response. Indeed, persistent stimulation by some proinflammatory cytokines, such as interferon γ and tumor necrosis factor α, could induce further processing of autoantigens and their presentation to T lymphocytes by macrophage-type immunocompetent cells. As a matter of fact, the prevalence of immune diseases among patients with CD seems proportional to the time of exposure to gluten[12], and many immune alterations disappear following the recognition of CD and appropriate treatment, just as it occurred in our patient.

## ACKNOWLEDGEMENT

The authors gratefully acknowledged Rosanna Abbate, MD (Dipartimento dell' area critica medico-chirurgica) and Antonio Calabrò, MD (Dipartimento di Fisiopatologia clinica, University of Florence), for their kind help in revising the manuscript.

## REFERENCES

1 **Cook HB**, Burt MJ, Collett JA, Whitehead MR, Frampton CM, Chapman BA. Adult coeliac disease: prevalence and clinical significance. *J Gastroenterol Hepatol* 2000; **15**: 1032-1036
2 **Farrell RJ**, Kelly CP. Celiac sprue. *New Eng J Med* 2002; **346**: 180-188
3 **Badenhoop K,** Dieterich W, Segni M, Hofmann S, Hufner M, Usadel KH, Hahn EG, Schuppan D. HLA DQ2 and/or DQ8 is associated with celiac disease-specific autoantibodies to tissue transglutaminase in families with thyroid autoimmunity. *Am J Gastroenterol* 2001; **96**: 1648-1649
4 **Hernell O**, Ivarsson A, Persson LA. Coeliac disease: effect of early feeding on the incidence of the disease. *Early Hum Dev* 2001; **65** (Suppl): S153-160
5 **Kennedy NP**, Feighery C. Clinical features of coeliac disease today. *Biomed Pharmacother* 2000; **54**: 373-380
6 **Fasano A**, Catassi C. Current approaches to diagnosis and treatment of celiac disease: an evolving spectrum. *Gastroenterology* 2001; **120**: 635-651
7 **Troncone R**, Greco L, Auricchio S. The controversial epidemiology of coeliac disease. *Acta Paediatr* 2000; **89**: 140-141
8 **Koop I**, Ilchmann R, Izzi L, Adragna A, Koop H, Barthelmes H. Detection of autoantibodies against tissue transglutaminase in patients with celiac disease and dermatitis herpetiformis. *Am J Gastroenterol* 2000; **95**: 2009-2014
9 **Gillett HR**, Freeman HJ. Serological testing in screening for adult celiac disease. *Can J Gastroenterol* 1999; **13**: 265-269
10 **Cooper BT**, Holmes GKT, Cooke WT. Coeliac disease and immunological disorders. *Br Med J* 1978; **1**: 537-539
11 **Collin P**, Reunala T, Pukkala E, Lappala P, Keyrilainen O, Pasternack A. Coeliac disease-associated disorders and survival. *Gut* 1994; **35**: 1215-1218
12 **Ventura A**, Magazzù G, Greco L. Duration of exposure to gluten and risk for autoimmune disorders in patients with celiac disease. *Gastroenterology* 1999; **117**: 297-303
13 **Collin P**, Salmi J, Hallstrom O, Oksa H, Oksala H, Maki M, Reunala T. High frequency of coeliac disease in adult patients with type-I diabetes. *Scand J Gastroenterol* 1989; **24**: 81-84
14 **Pocecco M**, Ventura A. Coeliac disease and insulin-dependent diabetes mellitus: a causal association. An Italian multicentre study. *Acta Paediatr* 1995; **84**: 1432-1433
15 **Lepore L**, Martelossi S, Pennesi M, Falcini F, Ermini ML, Ferrari R, Perticarari S, Presani G, Lucchesi A, Lapini M, Ventura A. Prevalence of coeliac disease in patients with juvenile chronic arthritis. *J Pediatr* 1996; **129**: 311-313
16 **Carroccio A**, Iannitto E, Montalto G, Tumminiello M, Campagna P, Lipari MG, Notarbartolo A, Iacono G. Sideropenic anemia and celiac disease: one study, two points of view. *Dig Dis Sci* 1998; **43**: 673-678
17 **Rabsztyn A**, Green PH, Berti I, Fasano A, Perman JA, Horvath K. Macroamylasemia in patients with celiac disease. *Am J Gastroenterol* 2001; **96**: 1096-1100
18 **Quilez C**, Martinez J, Gomez A, Trigo C, Palazon JM, Belda G, Perez-Mateo M. Chronic elevation of enzymes of pancreatic origin in asymptomatic patients. *Gastroenterol Hepatol* 1998; **21**: 209-211
19 **Yoshida E**, Tsuruoka T, Suzuki M, Asahara M, Okazaki T, Kadohno N, Kanno T. Sex and age distribution of patients with macroamylasemia found in the daily isoenzyme analysis. *Rinsho Byori* 1998; **46**: 473-478
20 **Rajvanshi P**, Chowdhury JR, Gupta S. Celiac sprue and macroamylasemia: potential clinical and pathophysiological implications. Case study. *J Clin Gastroenterol* 1995; **20**: 304-306

21 **Garcia-Gonzalez M**, Defarges-Pons V, Monescillo A, Hernandez F, Cano-Ruiz A. Macrolipasemia and celiac disease. *Am J Gastroenterol* 1995; **90**: 2233-2234

22 **Bonetti G**, Serricchio G, Giudici A, Bettonagli M, Vadacca GB, Bruno R, Coslovich E, Moratti R. Hyperamylasemia due to macroamylasemia in adult gluten enteropathy. *Scand J Clin Lab Invest* 1997; **57**: 271-273

23 **Barera G**, Bazzigaluppi E, Viscardi M, Renzetti F, Bianchi C, Chiumello G, Bosi E. Macroamylasemia attributable to gluten-related amylase autoantibodies: a case report. *Pediatrics* 2001; **107**: E93

24 **Rostoker G**, Laurent J, Andre C, Cholin S, Lagrue G. High levels of IgA antigliadin antibodies in patients who have IgA mesangial glomerulonephritis but not coeliac disease (letter). *Lancet* 1988; **1**: 356-357

25 **Sategna-Guidetti C**, Ferfoglia G, Bruno M, Pulitano R, Roccatello D, Amore A, Coppo R. Do IgA antigliadin and IgA antiendomysium antibodies show there is latent coeliac disease in primary IgA nephropathy? *Gut* 1992; **33**: 476-478

26 **Ots M**, Uibo O, Metskula K, Uibo R, Salupere V. IgA-antigliadin antibodies in patients with IgA nephropathy: the secondary phenomenon? *Am J Nephrol* 1999; **19**: 453-458

27 **Amore A**, Emancipator SN, Roccatello D, Gianoglio B, Peruzzi L, Porcellini MG, Piccoli G, Coppo R. Functional consequences of the binding of gliadin to cultured rat mesangial cells: bridging immunoglobulin A to cells and modulation of eicosanoid synthesis and altered cytokine production. *Am J Kidney Dis* 1994; **23**: 290-301

28 **Fornasieri A**, Sinico RA, Maldifassi P, Bernasconi P, Vegni M, D'Amico G. IgA-antigliadin antibodies in IgA mesangial nephropathy (Berger's disease). *Br Med J* 1987; **295**: 78-80

29 **Woodrow G**, Innes A, Boyd SM, Burden RP. A case of IgA nephropathy with coeliac disease responding to a gluten-free diet. *Nephrol Dial Transplant* 1993; **8**: 1382-1383

30 **Kaukinen K**, Collin P, Mykkanen AH, Partanen J, Maki M, Salmi J. Celiac disease and autoimmune endocrinologic disorders. *Dig Dis Sci* 1999; **44**: 1428-1433

31 **Berti I**, Trevisiol C, Tommasini A, Citta A, Neri E, Geatti O, Giammarini A, Ventura A, Not T. Usefulness of screening program for celiac disease in autoimmune thyroiditis. *Dig Dis Sci* 2000; **45**: 403-406

32 **Levine JS**, Branch DW, Rauch J. The antiphospholipid sindrome. *New Eng J Med* 2002; **346**: 752-763

33 **Stone S**, Khamashta MA, Poston L. Placentation, antiphospholipid syndrome and pregnancy outcome. *Lupus* 2001; **10**: 67-74

34 **Lerner A**, Blank M, Lahat N, Shoenfeld Y. Increased prevalence of autoantibodies in coeliac disease. *Dig Dis Sci* 1998; **43**: 723-726

35 **Di Sabatino A**, D'Alò S, Millimaggi D, Ciccocioppo R, Parroni R, Sciarpa G, Cifone MG. Apoptosis and peripheral blood lymphocyte depletion in coeliac disease. *Immunology* 2001; **103**: 435-440

36 **Chiurazzi F**, Poggi V, Greco L, Rotoli B. Lupus anticoagulant and coeliac disease: a case report. *Haematologica* 1987; **72**: 357-359

37 **Hozyasz KK**. Pregnancy outcomes in celiac women. *Am J Gastroenterol* 2000; **95**: 1373-1374

38 **Norgard B**, Fonager K, Sorensen HT, Olsen J. Birth outcomes of women with celiac disease: a nationwide historical cohort study. *Am J Gastroenterol* 1999; **94**: 2435-2440


**Edited by** Xu XQ

P.O.Box 2345, Beijing 100023,China
Fax: +86-10-85381893
E-mail: wjg@wjgnet.com www.wjgnet.com

World J Gastroenterol 2003;9(6):1381-1384
World Journal of Gastroenterology
Copyright ©2003 by The WJG Press ISSN 1007-9327

• CASE REPORT •

# Hepato-splenic lymphoma: a rare entity mimicking acute hepatitis: A case report

Federico Perfetto, Roberto Tarquini, Francesco Mancuso, Simonetta di Lollo, Silvia Tozzini, Giampiero Bellesi, Giacomo Laffi

**Federico Perfetto, Roberto Tarquini, Francesco Mancuso, Giacomo Laffi,** Department of Internal Medicine, University of Florence, Italy
**Simonetta di Lollo, Silvia Tozzini,** Department of Human Pathology and Oncology, University of Florence, Italy
**Giampiero Bellesi,** Department of Hematology, University of Florence, Italy
**Correspondence to:** Professor Giacomo Laffi, Department of Internal Medicine, University of Florence, Viale Pieraccini, 18, Zip Code 50139 Firenze, Italy. g.laffi@mednuc2.dfc.unifi.it
**Telephone:** +39-55-4223549 **Fax:** +39-55-4223549
**Received:** 2002-10-10 **Accepted:** 2002-11-04

## Abstract

We reported a case of non-Hodgkin's lymphoma where liver involvement was the predominant clinical manifestation. A 27-year old man presented wiht markedly elevated serum aspartate aminotrasferase, alanine aminotransferase and lactate dehydrogenase, reduced prothrombin activity, thrombocytopenic purpura and hepato-splenomegaly without adenopathy. Viral, toxic, autoimmune and metabolic liver diseases were excluded. Bone marrow biopsy showed an intracapillary infiltration of T-lymphocytes with no evidence of lipid storage disease. Because of a progressive spleen enlargement, splenectomy was performed. Histological examination showed lymphomatous intrasinuses invasion of the spleen. Immunohistochemical investigation revealed the T phenotype of the neoplastic cells: CD45+, CD45RO+, CD3+, CD4-, CD8-, TIA1-. About 50 % of the lymphoid cells expressed CD56 antigen. The diagnosis of hepatosplenic T cell lymphoma was done. The patient was treated with chemotherapy, which induced a complete remission. Eighteen months later, he had a first relapse with increased aspartate aminotransferase, alanine aminotransferase, lactate dehydrogenase, thrombocytopenic purpura and blast in the peripheral blood. In spite of autologous bone marrow transplantation, he died twenty months after the diagnosis. Even in the absence of a mass lesion or lymphoadenopathy, hepatosplenic T-cell lymphoma should be considered in the differential diagnosis of a patient whose clinical course is atypical for acute hepatic dysfunction.

Perfetto F, Tarquini R, Mancuso F, di Lollo S, Tozzini S, Bellesi G, Laffi G. Hepato-splenic lymphoma: a rare entity mimicking acute hepatitis: A case report. *World J Gastroenterol* 2003; 9 (6): 1381-1384
http://www.wjgnet.com/1007-9327/9/1381.asp

## INTRODUCTION

Liver and splenic involvement is commonly seen during a malignant lymphoma, but rarely occurs as a prominent clinical feature at diagnosis. Hepatosplenic lymphoma is a rare and poorly recognized entity[1] characterized by neoplastic proliferation of T-cell bearing a gd or, more rarely, ab clonal rearrangement of the receptor (TCR). This lymphoma shows a specific morphological pattern characterized by a preferential hepatic sinusoids and splenic red pulp involvement without lymphoadenopathy and discrete or absent bone marrow involvement. Moreover the diagnosis is complicated in several cases by the presence of misleading symptoms. We reported the case of a young man without palpable lymphoadenopathy and clinical and laboratory presentations resembling an acute liver disease.

## CASE REPORT

A 27-year old caucasian man was admitted in an Internal Medicine unit in February 1999 because of fever (38 ℃), malaise, anorexia, and erythematous macules and papules on the face, trunk and arms. The patient referred similar but transient cutaneous lesions in the previous two-months. Laboratory investigations yielded the following results: aspartate aminotransferase (AST) 240 IU/L (normal range: 0-37 IU/L), alanine aminotransferase (ALT) 520 IU/L (normal range: 0-40 IU/L), γ-glutamyl-transpeptidase (γ-GT) 46 IU/L (normal range: 11-43 IU/L), alkaline phosphatase (ALP) 298 IU/L (normal range: 60-270 IU/L) and platelets $120\times10^9$ /L (normal range: $130\text{-}400\times10^9$/L). Serological tests for Ebstein Barr virus (EBV) showed a positivity for nuclear antigen (IgG 248 ACU/ml) (normal value: <56 ACU/ml) whereas serology for hepatitis A (HAV), hepatitis B (HBV) and hepatitis C (HCV) viruses was negative. Physical examination showed a mild hepato-splenomegaly. There was no palpable lymphoadenopathy.

Two weeks later he was transferred to our Internal Medicine unit with the clinical diagnosis of "acute hepatitis with hepato-splenomegaly and recidivant purpuric exanthema". Physical examinations showed an enlarged tender liver (2 cm below the rib border) and splenomegaly (2 cm below the rib border) without peripheral lymphoadenopathy. The cutaneous lesions of the trunk and the face were already present as purpuric palpable papules. Fever was absent. Abdominal ultrasonography revealed a mild hepatomegaly and splenomegaly (major axis of 18 cm), without ascite and abdominal lymphoadenomegaly. Doppler sonography revealed an increased blood flow in the spleen and the portal vein without obstruction of the main hepatic veins. An upper gastrointestinal endoscopy did not reveal esophageal varices. Chest x-rays at the time of admission yielded normal findings. Liver function test showed AST 498 IU/L, ALT 958 IU/L, γ-GT 49 IU/L, ALP 426 IU/L, total bilirubin 1.15 mg/dl (normal range: 0.2-1.0 mg/dl) and lactate dehydrogenase (LDH) 1 234 U/L (normal range 190-450 IU/L). Peripheral blood counts showed hemoglobin 16.1 g/dl, hematocrit 45 %, leukocytes $4.9\times10^9$ /L with normal differential count and platelets $80\times10^9$/L. Coagulation indices showed prothrombin activity 53 % (normal range: 90-100 %), international normal ratio 1.4, activated partial thromboplastin time 53 sec (normal range: 25-40 sec) and fibrinogen 267 mg/dl (normal range: 200-400 mg/dl). Albumin levels were 4.25 g/dl (normal range: 3.3-5.1 g/dl) and γ-globulin were 1.44 g/dl (normal range:

0.84-1.44 g/dl). Serological tests were negative for HAV, HBV, HCV, cytomegalovirus and human herpes simplex N° 1, 2, and 6. EBV serologic findings were heterophile test (heterophile antibody) negative, viral capsid antigen (VCA) immunoglobulin IgM negative and IgG positive. Serological tests exploring infective agents able to induce an acute hepatitis such as Chlamydia pneumoniae, Bartonella spp, Borrelia Burgdorferi, Toxoplasma Gondii, Coxsackie virus groups A and B (N° 1-6) and Echovirus, were negative as well as the serological test for Rickettsie and Parvovirus B19. Results of serology for human immunodeficient virus (HIV) 1 and 2 including cDNA Polymerase Chain Reaction and the screening of the antigen p24 of HIV1 were negative. Serum α-fetoprotein and carcinoembryonic antigens were within the normal range. To exclude autoimmune disease, serological tests for anti-nuclear, anti-mitochondrial, anti-liver/kidney microsomial (LKM), and anti-smooth muscle (ASM) were performed but the results were negative; cryoglobulins and circulating immune complexes were absent. Serum ceruloplasmine levels, circulating serum copper levels, 24-h urine excretion of copper and α 1-antitrypsin levels were in the normal range and Kayser Fleischer rings were absent on slit-lamp examination. To exclude a thrombocytopenia induced by EDTA (pseudothrombocytopenia) blood was drawn on test tube with sodium citrate as anticoagulant but the result confirmed the presence of a true thrombocytopenia. Anti-platelet antibodies were negative in two consecutive different samples and reticulate platelets were in the normal range. Toxic (including also ingestion of hepatotoxic mushrooms such as Amanita Phalloides) and drugs inducing hepatitis were excluded by a careful and detailed personal and family history. During the following weeks, patient complained increasing fatigue and tenderness in the upper left quadrant and physical examination revealed an enlarged spleen that extended his lower pole 4-cm below the rib border. Liver function tests continued to rise with AST 658 IU/L, ALT 1 074 IU/L, γ-GT 72 IU/L, ALP 473 IU/L, and LDH 1 365 U/L. Serum β-2 microglobulin levels were 2.4 mg/dl; (normal range: 1.2-2.5 mg/dl). Coagulation indices showed prothrombin activity 51 %, international normal ratio 1.4, fibrinogen 146 mg/dl and activated partial thromboplastin time 42.4 sec without serological evidence of circulating anticoagulants such as lupus anticoagulant or anticardiolipin antibodies. A decreased activity of coagulation factor II (57 %; normal range: 70-120 %), VII (58 %; normal range: 70-120 %) and X (41 %; normal range: 70-120 %) were also demonstrated, despite i.v. Vitamin K treatment; factor VIII activity was also reduced (63.9 %; normal range: 70-150). The bleeding time was slightly prolonged (8 minutes and 20 seconds; normal range: 3-7 min.) Because of coagulopathy and thrombocytopenia percutaneous liver biopsy was not performed. Biopsy of the skin showed neither vasculitis findings nor lymphoproliferative disease. An abdominal CT scan revealed a massive enlargement of the spleen (20 cm of sagittal diameter and 14 cm of antero-posterior diameter) and mild hepatomegaly without either focal lesions or abdominal lymphoadenomegaly. Thorax and neck CT scan yielded normal findings. Although in type 1 Gaucher disease the liver function tests were not so seriously altered, the presence of hepatomegaly with a progressive and massive splenomegaly together with thrombocytopenia prompted us to undergo the patient to bone morrow examination and to a measurement of acid β-glucosidase activity in circulating leukocyte cells. Although β-glucosidase activity was slightly decreased (5.5 nmol/mg/h; normal range: 8-15.1 nmol/mg/h), the bone marrow examination did not reveal the presence of the characteristics of Gaucher cells with the typical "wrinkled paper" cytoplasm. However, an intracapillary T-lymphocytes infiltration was observed. The circulating leukocytes were $14.6\times10^9$/L (normal range: 4.8-8.5) with absolute lymphocytosis ($8.8\times10^9$/L, normal range: 1.6-2.4). Immunophenotype of circulating lymphocytes showed that CD3 positive lymphocytes were about $5.4\times10^9$/L (normal range: 1.1-1.7), CD4 positive lymphocytes were $2.5\times10^9$/L (normal range: 0.65-1.4), CD8 positive lymphocytes were $3.01\times10^9$/L (normal range: 0.32-0.90) with CD4 to CD8 ratio of 0.8 % (normal range: 1-1.5 %) and CD19 positive lymphocytes were $1.23\times10^9$/L (normal range: 0.2-0.4). Circulating T lymphocytes (65 % of overall; $5.65\times10^9$/L) bearing the ab type of TCR were 92.5 % (normal range: 90-95 %) while circulating T lymphocytes bearing gd TCR were about 7.5 % (normal range: 5-10 %). Over half (60 %) of circulating leukocytes were small to medium sized lymphoid cell with moderate amount of pale, agranular cytoplasm without villous projections. Some lymphocytes showed round or folding nucleus, with moderate clumped chromatin surrounding a small nucleolus. In spite of the opportunity to perform a transjugular liver biopsy, the presence of massive splenomegaly with pain in the left upper abdominal quadrant and early satiety, urged us to do splenectomy which was performed in April 1999. The histologic examination of the spleen revealed a hepatosplenic lymphoma. After the splenectomy, skin lesions disappeared, liver enzyme values progressively decreased and coagulation indices showed normalization in one week. As expected, platelets count increased until $738\times10^9$ /L one week after the splenectomy and decreased to $417\times10^9$/L one month later. In the post surgical period, patient was treated with 4 cycles of chemotherapy (Fi2/89; epirubicine, vincristine, bleomycine and cyclophosphamide). This resulted in a complete clinical remission with negative bone marrow biopsy. In view of autologous bone marrow transplantation (ABMT) he was treated with 2 cycles of chemotherapy (BAVEC-MiMA; BiCNU, adriblastine, vepeside, vincristine, mitoxantrone, methotrexate and cytosine arabinoside). In January 2000, he was submitted to three consecutive leukapheresis but, unfortunately, the number of peripheral circulating levels of CD34 positive cells was not sufficient for the ABMT and the patient refused new leukapheresis. Two other cycles of BAVEC-MiMA chemotherapy were performed as intensive consolidation therapy after the remission. One month later (May 2000), the patient was admitted to a hematological unit because of fatigue, malaise and erythematous papules of the face and trunk similar to those that characterized the beginning of the disease. Significant laboratory values included AST 225 IU/L, ALT 255 IU/L, LDH 1773 U/L, platelets $46\times10^9$/L and leukocytes $27.9\times10^9$/L, the latter characterized by medium and large size lymphocytes with cleaved and folding nucleus. The immunophenotype of circulating lymphocytes was NK (CD16+, CD56+, CD2+, CD7+; CD8 were expressed on about 63 % of NK population while CD3 was negative). He was treated with four weekly infusions of chemotherapy (MACOP-B; vincristine, adriamicine, bleomycine, cyclophosphamide, methotrexate and prednisone) with normalization of liver enzyme values, peripheral blood counts and skin lesions. The second relapse occured 10 weeks later. Patient was readmitted in the same hematological unit for salvage ABMT. One-month later, he developed an acute leukemia. The patient died in December 2000, twenty months after the diagnosis. Post-mortem examination was not performed.

## MATERIALS AND METHODS

Informed consent for all procedures was obtained from the patient. Bone marrow specimen was fixed in 10 % buffered formalin and processed according to standard technique. Paraffin sections were stained with hematoxylin-eosin, Giemsa,

PAS and Gomori method. Biopsy of the skin and specimens of the spleen were fixed in 10 % buffered formalin, and in B5; paraffin sections were stained with hematoxilin-eosin, Giemsa and PAS. An immunohistochemical investigation was performed on bone marrow and spleen sections according to streptavidin-biotin method. Monoclonal antibodies were used for detection of CD45, CD20, CD79a, CD10, CD45RO, CD30, CD15, CD56, CD8, CD4, TIA-1, AE1/AE3, EMA, HMB45, MIB1 antigens, and polyclonal antibodies for CD3 and S-100 protein detection. The positive reaction was revealed using diaminobenzidin as chromogen.

### *Histologic findings*

Biopsy of the skin showed a moderate aspecific lymphoid infiltration of perivascular space associated with erythrocytes. Bone marrow biopsy showed intense eritroid and megakaryocytic hyperplasia and a mild hypoplasia of myeloid compartment. Moreover an important intracapillary infiltration of medium-sized T-lymphocytes (CD45+, CD3+, scattered CD56+, CD 20- ) was observed (Figure 1). The spleen weight was 3 000 g. Microscopic examination showed the presence of a diffuse intrasinuses infiltrate in the red pulp of medium-sized T-lymphoid cells with round to irregular nuclei and moderately abundant pale cytoplasm (Figure 2). All neoplastic cells expressed CD45, CD45RO and CD3 membrane antigens (Figure 3), whereas they were CD4-, CD8- and TIA-1-. CD56 antigen was positive on about 50 % of the T-lymphoid cells (Figure 4). The diagnosis of hepatosplenic T cell lymphoma was done. Because of the unavailability of frozen sections, the analysis of gd TCR expression was not done.

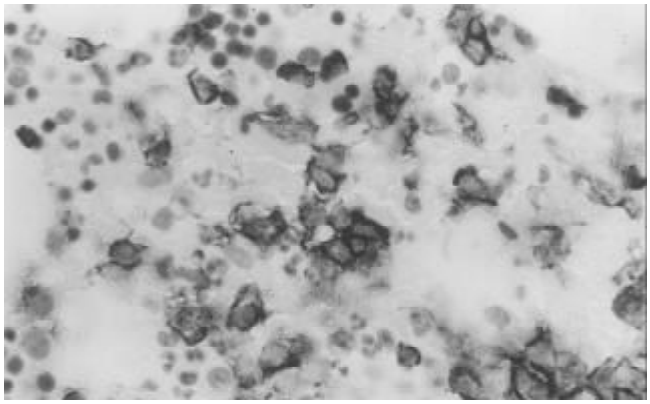

**Figure 1** Immunohistochemical analysis of the bone marrow: the neoplastic cells within sinuses were CD3 positive and scattered CD56 positive (insert).

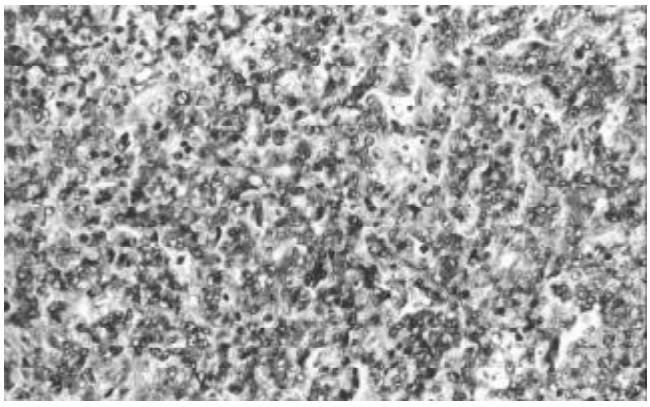

**Figure 2** Clusters of medium-sized cells seeped through the red pulp of spleen.

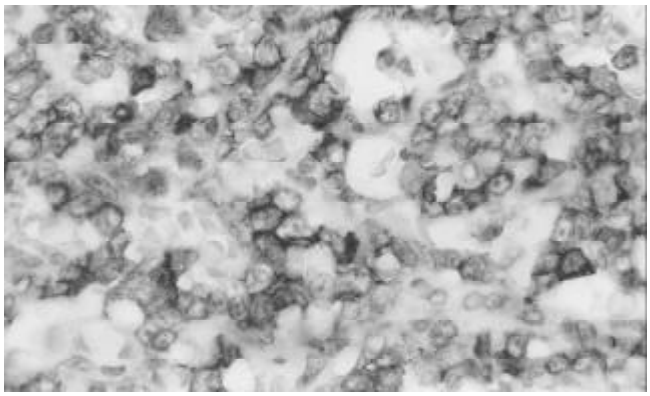

**Figure 3** The neoplastic cells were CD3 positive in the spleen.

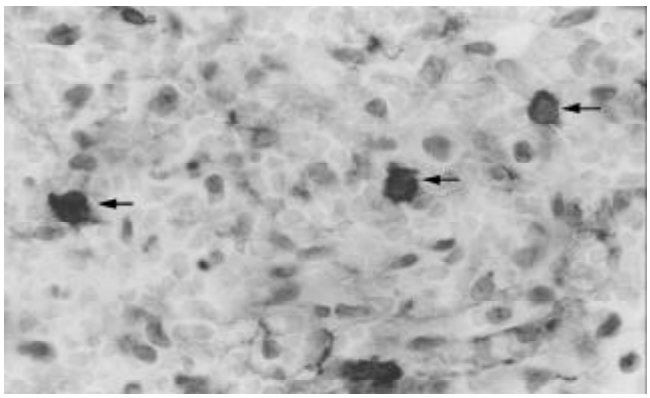

**Figure 4** The neoplastic cells were scattered CD56 positive (arrows) in the spleen.

## DISCUSSION

Lymphomatous involvement of the liver has been described in three clinical situations: disseminated disease, primary liver lymphoma and hepatosplenic T-cell lymphoma. Secondary hepatic involvement by lymphoma is relatively common and indicates advanced disease. Non-Hodgkin's primary lymphoma of the liver is an uncommon entity, often clinically indistinguishable from more commonly occurring primary carcinoma and metastatic neoplasms; the correct diagnosis is based on liver biopsy or even on post-mortem examination because of lacking of suggestive clinical or imaging features. The hepatosplenic T-cell lymphoma has been recognized by Farcet *et al.* in 1990[1] as a distinct entity characterized by a $\gamma\delta$ T lymphocytes sinusal infiltration of the red pulp of the spleen and by sinusoidal infiltration of the liver without lymph node involvement[2]. Because of its striking uniformity with respect to clinical, morphological and immunophenotypical features, this lymphoma was listed as a provisional entity in the Revised European-American Lymphoma (REAL) classification[3]. Later on, it has been incorporated as a distinct entity in the WHO classification of lymphoid neoplasms[4] and termed hepatosplenic $\gamma\delta$ T-cell lymphoma. Since then, to our knowledge, 45 cases have been described[5]. According to Weidmann revision, clinical symptoms at presentation are hepato-splenomegaly, constitutional symptoms and less frequently jaundice due to hepatic involvement. The predominant laboratory findings are reduced peripheral blood cells ranging from hemolytic anemia (Coombs negative) to thrombocytopenia or pancytopenia, high levels of LDH and mild increase of liver enzymes. Moreover, recently, 14 cases of hepatosplenic lymphoma expressing $\alpha\beta$ TCRs have been described[6].

These $\alpha\beta$ lymphomas fulfill all the clinical, morphological and immunophenotypical criteria required for the diagnosis

of hepatosplenic lymphoma, with the exception of the female preponderance (11/14 patients) and age of distribution (more wide than the γδ counterpart). Early diagnosis of this lymphoma, even if mandatory, is complicated in several cases because of the absence of lymphoadenomegaly, not specific bone marrow involvement and normal peripheral blood cell counts. The diagnosis of hepatosplenic T-cell lymphoma in the case we reported had considerable difficulties because its clinical and laboratory features were similar to acute hepatitis. As a matter of fact, the liver chemistry evaluation was typical of hepatic inflammatory disease with hepatocellular necrosis (about tenfold increase of AST and ALD and threefold increase of LDH) and impaired synthesis of liver coagulation factors whereas, the mild increase of ALP level together with normal levels of serum β-2 microglobulin and γ-GT were unusual for a lymphoproliferative disease of the liver. Probably these unusual laboratory findings were related to the quite exclusive sinusoidal infiltration by lymphoid cells without or with minimal portal involvement. However, this clinical presentation prompted us to exclude all causes of acute liver diseases such as viral hepatitis drugs, toxins, chemical ingestion and/or exposition, vascular abnormalities, autoimmune hepatitis and metabolic diseases. As the present case illustrated, an early diagnosis of hepatosplenic lymphoma was unlikely to be possible on bone marrow specimen alone. According to Galaurd[7] even when the hepatosplenic involvement is clear, the presence of few T-cells within bone marrow sinus is neither specific nor conclusive without a molecular analysis on frozen tissue. Liver biopsy, which is another way to confirm the diagnosis of hepatosplenic T-cell lymphoma, was not performed in this case because of the presence of coagulopathy and thrombocytopenia. Nevertheless, the presence of an intracapillary infiltrate by T lymphocytes on the bone marrow specimen as well as the progressive and symptomatic enlargement of the spleen prompted us to suspect the presence of a lymphoprolipherative disease and consequently to perform splenectomy. As reported in literature, splenectomy was the cornerstone for the diagnosis of hepatosplenic T-cell lymphoma. Immunophenotype studies on the spleen specimens showed the typical pattern of hepatosplenic T-cell lymphoma characterized by expression of CD45 and CD3 antigens and by double negativity for CD4 and CD8 antigens. The NK cell associated antigen CD56 expression has been reported in approximately 70-100 % of hepatosplenic T-cell lymphoma[8, 9]. The presence in the bone marrow of T-lymphocytes bearing the CD56 antigen could explain the late involvement of peripheral blood by lymphoid cell with NK immunophenotype. Furthermore, in contrast with other previous investigations, in all specimens of the spleen examined, neoplastic cells were negative for TIA-1 (restricted intracellular antigen, also called granular membrane protein of 17 Kd, GMP 17), a very sensitive marker of cytosol granules independent of their activation status. Concerning the recurrence of cutaneous skin lesions, a skin biopsy, performed early in the course of disease, showed only a moderate and aspecific lymphoid infiltration of perivascular spaces, without the morphological and immunophenotypical findings that characterized the peripheral lymphoma involving the skin. Although thrombocytopenia was not severe, a complete remission of skin lesions was achieved after its correction. It seems likely to ascribe these purpuric lesions to the reduced number of circulating platelets, but a cytotoxic activity of cutaneous T lymphocytes could have a role in the pathogenesis of these skin lesions. As the present case illustrated that the prognosis for this type of lymphoma is poor. Complete remission was reported only in few patients after chemotherapy (second and third generation regime for high-grade lymphomas), followed by autologous and allogenic bone marrow or peripheral stem cell transplantation. The median survival time was 8 months (range 0-42 month)[5].

In conclusion, the current report described the unusual clinical presentations of hepatosplenic lymphoma. This patient, in fact, shared several distinctive features including: 1) the initial clinical presentations mimicking an acute hepatitis, 2) the presence of cutaneous lesions, contemporary with the hepatosplenic involvement and 3) a negativity of TIA-1 expression of lymphoid T cells. Even in the absence of a mass lesion or lymphoadenopathy, hepatosplenic T-cell lymphoma should be included in the differential diagnosis of an acute hepatic dysfunction in young patient who shows no evidence of viral, toxic, autoimmune or metabolic liver disease.

## REFERENCES


1 **Farcet JP**, Gaulard P, Marolleau JP, Le Couedic JP, Henni T, Gourdin MF, Divine M, Haioun C, Zafrani S, Goossens M. Hepatosplenic T-cell lymphoma: sinusal / sinusoidal localization of malignant cells expressing the T-cell receptor gamma delta. *Blood* 1990; **75**: 2213-2219

2 **Gaulard P**, Zafrani S, Mavier P, Rocha FD, Farcet JP, Divine M, Haioun C, Piaudeau Y. Peripheral T cell lymphoma presenting as predominant liver disease: a report of three cases. *Hepatology* 1986; **6**: 864-868

3 **Harris NL**, Jaffe ES, Stein H, Banks PM, Chan JK, Cleary ML, Delsol G, De Wolf-Peeters C, Falini B, Gatter KC. A revised European-American Lymphoma of lymphoid neoplasms: a proposal from the International Lymphoma Study Group. *Blood* 1994; **84**: 1361-1392

4 **Harris NL**, Jaffe ES, Diebold J, Flandrin G, Muller-Hermelink HK, Vardiman J. Lymphoma classification-from controversy to consensus: the R.E.A.L. and WHO Classification of lymphoid neoplasms. *Ann Oncol* 2000; **11**: 3-10

5 **Weidmann E**. Hepatosplenic T cell lymphoma. A review on 45 cases since the first report describing the disease as a distinct lymphoma entity in 1990. *Leukemia* 2000; **14**: 991-997

6 **Macon WR**, Levy NB, Kurtin PJ, Salhany KE, Elkhalifa MY, Casey TT, Craig FE, Vnencak-Jones CL, Gulley ML, Park JP, Cousar JB. Hepatosplenic alpha beta lymphomas: a report of 14 cases and comparison with hepatosplenic gammadelta lymphomas. *Am J Surg Pathol* 2001; **25**: 285-296

7 **Gaulard P**, Kanavaros P, Farcet JP, Rocha FD, Haioun C, Divine M, Reyes F, Zafrani ES. Bone marrow histologic and immunohistochemical findings in peripheral T cell lymphoma: a study of 38 cases. *Hum Pathol* 1991; **22**: 331-338

8 **Cooke CB**, Krenacs L, Steller-Stevenson M, Greiner TC, Raffeld M, Kingma DW, Abruzzo L, Frantz C, Kaviani M, Jaffe ES. Hepatosplenic T cell lymphoma: a distinct clinicopathologic entity of cytotoxic gd T cell origin. *Blood* 1996; **88**: 4265-4274

9 **Salhany KE**, Feldman M, Kahn MJ, Perrit D, Schretzenmair RD, Wilson DM, DiPaola RS, Glick AD, Kant JA, Nowell PC Khan MJ. Hepatosplenic gammadelta lymphoma: ultrastructural, immunophenotypic, and functional evidence for cytotoxic T lymphocyte differentiation. *Hum Pathol* 1997; **28**: 674-685


**Edited by** Xu XQ and Zhu LH